Laurel A. Stadtmauer
Ilan Tur-Kaspa
Editors

Ultrasound Imaging in Reproductive Medicine

Advances in Infertility Work-up, Treatment, and ART

Springer

Ultrasound Imaging in Reproductive Medicine

Laurel A. Stadtmauer • Ilan Tur-Kaspa
Editors

Ultrasound Imaging in Reproductive Medicine

Advances in Infertility Work-up, Treatment, and ART

Springer

Editors
Laurel A. Stadtmauer, MD, PhD
Jones Institute for Reproductive Medicine
Department of Obstetrics and Gynecology
Eastern Virginia Medical School
Norfolk, VA
USA

Ilan Tur-Kaspa, MD
Institute for Human Reproduction (IHR)
Department of Obstetrics and Gynecology
The University of Chicago
Chicago, IL
USA

ISBN 978-1-4614-9181-1 ISBN 978-1-4614-9182-8 (eBook)
DOI 10.1007/978-1-4614-9182-8
Springer New York Heidelberg Dordrecht London

Library of Congress Control Number: 2013956430

Printed on acid-free paper

Springer is part of Springer Science+Business Media (www.springer.com)

A special thanks and dedication of the book to my parents Doris and Seymour, husband Ivan, and daughter Alessandra, who inspire me every day and have offered their love

Laurel A. Stadtmauer

This book is dedicated to the love of my life, my wife Hana Tur-Kaspa, and to our children Leeron, Adi, and Tomer, for their continuous love, support, and encouragement, and to the living memories of my parents, Miriam and Chaim Tur-Kaspa, that their wisdom and passion for education are an inspiration for us all

Ilan Tur-Kaspa

Foreword

It is with great pleasure that I introduce this book on *Ultrasound Imaging in Reproductive Medicine: Advances in Infertility Work-up, Treatment, and Assisted Reproductive Technology*. Ultrasound has proven to be essential in the care of the patient with infertility and in many aspects of reproductive medicine, and a high-quality book that encompasses what anyone in the field needs to know is a very valuable resource indeed.

This book is laid out in a very logical sequence, starting with general information about ultrasound safety in reproductive medicine, technique for 3D ultrasound and Doppler applications, and legal aspects of ultrasound imaging. The second part addresses the use of ultrasound in the infertility work-up starting with ultrasound of the ovary, the uterus, and the fallopian tube and male infertility. Each part addresses the normal changes followed by detailed chapters on specific abnormalities related to infertility. The third part focuses on ultrasound in infertility treatment with detailed description of the role of ultrasound in follicle monitoring, oocyte retrieval, embryo transfer, early pregnancy evaluation, ectopic pregnancy, and focused ultrasound for the treatment of fibroids.

A formidable team of authors with international prominence was assembled to contribute various chapters in their specific areas of expertise. The book is written in a style that is easy to read and is replete with ultrasound images, illustrating various normal and abnormal conditions. The reader will learn about various aspects of ultrasound imaging in reproductive medicine from world authority on the subject in a systematic and comprehensive fashion. Various chapters reflect the current state of the science in pelvic imaging as it relates to the evaluation and management of the infertile couple.

Kudos to Dr. Laural Stadtmauer and Dr. Ilan Tur-Kaspa, the book's editors, for their vision and hard work in accomplishing this masterpiece. Laurel is a gifted scientist, an actively practicing physician, and a superb gynecologic sonologist with tremendous expertise in advanced ultrasound imaging. Ilan is an internationally known expert in reproductive medicine and infertility and gynecologic ultrasound. Their skills and background present a special perspective as an editor that is evident throughout the book and translates into an evidence-based practical approach to ultrasound imaging.

This book belongs on the desk of any healthcare worker involved in the field of infertility. From my standpoint, this book will become the ultimate book on ultrasound in reproductive medicine.

Norfolk, Virginia — Alfred Z. Abuhamad, MD

Preface

Can one imagine infertility diagnosis and treatment without imaging? Ultrasound has become the main tool and has revolutionized the practice by reproductive specialists worldwide and is used daily by the authors. From the first encounter with the patients who have been suffering from infertility, ultrasound will be used for the evaluation of uterus and ovaries to rule out any abnormalities and evaluation of ovarian reserve. Ultrasound will be part of the monitor of a natural cycle, controlled ovarian hyperstimulation with oral and injectable medications, and for ART. It will then be used to confirm intrauterine pregnancy and for the investigation of a pregnancy of unknown location and evaluation and treatment of ectopic pregnancy.

Therefore, it was natural for us, the coeditors, who have been involved in advanced infertility work-up and treatment for about 20 years and have served as Chairs of the Reproductive Imaging Special Interest Group of the American Society for Reproductive Medicine (ASRM) to compile this book for gynecologists, infertility specialists, ultrasonographers, radiologists, and nurses involved in imaging and the diagnosis and treatment of the infertile couple. It is a practical book covering all normal findings and abnormalities found in women of reproductive age. Following this practical framework of the book, the chapters are covered in three parts and include the principles of ultrasound; the normal and abnormal uterus, fallopian tubes, and ovaries; and the use of ultrasound in infertility and ART treatments along with complications and ultrasound-guided techniques.

The authors have compiled many original ultrasound images with the chapters. All authors are all internationally recognized specialists in reproductive medicine as well as imaging, and their contribution made this book a unique comprehensive coverage of the modern role of ultrasound in reproductive medicine. We hope you find the book helpful in improving your evaluation and treatment of your patients and an enjoyable experience. See better, do ART better.

Norfolk, VA, USA — Laurel A. Stadtmauer, MD, PhD
Chicago, IL, USA — Ilan Tur-Kaspa, MD

Acknowledgments

Today one cannot imagine the practice of reproductive medicine without imaging. Over the last 20 years in practice, we have seen so many advances and improvements in ultrasound. See better, do ART better.

Special thanks to all of our mentors over the years, who trained us in the areas of ultrasound, and thanks to our patients whom we learn from daily.

Norfolk, VA, USA — Laurel A. Stadtmauer, MD, PhD
Chicago, IL, USA — Ilan Tur-Kaspa, MD

Contents

Contributors

Jacques S. Abramowicz, MD, FACOG, FAIUM Division of Maternal Fetal Medicine, Department of Obstetrics and Gynecology, Wayne State University, Hutzel Women's Hospital, Detroit, MI, USA

Alfred Z. Abuhamad, MD Department of Obstetrics and Gynecology, Eastern Virginia Medical School, Norfolk, VA, USA

Gautam N. Allahbadia, MD, DNB, FNAMS Rotunda-The Center for Human Reproduction, Mumbai, Maharashtra, India

Jane Arrington, RDMS Maternal Fetal Medicine, Eastern Virginia Medical School, Virginia Beach, VA, USA

Mark W. Austin, MD Department of Obstetrics and Gynecology, Riverside Regional Medical Center, Newport News, VA, USA

Renato Bauman, MD, PhD Department of Gynecology and Obstetrics, Sveti Duh Clinical Hospital, Zagreb, Croatia, Europe

Josef Blankstein, MD, ARDMS Department of Obstetrics and Gynecology, Rosalind Franklin University of Medicine and Science, Mount Sinai Hospital, Chicago, IL, USA

Silvina M. Bocca, MD, PhD Department of Obstetrics and Gynecology, The Jones Institute for Reproductive Medicine, Norfolk, VA, USA

Robert E. Brannigan, MD Department of Urology, Northwestern University, Feinberg School of Medicine, Chicago, IL, USA

Joel Brasch, MD Department of Obstetrics and Gynecology, Rosalind Franklin University of Medicine and Science, The Chicago Medical School, Chicago, IL, USA

Patricia Carrascosa, MD Maipu Diagnostics, Buenos Aires, Argentina

David D. Casalino, MD Department of Radiology, Northwestern University, Feinberg School of Medicine, Chicago, IL, USA

David P. Cohen, MD Department of Obstetrics and Gynecology/Section of Reproductive Endocrinology, University of Chicago Medical Center, Chicago, IL, USA

Edmond Confino, MD Repro/Endo, Infertility, Feinberg School of Medicine, Northwestern University, Chicago, IL, USA

Elosha Eiland, MD Department of Obstetrics and Gynecology, Meharry Medical College, Nashville, TN, USA

Donald L. Fylstra, MD Department of OBGYN, Medical University of South Carolina, Charleston, SC, USA

Bradley S. Hurst, MD Department of Obstetrics and Gynecology, Carolinas Healthcare System, Charlotte, NC, USA

Roohi Jeelani, MD Department of Obstetrics and Gynecology, Wayne State University, Detroit, MI, USA

Artemis Karkanaki, MD, MSc, PhD Third Department of Obstetrics and Gynecology, Hippokration General Hospital of Thessaloniki, Greece, Aristotle University of Thessaloniki, Thessaloniki, Greece

Jennifer F. Kawwass, MD Division of Reproductive Endocrinology and Infertility, Department of Gynecology and Obstetrics, Emory University School of Medicine, Atlanta, GA, USA

Alessandra Kovac College of Arts and Sciences, University of Virginia, Charlottesville, VA, USA

Shumal Malepati, MD Department of Obstetrics and Gynecology, Mount Sinai Hospital, Chicago, IL, USA

Ursula Reš Muravec, MD, MSc Department for infertility, Medical Center Dravlje, Ljubljana, Slovenia, Europe

Maximilian Murtinger, MD IVF Centers Prof. Zech, Bregenz, Austria

Emily N.B. Myer, MD Department of Obstetrics and Gynecology, Eastern Virginia Medical School, Norfolk, VA, USA

Ernest Hung Yu Ng, MD, FRCOG (UK) Department of Obstetrics and Gynaecology, The University of Hong Kong, Queen Mary Hospital, Pokfulam, Hong Kong, Hong Kong

Kamal Ojha, MRCOG Obstetrics and Gynecology, St. George's Hospital, London, Tooting, London, UK

Nikolaos Prapas, MD, MSc, PhD Third Department of Obstetrics and Gynecology, Hippokration General Hospital of Thessaloniki, Greece, Aristotle University of Thessaloniki, Thessaloniki, Greece

Beth W. Rackow, MD Department of Obstetrics and Gynecology, Columbia University Medical Center, Center for Women's Reproductive Care, New York, NY, USA

Gloria Richard-Davis, MD, FACOG Department of Obstetrics and Gynecology, Meharry Medical College, Nashville, TN, USA

Khaled Sakhel, MD, FACOG, FACS Division of Minimally Invasive and Robotic Surgery, Eastern Virginia Medical School, Norfolk, VA, USA

Donna R. Session, MD Division of Reproductive Endocrinology and Infertility, Department of Gynecology and Obstetrics, Emory University School of Medicine, Atlanta, GA, USA

James M. Shwayder, MD, JD Department of Obstetrics and Gynecology, University of Mississippi, Jackson, MS, USA

Laura Proud Smith, MD Department of Reproductive Endocrinology and Infertility, Reproductive Medicine and Surgery Center of Virginia, P.L.C, Charlottesville, VA, USA

Dietmar Spitzer, MD IVF Centers Prof. Zech, Salzburg, Austria

Laurel A. Stadtmauer, MD, PhD Department of Obstetrics and Gynecology, Eastern Virginia Medical School, Jones Institute for Reproductive Medicine, Norfolk, VA, USA

Dale W. Stovall, MD Department of Obstetrics and Gynecology, Riverside Regional Medical Center, Newport News, VA, USA

Carlos E. Sueldo, MD Department of Obstetrics and Gynecology (Rei Division), University of California San Francisco-Fresno, Clovis, CA, USA

Mette Toftager, MD, PhD Student Department of Gynecology and Obstetrics, Section of Infertility, Hvidovre University Hospital, Hvidovre, Denmark

Landon W. Trost, MD Department of Urology, Mayo Clinic, Rochester, MN, USA

Ilan Tur-Kaspa, MD Institute for Human Reproduction (IHR), Chicago, IL, USA

Department of Obstetrics and Gynecology, The University of Chicago, Chicago, IL, USA

Dimuthu Vinayagam, MB BS, BSc Obstetrics and Gynecology, St. George's Hospital, London, Tooting, London, UK

Steven L. Warsof, MD Department of Obstetrics and Gynecology, Eastern Virginia Medical School, Norfolk, VA, USA

Nicolas Herbert Zech, MD Department of Obstetrics and Gynecology, Medical University Graz, Bregenz, Austria

Part I

Ultrasound Technique

Ultrasound in Reproductive Medicine: Is It Safe?

1

Jacques S. Abramowicz

Introduction

The first published description of the clinical use of ultrasound in obstetrics and gynecology (ob/gyn) dates from 1958 [1] and describes the value of this new technology for the diagnosis of abdominal masses, specifically, ovarian cysts. Since then its use has increased exponentially and is ubiquitous in the daily practice of ob/gyn. Another field that has equally burgeoned is reproductive endocrinology and infertility. These two disciplines are strongly interconnected, in part because of the major progresses made in image quality and the introduction of new modalities, such as color and spectral Doppler or three-dimensional (3D) ultrasound, which has greatly facilitated diagnosis, interventions, and certain forms of therapy in fertility treatments and assisted reproductive technology. Because ultrasound is a waveform, with alternating positive and negative pressure, it has effects in tissues it traverses. These may be thermal and nonthermal (or mechanical). The question that bears asking is: can these effects be detrimental to the developing follicle, ovum, or early fetus? A publication describing premature ovulation in women whose ovaries were exposed to ultrasound is often quoted but dates from 1982 [2]. This chapter will briefly describe the physics of ultrasound and its interaction with live tissue, define bioeffects and on-screen indicators of potential risk, focus on ovarian scanning in ART, and discuss fetus susceptibility and safety measures. Bioeffects and safety of ultrasound in pregnancy, in general, and in later gestation, in particular, will not be addressed. The interested reader may consult various reviews on this topic [3–10]

A Short Review of Ultrasound Physics

Ultrasound is a waveform, characterized by various parameters: *frequency* is the number of cycles per second, measured in Hertz (Hz). Human ears can discern sounds at approximately 20–20,000 Hz. Diagnostic ultrasound is, generally, 2–15 million Hz (2–15 MHz). *Wavelength* is the distance between two corresponding points on a particular wave. It is inversely proportional to the frequency (0.2–1.5 mm). *Resolution* (i.e., the shortest distance between two points which allows these two points to be seen separately) depends on the wavelength: the axial resolution ranges between 2 and 4 wavelengths. Therefore, the smaller the wavelength (which corresponds to the higher the frequency), the better the resolution (the distance between the two points is smaller) but the lower the penetration. This explains why endovaginal probes have better resolution (higher frequency)

J.S. Abramowicz, MD, FACOG, FAIUM
Division of Maternal Fetal Medicine,
Department of Obstetrics and Gynecology,
Wayne State University, Hutzel Women's Hospital,
3990 John R Street, Detroit, MI 48201, USA
e-mail: jabramow@med.wayne.edu

L.A. Stadtmauer, I. Tur-Kaspa (eds.), *Ultrasound Imaging in Reproductive Medicine,*
DOI 10.1007/978-1-4614-9182-8_1, © Springer Science+Business Media New York 2014

but lower penetration, hence the need to be closer to the organs being examined. Diagnostic ultrasound is not continuous but pulsed. There are pulses separated by silent intervals. The number of pulses occurring in 1 s is the *pulse repetition frequency* (PRF). The fraction of time that the pulsed ultrasound is on (duty factor) is very important from a potential bioeffect aspect. When the PRF increases, so does the duty factor. Since the ultrasound wave is sinusoidal, there are alternating periods of positive and negative pressure which allow the wave to propagate through tissues by means of particles motions. The speed of propagation is related both to the beam and several of the tissue properties. The average speed of sound propagation in biological tissues is estimated at 1,540 m/s. When pressure is exerted on the resisting insonated tissue, work is produced. The ability of the wave to do this is its energy (in joules), and the rate at which the energy is transformed from one form to another is the *power* (in watts or milliwatts, mW). When expressed as a function of area unit (in cm^2), this is *intensity* (generally in mW/cm^2). Bioeffects are conventionally related to the acoustic intensity. As stated above, pulses of energy are intermingled with periods where no energy is emitted. When describing an ultrasound wave, several parameters can be described in relation to time or space. By combining peak and average values in time and space, six intensities can be defined. The spatial peak-temporal average (I_{SPTA}) is the most practical and most commonly referred to and corresponds to the energy averaged over a period of time. The maximal permitted values, based on various clinical application being considered, were first determined in 1976 by the US Food and Drug Administration (FDA) [11] but were modified in 1986 [12]. The most recent definition dates from 1992 [13]. These values (in mW/cm^2) are shown in Table 1.1 for the various applications (left column) as a function of the year they were implemented (modified from references [10–12]). The numbers in parentheses indicate the percentage increase, compared to the previously allowed intensity.

It is interesting to observe from Table 1.1 that, for fetal imaging, the I_{SPTA} was allowed to increase by a factor of almost 16 from 1976 to the most recent values in 1992, yet, as will be described below, all epidemiological information available regarding fetal effects predates 1992. A further remarkable fact is that intensity for ophthalmic examination has not changed from the original 17 mW/cm^2, a value approximately 42.5 times lower than the present allowed maximal value for fetal scanning. Furthermore, pelvic imaging (abdominal or transvaginal) is not specified in Table 1.1.

Table 1.1 Values of I_{SPTA} by modality and year of definition

	1976	1986	1992
Ophthalmic	17	17	17
Fetal imaging	46	94 (104 %)	720 (667 %)
Cardiac	430	430	720 (67 %)
Peripheral vessel	720	720	720

Adapted from Refs. [11–13]
All are derated values in mW/cm^2

Tissue Characteristics

When the ultrasound wave travels through a medium, its intensity diminishes with distance [14]. Biological tissues are nonhomogeneous and weakening (attenuation) of the signal results from *absorption* and *scattering,* as well as *reflection*. Absorption is the sound energy being converted to other forms of energy, and scattering is the sound being reflected in directions other than its original direction of propagation. Since attenuation is proportional to the square of sound frequency, it becomes evident why higher-frequency transducers have less penetration (but better resolution). Acoustic impedance can be described as the opposition to transmission of the ultrasound wave. It is proportional to the velocity of sound in the tissue (estimated at 1,540 ms/s, see above) and to the tissue density.

Instrument Outputs

Publications of various instruments outputs are available [15]. From a clinical standpoint, there is no easy way to verify the actual output of the instrument in use. In addition, each attached transducer will generate a specific output, further

complicated by which mode is being applied [16]. When comparing modes, the I_{SPTA} increases from B-mode (34 mW/cm^2, average) to M-mode to color Doppler to spectral Doppler (1,180 mW/cm^2). Average values of the temporal averaged intensity are 1 W/cm^2 in Doppler mode but can reach 10 W/cm^2 [17]. Therefore, precaution is needed when applying this mode. Most measurements are obtained from manufacturers' manuals, having been derived in laboratory conditions which may be different from real-life clinical conditions [18]. Furthermore, machine settings which are under the control of the clinician can alter the output. For instance, the degree of temperature elevation is proportional to the product of the amplitude of the sound wave by the pulse length and the PRF. Hence, it is evident why any change (augmentation) in these properties can add to the risk of elevating the temperature, a potential mechanism for bioeffects. The three important parameters under end-user control are the *operating mode (*including choice of *transducer),* the *system setup/output control,* and the *dwell time*.

1. *Scanning mode*: as mentioned above, B-mode carries the lowest risk and spectral Doppler the highest (with M-mode and color Doppler in between). High pulse repetition frequencies are used in pulsed Doppler techniques, generating greater temporal average intensities and powers than B- or M-mode and hence greater heating potential. In spectral Doppler, the beam needs to be held in relatively constant position over the vessel of interest, which may add to the risk of a larger increase in temporal average intensity. Naturally, *transducer choice* is of great consequence since transducer frequency will determine penetration, resolution, and field of view.
2. *System setup*: starting or default output power is very often high to allow better imaging, and end users will, generally, keep it as such, mostly out of lack of concern for bioeffects. Excellent, diagnostic images can be obtained at lower output powers (see Fig. 1.1). Recently major manufacturers have responded to requests from involved individuals and are now offering a low output power in Doppler as their default. Only if needed can the end user increase the power. Fine-tuning performed by the examiner to optimize the image influences output but with no visible effect (except if one follows TI and/or MI displays, see below). Controls that regularize output include *focal depth* (usually with greatest power at deeper focus but, occasionally on some machines, with highest power in the near field), *increasing frame rate*, and *limiting the field of view* (for instance, by high-resolution magnification or certain zooms). In Doppler mode, changing *sample volume* and/or *velocity range* (all done to optimize received signals) changes output. A very important control is receiver gain. It often has similar effects to the above controls on the recorded image but none on the output of the outgoing beam and is, therefore, completely safe to manipulate. In addition, over the years, as seen in Table 1.1, output of instruments has increased [17]
3. *Dwell time* is directly under the control of the examiner. It is the time during which the ultrasound beam remains at the same point in the tissue. Interestingly, dwell time is not taken into account in the calculation of the safety indices (TI and MI) nor, in general, until now, reported in clinical or experimental studies. Directly associated with dwell time is *examiner experience* in terms of knowledge of anatomy, bioeffects, instrument controls, and scanning techniques, since, presumably, the more experienced the examiner, the less scanning time is needed.

Ultrasound Bioeffects

Why is this even an issue? The average ultrasound professional (and the lay people) will state that ultrasound is obviously safe and that it is not X-rays [19]. Ultrasound, similarly to any sound, is a form of energy. The waveform has positive and negative pressures (see above). When such a waveform travels through *any* tissue, some of this energy is transformed into heat (thermal effects), and some may cause movements of tissues or membranes as well as some more complex mechanical results (nonthermal or

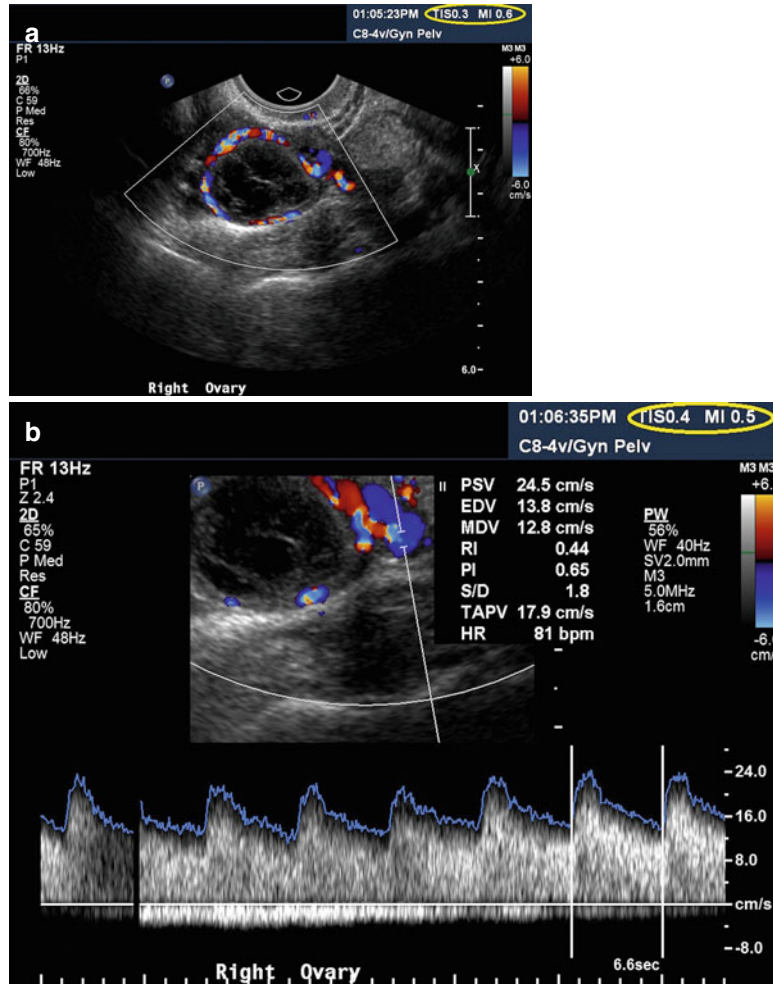

Fig. 1.1 Color (**a**) and spectral (**b**) Doppler of the corpus luteum. Please note the low TI (0.3 and 0.4, respectively) and MI (0.6 and 0.5, respectively) in both images

mechanical effects). Cavitation is one of these nonthermal effects. This refers to reaction of small gaseous bodies (bubbles) when exposed to an ultrasound field [20]. In inertial cavitation (formerly known as transient cavitation [21]), the bubble changes volume (expands under negative pressure and contracts under positive pressure) until the vibration amplitude of the bubble wall increases so much that the bubble implodes. This implosion generates highly localized shock waves and is also associated with extremely high local temperatures, up to 10,000 K [22]. This is localized on a tiny area and for a very brief moment, and no heat is actually exchanged (adiabatic reaction). However, in addition to the temperature elevation, the implosion may result in the generation of free radicals such as hydroxyl radicals and hydrogen [23]. If the bubble does not collapse during the ultrasound exposure, the condition is referred to as stable cavitation with the bubble oscillating as the waveform progresses. Absence of cavitation foci (gas bubbles), as is the case in fetal lungs and bowels and, presumably, in the vicinity of the ovary and the developing follicle, renders this phenomenon extremely improbable.

These effects occur whenever a tissue is insonated, thus the designation bioeffects [24]. Many in vitro models, such as cells or tissue cultures, have been used to investigate ultrasound bioeffects and to gain a better understanding of the possible mechanisms of interaction between ultrasound and biological tissue [25]. Studies on relatively simple nonmammalian organisms,

such as insects, amphibians, and avians, are helpful in understanding the mechanisms of interaction between ultrasound and biological systems [26]. However, from a clinical standpoint, bioeffect studies of mammalian species are of more relevance. Most of these studies were performed on small rodents, such as mice or rats. The extrapolation of experimental results to humans can be difficult, at best. A very comprehensive, albeit dated, review of the effects of ultrasound on mammalian development was prepared by Sikov [27]. He evaluated bioeffects depending on gestational age and thus attempted to extract information on the relation between exposure parameters and stage of development at exposure Experimental studies indicate that intact mammalian systems (in vivo) do not show a significant rise in temperature when exposed to pulsed imaging equipment [27–29]. However, peripheral vessel pulsed and continuous-wave (CW) Doppler equipment, when used for a relatively long time (1–10 min), may be an exception [30, 31]. Therefore, Doppler should be used with care, especially during applications in which Doppler is used for the assessment of blood velocities in ovarian vessels in ART and studies of the first trimester fetus [32]. Reports on the use of new technologies, such as three- and four-dimensional (3D/4D) ultrasound, are beginning to appear in the art literature [33], but these do not appear to expose tissues to higher levels of acoustic energy [34].

The Output Indices

Because of the two main mechanisms (described above) involved in bioeffects of ultrasound, a Standard for Real-Time Display of Thermal and Mechanical Indices on Diagnostic Ultrasound Equipment, generally known as the Output Display Standard or ODS, consisting of two indices—thermal (TI) and mechanical (MI)—was implemented in the USA around 1992–1994 [11, 13, 22]. Secondary to end users' desire for better imaging and as a result of discussions that involved the FDA, the AIUM, and the National Electrical Manufacturers Association (NEMA), in 1994 the FDA revised its guidance on diagnostic ultrasound 510(k) submissions to allow the use of the MI in place of the I_{SpPa} in determining substantial equivalence of devices. This revision assumes that on-system displays of numerical indices, including MI and TI, will inform the user about the potential for either thermal or nonthermal bioeffects associated with the actual examination settings of the imaging system. This enables the clinician to increase acoustic power output beyond the existing FDA guidelines when clinically warranted (see Table 1.1). Before the 1994 FDA revision, such an increase was not possible. The maximum available acoustic output was limited by the manufacturer's software, which would not allow the output to exceed FDA guidelines for maximum exposure. It must be stressed that with the implementation of the ODS, diagnostic ultrasound systems can have a higher output limit. With the higher limits comes the potential for increased risk to the patient, so the clinician must make a careful risk/benefit analysis. Therefore, the purpose of the ODS is to help the clinician implement the ALARA (as low as reasonably achievable) principle and minimize the potential for bioeffects. A very important aspect of the implementation of the ODS as explicitly emphasized in the original recommendations for adoption was education of the end users about bioeffects of ultrasound and safety-related issues. This particular goal appears to not have been very successful as indicated by the fact that 70–80 % of end users worldwide know very little about bioeffects and the safety indices [35–38]. Furthermore, sonographers and ob/gyn residents and fellows in the USA seem to be similarly unfamiliar [39, 40].

The thermal index (TI) provides some indication of potential temperature increase, and the mechanical index (MI) provides indication of potential for nonthermal (i.e., mechanical) effects [22, 25, 41]. The TI is the ratio of instantaneous total acoustic power to the acoustic power estimated to be required to increase tissue temperature by a maximum of 1 °C. It is an estimate of the maximal temperature rise at a given exposure. *It is not a measurement of the actual or assumed temperature*. Some correlation exists with

temperature rise in degrees Celsius, but in no way does TI allow an estimate or a guess as to what that temperature change *actually* is in the tissue. There are three variants: TI for soft tissue (TIS), for early pregnancy when ossification is minimal; TI for bones (TIB), to be used when the ultrasound beam impinges on bone, at or near the beam focus, such as late second and third trimesters of pregnancy; and TI for transcranial studies (TIC) when the transducer is essentially against bone, mostly for examinations in adult patients. In ART, TIS is recommended. These indices were required to be displayed if equal to or over 0.4. There are several issues with TI, in particular the fact it does not take exposure time into account. Thus, several authors have suggested modifications or frank changes in the way thermal effects can be assessed [42–44].

The MI has been developed as an on-screen indicator of the potential for nonthermal damage or cavitation-like phenomena related to B-mode operation. MI is inversely proportional to the center transducer frequency, i.e., the higher the frequency (as is used in ART), the lower the risk of mechanical effects. It is important to know that the MI is not based on actual in situ measurements. It is a theoretical formulation of the ratio of the pressure to the square root of the ultrasound frequency. Both the TI and MI can and should be followed as an indication of change in output during the clinical examination.

A complicating factor is uncertainties in TI (and MI) calculations. The error may be a factor of 2 or even 6. It is usual to consider a factor of 2 in risk evaluation. Hence, a TI of 2 may indicate a potential raise of temperature from 1 °C (half of 2) to 4 °C (two times 2). This limits their usefulness but, at the moment, this remains the best tool we have.

Ovarian Scanning

Although the first described use of ultrasound in ob/gyn was for the diagnosis of an ovarian cyst [1], most research and publications have concentrated on obstetrics. This, however, changed with the recognition that ultrasound could be used to closely follow the ovarian cycle [45] and, subsequently, with the realization that this was an excellent tool in induction of ovulation and many other ART procedures [46–48]. Questions regarding safety of the procedure were raised immediately with the rapid adaptation by clinicians [2, 49–51], with description of premature ovulation [2], reduced fertility in rats [49], reduction in pregnancy rates in ultrasound-monitored groups [50], and lower fertilization rate in women undergoing artificial insemination and who were monitored by ultrasound as compared with those who were not monitored by ultrasound, and furthermore, those who were monitored took significantly longer to become pregnant [51]. No mechanism for the findings is proposed in any of these publications. Later, Doppler assessment of ovarian vasculature was also introduced [52–56]. Intraovarian vessels can be interrogated by color and spectral Doppler to predict ovarian response [57]. The acoustic outputs of these modalities are much higher than in conventional grayscale B-mode, but excellent, diagnostic images may be obtained with low outputs as documented by low TI and MI, as can be seen in Fig. 1.1. Further novel technologies to investigate ovarian vasculature, described in various chapters in this book, include three-dimensional (3D) ultrasound [33, 58, 59] and the use of contrast agents [60, 61]. While 3D ultrasound appears safe [34], the injection of contrast agents into the body greatly increases the risks of harmful bioeffects by introducing cavitation foci (see above). Ovarian scanning carries specific worries. In transabdominal scanning, a lot of energy is absorbed by the (sometimes thick) subcutaneous layers. In endovaginal scanning, this "safety net" does not exist since the probe is relatively close to the organ of interest, thus less absorption occurs. Higher frequencies of the vaginal probes, however, are protective. In addition, besides the direct effects of the ultrasound waveform, probe heating has to be considered. It is known that the surface of the probe can heat up by several degrees Celsius [62]. Most of this heat is dissipated by the abdominal wall tissues before reaching the ovary (or the fetus), but much less heat loss occurs with the endovaginal approach.

Ultrasound and the Ovum

As stated in the introduction, a study from 1982 demonstrated premature ovulation in women who underwent ultrasound examination of the ovaries (B-mode) in the late follicular phase [2]. The authors compared patients in induced ovulation cycles and investigated timing of follicle rupture after the onset of LH surge or administration of hCG. Rupture never occurred before the 37th hour in control patients (no ultrasound in the follicular phase). However, ovulation (premature) was observed at 26–36 h in about 50 % of cases in the study group (ultrasound during the previous 3 days or in the 36 h immediately following the ovulatory stimulus). This study was very concerning but has never been reproduced. Since its description 30 years ago [47, 63], ultrasound-guided oocyte aspiration for in vitro fertilization and embryo transfer has now become routine. There are only a few, relatively dated, studies aimed at determining the interaction between ultrasound exposure and successful fertilization. Most are, in fact, concerned with success or lack thereof of the procedure in terms of pregnancy rates and not possible bioeffects. This has not been studied with epidemiological methods but is, arguably, as important as analysis of embryonic/fetal effects. Some researchers have reported deleterious effects of ultrasound on the menstrual cycle, particularly decrease in ovulation rates in mice [64] and premature ovulation [2], as well as reduced cumulative pregnancy rates in mice [49] and in humans [50]. Others have demonstrated no effects on the ovulation process or egg quality, including DNA and RNA synthesis [65], nor on fertilization rate and embryonic development following in vitro fertilization and embryo transfer [66]. In general, the clinically available data on ultrasound exposure of oocytes during meiosis are confusing. Some researchers reported a deleterious effect on the fertility of patients undergoing artificial insemination with a reduction in the cumulative rate of pregnancy [50]. A study of ultrasound exposure of meiotically active, preovulatory oocytes showed no differences between rats exposed to ultrasound after the LH surge and controls in terms of pregnancy rate, number of corpora lutea, implantations, pups, and mean pup and placental weights at autopsy on day 22 of pregnancy [67]. Others have claimed an increase in the success rate, allowing ultrasound monitoring of follicular growth [68], although, evidently, this is not a direct effect of ultrasound but of improved timing. An attempt to clarify this was described by Mahadevan and colleagues [66]. They wanted to determine how oocytes obtained under ultrasound guidance affected the pregnancy rate. The results obtained with 3.5 MHz probes suggest that exposure of human oocytes to ultrasonic waves during the different phases of meiosis does not significantly influence the developmental potential of the in vitro fertilized embryos. Unfortunately, no researcher describes any of the relevant exposure parameters discussed earlier, except for ultrasound frequency.

Embryo/Fetus Susceptibility

The growing embryo/fetus is particularly sensitive to external influences. For instance, certain medications or drug of abuse taken by the pregnant woman, exposure to X-rays, and elevated temperature, secondary to infectious diseases, are all known teratological agents [69]. This is especially true in the first 10–12 weeks of gestation. Gestational age is thus a vital issue when dealing with possible bioeffects: milder exposure during the preimplantation period can have similar consequences to more severe exposures during embryonic and fetal development and can result in prenatal death and abortion or a wide range of structural and functional defects.

Several studies on the influence of ultrasound exposure in the preimplantation period are available. For instance, pregnant rats were exposed to a 2.5 MHz ultrasound field on the second and third day of gestation, at spatial average intensities of 150 mW/cm^2, comparable to human exposure [70]. No increase in prenatal mortality was found. Similarly, no increase in the rate of postnatal malformation was found after 20 min exposures. In another experiment, pregnant mice were exposed to ultrasound in the first 3 days of

gestation [71]. Spatial average intensity was determined to be 1 W/cm^2. A decreased uninterrupted pregnancy rate was noted after exposure for 5 min on the third day and after exposure for 200 s on day 0. In addition, a reduction in neonatal weight (after delivery) was observed at certain thresholds for exposure on day 0 or 1. In another series of studies by the same authors [72], ultrasound exposure led to damage of maternal tissue, as reflected in increased mortality, decreased weight gain, and paralysis of the pups. One of the major concerns is whether ultrasound can raise the temperature of the developing embryo/fetus. This concern stems from the fact that, under certain conditions, ultrasound may indeed cause a rise of temperature and, on the other hand, it is well known that hyperthermia is teratogenic. Most at risk is the fetal central nervous system (CNS) due to a lack of compensatory growth of damaged neuroblasts [73]. In experimental animals the most common defects are of the neural tube as well as microphthalmia, cataract, and microencephaly, with associated functional and behavioral problems [74]. More subtle effects are possible, such as abnormal neuronal migration with unclear potential results [75]. Other prominent defects are seen in craniofacial development (more specifically facial clefts), the skeleton, the body wall, the teeth, and the heart [74]. Hyperthermia in utero (for instance, due to maternal influenza) has long been known to potentially induce structural anomalies in the fetus [76], but, relatively recently, it has been described as an environmental risk factor for psychological/behavioral disturbances [77] and, more particularly, schizophrenia [78]. It is stressed that these are *not ultrasound-induced* hyperthermia effects and that it is suggested that temperature elevation under 38.9 °C is probably not harmful. Yet, ultrasound has been shown to induce temperature increase in vivo [41], albeit not in humans. There is, however, a serious lack of data examining the effects of ultrasound while rigorously excluding other confounding factors. On the one hand, McClain and associates [79] exposed rats to 10 mW/cm^2 CW Doppler ultrasound for up to 2 h at frequencies of 2.25 and 2.5 MHz. The fetuses were examined on day 20, and no consistent increase in mortality was observed nor did the authors detect any other abnormalities. Evidence, however, of the possibility of ultrasonically produced embryolethal effects during organogenesis has been described [80]. Sikov and colleagues exposed an exteriorized rat uterus to various frequencies, some of them clinically relevant (0.8, 2, and 3.2 MHz), at day 9 and evaluated the offspring at day 20 [81]. The exposure was performed at different intensity levels, with exposure times at 5 or 15 min. No effect on fetal weight was observed, even at spatial average intensities as high as 30 W/cm^2, but prenatal mortality at 15–20 W/cm^2 (spatial average) clearly increased with increasing exposure time. The cause of this was ascribed to a thermal mechanism. A recent controversial study looked at neuronal migration in rat pups after maternal exposure to ultrasound [75]. Neurons of the cerebral neocortex in many animals (including humans) are generated during fetal life in the brain proliferative zones and then migrate to their final destinations by following an inside-to-outside sequence. In Ang's experiment neurons generated at embryonic day 16 and destined for the superficial cortical layers were chemically labeled in over 335 rats. A small but statistically significant number of neurons failed to acquire their proper position and remained scattered within inappropriate cortical layers and/or in the subjacent white matter when exposed to ultrasound for a total of 30 min or longer during the period of their migration. The magnitude of dispersion of labeled neurons was variable but increased with duration of exposure to ultrasound (although not linearly, with the most extended exposure yielding less effect than the one immediately lower). It is not clear whether a relatively small misplacement, in a relatively small number of cells that retain their origin cell class, is of any clinical significance. It is also important to note that there are several major differences between the experimental setup of Ang et al. and the clinical use of ultrasound in humans [8]. Most noticeable was the exposure duration, up to 7 h in Ang's setup, and the fact that scans were performed over a period of several days. Furthermore, embryos received whole-brain exposure to the

beam, which is rare in humans. Brains of mice are much smaller than those in humans and develop over days. This should not completely deter from the study which encourages caution. Another study which demonstrates potential harmful effects of ultrasound (when spectral Doppler is used) showed that even relatively short insonation of chick embryos to clinically relevant Doppler resulted in short-term and medium-term memory loss and a reduced ability to learn [82].

There are relatively few papers containing information which is pertinent from a human clinical standpoint and no epidemiological studies of ultrasound in early gestation. One scientific publication dating a few years indicated that fetal exposure was, most likely, within the upper limits, recommended, at that time [83]. A landmark study in the field of ultrasound bioeffects correlated temperature with exposure time [84]. No thermal bioeffects were observed at temperature elevations of 39 °C, regardless of how long the ultrasound exposure lasts. However, for each increasing degree of temperature elevation, to stay within safety limits, the duration of ultrasound examination must be reduced by a factor of four. More specifically, the review indicated that the maximum safe duration for a temperature of 43 °C is 1 min and for 42 °C it is 4 min. Similarly, at 41 °C the exposure time may be increased to 16 min, and at 40 °C the duration of examination may be as long as 64 min. Based on the data available, the survey concluded that if the maximum temperature rise during the ultrasound exposure is kept less than 2 °C, any biological effect (in an afebrile patient) is highly unlikely. As already addressed (see above) findings indicating that the ultrasound imaging transducer may act as a substantial heat source [62, 78] are of particular interest in ART and in the early stages of pregnancy because of the universal use of endovaginal scanning. The temperature at a clinically operated Doppler transducer was reported to increase by 10 °C when the Doppler was applied to skin with a standard coupling gel [78]. Although tissue heating from the transducer is most likely limited to the tissue volume in the immediate vicinity of the transducer, this effect has to be kept in mind for ultrasound examinations in which an endocavity (e.g., endovaginal) transducer is used, although in experiments, the effects on the fetus seemed to be negligible after 2 cm penetration [78].

It must be emphasized, once more, that there are very few human studies, and those which have been performed do not preclude the possibility that adverse effects may be found under certain conditions. One of the rare studies in humans examined activation of various substances involved in the apoptotic cascade, after exposures to diagnostic endovaginal ultrasound [85]. Pregnant patients scheduled for interruption of pregnancy at 7–8 weeks were scanned with 5 MHz endovaginal probes for 0, 10, 20, and 30 min. Chorionic villi were obtained 4 h later and analyzed for activation of caspase-3 and cytochrome release (believed to commit the cell to apoptosis). According to the authors, I_{SPTA} was 13 mW/cm^2. Unfortunately no indication on TI or MI is given. No or minimal activation of the above pathway was seen in controls (0 min exposure) or in those exposed for 10 min. The cleavage products of caspase-3 and cytochrome c were greatly increased after 20 and 30 min exposure, indicating a potential harmful effect of the ultrasound. Besides this study, all other published studies relate to scanning in the late first or second trimesters and not to ART or very early gestation. Epidemiological studies would be needed to clearly demonstrate an effect or lack thereof [10]. The very limited epidemiological data available indicate that no relation has been found between prenatal exposure to ultrasound and subsequent postnatal changes in children [86], but statistical considerations show that minor chemical and behavioral changes, long-term delayed effects, and certain genetic effects could easily escape detection [4].

Thus, it appears that in vivo exposure to ultrasound at spatial average intensities *below 1 W/cm*^{2} (which is arguably the case in ART as well as early gestation) does not affect embryos/fetuses in the early stages of gestation. Limited data, however, suggest that levels of ultrasound of 1 W/cm^2 may lead to undesirable changes in maternal tissue. If one considers together the

facts that hyperthermia is potentially harmful to the fetus and that ultrasound may, under certain circumstances, elevate tissue temperature, then precaution has to be recommended, particularly in early gestation and especially with modes known to emit higher acoustic energy levels (such as pulsed Doppler [87]). This recommendation is supported by experimental data. Further prospective studies on ultrasound safety in ART and pregnancy are highly recommended.

Safety Aspects of Ultrasound in Ovulation Induction and Early Gestation

There are many valid medical indications to perform ultrasound in early gestation [88]. These include, among others, bleeding, accurate gestation dating, confirmation of viability, and verification of number of fetuses. In addition, ultrasound is invaluable in ART. All of these examinations are primarily performed with B-mode, a mode with relatively low acoustic output. However, more recently, screening for genetic abnormalities and early assessment of structural abnormalities are described in the literature in early (11–15 weeks) pregnancy. While most of these are also performed with B-mode, Doppler is often used to detect blood vessels and/or to visualize and analyze cardiac valves, potentially exposing the fetus to much higher energy levels. One needs to keep in mind that, even with B-mode, dwell time is important since prolonged examination can result in higher exposure levels.

The evidence of ultrasonically induced bioeffects in humans is perhaps the most important information from the clinician's point of view. As pointed out by Ziskin and Petitti, "No matter how many laboratory experiments show a lack of effect from diagnostic ultrasound, it will always be necessary to study directly its effect in human populations before any definitive statement regarding risk can be made." [4] Indeed, a lack of demonstrated effects is not equivalent to a factual lack of effects. All published epidemiological studies in humans were performed with pre-1992 machines, a time when the maximal acoustic output of medical ultrasound instruments was allowed to be greatly increased [89]. The words of Francis Duck in 1999 are still particularly valid: "No epidemiological or other evidence was then or is now available to support the assertion of safety at these higher exposures." [90]

Summary and Recommendations

Several statement and guidelines are available [91–97]. As already mentioned, based on various sources, it appears that acoustic output (as expressed by various intensities) can be much higher in Doppler mode: for instance, 34 mW/cm^2 for the I_{SPTA} in B-mode versus 1,180 mW/cm^2 for spectral Doppler and with color Doppler somewhat in between [98]. Concerns about the fact that outputs are much higher in Doppler applications were already expressed approximately 10 years ago in three editorials [90, 99, 100]. In one of these, the question was even raised whether research involving Doppler in the first trimester should even be considered for publication [100]. Despite this, as detailed above, ultrasound is routine in ART, and in more recent years, there has been a recrudescence in the usage of Doppler in the 1st trimester and furthermore in the early stages of the first trimester. A very important recommendation, already mentioned, is to limit exposure to be as short as possible, compatible with an adequate diagnosis (as low as reasonably achievable [ALARA] principle). A very useful method to keep risk at a minimum is to use published guidelines in the USA [91] as well as BMUS-recommended limits [98]. These can be summarized in a few easy-to-remember bullet points:

- Perform a scan only when medically indicated.
- Know your machine and how controls change the output.
- Start at low output and increase only when necessary.
- Keep TI and MI below 1.
- Watch the clock and keep the examination as brief as possible (but enough to obtain diagnostic accuracy).
- Be cautious when using Doppler.

Diagnostic ultrasound is an extremely powerful tool in the hands of experienced physicians, sonographers, nurses, and other users. The decision regarding the risks and benefits can be made only by the individual responsible for applying the ultrasound to the patient. This is a clinical responsibility but also an ethical and legal one. Education of end users is primordial in this regard.

References

1. Donald I, Macvicar J, Brown TG. Investigation of abdominal masses by pulsed ultrasound. Lancet. 1958;1:1188–95.
2. Testart J, Thebault A, Souderes E, Frydman R. Premature ovulation after ovarian ultrasonography. Br J Obstet Gynaecol. 1982;89:694–700.
3. Salvesen KA, Vatten LJ, Jacobsen G, et al. Routine ultrasonography in utero and subsequent vision and hearing at primary school age. Ultrasound Obstet Gynecol. 1992;2(243–4):5–7.
4. Ziskin MC, Petitti DB. Epidemiology of human exposure to ultrasound: a critical review. Ultrasound Med Biol. 1988;14:91–6.
5. Nyborg WL. Biological effects of ultrasound: development of safety guidelines. Part II: general review. Ultrasound Med Biol. 2001;27:301–33.
6. Marinac-Dabic D, Krulewitch CJ, Moore Jr RM. The safety of prenatal ultrasound exposure in human studies. Epidemiology. 2002;13:S19–22.
7. Salvesen KA. EFSUMB: safety tutorial: epidemiology of diagnostic ultrasound exposure during pregnancy-European committee for medical ultrasound safety (ECMUS). Eur J Ultrasound. 2002;15:165–71.
8. Abramowicz JS. Prenatal exposure to ultrasound waves: is there a risk? Ultrasound Obstet Gynecol. 2007;29:363–7.
9. Church CC, Miller MW. Quantification of risk from fetal exposure to diagnostic ultrasound. Prog Biophys Mol Biol. 2007;93:331–53.
10. Abramowicz JS, Fowlkes JB, Stratmeyer ME, Ziskin MC. Epidemiology of ultrasound bioeffects. In: Sheiner E, editor. Textbook of epidemiology in perinatology. New York: Nova Science Publishers, Inc.; 2010.
11. FDA, Center for Devices and Radiological Health. 501(k) guide for measuring and reporting acoustic output of diagnostic ultrasound medical devices; 1985. http://www.fda.gov/MedicalDevices/ProductsandMedicalProcedures/DeviceApprovalsandClearances/510kClearances/default.htm. Accessed on March 2013.
12. US Food and Drug Administration (FDA). Diagnostic ultrasound guidance update. Rockville: Center for Devices and Radiological Health; 1987.
13. AIUM/NEMA. American Institute of Ultrasound in Medicine and the National Electrical Manufacturers' Association. Standard for real-time display of thermal and mechanical acoustic output indices on diagnostic ultrasound devices. Laurel/Rosslyn: American Institute of Ultrasound in Medicine (AIUM); 1992.
14. Insana MF. Sound attenuation in tissue. In: Goldman IW, Fowlkes JB, editors. Medical CT and ultrasound: current technology and applications. College Park: American Association of Physicists in Medicine; 1995.
15. Henderson J, Willson K, Jago JR, Whittingham TA. A survey of the acoustic outputs of diagnostic ultrasound equipment in current clinical use. Ultrasound Med Biol. 1995;21:699–705.
16. Martin K. The acoustic safety of new ultrasound technologies. Ultrasound. 2010;18:110–8.
17. Duck FA, Henderson J. Acoustic output of modern instruments: is it increasing? In: Barnett SB, Kossoff G, editors. Safety of diagnostic ultrasound. New York/London: The Parthenon Publishing Group; 1998.
18. Jago JR, Henderson J, Whittingham TA, Willson K. How reliable are manufacturer's reported acoustic output data? Ultrasound Med Biol. 1995;21:135–6.
19. Zhu WH, Miller MW, Cox C. Lack of increase in cell transformation frequency of C3H cells after exposure to pulsed ultrasound. Ultrasonics. 1991;29:81–4.
20. Church CC. Spontaneous homogeneous nucleation, inertial cavitation and the safety of diagnostic ultrasound. Ultrasound Med Biol. 2002;28:1349–64.
21. Barnett SB, ter Haar GR, Ziskin MC, Nyborg WL, Maeda K, Bang J. Current status of research on biophysical effects of ultrasound. Ultrasound Med Biol. 1994;20:205–18.
22. Abbott JG. Rationale and derivation of MI and TI–a review. Ultrasound Med Biol. 1999;25:431–41.
23. Wu J, Nyborg WL. Ultrasound, cavitation bubbles and their interaction with cells. Adv Drug Deliv Rev. 2008;60:1103–16.
24. O'Brien Jr WD. Ultrasound-biophysics mechanisms. Prog Biophys Mol Biol. 2007;93:212–55.
25. NCRP. (National Council on Radiation Protection and Measurements). Exposure criteria for medical diagnostic ultrasound: II. Criteria based on all known mechanisms. Report No. 140. Bethesda; 2002.
26. Sikov MR. Effect of ultrasound on development. Part 1: introduction and studies in inframammalian species. Report of the bioeffects committee of the American Institute of Ultrasound in Medicine. J Ultrasound Med. 1986;5:577–83.
27. Sikov MR. Effect of ultrasound on development. Part 2: studies in mammalian species and overview. J Ultrasound Med. 1986;5:651–61.
28. Stratmeyer ME, Christman CL. Biological effects of ultrasound. Women Health. 1982;7:65–81.
29. National Council on Radiation Protection and Measurements. Biological effects of ultrasound: mechanisms and clinical implications. Bethesda: National Council on Radiation; 1984.

30. Stewart HF, Stratmeyer ME. An overview of ultrasound theory, measurement, medical applications and biological effects. US Department of Health and Human Services Publications; FDA 82-8190, US Government Printing Office: 1982.
31. Thomenius KE, Lewin PA. Ultrasound bioeffects 1991. Ultrasound Q. 1991;9:111–37.
32. Dickey RP. Doppler ultrasound investigation of uterine and ovarian blood flow in infertility and early pregnancy. Hum Reprod Update. 1997;3:467–503.
33. Engels V, Sanfrutos L, Perez-Medina T, et al. Periovulatory follicular volume and vascularization determined by 3D and power Doppler sonography as pregnancy predictors in intrauterine insemination cycles. J Clin Ultrasound. 2011;39:243–7.
34. Sheiner E, Hackmon R, Shoham-Vardi I, et al. A comparison between acoustic output indices in 2D and 3D/4D ultrasound in obstetrics. Ultrasound Obstet Gynecol. 2007;29:326–8.
35. Marsal K. The output display standard: has it missed its target? Ultrasound Obstet Gynecol. 2005;25:211–4.
36. Sheiner E, Abramowicz JS. Clinical end users worldwide show poor knowledge regarding safety issues of ultrasound during pregnancy. J Ultrasound Med. 2008;27:499–501.
37. Akhtar W, Arain MA, Ali A, et al. Ultrasound biosafety during pregnancy: what do operators know in the developing world?: national survey findings from Pakistan. J Ultrasound Med. 2011;30:981–5.
38. Sharon N, Shoham-Vardi I, Aricha-Tamir B, Abramowicz JS, Sheiner E. [What do ultrasound performers in Israel know regarding safety of ultrasound, in comparison to the end users in the United States?]. Harefuah. 2012;151:146–9, 90.
39. Bagley J, Thomas K, DiGiacinto D. Safety practices of sonographers and their knowledge of the biologic effects of sonography. J Diagn Med Sonography. 2011;27:252–61.
40. Houston LE, Allsworth J, Macones GA. Ultrasound is safe… right?: resident and maternal-fetal medicine fellow knowledge regarding obstetric ultrasound safety. J Ultrasound Med. 2011;30:21–7.
41. Nyborg WL. History of the American Institute of Ultrasound in Medicine's efforts to keep ultrasound safe. J Ultrasound Med. 2003;22:1293–300.
42. Karagoz I, Kartal MK. A new safety parameter for diagnostic ultrasound thermal bioeffects: safe use time. J Acoust Soc Am. 2009;125:3601–10.
43. Ziskin MC. The thermal dose index. J Ultrasound Med. 2010;29:1475–9.
44. Bigelow TA, Church CC, Sandstrom K, et al. The thermal index: its strengths, weaknesses, and proposed improvements. J Ultrasound Med. 2011;30:714–34.
45. Queenan JT, O'Brien GD, Bains LM, Simpson J, Collins WP, Campbell S. Ultrasound scanning of ovaries to detect ovulation in women. Fertil Steril. 1980;34:99–105.
46. Vesper B, Schulte HR. [Ultrasonic follow-up check of overstimulation by gonadotrophin therapy (author's transl)]. Zentralbl Gynakol. 1980;102:791–6.
47. Lenz S, Lauritsen JG, Kjellow M. Collection of human oocytes for in vitro fertilisation by ultrasonically guided follicular puncture. Lancet. 1981;1:1163–4.
48. Renaud R, Ehret C, Dervain I, Plas-Roser S, Aron C, Spira A. [Ovarian sonography: a new way of monitoring ovulation induction treatments]. Bull Acad Natl Med. 1981;165:353–8.
49. Bologne R, Demoulin A, Schaaps JP, Hustin J, Lambotte R. [Influence of ultrasonics on the fecundity of female rats]. C R Seances Soc Biol Fil. 1983;177:381–7.
50. Demoulin A, Bologne R, Hustin J, Lambotte R. Is ultrasound monitoring of follicular growth harmless? Ann N Y Acad Sci. 1985;442:146–52.
51. Quereux C, Mazili ML, Desroches A, et al. Does ultrasound have an adverse effect on the fertility of women? J Gynecol Obstet Biol Reprod (Paris). 1986;15:159–64.
52. Feichtinger W, Putz M, Kemeter P. [Transvaginal Doppler sonography for measuring blood flow in the pelvis]. Ultraschall Med. 1988;9:30–6.
53. Deutinger J, Reinthaller A, Bernaschek G. Transvaginal pulsed Doppler measurement of blood flow velocity in the ovarian arteries during cycle stimulation and after follicle puncture. Fertil Steril. 1989;51:466–70.
54. Fleischer AC. Ultrasound imaging–2000: assessment of utero-ovarian blood flow with transvaginal color Doppler sonography; potential clinical applications in infertility. Fertil Steril. 1991;55:684–91.
55. Campbell S, Bourne TH, Waterstone J, et al. Transvaginal color blood flow imaging of the periovulatory follicle. Fertil Steril. 1993;60:433–8.
56. Abramowicz JS, Jaffe R, Pierson R. Transvaginal color Doppler assessment of uterine and ovarian blood flow during normal and abnormal cycles. In: Jaffe R, Pierson R, Abramowicz JS, editors. Imaging in infertility and reproductive endocrinology. Philadelphia: J.B. Lippincott; 1994.
57. Altundag M, Levi R, Adakan S, et al. Intraovarian stromal artery Doppler indices in predicting ovarian response. J Reprod Med. 2002;47:886–90.
58. Jarvela IY, Sladkevicius P, Kelly S, Ojha K, Campbell S, Nargund G. Quantification of ovarian power Doppler signal with three-dimensional ultrasonography to predict response during in vitro fertilization. Obstet Gynecol. 2003;102:816–22.
59. Merce LT, Gomez B, Engels V, Bau S, Bajo JM. Intraobserver and interobserver reproducibility of ovarian volume, antral follicle count, and vascularity indices obtained with transvaginal 3-dimensional ultrasonography, power Doppler angiography, and the virtual organ computer-aided analysis imaging program. J Ultrasound Med. 2005;24:1279–87.
60. Marret H, Brewer M, Giraudeau B, Tranquart F, Voelker K, Satterfield W. Ovine model to evaluate ovarian vascularization by using contrast-enhanced sonography. Comp Med. 2005;55:150–5.
61. Marret H, Brewer M, Giraudeau B, Tranquart F, Satterfield W. Assessment of cyclic changes of

microvessels in ovine ovaries using Sonovue contrast-enhanced ultrasound. Ultrasound Med Biol. 2006;32:163–9.
62. Duck FA, Starritt HC, ter Haar GR, Lunt MJ. Surface heating of diagnostic ultrasound transducers. Br J Radiol. 1989;62:1005–13.
63. Gleicher N, Friberg J, Fullan N, et al. EGG retrieval for in vitro fertilisation by sonographically controlled vaginal culdocentesis. Lancet. 1983;2:508–9.
64. Heyner S, Abraham V, Wikarczuk ML, Ziskin MC. Effects of ultrasound on ovulation in the mouse. Gamete Res. 1989;22:333–8.
65. Heyner S, Abraham V, Wikarczuk ML, Ziskin MC. Effects of ultrasound on DNA and RNA synthesis in preimplantation mouse embryos. Mol Reprod Dev. 1990;25:209–14.
66. Mahadevan M, Chalder K, Wiseman D, Leader A, Taylor PJ. Evidence for an absence of deleterious effects of ultrasound on human oocytes. J In Vitro Fert Embryo Transf. 1987;4:277–80.
67. Williams SR, Rothchild I, Wesolowski D, Austin C, Speroff L. Does exposure of preovulatory oocytes to ultrasonic radiation affect reproductive performance? J In Vitro Fert Embryo Transf. 1988;5:18–21.
68. Kerin JF. Determination of the optimal timing of insemination in women. In: Richardson D, Joyce D, Symonds M, editors. Frozen human semen. London: Royal College of Obstetrics and Gynaecology; 1979. p. 105–32.
69. Brent RL, Beckman DA, Landel CP. Clinical teratology. Curr Opin Pediatr. 1993;5:201–11.
70. Takeuchi H, Nakazawa T, Kumakiri K, Kusano R. Experimental studies on ultrasonic Doppler method in obstetrics. Acta Obstet Gynaecol Jpn. 1970;17:11–6.
71. Stolzenberg SJ, Torbit CA, Edmonds PD, Taenzer JC. Effects of ultrasound on the mouse exposed at different stages of gestation: acute studies. Radiat Environ Biophys. 1980;17:245–70.
72. Stolzenberg SJ, Edmonds PD, Torbit CA, Sasmore DP. Toxic effects of ultrasound in mice: damage to central and autonomic nervous systems. Toxicol Appl Pharmacol. 1980;53:432–8.
73. Brodal P. Restitution of function after brain damage. In: Brodal P, editor. The central nervous system Structure and function. 4th ed. New York: Oxford University Press; 2010. p. 147–56.
74. Edwards MJ, Saunders RD, Shiota K. Effects of heat on embryos and foetuses. Int J Hyperthermia. 2003;19:295–324.
75. Ang ESBC, Gluncic V, Duque A, Schafer ME, Rakic P. Prenatal exposure to ultrasound waves impacts neuronal migration in mice. Proc Natl Acad Sci U S A. 2006;103:12903–10.
76. Graham Jr JM, Edwards MJ, Edwards MJ. Teratogen update: gestational effects of maternal hyperthermia due to febrile illnesses and resultant patterns of defects in humans. Teratology. 1998;58:209–21.
77. Stalberg K, Haglund B, Axelsson O, Cnattingius S, Pfeifer S, Kieler H. Prenatal ultrasound and the risk of childhood brain tumour and its subtypes. Br J Cancer. 2008;98:1285–7.
78. Calvert J, Duck F, Clift S, Azaime H. Surface heating by transvaginal transducers. Ultrasound Obstet Gynecol. 2007;29:427–32.
79. McClain RM, Hoar RM, Saltzman MB. Teratologic study of rats exposed to ultrasound. Am J Obstet Gynecol. 1972;114:39–42.
80. Sikov MR, Hildebrand BP. Embryotoxicity of ultrasound exposure at nine days of gestation in the rat. In: White D, Braun RE, editors. Ultrasound in medicine. New York: Plenum Press; 1977.
81. Sikov MR, Hildebrand BP. Effects of ultrasound on the prenatal development of the rat. Part 1. 3.2 MHz continuous wave at nine days of gestation. J Clin Ultrasound. 1976;4:357–63.
82. Schneider-Kolsky ME, Ayobi Z, Lombardo P, Brown D, Kedang B, Gibbs ME. Ultrasound exposure of the foetal chick brain: effects on learning and memory. Int J Dev Neurosci. 2009;27:677–83.
83. Hussain R, Kimme-Smith C, Tessler FN, Perrella RR, Grant EG, Sandstrom K. Fetal exposure from endovaginal ultrasound examinations in the first trimester. Ultrasound Med Biol. 1992;18:675–9.
84. Miller MW, Ziskin MC. Biological consequences of hyperthermia. Ultrasound Med Biol. 1989;15:707–22.
85. Zhang J, Zhou F, Song Y, Ying W, Zhang Y. Long dwell-time exposure of human chorionic villi to transvaginal ultrasound in the first trimester of pregnancy induces activation of caspase-3 and cytochrome C release. Biol Reprod. 2002;67:580–3.
86. Abramowicz JS, Fowlkes JB, Skelly AC, Stratmeyer ME, Ziskin MC. Conclusions regarding epidemiology for obstetric ultrasound. J Ultrasound Med. 2008;27:637–44.
87. Sheiner E, Shoham-Vardi I, Pombar X, Hussey MJ, Strassner HT, Abramowicz JS. An increased thermal index can be achieved when performing Doppler studies in obstetric sonography. J Ultrasound Med. 2007;26:71–6.
88. AIUM. AIUM practice guideline for the performance of obstetric ultrasound examination. J Ultrasound Med. 2010;29:157–66.
89. Miller MW, Brayman AA, Abramowicz JS. Obstetric ultrasonography: a biophysical consideration of patient safety–the "rules" have changed. Am J Obstet Gynecol. 1998;179:241–54.
90. Duck FA. Is it safe to use diagnostic ultrasound during the first trimester? Ultrasound Obstet Gynecol. 1999;13:385–8.
91. Nelson TR, Fowlkes JB, Abramowicz JS, Church CC. Ultrasound biosafety considerations for the practicing sonographer and sonologist. J Ultrasound Med. 2009;28:139–50.
92. Safety Group of the British Medical Ultrasound Society (BMUS). Guidelines for the safe use of diagnostic ultrasound equipment. Ultrasound. 2010;18:52–9.
93. Abramowicz JS. Fetal Doppler: how to keep it safe? Clin Obstet Gynecol. 2010;53:842–50.
94. Abramowicz JS, Sheiner E. Ultrasound bioeffects and safety: what the practitioner should know. In:

Fleischer AC, Manning FA, Jeanty P, Romero R, editors. Sonography in obstetrics and gynecology-principles and practice. 7th ed. New York: McGraw-Hill; 2010.
95. AIUM. AIUM Official Statement. Statement on the safe use of Doppler ultrasound during 11-14 week scans (or earlier in pregnancy); 2011. http://aium.org/officialstatements/42. Accessed on March 2013.
96. AIUM. AIUM Official Statement. Prudent use in pregnancy; 2012. http://aium.org/officialstatements/33. Accessed on March 2013.
97. AIUM. AIUM As Low As Reasonably Achievable (ALARA) principle; 2012. http://aium.org/officialstatements/39. Accessed on March 2013.
98. Ter Haar G. Ultrasound imaging: safety consideration. Interface Focus. 2011;1(14):686–97. doi:10.1098/rsfs.2011.0029. Epub 2011 May 25.
99. Chervenak FA, McCullough LB. Research on the fetus using Doppler ultrasound in the first trimester: guiding ethical considerations. Ultrasound Obstet Gynecol. 1999;14:161.
100. Campbell S, Platt L. The publishing of papers on first-trimester Doppler. Ultrasound Obstet Gynecol. 1999;14:159–60.

Principles of 3D Ultrasound

2

Maximilian Murtinger, Dietmar Spitzer,
and Nicolas Herbert Zech

Introduction

Ultrasound (US) performance is a noninvasive, painless procedure. Its applications are essential for IVF (in vitro fertilization) therapy; employed US frequencies range between 1 and 18 MHz, which have no known harmful effects to the patients, their gametes, or embryos [1, 2].

Two-dimensional ultrasound (2D US) has been used in medical applications for decades, notably in artificial reproduction technology (ART). Interestingly, the first commercial three-dimensional visualization was achieved not by US but by magnetic resonance imaging (MRI) and computed tomography (CT). However, the first reports on 3D US appeared in the early 1980s, almost simultaneously with the appearance of CT and MRI [3–5]. Nevertheless, 3D US suffered from several initial problems. As a result, more than one decade passed before the first commercial 3D US became available and was introduced for clinical applications. This was due to several factors. First, the development of 3D US imaging had been limited by computing power, which, until the last decade, restricted 3D reconstruction to offline work stations. Second, the clinical approach was handicapped by problems intrinsic to US imaging: speckle, clutter, grating lobe, and other artifacts [6]. Additionally, in the past the storage of 3D images was unfeasible due to the limited storage capacity of the computers as well as the post-processing procedures, which are now considerably facilitated by highly efficient hardware and software. With the new data processors, the reconstruction procedure of 2D scans into 3D structures can be carried out within a few seconds after the images have been acquired. Three-dimensional images can also be generated with 2D ultrasound computed tomography, either by shifting the measurement arrangement or by moving the analyzed object. By this approach, at each step only one layer is recorded, which is then composed to a full-dimensional structure. Therefore, even with conventional US scanners, a composited 3D imaging (spatial compounding) can be generated. Important for this technique is the matching of the set of 2D images. The 3D images are calculated by combining the information on the position and angulation of the images. The required positional information is obtained either by the conventional probe, the position of the transducer measured, or by using a special scanner. However, a system for positioning and orientation of the scanner is still needed. To

M. Murtinger, MD
IVF Centers Prof. Zech,
Römerstrasse 2, Bregenz 6900, Austria
e-mail: m.murtinger@ivf.at

N.H. Zech, MD (✉)
Department of Obstetrics and Gynecology,
Medical University Graz,
Römerstrasse 2, 6900 Bregenz, Austria
e-mail: n.zech@ivf.at

D. Spitzer, MD
IVF Centers Prof. Zech, Innsbrucker
Bundesstrasse 35, Salzburg 5000, Austria
e-mail: d.spitzer@salzburg.ivf.at

L.A. Stadtmauer, I. Tur-Kaspa (eds.), *Ultrasound Imaging in Reproductive Medicine*,
DOI 10.1007/978-1-4614-9182-8_2,

reduce the number of orientations, special types of ultrasound transducer systems were developed, allowing the acquisition of information through only one viewing direction by electronic focusing.

In 1984, Kazunori Baba first described a 3D ultrasound system. In 1986, he was the first person on the globe to obtain 3D images of a 19-week fetus by processing the raw 2D images on a minicomputer in 1986 [7, 8]. In 1987 Olaf T. von Ramm and Steven W. Smith patented "An acoustic pulse echo imaging system capable of producing an image of a three-dimensional object utilizing a two-dimensional display. In the system angular relationships of targets at all ranges are maintained for display. The system uses a two-dimensional transducer array of piezoelectric elements; the array is steered to assume transmit and receive orientations in both azimuth and elevation by producing (1) a directed transmit pulse and many similarly directed receive orientations or (2) a non-directed transmit pulse and many directed receive orientations. For each transmit pulse a parallel processing system produces several unique image points whose locations in the image correspond to the tangents of the angles of the receive orientations in the azimuth and elevation planes. The brightness of each image point is the weighted integral of the echo data received along each receive path. As an option, range discrimination capability is provided by means of a range dependent gain control, brightness shading as a function of range or a color display in which data originating from different ranges is displayed in different hues [9]."

Two years later, the first commercially available 3D US instrument was marketed in 1989 by the Austrian company Kretztechnik (Zipf/Austria) which was founded by the engineer Paul Kretz after the Second World War.

This instrument, the Combison 330 equipped with 7.5 MHz and integrated 3D system was presented at the French radiology congress in Paris in 1989 [10]. It utilized mechanical abdominal volume scan transducers with the mechanical swept-volume approach. Although the acquisition of the volume took only 1–2 s, rendering of the image took up to almost 20 min on an external computer. However, the rendering was also limited in ability to provide a set of orthogonal planes orientated images in strict relation to the axis of the probe. Additionally, special scan transducers were needed for this instrument. They had to be held by their larger side, thus making them rather difficult to handle. This drawback was removed in the majority of the later US instruments by a 90° rotation of the 3D US device. In 1998, the Voluson 530D 3D system implemented a technology that displayed not only the 3D sectional images, but also processed the data of the entire volume in real time. With the commercial launch of this 3D instrument platform, 3D ultrasound technology competed with the higher priced CT and MRI instruments; it allowed effective grayscale imaging, spectral Doppler, color Doppler, and Angio Color Imaging [11]. Two years later, the medical equipment manufacturer GE Healthcare introduced a new generation of clinical US systems, the Voluson 730 with real-time acquisition of volumes (16 volumes/s). Now, it is possible to detect and analyze even moving objects such as a fetus. With the beginning of the new millennium, several new software programs became available that significantly improved the image quality.

Currently, numerous 3D US instruments are available (most of them semi- or fully automated), and it is extremely likely that dozens of new machines will become available in the next few years. The systems have become faster and more advanced. Furthermore, the number of compatible software programs exceeds the amount of instruments sold. Virtual navigation, different modes of presentation (such as tomographic ultrasound imaging (TUI) volume, contrast imaging (VCI) and automated volume calculation (SonoAVC), computer-aided analysis (VOCAL) calculation), and other techniques are now available; they are reliable, fast, and user friendly [12]. With these features, the possibilities for clinical application become almost unlimited; furthermore, use is increasing in the clinical setting. Many post-processing tools such as speckle reduction imaging, electronic scalpel, and filters for brightness and contrast facilitate handling. Data transfer and long-term storage are now possible without any quality

loss. Although most procedures are still conducted with 2D scans, for a number of reasons, it is likely that the 3D technology will be a supplementary tool—and in some cases, a replacement—for 2D instruments in the field of ART in the future.

Basic Techniques of 3D US

The basic techniques of 3D US systems are almost identical to those of 2D systems because they use the same frequencies and wavelengths. According to the US Food and Drug Administration (FDA), the limit for obstetrical ultrasound is 94 mW/cm^2 for the spatial peak temporal average intensity and 190 W/cm^2 for spatial peak pulse average for fetal imaging [13]. The principles of 3D Doppler US technology are not a subject of this chapter but are summarized in detail in a previous chapter.

Three-dimensional sonography in medicine comprises data acquisition, analysis and processing of volume, image animation and finalizing of the image, and data storage [14]. In principle, there are three (respectively four) ways of achieving 3D data:

1. The tracked freehand method: Freehand 3D ultrasound allows intraoperative imaging of volumes of interest in a rapid and flexible manner [15]. This technique requires manual movement of the probe through the ROI (region of interest). However, as a prerequisite the exact angulation and position of the US transducer are needed.
2. The untracked freehand systems: With these systems, the operator moves the transducer in a regular motion, while the 2D images are performed. For a 3D image a linear or angular spacing between the single images is assumed. The major disadvantage of this technique is that exact local positioning is not possible and measurements, especially for volumes, are highly inaccurate.
3. A three-dimensional visualization can be intrinsically achieved by 2D transducer arrays: These arrays generate pyramidal pulses of the US and the echoes are converted into 3D images. The advantage is that the transducer can remain stationary and electronic scanning can be used to sweep a broad ultrasound beam over the entire volume under examination [16].
4. A fourth possibility is mechanical assemblies: The transducer is moved either (1) linear, (2) tilted, or (3) in a rotational movement about its central axis by a mechanical assembly.

Reconstruction and Visualization of 3D Images and Post-processing

Software programs for reconstruction (rendering) and imaging play a dominant role in 3D US. Several algorithms have been developed allowing for perfect visualization, manipulation, and processing of the received 3D images. It is apparent that the progress in software development was—and still is—the key to success for this technique. Currently, numerous visualization modalities are available:

1. Multi-planar view: This was the first available visualization mode in 3D US. The display presents the three orthogonal planes simultaneously: the longitudinal, transverse, and coronal planes. The dataset can then be rotated or sliced in order to view the region of interest (ROI). The multi-planar view displays the exact spatial relationships between the three planes.
2. The tomographic ultrasound imaging (TUI) or multi-slice technique: TUI allows for a comprehensive sequential analysis of the desired organ (Fig. 2.1). The same imaging principle is employed in CT and MRI. For example, tomographic ultrasound imaging has been reported to greatly simplify pelvic floor assessment [17].
3. The static volume contrast imaging (VCI) mode: This mode allows for the receipt of information from adjacent slices in a volume. This imaging mode was especially developed to enhance the contrast between tissues or organs that would appear similar on conventional 2D US [18]. VCI is currently applied for detecting thoracic abnormalities [18] or imaging fetal pelvic anatomy [19]; it was found to be superior to 2D US in these studies.

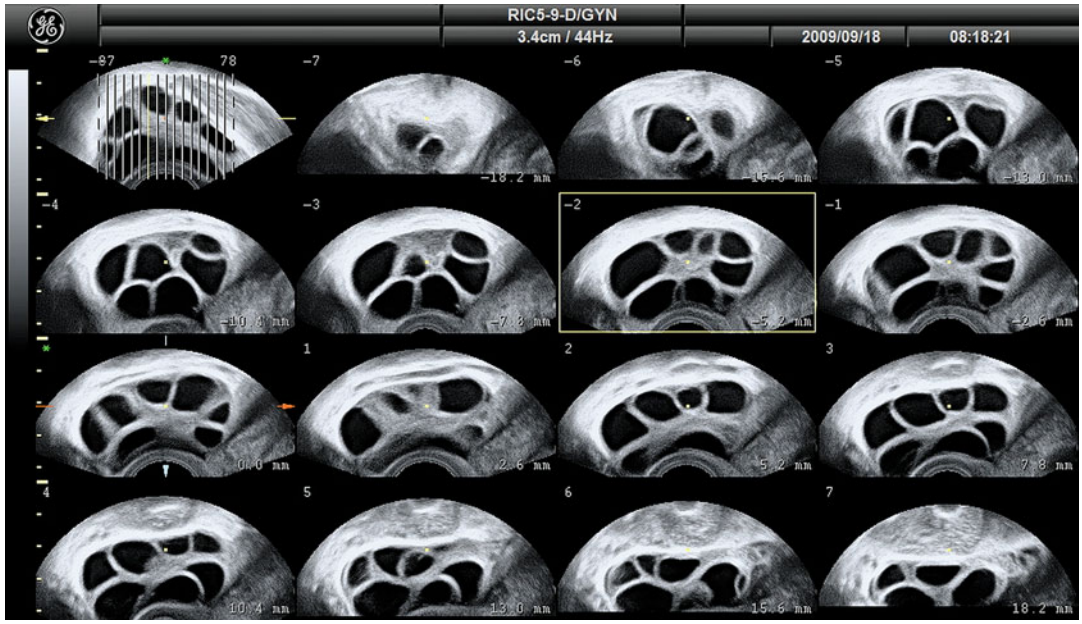

Fig. 2.1 Tomographic ultrasound image (TUI) of multiple follicles in a stimulated ovary

4. Inversion mode: In inversion mode, volumes are displayed in their entirety as an echogenic area, while the grayscale portions of the image are rendered as transparent. Some IVF and obstetrical applications could benefit from this method [20].
5. Transparency mode: The transparency mode (also known as maximum mode) images regions with high echo density in a glass-like mode. This mode is mostly used for imaging of cartilaginous structures. With this mode, high-echogenic voxels are higher valued.
6. The surface-rendering mode helps to detect and display the surface of the structures. It is most commonly used for the evaluation of ovarian tumors [21, 22]. This technique allows surface reconstruction of conspicuous parietal structures [21].
7. Glass-body rendering: Glass-body rendering (GBR) imaging is a combination of the transparency and color or power Doppler mode. It is very suitable for gynecologic applications; however, it is most useful for vessel imaging. In this mode the rendering algorithm is based on the simultaneous representation of gray and color Doppler scale [23].
8. Four-dimensional image techniques: The four-dimensional image techniques (such as the spatiotemporal image correlation (STIC)) allow for procedures such as echocardiography of the fetal heart [24, 25]. The received data is acquired by a single, automatic volume sweep; subsequently, the software analyzes the data according to their spatial and temporal domain and processes a 4D cine sequence. Prior to the launch of these 4D techniques, the examination of the fetal heart with conventional US was often difficult.
9. OmniView: OmniView (GE Medical Systems, Kretztechnik, Zipf, Austria) is a recently developed display technology for 3D and 4D US that allows integration of volume datasets and the simultaneous display of up to three independent (non-orthogonal) planes by manually drawing straight or curved lines from any direction or angle [26].

Although many 3D US display techniques have been employed (more than the ones described in this chapter), the two most commonly used are multi-planar reformatting and volume contrast rendering. Image quality has improved since the 1990s; nevertheless,

the final quality still depends on the accuracy of the scanned volumes (also see next paragraph). Nevertheless, as previously mentioned, various software-based tools are currently available. Post-processing is done via the electronic scalpel (Kretztechnik, Zipf, Austria), contrast and brightness regulation, or speckle reduction imaging (SRI). SRI was established on the Voluson platform in 2004 by GE Healthcare. The electronic scalpel allows for the removal of pre-located obscuring structures in three steps: (1) rotation of the rendered image into a position where the obscuring structures can be cut; (2) the selection of the cutting mode; and (3) creation of the outline for the cut and activation of the cutting mode [27]. Speckles are recurrent problems in sonography due to interference of ultrasound echoes; they produce difficulties in differentiating anatomical structure. Many approaches have been attempted with the goal of reducing or even of eliminating speckles. Most significantly, the increased computer processing power and speed of calculation within recent years have allowed more complex image-processing techniques to reduce these artifacts without impairing image quality [28]. In addition, filtering is widely used for undesired echoes that are a recurrent phenomenon in sonography. Filtering allows the suppression of unwanted background noise or the enhancement of the desired information (suppressing and enhancing filters) [29].

Initially, data storage was a problem with 3D technology. This problem has been resolved by the improved storage capacity of the hard disk. The acquired data can be readily stored without quality loss either at the US systems itself or on external media (CD, DVD, USB, or external hard drive). The data can still be post-processed with medical software and can be transferred, for example, via (virtual private network) VPN tunneling to another physician. Most importantly, the data can be reloaded and subjected to an additional expert opinion or used for education [30]. This is an invaluable feature. Currently, this capability facilitates optimal patient care. Moreover, it might reduce medical malpractice and might prove to be an essential step towards standardization in this field.

Advantages and Shortcomings of 3D US Techniques

Three-dimensional US allows visualization of all three image planes (sagittal, transverse, and coronal) of the analyzed object, including planes not accessible by 2D US. The viewed planes can be chosen or changed by the user to view the desired region under investigation. Using the conventional 2D technique, the referring physician often had to integrate all the received 2D images in a three-dimensional form to obtain an impression about the anatomy and possible pathologies.

The use of 2D ultrasound for measurement of organs, such as the uterus or follicle volume, is variable and at times inaccurate. Some diagnostic and treatment IVF procedures require accurate volume measurements (such as follicle monitoring). The accurate acquisition of volumes is only possible with 3D US, especially when the analyzed structures are not spherical but complex (i.e., follicles within a multi-follicular growth complex; this problem will be discussed in a subsequent chapter). 3D US is a relatively new technique for gynecology and IVF. However, studies have already been published reporting high accuracy.

Use of the 3D technique together with the appropriate software allows for the accessed 3D volumes to be digitally stored. This is a tremendous advantage for later post-processing and evaluation. Thus, the stored data can be reformatted and analyzed in various ways. Beyond all the technical improvements, 3D US is still based on conventionally received 2D US data. Thus, poor US scanning techniques cannot be improved by this innovative technique. Inadequate resolution of 2D scans results in poor image quality of the three-dimensional structures. Therefore the 2D scans must be optimized in regard to (1) brightness, (2) the depth of field, and (3) the correct positioning of focus. The correct setting to

achieve the optimal 2D scan is therefore a prerequisite for the best possible 3D calculation.

In addition, most artifacts, which are common in 3D or 4D US, are also similar to those of 2D US because both techniques are based on the same principle. Improper calibration and operation is one major source of the production of inferior data as well as for poor interobserver reliability. This holds true for both, 2D and 3D US. One exception might be the appearance of artifacts due to the movement of the examined objects with 4D US. However, the application of 4D US does not play a dominant role in ART because most of the analyzed structures are immotile. However, it is not unequivocally clear whether the 4D technique might be of future value for ART. For example, endometrial blood flow analyzed by 4D US might become an additional parameter for the prediction of embryo implantation in the future.

The 3D visualization technique offers no additional advantages in regard of reducing the aforementioned artifacts. The effective improvements of US imaging is due to accompanying post-processing software. However, this technical processing cannot be regarded separately as these are integrated components of high-quality 3D instruments.

The rapidly increasing processing power was also one basic requirement for the introduction of portable US systems. This innovation, together with standardized higher image quality, standardized image storage, and compression techniques such as the Digital Imaging and Communications in Medicine (DICOM) standard, enables a medical network and improved patient care.

Applications of 3D Ultrasound in ART

Several clinical trials have demonstrated the superiority of 3D systems compared to conventional 2D US. The images of the structure's surfaces become fully apparent (as a result of their three-dimensional nature). The detailed advantages of the 3D sonography, especially for IVF, are discussed within the Chap. 20. However, studies concerning 3D US in the context of IVF therapies are still limited. Conversely, 3D US in monitoring is commonly used during pregnancy and a crucial tool in prenatal diagnosis because the volumes of fetal organs can be accessed more accurately by the new 3D techniques rather than by conventional 2D US. Thus, fetal anomalies can be recognized more readily [31, 32].

The applications of 3D US in IVF are also summarized in the Chap. 20. However, an overview of the applications of 3D sonography will be presented here. The investigation of the uterus, ovaries, and fallopian tubes are a prerequisite of an IVF cycle. Uterine pathology such as myomas, malformations (see Figs. 2.2 and 2.3) and carcinomas can significantly impair the outcome of IVF therapy [33], and sometimes patient health. In addition to MRI and CT, 2D US was and is currently used for the detection of congenital malformations of the female reproductive system. However, it lacks specificity and image quality [34–37]. Three-dimensional sonography allows a more accurate calculation of the uterine volume. It also allows a more precise estimation of endometrial morphology and volume. Endometrial volume and morphology are the most crucial factors for IVF success. Nonoptimal endometrial lining or a small endometrial volume impacts embryo implantation. In these cases, it might be prudent to consider embryo cryopreservation and opt for a cryocycle [38]. In addition, 3D techniques such as 3D Doppler enable the visualization of endometrial blood flow and neovascularization of cervical carcinomas, which are completely beyond the scope of conventional 2D US.

Imaging modes such as the glass-body mode are the most optimal for the recognition of tumor-feeding vessels. The glass-body mode is a very good method for hysterosalpingo-contrast-sonography (HyCoSy) to detect abnormal varicosity in the adnexal region. The use of 3D US dramatically facilitates HyCoSy and provides a better assessment of tubal patency [39]. Furthermore, 3D US techniques enable an estimation of the ovarian reserve and can be applied during follicle monitoring [40]. Thus, particular automated systems such as the

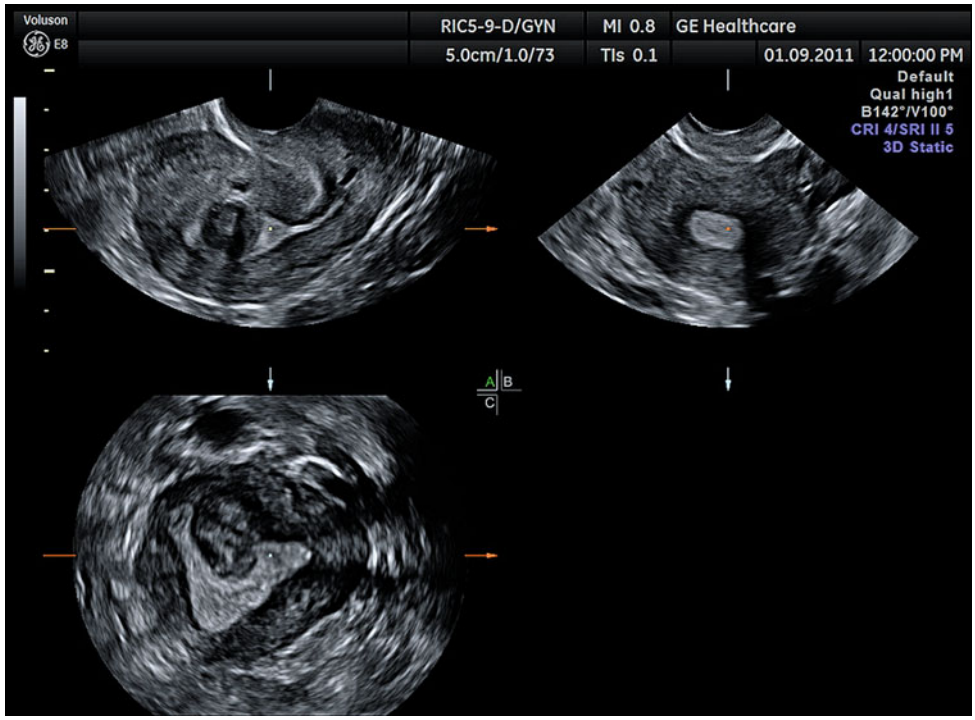

Fig. 2.2 3D image of a uterine myoma (Voluson E8)

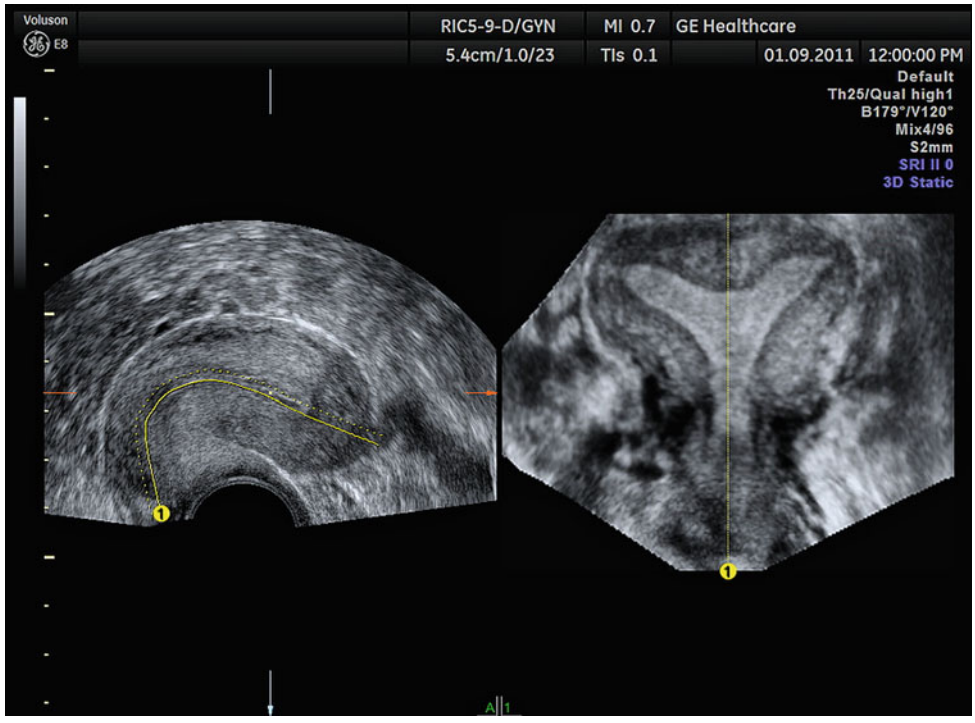

Fig. 2.3 3D image of uterus arcuatus (Voluson E8)

SonoAVC (GE Medical Systems, Kretztechnik, Zipf, Austria) are user-friendly systems, which can accurately determine follicle number and size.

Currently, 3D ultrasound is widely used for monitoring the course of pregnancy. It allows imaging the developing fetus. With the quality 3D images that this type of ultrasound produces, physicians can clearly assess the health condition of the infant or any anomalies, such as cleft palate, spina bifida, anencephaly, and cardiac defects. It provides quantifiable nuchal scan measurements to facilitate the calculation of the risk of chromosomal defects such as Down syndrome [41]. In addition, it facilitates gender determination [42]. 3D ultrasound is not only applied in fetal and gynecologic imaging, but also in other medical procedures such as surgeries or biopsies [43, 44]. Moreover, 3D US is being adopted by other medical fields such as cardiology and neurology [45–47]. Furthermore, it is used in several other fields and its application is at the forefront of current medical technology.

Conclusions

Three-dimensional US opens up new clinical applications and facilitates many of the procedures originally performed with 2D US. The advantages of this relatively new, noninvasive technique have been reported in many specialties. Only a few limitations must be kept in mind, such as the more complex interface that requires a steeper learning curve. However, the advantages it provides not only in the field of ART is striking, and instruments as well as supporting software programs are becoming more and more user friendly. Operation of the systems has become facilitated and the processing time has been significantly shortened. The progress in software regarding imaging and image remodeling as well as the variety of imaging modes facilitates optimal diagnosis and therapy. Three-dimensional sonography has been adopted by several medical fields such as prenatal care, and it is becoming increasingly acceptable as a diagnostic tool. There is no doubt that this innovative method will also be fully established in ART.

References

1. Mahadevan M, Chalder K, Wiseman D, Leader A, Taylor PJ. Evidence for an absence of deleterious effects of ultrasound on human oocytes. J In Vitro Fert Embryo Transf. 1987;4:277–80.
2. Hershkovitz R, Sheiner E, Mazor M. Ultrasound in obstetrics: a review of safety. Eur J Obstet Gynecol Reprod Biol. 2002;101:15–8. Review.
3. Brinkley JF, Muramatsu SK, McCallum WD, Popp RL. In vitro evaluation of an ultrasonic three-dimensional imaging and volume system. Ultrason Imaging. 1982;4:126–39.
4. Rinck PA, Petersen SB. Muller RN [NMR-whole body tomography: a new imaging method]. Radiologe. 1983;23:341–6.
5. Vannier MW, Marsh JL, Warren JO. Three-dimensional CT reconstruction images for craniofacial surgical planning and evaluation. Radiology. 1984;150:179–84.
6. Lees W. Ultrasound imaging in three and four dimensions. Semin Ultrasound CT MR. 2001;22:85–105. Review.
7. Baba K, Satoh K. Development of a system for ultrasonic fetal three-dimensional reconstruction. Acta Obstet Gynaecol Jpn. 1986;38:1385.
8. Baba K, Satch K, Sakamoto S, Oka T, Shiego I. Development of an ultrasonic system for three-dimensional reconstruction of the fetus. J Perinat Med. 1989;17:19–24.
9. Von Ramm OT, Smith SW. Three-dimensional imaging system.1987. United States Patent 4694434. http://www.freepatentsonline.com/4694434.html. Last accessed on 23 May 2013.
10. OBGYN.NET. Kretz museum tour – the history of ultrasound. http://hcp.obgyn.net/conference-insider/display/article/1760982/1953224. Last accessed on 23 May 2013.
11. Brandl H, Gritzky A, Haizinger M. 3D ultrasound: a dedicated system. Eur Radiol. 1999;9:331–3. Review.
12. Alcazar JL. The use of three-dimensional ultrasound in gynecological patients. Donald Sch J Ultrasound Obstet Gynecol. 2008;2:10–6.
13. Miller DL. Safety assurance in obstetrical ultrasound. Semin Ultrasound CT MR. 2008;29:156–64. Review.
14. Merz E. 3D ultrasound in prenatal diagnosis. Curr Obstet Gynecol. 1999;9:93–100.
15. Zhang H, Banovac F, White A, Cleary K. Freehand 3D ultrasound calibration using an electromagnetically tracked needle. Available from: http://proceedings.spiedigitallibrary.org/proceeding.aspx?articleid=1276235. Last Accessed on 23 May 2013.
16. Fenster A, Downey DB, Cardinal HN. Three-dimensional ultrasound imaging. Phys Med Biol. 2001;46:R67–99. Review.
17. Dietz HP, Shek KL. Tomographic ultrasound imaging of the pelvic floor: which levels matter most? Ultrasound Obstet Gynecol. 2009;33:698–703.

18. Ruano R. Recent advances in sonographic imaging of fetal thoracic structures. Expert Rev Med Devices. 2005;2:217–22. Review.
19. Jouannic JM, Rosenblatt J, Demaria F, Jacobs R, Aubry MC, Benifla JL. Contribution of three-dimensional volume contrast imaging to the sonographic assessment of the fetal uterus. Ultrasound Obstet Gynecol. 2005;26:567–70.
20. Benacerraf BR. Inversion mode display of 3D sonography: applications in obstetric and gynecologic imaging. AJR Am J Roentgenol. 2006;187:965–71. Review.
21. Weber G, Merz E, Bahlmann F, Macchiella D. Ultrasound assessment of ovarian tumors–comparison between transvaginal 3D technique and conventional 2-dimensional vaginal ultrasonography. Ultraschall Med. 1997;18:26–30.
22. Campbell S. The potential diagnostic capabilities of three-dimensional surface rendering. Ultrasound Obstet Gynecol. 1999;14:148.
23. Turan S, Turan O, Baschat AA. Three- and four-dimensional fetal echocardiography. Fetal Diagn Ther. 2009;25:361–72. Review.
24. Adriaanse BM, Tromp CH, Simpson JM, Van Mieghem T, Kist WJ, Kuik DJ, Oepkes D, Van Vugt JM, Haak MC. Interobserver agreement in detailed prenatal diagnosis of congenital heart disease by telemedicine using four-dimensional ultrasound with spatiotemporal image correlation. Ultrasound Obstet Gynecol. 2012;39:203–9.
25. Hongmei W, Ying Z, Ailu C, Wei S. Novel application of four-dimensional sonography with B-flow imaging and spatiotemporal image correlation in the assessment of fetal congenital heart defects. Echocardiography. 2012;29:614–9.
26. Yeo L, Romero R, Jodicke C, Oggè G, Lee W, Kusanovic JP, Vaisbuch E, Hassan S. Four-chamber view and 'swing technique' (FAST) echo: a novel and simple algorithm to visualize standard fetal echocardiographic planes. Ultrasound Obstet Gynecol. 2011; 37:423–31.
27. Merz E, Miric-Tesanic D, Welter C. Value of the electronic scalpel (cut mode) in the evaluation of the fetal face. Ultrasound Obstet Gynecol. 2000;16:564–8.
28. Powers J, Kremkau F. Medical ultrasound systems. Interface Focus. 2011;1:477–89.
29. Udupa JK. Three-dimensional visualization and analysis methodologies: a current perspective. Radiographics. 1999;19:783–806. Review.
30. Nelson TR, Pretorius DH, Lev-Toaff A, Bega G, Budorick NE, Hollenbach KA, Needleman L. Feasibility of performing a virtual patient examination using three-dimensional ultrasonographic data acquired at remote locations. J Ultrasound Med. 2001;20:941–52.
31. Merz E, Abramowicz JS. 3D/4D ultrasound in prenatal diagnosis: is it time for routine use? Clin Obstet Gynecol. 2012;55:336–51. Review.
32. Rizzo G, Pietrolucci M, Aiello E, Mammarella S, Bosi C, Arduini D. The role of three-dimensional ultrasound in the diagnosis of fetal congenital anomalies: a review. Minerva Ginecol. 2011;63:401–10. Review.
33. Bulletti C, DE Ziegler D, Levi Setti P, Cicinelli E, Polli V, Stefanetti M. Myomas, pregnancy outcome, and in vitro fertilization. Ann N Y Acad Sci. 2004; 1034:84–92.
34. Raga F, Bonilla-Musoles F, Blanes J, Osborne NG. Congenital Müllerian anomalies: diagnostic accuracy of three-dimensional ultrasound. Fertil Steril. 1996; 65:523–8.
35. Wu MH, Hsu CC, Huang KE. Detection of congenital müllerian duct anomalies using three-dimensional ultrasound. J Clin Ultrasound. 1997;25:487–92.
36. Ghi T, Casadio P, Kuleva M, Perrone AM, Savelli L, Giunchi S, et al. Accuracy of three-dimensional ultrasound in diagnosis and classification of congenital uterine anomalies. Fertil Steril. 2009;92:808–13.
37. Rosendahl M, Ernst E, Rasmussen PE, Andersen CY. True ovarian volume is underestimated by two-dimensional transvaginal ultrasound measurement. Fertil Steril. 2010;93:995–8.
38. Vanderzwalmen P, Zech NH, Ectors F, Stecher A, Lejeune B, Vanderzwalmen S, Wirleitner B. Blastocyst transfer after aseptic vitrification of zygotes: an approach to overcome an impaired uterine environment. Reprod Biomed Online. 2012;25:591–9.
39. Sladkevicius P, Ojha K, Campbell S, Nargund G. Three-dimensional power Doppler imaging in the assessment of Fallopian tube patency. Ultrasound Obstet Gynecol. 2000;16:644–7.
40. Deb S, Campbell BK, Clewes JS, Raine-Fenning NJ. Quantitative analysis of antral follicle number and size: a comparison of two-dimensional and automated three-dimensional ultrasound techniques. Ultrasound Obstet Gynecol. 2010;35:354–60.
41. Shaw SW, Hsieh TT, Hsu JJ, Lee CL, Cheng PJ. Measurement of nuchal volume in the first trimester down screening using three-dimensional ultrasound. Prenat Diagn. 2009;29:69–73.
42. Youssef A, Arcangeli T, Radico D, Contro E, Guasina F, Bellussi F, Maroni E, Morselli-Labate AM, Farina A, Pilu G, Pelusi G, Ghi T. Accuracy of fetal gender determination in the first trimester using three-dimensional ultrasound. Ultrasound Obstet Gynecol. 2011;37:557–61.
43. Jang M, Kim SM, Lyou CY, Choi BS, Choi SI, Kim JH. Differentiating benign from malignant thyroid nodules: comparison of 2- and 3- dimensional sonography. J Ultrasound Med. 2012;31:197–204.
44. Smeenge M, de la Rosette JJ, Wijkstra H. Current status of transrectal ultrasound techniques in prostate cancer. Curr Opin Urol. 2012;22:297–302. Review.
45. Downey DB, Fenster A. Vascular imaging with a three-dimensional power Doppler system. AJR Am J Roentgenol. 1995;165:665–8.
46. Houck RC, Cooke JE, Gill EA. Live 3D echocardiography: a replacement for traditional 2D echocardiography? AJR Am J Roentgenol. 2006;187:1092–106. Review.
47. Pooh RK, Kurjak A. 3D and 4D sonography and magnetic resonance in the assessment of normal and abnormal CNS development: alternative or complementary. J Perinat Med. 2011;39:3–13.

Two-Dimensional and Three-Dimensional Doppler in Reproductive Medicine

3

Ernest Hung Yu Ng

Introduction

In vitro fertilisation (IVF) is an effective treatment for various causes of infertility and typically involves multiple follicular development, oocyte retrieval and embryo transfer after fertilisation. Multiple embryos are still being replaced in order to compensate for their low implantation potential, which have remained steady at 20–30 % for a long time. Development of multiple follicles in response to gonadotrophin stimulation is considered as the key factor leading to successful outcome. Successful implantation is dependent on interaction between a good quality embryo and a receptive endometrium.

Ultrasound is essential during the IVF treatment for monitoring the ovarian response to gonadotrophin and guiding the transvaginal aspiration of oocytes and transfer of embryos to the uterine cavity. Angiogenesis plays a critical role in various female reproductive processes such as development of a dominant follicle, formation of a corpus luteum, growth of endometrium and implantation [1, 2]. This chapter covers the use of two dimensional (2D) and three dimensional (3D), in particular the role of endometrial and subendometrial blood flow determined in predicting the IVF success and the role of ovarian stromal blood flow determined in predicting ovarian response to gonadotrophin stimulation.

E.H.Y. Ng, MD, FRCOG (UK)
Department of Obstetrics and Gynaecology,
The University of Hong Kong, Queen Mary Hospital,
Pokfulam, Hong Kong, Hong Kong
e-mail: nghye@hku.hk

Endometrial Blood Flow

Ultrasound examination of the endometrium serves a non-invasive evaluation of the endometrium during IVF treatment [3]. Parameters such as endometrial thickness, endometrial pattern, endometrial volume and Doppler study of uterine arteries and the endometrium are most commonly used to evaluate the endometrial receptivity. Endometrial thickness and pattern have low positive predictive value and specificity for the IVF outcome [4, 5], whereas endometrial volume measured by 3D ultrasound is not predictive of pregnancy [6–9].

Assessment of endometrial blood flow gives a physiological dimension to the anatomical ultrasound parameters. A good blood flow towards the endometrium is usually considered as an essential requirement for successful implantation. Jinno et al. [10] measured endometrial tissue blood flow in infertile patients by the intrauterine laser Doppler technique between days 4 and 6 of the luteal phase of a spontaneous cycle preceding IVF. The IVF pregnancy rate was significantly higher in women with endometrial tissue blood flow of at least 29 mL/min/100 g of tissue than in women with lower values (42 % vs. 15 %, respectively, $P < 0.05$).

Endometrial blood flow comes from the radial artery, which divides after passing through the

L.A. Stadtmauer, I. Tur-Kaspa (eds.), *Ultrasound Imaging in Reproductive Medicine*,
DOI 10.1007/978-1-4614-9182-8_3,

myometrial-endometrial junction to form the basal arteries that supply the basal portion of the endometrium and the spiral arteries that continue up towards the endometrium. Endometrial blood flow can be determined by colour and power Doppler ultrasound. Power Doppler imaging is more sensitive than colour Doppler imaging at detecting low-velocity flow and hence improves the visualisation of small vessels [11]. In combination with 3D ultrasound, power Doppler can objectively examine both endometrial and subendometrial blood flow.

Blood Flow of Uterine Vessels

Doppler study of uterine vessels reflecting downstream impedance to flow is assumed to reflect the endometrial blood flow. It is usually expressed as the pulsatility index (PI) and the resistance index (RI) (Fig. 3.1). PI is calculated as the peak systolic velocity (PSV) minus end-diastolic velocity divided by the mean, whereas RI is the ratio of PSV minus end-diastolic velocity divided by PSV.

Flow velocity waveforms are obtained from the ascending main branch of the uterine artery

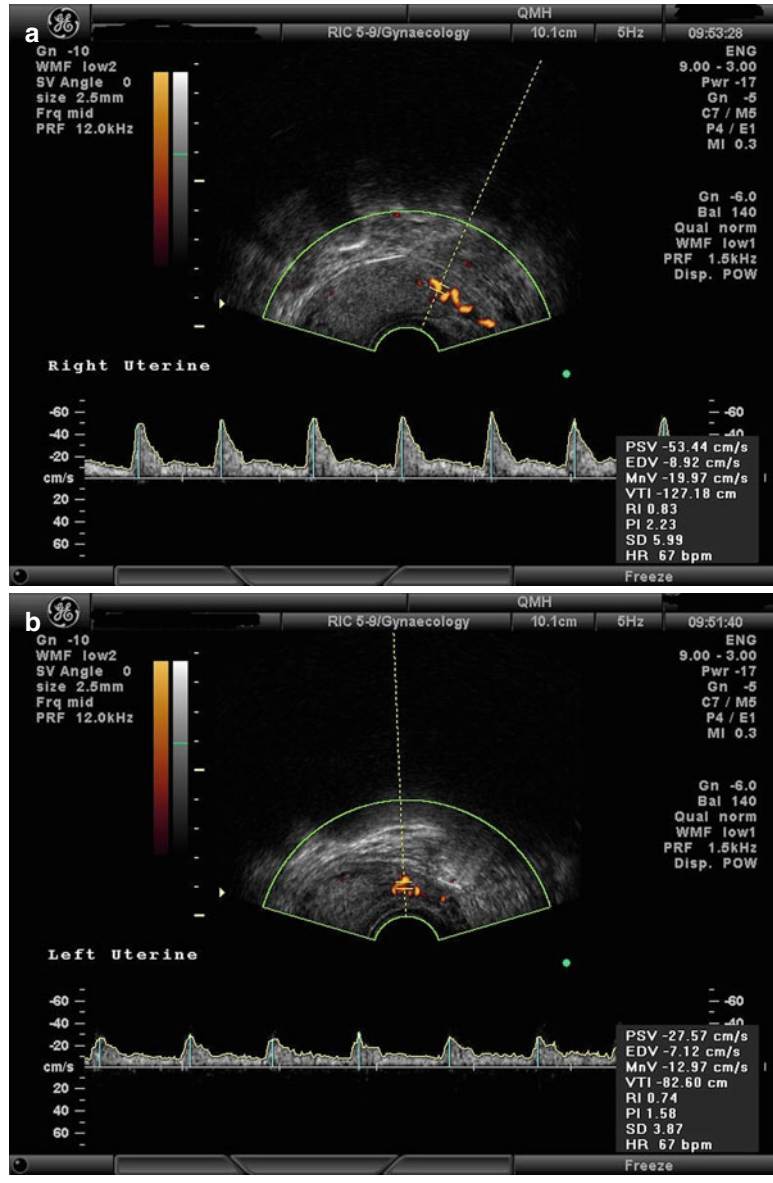

Fig. 3.1 Right (**a**) and left (**b**) uterine blood flow measured by 2D Doppler ultrasound

on the right and left side of the cervix in a longitudinal plane before it enters the uterus. The 'gate' of the Doppler is positioned when the vessel with good colour signals is identified on the screen. The PI and RI of the uterine arteries were calculated electronically when three similar, consecutive waveforms of good quality were obtained.

Good uterine blood flow as shown by low PI or RI is correlated with successful IVF outcomes [12, 13]. Steer et al. [12] classified PI measured on the day of ET as low, medium and high in the ranges of 0–1.99, 2.00–2.99 and ≥3.00, respectively, and reported a 35 % implantation failure when PI was >3.0. Using a PI upper limit of 3.0 [12] or 3.3 [13], the uterine Doppler flow indices have a high negative predictive value and sensitivity (in the ranges of 88–100 % and 96–100 %, respectively) and a relatively higher range of positive predictive value and specificity (44–56 % and 13–35 %, respectively) when compared with endometrial thickness and pattern [5].

Uterine artery Doppler study may not reflect the actual blood flow to the endometrium as the major compartment of the uterus is the myometrium and there is collateral circulation between uterine and ovarian vessels. I have shown 2D Doppler study of uterine vessels is a poor reflection of subendometrial blood flow by 3D power Doppler in both stimulated and natural cycles as endometrial and subendometrial 3D Doppler flow indices were similar among patients with averaged uterine PI <2.0, 2.0–2.99 and ≥3.0. [14].

Endometrial and Subendometrial Blood Flow by 2D Doppler

Endometrial and subendometrial blood flow examined by colour (Table 3.1) and power Doppler (Table 3.2) was correlated with implantation or pregnancy rates during IVF treatment. 2D Doppler flow indices of spiral arteries such as PI and PSV are not predictive of pregnancy [8, 19, 22], although Battaglia et al. [16] and Kupesic et al. [23] found significantly lower spiral artery PI in pregnant cycles than nonpregnant cycles.

Yang et al. [18] used a computer software to measure the area and intensity of colour signals present in the endometrium in a longitudinal axis, i.e. intraendometrial power Doppler area (EDPA). Significantly higher EDPA was found in pregnant cycles than nonpregnant cycles (8.8 mm^2 vs. 5.8 mm^2 respectively). Patients with EDPA <5 mm^2 had significantly lower pregnancy rate (23.5 % vs. 47.5 %; $P=0.021$) and implantation rate (8.1 % vs. 20.2 %; $P=0.003$) than those with ≥5 mm^2. Contart et al. [20] graded endometrial blood flow by the visualisation of power Doppler in the quadrants in the fundal region of

Table 3.1 Summary of studies of endometrial blood flow by 2D colour Doppler

Study	IVF cycles	USS parameters	USS day	Results
Popovic-Todorovic et al. [15]	96 cycles using a long protocol	Spiral PI and PSV	hCG	No difference in subendometrial PI and PSV between pregnant and nonpregnant cycles
		Presence of endometrial and subendometrial flow		Absent subendometrial flow associated with no pregnancy
Battaglia et al. [16]	60 cycles	Uterine and spiral PI	OR	Uterine and spiral PI lower in pregnant than nonpregnant cycles
		Presence of endometrial blood flow		Absent subendometrial flow associated with no pregnancy
Chien et al. [17]	623 cycles using ultrashort and ultralong protocols	Uterine and spiral PI and RI	ET	Significantly lower implantation and pregnancy rates in patients without endometrial/subendometrial flow
		Presence of endometrial and subendometrial (<10 mm) blood flow		Presence of subendometrial flow 5.9 times to become pregnant than those with absent flow

USS ultrasound, *PI* pulsatility index, *PSV* peak systolic velocity, *OR* oocyte retrieval, *ET* embryo transfer

Table 3.2 Summary of studies of endometrial blood flow by 2D power Doppler

Study	IVF cycles	USS parameter	USS day	Results
Yang et al. [18]	95 cycles using long and short protocols Endometrium ≥10 mm	Intraendometrial power Doppler area (EDPA) <5 mm^2; ≥5 mm^2	OR	Higher EDPA in pregnant cycles Lower implantation and pregnancy rates when EDPA <5 mm^2
Yuval et al. [19]	156 cycles using a long protocol	PI and RI	OR and ET	No difference in any USS parameters between pregnant and nonpregnant cycles
Contart et al. [20]	185 cycles using a long protocol	Fundal region along transverse plan; grades I, II, III and IV according to visualisation of power Doppler in the quadrants	hCG	Implantation and pregnancy rates similar in all grades of endometrial vascularity
Schild et al. [8]	135 cycles using a long protocol; first cycle only	PI and PSV of vessels in endometrium and subendometrial area (<5 mm)	OR	No difference in spiral artery PI and PSV between pregnant and nonpregnant cycles Non-detectable spiral blood flow was not associated with a lower implantation rate
Maugey-Laulon et al. [21]	144 cycles using a long protocol	Presence of endometrial and subendometrial blood flow	ET	Absent endometrial and subendometrial flow associated with a lower pregnancy rate

USS ultrasound, *PI* pulsatility index, *PSV* peak systolic velocity, *OR* oocyte retrieval, *ET* embryo transfer

the transverse plane but could not demonstrate any predictive value of such grading system.

Presence of endometrial and subendometrial blood flow can be identified easily in 2D Doppler ultrasound. Absent endometrial and subendometrial blood flow has been shown to be associated with no pregnancy [16, 22] or a significantly lower pregnancy rate [17, 21].

Endometrial and Subendometrial Blood Flow by 3D Doppler

3D power Doppler ultrasound with the aid of the VOCAL® (Virtual Organ Computer-Aided Analysis) imaging program for the 3D power Doppler histogram can be used to measure the endometrial volume and indices of blood flow within the endometrium (Fig. 3.2). Vascularisation index (VI), which measures the ratio of the number of colour voxels to the number of all the voxels, is thought to represent the presence of blood vessels (vascularity) in the endometrium, and this was expressed as a percentage (%) of the endometrial volume. Flow index (FI), the mean power Doppler signal intensity inside the endometrium, is thought to express the average intensity of flow. Vascularisation flow index (VFI) is a combination of vascularity and flow intensity [24].

The subendometrium can be examined through the application of 'shell imaging' which allows the user to generate a variable contour that parallels the originally defined surface contour. The VI, FI and VFI of the subendometrial region are obtained accordingly (Fig. 3.3). The intraobserver reliability and interobserver reliability of endometrial and subendometrial blood flow by 3D power Doppler have been confirmed to be high with all measurements obtaining an intraclass correlation of above 0.9 [25, 26].

Studies addressing the role of endometrial and subendometrial blood flow measured by 3D Doppler in IVF treatment are summarised in Table 3.3. Schild et al. [27] measured the subendometrial blood flow after pituitary downregulation but prior to ovarian stimulation

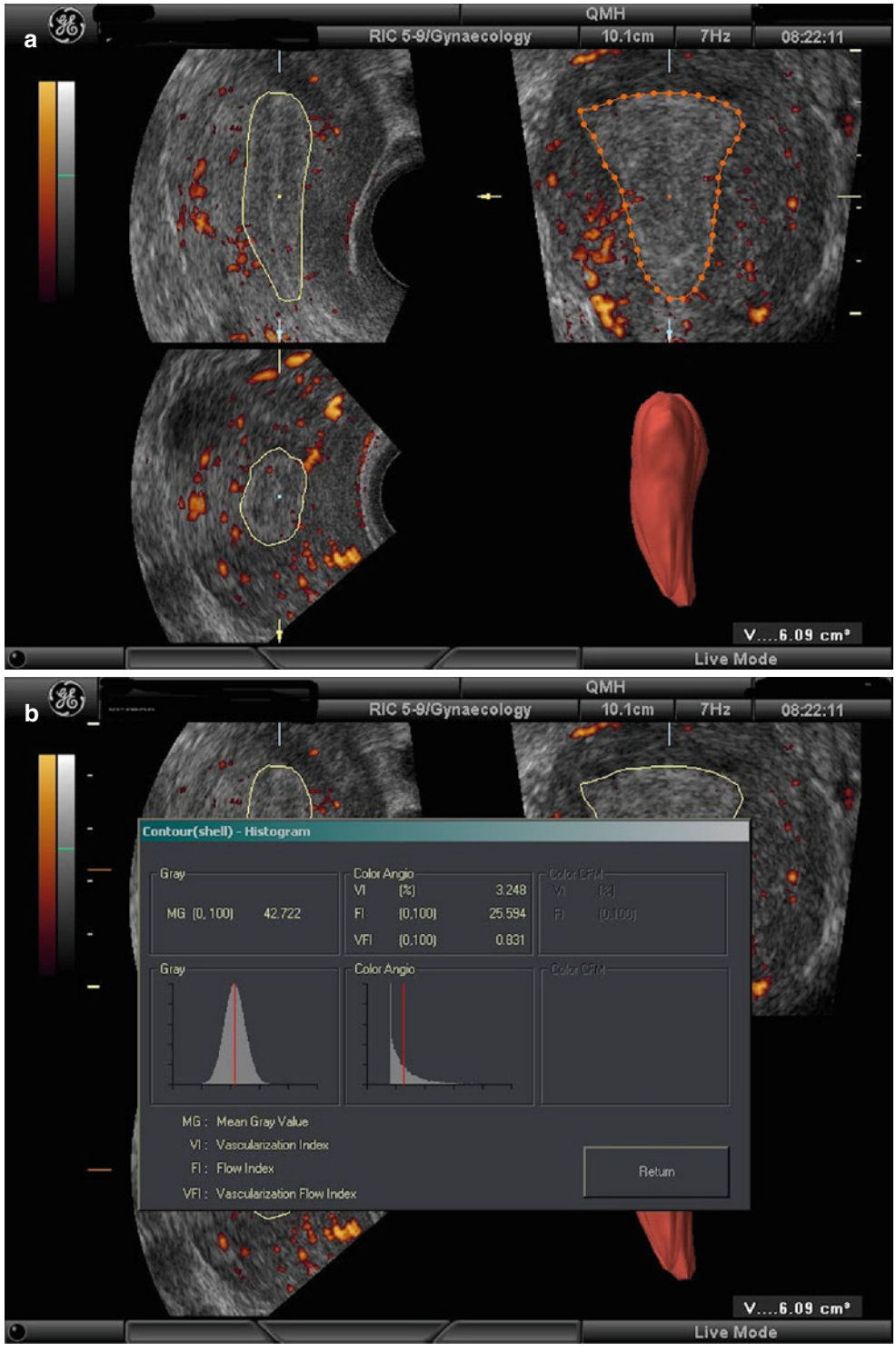

Fig. 3.2 Endometrial volume (**a**) and blood flow (**b**) measured by 3D Doppler ultrasound

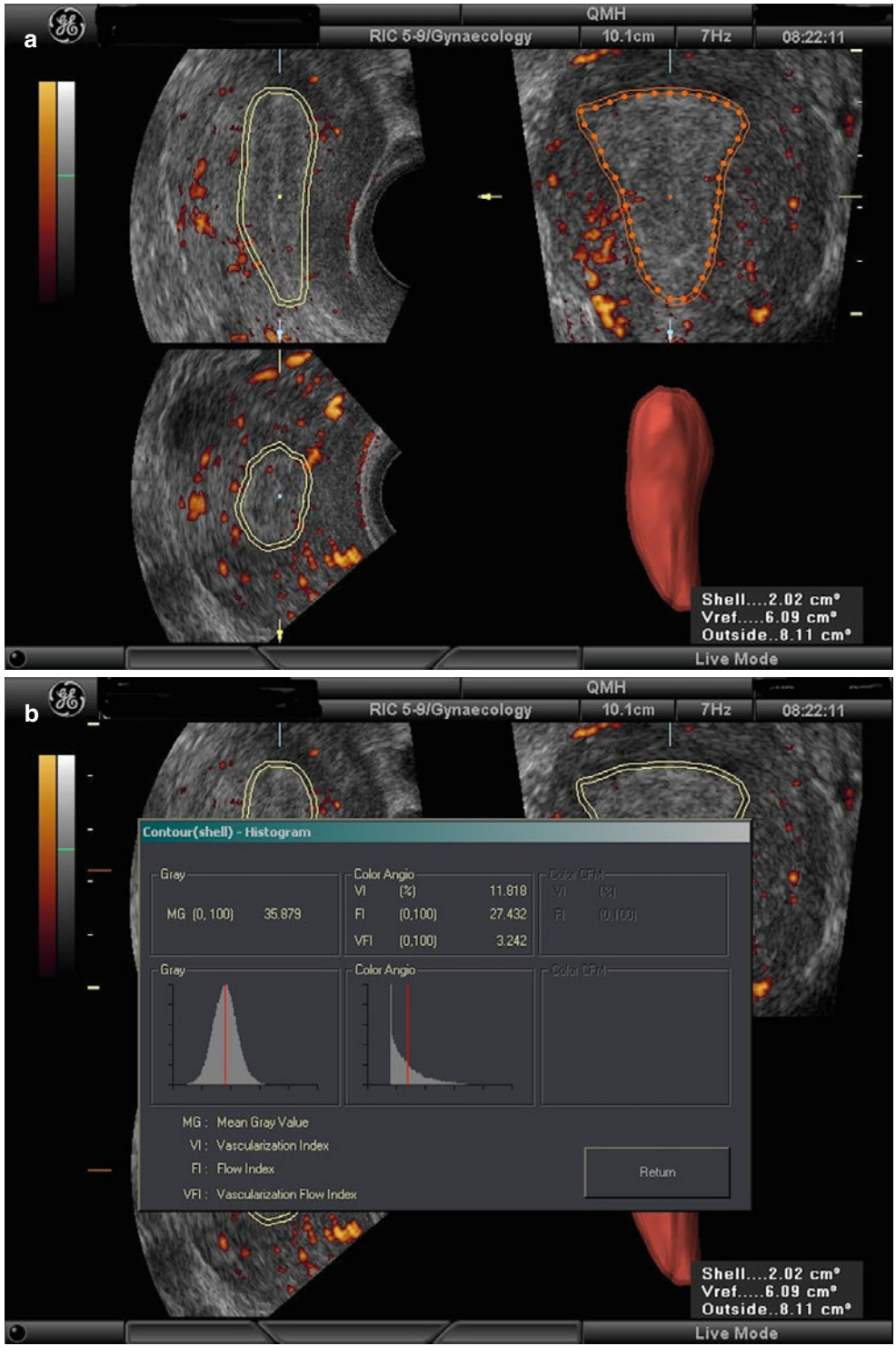

Fig. 3.3 Subendometrial volume (**a**) and blood flow (**b**) measured by 3D Doppler ultrasound

Table 3.3 Summary of studies of endometrial and subendometrial blood flow by 3D power Doppler ultrasound

Study	IVF cycles	Inclusion/exclusion criteria	USS day	Results
Schild et al. [27]	75 cycles using a long protocol ET 2 days after TUGOR	Inclusion criteria Downregulation confirmed (endometrium <5 mm, no ovarian cyst of >2.5 cm, serum oestradiol <60 pg/mL)	Before stimulation	Subendometrial VI, FI and VFI lower in pregnant than nonpregnant cycles Subendometrial FI is the strongest predictive factor for IVF in logistic regression analysis
Kupesic et al. [23]	89 cycles using a long protocol Blastocyst transfer 5 days after TUGOR	Inclusion criteria Serum FSH < 10 IU/L No fibroid, ovarian cysts and ovarian endometriosis	ET (hCG +7)	Higher subendometrial FI in pregnant cycles
Wu et al. [28]	54 cycles; first cycle only (details of ovarian stimulation and ET not given)	Inclusion criteria Age <38 years Normal uterine cavity Serum FSH <15 IU/L ≥2 good quality embryos	hCG	Subendometrial VFI higher in pregnant cycles
Dorn et al. [29]	42 cycles using a long protocol	Exclusion criteria Polycystic ovary syndrome Endometrium <6 mm Gynaecological surgery	OR	No difference in subendometrial VI, FI and VFI between pregnant and nonpregnant cycles
Järvelä et al. [30]	35 cycles using a long protocol ET 2 days after TUGOR	Exclusion criteria Uterine fibroids Endometriosis Single ovary Previous operation on uterus or salpingectomy	After stimulation and OR	No difference in endometrial and subendometrial VI between pregnant and nonpregnant cycles on both days
Ng et al. [31]	451 cycles using a long protocol; first cycle only ET 2 days after TUGOR	Inclusion criteria Normal uterine cavity on scanning	OR	Endometrial VI and VFI lower in pregnant cycles
Ng et al. [32]	193 cycles Frozen-thawed embryo transfer cycles	Inclusion criteria Normal uterine cavity	LH +1	No difference in endometrial and subendometrial 3D Doppler flow indices between pregnant and nonpregnant cycles

(continued)

Table 3.3 (continued)

Study	IVF cycles	Inclusion/exclusion criteria	USS day	Results
Mercè et al. [33]	80 cycles using a long protocol	Inclusion criteria First cycle Normal uterine cavity Serum FSH <10 IU/L Regular cycles Non-smokers	hCG	Higher endometrial VI, FI and VFI in pregnant cycles
Ng et al. [34]	293 cycles using a long protocol ET 2 days after OR	Inclusion criteria First cycle Normal uterine cavity	OR and ET	No difference in endometrial and subendometrial 3D Doppler flow indices on the 2 days and changes in these indices between pregnant and nonpregnant cycles

USS ultrasound, *VI* vascularisation index, *FI* flow index, *VFI* vascularisation flow index, *OR* oocyte retrieval, *ET* embryo transfer

and showed that subendometrial VI, FI and VFI were significantly lower in pregnant cycles than nonpregnant ones. Logistic regression analysis found that the subendometrial FI was the strongest predictive factor for the pregnancy outcome among other 3D Doppler flow indices.

Kupesic et al. [23] performed 3D ultrasound examination on the day of blastocyst transfer and found that subendometrial FI was significantly higher in pregnant cycles. Subendometrial VI and VFI were similar between pregnant and nonpregnant patients. Wu et al. [28] measured subendometrial blood flow on the day of hCG and demonstrated that subendometrial VFI was significantly higher in the pregnant group. Subendometrial VI and FI were also similar between pregnant and nonpregnant cycles. Subendometrial VFI was superior to subendometrial VI, subendometrial FI and endometrial volume in predicting the successful outcome in the receiver-operating characteristics (ROC) curve analysis.

On the day of oocyte retrieval, Dorn et al. [29] compared the subendometrial blood flow before and after an intravenous administration of Levovist, which is a contrast agent and consists of 99.9 % of D-galactose. All subendometrial 3D Doppler flow indices after the administration of the contrast agent were significantly higher than those without the contrast agent. However, all subendometrial 3D Doppler flow indices with and without the contrast agent were comparable between pregnant and nonpregnant cycles. The results of this study suggested that the use of 3D power Doppler ultrasound under a contrast agent during IVF treatment provided no additional advantage over the conventional 3D power Doppler ultrasound examination.

Järvelä et al. [30] determined endometrial and subendometrial VI after gonadotrophin stimulation but before hCG administration and again the day of oocyte retrieval. There were no differences between the pregnant and nonpregnant groups in endometrial and subendometrial VI on either day examined. I have published the largest study involving 451 transfer cycles [31]. Patients in the pregnant group had significantly lower uterine RI, endometrial VI and VFI than those in the nonpregnant group. Endometrial thickness, endometrial volume, endometrial pattern, uterine PI, endometrial FI and subendometrial VI, FI and VFI were similar between the nonpregnant and pregnant groups. The number of embryos replaced and endometrial VI were the only two predictive factors for pregnancy in a logistic multiple regression analysis. ROC curve analysis revealed that the area under the curve was around 0.5 for all ultrasound parameters for endometrial receptivity. Implantation and pregnancy rates were comparable for patients with and without endometrial and subendometrial blood flow [31].

The age of women, their smoking habits, their types of infertility and parity and causes of subfertility had no effect on all endometrial and subendometrial 3D Doppler flow indices [35]. Endometrial blood flow was negatively affected by serum oestradiol concentration on the day of hCG. Indeed, endometrial and subendometrial 3D Doppler flow indices in the stimulated cycles were significantly lower than those in the natural cycles of the same patients undergoing IVF treatment [36].

Uterine PI, uterine RI, endometrial and subendometrial 3D Doppler flow indices were comparable between the nonpregnant and pregnant groups' frozen-thawed embryo transfer cycles using natural or clomiphene-induced cycles [32]. On the other hand, endometrial and subendometrial blood flow was significantly higher in pregnant patients with live birth following IVF and frozen-thawed embryo transfer treatment [37].

Mercè et al. [33] found that endometrial 3D power Doppler flow indices were statistically significantly higher in the pregnant group. The area under ROC curve was statistically significant for endometrial VI, FI and VFI when no grade 1 embryos or only one was transferred, but not when two or three grade 1 embryos were transferred.

Changes in Endometrial and Subendometrial Blood Flow

Ultrasound examination was performed on the day of hCG [28, 33], oocyte retrieval [29–31] and blastocyst transfer [23]. There is no consensus when the ultrasound examination for

assessing endometrial receptivity in IVF treatment should be done. The day of the ultrasound examination in these studies was chosen for logistic reasons.

Endometrial blood flow changes throughout the menstrual cycle [38]. Raine-Fenning et al. [38] showed that endometrial and subendometrial blood flow by 3D ultrasound increased during the proliferative phase, peaking around 3 days prior to ovulation before decreasing to a nadir 5 days post-ovulation. Hypoxia in the endometrium may play a beneficial role for implantation as the expression of vascular endothelial growth factor is upregulated by hypoxia [39] and relatively low oxygen tension was present around the blastocyst during the time of implantation [40].

Endometrial and subendometrial blood flow was measured on the days of hCG and ET [34]. Patients in nonpregnant and pregnant groups had comparable 3D Doppler flow indices of endometrial and subendometrial regions measured on either day. Percentage changes in endometrial and subendometrial 3D Doppler flow indices between these 2 days were also similar. Again, none of the ultrasound parameters was predictive of pregnancy in a multiple logistic regression analysis and the ROC curve analysis.

Prediction of Ovarian Response to Gonadotrophin

Development of multiple follicles in response to ovarian stimulation is the key factor leading to a successful outcome of IVF treatment. Poor ovarian response is associated with lower pregnancy rates, while exaggerated ovarian response leads to an increased risk of ovarian hyperstimulation syndrome. Prediction of ovarian responses prior to gonadotrophin stimulation is useful in counselling patients and helpful in tailoring the dosage of gonadotrophin to individual patients. A number of ultrasound parameters have been examined to predict the ovarian response to gonadotrophins, including ovarian volume, antral follicle count [41] and ovarian stromal blood flow [15, 42–45].

Folliculogenesis in the human ovary is a complex process regulated by a variety of endocrine and paracrine signals [46]. It has been suggested that the availability of an adequate vascular supply to provide endocrine and paracrine signals may play a key role in the regulation of follicle growth [47]. It is postulated that increased ovarian stromal blood flow may lead to a greater delivery of gonadotrophins to the granulosa cells of the developing follicles.

Ovarian Stromal Blood Flow by 2D Doppler

Ovarian stromal blood flow can be assessed by colour Doppler and power Doppler ultrasound. Power Doppler is better suited to the study of the ovarian stromal blood flow as it is more sensitive to lower velocities and essentially angle independent [11, 48]. Flow velocity waveforms were obtained from stromal blood vessels away from the ovarian capsule, if present. The ‘gate’ of the Doppler was positioned when the vessel with good colour signals was identified on the screen. PI, RI and peak systolic blood flow velocity (PSV) of stromal vessels was calculated electronically when three similar, consecutive waveforms of good quality were obtained.

Zaidi et al. [42] showed that mean ovarian stromal PSV prior to pituitary downregulation was significantly correlated with the number of follicles, after controlling for patients’ age. Patients with >6 follicles at retrieval had significantly higher velocity than those <6 follicles (10.2 ± 5.8 cm/s vs. 5.2 ± 4.2 cm/s). Similarly, Engmann et al. [43] demonstrated that ovarian stromal PSV after pituitary downregulation was the most important independent predictor of the number of oocytes obtained in patients with normal basal FSH concentration, when compared with age of women, basal FSH concentration, E2 concentration or FSH:LH ratio. Bassil et al. [49] reported that women with RI of ovarian blood flow >0.56 had a significantly longer stimulation and a significantly lower mean number of oocytes retrieved. Both BMI and AFC were not included in these three studies.

Popovic-Todorovic et al. [15] evaluated ovarian stromal blood by 2D power Doppler ultrasound and a semi-quantitative score was allocated to each ovary according to the number and area of the power Doppler signals. Total Doppler score was the sum of scores for each ovary: score 1 for poor flow, score 2 for moderate flow and score 3 for good flow. The number of oocytes was predicted by AFC, total Doppler score, serum testosterone concentration and smoking status.

In a prospective study, 136 women aged <40 years with basal FSH concentration <10 IU/L received a standard regimen of ovarian stimulation in their first IVF cycle [50]. The ovarian stromal blood flow measured by 2D power Doppler was compared to age of women, body mass index, basal FSH concentration and AFC in the prediction of the ovarian response. Basal FSH concentration achieved the best predictive value in relation to the number of oocytes obtained, followed by AFC and BMI. AFC was the only predictive factor of serum oestradiol concentration on the day of hCG, while BMI was predictive of the gonadotrophin dosage. Ovarian stromal blood flow indices measured by power Doppler ultrasound had no predictive value for the ovarian response.

Ovarian Stromal Blood Flow by 3D Doppler

I further evaluated the role of ovarian stromal blood flow by 3D power Doppler. Age of women, BMI, basal FSH concentration, AFC and ovarian stromal vascularity indices measured by 3D power Doppler were compared in 111 women aged <40 years old with basal FSH concentration <10 IU/L in their first IVF cycle [51]. The results indicated that AFC achieved the best predictive value in relation to the number of oocytes obtained, followed by age of women and BMI. Basal FSH concentration was the only predictive factor for the duration and dosage of gonadotrophin used. Mean ovarian 3D power Doppler flow indices were not predictive of pregnancy in a multiple logistic regression analysis.

Therefore, ovarian stromal blood flow measured after pituitary downregulation by both 2D and 3D power Doppler was not predictive of the ovarian response in terms of the number of oocytes obtained, the duration and dose of FSH used and maximum serum E2 concentrations. These results were in line with those of previous studies assessing ovarian stromal blood flow in fertile Chinese women [52, 53]. There was no effect of age on mean PSV of ovarian stromal blood vessels determined by 2D colour Doppler ultrasound. Using 3D Doppler ultrasound, ovarian stromal vascularity was significantly lower in fertile Chinese women aged ≥41 years, and the rate of decline of total ovarian vascularity index was only 0.18 % per year [53]. These data strongly suggest that reduction in ovarian stromal blood flow with increasing age is a relatively late phenomenon, and ovarian stromal blood flow is unlikely an early marker for ovarian response.

Conclusion

Angiogenesis plays a critical role in various female reproductive processes such as folliculogenesis, formation of a corpus luteum, growth of endometrium and implantation. Assessment of blood flow by Doppler ultrasound may add a physiological dimension to the anatomical USS parameters, but for the time being, 2D and 3D Doppler study of the endometrium and the ovary has no definite benefit in routine patient care in IVF treatment.

References

1. Abulafia O, Sherer DM. Angiogenesis of the ovary. Am J Obstet Gynecol. 2000;182:240–6.
2. Smith SK. Regulation of angiogenesis in the endometrium. Trends Endocrinol Metab. 2001;12:147–51.
3. Ng EHY, Ho PC. The role of ultrasound parameters in the prediction of pregnancy during in vitro fertilization treatment. Expert Rev Obstet Gynaecol. 2008;3:503–14.
4. Turnbull LW, Lesny P, Killick SR. Assessment of uterine receptivity prior to embryo transfer: a review of currently available imaging modalities. Hum Reprod Update. 1995;1:505–14.
5. Friedler S, Schenker JG, Herman A, Lewin A. The role of ultrasonography in the evaluation of

endometrial receptivity following assisted reproductive treatments: a critical review. Hum Reprod Update. 1996;2:323–35.
6. Raga R, Bonilla-Musoles F, Casan EM, Klein O, Bonilla F. Assessment of endometrial volume by three-dimensional ultrasound prior to embryo transfer: clues to endometrial receptivity. Hum Reprod. 1999;14:2851–4.
7. Yaman C, Ebner T, Sommergruber M, Polz W, Tews G. Role of three-dimensional ultrasonographic measurement of endometrium volume as a predictor of pregnancy outcome in an IVF-ET program. A preliminary study. Fertil Steril. 2000;74:797–801.
8. Schild RL, Knoblock C, Dorn C, Fimmers R, van der Ven H, Hansmann M. Endometrial receptivity in an in vitro fertilization program as assessed by spiral artery blood flow, endometrial thickness, endometrial volume, and uterine artery Blood flow. Fertil Steril. 2001;75:361–6.
9. Ng EHY, Yeung WSB, Ho PC. Endometrial and subendometrial vascularity significantly lower in patients with endometrial volume<=2.5ml. Reprod Biomed Online. 2009;18:262–8.
10. Jinno M, Ozaki T, Iwashita M, Nakamura Y, Kudo A, Hirano H. Measurement of endometrial tissue blood flow: a novel way to assess uterine receptivity for implantation. Fertil Steril. 2001;76:1168–74.
11. Guerriero S, Ajossa S, Lai MP, Risalvato A, Paoletti AM, Melis GB. Clinical applications of colour Doppler energy imaging in the female reproductive tract and pregnancy. Hum Reprod Update. 1999;5:515–29.
12. Steer CV, Campbell S, Tan SL, Crayford T, Mills C, Mason BA, et al. The use of transvaginal colour flow imaging after in vitro fertilization to identify optimum uterine conditions before embryo transfer. Fertil Steril. 1992;57:372–6.
13. Coulam CB, Bustillo M, Soenksen DM, Britten S. Ultrasonographic predictors of implantation after assisted reproduction. Fertil Steril. 1994;62:1004–10.
14. Ng EHY, Chan CCW, Tang OS, Yeung WSB, Ho PC. Relationship between uterine blood flow and endometrial and subendometrial blood flow during stimulated and natural cycles. Fertil Steril. 2006;85:721–7.
15. Popovic-Todorovic B, Loft A, Lindhard A, Bangsboll S, Andersson AM, Andersen AN. A prospective study of predictive factors of ovarian response in 'standard' IVF/ICSI patients treated with recombinant FSH. A suggestion for a recombinant FSH dosage normogram. Hum Reprod. 2003;18:781–7.
16. Battaglia C, Artini PG, Giulini S, Salvatori M, Maxia N, Petraglia F, et al. Colour Doppler changes and thromboxane production after ovarian stimulation with gonadotrophin-releasing hormone agonist. Hum Reprod. 1997;12:2477–82.
17. Chien LW, Au HK, Chen PL, Xiao J, Tseng CR. Assessment of uterine receptivity by the endometrial-subendometrial blood flow distribution pattern in women undergoing in vitro fertilization-embryo transfer. Fertil Steril. 2002;78:245–51.
18. Yang JH, Wu MY, Chen CD, Jiang MC, Ho HN, Yang YS. Association of endometrial blood flow as determined by a modified colour Doppler technique with subsequent outcome of in-vitro fertilization. Hum Reprod. 1999;14:1606–10.
19. Yuval Y, Lipitz S, Dor J, Achiron R. The relationship between endometrial thickness, and blood flow and pregnancy rates in in-vitro fertilization. Hum Reprod. 1999;14:1067–71.
20. Contart P, Baruffi RL, Coelho J, Mauri AL, Petersen C, Franco Junior JG. Power Doppler endometrial evaluation as a method for the prognosis of embryo implantation in an ICSI program. J Assist Reprod Genet. 2000;17:329–34.
21. Maugey-Laulon B, Commenges-Ducos M, Jullien V, Papaxanthos-Roche A, Scotet V, Commenges D. Endometrial vascularity and ongoing pregnancy after IVF. Eur J Obstet Gynecol Reprod Biol. 2002;104:137–43.
22. Zaidi J, Campbell S, Pittrof FR, Tan SL. Endometrial thickness morphology, vascular penetration and velocimetry in predicting implantation in an IVF program. Ultrasound Obstet Gynecol. 1995;6:191–8.
23. Kupesic S, Bekavac I, Bjelos D, Kurjak A. Assessment of endometrial receptivity by transvaginal colour Doppler and three-dimensional power Doppler ultrasonography in patients undergoing in vitro fertilization procedures. J Ultrasound Med. 2001;20:125–34.
24. Pairleitner H, Steiner H, Hasenoehrl G, Staudach A. Three-dimensional power Doppler sonography: imaging and quantifying blood flow and vascularization. Ultrasound Obstet Gynecol. 1999;14:139–43.
25. Raine-Fenning NJ, Campbell BK, Clewes JS, Kendall NR, Johnson IR. The reliability of virtual organ computer-aided analysis (VOCAL) for the semiquantification of ovarian, endometrial and subendometrial perfusion. Ultrasound Obstet Gynecol. 2003;22:633–9.
26. Raine-Fenning NJ, Campbell BK, Clewes JS, Kendall NR, Johnson IR. The interobserver reliability of three-dimensional power Doppler data acquisition within the female pelvis. Ultrasound Obstet Gynecol. 2004;23:501–8.
27. Schild RL, Holthanus S, Alquen JD, Fimmers R, Dorn C, van der Ven H, Hansmann M. Quantitative assessment of subendometrial blood flow by three-dimensional-ultrasound is an important predictive factor of implantation in an in-vitro fertilization programme. Hum Reprod. 2000;15:89–94.
28. Wu HM, Chiang CH, Huang HY, Chao AS, Wang HS, Soong YK. Detection of the subendometrial vascularization flow index by three-dimensional ultrasound may be useful for predicting the pregnancy rate for patients undergoing in vitro fertilization-embryo transfer. Fertil Steril. 2003;79:507–11.
29. Dorn C, Reinsberg J, Willeke C, Wendt A, van der Ven H, Schild RL. Three-dimensional power Doppler ultrasound of the subendometrial blood flow under the administration of a contrast agent (Levovist). Arch Gynecol Obstet. 2004;270:94–8.

30. Järvelä IY, Sladkevicius P, Kelly S, Ojha K, Campbell S, Nargund G. Evaluation of endometrial receptivity during in-vitro fertilization using three-dimensional power Doppler ultrasound. Ultrasound Obstet Gynecol. 2005;26:765–9.
31. Ng EHY, Chan CCW, Tang OS, Yeung WSB, Ho PC. The role of endometrial and subendometrial blood flow measured by three-dimensional power Doppler ultrasound in the prediction of pregnancy during in vitro fertilization treatment. Hum Reprod. 2006;21: 164–70.
32. Ng EHY, Chan CCW, Tang OS, Yeung WSB, Ho PC. The role of endometrial and subendometrial vascularity measured by three-dimensional power Doppler ultrasound in the prediction of pregnancy during frozen-thawed embryo transfer cycles. Hum Reprod. 2006;21:612–1617.
33. Mercè LT, Barco MJ, Bau S, Troyano J. Are endometrial parameters by three-dimensional ultrasound and power Doppler angiography related to in vitro fertilization/embryo transfer outcome? Fertil Steril. 2008; 1:111–7.
34. Ng EHY, Chan CCW, Tang OS, Yeung WSB, Ho PC. Changes in endometrial and subendometrial blood flows in IVF. Reprod Biomed Online. 2009;18: 269–75.
35. Ng EHY, Chan CCW, Tang OS, Yeung WSB, Ho PC. Factors affecting endometrial and subendometrial blood flow measured by three-dimensional power Doppler ultrasound during in vitro fertilization treatment. Hum Reprod. 2006;21:1062–9.
36. Ng EHY, Chan CCW, Tang OS, Yeung WSB, Ho PC. Comparison of endometrial and subendometrial blood flow measured by three-dimensional power Doppler ultrasound between stimulated and natural cycles in the same patients. Hum Reprod. 2004;19:2385–90.
37. Ng EHY, Chan CCW, Tang OS, Yeung WSB, Ho PC. Endometrial and subendometrial vascularity is higher in pregnant patients with live birth following ART than in those who suffer a miscarriage. Hum Reprod. 2007;22:134–1141.
38. Raine-Fenning NJ, Campbell BK, Kendall NR, Clewes JS, Johnson IR. Quantifying the changes in endometrial vascularity throughout the normal menstrual cycle with three-dimensional power Doppler angiography. Hum Reprod. 2004;19:330–8.
39. Sharkey AM, Day K, McPherson A, Malik S, Licence D, Smith SK, et al. Vascular endothelial growth factor expression in human endometrium is regulated by hypoxia. J Clin Endocrinol Metab. 2000;85:402–9.
40. Graham CH, Postovit LM, Park H, Canning MT, Fitzpatrick TE. Adriana and Luisa Castellucci award lecture 1999: role of oxygen in the regulation of trophoblast gene expression and invasion. Placenta. 2000;21:443–50.
41. Broekmans FJ, Kwee J, Hendriks DJ, Mol BW, Lambalk CB. A systematic review of tests predicting ovarian reserve and IVF outcome. Hum Reprod Update. 2006;12:685–718.
42. Zaidi J, Barber J, Kyei-mensah A, Bekir J, Campbell S, Tan SL. Relationship of ovarian stromal blood flow at the baseline ultrasound scan to subsequent follicular response in an in vitro fertilization program. Obstet Gynecol. 1996;88:779–84.
43. Engmann L, Sladkevicius P, Agrawal R, Bekir JS, Campbell S, Tan SL. Value of ovarian stromal blood flow velocity measurement after pituitary suppression in the prediction of ovarian responsiveness and outcome of in vitro fertilization treatment. Fertil Steril. 1999;71:22–9.
44. Kupesic S, Kurjak A. Predictors of IVF outcome by three-dimensional ultrasound. Hum Reprod. 2002;17: 950–5.
45. Kupesic S, Kurjak A, Bjelos D, Vujisic S. Three-dimensional ultrasonographic ovarian measurements and in vitro fertilization outcome are related to age. Fertil Steril. 2003;79:190–7.
46. McGee EA, Hsueh AJ. Initial and cyclic recruitment of ovarian follicles. Endocr Rev. 2000;21:200–14.
47. Redmer D, Reynolds L. Angiogenesis in the ovary. Rev Reprod. 1996;1:182–92.
48. Rubin JM, Bude RO, Carson PL, Bree RL, Adler RS. Power Doppler US: a potentially useful alternative to mean frequency- based colour Doppler US. Radiology. 1994;190:853–6.
49. Bassil S, Wyns C, Toussaint-Demylle D, Nisolle M, Gordts S, Donnez J. The relationship between ovarian vascularity and the duration of stimulation in in-vitro fertilization. Hum Reprod. 1997;12:1240–5.
50. Ng EHY, Tang OS, Chan CCW, Ho PC. Ovarian stromal blood flow in the prediction of ovarian response during in vitro fertilization treatment. Hum Reprod. 2005;20:3147–51.
51. Ng EHY, Chan CCW, Tang OS, Ho PC. Ovarian stromal vascularity is not predictive of ovarian response and pregnancy. Reprod Biomed Online. 2006;12:43–9.
52. Ng EHY, Fong DYT, Yeung WSB, Ho PC. Effects of age on hormonal and ultrasound markers of ovarian reserve in Chinese women with proven fertility. Hum Reprod. 2003;18:2169–74.
53. Ng EHY, Chan CCW, Yeung WSB, Ho PC. Effect of age on ovarian stromal flow measured by three-dimensional ultrasound with power Doppler in Chinese women with proven fertility. Hum Reprod. 2004;19:2132–7.

Legal Aspects of Ultrasound Imaging in Reproductive Medicine

4

James M. Shwayder

Legal Aspects of Ultrasound Imaging in Reproductive Medicine

Medical liability concerns all providers and has great impact on the health system. Recognizing the prime areas of risk and proactively addressing these issues can reduce the frequency and severity of litigation. However, liability now extends to billing fraud, which can be even more financially devastating.

The elements of malpractice include the following: (1) the duty to care for a patient; (2) a breach of that duty, i.e., a breach of the standard of care; (3) that breach is the proximate cause of an adverse outcome or complication; and (4) damages result that are compensable. If any one of these elements is not met, then the action fails or in other words defensible. Litigation in ultrasound imaging focuses on two areas: (1) the proper performance of the study with acquisition of images suitable to render a diagnosis and (2) errors surrounding study interpretation and reporting.

J.M. Shwayder, MD, JD
Department of Obstetrics and Gynecology,
University of Mississippi, 2500 North State Street,
Room L305 (for FedEx or UPS), Jackson,
MS 39216, USA
e-mail: jshwayder@umc.edu

Performance of the Ultrasound Study

Litigation in this area tends to focus on the following:

1. Inadequate training of the person performing the ultrasound study
2. Inadequate and thus negligent performance of the study, with inadequate or incomplete images
3. Inadequate supervision of the sonographer
4. Lost or misplaced images
5. Inadequate equipment maintenance

Personnel Performing Ultrasound Examinations

There are specific issues that are unique to ultrasound. Ultrasound performance is often delegated to other personnel. The American Institute of Ultrasound in Medicine (AIUM) accreditation guidelines require that all persons who perform ultrasounds, other than physicians, are either RDMS (Registered Diagnostic Medical Sonographer) certified or eligible [1]. However, many reproductive medicine practices use nurses, nurse practitioners, or other personnel who do not meet these criteria to perform ultrasound. In 2009, the American Institute of Ultrasound in Medicine (AIUM) and the American Society of Reproductive Medicine

L.A. Stadtmauer, I. Tur-Kaspa (eds.), *Ultrasound Imaging in Reproductive Medicine*,
DOI 10.1007/978-1-4614-9182-8_4,

(ASRM) issued a consensus statement regarding focused ultrasounds in reproductive medicine [2]. Ultrasounds for follicular monitoring are intended to provide specific diagnostic information comprising the number and size of developing follicles, as well as uterine evaluation including endometrial thickness and morphology. These are considered limited ultrasounds, rather than complete diagnostic sonographic studies. The consensus is that such limited examinations are within the scope of practice of a nurse with specific training and with appropriate physician supervision in an infertility practice. However, it states that a comprehensive ultrasound examination should have been performed within the prior 4–6 months to exclude significant gynecologic pathology.

A caution is that the position of AIUM and ASRM on nurses performing ultrasound examinations pertains to the limited studies appropriate for monitoring ovulation induction. If the practice performs comprehensive diagnostic studies, according to AIUM guidelines, these should be performed by physicians or appropriately trained and qualified personnel. If not, the physician is at increased legal risk in the event of misdiagnosis.

Adequacy of the Ultrasound Study

Images obtained should conform with the guidelines set forth by AIUM [3–5]. Incomplete studies expose the physician to increased risk as the lack of images supporting the reported diagnosis reduces defensibility. Also, the lack of a documented complete study can expose the physician to a claim of insurance fraud specifically billing for a higher level of service than supported by documentation.

Ultrasound Supervision

The Centers for Medicare and Medicaid Services (CMS) states, with one exception, that "general supervision" of personnel performing ultrasounds is required. "General supervision" dictates that the physician's presence is not required during the performance of the procedure. However, the training of the nonphysician personnel who perform the diagnostic procedure and equipment maintenance are the responsibility of the physician [6]. Thus, any errors resulting from inadequately performed ultrasound studies fall within legal concept of respondeat superior. This concept holds the employer, or physician, liable for the wrong of an employee if it was committed within the scope of employment [7]. The exception to this supervision level is in the performance of sonohysterography that requires "personal supervision." Personal supervision requires the physician's presence in the room during the performance of the procedure. In most instances this requirement is met when the physician inserts the catheter and instills fluid while the ultrasound is performed. Similar requirements exist for sonosalpingography. If the physician is not available for immediate consultation, then guidelines should be established that address immediate communication with the supervising physician. In addition, callback mechanisms should be established when further evaluation of the patient is required.

Image Acquisition and Retention

Images obtained should conform with the guidelines set forth by AIUM [3–5]. Ideally, images should be retained in a digital format to maximize retention of image quality for a more extended time. At a minimum, thermal print images of critical findings should remain in the medical record. The images, as well as the report, should be retained for the statute of limitations as required in the applicable jurisdiction.

Equipment Maintenance

AIUM accreditation specifies that preventive maintenance and resolution testing should be done on an annual basis. This maintenance is critical to assure optimum performance and is recommended regardless of accreditation status. Ultrasound performance with outmoded technology or with machines that are not properly maintained exposes the physician to additional risk.

Study Interpretation and Reporting

Ultrasound litigation surrounding ultrasound remains most frequent with obstetrical ultrasound. However, gynecologic ultrasound is now the second most common cause of ultrasound-related litigation [8]. The most common causes of liability actions comprise the following: (1) perception errors, (2) interpretation errors, (3) failing to suggest the next appropriate procedure, and (4) failure to communicate significant abnormal findings [9].

Perception errors occur when an abnormality is seen in retrospect but it was missed when interpreting the initial study [10]. An example would be an adnexal mass with a gestational sac, consistent with an ectopic pregnancy, which was not identified on the initial study but identified on subsequent review. Although the error rate in radiology is approximated at 30 % [10], this rate is not accepted when errors occur. The critical question is: "Was it below the standard of care for the physician not to have seen the abnormality?" [11] These cases are difficult to defend with almost 80 % of cases decided against the physician if the case goes to jury verdict [11]. Thus, most of these suits are settled. The best defense is (1) a complete examination performed in a systematic fashion, evaluating all appropriate structures; (2) appropriate and adequate image documentation; (3) appropriate and reasonable interpretation of the findings; and (4) ongoing continuing education for the interpreting physician.

Interpretation errors occur when the abnormality is perceived but is incorrectly described [9]. One example that is becoming a more frequent source of litigation is the misdiagnosis of an "ectopic pregnancy." In this instance an early intrauterine pregnancy, with no visualized gestational sac, and a corpus luteum is diagnosed as an ectopic pregnancy, with subsequent administration of methotrexate. A more common error is when a normal variant is called abnormal, such as a corpus luteum diagnosed as a malignancy. The converse is when a malignant lesion is called benign, such as a complex ovarian mass diagnosed as a benign lesion. These errors often occur due to lack of knowledge or faulty judgment of the interpreting physician. The best defense is available when the interpretation includes an appropriate differential diagnosis, particularly if it includes the correct diagnosis. As these cases are subject to interpretation, they tend to be more defensible, with 75 % won if the case goes to jury verdict [11].

Failing to suggest the next appropriate procedure places the interpreting physician at risk of litigation and liability. The prudent physician or radiologist should suggest the next appropriate study or procedure based upon the findings and clinical information. The recommended study should add meaningful information to clarify or confirm the diagnosis [12]. This is particularly apropos when performing and interpreting ultrasound studies referred from outside physicians. An example is when a study is consistent with a pregnancy of unknown location. The appropriate recommendation would be serial hCG levels and a repeat ultrasound as clinically indicated.

Failure to communicate significant abnormal findings on an ultrasound again places the interpreting physician at risk for liability. Two examples are the diagnosis of an ectopic pregnancy or an ovarian malignancy without prompt notification of the referring physician. These findings place the patient at significant risk and merely providing a written report is not adequate. Practices should have established protocols or guidelines for notifying referring physicians of sonographic results, particularly for those cases with critical findings. It is preferred that all studies have a final reading and report issued within 24 h of the original procedure. Following these protocols and guidelines provide the best defense for the physician [9].

New Horizons in Ultrasound Liability

First-Trimester Ultrasound

Identifying the early embryo and cardiac activity is an emotional event for patients. One should avoid the temptation to demonstrate the fetal heart rate with Doppler sonography as this exposes the early embryo to higher than ideal

energy. All ultrasound studies should be performed with the ALARA (as low as reasonably achievable) principle as the standard. This minimizes fetal exposure and the potential risk to the developing fetus.

Some physicians defer referral to an obstetrical or maternal-fetal medicine specialist until the early second trimester. This habit should be carefully scrutinized in light of advances in antenatal diagnosis. ACOG recommends antenatal screening for all patients prior to 20 weeks of gestation [13]. First-trimester screening with nuchal translucency, integrated and sequential testing in the first and second trimesters, and maternal blood screening for fetal cell-free DNA are all options for earlier detection of chromosomal abnormalities. However, counseling and appropriate referral are crucial to the effective use of these diagnostic modalities. In addition, there is increasing evidence that screening for anatomic abnormalities may be feasible in the first trimester. With this background, if one is not prepared to provide the necessary counseling and screening, it may be prudent to refer patients once cardiac activity is demonstrated, such that appropriate counseling and screening may be performed.

Healthcare Fraud

Increasing liability exists related to inappropriate billing for ultrasound-related procedures. Insurance fraud is assuming a greater role in liability in a physician's practice. In reproductive medicine, one must be cautious to avoid liability exposure for fraud. For example, infertility services may not be covered by a patient's insurance plan. In such cases, patients may request a change in the diagnostic codes to gain insurance coverage. Pursuing such action, when not clinically appropriate, exposes one to the claim of insurance fraud, with devastating consequences, ranging from monetary penalties (up to $11,000 per instance); exclusion from governmental payers, such as Medicare, Medicaid, and Tri-Care; closing of one's office; and even prison sentences. One must remind patients of these potential consequences and resist such actions.

Intent to commit fraud is not necessary to face litigation and liability. However, compliance programs can mitigate damages and penalties when in place and functioning. Guidance for even individual and small group practices has been provided by the Office of the Inspector General [14]. This includes the following recommendations:

1. *Conduct internal monitoring and auditing.* Audits should be conducted at least every 6 months with a representative set of patient charts.
2. *Implement compliance and practice standards*. Practice standards should be adopted and adhered to.
3. *Designate a compliance officer or contact*. It is recommended that the compliance officer should not be the same person responsible for coding and bill submission. An "independent" person is best suited to detect billing and coding irregularities.
4. *Conduct appropriate training and education*. The physicians and their staffs should receive ongoing education, with appropriate updates, to remain up-to-date on proper coding and billing practices.
5. *Respond appropriately to detected offenses and develop corrective action*. If inappropriate payments are detected, the practice should return these promptly. Further, education and actions to correct any detected irregularities are to be instituted upon discovery.
6. *Develop open lines of communication*. The physician should maintain an environment that encourages compliance, open communication, and transparency.
7. *Enforce disciplinary standards through well-publicized guidelines*. Discipline for intentional coding or billing irregularities should be established, published, and enforced.

Conclusion

This chapter has addressed several areas of potential liability related to ultrasound imaging in reproductive medicine. Discussed are strategies and practices that minimize liability exposure and risk. Unfortunately, the potential

for a liability action exists even if all of the recommendations are followed. However, a case is more defensible when these best practices are followed.

References

1. AIUM. Standards and guidelines for the accreditation of ultrasound practices. AIUM Ultrasound Practice Accreditation; December 17, 2010: http://www.aium.org/accreditation/accreditation.aspx. Accessed 11 July 2012.
2. AIUM, ASRM. AIUM practice guideline for ultrasonography in reproductive medicine. http://www.aium.org/accreditation/accreditation.aspx. 2009. Accessed 6 July 2012.
3. AIUM. AIUM practice guideline for the performance of sonohysterography. http://www.aium.org/accreditation/accreditation.aspx. 2007. Accessed 20 July 2012
4. AIUM. AIUM practice guideline for the performance of pelvic ultrasound examinations. http://www.aium.org/accreditation/accreditation.aspx. 2009. Accessed 19 July 2012.
5. AIUM. Guidelines for performance of a focused reproductive endocrinology and infertility scan. http://www.aium.org/resources/guidelines/reproductiveEndo.pdf. 2012. Accessed 4 June 2012.
6. CMS. Medicare requirements for physician supervision of sonographers. http://www.cms.gov/Medicare/Medicare-Fee-for-Service-Payment/PhysicianFeeSched/PFS-Relative-Value-Files.html. Accessed 12 Mar 2012.
7. Garner BA, editor. Black's law dictionary. 8th ed. St. Paul: West Group; 2004.
8. Sanders RC. Changing patterns in ultrasound-related litigation. J Ultrasound Med. 2003;22:1009–15.
9. Raskin MM. Liability of radiologists. Legal medicine. 6th ed. Philadelphia: Mosby; 2004. p. 456–60.
10. Berlin L, Hendrix R. Perceptual errors and negligence. Am J Roentgenol. 1998;170(4):863–7.
11. Berlin L. Malpractice issues in radiology: defending the "missed" radiographic diagnosis. Am J Roentgenol. 2001;176:317–32.
12. Montgomery v. South County Radiologists, Inc., 49 S.W.2s 191 (2001).
13. ACOG. Screening for fetal chromosomal abnormalities. ACOG Practice Bull. 2007;77(January):1–11.
14. Foley & Lardner. OIG issues final compliance program guidance for individual and small group physician practices. Milwaukee: Foley & Lardner; 2000.

Part II

Ultrasound in Infertility Workup

The Normal Ovary (Changes in the Menstrual Cycle)

5

Renato Bauman and Ursula Reš Muravec

The ovaries are two small, almond-shaped organs located on either side of the uterus, attached by the ovarian ligament to the uterine fundus by the suspensory ligaments to the pelvic side wall and by mesovarium to the broad ligament. Traditionally the ovaries can be visualized by transabdominal approach using the full bladder for better ultrasonographic visualization. With the full bladder, the intestines are pulled up and an acoustic window that allows the distinction of the female genital organs is created. The visualization can be compromised by the quantity of the abdominal fat tissue and/or abdominal scars. Ovaries are imaged as homogeneous, hypoechogenic ovoid structures with slightly echogenic central part.

Today the transvaginal approach is a golden standard for the estimation of the ovary. The closeness of the probe and the visualized organ allows the use of higher frequency probes that give better resolution and offer more detailed visualization.

R. Bauman, MD, PhD
Department of Gynecology and Obstetrics,
Sveti Duh Clinical Hospital, Sveti Duh 64,
Zagreb 10000, Croatia, Europe
e-mail: baumanrenato@gmail.com,
renato.bauman@zg.t-com.hr

U.Reš Muravec, MD Msc (✉)
Department for infertility, Medical Center Dravlje,
Ulica bratov Babnik 10, Ljubljana
1000, Slovenia, Europe
e-mail: ursula.res@gmail.com

Transabdominal Ultrasound

The ovaries can be displayed along with the uterine body in transverse plane if they are not too distant from the uterus. According to the position of the ovaries, that in normal circumstances can be variable, there is a real possibility that both ovaries could not be seen on the scan in the same time/image. In this situation in order to detect the second ovary, the examiner should move the probe cranially or caudally. If the ovary is located more cranially and near the pelvic wall, there is a realistic possibility that this ovary could be covered by the intestine and so it could not be visualized and examined. Same is the situation with small postmenopausal ovaries that due to the size often cannot be distinguished from the intestines.

Full bowel loops can be misdiagnosed as an ovary, but if the examiner is patient enough to wait the peristaltic wave, it will solve the problem; otherwise the examiner has to verify the position of the iliac vessels in order to longitudinally find the position of the ovary.

Transvaginal Ultrasound

Alfred Kratochwil is considered to be the father of transvaginal ultrasound. He described in 1969 his experience with the new endovaginal sonography technique using the probe attached to the colposcope [1]. Due to the low quality of the obtained images, the technique was abandoned until the mid-1980s when the first endovaginal

L.A. Stadtmauer, I. Tur-Kaspa (eds.), *Ultrasound Imaging in Reproductive Medicine*,
DOI 10.1007/978-1-4614-9182-8_5,

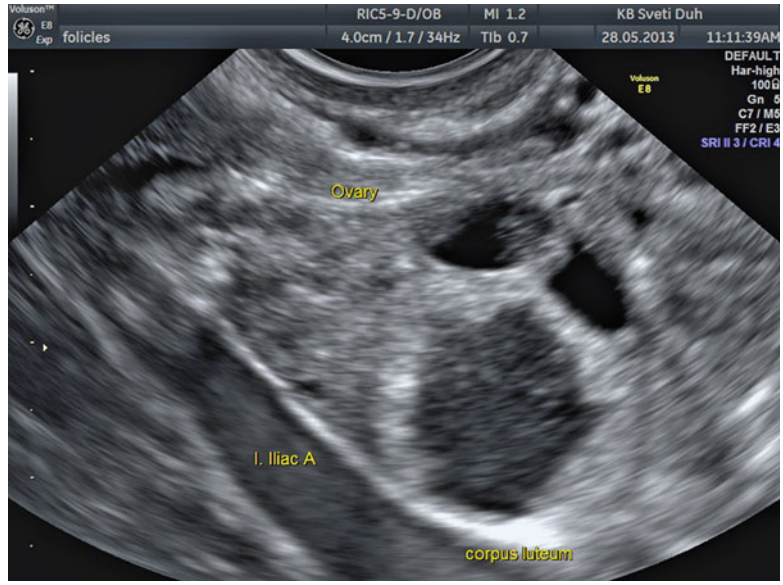

Fig. 5.1 Transvaginal image of ovary with the corpus luteum, note the iliac vessels

probe with the visible angle of 240° that allowed panoramic view of the genital organs was put in market. The first meeting about endovaginal ultrasound was organized in Hamburg, Germany, in 1985 by L. Popp [2]. First accepted with skepticism, the new technique was quickly adopted in the majority of sonography centers, first in Germany and then all over the world. Because of the numerous advantages in pelvic sonography, the endovaginal technique today is essential for quality examination of the female pelvis.

Ovaries can be visualized with the probe moved laterally of the uterus towards the pelvic wall in the longitudinal or sagittal section. Ovaries have ellipsoid shape, with relatively hypoechogenic structure and homogenic echotexture, and often are positioned near the iliac blood vessels (Fig. 5.1). Using probes with the wide angle of insonation, it is possible to visualize in the same frontal section of both ovaries if they are positioned in the same plane. Regularly each ovary is visualized separately. In order to compare the ovaries, it is useful to divide the image in two parts and then visualize both ovaries (Fig 5.2.).

In fertile women ovaries are usually easily visualized because they are relatively big and have follicles and/or corpus luteum, structures that are easy to recognize using transvaginal ultrasound. The average size of the ovaries in premenopausal women is 3.5 × 2.5 × 1.5 cm (length × height × width) and in postmenopausal women is 2.0 × 1.5 × 1.0 cm. In order to measure, it is important to visualize the ovary in the frontal and sagittal plane. Three dimensions could be obtained, and the volume can be calculated using the ellipsoid formula (V = 4/3 × 3.14 × (D1/2 × D2/2 × D3/2)) [3] or the simplified ellipsoid formula (V = 1/2 × length × height × width). Difficulties in the visualization of normal ovaries can be caused by extreme cranial position of the ovary or in case of severe adhesions in the pelvis.

Postmenopausal Ovaries

Ovarian volume and diameter decrease with age, consequently making postmenopausal ovaries appear small hypoechoic structures. The absence of follicles results in difficult sonographic visualization and often may not be detected. Premenopausal ovaries can be visualized in 96 % and postmenopausal in 62–65 % of cases [3, 4].

Premenarchal Ovaries

Before, sexarche ovaries can be visualized by transabdominal ultrasound using the full bladder technique or by transrectal approach using the transvaginal probe. The images obtained transrectally are quite similar to those obtained

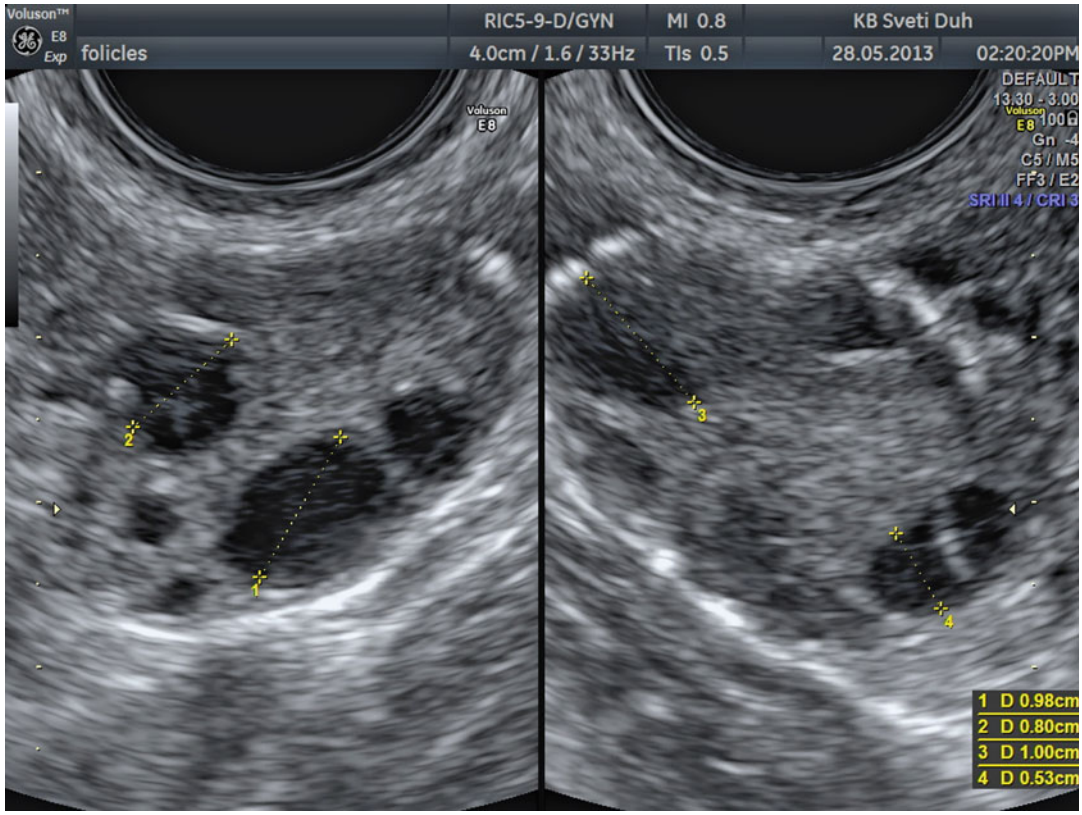

Fig 5.2 Transvaginal image of both ovaries in early first phase

transvaginally. In children before 5 years of age, ovaries have a volume of less than 1 cm. Before puberty ovaries are small hypoechoic structures that measure less than 2 cm in diameter. Few years before menarche small anechoic structures with sharp borders measuring 5–9 mm can be visualized, indicating the start of folliculogenesis.

In the years of adolescence, until the hypothalamus-hypophysis-ovary axis is not fully mature, ovaries are visualized with the variety of growing follicles of different sizes. Anovulation is common, and these large ovaries with a lot of follicles can often be misdiagnosed as polycystic ovaries.

Reproductive Age Ovaries

Changes in the morphological appearance of the ovary which can be detected by ultrasound come due to rhythmic changes in the secretion of female hormones FSH and LH. Ovaries pass through the menstrual cycle, in which we distinguish follicular phase, ovulation, and luteal phase. Ultrasound provides insight into the psychological changes during the ovarian cycle and allows accurate and reproducible investigations of follicular size, development, and growth during the follicular phase [5].

Newborn girl has two million follicles and before puberty 300,000 follicles are still present. For their development gonadotropins are not required. Since the mid-fetal life until menopause, there is a permanent reduction in the number of follicles, and only 400 (100–1,000) follicles will achieve preovulatory maturation and ovulate until menopause.

The majority of primordial of follicles will go through the process of atresia.

In the first 5 days of the cycle, FSH levels are high in order to stimulate the development of a primary follicle in the ovary. A primary follicle measures 40 μm; it has one layer of granulosa cells and an oocyte. By further growth and multiplication

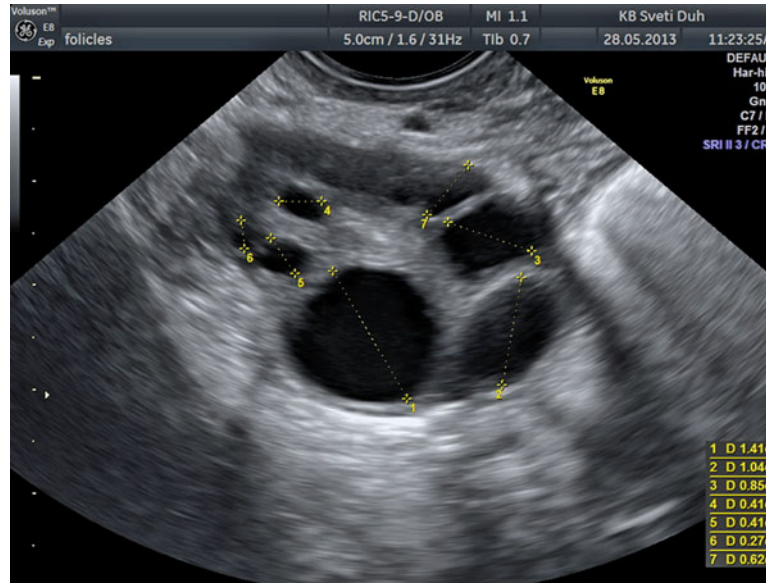

Fig 5.3 Transvaginal image of a normal ovary in the first phase, note the dominant follicle

of cells, a preantral follicle is developed. Preantral follicle has a diameter of only 150 μm, and it is not detectable by ultrasound.

Between fifth and seventh day of the cycle, secondary antral follicles can be detected and are presented as anechoic spheroid zones inside the ovary, approximately 2–3 mm in diameter. These are the first follicular structures that may be visualized by common ultrasound devices [5].

With further selection one dominant follicle is being elected while other follicles go into atresia. The dominant follicle can be detected between 8th and 12th day of the cycle when its size and growing pattern are clearly superior to other visualized follicles (Fig. 5.3). The remaining follicles can continue with their growth but just up to 14 mm in diameter. In up to 10 % of maturely menstrual cycles, sonography can detect two dominant follicles [6].

The diameter is measured from one internal follicle wall to the other if the follicle is roundly shaped. If we are measuring an oval follicle, we have to measure three distances (the longest, the shortest, and the oblique) and then calculate the median: $DF = (D1 + D2 + D3)/3$.

The dominant follicle has a linear daily diameter growth of 2–3 mm per day, and at the moment of ovulation, the diameter of the dominant follicle is 18–27 mm [7].

This variety at the time of ovulation limits the use of follicle diameter for ovulation prediction.

In order to predict ovulation serial follicle, measurements have to be done in more than two menstrual cycles in each patient. In the majority of patients, a uniform pattern of morphologic sonographic changes prior to ovulation can be established, and the knowledge of follicle diameter and endometrial thickness and shape can help in infertility procedures during the natural cycle. Unfortunately not all patients have a uniform pattern and ovulate with different sizes of dominant follicles.

Besides follicle diameter other sonographically visualized morphologic changes could help in the detection of ovulation. In more than 20 % of follicles >18 mm, a cumulus oophorus can be visualized and is seen as a small anechoic part in the lumen of the dominant follicle that presents the detachment of granulosa cells containing the oocyte.

Twenty-four hours before the ovulation, a hypoechogenic line surrounding the preovulatory follicle can be visualized; it presents the separation of theca cells from internal granulosa cells. The theca cells are at that time hypervascularized and edematous, and these changes can be even better visualized using color Doppler (Fig. 5.4).

Before ovulation the internal wall of the preovulatory follicle can be slightly hyperechoic

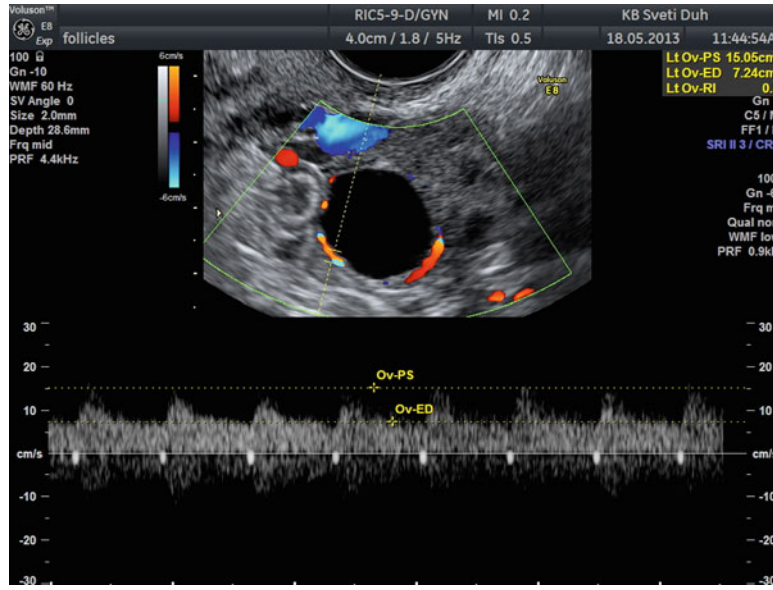

Fig 5.4 Transvaginal color Doppler image of perifollicular vascularization of preovulatory follicle

with irregular internal borders. It is important to always check the endometrium because its thickness and shape correlates with the serum estradiol level and endometrial findings can help in predicting the ovulation.

The key sonographic markers of ovulation are disappearance of or sudden decrease in follicle size (the most frequent sign of ovulation with the sensitivity of 84 %), appearance of ultrasonic echoes in the follicle, irregularity of follicle wall and free fluid in the pouch of Douglas (in 77 % of cases on the day of ovulation) [5, 8], and secretory changes of the endometrium.

After the ovulation the follicle is transformed in corpus hemorrhagicum with internal echoes. The corpus luteum is afterwards created with the vascularization and luteinization of granulosa cells. Sonographic appearance can be variable in size and shape [9]. The size is generally reduced and is visualized as a structure with thick hyperechogenic walls enclosing the hypoechoic center (Fig. 5.1). It is well known that corpus luteum can also look like many pathologic changes of the ovary (endometriosis, cystic teratoma, and other benign or even malignant tumors), and sometimes it is absolutely necessary to perform an ultrasound examination after the menstruation in order to differentiate the possible pathology.

The corpus luteum vanishes before the start of next menstrual cycle, and the presence of corpus luteum 12 or more days after ovulation can be a first sign of pregnancy.

Color Doppler of the Normal Ovary

Transvaginal color Doppler (TVCD) plays an important role in better understanding the physiology of the menstrual cycle. This technique was intensively studied in the beginning of the 1990s, and many studies proved the usefulness in detection of vascular changes in the uterus and the ovary [10–15].

The blood supply of the ovary has two sources: ovarian artery and the ovarian branch of the uterine artery that anastomoses and forms an arch in the ovarian hilus. Color Doppler signals of the uterine artery can be found on the lateral border of the ovary. The impedance indices found in the ovarian artery correlate with the menopausal status. Before menarche and after menopause, the ovarian artery is difficult to visualize because the ovaries are very poorly vascularized at that time. The resistance to blood flow is high and so are the flow indices (RI = resistance index, PI = pulsatility index). During the reproductive age, there is a difference in vascularization depending on which

ovary is the dominant follicle growing and where the resistance to blood flow is lower in comparison to the non-dominant side. It is absolutely logic that a growing follicle or the corpus luteum needs more vascularization, and so we register lower flow indices. As ovarian arteries are not easy to find, in order to perform objective measurements in practice, we estimate the intraovarian blood flow that changes during the age and the cycle. Before puberty and after menopause, blood flow should not be detected in the ovaries using color Doppler. Any positive vascularization in that time of life in the ovaries has to raise suspicion about possible pathology of the vascularized ovary [11, 12].

TVCD in Preovulatory Phase

Perifollicular blood flow can be detected when a dominant follicle has a diameter of >10 mm. Few days prior to ovulation, the RI is around 0.54 ± 0.04. Two days before ovulation, the RI starts to decline while at ovulation the RI is 0.44 ± 0.04. The flow velocity is increasing as the RI gets lower, and even if the RI is not changing, the peak systolic velocity rises on the onset of ovulation. Angiogenesis and dilatation of newly formed vessels between the theca and granulosa layer and changes in the follicular wall could be necessary for follicular rupture [13]. In case of luteinized unruptured follicle, a failure of blood velocity to peak in the preovulatory period is observed that proves that adequate vascularization is necessary for achieving ovulation [14].

The vascularization in the polycystic ovaries is detected in the hyperechoic stroma, and waveforms showed mean RI = 0.54 but without cyclic changes caused by hormonal steady state (anovulation). There are also no changes in the Doppler indices in the uterine artery that are usually found in regular menstrual cycles. The vascularization of the uterus and the ovary is hormonally dependent, and Doppler measurements reflect cyclic hormonal changes in the female genital organs.

The perifollicular vascularity is a constant challenge for clinicians and researchers. It is known that it correlates well with the level of follicular oxygenation. Oocytes from severe hypoxic follicles are associated with high frequency of abnormalities in the organization of the chromosomes. Color Doppler analysis of perifollicular blood may provide an indirect sign of the developmental competence of the oocyte [15]. In the stimulated cycles there is a correlation of higher peak systolic velocity (PSV > 10 cm/s) in follicles with subsequent fertilized oocytes [16]. However, in the natural cycles Doppler indices of perifollicular blood flow as predictors of oocyte quality are still of limited value [17]. Three-dimensional reconstruction of power Doppler perifollicular vascular network could be a better predictor for oocyte competence in natural cycles [18, 19].

TVCD is very reliable in confirming ovulation. A marked drop in blood flow indices and rise of blood flow velocities in the early luteal phase are signs of prominent vascularization and corpus luteum formation. Color Doppler findings added to ovarian morphology changes mentioned above accurately confirm ovulation.

TVCD and the Corpus Luteum

The formation of the corpus luteum is a key event in the reproductive life and also plays an important role in early pregnancy support. Immediately after ovulation blood vessels of the theca layer invade the cavity of the ruptured follicle (Fig. 5.5). There is a dramatic increase of the amount of blood flow with increased velocity and low impedance to blood flow. The RI is low (0.43 ± 0.04), remains at the same level for 4–5 days, and then gradually rises to a level of 0.49 ± 0.04, which is still lower than in the follicular phase (Fig. 5.6).

If the pregnancy is achieved, corpus luteum has prominent blood flow with low Doppler indices (RI = 0.45 ± 0.04) and similar vascularization is detected during the 1st trimester. In cases of threatened abortion (p<0,01), missed abortion (p<0,01), and incomplete abortion (p<0,01), the resistance and pulsatility indices are significantly higher than in the normal pregnancy. There is a correlation between vascularization indices of the corpus luteum and hormonal levels of HCG, estradiol, and progesterone.

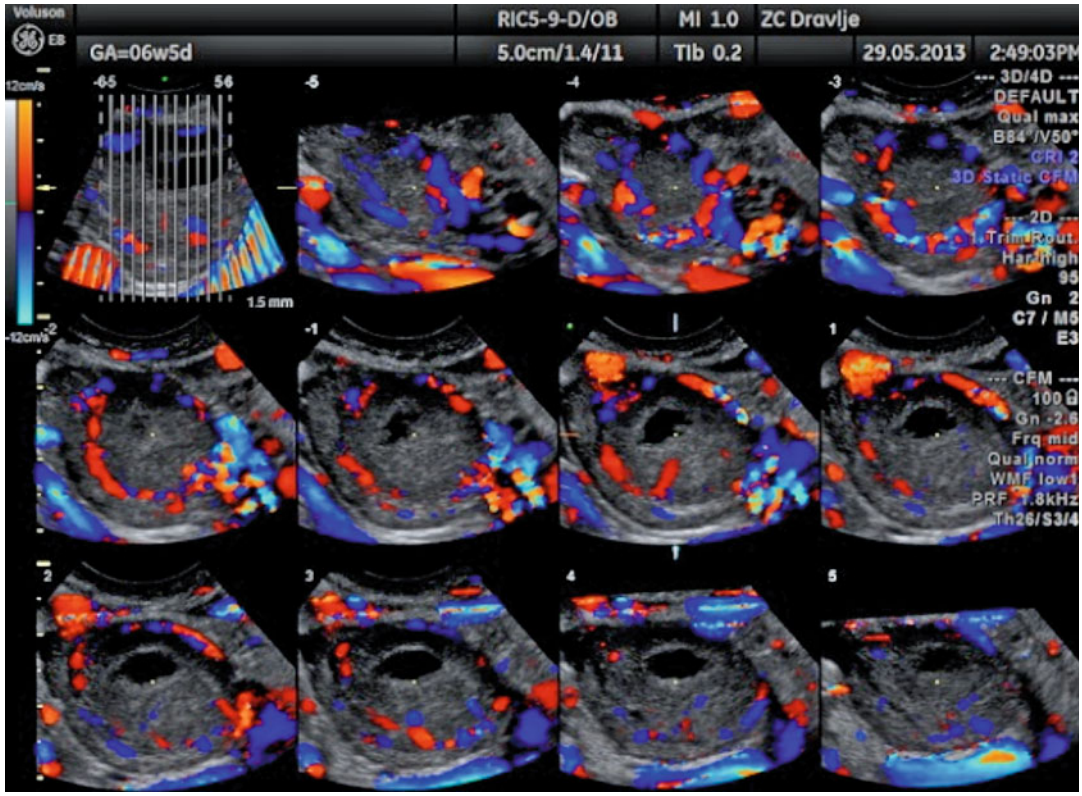

Fig. 5.5 Color Doppler image of vascularization of the corpus luteum

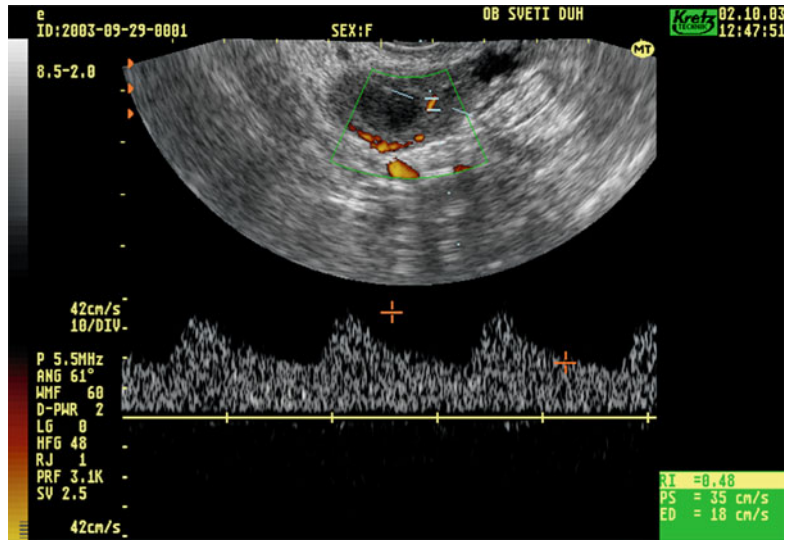

Fig. 5.6 Transvaginal color Doppler image of corpus luteum blood flow

After the 23rd day of cycle, if there is no pregnancy, the corpus luteum starts its regression. The color flow signals are poor, and the Doppler indices are getting higher until menstruation and the start of the new cycle. At that time there is no color flow detected in the ovary.

Luteal phase defect could be assessed noninvasively by transvaginal color Doppler measurements of the blood flow in the corpus luteum. The mean RI in the defect luteal phase is significantly higher (RI = 0.56 ± 0.04; $p < 0{,}001$) compared to controls [20].

Three-Dimensional Ultrasound Visualization of the Normal Ovary

Volume of the Ovary

With the three-dimensional ultrasound (3D US), the image of the ovary could be obtained in all three dimensions. Storage capacities, reconstruction of the volume images, and simultaneous viewing of all three orthogonal planes are the main advantages of this method.

The volume of the ovary can be calculated using the simplified ellipsoid [3] formula (V = 1/2 × length × height × width) or sonographic formula (ovary = length × height × width × 0.5236).

Volume of the ovary can be measured even more precisely with semiautomatic VOCAL (virtual organ computer-aided analysis) technique (Fig. 5.7). VOCAL is a 3D software technology (General Electrics Healthcare, Kretz, Austria) program where the ovary is rotated around one axis from 6 to 30 times (every 30°, 15°, 9°, or 6° rotation angles), and in every step it is required to outline the ovarian borders. If the 30° step is chosen, the ovary is rotated six times. The software estimates the volume from these six planes of the ovary.

The ovarian volume in the reproductive age of the women inversely correlates with age, and a statistically significant decrease in ovarian volume starts at 30 years of age [21, 22].

It is reported that average volume of the ovary by the age of 1 year is 0.26 cm^3 measured by transabdominal probe and increases steadily to an average of 1 cm^3 by 13 years of age [23]. The mean ovarian volume in nulliparous women in reproductive age is 7.8 cm^3 (2.6 SD), and it decreases to 3.4 cm^3 (1.3 SD) in the first 5 years of menopause. After 5 years of menopause, it shrinks to mean volume of 2.5 cm^3 (1.3 SD), and later in menopause it can become undetectable [3].

Measurement of ovarian volume to predict ovarian reserve and responsiveness is limited and it is useful only at the extremes of reproductive live. The novel ultrasound markers for the ovarian reserve, such as AFC (antral follicle count), AMH, and age, predict the responsiveness to gonadotropins much better [24, 25].

Antral Follicle Count (AFC)

AFC is one of the markers of the ovarian reserve. Together with the AMH and age, it is considered as the best marker for ovarian reserve [26]. AFC is used to predict the response to the gonadotropin stimulation during assisted reproductive technology treatment.

AFC informs the clinician about quantitative and not the qualitative ovarian reserve. AFC correlates well with the number of oocytes retrieved after gonadotropin stimulation and not so good with the pregnancy results [26].

With advanced reproductive age AFC decreases [27–31]. AFC declines progressively over the time, with annual losses of 0.35–0.95 antral follicles per year [27, 31, 32]. The age-related nomograms in infertile women for the 3rd, 10th, 25th, 50th, 75th, 90th, and 97th percentiles for AMH and AFC were produced [31].

There is intra-cycle and inter-cycle variability, variability in the clinical definitions, and technical methods used to count and measure the volume of antral follicles. The practical recommendations for better standardization came out in 2010 [31]. It is recommended to count the cohort of 2–10 mm follicles between day 2 and 4 of menstrual cycle [31].

The technique used for AFC can be as follows:

- 2D scrolling through each ovary (manual counting of all antral follicles in the scroll)
- 2D counting of the antral follicles in one plane
- 3D SonoAVC (sonography-based automated volume count) (Fig. 5.8)

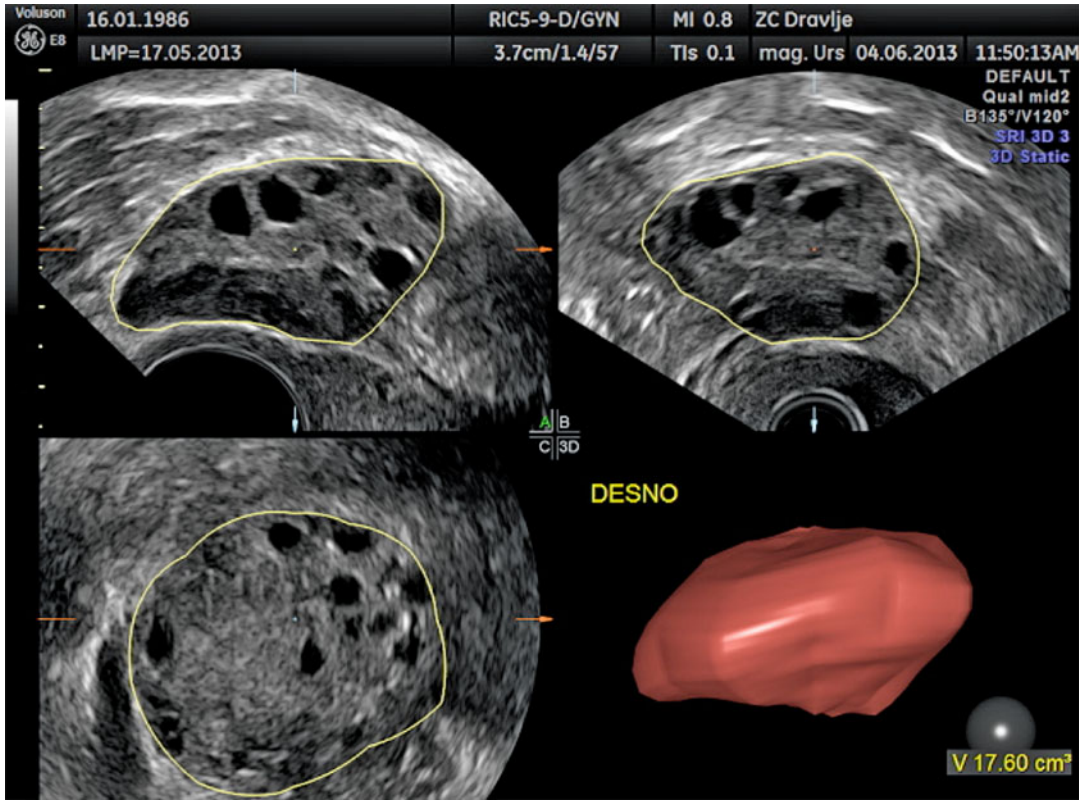

Fig. 5.7 3D volume measurement of the ovary with VOCAL

SonoAVC (General Electrics Healthcare, Kretz, Austria) is a novel ultrasound technique which can be used for the ultrasonographically hypoechogenic structures, such as the follicles. SonoAVC identifies hypoechogenic structures and their approximate shape in the selected 3D matrix and explorate the volume. It automatically recognizes the follicular borders in 3D and does a follicle volume assessment for each follicle in a selected volume box. The numbers and volumes of antral follicles are reported.

3D of the Dominant Follicle, Ovulation, and Formation of Corpus Luteum

The majority of small growing follicles are round and can be easily measured by 2D US, either with one, two, or three perpendicular diameters. The dominant follicle usually changes the shape from round to oval before the ovulation. More precise measurement can be made with 3D ultrasound comparing to 2D US measurements. 3D measurement of the dominant follicle can be obtained in three ways: first, classical with x, y, and z diameters as described before; second, with semimanual technique VOCAL described before; and third by automated technique SonoAVC (Fig. 5.9).

The measurements of VOCAL, SonoAVC, and actual volume of dominant follicle were comparable – the median actual volume of dominant follicle on the day of aspiration was 3.6 ml, with ranges from 2.9 to 8.0 ml [33]. SonoAVC is considered as a rapid and simple technique, with a good reproducibility and reliability [33].

On the basis of the dominant follicle volume measured with SonoAVC method, new criteria for timing hCG administration or planning the oocyte retrieval can be established [34]. Follicles with the measured volume ≥ 0.6 cm^3 on the day

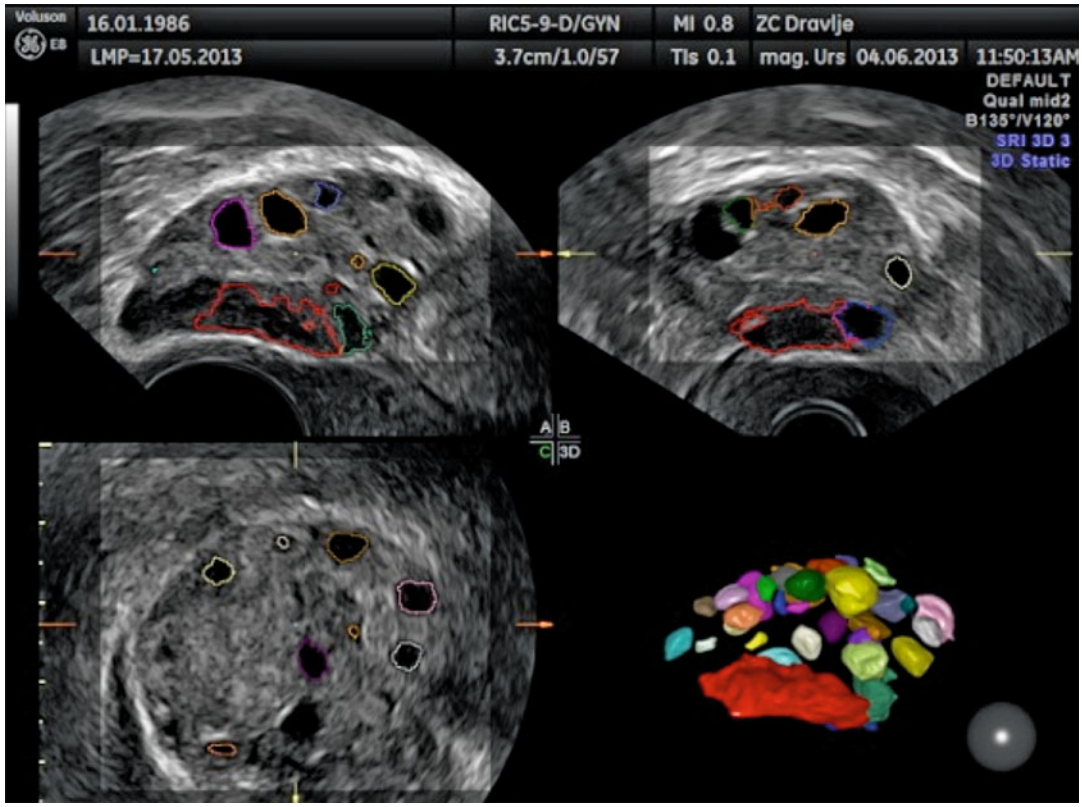

Fig. 5.8 Antral follicle count (AFC) measured by 3D US SonoAVC

of hCG administration are associated with the finding of mature oocytes at the time of egg retrieval [34].

Additionally with 3D US a cumulus oophorus can be visualized with the surface view, much better than with conventional 2D US (Fig. 5.10).

After ovulation the morphological changes in ruptured follicle can be even better observed with 3D US than with classical 2D ultrasound: decrease in follicle size can be measured with VOCAL or SonoAVC, appearance of ultrasonic echoes and irregularity of the follicular walls can be seen on 3D slices of the ruptured follicle, and volume of the free fluid in the cul-de-sac can be measured with SonoAVC. Currently there is not enough data that 3D US following of the natural cycle is superior to conventional 2D US.

3D Power Doppler of the Preovulatory Follicle and Corpus Luteum

As it is well known from 2D color Doppler US scanning, the vascularization in the ovary changes during the menstrual cycle. With the 2D US the vascular indices (RI, PI) are measured just in one vessel selected very subjectively. 3D US vascularization gives schematical information about all vessels (sonographic angiogram) and additionally quantifying blood flow in the selected volume. 3D vascular indices can be measured: vascular index (VI), flow index (FI), and VFI (vascular flow index).

The vascularization index (VI) gives information in percent [%] about the amount of color values (vessels) in that volume of interest. The VI is calculated by dividing the figure of color values by

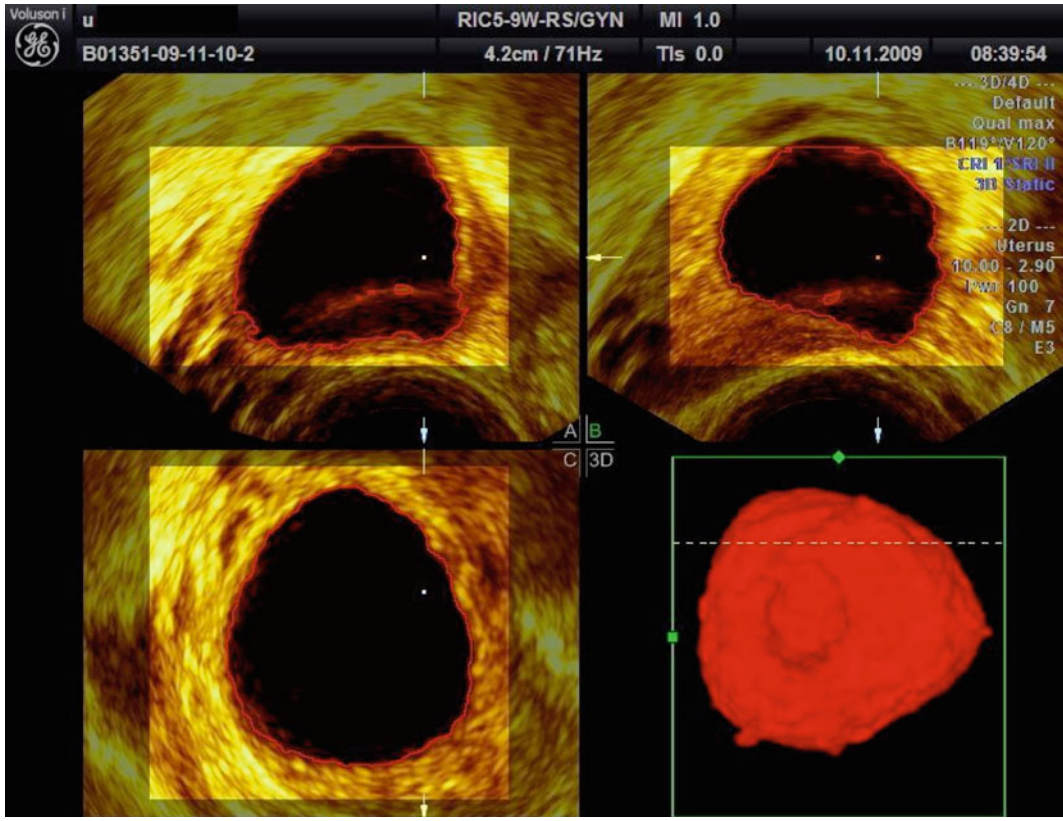

Fig. 5.9 3D measurement of the dominant follicle with SonoAVC

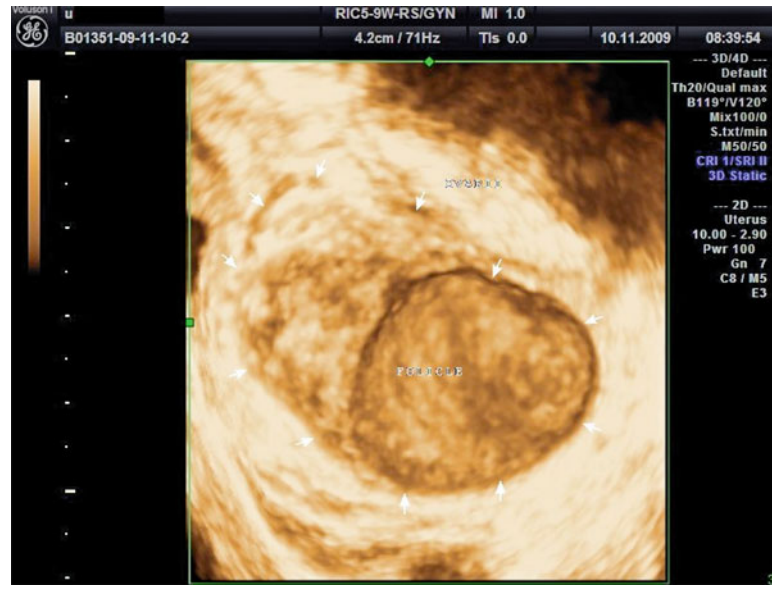

Fig. 5.10 3D surface view of the dominant follicle and cumulus oophorus (darker), with arrows is marked the whole ovary

the figure of total voxels minus the background voxels. Flow index (FI) measures the mean blood flow intensity. The figure ranges from 0 to 100. FI is calculated as the ratio of weighted color values (weighted by their amplitudes) to the number of the color values. The vascularization-flow index (VFI) gives combined information of vascularization and mean blood flow intensity. The figure of the VFI is also dimensionless and ranges from 0 to 100. It is calculated by dividing the weighted color values (weighted by their amplitudes) by the total voxels minus the background voxels.

3D vascular indices can be measured in the selected volume (ovary, dominant follicle, corpus luteum) in different phases of the menstrual cycle. In the follicular phase, the vascularization around the dominant follicle increases, the sonographic angiogram of the dominant follicle shows the angioarchitecture in the whole dominant follicle, as shown schematically with the color Doppler (Fig. 5.11). During the normal menstrual cycle, typical changes in vascular indices were noted [35–37]. Vascular indices (VI, FI, VFI) slowly increase during follicular phase in dominant follicle [35, 36]. In the late follicular phase, there is a short vascular depression in all indices. After ovulation very important vascular changes take place in the ruptured follicle. There is an increase vessel formation and blood supply and increase in velocities are noted. In a ruptured follicle (Fig. 5.12) increase in vascular index (VI), flow index (FI), and VFI (vascular flow index)

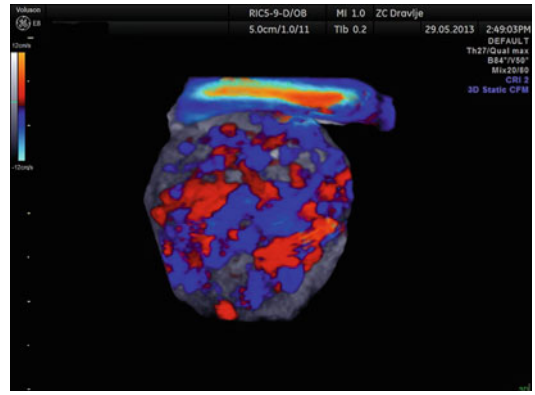

Fig 5.11 3D color Doppler vascularization of dominant follicle before ovulation

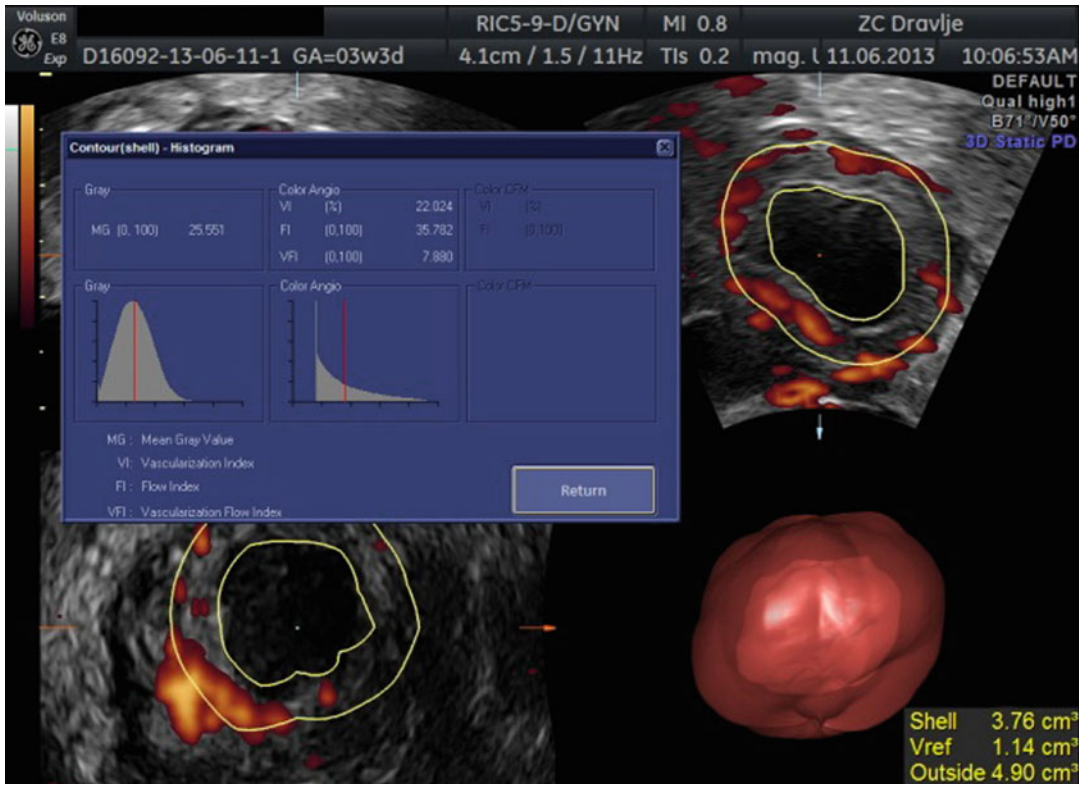

Fig. 5.12 3D vascularization of the corpus luteum with VI, FI, and VFI index

can be noted in the first 7 days after ovulation [35–37]. VFI in corpus luteum 7 days after ovulation is on average 3.1 times higher than 1 day before the ovulation [35]. In the late luteal phase, the indices do not change significantly [35, 36].

The 3D sonographic angiogram is very useful because it is relatively easy to obtain and it gives a good impression on whole vascularization in selected volume. 3D vascularization indices are currently used mostly for research purposes, and broad clinical use is still limited due to technical problems, need for good equipment, and experience of the clinicians.

References

1. Kratochwill A. Ein neues vaginales Schnittbildverfahren. Geburtshilfe Frauenheilkd. 1969;29:379–85.
2. Popp LW. Gynaekologische Endosonographie. Quickborn: Klemke; 1986.
3. Merz E, Miric-Tesanic D, Weber G, Bahlmann F. Sonographic size of the uterus and ovaries in pre- and postmenopausal women. Ultrasound Obstet Gynecol. 1996;7:1–5.
4. Sladkevicius P, Valentin L, Marsal K. Transvaginal grey-scale and Doppler ultrasound examinations of the uterus and ovaries in healthy postmenopausal women. Ultrasound Obstet Gynecol. 1995;6:81–90.
5. Vlaisavljevic V. Echographic evidence of follicle development and maturation. Donald Sch J Ultrasound Obstet Gynecol. 2011;5(3):267–72.
6. Picker RH, Smith DH, Tucker MH, Saunders DM. Ultrasonic signs of imminent ovulation. J Clin Ultrasound. 1983;11:1–2.
7. Matijevic R, Grgic O. Predictive values of ultrasound monitoring of the menstrual cycle. Curr Opin Obstet Gynecol. 2005;17:405–10.
8. Jarvela IY, Sladkevicius P, Kelly S, Ojha K, Nargund G, Campbell S. Three dimensional sonographic and Power Doppler characterization of ovaries in late follicular phase. Ultrasound Obstet Gynecol. 2003;22(5):520–6.
9. Deichert U, Daume E. Zyklische Veranderungen am Ovar. In: Deichert U, Ducla V, Schlief R, editors. Funktionelle Sonographie in Gynakologie und Reproduktionsmedizin. Berlin: Springer; 1993. p. 71–132.
10. Collins WP, Jurkovic D, Waterstone J, Campbell S. Ovarian morphology, endocrine function and intrafollicular blood flow during periovulatory period. Hum Reprod. 1991;6:319–24.
11. Kurjak A, Schulman H, Sosic A, Zalud I, Shalan H. Transvaginal ultrasound, color flow and Doppler waveform of the postmenopausal adnexal mass. Obstet Gynecol. 1992;80:917–21.
12. Kurjak A, Kupesic S. Ovarian senescence and its significance on uterine and ovarian perfusion. Fertil Steril. 1995;64:532–7.
13. Bourne T, Jurkovic D, Waterstone J, Campbell S, Collins WP. Intrafollicular blood flow during human ovulation. Ultrasound Obstet Gynecol. 1991;1:53–9.
14. Kupesic S, Kurjak A. Uterine and ovarian perfusion during the periovulatory period assessed by transvaginal color Doppler. Fertil Steril. 1993;3:439–43.
15. Van Blerkom J, Antczak M, Schrader R. The developmental potential of the human oocyte is related to the dissolved oxygen content of follicular fluid: association with vascular endothelial growth factor levels and perifollicular blood flow characteristics. Hum Reprod. 1997;12:1047–55.
16. Nargund G, Doyle PE, Bourne TH, Parsons JH, Cheng WC, Campbell S, et al. Ultrasound derived indices of follicular blood flow before hCG administration and the prediction of oocyte recovery and preimplantation embryo quality. Hum Reprod. 1996;11:2512–7.
17. Lovrec VG, Vlaisavljevic V, Reljic M. Dependence of the in-vitro fertilization capacity of the oocyte on perifollicular flow in the preovulatory period of unstimulated cycles. Wien Klin Wochenschr. 2001;113 Suppl 3:21–6.
18. Vlaisavljevic V, Reljic M, Lovrec VG, Zazula D, Sergent N. Measurement of perifollicular blood flow of the dominant preovulatory follicle using three-dimensional power Doppler. Ultrasound Obstet Gynecol. 2003;22:520–6.
19. Vlaisavljevic V, Borko E, Radakovic B, Zazula D, Dosen M. Changes in perifollicular vascularity after administration oh human chorionic gonadotropin measured by quantitative three-dimensional power Doppler ultrasound. Wien Klin Wochenschr. 2010;122 Suppl 2:85–90.
20. Kupesic S, Kurjak A, Vujisic S, Petrovic M. Luteal phase defect: comparison between Doppler velocimetry, histological and hormonal markers. Ultrasound Obstet Gynecol. 1997;9:105–12.
21. Pavlik EJ, DePriest PD, Gallion HH, Ueland FR, Reedy MB, Kryscio RJ, et al. Ovarian volume related to age. Gynecol Oncol. 2000;77:410–2.
22. Kupesic S, Kurjak A, Bjelos D, Vujisic S. Three-dimensional ultrasonographic ovarian measurements and in vitro fertilization outcome are related to age. Fertil Steril. 2003;79:190–7.
23. Bernaschek G, Lubec G, Schaller A. Sonographische Untersushungen uber das Wachstum von Uterus und Ovarien zwischen dem 1.-14. Lebensjahr. Geburtshilfe Frauenheilkd. 1984;44:727–30.
24. Jayaprakasan K, Campbell B, Hopkisson J, Johnson I, Reine-Fenning N. A prospective, comparative analysis of anti-Mullerian hormone, inhibin-B, and three-dimensional ultrasound determinants of ovarian reserve in the prediction of poor response to control ovarian stimulation. Fertil Steril. 2010;3:855–64.
25. Henriks DJ, Kwee WS, Mol BW, te Velde ER, Broekmans FJ. Ultrasonography as a tool for the

prediction of outcome in IVF patients: a comparative meta-analysis of ovarian volume and antral follicle count. Fertil Steril. 2007;87:764–75.
26. Broekmans F, de Zieger D, Howles C, Gougeon A, Trew G, Olivennes F. The antral follicle count: practical recommendations for better standardization. Fertil Steril. 2010;94(3):1044–51.
27. Ruess ML, Kline J, Santos R, Levin B, Timor-Tritsch I. Age and the ovarian follicle pool assessed with transvaginal ultrasonography. Am J Obstet Gynecol. 1996;174:624–7.
28. Scheffer GJ, Broekmans FJ, Looman CW, Blankenstein M, Fauser BCJM, de Jong FH, et al. The number of antral follicles in normal women with proven fertility is the best reflection of the reproductive age. Hum Reprod. 2003;18: 700–6.
29. Chang MW, Chiang CH, Hsieh TT, Soong YK, Hsu KH. Use of antral follicle count to predict the outcome of assisted reproductive technologies. Fertil Steril. 1998;69:505–10.
30. Kline J, Kinney A, Kelly A, Reuss ML, Levin B. Prediction of antral follicle count during reproductive years. Hum Reprod. 2005;20:2179–89.
31. Almog B, Shehata F, Suissa S, Holzer H, Shalom-Paz E, La Marca A. Age-related nomograms of serum antimullerian hormone levels in a population of infertile women: a multicenter study. Fertil Steril. 2011;7: 2359–63.
32. Ng EH, Yeung WS, Fong DY, Ho PC. Effects of age on hormonal and ultrasound markers of ovarian reserve in Chinese women with proven fertility. Hum Reprod. 2003;18:2169–74.
33. Salama S, Arbo E, Lamazou F, Levaillant JM, Frydman R, Fanchin R. Reproducibility and reliability of automated volumetric measurement of single preovulatory follicles using SonoAVC. Fertil Steril. 2010;93:2069–73.
34. Rodriguez-Fuentes A, Hernandez J, Garcia-Guzman R, Chinea E, Iaconianni L, Palumbo A. Prospective evaluation of automated follicle monitoring in 58 in vitro fertilization cycles: follicular volume as a indicator of oocyte maturity. Fertil Steril. 2010;93:616–20.
35. Jokubkiene L, Sladkevicius P, Rovas L, Valentin L. Assessment of changes in volume and vascularity of the ovaries during the normal menstrual cycle using three-dimensional power Doppler ultrasound. Hum Reprod. 2006;10:2661–8.
36. Hope JM, Long K, Kudla M, Arslan A, Tsymbal T, Strok I, et al. Three-dimensional power Doppler angiography of cyclic ovarian blood flow. J Ultrasound Med. 2009;8:1043–52.
37. Engels V, Sanfrutos L, Perey-Medina T, Alvarez P, Zapardiel I, Godoy-Tunidor S, et al. Periovulation follicular volume and vascularization determined by 3D and power Doppler sonography as pregnancy predictors in intrauterine insemination cycles. J Clin Ultrasound. 2011;5:243–7.

Ovarian Reserve and Ovarian Cysts

6

Laurel A. Stadtmauer, Alessandra Kovac,
and Ilan Tur-Kaspa

Introduction

Ultrasound has become the most widely used and important tool in the diagnosis and treatment of infertility and IVF. Measuring the antral follicle count (AFC) is one of the best predictors for estimating ovarian reserve. This initial ultrasound exam will immediately affect the management of the patient and help determine IVF stimulation protocols. The initial exam also picks up benign and malignant ovarian masses and the most common cysts are covered in the chapter. Doppler modalities of ultrasound allow identification of the direction and magnitude of blood flow and calculation of velocity and can help distinguish benign from malignant masses. Three-dimensional (3D) transvaginal ultrasound (TVS) techniques allow the identification and quantification of hypoechoic regions within a three-dimensional ultrasound (3D) data set and provide a precise estimation of their absolute dimensions, mean diameters, and volumes. Accurate evaluation of size and volume of complex structured follicles is facilitated. This chapter is aimed to review how ultrasound is used to maximize ART outcome by evaluation of the ovary and assessing ovarian reserve.

Definition of Ovarian Reserve

Ovarian reserve is a term that reflects the number of oocytes that are available for procreation. There are biochemical and morphological markers which will be discussed in this chapter. The most common ultrasound morphological markers are antral follicle counts in 2 or 3 dimensions, ovarian volume, and ovarian blood flow to the stroma.

The ovaries contain several subtypes of follicles: the primordial follicles (≤0.05 mm diameter), primary follicles, secondary follicles, preantral follicles, and antral follicles (>2 mm diameter). Primordial follicles consist of the oocyte with a thin layer of granulosa and stromal cells which cannot be seen on ultrasound. The gonadotropin-dependent stage (antral follicles) can be visualized on ultrasound as small cysts. As a follicle grows, it develops follicular fluid which can be seen by ultrasound. Antral follicles are visible and measure from 2 to 10 mm and represent the pool of follicles recruited in the

L.A. Stadtmauer, MD, PhD (✉)
Department of Obstetrics and Gynecology,
Eastern Virginia Medical School, Jones Institute
for Reproductive Medicine, 601 Colley Avenue,
Norfolk, VA 23507, USA
e-mail: stadtmla@evms.edu

A. Kovac
College of Arts and Sciences, University of Virginia,
Charlottesville, VA 22904, USA
e-mail: aak4df@virginia.edu

I. Tur-Kaspa, MD
Institute for Human Reproduction (IHR),
Department of Obstetrics and Gynecology,
The University of Chicago, 409 W. Huron St.,
Chicago, IL 60654, USA
e-mail: drtk@infertilityihr.com

L.A. Stadtmauer, I. Tur-Kaspa (eds.), *Ultrasound Imaging in Reproductive Medicine*,
DOI 10.1007/978-1-4614-9182-8_6, © Springer Science+Business Media New York 2014

follicular phase for ovulation. The antral follicle count (AFC) is the total number of follicles counted in 2D or 3D per ovary and correlates well with the number of recruitable mature oocytes for IVF. The recruitment process occurs over 3 months.

Before initiating ovarian stimulation, the baseline day 3D US is a prerequisite for planning the IVF therapy in detail; it can estimate the ovarian reserve, which can be done most accurately by an AFC. During an IVF stimulation with gonadotropins, the largest follicles reach a diameter of 17–24 mm prior to human chorionic gonadotropin (hCG) trigger. The retrieval of a large number of good quality oocytes increases the likelihood of a high fertilization rate and an adequate number of high quality embryos.

Female reproductive ageing is a process that will reduce fecundity (the ability to have a viable embryo implanted). The process of ageing involves decrease in both the quantity and quality of the oocytes within the follicles. At 4 months of fetal life, the germ cells are surrounded by the somatic cells forming the primordial follicles, containing the peak number of oocytes at six to seven million. At birth, there are one million oocytes, with loss by atresia. It further decreases to 300,000–500,000 follicles at menarche. Throughout life, follicles leave the primordial pool and enter the growing recruitable pool taking about 85 days or three menstrual cycles to reach ovulation. The majority of follicles undergo atresia, until rescued by the FSH at puberty by the activation of the pituitary-gonadal axis. Rate of decline of follicles during the reproductive years is steady at approximately 1,000 follicles per month. The rate of decline rapidly increases after 37 years of age. The loss in the quality is due to increased rate of meiotic nondisjunction leading to increased rate of aneuploidy in early embryos at higher female ages. At menopause of average age of 51, the number of follicles remaining will be less than 1,000 [1].

The first noticeable sign of reproductive ageing is shortening of the cycle by 2–3 days due decrease in the follicular phase by early selection and maturation of the dominant follicle. These signs occur relatively late much after changes in the quantity and quality of the oocytes have occurred.

Antral Follicle Count and Ovarian Reserve

The estimation of antral follicle count and antral follicle size performed by TVUS is currently the most reliable method and gives the best correlation with retrieved oocytes [2–4]; moreover, it is easy to perform and is noninvasive. The definition of AFC is the number of follicles in both ovaries added up that can be recruited with the threshold dose of gonadotropins for each particular patient. Therefore, the AFC determined by ultrasound on day 2 or 3 of the cycle, notably by 2D or 3D techniques, is the best predictor for poor ovarian response, ovarian hyperstimulation syndrome (OHSS), oocytes collected, and live birth rates [2–6]. Decreased AFC of 3 is shown in Fig. 6.1. Only a small number of ovarian follicles are highly responsive to FSH during an IVF stimulation. The number of these antral follicles represents the "recruitable or selectable follicles." The antral follicle count (AFC) reflects the ovarian reserve and is predictive of the IVF outcome in regard to the number of yielded oocytes in response to hormonal stimulation. Fratterelli and colleagues correlated the AFC with the number of mature follicles ($r=0.52$) and the number of oocytes ($r=0.38$) and found the AFC <4 was associated with a high cancellation rate and poor

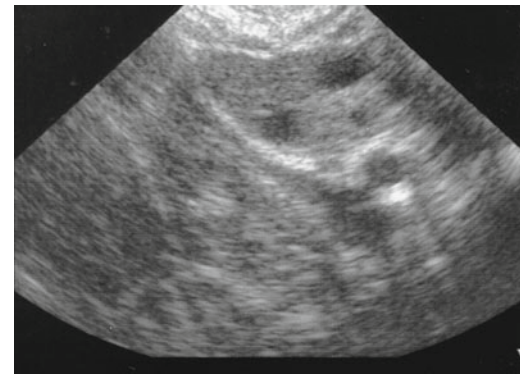

Fig. 6.1 Decreased ovarian reserve with AFC of 3

pregnancy rates [7]. For the high responders the cutoff level of >14 antral follicles has the best combination of sensitivity and specificity for predicting a hyper-response with values close to 90 %. It is important in selection of the protocol and gonadotropin dosage which will lead to decreasing OHSS and cancelled cycles. The accurate assessment of the ovarian reserve is a way to individualize optimal therapy. Ovarian volume also correlates with the AFC and can be measured by TVS [8].

Standard AFC assessment was, and still is, performed primarily with 2D US imaging. Although this modality might be sufficient in some cases, there might be some uncertainties and disadvantages.

3D AFC is more reproducible and accurate but the method is less standardized, and 3D technology may not be freely available for all reproductive endocrinologists. Figure 6.2a, b shows 3D antral follicle count. The 3D count can be performed in inverse mode as shown (Fig. 6.2a). It should be noted that it is imperative to distinguish between the total antral follicle count (TAFC), including follicles >6 mm in diameter; however, the number of small antral follicles is more predictive of number of oocytes retrieved. AFC is also a predictor of pregnancy loss and low AFC correlates with 4× increase in early miscarriages [9].

Endocrine Markers of Ovarian Reserve

Endocrine markers of ovarian reserve are antimüllerian hormone (AMH) and inhibin B which are direct markers of quantity and follicular cohort numbers. Indirect markers are basal day 3 FSH and estradiol (E2) levels [10–16], and high levels indicate a decreased number of small antral follicles. Both AFC and AMH predict similarly the response to treatment, but ultrasound is the only method so far that allows a direct assessment of each ovary separately. Identification of participants who are likely to respond poorly during IVF treatment is clinically relevant as the couple can be counseled regarding cycle cancellation and lower chance of success. Pretreatment AFC and AMH were found to be the most significant predictors of the number of oocytes retrieved especially for low and high responders in multiple studies including a meta-analysis by Hendricks et al. [2, 10–16]. These studies showed that AFC and AMH demonstrated similar predictive power based on ROC area under the curve (AUC) analysis and correlated with oocyte number better than other parameters such as FSH or age. However, all these parameters correlate less well with pregnancy outcomes, which is a more important outcome for the patient than oocyte number. In addition, AMH and AFC have been shown to be the best predictors of OHSS in women undergoing ovarian stimulation for IVF. The advantage of AMH is that it is not operator or cycle day dependent. A cutoff level of >3.3 ng/mL determines the risk of OHSS with a 90 % sensitivity,71 % specificity, and 61 % PPV, and a cutoff value of AFC >8 predicts the risk of OHSS with a 78 % sensitivity, 65 % specificity, and 53 % PPV [17].

The validity of AFC for ovarian reserve comes from studies showing a direct correlation with the number of nongrowing follicles viewed on histologic sections [18]. On the other hand, ovarian volume, vascularity, and perfusion had no significant value in predicting poor ovarian response and all are inferior to AFC [19]. The hypothesis that aneuploidy is negatively associated with the quantity of oocytes in the ovary is supported by studies showing decrease AFC in women with spontaneous abortions after IVF. The conclusions are not supported by all studies possibly because some lack power and it may depend on the mechanism of diminished ovarian reserve. In many women with low AFC, especially at a young age, there is a decrease in quantity but not in quality of the oocytes.

3D Ultrasound and Ovarian Volume

Ovarian volume can be calculated by measuring each ovary in three perpendicular directions and applying the formula of the ellipsoid ($D1 \times D2 \times D3 \times \pi/6$). Ovarian volume can also

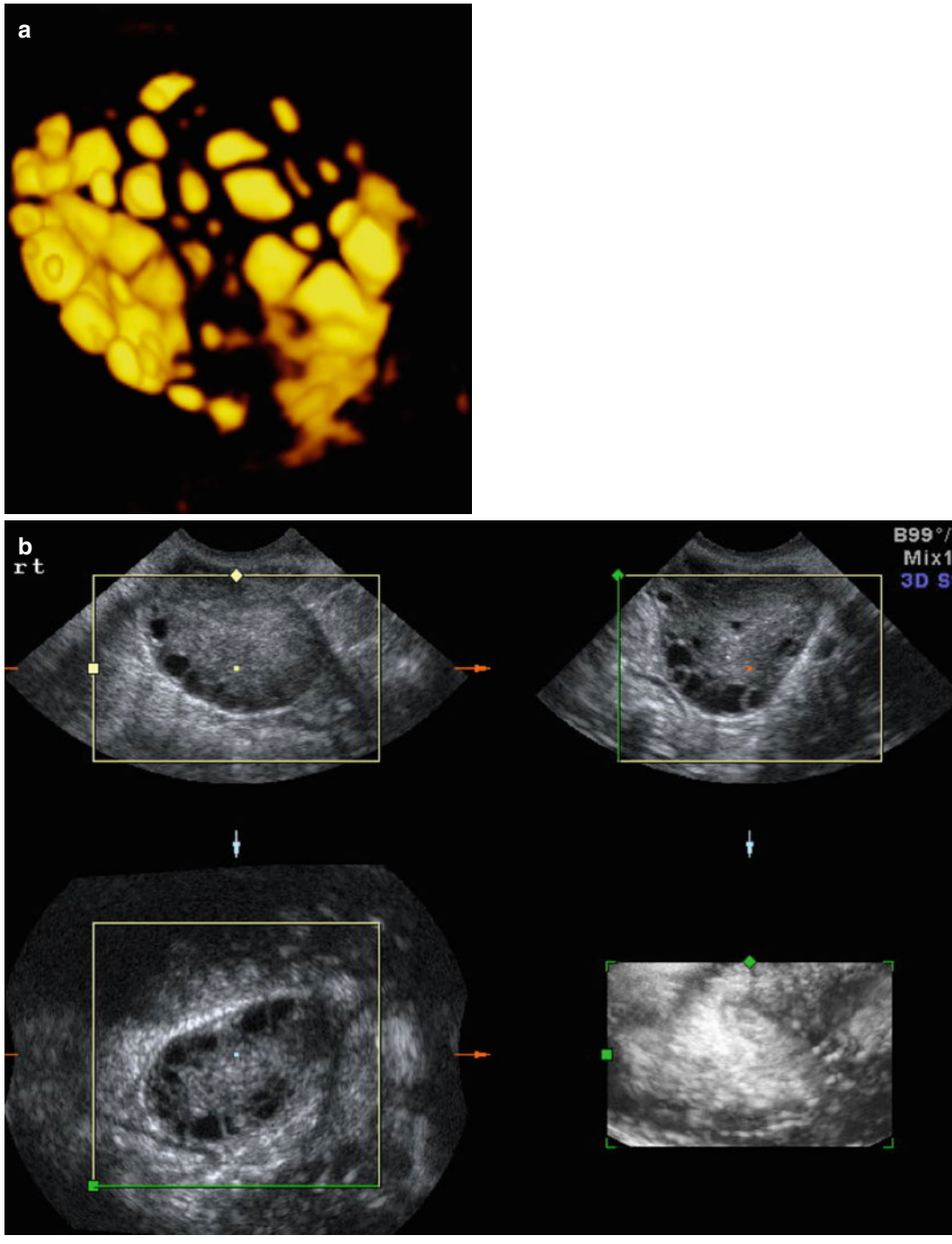

Fig. 6.2 (**a**) 3D AFC in inverse mode (**b**) Multiplanar view of ovary with antral follicle count

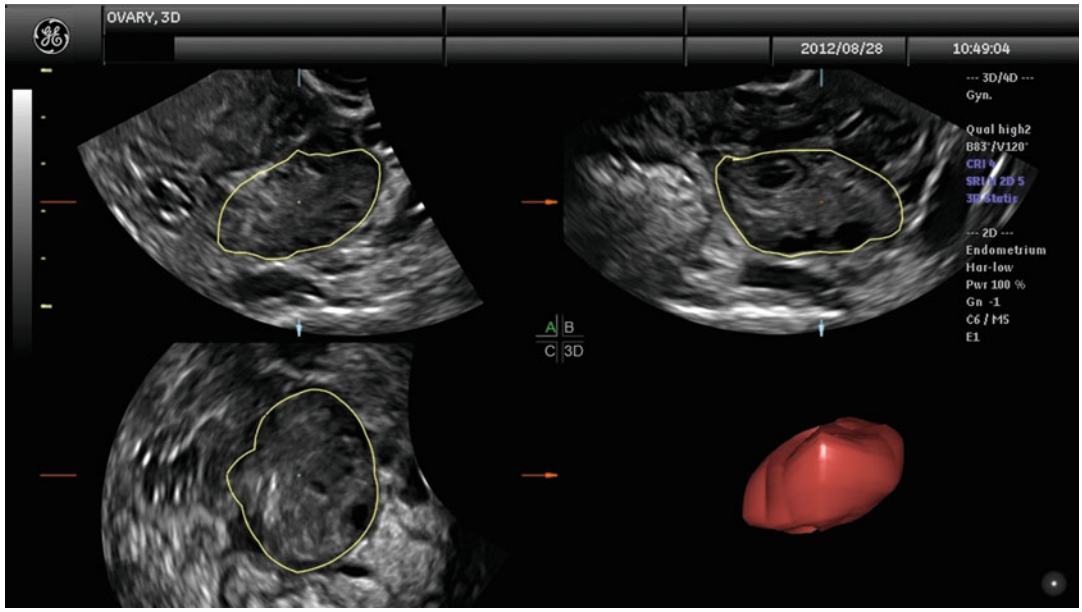

Fig. 6.3 Ovarian volume with VOCAL program. (**a**–**c**) Multiplaner view of ovary with ovarian volume

be automatically calculated using the software called "virtual organ computer-aided analysis" or VOCAL (Fig. 6.3). This imaging program calculates organ volume from the areas of the three orthogonal sections, sagittal, transverse, and coronal views, and allows very precise calculation of ovarian volumes. However, ovarian volume can be affected by ovarian cysts. Ovarian volume and antral follicle volume can now be automated. Three-dimensional US is an excellent technique for calculating ovarian volume very precisely using the VOCAL program and observing the ovary with rotating angles. Low ovarian reserve and poor response to controlled ovarian hyperstimulation in ART are associated with volumes <3 cm^3 as seen by Lass and colleagues with increased cancellation rates [20]. Polycystic ovaries are associated with volumes >6.6 cm^3. Ovarian hyperstimulation syndrome (OHSS) is associated with increased ovarian volume [21, 22]. However, total volume of the ovaries detected by transvaginal ultrasound is not better than the AFC in predicting parameters.

The studies of IVF patients have demonstrated that 3D ultrasound volume measurements for follicles correlate better with the volume of aspirated follicular fluid than 2D ultrasound measurements [22]. One of the most frequently employed applications is the sonography-based Automated Volume Calculation (SONO-AVC; GE Medical Systems, Zipf, Austria). The application of SonoAVC for IVF was first described by Raine-Fenning et al. [23]. Studies with SonoAVC have not shown a clear benefit in improving IVF outcomes [24]. Even if there is no clinical benefit, the advantages of SonoAVC may be a time decrease during the ultrasound as the ovarian volumes are saved and can be calculated later. This may lead to less discomfort for the patients. However, there is time required for manual assessment of the 3D data which should be added to the time in scanning and the technique needs to be learned and reproducibility documented. Rodriguez Fuentes analyzed the impact of SonoAVC on time and the clinical outcome of IVF treatment. They found reduced time saving of 4 min per case after including the post-processing time [24]. Their study has shown that SonoAVC provides different results from those of 2D ultrasound imaging when the size of the follicle is considered.

Evaluation of Ovarian Stroma Flow with 3D Ultrasound

It is possible that poor ovarian vascularization impairs access of gonadotropins to the ovarian follicles. Power Doppler US in combination with 3D US and VOCAL is a very good approach for correlating the ovarian vascular network with the ovarian response to ART. The significance of ovarian stromal blood flow with ovarian reserve was studied [19]. Variably, some studies show correlation of undetectable basal ovarian stromal blood flow with poor response and others did not.

Ovarian Cysts and Masses

Ovarian cysts are important to diagnose by ultrasound in the infertile patient and can affect the ovarian volume. In addition, ovarian cysts and masses can be picked up on baseline ultrasounds for ovarian reserve. The most common ovarian cysts seen in infertility patients are simple functional cysts, hemorrhagic cysts, endometriomas, and dermoid cysts. Studies verify that evaluation of ovarian masses by basic ultrasound based on morphology is equal to other methods with a sensitivity of 88–100 % and a specificity of 62–96 % for predicting malignancy [25]. The majority of ovarian masses that will be seen on the baseline ultrasound will be one of the big 6. This includes functional cysts or follicles, corpus luteum cyst, hemorrhagic cysts, endometriomas polycystic ovaries, and benign cystic teratomas (dermoids). Functional cysts are the most common cystic masses seen on ultrasound in the reproductive age group. These cysts tend to stay less than 10 cm and regress after 1–2 cycles and are either follicular cysts or luteal cysts. A functional follicle can develop when ovulation fails to occur and is simple in ultrasound appearance (Fig. 6.4). If they are small (<3 cm) and not hormonally active, they do not need to be treated before ART. However, patients with large simple ovarian cysts may have lower response to stimulation, and ovarian cyst aspiration immediately prior to ovarian stimulation has been shown to be beneficial [26]. A corpus

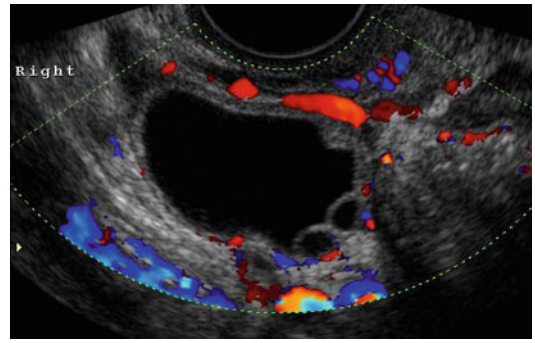

Fig. 6.4 Follicular cyst

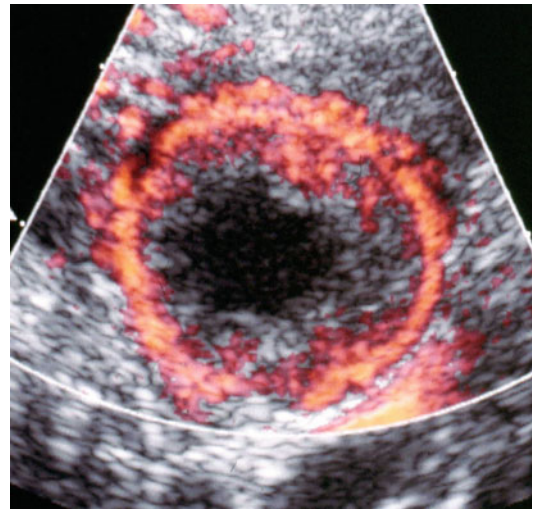

Fig. 6.5 Corpus luteum (with ring of fire)

luteum cyst is more solid in appearance, and Doppler US demonstrates prominent peripheral blood flow with a low-resistance waveform (Fig. 6.5). Typically this cyst can resolve in a few weeks and is asymptomatic but can grow and cause pain, rupture, or torsion. A hemorrhagic cyst can develop from hemorrhage into a corpus luteum. Acutely there is clot and the clot may retract and resolve. It will jiggle with the movement of the transducer and fibrin strands are seen (Fig. 6.6).

An endometrioma is also a very common finding in the infertile patient and is a sign of the presence of endometriosis in other areas [27, 28]. The typical endometrioma is a unilocular cyst with homogeneous low-level internal echogenicity (ground glass echogenicity)

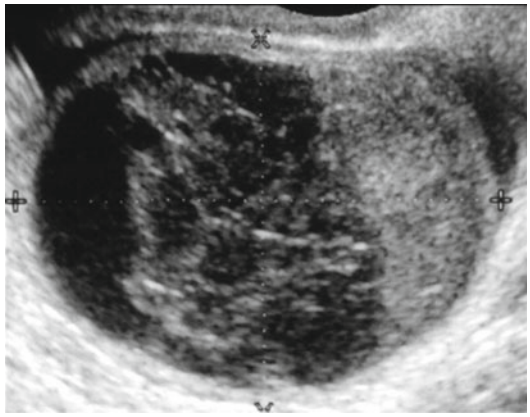

Fig. 6.6 Resolving hemorrhagic cyst

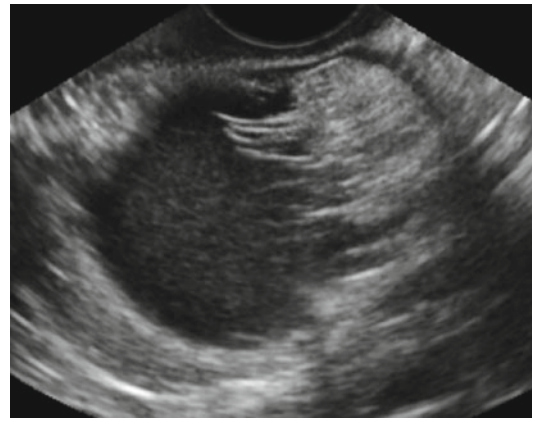

Fig. 6.8 Dermoid cyst with hair

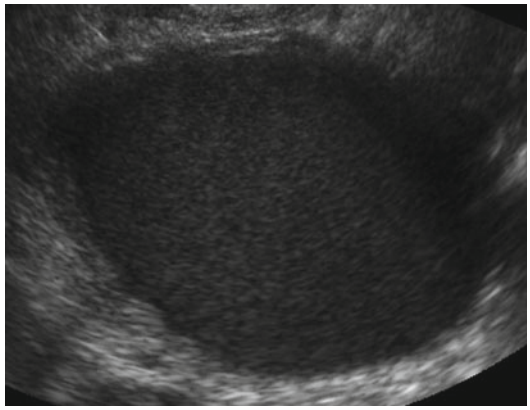

Fig. 6.7 Endometrioma

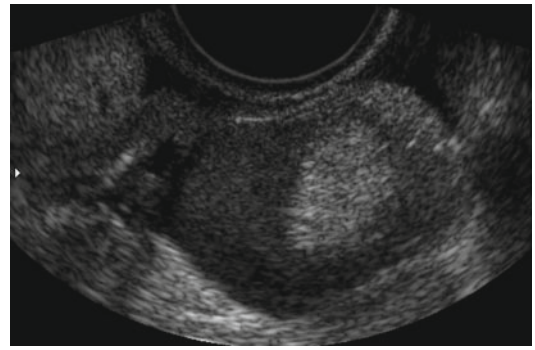

Fig. 6.9 Dermoid cyst "tip of the iceberg" sign

of the cyst fluid (Fig. 6.7). With respect to endometrioma, a correct diagnosis is important for infertility with possible need for ART. Transvaginal ultrasonography is the imaging of choice to differentiate ovarian endometriomas from other adnexal masses [29, 30]. Studies show that an endometrioma is associated with lower response to ovarian stimulation; however, removing the endometrioma can also affect ovarian response and may significantly diminish ovarian reserve as the base of the ovary is usually burned and the cyst wall is stripped with damage of follicles [31]. The trend has become to stimulate with the endometriomas present unless symptomatic and less surgery is necessary to enhance fertility [32].

Polycystic ovaries are covered below. Dermoid cysts can present as solid hyperechoic heterogeneous masses with a mixed pattern of solid and cystic areas. They may contain calcifications, fat, and hair. The hair can disperse in the surrounding fluid as seen in Fig. 6.8. If the "hair ball" floats in the sebum, there is an appearance of a tip of the iceberg sign (Fig. 6.9). They should be removed prior to IVF if they are causing pain or if there is a question of malignancy. Puncture during oocyte retrieval should be avoided due to high risk of peritonitis.

Other extraovarian lesions include hydrosalpinges, paraovarian cysts, and peritoneal inclusion cysts that may be picked up on baseline ultrasound. These are benign and will be covered in other chapters. Features that are worrisome for primary epithelial malignancy include cysts with thick septations or vascularized areas of focal wall thickening, solid masses, and ascites (Fig. 6.10).

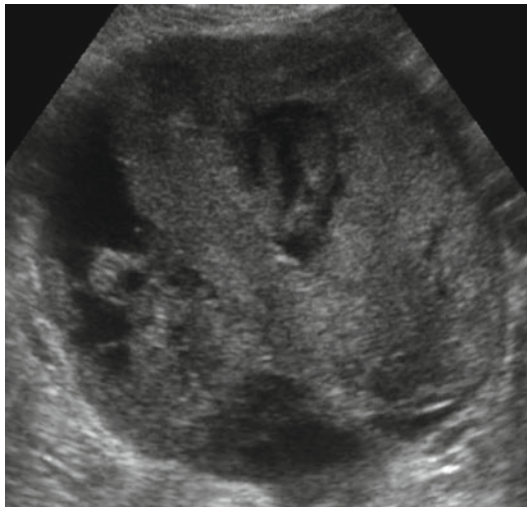

Fig. 6.10 Ovarian cancer

Ultrasound and Polycystic Ovary (PCO)

Polycystic ovary syndrome (PCOS) is one of the most common endocrine disorders impairing female fertility; it has been reported to occur in about 20 % of the general female population and in up to 50 % of women undergoing IVF therapy [33, 34]. It is covered in detail in another chapter but will be discussed briefly here. Ultrasound is one of the criteria for the diagnosis of polycystic ovarian syndrome (PCOS) based on the Rotterdam consensus conference. Current data suggest that polycystic ovaries detected by transvaginal ultrasonography may be found in approximately 75 % of women with a clinical diagnosis of PCOS [35, 36]. However, it is not a rule that all women with polycystic ovaries will demonstrate the clinical and biochemical features of PCOS, oligomenorrhea, and/or hyperandrogenism. Polycystic ovaries per se, even without PCOS, constitute a risk factor for the development of ovarian hyperstimulation syndrome (OHSS) and the stimulation protocol chosen should reflect this [37]. AMH is also an excellent marker for PCOS and OHSS.

Transvaginal ultrasound is a highly sensitive method for identification of PCO. The most commonly used criteria today are those proposed by Dewailly and colleagues with a string of pearls pattern [38, 39] where the antral follicles

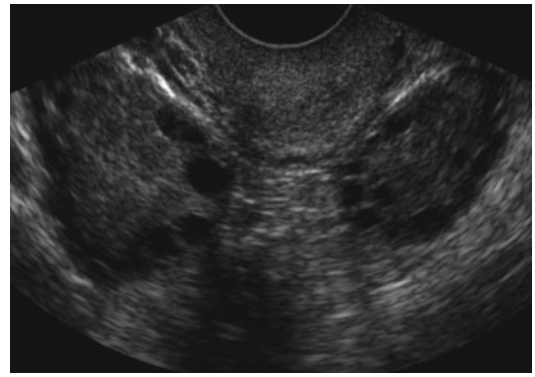

Fig. 6.11 PCOS

are arranged peripherally with a dense core of ovarian stroma (Fig. 6.11). This was reaffirmed in the Rotterdam 2003 consensus [40]. The transvaginal definition is based on the presence of an ovarian volume of greater than 10 cm^3 (milliliters) >12 small follicles in a single ovary. Comparisons between transabdominal and transvaginal ultrasound do not find significant differences in the detection rate of PCO. The 3D ultrasound and the use of color and pulsed Doppler ultrasound showing increased ovarian blood flow are techniques which further enable the identification of PCO, but are not mandatory for the diagnosis [39]. No other imaging modality, such as magnetic resonance imaging (MRI) for the visualization of the ovaries, are needed for the diagnosis of PCO and should not be used use as routine examination.

The new automated 3D US techniques facilitate the exclusion of a false-positive PCOS diagnosis and reflect pathophysiological changes in these patients in a more accurate manner. An early detection of PCOS is highly recommended for women undergoing IVF treatment due to the elevated risk for OHSS. Unfortunately, because 3D ultrasound is a relatively new imaging modality, the Rotterdam criteria only take 2D US sonography into account.

At present, only a few studies have evaluated the use of 3D US for PCOS patients [41, 42]; furthermore, to date, only one study has addressed automated 3D US (SonoAVC) [42]. In a retrospective cohort study, Allemand et al. [41] analyzed 29 normoandrogenic, ovulatory women

with tubal or male factor infertility and 10 PCOS women with chronic anovulation and clinical or biochemical hyperandrogenism. Mean follicle number/ovary (FNPO) as well as the maximal number of follicles in a single sonographic plane (FSSP) were determined by 3D TVUS; simultaneously, the ovarian volume was determined by 2D TVUS. Interestingly, the authors postulated a considerably higher threshold of antral follicles (20 or more) for PCOS patients, which is a considerably higher threshold than that of the Rotterdam criteria. The authors explained this discrepancy by the identification of more follicles by 3D US. The weakness of this study is the small number of patients, the missing direct comparison to 2D US, and the low sensitivity (true positive rate) using receiver-operating characteristics (ROCs). According to most publications dealing with 3D US in PCOS patients, there is a broad agreement about increased ovarian volume of polycystic ovaries [42–45]. Nevertheless there is still disagreement regarding ovarian vascularity, stromal changes, and cutoff values for antral follicles.

Antral Follicle Count and SonoAVC

The antral follicle count in 2D and 3D are generally similar although 3D ultrasound is superior for the high antral follicle population. In the inversion mode, follicles which appear white can be counted easily. Image or volume rotation using the cine-loop facilitates the process (Fig. 6.2a). Assisted reproductive techniques including in vitro fertilization (IVF) and ovulation induction require close monitoring of follicular development. Follicular development is commonly assessed with transvaginal ultrasounds during which each follicle is measured in 2 or 3 dimensions. As there are often 10–20 follicles, this is very time consuming. In addition follicular boarders are irregular, and hence this method has poor reproducibility and is often an inaccurate assessment of follicular volume. Recently a new software program, the automated follicular assessment using segmental topology or FAST program, was developed in order to automate the follicular measurements. Therefore, our objective was to determine the accuracy, reproducibility, and efficiency of this novel program. This will be discussed further in another chapter.

One disadvantage of 2D for antral follicle counts involves inter- and intra-observer reproducibility. Of note, only a handful of studies compare the accuracy of ultrasound in regard to AFC and inter- and intra-observer reliability. Scheffer et al. [46] described the value of AFC determined by AVC needed for the improvement of standardization. They compared healthy volunteers with proven fertility to patients visiting an infertility clinic. For each patient, 2D or 3D TVS was conducted for AFC (2–10 mm) and interobserver reliability was calculated. Both techniques were adequate when only a few follicles were present; however, when higher AFCs occurred, the reproducibility decreased with the 2D technique. In addition to this report, studies by the group of Raine-Fenning [23, 47, 48] demonstrated an improvement of interobserver/intraobserver reliability by the application of 3D methods (in particular by automated systems, such as SonoAVC).

The SonoAVC software is especially designed for the automatic detection of multifollicular growth and to overcome the aforementioned problems of follicle observation by 2D US [22, 24, 47, 49–55]. This software allows not only the display of single follicles in 3D but also automatically calculates the number and volume of hypoechoic structures in a 3D echo-derived data set; furthermore, it provides estimations regarding the absolute dimensions of follicles. The only necessary requirement is adjustment of the ROI box over the entire ovary to include only the information which is needed for calculation and to check during postprocessing. Measurements are based on calculation of the largest diameters in three orthogonal planes: the mean follicle diameter, the follicular volume, and the volume-based diameter of the follicle. Thus, the volume is calculated via the voxel count within hypoechoic structures. The true volume can be measured, and SonoAVC calculates the follicle diameter by rendering

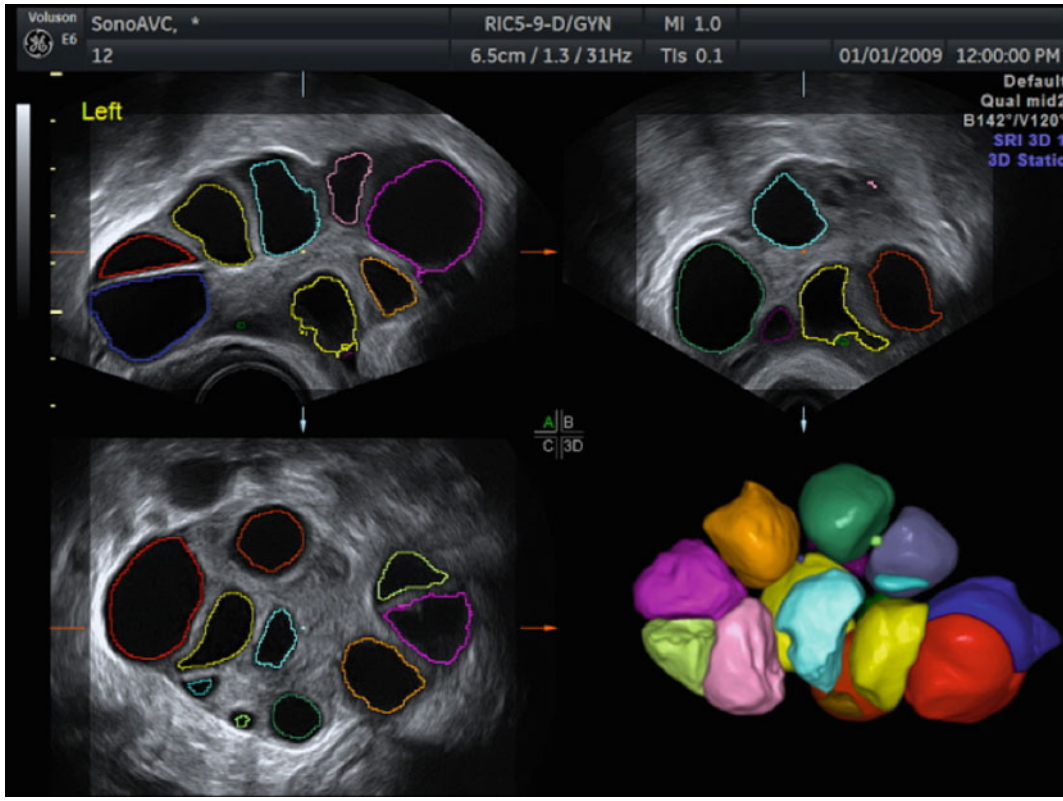

Fig. 6.12 SonoAVC

the follicle as a perfect sphere. This results in the visualization of sono-anatomic details, which could not previously be recognized. A major advantage of this sono-anatomic rendering is that individual structures are color coded (Fig. 6.12) allowing the exact count, which is needed for the determination of factors such as ovarian reserve.

Conclusions

AFC is highly predictive for the ovarian reserve reflected by the number of oocytes retrieved on stimulation and strongly associated with the serum AMH level. This is helpful for counseling the patient and determining the stimulation protocol. The estimation of the ovarian response by US is simple and noninvasive; thus, it is an advisable procedure. The reliability of this method is probably increased with 3D instruments. There are several advantages of the new 3D US techniques. New software systems such as SonoAVC allow decreased inter- and intrapersonal variability in the processing, readout, and interpretation of ultrasound scans. While manual post-processing of US scans is required, this can be performed at a later time once the patient is off the table. The ultrasound definition of PCOS may need modification incorporating the 3D automated technology.

References

1. Faddy MJ, Gosden RG, Gougeon A, Richardson SJ, Nelson JF. Accelerated disappearance of ovarian follicles in mid-life: implications for forecasting menopause. Hum Reprod. 1992;7:1342–6.
2. Hendriks DI, Mol BW, Bancsi LF, Te Velde ER, Broekmans FI. Antral follicle count in the prediction of poor ovarian reserve and IVF outcome after in vitro fertilization :a meta-analysis and comparison with basal FSH level. Fertil Steril. 2005;83:291–310.
3. Broekmans FJ, Kwee J, Hendriks DJ, Mol BW, Lambalk CB. A systematic review of tests predicting ovarian reserve and IVF outcome. Hum Reprod Update. 2006;12:685–718.

4. Muttukrishna S, McGarrigle H, Wakim R, Khadum I, Ranieri DM, Sethal P. Antral follicle count, antimullerian hormone and inhibin B: predictors of ovarian response in assisted reproductive technology? BJOG. 2005;112:1384–90.
5. Johnson NP, Bagrie EM, Coomarasamy A, Bhattacharya S, Shelling AN, Jessop S, Farquhar C, Khan KS. Ovarian reserve tests for predicting fertility outcomes for assisted reproductive technology: The International Systematic Collaboration of Ovarian Reserve Evaluation protocol for a systematic review of ovarian reserve test accuracy. BJOG. 2006;113: 1472–80.
6. Jayaprakasan K, Deb S, Batcha M, Hopkisson J, Johnson I, Campbell B, et al. The cohort of antral follicles measuring 2–6 mm reflects the quantitative status of ovarian reserve as assessed by serum levels of anti-Mullerian hormone and response to controlled ovarian stimulation. Fertil Steril. 2010;94:1775–81.
7. Fratterelli JL, Lauria-Costab DF, Miller BT, Bergh PA, Scott RT. Basal antral follicle number and mean ovarian diameter predict cycle cancellation and ovarian responsiveness in assisted reproductive technology cycles. Fertil Steril. 2000;7:512–7.
8. Danninger B, Brunner M, Obruca A, Feichtinger W. Prediction of ovarian hyperstimulation syndrome by ultrasound volumetric assessment [corrected] of baseline ovarian volume prior to stimulation. Hum Reprod. 1996;11:1597–9.
9. Jayaprakasan K, Hilwah N, Kendall NR, Hopkisson JF, Campbell BK, Johnson IR, et al. Does 3D ultrasound offer any advantage in the pretreatment assessment of ovarian reserve and prediction of outcome after assisted reproduction treatment? Hum Reprod. 2007;22:1932–41.
10. van der Stege JG, van der Linden PJ. Useful predictors of ovarian stimulation response in women undergoing in vitro fertilization. Gynecol Obstet Invest. 2001;52:43–6.
11. Karande VC. Managing and predicting low response to standard in vitro fertilization therapy: a review of the options. Treat Endocrinol. 2003;2:257–72.
12. Muasher SJ, Oehninger S, Simonetti S, Matta J, Ellis LM, Liu HC, Jones GS, Rosenwaks Z. The value of basal and/or stimulated serum gonadotropin levels in prediction of stimulation response and in vitro fertilization outcome. Fertil Steril. 1988;50(2):298–307.
13. Broekmans FJ, Knauff EA, te Velde ER, Macklon NS, Fausser BC. Female reproductive ageing: current knowledge and future trends. Trends Endocrinol Metab. 2007;18:58–65.
14. Broer SL, Mol BWJ, Hendriks D, Broekmans FJM. The role of antimullerian hormone in prediction of outcome after IVF: comparison with the antral follicle count. Fertil Steril. 2009;91:705–14.
15. Hazout A, Bouchard P, Seifer DB, Aussage P, Junca AM, Cohen-Bacrie P. Serum anti-müllerian hormone/müllerian-inhibiting substance appears to be a more discriminatory marker of assisted reproductive technology outcome than follicle-stimulating hormone, inhibin B, or estradiol. Fertil Steril. 2004;82: 1323–9.
16. Riggs RM, Duran EH, Baker MW, Kimble TD, Hobeika E, Yin L, Matos-Bodden L, Leader B, Stadtmauer L. Assessment of ovarian reserve with antimullerian hormone: a comparison of the predictive value of antimullerian hormone, follicle-stimulating hormone, inhibin B and age. Am J Obstet Gynecol. 2008;199:202e1–8.
17. Ocal P, Sahmay S, Cetin M, Irez T, Guralp O, Cepni I. Serum anti-Müllerian hormone and antral follicle count as predictive markers of OHSS in ART cycles. J Assist Reprod Genet. 2011;28:1197–203.
18. Hansen KR, et al. Correlation of ovarian reserve tests with histologically determined primordial follicle number. Fertil Steril. 2011;95:855–64.
19. Jayaprakasan K, Al-Hasie H, Jayaprakasan R, Campbell B, Hopkisson J, Johnson I, Raine-Fenning N. The three-dimensional ultrasonographic ovarian vascularity of women developing poor ovarian response during assisted reproduction treatment and its predictive value. Fertil Steril. 2009;92(6): 1862–9.
20. Lass A, Brinsden P. The role of ovarian volume in reproductive medicine. Hum Reprod Update. 1999;5: 256–66.
21. McDougall MJ, Tan SL, Jacobs HS. IVF and the ovarian hyperstimulation syndrome. Hum Reprod. 1992;5:597–600.
22. Ata B, Tulandi T. Ultrasound automated volume calculation in reproduction and in pregnancy. Fertil Steril. 2011;95:2163–70. Review.
23. Raine-Fenning N, Jayaprakasan K, Clewes J, Joergner I, Bonaki SD, Chamberlain S, et al. SonoAVC: a novel method of automatic volume calculation. Ultrasound Obstet Gynecol. 2008;31: 691–6.
24. Rodriguez-Fuentes A, Hernandez J, Garcia-Guzman R, Chinea E, Iaconianni L, Palumbo A. Prospective evaluation of automated follicle monitoring in 58 in vitro fertilization cycles: follicular volume as a new indicator of oocyte maturity. Fertil Steril. 2010;93: 616–20.
25. Valentine L, Ameye L, Savelli L, et al. Adnexal masses difficult to classify as benign or malignant using subjective assessment of grey-scale and Doppler ultrasound findings: logistic regression models do not delp. Ultrasound Obstet Gynecol. 2011;38(4):456–65.
26. Firouzabadi RD, Sekhavat L, Javedani M. The effect of ovarian cyst aspiration on IVF treatment with GnRH. Arch Gynecol Obstet. 2010;281(3):545–9.
27. Okaro E, Condous G, Khalid A, Timmerman D, Ameye L, Van Huffel S, Bourne T. The use of ultrasound-based 'soft markers' for the prediction of pelvic pathology in women with chronic pelvic pain, can we reduce the need for laparoscopy? BJOG. 2006;113:251–6.
28. Raine-Fenning N, Jayaprakasan K, Deb S. Three – dimensional ultrasonographic characteristics of endometriomata. Ultrasound Obstet Gynecol. 2008; 31:718–24.
29. Asch E, Levine D. Variations in appearance of endometriomas. J Ultrasound Med. 2007;26:993–1002.

30. Kumfer MC, Schwimer SR, Lebovic J. Transvaginal sonographic appearance of endometriomas: spectrum of findings. J Ultrasound Med. 1992;11:129–33.
31. Somigliana E, Vercellini P, Viganó P, Ragni G, Crosignani PG. Should endometriomas be treated before IVF-ICSI cycles? Hum Reprod Update. 2006;12:57–64.
32. Bernardi LA, Pavone ME. Endometriosis and update on management. Womens Health (Lond Engl). 2013;9(3):233–50.
33. Balen A, Michelmore K. What is polycystic ovary syndrome? Are national views important? Hum Reprod. 2002;17:2219–27.
34. Polson DW, Adams J, Wadsworth J, Franks S. Polycystic ovaries–a common finding in normal women. Lancet. 1988;1:870–2.
35. Alborzi S, Khodaee R, Parsanejad ME. Ovarian size and response to laparoscopic ovarian electrocauterization in polycystic ovarian disease. Int J Gynaecol Obstet. 2001;74:269–74.
36. Amer SA, Li TC, Bygrave C, Sprigg A, Saravelos H, Cooke ID. An evaluation of the inter-observer and intra-observer variability of the ultrasound diagnosis of polycystic ovaries. Hum Reprod. 2002;17:1616–22.
37. Jacobs HS. Polycystic ovaries and polycystic ovary syndrome. Gynecol Endocrinol. 1987;1:113–31. Review.
38. Kousta E, White DM, Cela E, McCarthy MI, Franks S. The prevalence of polycystic ovaries in women with infertility. Hum Reprod. 1999;14:2720–3.
39. Dewailly D, Gronier H, Poncelet E, Robin G, Leroy M, et al. Diagnosis of polycystic ovary syndrome (PCOS): revisiting the threshold values of follicle count on ultrasound and of the serum AMH level for the definition of polycystic ovaries. Hum Reprod. 2011;26:3123–9.
40. Rotterdam ESHRE/ASRM-Sponsored PCOS Consensus Workshop Group. Revised 2003 consensus on diagnostic criteria and long-term health risks related to polycystic ovary syndrome. Fertil Steril. 2004;81:19–25.
41. Allemand MC, Tummon IS, Phy JL, Foong SC, Dumesic DA, Session DR. Diagnosis of polycystic ovaries by three-dimensional transvaginal ultrasound. Fertil Steril. 2006;85:214–9.
42. He LR, Zhou LX, Pan RK, Zhang X. [Clinical significance of counting follicles in diagnosis of polycystic ovary syndrome by the three-dimensional ultrasound imaging with sonography based automated volume calculation method]. Zhonghua Fu Chan Ke Za Zhi. 2011;46:350–4.
43. Kyei-Mensah AA, Lin Tan S, Zaidi J, Jacobs HS. Relationship of ovarian stromal volume to serum androgen concentrations in patients with polycystic ovary syndrome. Hum Reprod. 1998;13:1437–41.
44. Järvelä IY, Mason HD, Sladkevicius P, Kelly S, Ojha K, Campbell S, et al. Characterization of normal and polycystic ovaries using three-dimensional power Doppler ultrasonography. J Assist Reprod Genet. 2002;19:582–90.
45. Pan HA, Wu MH, Cheng YC, Li CH, Chang FM. Quantification of Doppler signal in polycystic ovary syndrome using three-dimensional power Doppler ultrasonography: a possible new marker for diagnosis. Hum Reprod. 2002;17:201–6.
46. Scheffer GJ, Broekmans FJ, Bancsi LF, Habbema JD, Looman CW, Te Velde ER. Quantitative transvaginal two- and three-dimensional sonography of the ovaries: reproducibility of antral follicle counts. Ultrasound Obstet Gynecol. 2002;20:270–5.
47. Raine-Fenning N, Jayaprakasan K, Chamberlain S, Devlin L, Priddle H, Johnson I, et al. Automated measurements of follicle diameter: a chance to standardize? Fertil Steril. 2009;91:1469–72.
48. Raine-Fenning N, Jayaprakasan K, Deb S, Clewes J, Joergner I, Dehghani Bonaki S, Johnson I. Automated follicle tracking improves measurement reliability in patients undergoing ovarian stimulation. Reprod Biomed Online. 2009;18(5):658–63.
49. Deutch TD, Joergner I, Matson DO, Oehninger S, Bocca S, Hoenigmann D, Abuhamad A. Automated assessment of ovarian follicles using a novel three-dimensional ultrasound software. Fertil Steril. 2009;92(5):1562–8.
50. Raine-Fenning N, Deb S, Jayaprakasan K, Clewes J, Hopkisson J, Campbell B. Timing of oocyte maturation and egg collection during controlled ovarian stimulation: a randomized controlled trial evaluating manual and automated measurements of follicle diameter. Fertil Steril. 2010;94:184–8.
51. Ben-Haroush A, Farhi J, Zahalka Y, Sapir O, Meizner I, Fisch B. Small antral follicle count (2–5 mm) and ovarian volume for prediction of pregnancy in in vitro fertilization cycles. Gynecol Endocrinol. 2011;27(10):748–52.
52. Deb S, Jayaprakasan K, Campbell BK, Clewes JS, Johnson IR, Raine-Fenning NJ. Intraobserver and interobserver reliability of automated antral follicle counts made using three-dimensional ultrasound and SonoAVC. Ultrasound Obstet Gynecol. 2009;33:477–83.
53. Deb S, Campbell BK, Clewes JS, Raine-Fenning NJ. Quantitative analysis of antral follicle number and size: a comparison of two-dimensional and automated three-dimensional ultrasound techniques. Ultrasound Obstet Gynecol. 2010;35:354–60.
54. Jayaprakasan K, Campbell BK, Clewes JS, Johnson IR, Raine-Fenning NJ. Three-dimensional ultrasound improves the interobserver reliability of antral follicle counts and facilitates increased clinical work flow. Ultrasound Obstet Gynecol. 2008;31:439–44.
55. Forman RG, Robinson J, Yudkin P, Egan D, Reynolds K, Barlow DH. What is the true follicular diameter: an assessment of the reproducibility of transvaginal ultrasound monitoring in stimulated cycles. Fertil Steril. 1991;56:89–92.

Ultrasound and PCOS

7

Nikolaos Prapas and Artemis Karkanaki

The Definition of Polycystic Ovary Syndrome

Polycystic ovary syndrome (PCOS) is a common medical entity, of great scientific interest, affecting up to 10 % of women of reproductive age [1, 2]. Until 2003, when the presence of polycystic ovarian morphology was included, the diagnosis of PCOS was based on the presence of clinical or laboratory evidence of hyperandrogenemia and chronic oligo- or anovulation [3]. Despite the name of this syndrome, the polycystic ovarian morphology was not considered pathognomonic for the diagnosis until the Consensus Workshop held in Rotterdam in 2003 [4, 5]. Thereafter, the sonographic evidence of polycystic morphology was recognized as an equal diagnostic criterion of the syndrome and was further defined and simplified into the existence of either 12 or more follicles of 2–9 mm of diameter or an increased ovarian volume of more than 10 cm^3 on both or even one ovary. Importantly, the polycystic ovarian morphology should not be confused with the syndrome, since the diagnosis of PCOS presupposes the existence of one more diagnostic criterion at least.

It should be emphasized that the diagnosis is posed after the exclusion of any other etiology that mimics the clinical expression of PCOS, as thyroid dysfunction, hyperprolactinemia, congenital adrenal hyperplasia (including nonclassical), Cushing's syndrome, androgen-secreting tumors, and idiopathic hirsutism.

Thus, four distinct clinical phenotypes of PCOS are recognized, according to the combination of manifestations [6]. The distinct phenotypes are seen in Table 7.1. The first two phenotypes, already diagnosed by the old criteria of National Institutes of Health of 1990 [3], are widely characterized as the "classic PCOS." The last two groups, "newer PCOS," comprise additional phenotypes that aroused after the new diagnostic criteria of Rotterdam [4, 5], and both include the polycystic ovarian morphology as a feature in contrast to the classic PCOS phenotypes. However, despite the consented criteria there is still uncertainty concerning the importance of each syndrome feature and the severity

N. Prapas, MD, MSc, PhD
A. Karkanaki, MD, MSc, PhD (✉)
Third Department of Obstetrics and Gynecology, Hippokratio General Hospital of Thessaloniki, Greece, Aristotle University of Thessaloniki, 49 Str. Konstantinoupoleos, Thessaloniki, 54642, Greece
e-mail: nikos@iakentro.gr; kartemis2004@hotmail.com

Table 7.1 The four phenotypes of PCOS

Phenotypes	1	2	3	4
Anovulation	+	+	−	+
Hyperandrogenemia	+	+	+	−
Polycystic ovarian morphology	+	−	+	+
	Classic PCOS		Newer PCOS	

L.A. Stadtmauer, I. Tur-Kaspa (eds.), *Ultrasound Imaging in Reproductive Medicine*,
DOI 10.1007/978-1-4614-9182-8_7, © Springer Science+Business Media New York 2014

of the metabolic and reproductive dysfunction every phenotype implies [6, 7].

The unstable and relatively common finding (20–25 %) of polycystic ovarian morphology in the general population [8, 9] triggered the opposition of Androgen Excess Society which stated that PCOS is a primarily androgen excess disorder and this feature should be a prerequisite for the diagnosis of the syndrome. Subsequently, according to Androgen Excess Society, one of the two newer phenotypes with polycystic ovarian morphology and anovulation could not be defined as PCOS [10]. However, this opinion is not widely accepted and is currently under investigation.

The Polycystic Ovarian Morphology

The polycystic ovarian morphology, as defined in Rotterdam, is conditioned by two elements, the presence of 12 or more follicles (2–9 mm of diameter) and/or ovarian volume more than 10 cm^3, in a single or both ovaries. This definition leaves no margin for subjective assessments regarding the diagnosis which can be set even with polycystic morphology in a single ovary. Women taking an oral contraceptive pill cannot be diagnosed as the pill reduces the ovarian volume despite the possible persistence of polycystic morphology [4, 5, 11]. In the case of a dominant follicle (>10 mm) or a corpus luteum, the ultrasonography should be repeated in the next cycle while an abnormal cyst or ovarian asymmetry requires further investigation [4, 5, 12].

The use of state-of-the-art equipment and well-trained operators are some of the technical requirements that should be met for successful examination. Furthermore, the transvaginal approach, whenever possible, and especially in obese women, is highly recommended. Importantly, the scan should be performed during the early follicular phase (days 3–5) of a spontaneous cycle in women with regular cycles and of a progesterone-induced bleeding episode or randomly in women with irregular cycles [4, 5]. The time of the day is meaningful only if Doppler examination is performed due to the diurnal variation in uterine and ovarian blood flow [13, 14].

The current definition of polycystic ovarian morphology makes no reference to the distribution of the follicles, the stromal brightness (echogenicity) and volume as well as to the uterine size and its relationship to the ovarian size, and, finally, to the blood flow through the uterine and ovarian arteries, including the intraovarian stromal blood flow.

The typical polycystic ovary was initially described by Adams et al. as an enlarged ovary with highly vascular and hyperechogenic stroma, compared to the cortex, and with many small follicles arranged in the periphery [15]. The follicles are at least ten and their diameter ranges between 2 and 8 mm, but are usually symmetrical and measure between 2 and 5 mm. The growth of these gonadotropin-dependent antral follicles is halted due to the aberrant folliculogenesis of the syndrome. Interestingly, the cohort of small follicles of 2–5 mm of diameter seems to be a better indicator of the ovarian reserve [16] and is negatively determined by the age [17].

On the other hand, the term multifollicular ovary refers to an ovary with many small follicles of variable size, scattered through an increased amount of stroma, but not in the classic type of "necklace" as in the polycystic ovary. The multicystic ovary may represent a milder disturbance of the ovary where normal folliculogenesis happens to some degree [18]. Multicystic ovaries are common in early adolescence and in the majority regress without evolving to PCOS [19].

Asymptomatic women with only polycystic ovarian morphology are commonly found in the general population up to 32 % of women [20]. These women may conceal some mild abnormalities of androgen secretion, insulin sensitivity, and glucose metabolism [21–23], though the data are still contradictory [20]. The sole presence of polycystic ovarian morphology seems to recede with age, and especially after the age of 35 years [20, 24]. However, when women with polycystic ovarian morphology are subjected to controlled ovarian stimulation and ovulation, as an infertility treatment, they behave like women with PCOS and are faced with an increased risk of

hyperstimulation and ovarian hyperstimulation syndrome (OHSS) [25–27]. Indeed, Swanton et al. found that the rates of severe OHSS were similar between women with polycystic ovarian morphology and PCOS and significantly higher compared to controls [25]. In spite of significantly lower doses of FSH, women with both polycystic ovarian morphology and PCOS responded with higher estradiol level numbers of retrieved oocytes to controlled ovarian stimulation [26, 28, 29].

Furthermore, serum, basal anti-Mullerian hormone (AMH) levels of women with polycystic ovarian morphology were found intermediate between controls and women with PCOS, despite the low androgen levels, suggesting a granulosa cell abnormality [30]. Likewise, AMH concentrations and follicle numbers, after controlled ovarian stimulation, were shown higher in women with polycystic ovarian morphology compared to controls and lower compared to PCOS patients with polycystic ovarian morphology and hyperandrogenism [31].

Regardless of the response and the possibility of OHSS, there was no difference in fertilization, implantation, clinical pregnancy, and live birth rates among women with polycystic ovarian morphology and PCOS and controls [25, 26, 32]. Importantly, women with polycystic ovarian morphology had similar oocyte and embryo quality with women with PCOS, but significantly lower miscarriage rates [28].

In conclusion, the ultrasound assessment of polycystic ovarian morphology is very useful for the diagnosis of the PCOS and possibly its severity and prognosis, the surveillance of the controlled ovarian stimulation in such patients, the prediction of outcome following fertility treatments, the diagnosis of OHSS, the decision of turning to in vitro oocyte maturation in these women, and the diagnosis of other genital tract anomalies and even endometrial hyperplasia that are often overlooked [4, 5, 25, 33, 34]. A point to consider during every ultrasound scanning is that the diagnosis of polycystic ovarian morphology does not exclude other underlying causes of infertility as well as internal genitalia malformations.

Follicle Number and Size

The antral follicle count (AFC) is a direct quantitative marker of ovarian reserve and responsiveness [35]. The follicular number shows an annual loss of 0.35–0.95 antral follicles per year following the reproductive ageing of women [36]. There is a high correlation between AFC and reproductive age which is widely applicable in assisted reproduction treatments [37, 38]. The visible follicle by ultrasound means is the result of a sophisticated journey of an oocyte through the reproductive life of a female. A follicle is an oocyte surrounded by granulosa cells. The follicle grows by a small increase in the oocyte volume, a significant proliferation of the surrounding granulosa cells, and an expansion of the antral cavity. There are three stages of follicles: primordial, early growing, and antral [39, 40].

Primordial follicles have a very small size of less than 0.05 mm and are not visible [41]. Early growing follicles are less than 2 mm and comprise of large primary, secondary, preantral, early antral, and small antral follicles [39]. Several months are required for a new growing follicle to reach the preantral stage (0.15 mm) and 70 additional days to reach the size of 2 mm. Early growing follicle growth is unaffected by cyclic hormonal fluctuations and is regulated by subtle interactions between FSH and local factors produced by theca and granulosa cells, as well as the oocyte [42].

Only a small number of preantral follicles progress to antral stage which are more than 2 mm and become selectable during the late follicular phase [43]. From the time they enter the selectable stage during the late luteal phase, follicles become sensitive to cyclic changes of FSH in terms of granulosa cell proliferation. These are the follicles that contribute to the hormonal cyclic profile depicted in the classic diagram of the menstrual cycle. Indeed, as the follicle develops, its responsiveness to gonadotropins progressively increases under the control of local factors acting in an autocrine/paracrine fashion [42].

The number of these selectable follicles, especially the small antral (2–5 mm), is believed to reflect the number of remaining primordial

follicles and, thus, the ovarian reserve [44]. Their number is also strongly correlated with serum AMH levels [45]. The larger follicles >6 mm are totally gonadotropin dependent and one of them will evolve to dominant during the next follicular phase, while the rest will become atretic. So, in this phase, all other healthy follicles with granulosa cell activity tend not to exceed 6 mm, suggesting that all larger follicles are possibly atretic and do not reflect the actual reproductive capability of the woman [46, 47]. Exogenous gonadotropin administration during IVF rescues these small antral follicles from atresia and promotes their growth. Eventually, the retrieved oocytes by follicle aspiration come from this cohort of visible follicles.

PCOS is related to an excess in small antral follicles of 2–5 mm [16]. Although the pool of growing primary and secondary follicles in women with the syndrome is two- to threefold that of normal ovaries, the pool of primordial follicles is normal [48]. This excess is drastically involved in the follicular arrest of PCOS, presumably through an auto-inhibiting effect that could involve AMH. Still, the 6–9 mm follicles also appear to be affected by the unfavorable environment of the syndrome [49].

The follicle number, using two-dimensional (2D) ultrasound, is estimated both in longitudinal and anteroposterior cross sections of the ovaries, as the performer slowly moves the transducer from one side of the ovary to the other. After the identification of the ovary, a scout sweep is performed in the two planes and the largest follicle is localized. Then the counting is performed starting from the outer ovarian margin to the opposite. The procedure is repeated with the contralateral ovary [39]. It has been observed that the number of follicles counted by 2D is overestimated compared to oocytes retrieved, and even more in ovaries with many follicles as the polycystic when they are stimulated, possibly because of double counting (repetitions) and inclusion of atretic follicles [39, 50].

The size of follicles in 2D ultrasonography is expressed as the mean of the diameters measured on the two aforementioned sections [4, 5]. However, in clinical practice, three techniques are applied [51]. The first includes a single measurement of the maximal diameter in the longitudinal plane; the second includes an additional measurement of a diameter at 90° to the first; and the third is expanded to the measurement of a perpendicular to the previous two diameters in the transverse plane, after manual rotation of the transducer. In the latter two cases, the diameter is the mean of the two or three diameters, respectively.

Alternatively, the size of a follicle could be defined by its volume. For optimal in vitro fertilization (IVF) outcome, the follicular fluid volume should be more than 1 and up to 7 mL, which corresponds to a spheroid follicle of diameter of 12–24 mm [52]. The follicular volume can be calculated by 2D ultrasound from the mean diameter using the formula of a sphere: $4/3 \times \pi \times$ diameter [53]. When the mean diameter is estimated by the three follicular diameters, as described above, it is more accurate [51]. Follicles scarcely have the shape of a sphere; they usually are more elliptical, and therefore, the formula of a sphere does not provide an accurate estimation of the volume [54].

This matter has been addressed by the three-dimensional (3D) calculation of follicular volume which can be assessed by two ways: manually and automatically. The manual measurement is performed more often by the program Virtual Organ Computer-aided Analysis (VOCAL®). Initially, the data is acquired by an automatic mechanical sweep of the region ensuring that the entire ovary is included. The process is repeated for the contralateral ovary and the data are saved. The data are then processed using VOCAL. Each follicle is delineated manually by tracing around its perimeter and the volume of interest is calculated automatically.

The automatic technique is performed by the program Automatic Volume Calculation (SonoAVC®). The data are captured as described above and then processed by SonoAVC after right positioning. This program identifies every single follicle with a specific color and then automatically calculates the mean diameter (relaxed sphere diameter), the maximum dimensions (x, y, z), and the follicle volume (Fig. 7.1). This later method is highly valid and provides more

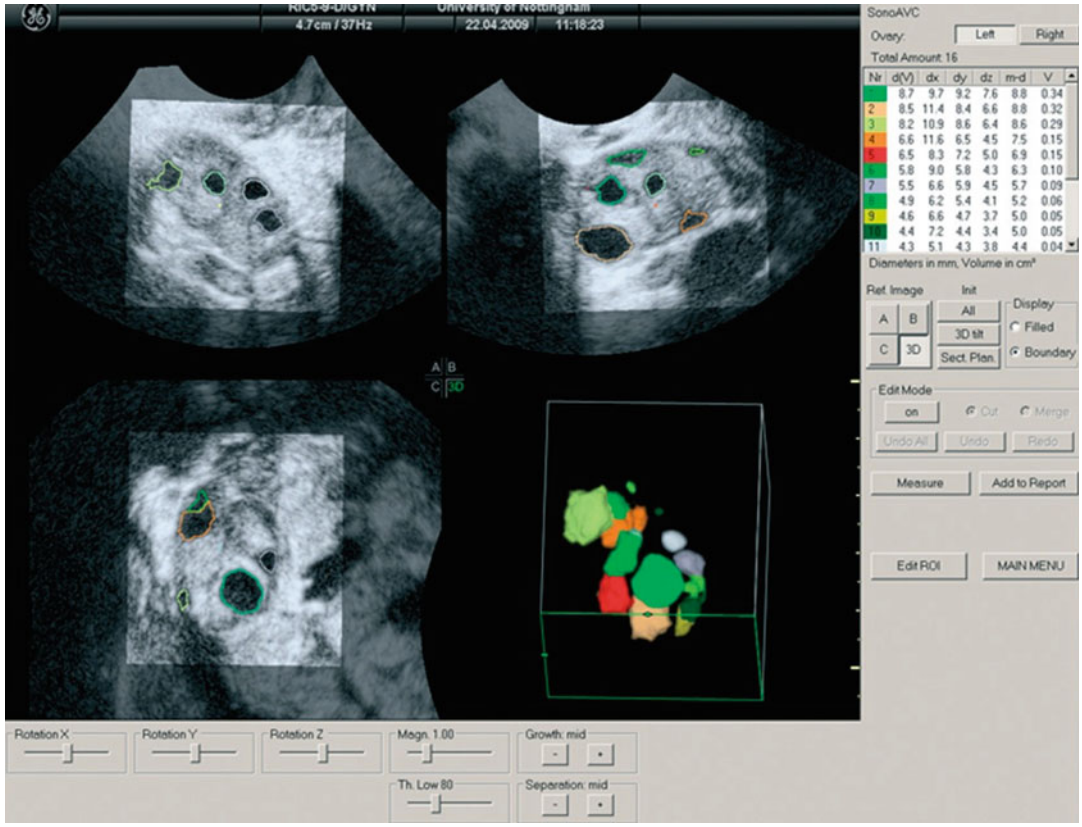

Fig. 7.1 Multiplanar display of an ovarian three-dimensional ultrasound dataset by SonoAVC. Each follicle has a specific color and its measurements are displayed on the right side (Reprinted from Deb et al. [47]. With permission from John Wiley & Sons, Inc.)

accurate values than those estimated from 2D measurements and automated measurements of follicular diameter as well as calculated using VOCAL [50, 51, 55].

Antral follicle count can also be performed by 3D ultrasound. Data are acquired as described above. There are three ways to count the follicles. In the first, the observer counts manually the follicles in a multiplanar view that is using all three perpendicular planes simultaneously in order to enhance the spatial awareness. In the second way, the ovary is defined by VOCAL, inversion mode is applied and the follicles are displayed without the surrounding ovarian tissue, and, finally, the counting is performed in multiplanar view (Figs. 7.2 and 7.3). In the last way, SonoAVC displays every single follicle in a specific color in an inversion mode, again without the ovarian tissue (Fig. 7.1). SonoAVC can distinguish follicles of 1–2 mm of diameter and provides the option of post-procession where manually the observer picks any missed follicles or excludes any that has been included incorrectly. Post-procession seems necessary since SonoAVC misses follicles of random sizes that are easily recognized in the multiplanar view due to their specific color [57].

Ovarian Volume

Women with PCOS have a larger ovarian volume [12, 15, 16, 58, 59]. The ovarian volume declines with age as the follicle both in women with PCOS and controls, but this decline does not correlate so well with age as the follicle number does [36, 60, 61]. The pattern of the ovarian volume falling in women with PCOS is different because declines less markedly than of controls despite

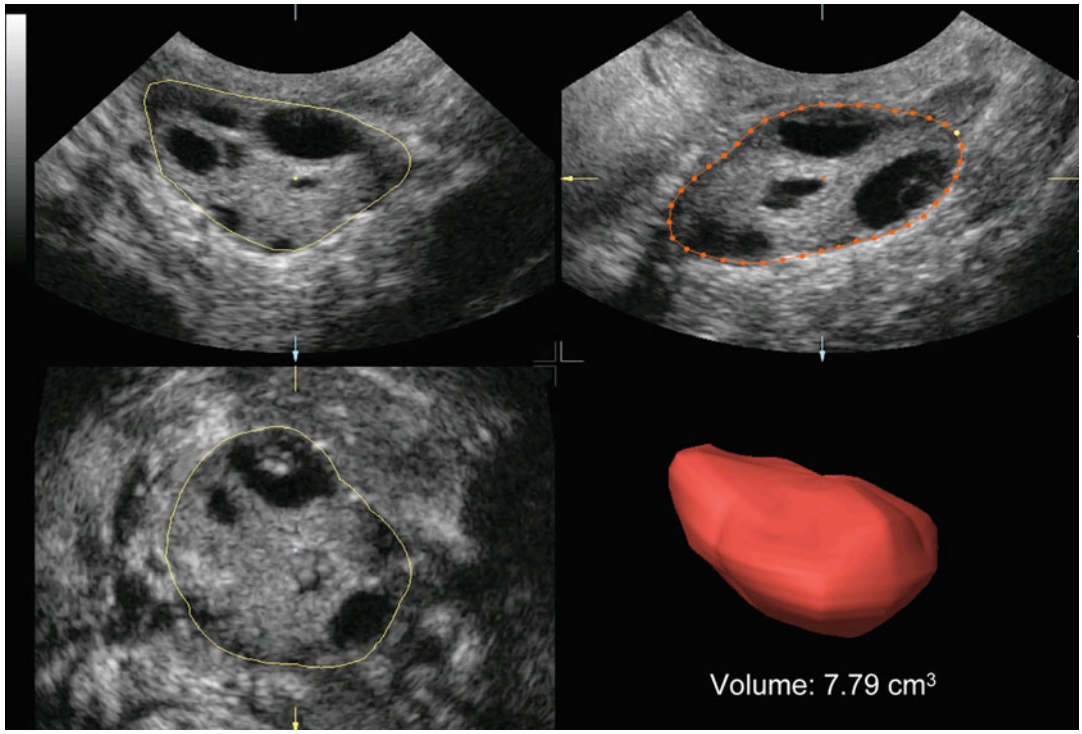

Fig. 7.2 Ovarian volume calculation using VOCAL before the application of inversion mode (Reprinted from Jayaprakasan et al. [56]. With permission from Oxford University Press)

the similar decline in follicle number. This fact suggests that the stroma plays a significant role [61, 62] and also the size of the follicles, because the decrease with age affects mainly the number of small follicles (2–6 mm) but not of bigger follicles (7–10 mm) in women with PCOS [63]. Alsamarai et al. demonstrated a linear decline in ovarian volume and concluded that age-dependent criteria for the diagnosis of PCOS are necessary [61]. This point could be of value in assisted reproduction field as the patients are very often more than 40 years old, but still in danger for OHSS.

The calculation of the ovarian volume is performed either using the formula for a prolate ellipsoid (0.5233 × length × width × thickness) [4, 5] or automatically by the software of the ultrasound equipment just outlining the ovary. The simplified formula, 0.5 × length × width × thickness, is practical and easy to use. The polycystic ovarian morphology is diagnosed when the ovarian volume exceeds 10 cm^3 [4, 5]. This consensus definition was based on the findings of studies that investigated the sensitivity and specificity of a diagnostic cutoff level [16, 58, 59]. However, other volume thresholds have been proposed subsequently [64, 65].

Again 3D ultrasound provides a more reliable, accurate, and reproducible assessment of ovarian volume than the 2D-based methods, with better spatial information and the ability to correct any shape irregularities [66–68]. 3D ultrasound also confirmed the greater ovarian volume of women with PCOS [69–72]. There two ways to calculate the ovarian volume: the conventional full planar technique and the VOCAL program. During the conventional method, the observer scrolls through one plane of the multiplanar display and simultaneously delineates the ovary in a different plane [68, 72]. With VOCAL program, the observer manually defines the contour of the ovary, while the dataset is rotated through 180° [72] (Fig. 7.4). Raine-Fenning et al. compared the two techniques and found that measurements with VOCAL program are superior to conventional, though comparable [72, 74].

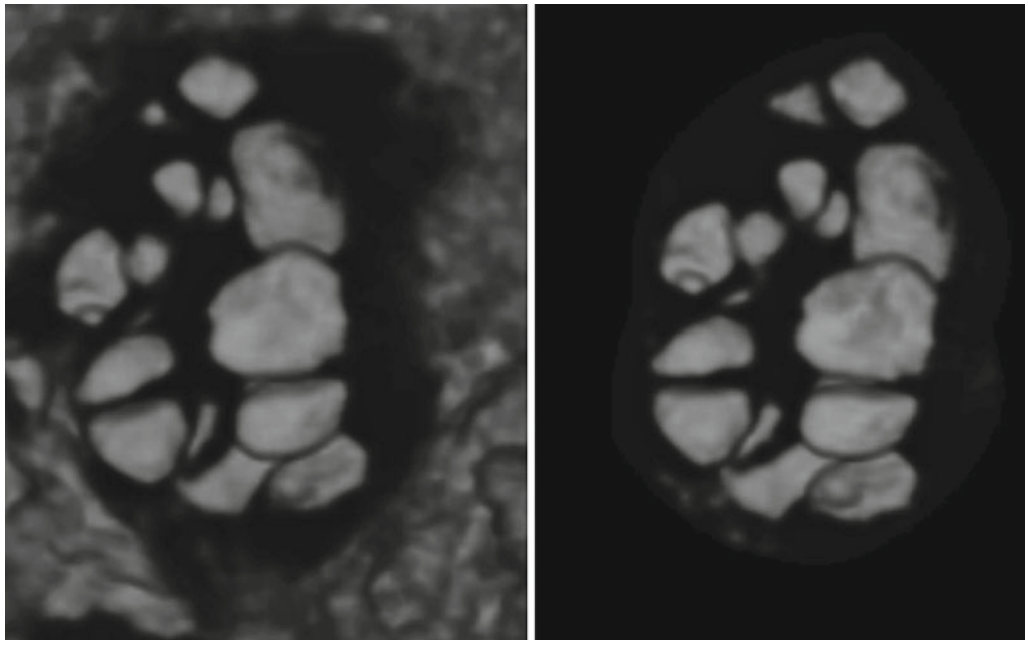

Fig. 7.3 Ovarian volume calculation using VOCAL after application of inversion mode (Reprinted from Jayaprakasan et al. [56]. With permission from Oxford University Press)

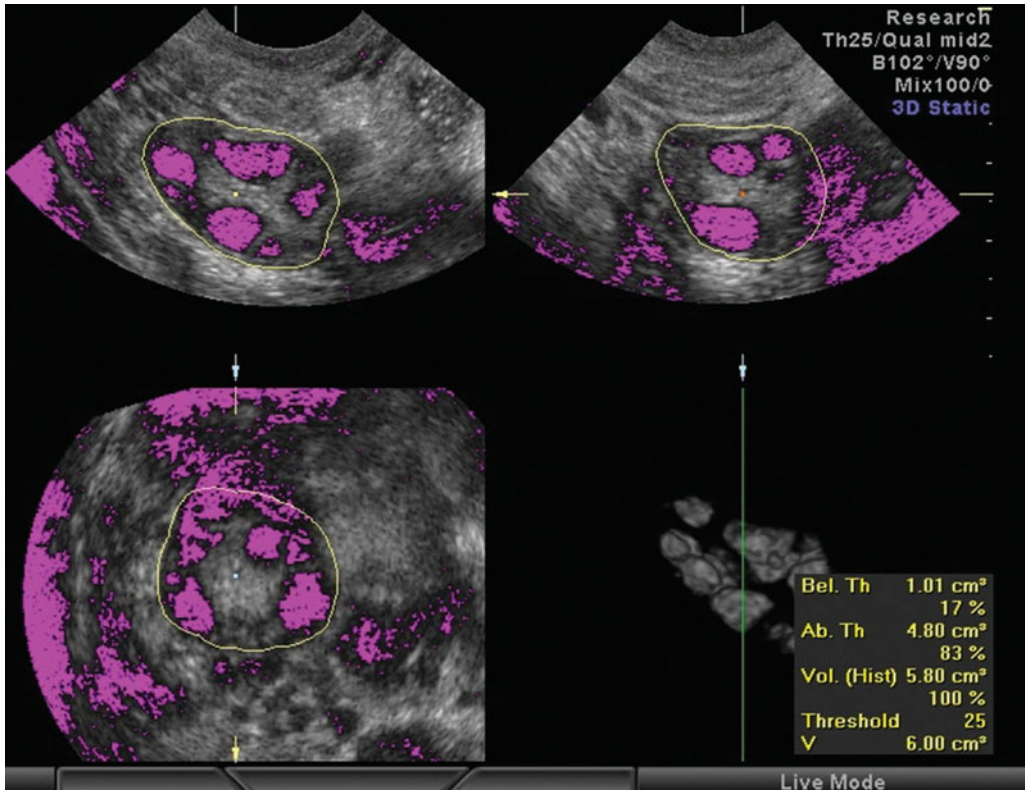

Fig. 7.4 Calculation of stromal volume determining the stromal and follicular area by setting a threshold of voxels (Reprinted from Lam et al. [73]. With permission from Oxford University Press)

Stromal Area, Volume, and Echogenicity

Despite the fact that increased stromal area and echogenicity are not included to the diagnostic criteria of PCOS, they are still characteristic ultrasonographic features of the syndrome [59, 75]. Patients with PCOS present higher stromal area and volume [59, 62, 73, 75–79] with the exception of a Chinese PCOS population [69]. Stromal hypertrophy is a common and specific indicator of ovarian hyperandrogenism [75]. The hypertrophic theca cells in the stroma of women with PCOS produce higher amounts of androgens [77]. Indeed, ovarian stromal area was found to correlate with androgen levels and Free Androgen Index (FAI) [62, 75, 80]. In clinical practice, the measurement of ovarian volume is a good surrogate for the stromal volume, because increased stromal volume is the main cause of ovarian enlargement in PCOS, except for patients taking contraceptive pills [4, 5, 12, 75].

Another marker of stromal hypertrophy is the stromal area to total ovarian area ratio (S/A). S/A is the stromal area defined by the periphery of the hyperechoic stroma divided by the total ovarian area defined by the perimeter of the ovary in the maximum plane section [81, 82]. Women with PCOS have a higher S/A value when compared to women with polycystic ovarian morphology or controls, whereas the last two groups do not differ significantly [79]. Furthermore, S/A ratio in women with PCOS correlates well with androstenedione, testosterone 17a-hydroxyprogesterone, FAI, and insulin levels [75, 79, 80, 82, 83]. S/A ratio could be the most efficient ultrasound performance for hyperandrogenism [34, 82]. In this line, a cutoff value of S/A of 0.32 is the best predictor of elevated androstenedione and testosterone levels. This cutoff value could be used in everyday clinical practice and even included in the diagnostic criteria of the syndrome [82, 83].

2D ultrasound measurement of stromal area can by performed by two ways: the manual and the semiautomatic. In the first method, the area is calculated using the formula for an ellipse: $\pi/4 \times \text{length} \times \text{width}$ ($0.78 \times \text{length} \times \text{width}$ or simplified to $0.8 \times \text{length} \times \text{width}$). In the second method the stromal area is defined by delineating its perimeter and is then calculated automatically by the ultrasound machine [12]. 3D measurement of stromal volume is achieved either after the calculation and subtraction of the total follicular volume from the total ovarian volume [62, 77] (these 3D techniques have already been described in the previous paragraphs) or using VOCAL program and by determining a limit area (number of voxels) which determines the stromal and follicular area (Fig. 7.4). Thus, above and below the limit are calculated the stromal and the follicular area, respectively [77].

Stromal echogenicity had been a key feature for many years [59, 84, 85] until the first more objective assessments showed that there was no significant difference in stromal echogenicity between women with PCOS and controls [76, 86]. 2D ultrasound measurement of stromal echogenicity can be either a subjective operator assessment [59, 84, 85] or an objective calculation derived by the intensity level of the ultrasound pixels within the stroma displayed on the sonographic image [81]. The difference found with the first subjective measurements was attributed to increased volume of ovarian stroma in relation to the lower mean echodensity of the ovary due to the higher number of follicles [76]. Another marker of echogenicity is the stromal index which is the ratio of the mean stromal echogenicity to the mean ovarian (total) echogenicity [86]. Stromal index was found higher in PCOS [76] but this was not confirmed [86].

3D ultrasound assessments of stromal echogenicity were in accordance with the 2D objective calculations which showed no difference between women with PCOS and controls [77, 78, 87, 88]. The 3D assessment of echogenicity is performed by the mean gray (MG) value that is calculated automatically by the VOCAL program (Fig. 7.5). The MG value represents the mean tissue density of a defined area and is calculated by the mean signal intensity of the gray-scale voxels [77, 87, 88]. 3D ultrasound is considered more appropriate for the quantification of the stromal echogenicity especially for research purposes [71].

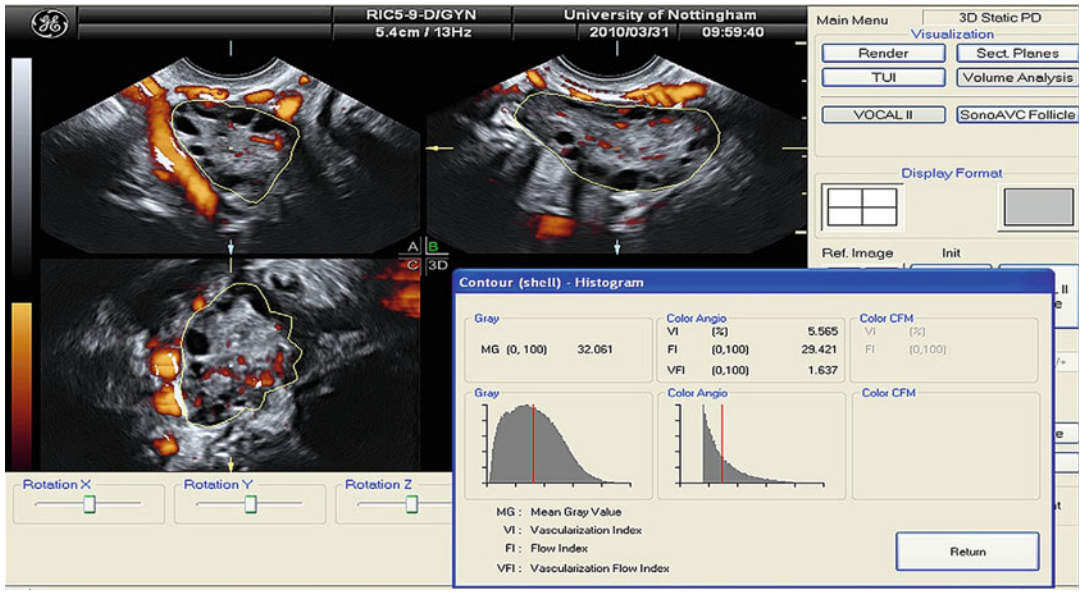

Fig. 7.5 Mean gray value (MG) and 3D power Doppler indices within the ovarian volume delineated using VOCAL (Reprinted from Deb et al. [89]. With permission from Elsevier)

Ovarian Stromal Blood Flow

The ovarian stromal blood flow was traditionally believed to be higher in women with PCOS compared to controls [12, 70, 90–95] until the publication of some contradictory studies [77, 78, 96, 97]. The higher blood flow was explained by the reduced resistance in the ovarian and stromal vessels found by some investigators [92, 93]. Interestingly, the results of both 2D and 3D ultrasound examinations are conflicting. The controversy in literature could be explained by the different study designs, selection of controls, criteria used for the definition of PCOS, the lack of hormonal assessments, the variety in ultrasound equipment and settings, and, finally, the arbitrary selection of vessels in 2D ultrasound [77, 97].

2D ultrasound assessment of blood flow could be subjective through color Doppler maps that are no longer used or objective by measuring flow velocity and resistance with pulsed-wave Doppler (PWD). PWD is used to depict the flow velocity waveform from the vessel of interest. Angle correction is applied whenever necessary to fit the incident beam. The waveforms are then analyzed manually (at least three optimal waveforms in a row) or automatically to calculate peak systolic velocity (PSV), end-diastolic velocity (EDV), resistance index (RI), pulsatility index (PI), and, lately, capacitance index (CI), which is the area under the curve for the diastolic part of the waveform, and S/D ratio that is the ratio of the PSV divided by the EDV [77, 97]. A strong correlation was reported between stromal PI and LH/FSH [98].

3D ultrasound assessment of blood flow is easy to perform. When the power Doppler signal is optimal, the 3D volume box is opened and a 3D sweep scan is performed. Then the VOCAL program quantifies the information using the histogram facility, and the blood flow indices are calculated automatically (Fig. 7.5). Vascularization index (VI) represents the ratio of color voxels within the total dataset relative to both color and gray information, providing, thus, an indication of the number and/or size of the vessels lying in the area of interest and, therefore, the degree of vascularity. Flow index (FI) is the mean power Doppler intensity, and as the intensity of the signal is dependent on the number of erythrocytes within a given volume at any time, this index is considered reflective of the volume

flow rate. Vascularization flow index (VFI) represents the ratio of the weighted color voxels to total voxels and gives a unified value for both vascularity and volume flow reflecting the tissue perfusion [99].

These indices are all significantly affected by volume flow, attenuation, vessel number, and erythrocyte density, but in different ways. The VI and VFI seem to have a more predictable relationship, whereas the FI often demonstrates a more complex cubic relationship that is not always logical. Further work is required before a better understanding of 3D power Doppler ultrasound imaging is achieved [100]. However, the findings are controversial even with 3D power Doppler. Some studies showed increased vascularity and blood flow in the ovaries of women with PCOS [88, 101–103] explained possibly by the higher vascular endothelial growth factor (VEGF), while others did not report any significant difference [69, 77, 78, 87, 88]. Higher ovarian VFI was correlated with lower BMI, hyperandrogenism, greater LH/FSH values, ovarian volumes, and follicle numbers [77, 78, 103]. The 3D ultrasound approach is preferable because it provides the possibility to examine the blood flow and vascularization in the whole ovary, avoiding the arbitrary selection of a single vessel, or even to define a region and calculate separately the flow within and around this region [71, 104].

Uterine Size and Perfusion

Literature references upon uterine ultrasound characteristics in PCOS are scarce. The uterine volume has been found either smaller [105, 106] or bigger [15, 107] in women with PCOS and lower in 40 % of adolescent with the syndrome [108], and also in correlation with LH [107]. In few studies, a new criterion was suggested, the ratio of ovarian to uterine volume with an upper limit of 1.0 which was doubted and abandoned [106, 109]. Endometrial thickness was diverse in women and adolescents with PCOS [108, 110, 111] without correlation with the time interval since the last period [108]. Nevertheless, in a recent study, there was no difference in endometrial thickness and volume between women with PCOS and controls [112].

The uterine and endometrial blood flow was found lower in women with PCOS [91, 92, 103, 108, 113–117] with the exemption of a recent study [112]. The lower uterine and endometrial blood perfusion is reflected in higher values of Doppler indices as PI and RI in PCOS and is correlated with obesity and hyperandrogenemia (higher levels of androstenedione, DHEAS, and LH/FSH) [91, 92, 116, 117]. Furthermore, uterine perfusion increases with exogenous estrogen and progesterone as well as antiandrogen administration [113, 118], while there is a significant negative correlation between estrogens and uterine PI [119]. This impaired uterine perfusion was associated with metabolic disorders and risk factors for cardiovascular events [114, 115]. The only study to investigate the endometrial blood flow with 3D Doppler did not reveal any significant difference between PCOS and controls in 2D pulsed-wave (uterine arteries) and 3D power Doppler (endometrial and subendometrial blood flow) indices, apart from significantly disturbed endometrial perfusion in women with PCOS and clinical signs of hyperandrogenemia diagnosed only by 3D Doppler [112].

Ultrasound and Assisted Reproduction Outcome

The poorer clinical outcome of assisted reproduction in women with PCOS has been associated with adverse factors interfering with every stage of therapeutic process from impaired folliculogenesis and lower quality oocytes to higher incidence of recurrent miscarriages. Despite the importance, there are no sufficient knowledge regarding the clinical outcome in women with PCOS, and in some fields the data are contradictory. In general, ultrasound is considered helpful to predict fertility outcome in PCOS [34]; however, it seems that the most important contribution, currently, is the diagnosis of polycystic ovarian morphology.

Ovarian drilling is an effective, although interventional, therapy of anovulatory infertility in women with PCOS. The success of ovarian drilling could be estimated with ultrasound given that the ovarian volume reduces 3 weeks after intervention [120] and also the stromal blood flow in the early follicular phase of the first post-operative cycle or 3 months after drilling [101, 102, 121]. The 3D Doppler assessment showed significantly higher ovarian stromal VI, FI, and VFI coexisting with higher AMH levels in PCOS compared to controls before drilling and decreased ovarian blood flow and AMH concentrations after drilling [101, 102]. Though, there was no difference in stromal blood perfusion between responders (spontaneous ovulation after ovarian drilling) and nonresponders with PCOS [102] and any clinical outcome report.

The basal stromal flow measurement is considered to have no predictive value in PCOS with regard to pregnancy, since the flow indices between conception and non-conception cycles in women with PCOS undergoing IVF are similar [97, 122]. Nevertheless, the stromal blood perfusion has been proven the most relevant predictor of ovarian response to controlled ovarian stimulation compared to ovarian or stromal volume [76, 122]. Jarvela et al. compared the vascularization per follicle between women with PCOS and controls, after pituitary suppression during IVF. Women with PCOS had lower ovarian vascularization per follicle and demanded lower doses of FSH to achieve a similar level of vascularization after stimulation with FSH and hCG administration [87]. Moreover, there was a significant positive correlation between the number of retrieved oocytes and vascularized ovarian volume after stimulation. Still, the calculation of ovarian vascularization per follicle was ambiguous and there was no report to clinical outcome.

PCOS is also associated with recurrent miscarriages [123]. Likewise, hyperandrogenemia has been reported as a serious etiology of recurrent pregnancy loss, regardless of PCOS, possibly due to lower endometrial and subendometrial blood perfusion secondary to elevated uterine arterial resistance [124–131]. Altogether, higher uterine resistance and lower ovarian stromal resistance, as reported in women with PCOS due to hyperandrogenemia and unopposed estrogens, are indicative of failure of conception in IVF and recurrent miscarriage. Thus, further research and maybe threshold value establishment, especially, in 3D power Doppler could contribute to a prognosis algorithm of failed implantation and miscarriage in women with PCOS undergoing assisted reproduction.

Ultrasound and Prevention of OHSS

Ovarian hyperstimulation syndrome is a rare (less than 5 %) but serious iatrogenic complication of controlled ovarian hyperstimulation, concerning particularly patients with PCOS, with significant health risk for the affected women [132–135]. A great number of women undergoing controlled ovarian stimulation develop mild OHSS with symptoms such as abdominal bloating and discomfort; however, the development of moderate and severe OHSS could be fatal [133, 136]. Therefore, the identification of women who could manifest moderate or severe OHSS during ovarian stimulation is important, as would allow adequate designing or modification of the stimulation protocol and dose of gonadotropin to reduce the risk. Currently, AMH and antral follicle count are the most prominent predictive factors [137]. Several thresholds for follicle number have also been proposed up to date, as >20 or >14 and >18 but not conclusively [137, 138].

Nevertheless, other predictive factors and models including age, number of follicles, estrogen concentrations, and ovarian blood flow have been proposed [71, 137–139]. Doppler blood flow velocities in the ovarian vessels were found higher in women who developed OHSS [139]. Though, a recent study with 3D ultrasound assessments showed that women who develop OHSS do not demonstrate increased ovarian blood flow and the only discriminative factor was the significantly higher antral follicle count [140]. A possible increase in blood flow in parallel with higher VEGF and gonadotropin levels could trigger OHSS [101, 141], while a decrease

in stromal blood flow after ovarian drilling could reduce the occurrence of OHSS [101].

In any case, the ultrasound finding of polycystic ovarian morphology, even in the absence of PCOS, is a serious predisposing factor for OHSS [12, 25] and should be taken into account when designing a controlled stimulation protocol or planning the cycle monitoring. Prompt modification and alertness for symptoms is advised.

Future Points

Ultrasound examination has an outstanding position in the diagnosis and management of women with PCOS. However, there is still place for improvement and many matters that should be addressed. The research regarding the ultrasound evaluation and the diagnostic and prognostic markers of PCOS is insufficient. The methodology and mainly the diagnostic criteria applied in existing studies are not unanimous and widely accepted. The heterogenous phenotypic spectrum of the syndrome renders necessary the clustered investigation both of clinical and ultrasound indices as well as the correlation of hormonal findings with the clinical practice. Definitely, literature regarding ultrasound characteristics of women with PCOS who undergo assisted reproduction therapies is scarce. Finally, the application of 3D ultrasound seems promising, at least in research level, as it provides better spatial awareness, more objective volumetric and vascularization assessment, reduced scanning time, and better intra- and interobserver variability, despite the higher cost and training requirements. Nevertheless, 3D ultrasound does not seem to add much in clinical practice for the present.

References

1. Franks S. Polycystic ovary syndrome. N Engl J Med. 1995;333:853–61. Erratum in: N Engl J Med. 1995; 333:1435.
2. Diamanti-Kandarakis E, Kouli CR, Bergiele AT, Filandra FA, Tsianateli TC, Spina GG, Zapanti ED, Bartzis MI. A survey of the polycystic ovary syndrome in the Greek island of Lesbos: hormonal and metabolic profile. J Clin Endocrinol Metab. 1999;84: 4006–11.
3. Zawadzki JA, Dunaif A. Diagnostic criteria for polycystic ovary syndrome: towards a rational approach. In: Dunaif A, Givens JR, Haseltine FP, Merriam GR, editors. Polycystic ovary syndrome. Boston: Blackwell Scientific; 1992. p. 377–84.
4. The Rotterdam ESHRE/ASRM-sponsored PCOS consensus workshop group. Revised 2003 consensus on diagnostic criteria and long-term health risks related to polycystic ovary syndrome (PCOS). Hum Reprod. 2004;19:41–7.
5. The Rotterdam ESHRE/ASRM-sponsored PCOS consensus workshop group. Revised 2003 consensus on diagnostic criteria and long-term health risks related to polycystic ovary syndrome (PCOS). Fertil Steril. 2004;81:19–25.
6. Karkanaki A, Piouka A, Katsikis I, Farmakiotis D, Macut D, Panidis D. Adiponectin levels reflect the different phenotypes of polycystic ovary syndrome: study in normal weight, normoinsulinemic patients. Fertil Steril. 2009;92:2078–81.
7. Diamanti-Kandarakis E, Panidis D. Unraveling the phenotyping map of polycystic ovary syndrome (PCOS): a prospective study of 634 women with PCOS. Clin Endocrinol (Oxf). 2007;67:735–42.
8. Polson DW, Adams J, Wadsworth J, Franks S. Polycystic ovaries-a common finding in normal women. Lancet. 1988;1:870–2.
9. Clayton RN, Ogden V, Hodgkinson J, Worswick L, Rodin DA, Dyer S, et al. How common are polycystic ovaries in normal women and what is their significance for the fertility of the population? Clin Endocrinol (Oxf). 1992;37:127–34.
10. Azziz R, Carmina E, Dewailly D, Diamanti-Kandarakis E, Escobar-Morreale HF, Futterweit W, Janssen OE, Legro RS, Norman RJ, Taylor AE, Witchel SF, Androgen Excess Society. Positions statement: criteria for defining polycystic ovary syndrome as a predominantly hyperandrogenic syndrome: an Androgen Excess Society guideline. J Clin Endocrinol Metab. 2006;91:4237–45.
11. Christensen JT, Boldsoen J, Westergaard JG. Ovarian volume in gynecologically healthy women using contraception or using IUD. Acta Obstet Gynecol Scand. 1997;76:784–9.
12. Balen AH, Laven JSE, Tan SL, Dewailly D. Ultrasound assessment of the polycystic ovary: international consensus definitions. Hum Reprod. 2003;9:505–14.
13. Zaidi J, Jurkovic D, Campbell S, Pitroff R, McGregor A, Tan SL. Description of circadian rhythm in uterine artery blood flow indices during the peri-ovulatory period. Hum Reprod. 1995;10:1642–6.
14. Zaidi J, Tan SL, Pitroff R, Campbell S, Collins W. Blood flow changes in the intra-ovarian arteries during the peri-ovulatory period-relationship to the time of day. Ultrasound Obstet Gynecol. 1996;7:135–40.
15. Adams J, Franks S, Polson DW, Mason HD, Abdulwahid N, Tucker M, Morris DV, Price J, Jacobs HS. Multifollicular ovaries: clinical and endocrine

features and response to pulsatile gonadotropin releasing hormone. Lancet. 1985;2:1375–9.
16. Jonard S, Robert Y, Cortet-Rudelli C, Pigny P, Decanter C, Dewailly D. Ultrasound examination of polycystic ovaries: is it worth counting the follicles? Hum Reprod. 2003;18:598–603.
17. Jonard S, Dewailly D, Pigny P, Robert Y, Decanter C. What are the determinants of the antral follicle number at ovarian ultrasonography (U/S) in PCOS? ESHRE Congress, Madrid, 29 June to 3 July 2003, oral communication, 0–119. Hum Reprod. 2003;18 Suppl 1:42.
18. Raine-Fenning N. What's in a number? The polycystic ovary revisited. Hum Reprod. 2011;11:3118–22.
19. Balen AH, Dunger D. Pubertal maturation of the internal genitalia. Ultrasound Obstet Gynecol. 1995; 6:164–5.
20. Johnstone EB, Rosen MP, Neril R, Trevithick D, Sternfeld B, Murphy R, Addauan-Andersen C, McConnell D, Pera RR, Cedars MI. The polycystic ovary post-rotterdam: a common, age-dependent finding in ovulatory women without metabolic significance. J Clin Endocrinol Metab. 2010;95:4965–72.
21. Azziz R, Carmina E, Dewailly D, Diamanti-Kandarakis E, Escobar-Morreale HF, Futterweit W, Janssen OE, Legro RS, Norman RJ, Taylor AE, Witchel SF, Task Force on the Phenotype of the Polycystic Ovary Syndrome of The Androgen Excess and PCOS Society. The Androgen Excess and PCOS Society criteria for the polycystic ovary syndrome: the complete task force report. Fertil Steril. 2009;91:456–88.
22. Adams JM, Taylor AE, Crowley Jr WF, Hall JE. Polycystic ovarian morphology with regular ovulatory cycles: insights into the pathophysiology of polycystic ovarian syndrome. J Clin Endocrinol Metab. 2004;89:4343–50.
23. Kousta E, Cela E, Lawrence N, Penny A, Millauer B, White D, et al. The prevalence of polycystic ovaries in women with a history of gestational diabetes. Clin Endocrinol (Oxf). 2000;53:501–7.
24. Koivunen R, Laatikainen T, Tomas C, Huhtaniemi I, Tapanainen J, Martikainen H. The prevalence of polycystic ovaries in healthy women. Acta Obstet Gynecol Scand. 1999;78:137–41.
25. Swanton A, Storey L, McVeigh E, Child T. IVF outcome in women with PCOS, PCO and normal ovarian morphology. Eur J Obstet Gynecol Reprod Biol. 2010;149:68–71.
26. Esinler I, Bayar U, Bozdag G, Yarali H. Outcome of intracytoplasmic sperm injection in patients with polycystic ovary syndrome or isolated polycystic ovaries. Fertil Steril. 2005;84:932–7.
27. McDougall MJ, Tan SL, Jacobs HS. IVF and the ovarian hyperstimulation syndrome. Hum Reprod. 1992;5:597–600.
28. Sahu B, Ozturk O, Ranierri M, Serhal P. Comparison of oocyte quality and intracytoplasmic sperm injection outcome in women with isolated polycystic ovaries or polycystic ovarian syndrome. Arch Gynecol Obstet. 2008;277:239–44.
29. Elting MW, Kwee J, Schats R, Rekers-Mombarg LT, Schoemaker J. The rise of estradiol and inhibin B after acute stimulation with follicle-stimulating hormone predict the follicle cohort size in women with polycystic ovary syndrome, regularly menstruating women with polycystic ovaries, and regularly menstruating women with normal ovaries. J Clin Endocrinol Metab. 2001;86:1589–95.
30. Catteau-Jonard S, Bancquart J, Poncelet E, Lefebvre-Maunoury C, Robin G, Dewailly D. Polycystic ovaries at ultrasound: normal variant or silent Polycystic Ovary Syndrome? Ultrasound Obstet Gynecol. 2012;40(2):223–9. doi:10.1002/uog.11202.
31. Eldar-Geva T, Margalioth EJ, Gal M, Ben-Chetrit A, Algur N, Zylber-Haran E, Brooks B, Huerta M, Spitz IM. Serum anti-Mullerian hormone levels during controlled ovarian hyperstimulation in women with polycystic ovaries with and without hyperandrogenism. Hum Reprod. 2005;20:1814–9.
32. Engmann L, DiLuigi A, Schmidt D, Nulsen J, Maier D, Benadiva C. The use of gonadotropin-releasing hormone (GnRH) agonist to induce oocyte maturation after cotreatment with GnRH antagonist in high-risk patients undergoing in vitro fertilization prevents the risk of ovarian hyperstimulation syndrome: a prospective randomized controlled study. Fertil Steril. 2008;89:84–91.
33. Son WY, Tan SL. Laboratory and embryological aspects of hCG-primed in vitro maturation cycles for patients with polycystic ovaries. Hum Reprod Update. 2010;16:675–89.
34. Nardo LG, Gelbaya TA. Evidence-based approach for the use of ultrasound in the management of polycystic ovary syndrome. Minerva Ginecol. 2008;60: 83–9.
35. Broekmans FJ, Kwee J, Hendriks DJ, Mol BW, Lambalk CB. A systematic review of tests predicting ovarian reserve and IVF outcome. Hum Reprod Update. 2006;12:685–718.
36. Scheffer GJ, Broekmans FJ, Dorland M, Habbema JD, Looman CW, te Velde ER. Antral follicle counts by transvaginal ultrasonography are related to age in women with proven natural fertility. Fertil Steril. 1999;72:845–51.
37. Kline J, Kinney A, Kelly A, Reuss ML, Levin B. Predictors of antral follicle count during the reproductive years. Hum Reprod. 2005;20:2179–89.
38. Broer SL, Mol BW, Hendriks D, Broekmans FJ. The role of antimüllerian hormone in prediction of outcome after IVF: comparison with the antral follicle count. Fertil Steril. 2009;91:705–14.
39. Broekmans FJM, de Ziegler D, Howles CM, Gougeon A, Trew G, Olivennes F. The antral follicle count: practical recommendations for better standardization. Fertil Steril. 2010;94:1044–51.
40. Craig J, Orisaka M, Wang H, Orisaka S, Thompson W, Zhu C, et al. Gonadotropin and intra-ovarian signals regulating follicle development and atresia: the delicate balance between life and death. Front Biosci. 2007;12:3628–39.

41. Charleston JS, Hansen KR, Thyer AC, Charleston LB, Gougeon A, Siebert JR, et al. Estimating human ovarian non-growing follicle number: the application of modern stereology techniques to an old problem. Hum Reprod. 2007;22:2103–10.
42. Gougeon A. Human ovarian follicular development: from activation of resting follicles to preovulatory maturation. Ann Endocrinol (Paris). 2010;71: 132–43.
43. Gougeon A. Regulation of ovarian follicular development in primates: facts and hypotheses. Endocr Rev. 1996;17:121–55.
44. Broekmans FJ, Faddy MJ, Scheffer G, te Velde ER. Antral follicle counts are related to age at natural fertility loss and age at menopause. Menopause. 2004;11:607–14.
45. van Rooij IA, Broekmans FJ, te Velde ER, Fauser BC, Bancsi LF, de Jong FH, et al. Serum anti-Mullerian hormone levels: a novel measure of ovarian reserve. Hum Reprod. 2002;17:3065–71.
46. Gougeon A. Ovarian follicular growth in humans: ovarian ageing and population of growing follicles. Maturitas. 1998;30:137–42.
47. Deb S, Campbell BK, Clewes JS, Raine-Fenning NJ. Quantitative analysis of antral follicle number and size: a comparison of two-dimension and automated three-dimension ultrasound techniques. Ultrasound Obstet Gynecol. 2010;35:354–60.
48. Webber LJ, Stubbs S, Stark J, Trew GH, Margara R, Hardy K, Franks S. Formation and early development of follicles in the polycystic ovary. Lancet. 2003;362: 1017–21.
49. Dewailly D, Catteau-Jonard S, Reyss AC, Maunoury-Lefebvre C, Poncelet E, Pigny P. The excess in 2–5 mm follicles seen at ovarian ultrasonography is tightly associated to the follicular arrest of the polycystic ovary syndrome. Hum Reprod. 2007;22:1562–6.
50. Raine-Fenning N, Jayaprakasan K, Clewes J. Automated follicle tracking facilitates standardization and may improve work flow. Ultrasound Obstet Gynecol. 2007;30:1015–8.
51. Raine-Fenning N, Jayaprakasan K, Clewes J, Joergner I, Bonaki SD, Chamberlain S, Devlin L, Priddle H, Johnson I. SonoAVC: a novel method of automatic volume calculation. Ultrasound Obstet Gynecol. 2008;31:691–6.
52. Wittmaack FM, Kreger DO, Blasco L, Tureck RW, Mastroianni Jr L, Lessey BA. Effect of follicular size on oocyte retrieval, fertilization, cleavage, and embryo quality in in vitro fertilization cycles: a 6-year data collection. Fertil Steril. 1994;62:1205–10.
53. Amer A, Hammadeh ME, Kolkailah M, Ghandour AA. Three-dimensional versus two-dimensional ultrasound measurement of follicular volume: are they comparable? Arch Gynecol Obstet. 2003;268: 155–7.
54. Penzias AS, Emmi AM, Dubey AK, Layman LC, DeCherney AH, Reindollar RH. Ultrasound prediction of follicle volume: is the mean diameter reflective? Fertil Steril. 1994;62:1274–6.
55. Ata B, Tulandi T. Ultrasound automated volume calculation in reproduction and in pregnancy. Fertil Steril. 2011;95:2163–70.
56. Jayaprakasan K, Hilwah N, Kendall NR, Hopkisson JF, Campbell BK, Johnson IR, Raine-Fenning NJ. Does 3D ultrasound offer any advantage in the pretreatment assessment of ovarian reserve and prediction of outcome after assisted reproduction treatment? Hum Reprod. 2007;22:1932–41.
57. Deb S, Jayaprakasan K, Campbell BK, Clewes JS, Johnson IR, Raine-Fenning NJ. Intraobserver and interobserver reliability of automated antral follicle counts made using three-dimensional ultrasound and SonoAVC. Ultrasound Obstet Gynecol. 2009;33: 477–83.
58. Van Santbrink EJ, Hop WC, Fauser BC. Classification of normogonadotropin infertility: polycystic ovaries diagnosed by ultrasound versus endocrine characteristics of PCOS. Fertil Steril. 1997;67:452–8.
59. Pache TD, Hop WC, Wladimiroff JW, Schipper J, Fauser BC. How to discriminate between normal and polycystic ovaries. Radiology. 1992;17:589–93.
60. Erdem A, Erdem M, Biberoglu K, Hayit O, Arslan M, Gursoy R. Age-related changes in ovarian volume, antral follicle counts and basal FSH in women with normal reproductive health. J Reprod Med. 2002;47: 835–9.
61. Alsamarai S, Adams JM, Murphy MK, Post MD, Hayden DL, Hall JE, Welt CK. Criteria for polycystic ovarian morphology in polycystic ovary syndrome as a function of age. J Clin Endocrinol Metab. 2009;94: 4961–70.
62. Kyei-Mensah A, Tan SL, Zaidi J, Jacobs HS. Relationship of ovarian stromal volume to serum androgen concentrations in patients with polycystic ovary syndrome. Hum Reprod. 1998;13: 1437–41.
63. Haadsma ML, Bukman A, Groen H, Roeloffzen EM, Groenewoud ER, Heineman MJ, et al. The number of small antral follicles (2-6mm) determines the outcome of endocrine ovarian reserve tests in a subfertile population. Hum Reprod. 2007;22:1925–31.
64. Allemand MC, Tummon IS, Phy JL, Foong SC, Dumesic DA, Session DR. Diagnosis of polycystic ovaries by three-dimensional transvaginal ultrasound. Fertil Steril. 2006;85:214–9.
65. Dewailly D, Gronier H, Poncelet E, Robin G, Leroy M, Pigny P, Duhamel A, Catteau-Jonard S. Diagnosis of polycystic ovary syndrome (PCOS): revisiting the threshold values of follicle count on ultrasound and of the serum AMH level for the definition of polycystic ovaries. Hum Reprod. 2011;26:3123–9.
66. Jayaprakasan K, Campbell BK, Clewes JS, Johnson IR, Raine-Fenning NJ. Three-dimensional ultrasound improves the interobserver reliability of antral follicle counts and facilitates increased clinical work flow. Ultrasound Obstet Gynecol. 2008;31:439–44.
67. Raine-Fenning NJ, Campbell BK, Clewes JS, Johnson IR. The interobserver reliability of ovarian volume measurement is improved with

three-dimensional ultrasound, but dependent upon technique. Ultrasound Med Biol. 2003;29:1685–90.
68. Kyei-Mensah A, Maconochie N, Zaidi J, Pittrof R, Campbell S, Tan SL. Transvaginal three-dimensional ultrasound: accuracy of ovarian follicular volume measurements. Fertil Steril. 1996;65:371–6.
69. Ng EH, Chan CC, Yeung WS, Ho PC. Comparison of ovarian stromal blood flow between fertile women with normal ovaries and infertile women with polycystic ovary syndrome. Hum Reprod. 2005;20:1881–6.
70. Pan HA, Wu MH, Cheng YC, Li CH, Chang FM. Quantification of Doppler signal in polycystic ovarian syndrome using 3D power Doppler ultrasonography. Hum Reprod. 2002;17:2484–8.
71. Lam PM, Raine-Fenning NJ. The role of three-dimensional ultrasonography in polycystic ovary syndrome. Hum Reprod. 2006;21:2209–15.
72. Raine-Fenning NJ, Clewes JS, Kendall NR, Bunkheila AK, Campbell BK, Johnson IR. The interobserver reliability and validity of volume calculation from three-dimensional ultrasound datasets in the in vitro setting. Ultrasound Obstet Gynecol. 2003;21:283–91.
73. Lam PM, Johnson IR, Raine-Fenning NJ. Three-dimensional ultrasound features of the polycystic ovary and the effect of different phenotypic expressions on these parameters. Hum Reprod. 2007;22:3116–23.
74. Dewailly D, Robert Y, Helin I, Ardaens Y, Thomas-Desrousseaux P, Lemaitre L, Fossati P. Ovarian stromal hypertrophy in hyperandrogenic women. Clin Endocrinol (Oxf). 1994;41:557–62.
75. Buckett WM, Bouzayen R, Watkin KL, Tulandi T, Tan SL. Ovarian stromal echogenicity in women with normal and polycystic ovaries. Hum Reprod. 1999;14: 618–21.
76. Yoo RY, Sirlin CB, Gottschalk M, Chang RJ. Ovarian imaging by magnetic resonance in obese adolescent girls with polycystic ovary syndrome: a pilot study. Fertil Steril. 2005;84:985–95.
77. Lam P, Raine-Fenning NJ, Cheung L, Haines C. Three-dimensional ultrasound features of the polycystic ovary in Chinese women. Ultrasound Obstet Gynecol. 2009;34:196–200.
78. Fulghesu AM, Ciampelli M, Belosi C, Apa R, Pavone V, Lanzone A. A new ultrasound criterion for the diagnosis of polycystic ovary syndrome: the ovarian stroma/total area ratio. Fertil Steril. 2001;76:326–31.
79. Pache TD, de Jong FH, Hop WC, Fauser BCJM. Association between ovarian changes assessed by transvaginal sonography and clinical and endocrine signs of the polycystic ovary syndrome. Fertil Steril. 1993;59:544–9.
80. Lam PM, Raine-Fenning N. Polycystic ovarian syndrome: a misnomer for an enigmatic disease. Ultrasound Obstet Gynecol. 2009;33:621–7.
81. Fulghesu A, Angioni S, Frau E, Belosi C, Apa R, Mioni R, Xamin N, Capobianco GP, Dessole S, Fruzzetti F, Lazzarini V, Minerba L, Melis GB, Lanzone A. Ultrasound in polycystic ovary syndrome-the measuring of ovarian stroma and relationship with circulating androgens: results of a multicentric study. Hum Reprod. 2007;22:2501–8.
82. Belosi C, Selvaggi L, Apa R, Guido M, Romualdi D, Fulghesu AM, Lanzone A. Is the PCOS diagnosis solved by ESHRE/ASRM 2003 consensus or could it include ultrasound examination of the ovarian stroma? Hum Reprod. 2006;21:3108–15.
83. Ardaens Y, Robert Y, Lemaitre L, Fossati P, Dewailly D. Polycystic ovarian disease: contribution of vaginal endosonography and reassessment of ultrasonic diagnosis. Fertil Steril. 1991;55:1062–8.
84. Pache TD, Hop WC, Wladimiroff JW, Schipper J, Fauser BCJM. Transvaginal sonography and abnormal ovarian appearance in menstrual cycle disturbances. Ultrasound Med Biol. 1991;17:589–93.
85. Al-Took S, Watkin K, Tulandi T, Tan SL. Ovarian stromal echogenicity in women with clomiphene citrate-sensitive and clomiphene citrate-resistant polycystic ovary syndrome. Fertil Steril. 1999;71: 952–4.
86. Jarvela IY, Mason HD, Sladkevicius P, Kelly S, Ojha K, Campbell S, Nargund G. Characterization of normal and polycystic ovaries using three-dimensional power Doppler ultrasonography. J Assist Reprod Genet. 2002;19:582–90.
87. Pascual MA, Graupera B, Hereter L, Tresserra F, Rodriguez I, Alcazar JL. Assessment of ovarian vascularization in the polycystic ovary by three-dimensional power Doppler ultrasonography. Gynecol Endocrinol. 2008;24:631–6.
88. Agrawal R, Sladkevicius P, Engmann L, Conway GS, Payne NN, Bekis J, Tan SL, Campbell S, Jacobs HS. Serum vascular endothelial growth factor concentrations and ovarian stromal blood flow are increased in women with polycystic ovaries. Hum Reprod. 1998; 13:651–5.
89. Deb S, Jayaprakasan K, Campbell BK, Clewes JS, Raine-Fenning NJ. The interovarian variation in three-dimensional ultrasound markers of ovarian reserve in women undergoing baseline investigation for subfertility. Fertil Steril. 2011;95:667–72.
90. Aleem FA, Predanic M. Transvaginal color Doppler determination of the ovarian and uterine blood flow characteristics in polycystic ovary disease. Fertil Steril. 1996;65:510–6.
91. Ozkan S, Vural B, Caliskan E, Bodur H, Turkoz E, Vural F. Color Doppler sonographic analysis of uterine and ovarian artery blood flow in women with polycystic ovary syndrome. J Clin Ultrasound. 2007;35: 305–13.
92. Loverro G, Vicino M, Lorusso F, Vimercati A, Greco P, Selvaggi L. Polycystic ovary syndrome: relationship between insulin sensitivity, sex hormone levels and ovarian stromal blood flow. Gynecol Endocrinol. 2001;15:142–9.
93. Zaidi J, Campbell S, Pittrof R, Kyei-Mensah A, Shaker A, Jacobs HS, Tan SL. Ovarian stromal blood flow in women with polycystic ovaries-a possible new marker for diagnosis? Hum Reprod. 1995;10: 1992–6.

94. Dolz M, Osborne NG, Blanes J, Raga F, Abad-Velasco L, Villalobos A, Pellicer A, Bonilla-Musoles F. Polycystic ovarian syndrome: assessment with color Doppler angiography and three-dimensional ultrasonography. J Ultrasound Med. 1999;18: 303–13.
95. Tugrul S, Oral O, Guclu M, Kutlu T, Uslu H, Pekin O. Significance of Doppler ultrasonography in the diagnosis of polycystic ovary syndrome. Clin Exp Obstet Gynecol. 2006;33:154–8.
96. Younis JS, Jadaon JE, Haddad S, Izhaki I, Ben-Ami M. Prospective evaluation of basal stromal Doppler studies in women with good ovarian reserve and infertility undergoing in vitro fertilization-embryo transfer treatment: patients with polycystic ovary syndrome versus ovulatory patients. Fertil Steril. 2011;95:1754–8.
97. Battaglia C, Genazzani AD, Salvatori M, Giulini S, Artini PG, Genazzani AR, Volpe A. Doppler, ultrasonographic and endocrinological environment with regard to the number of small subcapsular follicles in polycystic ovary syndrome. Gynecol Endocrinol. 1999;13:123–9.
98. Pairleitner H, Steiner H, Hasenoehrl G, Staudach A. Three dimensional power Doppler sonography: imaging and quantifying blood flow and vascularization. Ultrasound Obstet Gynecol. 1999;14:139–43.
99. Raine-Fenning NJ, Nordin NM, Ramnarine KV, Campbell BK, Clewes JS, Perkins A, Johnson IR. Determining the relationship between three-dimensional power Doppler data and true blood flow characteristics: an in-vitro flow phantom experiment. Ultrasound Obstet Gynecol. 2008;32:540–50.
100. El Behery MM, Diab AE, Mowafy H, Ebrahiem MA, Shehata AE. Effect of laparoscopic ovarian drilling on vascular endothelial growth factor and ovarian stromal blood flow using 3-dimensional power Doppler. Int J Gynaecol Obstet. 2011;112:119–21.
101. Elmashad AI. Impact of laparoscopic ovarian drilling on anti-Mullerian hormone levels and ovarian stromal blood flow using three-dimensional power Doppler in women with anovulatory polycystic ovary syndrome. Fertil Steril. 2011;95:2342–6.
102. Mala YM, Ghosh SB, Tripathi R. Three-dimensional power Doppler imaging in the diagnosis of polycystic ovary syndrome. Int J Gynaecol Obstet. 2009;105: 36–8.
103. Raine-Fenning NJ, Campbell BK, Clewes JS, Kendall NR, Johnson IR. The interobserver reliability of three-dimensional power Doppler data acquisition within the female pelvis. Ultrasound Obstet Gynecol. 2004;23:501–8.
104. Hann LE, Hall DA, McArdle CR, Seibel M. Polycystic ovarian disease: sonographic spectrum. Radiology. 1984;150:531–4.
105. Orsini LF, Venturoli S, Lorusso R, Pluchinotta V, Paradisi R, Bovicelli L. Ultrasonic findings in polycystic ovarian disease. Fertil Steril. 1985;43: 709–14.
106. Balen AH, Conway GS, Kaltsas G, Techatrasak K, Manning PJ, West C, Jacobs HS. Polycystic ovary syndrome: the spectrum of the disorder in 1741 patients. Hum Reprod. 1995;10:2107–11.
107. Shah B, Parnell L, Milla S, Kessler M, David R. Endometrial thickness, uterine, and ovarian ultrasonographic features in adolescents with polycystic ovarian syndrome. J Pediatr Adolesc Gynecol. 2010;23:146–52.
108. Parisi L, Tramonti M, Casciano S, Zurli A, Gazzarini O. The role of ultrasound in the study of polycystic ovarian disease. J Clin Ultrasound. 1982; 10:167–72.
109. Peri N, Levine D. Sonographic evaluation of the endometrium in patients with a history or an appearance of polycystic ovarian syndrome. J Ultrasound Med. 2007;26:55–9.
110. Vanky E, Kjøtrød S, Salvesen KA, Romundstad P, Moen MH, Carlsen SM. Clinical, biochemical and ultrasonographic characteristics of Scandinavian women with PCOS. Acta Obstet Gynecol Scand. 2004;83:482–6.
111. Lam P, Johnson I, Raine-Fenning N. Endometrial blood flow is impaired in women with polycystic ovarian syndrome who are clinically hyperandrogenic. Ultrasound Obstet Gynecol. 2009;34: 326–34.
112. Ajossa S, Guerriero S, Paoletti AM, Orrù M, Melis GB. The antiandrogenic effect of flutamide improves uterine perfusion in women with polycystic ovary syndrome. Fertil Steril. 2002;77:1136–40.
113. Ajossa S, Guerriero S, Paoletti AM, Orrù M, Melis GB. Hyperinsulinemia and uterine perfusion in patients with polycystic ovary syndrome. Ultrasound Obstet Gynecol. 2002;20:276–80.
114. Chekir C, Nakatsuka M, Kamada Y, Noguchi S, Sasaki A, Hiramatsu Y. Impaired uterine perfusion associated with metabolic disorders in women with polycystic ovary syndrome. Acta Obstet Gynecol Scand. 2005;84:189–95.
115. Battaglia C, Artini PG, Genazzani AD, Sgherzi MR, Salvatori M, Giulini S, Volpe A. Color Doppler analysis in lean and obese women with polycystic ovary syndrome. Ultrasound Obstet Gynecol. 1996;7: 342–6.
116. Battaglia C, Artini PG, D'Ambrogio G, Genazzani AD, Genazzani AR. The role of color Doppler imaging in the diagnosis of polycystic ovary syndrome. Am J Obstet Gynecol. 1995;172:108–13.
117. de Ziegler D, Bessis R, Frydman R. Vascular resistance of uterine arteries: physiological effects of estradiol and progesterone. Fertil Steril. 1991;55: 775–9.
118. Killam AP, Rosenfeld CR, Battaglia FC, Makowski EL, Meschia G. Effect of estrogens on the uterine blood flow of oophorectomized ewes. Am J Obstet Gynecol. 1973;115:1045–52.
119. Tulandi T, Watkin K, Tan SL. Reproductive performance and three dimensional ultrasound volume

determination of polycystic ovaries following laparoscopic ovarian drilling. Int J Fertil Womens Med. 1997;42:436–40.
120. Wu MH, Huang MF, Tsai SJ, Pan HA, Cheng YC, Lin YS. Effects of laparoscopic ovarian drilling on young adult women with polycystic ovarian syndrome. J Am Assoc Gynecol Laparosc. 2004;11: 184–90.
121. Engmann L, Sladkevicius P, Agrawal R, Bekir JS, Campbell S, Tan SL. Value of ovarian stromal blood flow velocity measurement after pituitary suppression in the prediction of ovarian responsiveness and outcome of in vitro fertilization treatment. Fertil Steril. 1999;71:22–9.
122. Cocksedge KA, Li TC, Saravelos SH, Metwally M. A reappraisal of the role of polycystic ovary syndrome in recurrent miscarriage. Reprod Biomed Online. 2008;17:151–60.
123. Okon MA, Laird SM, Tuckerman EM, Li TC. Serum androgen levels in women who have recurrent miscarriages and their correlation with markers of endometrial function. Fertil Steril. 1998;69:682–90.
124. Li TC, Spuijbroek MD, Tuckerman E, Anstie B, Loxley M, Laird S. Endocrinological and endometrial factors in recurrent miscarriage. BJOG. 2000; 107:1471–9.
125. Cocksedge KA, Saravelos SH, Wang Q, Tuckerman E, Laird SM, Li TC. Does free androgen index predict subsequent pregnancy outcome in women with recurrent miscarriage? Hum Reprod. 2008;23: 797–802.
126. Ferreira AM, Pires CR, Moron AF, Araujo Júnior E, Traina E, Mattar R. Doppler assessment of uterine blood flow in recurrent pregnancy loss. Int J Gynaecol Obstet. 2007;98:115–9.
127. Nakatsuka M, Habara T, Noguchi S, Konishi H, Kudo T. Impaired uterine arterial blood flow in pregnant women with recurrent pregnancy loss. J Ultrasound Med. 2003;22:27–31.
128. Habara T, Nakatsuka M, Konishi H, Asagiri K, Noguchi S, Kudo T. Elevated blood flow resistance in uterine arteries of women with unexplained recurrent pregnancy loss. Hum Reprod. 2002;17:190–4.
129. Ng EH, Chan CC, Tang OS, Yeung WS, Ho PC. Endometrial and subendometrial vascularity is higher in pregnant patients with livebirth following ART than in those who suffer a miscarriage. Hum Reprod. 2007;22:1134–41.
130. Mercé LT, Barco MJ, Bau S, Troyano J. Are endometrial parameters by three-dimensional ultrasound and power Doppler angiography related to in vitro fertilization/embryo transfer outcome? Fertil Steril. 2008;89:111–7.
131. Zohav E, Orvieto R, Anteby EY, Segal O, Meltcer S, Tur-Kaspa I. Low endometrial volume may predict early pregnancy loss in women undergoing in vitro fertilization. J Assist Reprod Genet. 2007;24: 259–61.
132. Mathur R, Kailasam C, Jenkins J. Review of the evidence base of strategies to prevent ovarian hyperstimulation syndrome. Hum Fertil (Camb). 2007;10: 75–85.
133. Mathur R, Evbuomwan I, Jenkins J. Prevention and management of ovarian hyperstimulation syndrome. Curr Obstet Gynaecol. 2005;15:132–8.
134. Royal College of Obstetricians and Gynaecologists (RCOG). The management of ovarian hyperstimulation syndrome. RCOG green-top guideline number 5. London: RCOG Press; 2006. p. 1–11.
135. Delvigne A, Rozenberg S. Epidemiology and prevention of ovarian hyperstimulation syndrome (OHSS): a review. Hum Reprod Update. 2002;8:559–77.
136. Papanikolaou EG, Pozzobon C, Kolibianakis EM, Camus M, Tournaye H, Fatemi HM, Van Steirteghem A, Devroey P. Incidence and prediction of ovarian hyperstimulation syndrome in women undergoing gonadotropin-releasing hormone antagonist in vitro fertilization cycles. Fertil Steril. 2006;85:112–20.
137. Papanikolaou EG, Humaidan P, Polyzos NP, Tarlatzis B. Identification of the high-risk patient for ovarian hyperstimulation syndrome. Semin Reprod Med. 2010;28:458–62.
138. Kwee J, Elting ME, Schats R, McDonnell J, Lambalk CB. Ovarian volume and antral follicle count for the prediction of low and hyper responders with in vitro fertilization. Reprod Biol Endocrinol. 2007;15:5–9.
139. Agrawal R, Conway G, Sladkevicius P, Tan SL, Engmann L, Payne N, Bekir J, Campbell S, Jacobs H. Serum vascular endothelial growth factor and Doppler blood flow velocities in in vitro fertilization: relevance to ovarian hyperstimulation syndrome and polycystic ovaries. Fertil Steril. 1998;70:651–8.
140. Jayaprakasan K, Jayaprakasan R, Al-Hasie HA, Clewes JS, Campbell BK, Johnson IR, Raine-Fenning NJ. Can quantitative three-dimensional power Doppler angiography be used to predict ovarian hyperstimulation syndrome? Ultrasound Obstet Gynecol. 2009;33:583–91.
141. Agrawal R, Conway GS, Sladkevicius P, Payne NN, Bekir J, Campbell S, et al. Serum vascular endothelial growth factor (VEGF) in the normal menstrual cycle: association with changes in ovarian and uterine Doppler blood flow. Clin Endocrinol (Oxf). 1999;50:101–6.

The Normal Uterus

8

Khaled Sakhel and Alfred Z. Abuhamad

Uterus

The uterus is a muscular organ whose purpose is to provide the implantation site and nutrients to the developing fetus. It is located in the true pelvis and lies between the urinary bladder anteriorly and the rectosigmoid colon posteriorly. The space between the uterus and the rectosigmoid is the posterior cul-de-sac which is the most dependent area in the peritoneal cavity and where fluid tends to accumulate.

There are three main anatomic components of the uterus which are the upper part or fundus that lies superior to the fallopian tube ostia, the main body or corpus, and the cervix. The lower segment of the corpus is sometimes termed the isthmus. The corpus is made up of the muscular myometrium and the endometrium. The endometrium is hormonally responsive and undergoes changes in response to ovarian hormones during a menstrual cycle. These changes prepare for the implantation of the fertilized ovum. The myometrium does not undergo significant anatomic changes in response to the menstrual cycle.

K. Sakhel, MD, FACOG, FACS (✉)
Division of Minimally Invasive and Robotic Surgery,
Eastern Virginia Medical School, 825 Fairfax Ave,
Suite 310, Norfolk, VA 23507, USA
e-mail: sakhelk@evms.edu

A.Z. Abuhamad, MD
Department of Obstetrics and Gynecology,
Eastern Virginia Medical School,
825 Fairfax Ave, Suite 310, Norfolk,
VA 23507, USA

This chapter discusses and illustrates the sonography of a normal uterus including the uterine myometrium, endometrium and cervix. It also highlights the changes that occur during a normal menstrual cycle.

The uterus can be evaluated by transabdominal (transvesical) sonography (TAS) and transvaginal sonography (TVS). Two other techniques including the transrectal and translabial approach are seldom used and are usually reserved in patients where neither TAS nor TVS is feasible.

The advantage of TAS is the ability to assess the upper pelvis especially in patients with larger uteri that are greater than 12 weeks in size. Disadvantages of the TAS approach include the requirement of a full bladder and a limited image resolution especially in patients with a higher body mass index (BMI) as well as in patients with lower abdominal scars from prior surgery.

The TVS approach is clearly superior in imaging quality due to the use of higher-frequency probes and is by far the most commonly used method for imaging of the pelvis. It is limited, however, by depth of penetration of the transvaginal ultrasound probe and therefore can only assess structures in the true pelvis which is adequate in most cases. For TVS the patient is asked to empty her bladder and lie supine in the lithotomy position with the legs flexed. The uterus can be evaluated using the traditional 2-dimensional (2-D) probe which portrays the image in the sagittal and transverse planes. It can also be evaluated using a 3-dimensional (3-D) probe which can portray a reconstructed coronal image of the uterus [1].

L.A. Stadtmauer, I. Tur-Kaspa (eds.), *Ultrasound Imaging in Reproductive Medicine*,
DOI 10.1007/978-1-4614-9182-8_8,

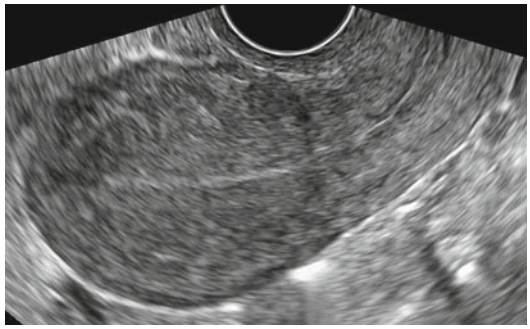

Fig. 8.1 Midsagittal plane showing an immediate postmenstrual cycle thin endometrium (type A) with an anteverted uterus

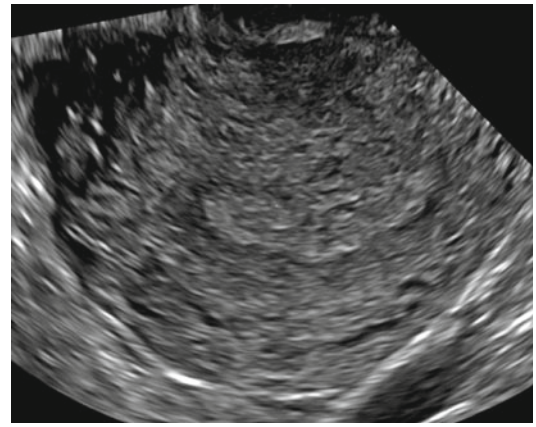

Fig. 8.2 Midtransverse plane of the uterus

The American Institute for Ultrasound in Medicine (AIUM) has put forth practice guidelines for the "Performance of Pelvic Ultrasound Examinations," "Ultrasonography in Reproductive Medicine," and "Focused Reproductive Endocrinology and Infertility Scan." These are helpful in establishing indications and reporting requirements [2–4].

Sonography of the uterus includes examination for size, shape, contour, orientation, and appearance of the myometrium, endometrium, and cervix. Unless the fallopian tubes are distended with fluid, they are not usually apparent during routine pelvic sonography. In addition the cul-de-sac is routinely evaluated for scar tissue, fluid, and masses [2–4].

The uterus is first imaged in its long axis on the midsagittal plane which is obtained by optimizing the long axis of the echogenic endometrium. The midsagittal plane allows the visualization of a cross section of the myometrium, endometrium, cervix, cul-de-sac, rectum, and bladder (Fig. 8.1). In this plane, the angle between the cervix and uterus can be measured. The midtransverse plane is perpendicular to the midsagittal plane and can be obtained by rotating the probe 90° clockwise or counterclockwise. It allows visualization of a cross section of the uterine structures at different levels from fundus to outer cervical os (Fig. 8.2). The 3-D ultrasound probe, when available, can acquire a volume of the uterus, and the software will use the data to generate and display a coronal image (Fig. 8.3). The coronal plane is that plane that bisects the uterus parallel to the plane of the ultrasound bed and the supine body. This has been shown to be especially helpful in detecting Mullerian anomalies and for IUD localization [1]. The Z technique is a simple technique that describes the steps required for the display of the mid-coronal plane out of a 3-D volume of the uterus [5].

Measurements of the uterus include the length, height, and width. The length and height are measured in the midsagittal plane, whereas the width is measured in the transverse plane [6, 7]. The length is measured from outer serosal surface of the fundus to the external os of the cervix. If volume assessment of the uterus is required, then the cervical length should be excluded from the height measurement. Uterine volume may be calculated using the formula: volume = length × width × height × 0.52. The length of a normal nulliparous uterus is 6–8.5 cm, and in multiparous women, it is 8–10.5 cm. The height is measured from anterior to posterior serosal surfaces and perpendicular to the long axis of the uterus. The height of the normal uterus in nulliparous women is 2–4 cm, and in multiparous women, it is 4–6 cm. The width of the corpus is taken at the widest region of the uterus on a transverse plane. The width of a nulliparous uterus is 3–5 and 4–6 cm in multiparous women.

The orientation of the uterus is described in the anteroposterior and right-left dimensions in relation to the supine body. The orientation is

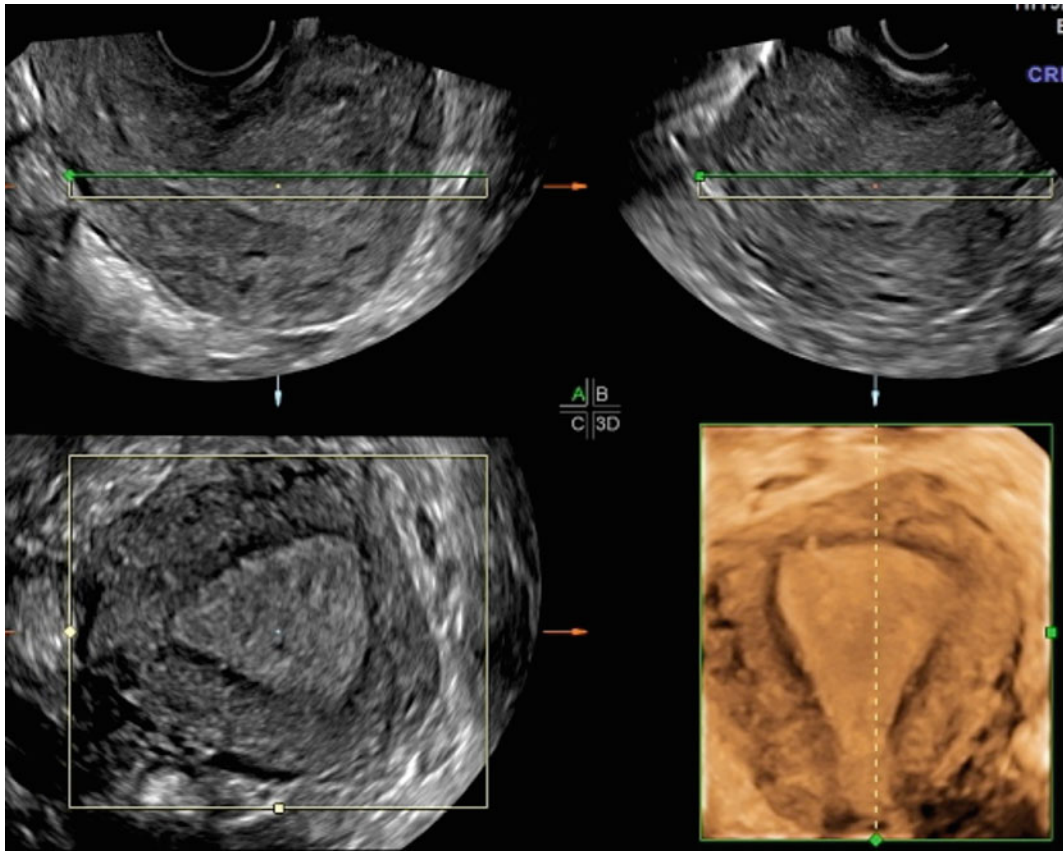

Fig. 8.3 The three orthogonal planes sagittal, transverse, and coronal planes as well as the rendered image. The coronal image also portrays the hypoechoic junctional zone of the myometrium

noted once the optimum midsagittal image is obtained using the echogenic endometrium for guidance. The direction of the ultrasound probe can provide the right to left orientation. The orientation in the anteroposterior dimension is described in terms of version and flexion which require image processing. The uterus is said to be flexed or angled across the isthmus when there is an angle between the cervix and the corpus of the uterus (Fig. 8.4). The anteroflexed and retroflexed uteri can pose a challenge to procedures that require access to the endometrial cavity. If there is no angulation between the cervix and the corpus, the uterus is described in terms of version (Figs. 8.1 and 8.5). It is important to describe and report the orientation of the uterus as part of the ultrasound examination. This information is helpful if uterine instrumentation is required.

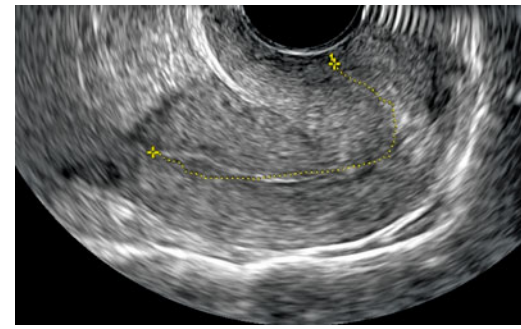

Fig. 8.4 Anteroflexed uterus with the *traced line* showing the sharp angle between the cervix and the endometrial cavity

Myometrium

The uterine myometrium is made of a homogeneous layer of smooth muscle and blood vessels. The uterine arteries reach the uterus at the level

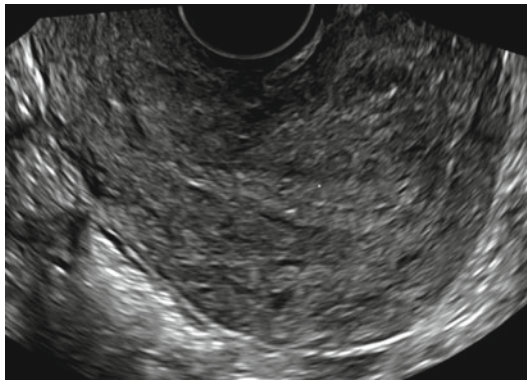

Fig. 8.5 Retroverted uterus with minimal angulation between the cervix and the endometrial cavity

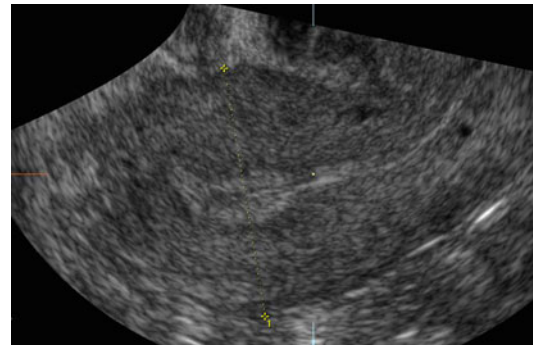

Fig. 8.6 Trilaminar endometrium (type B) under the influence of increasing estradiol in the early proliferative phase

of the cardinal ligaments and divide into ascending and descending branches that travel within the layers of the broad ligament along the lateral wall. Sonographically the normal myometrium has a medium echogenicity, less than the endometrium, with a granular echotexture. The myometrium can be divided into three layers. The inner or junctional myometrium, which abuts the endometrium, is thin and hypoechoic compared to the thicker homogeneous middle layer (Fig. 8.3) [7, 8]. Thickening of this layer has been shown to be associated with adenomyosis [9]. The arcuate vessels separate the middle and outer layer which is also thin and slightly less echogenic than the middle layer. The myometrium does not appear to change sonographically during the course of the menstrual cycle.

Endometrium

The uterine endometrium is the site of dynamic changes in response to ovarian hormones during the menstrual cycle. It can be divided into the inner functional layer that sloughs during menses and the outer basal layer which abuts the myometrial junctional layer. The changes that occur during the menstrual cycle can be seen sonographically [7, 8, 10–17].

The immediate postmenstrual endometrium is a thin echogenic line (type A) at the intersection of anterior and posterior uterine walls and normally measures 3–8 mm (Fig. 8.1). Assessing the endometrial thickness in patients presenting with postmenopausal bleeding is an important step in the overall evaluation process. It is important to know that a thin endometrium in that setting, typically at less than 5 mm, has been correlated in multiple studies with the absence of endometrial cancer. When measuring endometrial thickness on ultrasound, it is critical to ensure that the uterus is in a midsagittal plane, the whole endometrial stripe is seen from the fundus to the endocervix, the thickest portion is measured, and the image is clear and magnified.

Under the influence of increasing estradiol hormone levels secreted by the growing ovarian follicles, endometrial proliferation occurs. Sonographically this is seen as thickening of the lining into the so-called trilaminar layer (type B) with an anterior and posterior hypoechoic layer separated in the midline by a hyperechogenic central line (Fig. 8.6). During the late proliferative period and near the time of ovulation, endometrial lining is 8–12 mm in thickness with an accentuated trilaminar appearance (type C, Fig. 8.7).

The post-ovulatory endometrial lining, under the influence of progesterone hormone secreted by the corpus luteum, is characterized by loss of the trilaminar appearance and the development of a uniformly hyperechoic stripe (type D, Fig. 8.8).

The implantation, pregnancy, and live birth rates following in vitro fertilization (IVF) are affected by the midcycle endometrial thickness [14, 18–23]. Studies have shown that a midcycle endometrial thickness less than 8 mm was associated with poor IVF outcome as compared to at least 9 mm thickness. There is conflicting

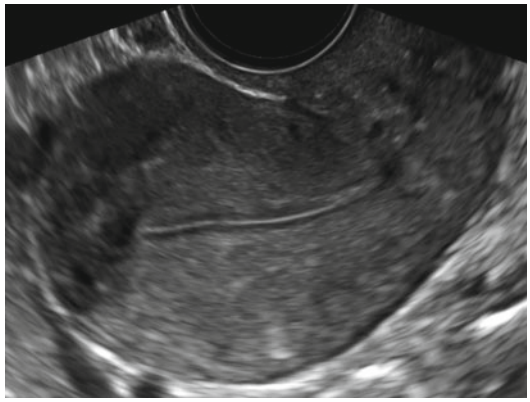

Fig. 8.7 Late proliferative phase endometrium with an accentuated trilaminar pattern (type C)

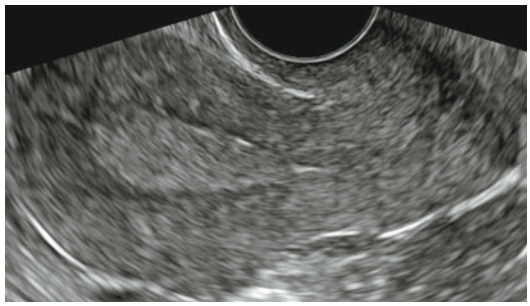

Fig. 8.8 Luteal phase endometrium showing a homogenously thickened hyperechoic stripe (type D)

evidence as to the detrimental effect of increased endometrial thickness beyond 12 mm. Cases of successful pregnancies in patients with endometrial thickness as low as 4 mm have also been reported [24].

Cervix

The cervix can be divided into the portio vaginalis or ectocervix, the endocervix, and the endocervical canal. It is amenable to imaging using TAS, TVS, and translabial sonography.

Clinically the presence of endocervical mucus has been used in the assessment of the presence of increasing estradiol levels and the lead follicle. Scoring methods of the cervical mucus including the Insler and Moghissi that looked at the amount, consistency, Spinnbarkeit, and ferning were introduced [25, 26]. However, these often needed

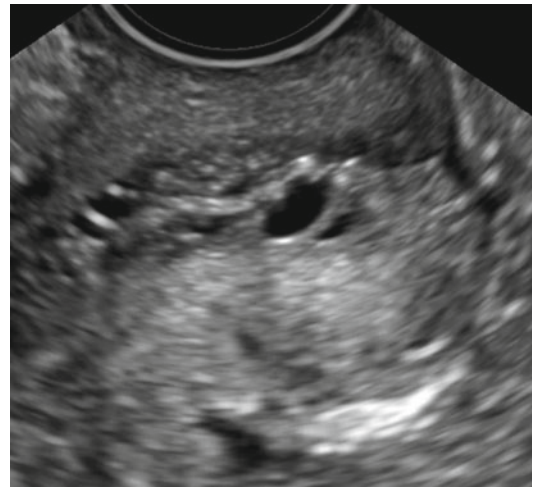

Fig. 8.9 Cervix with nabothian cysts (*thin arrows*) and blood (*thick arrows*) during menses

to be performed repeatedly which is not practical and uncomfortable for the patient. Ultrasound assessment of the cervix, in conjunction with the pelvic sonography being performed, has been introduced to look at the changes associated with the menstrual cycle [27].

Sonographically the cervical stroma is usually of the same consistency as the myometrium. The endocervical canal is normally spindle shaped and begins at the bottle neck where the endometrium tapers off. The presence of anechoic pockets within the cervix represents nabothian cysts and is a normal finding. The cervical stroma is not affected by the hormonal changes. The changes are limited to the endocervix and the appearance of cervical mucus. The endocervix during menses is noted to contain complex fluid with blood and mucus (Fig. 8.9). After the cessation of menses, the endocervix is noted to be thin and relatively hypoechogenic (Fig. 8.10). The endocervix is noted to increase in echodensity starting on cycle day 7 or when the leading follicle is 11 mm, endometrial thickness of 5.8 mm, and estradiol levels of around 289 pmol/l (Fig. 8.11). In addition, cervical mucus can be observed within the endocervical canal as of cycle day 13, or when the lead follicle is 16.8 mm, endometrial thickness 7.5 mm, or estradiol level exceeds 500 pmol/l (Fig. 8.12) [27].

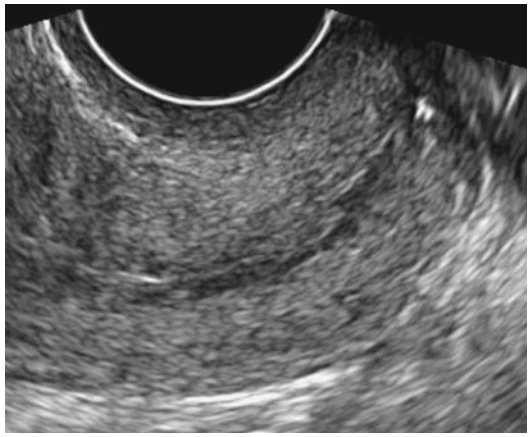

Fig. 8.10 Cervix in early proliferative phase after menses showing a thin endocervix

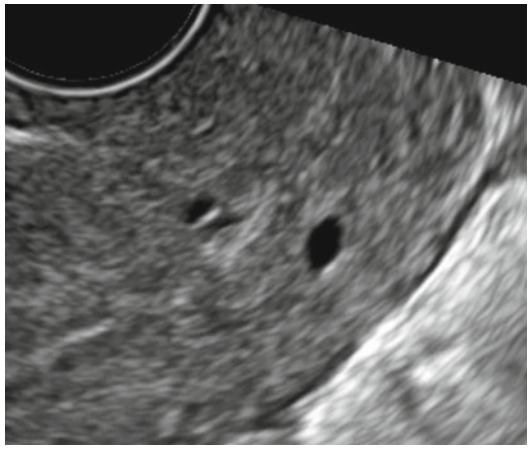

Fig. 8.11 Cervix in mid-proliferative phase showing a thicker and hyperechoic endocervix and presence of nabothian cysts

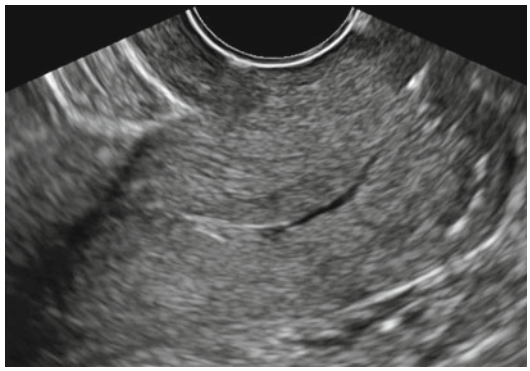

Fig. 8.12 Cervix at day 13 of cycle showing mucus in the endocervix under the effect of increasing estradiol

References

1. Sakhel K, Benson CB, Platt LD, Goldstein SR, Benacerraf BR. Begin with the basics: role of 3-dimensional sonography as a first-line imaging technique in the cost-effective evaluation of gynecologic pelvic disease. J Ultrasound Med. 2013;32(3):381–8.
2. American College of Nurse-Midwives (ACNM); American College of Obstetricians and Gynecologists (ACOG); American College of Osteopathic Obstetricians and Gynecologists (ACOOG); American Society for Reproductive Medicine–Society for Reproductive Endocrinology and Infertility (ASRM-SREI); Association of Women's Health, Obstetric and Neonatal Nurses (AWHONN). AIUM practice guideline for the performance of a focused reproductive endocrinology and infertility scan. J Ultrasound Med. 2012;31(11):1865–74.
3. American Institute of Ultrasound in Medicine. AIUM practice guideline for the performance of pelvic ultrasound examinations. J Ultrasound Med. 2010;29(1):166–72.
4. American Institute of Ultrasound in Medicine; Society for Reproductive Endocrinology and Infertility; American Society of Reproductive Medicine. AIUM practice guideline for ultrasonography in reproductive medicine. J Ultrasound Med. 2009;28(1):128–37.
5. Abuhamad AZ, Singleton S, Zhao Y, Bocca S. The Z technique: an easy approach to the display of the mid-coronal plane of the uterus in volume sonography. J Ultrasound Med. 2006;25(5):607–12.
6. Merz E, Miric-Tesanic D, Bahlmann F, Weber G, Wellek S. Sonographic size of uterus and ovaries in pre- and postmenopausal women. Ultrasound Obstet Gynecol. 1996;7(1):38–42.
7. Poder L. Ultrasound evaluation of the uterus. In: Callen PW, editor. Ultrasonography in obstetrics and gynecology. 5th ed. Philadelphia: Saunders Elsevier; 2008. p. 919–41.
8. Mitchell DG, Schonholz L, Hilpert PL, Pennell RG, Blum L, Rifkin MD. Zones of the uterus: discrepancy between US and MR images. Radiology. 1990;174(3 Pt 1):827–31.
9. Sakhel K, Abuhamad A. Sonography of adenomyosis. J Ultrasound Med. 2012;31(5):805–8.
10. Fleischer AC, Kalemeris GC, Entman SS. Sonographic depiction of the endometrium during normal cycles. Ultrasound Med Biol. 1986;12(4):271–7.
11. Fleischer AC, Pittaway DE, Beard LA, Thieme GA, Bundy AL, James Jr AE, Wentz AC. Sonographic depiction of endometrial changes occurring with ovulation induction. J Ultrasound Med. 1984;3(8):341–6.
12. Randall JM, Fisk NM, McTavish A, Templeton AA. Transvaginal ultrasonic assessment of endometrial growth in spontaneous and hyperstimulated menstrual cycles. Br J Obstet Gynaecol. 1989;96(8):954–9.
13. Randall JM, Templeton A. Transvaginal sonographic assessment of follicular and endometrial growth in spontaneous and clomiphene citrate cycles. Fertil Steril. 1991;56(2):208–12.

14. Gonen Y, Casper RF, Jacobson W, Blankier J. Endometrial thickness and growth during ovarian stimulation: a possible predictor of implantation in in vitro fertilization. Fertil Steril. 1989;52(3):446–50.
15. Lenz S, Lindenberg S. Ultrasonic evaluation of endometrial growth in women with normal cycles during spontaneous and stimulated cycles. Hum Reprod. 1990;5(4):377–81.
16. Santolaya-Forgas J. Physiology of the menstrual cycle by ultrasonography. J Ultrasound Med. 1992;11(4): 139–42.
17. Bakos O, Lundkvist O, Bergh T. Transvaginal sonographic evaluation of endometrial growth and texture in spontaneous ovulatory cycles-a descriptive study. Hum Reprod. 1993;8(6):799–806.
18. Barker MA, Boehnlein LM, Kovacs P, Lindheim SR. Follicular and luteal phase endometrial thickness and echogenic pattern and pregnancy outcome in oocyte donation cycles. J Assist Reprod Genet. 2009;26: 243–9.
19. McWilliams GD, Frattarelli JL. Changes in measured endometrial thickness predict in vitro fertilization success. Fertil Steril. 2007;88:74–81.
20. Amir W, Micha B, Ariel H, Liat LG, Jehoshua D, Adrian S. Predicting factors for endometrial thickness during treatment with assisted reproductive technology. Fertil Steril. 2007;87:799–804.
21. Richter KS, Bugge KR, Bromer JG, Levy MJ. Relationship between endometrial thickness and embryo implantation, based on 1,294 cycles of in vitro fertilization with transfer of two blastocyst-stage embryos. Fertil Steril. 2007;87:53–9.
22. Kovacs P, Matyas S, Boda K, Kaali SG. The effect of endometrial thickness on IVF/ICSI outcome. Hum Reprod. 2003;18:2337–41.
23. Noyes N, Hampton BS, Berkeley A, Licciardi F, Grifo J, Krey L. Factors useful in predicting the success of oocyte donation: a 3-year retrospective analysis. Fertil Steril. 2001;76:92–7.
24. Sundstrom P. Establishment of a successful pregnancy following in-vitro fertilization with an endometrial thickness of on more than 4 mm. Hum Reprod. 1998;13:1550–2.
25. Insler V, Melmed H, Eichenbrenner I, Serr DM, Lunenfeld B. The cervical score, a simple semiquantitative method for monitoring of the menstrual cycle. Int J Gynaecol Obstet. 1972;10:223–8.
26. Moghissi KS. Postcoital test: physiologic basis, technique, and interpretation. Fertil Steril. 1976;27: 117–29.
27. Duijkers IJ, Klipping C. Ultrasonographic assessment of endocervix and cervical mucus in ovulatory menstrual cycles. Eur J Obstet Gynecol Reprod Biol. 2000;93(1):13–7.

Congenital Uterine Anomalies

9

Beth W. Rackow

Abbreviations

2DUS	Two-dimensional ultrasonography
3DUS	Three-dimensional ultrasonography
CT	Computed tomography
DES	Diethylstilbestrol
HSG	Hysterosalpingography
MA	Müllerian anomalies
MR	Magnetic resonance
MRI	Magnetic resonance imaging
MRKH	Mayer-Rokitansky-Küster-Hauser syndrome
RPL	Recurrent pregnancy loss
SIS	Saline-infusion sonography

Introduction

Congenital anomalies of the female reproductive tract or Müllerian anomalies (MA) may involve the uterus, cervix, fallopian tubes, or vagina. Of the Müllerian anomalies, uterine anomalies are the most common; prevalence rates range from 3 to 8 % of fertile and infertile women [1–5]. The true incidence of uterine anomalies in the general population, cited as 0.5 % [6], is hard to determine because reproduction is not always affected; thus, some individuals are asymptomatic and unidentified, and accurate assessment and diagnosis has not always occurred [4, 5, 7]. The etiology of MA is poorly understood; the majority of MA are infrequent and sporadic, although some familial clustering occurs, and MA are generally attributed to polygenic and multifactorial causes [8, 9]. This chapter will review the embryologic development of the female reproductive tract, classification of congenital uterine anomalies, gynecologic and obstetric presentations of congenital uterine anomalies, imaging techniques, and management options for uterine anomalies.

B.W. Rackow, MD
Department of Obstetrics and Gynecology,
Columbia University Medical Center,
Center for Women's Reproductive Care,
1790 Broadway, New York, NY 10019, USA
e-mail: bwr2113@columbia.edu

Embryology of the Female Reproductive Tract

While genetic sex is determined at the time of fertilization, male or female phenotype is not defined until after the sixth week of development. Early in embryologic development, both the Wolffian, (mesonephric) and Müllerian (paramesonephric) ducts are present. The paired Wolffian ducts connect the embryologic kidney (mesonephros) to the cloaca between 5 and 10 weeks of gestation; development of the functional kidney (metanephros) is stimulated by an outgrowth of the Wolffian duct, the ureteric bud. Müllerian duct development occurs concomitant with the development of the urinary tract, and kidney and ureteral anomalies are associated with MA; renal anomalies include agenesis, ectopic location, or abnormal anatomy [10]. Although gonadal development begins at the same time as Müllerian duct

L.A. Stadtmauer, I. Tur-Kaspa (eds.), *Ultrasound Imaging in Reproductive Medicine*,
DOI 10.1007/978-1-4614-9182-8_9,

development, at 6 weeks of gestation, the two processes are separate and distinct; females with MA usually have normal ovaries and steroid hormone production.

Normal development of the female tract involves a complex series of events, and failure of any part of this process can result in a Müllerian anomaly. Paired Müllerian ducts arise from coelomic epithelium along the lateral walls of the urogenital ridge, and these solid ducts are present by week 6 of development. In the absence of Müllerian-inhibiting substance released from the male gonad, the Müllerian ducts proliferate while the Wolffian ducts regress. The Müllerian ducts elongate caudally and cross the Wolffian ducts medially, and midline fusion of the ducts forms the primitive uterovaginal structure. By week 10 of development, fusion occurs between the caudal end of the joined Müllerian ducts and the urogenital sinus. Subsequently, the unified Müllerian ducts undergo internal canalization which results in two lumens divided by a midline septum. Resorption of the septum commonly occurs in a caudal to cranial direction. The fused caudal portion of the Müllerian ducts becomes the uterus, cervix, and upper vagina, and the unfused cranial portion becomes the fallopian tubes. Uterine development is completed by week 20 of development.

The lower vagina has a separate embryologic origin. At week 10, when the fused Müllerian ducts connect with the urogenital sinus, the sinovaginal bulbs develop and proliferate toward the caudal end of the uterovaginal canal, forming a solid vaginal plate that elongates with time. The central cells of the vaginal plate degenerate in a caudal to cranial direction, forming a hollow structure. Vaginal development is also complete by week 20 of development. The hymenal membrane originates from the sinus tubercle and separates the vaginal lumen from the urogenital sinus. The central epithelial cells usually degenerate prior to birth, achieving a patent structure with a thin fold of mucus membrane at the introitus.

Although the caudal-to-cranial direction of Müllerian duct fusion and septal resorption is the traditional theory of female reproductive tract development, unusual MA have been documented that are exceptions to this order of progression. Examples include a complete septate uterus with a double cervix and vaginal septum, and a normal uterus and cervix with an isolated longitudinal vaginal septum [11–14]. Hence, medial fusion of the Müllerian ducts can proceed in a caudal or cranial direction or both [15].

Classification of Müllerian Anomalies

Müllerian anomalies are commonly classified into three categories: agenesis and hypoplasia, lateral fusion defects, and vertical fusion defects. Reproductive tract abnormalities due to in utero exposure to diethylstilbestrol (DES) comprise a fourth group of anomalies. *Agenesis and hypoplasia* can occur for a portion of or an entire Müllerian duct, or for both ducts, affecting one or multiple Müllerian structures. *Lateral fusion defects* are the most common category of Müllerian defects and originate due to failure of migration of one or both ducts, midline fusion of the ducts, or absorption of the midline septum between the ducts. A range of anomalies can occur including symmetric or asymmetric and nonobstructed or obstructed Müllerian structures. *Vertical fusion defects* occur due to disordered fusion of the Müllerian ducts with the urogenital sinus or abnormal vaginal canalization and may present with menstrual flow obstruction.

Although there is no universally accepted standard classification for Müllerian anomalies, the American Fertility Society classification system from 1988 is commonly utilized and provides a standardized nomenclature to describe anomalies (Fig. 9.1) [4, 16]. This classification system focuses on the major categories of uterine anomalies and describes them based on their embryologic etiology. Hypoplasia/agenesis (category I) and unicornuate (category II) denote anomalies with developmental failure of one or both Müllerian ducts; didelphys (category III) and bicornuate (category IV) describe anomalies involving a varying degree of failure of midline fusion; septate (category V) and arcuate (category

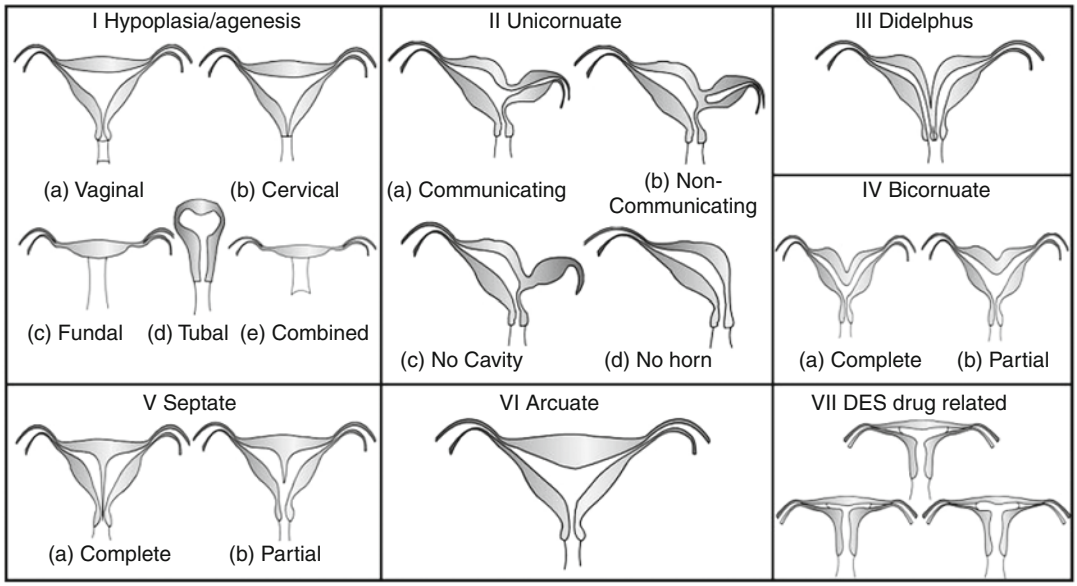

Fig. 9.1 Classification of uterine anomalies according to the American Fertility Society [16]. DES, diethylstilbestrol (Reprinted Bermejo et al. [17]. With permission from John Wiley & Sons, Inc.)

VI) identify anomalies with some degree of failure of resorption of the midline septum. DES drug-related anomalies (category VII) are a separate category of anomalies and will not be discussed in this chapter. With this classification system, associated anomalies of the vagina, cervix, fallopian tubes, and urinary system must be documented separately. Two additional issues with this classification system are the inability to fully describe a uterine anomaly when multiple abnormalities are present (i.e., septate uterus with duplicated cervix) and the lack of specific diagnostic criteria to enable differentiation between bicornuate, septate, and arcuate uteri [4, 11, 18, 19]. Hence, complex anomalies need to be described according to the component parts.

Overview of the Uterine Anomalies

Unicornuate Uterus

The unicornuate uterus arises due to agenesis or hypoplasia of one of the two Müllerian ducts. The unicornuate uterus is a functional uterus with a normal-appearing cervix and a single fallopian tube, and the contralateral side may have a variety of configurations: agenesis or a rudimentary horn in 74 % [6]. The rudimentary horn can be noncommunicating (70 to 90 %) or communicating with the unicornuate uterus and may contain functional endometrium [20]. Women with a rudimentary uterine horn containing functional endometrium may present with cyclic or chronic pain, endometriosis, or a horn gestation [20]. Nonfunctional rudimentary horns are usually asymptomatic. Lastly, the unicornuate uterus is associated with a 40 % incidence of renal anomalies, usually ipsilateral to the anomalous side [20–22].

Uterus Didelphys

The uterus didelphys results from complete failure of lateral fusion of the two Müllerian ducts; duplication of the Müllerian structures is the result. Anatomically, these women have two unicornuate uteri, two separate endometrial cavities, and two cervices. In the majority of women with a uterus didelphys, vaginal duplication also occurs and a longitudinal vaginal septum is

present. Additionally, this anomaly can present with an obstructed hemivagina and associated ipsilateral renal anomaly [23, 24].

Bicornuate Uterus

Incomplete lateral fusion of the Müllerian ducts at the fundus results in a bicornuate uterus. Commonly, a single cervix and two endometrial cavities are present. Variability exists in the extent of separation between the two cavities, with maximal separation extending down to the internal cervical os (complete bicornuate). A fundal indentation of at least 1 cm has been found to be reliable for differentiating a bicornuate from a septate uterus [11, 25–28]. Although a normal vagina is commonly present, a longitudinal vaginal septum can occur with the bicornuate uterus [14].

Septate Uterus

The septate uterus occurs due to a defect in resorption of the midline division between the two fused Müllerian ducts, and a fibromuscular septum remains. The degree of septation can vary from complete, extending from the uterine fundus through the cervix, to partial, in which a portion of the caudal aspect of the septum is resorbed. Since the Müllerian ducts are completely fused, a normal external fundal contour is present despite a complete or partial division of the endometrial cavity. A longitudinal vaginal septum is a common finding with a complete septate uterus and can also occur with a partial septate uterus [14]. Endometriosis is also associated with septate uteri and has been documented in 30 % of fertile and infertile women with septate uteri [29, 30].

Arcuate Uterus

The arcuate uterus demonstrates a slight, rounded midline septum with a broad fundus and sometimes has a small indentation at the fundus. It has been characterized as a variant of normal uterine anatomy or a uterus with a small partial septum [16], or a bicornuate uterus. Appropriate imaging to define uterine anatomy is essential so as not to misclassify a uterus as arcuate instead of partial septate or bicornuate, which have different reproductive implications.

Müllerian Agenesis

The most extreme of the Müllerian anomalies is Müllerian agenesis, otherwise known as Mayer-Rokitansky-Küster-Hauser (MRKH) syndrome, which occurs due to agenesis or hypoplasia of the Müllerian ducts and affects approximately 1 in 5,000 females [31]. Müllerian agenesis involves congenital absence of the vagina and variable uterine development that ranges from agenesis to hypoplastic and rudimentary structures. One study demonstrated that in females with MRKH, 87 % had Müllerian remnants, 26 % of the remnants were cavitated and contained endometrial mucosa, 7 % had a Müllerian remnant measuring >4 cm, and 30 % had anomalies of the urinary tract [32]. Along with urologic anomalies, Müllerian agenesis is associated with other extragenital anomalies involving skeletal, cardiac, and auditory systems and digits and palate [33, 34].

Clinical Presentation of Congenital Uterine Anomalies

Although many females with congenital uterine anomalies are asymptomatic and a late diagnosis may occur during evaluation of infertility [35, 36], it is important to recognize several gynecologic and obstetric signs and symptoms that may indicate a uterine disorder (Table 9.1). Müllerian agenesis presents with primary amenorrhea. Women with an obstructive anomaly may report cyclic or noncyclic pelvic pain and dysmenorrhea, and these symptoms can begin several months after menarche or into adulthood. Obstructive uterine anomalies are associated with hematometra, retrograde menstruation, and endometriosis [21, 37]. Endometriosis is a common finding in women with obstructive and nonobstructive Müllerian anomalies

Table 9.1 Clinical presentation of uterine anomalies

Gynecology	Obstetrics
Pelvic pain, cyclic or noncyclic	Pregnancy loss: first and second trimester
Dysmenorrhea	Cervical incompetence
Primary amenorrhea with pain	Preterm labor and delivery
Primary amenorrhea without pain	Intrauterine growth restriction
Hematometra	Placental abruption
Abnormal uterine bleeding	Intrauterine fetal demise
Dyspareunia	Malpresentation
	Cesarean delivery
	Pregnancy-induced hypertension (related to renal abnormalities)
	Pregnancy in rudimentary uterine horn

and is a known etiology of infertility [29, 37]. Abnormal bleeding can also occur with uterine anomalies and has been associated with septate uteri [29]. Furthermore, vaginal anomalies may occur in conjunction with uterine anomalies, and abnormal bleeding may be due to a partial or microperforate vaginal obstruction or a longitudinal vaginal septum. A nonobstructive vaginal anomaly such as a longitudinal vaginal septum, which is associated with septate and didelphys uteri, may be a woman's first presentation with a uterine anomaly; associated symptoms include difficulty with tampon insertion, bleeding around one tampon (two are required), and dyspareunia. Hence, if a vaginal anomaly is identified, then uterine imaging is warranted [14].

In obstetrics, congenital uterine anomalies are associated with a higher rate of poor obstetric outcomes: recurrent pregnancy loss (RPL), first and second trimester pregnancy loss, intrauterine growth restriction, preterm labor and delivery, placental abruption, malpresentation, and intrauterine fetal demise [1, 7, 21, 38, 39]. Among women with RPL, the incidence of uterine anomalies is highly variable and ranges from 6 to 38 %, but based on meta-analyses is likely closer to 12 to 16 % and is as high as 25 % in women with second trimester pregnancy loss [3–5, 40]. Uterine dysfunction may occur due to diminished cavity size, insufficient musculature, impaired ability to distend, abnormal myometrial and cervical function, inadequate vascularity, or abnormal endometrial development [1, 3, 8, 22, 41–46]. Due to higher rates of malpresentation, an increased rate of cesarean delivery can be seen with uterine anomalies. Additional obstetric complications such as cervical incompetence [47], pregnancy-induced hypertension (due to renal anomalies), and antepartum and postpartum bleeding are also associated with congenital uterine anomalies. Lastly, pregnancy may occur in an obstructed or rudimentary uterine horn. These pregnancies are surgical emergencies due to an 89 % rate of rupture and the related morbidity and mortality [20].

Imaging of Congenital Uterine Anomalies

Initial testing to evaluate pelvic anatomy, especially in infertile women, may include hysterosalpingography (HSG) and two-dimensional ultrasonography (2DUS). While these modalities are useful for the initial assessment of uterine anomalies, additional testing may be warranted such as saline-infusion ultrasonography (SIS), magnetic resonance imaging (MRI), and the increasingly common technique of three-dimensional ultrasonography (3DUS). The benefit of 3DUS and MRI is the ability to simultaneously assess the uterine fundus and cavity [17]. However, there are inherent strengths and limitations to each imaging technique; thus, a combination of several techniques may be necessary to evaluate a uterine anomaly. Although surgical evaluation (i.e., laparoscopy, hysteroscopy, laparotomy) has been considered the gold standard for evaluation of complex Müllerian anomalies [18, 41], with readily available diagnostic imaging, surgery is infrequently necessary for evaluation and diagnosis of anomalies. Surgical intervention with hysteroscopy and/or laparoscopy may only be necessary when the uterine anomaly is amenable to surgery and the intervention is clinically necessary [4, 48, 49]. This discussion

will review all available imaging techniques and will focus on the evolving technique of 3-D ultrasonography.

Hysterosalpingography

A common procedure for evaluation of tubal patency in women with infertility, HSG can also provide information about the contour of the uterine cavity. In a woman with a uterine anomaly, the HSG may identify patent canals and any complex communications, but is unable to adequately evaluate the external uterine contour and, hence, cannot reliably differentiate between uterine anomalies [4, 11, 35]. When a uterine anomaly is identified, assessment of the external uterine contour can be achieved with 2DUS, 3DUS, and/or SIS. In one study, HSG correctly diagnosed 55 % of septate and bicornuate uteri, and the addition of ultrasonography improved this result to 90 % [50]. Since the HSG involves exposure to ionizing radiation, in young women with desired fertility, this test should only be ordered when clinically indicated.

Two-Dimensional Ultrasonography

Two-dimensional transabdominal or transvaginal ultrasonography is a common initial technique for assessing pelvic structures. It effectively visualizes the uterine structure and endometrial contour, can detect a pelvic mass or hematometra, confirms the presence of ovaries, and can be used to evaluate the kidneys. When 2DUS is performed in the secretory phase of the menstrual cycle, better visualization of the endometrium and internal uterine contour can be achieved [51, 52]. A compilation of 2DUS studies for uterine anomalies noted a pattern of low sensitivity and high specificity; although 2DUS can only identify about half of the uterine anomalies present, the diagnosis of an anomaly is highly likely to be correct [4]. When indicated, *saline infusion sonography* can be employed to further assess the internal and external uterine contours and can accurately diagnose uterine anomalies as well as identify other intracavitary abnormalities such as polyps, myomas, or adhesions [4, 49, 53].

Pelvic Magnetic Resonance Imaging

Pelvic MRI is a sensitive and specific imaging modality for evaluating Müllerian anomalies [11, 54]. MRI provides detailed delineation of internal and external uterine contours, can differentiate between a myometrial and fibrous uterine division, can differentiate between a septate cervix and duplicated cervix, can diagnose vaginal anomalies, and can identify if a rudimentary uterine horn contains functional endometrium [11, 17]. Furthermore, MRI can also assess renal morphology and location. Although costly, this noninvasive imaging modality is less expensive than surgery [18]. Pelvic MRI may not be necessary for every patient with a uterine anomaly and may be best utilized for the evaluation of complex Müllerian anomalies [17, 36].

A number of studies have evaluated the efficacy of MRI to assess surgically confirmed uterine anomalies [18, 55–58]. A range of sensitivity (29 to 100 %) and specificity (33 to 100 %) and positive predictive value (83 to 100 %) and negative predictive value (25 to 100 %) was identified. The ability of MRI to detect and correctly diagnose a uterine anomaly can be limited by the availability of technically adequate images which may be influenced by the MRI machine and software utilized and requires image interpretation by a practitioner with experience in the diagnosis of uterine anomalies [18, 49].

Three-Dimensional Ultrasonography

Three-dimensional ultrasonography (3DUS) is a relatively new imaging technique that provides detailed and highly accurate views of pelvic anatomy; it constructs three-dimensional volumes from a series of two-dimensional images [18, 27]. After the volume is created, it can be stored and any section of a structure can be examined. With uterine anomalies, the ability to visualize the coronal section of the uterus is invaluable for assessing the architecture of the endometrial cavity and the uterine fundus (Fig. 9.2) [17, 27, 48, 59, 60]. Therefore, by evaluating the internal and external uterine contours, 3DUS is able to reliably differentiate between various uterine

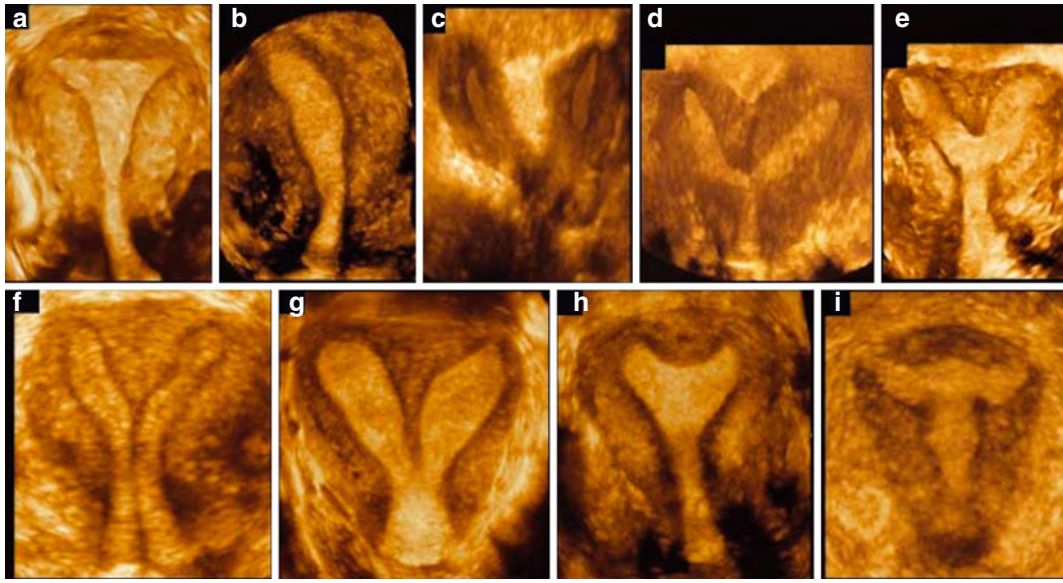

Fig. 9.2 Three-dimensional rendered coronal ultrasound images demonstrating different uterine anomalies using the American Fertility Society classification [16]: (**a**) normal uterus; (**b**) unicornuate uterus; (**c**) didelphic uterus; (**d**) complete bicornuate uterus; (**e**) partial bicornuate uterus; (**f**) complete septate uterus; (**g**) partial septate uterus; (**h**) arcuate uterus; (**i**) uterus with diethylstilbestrol (DES) drug-related malformations (Reprinted Bermejo et al. [17]. With permission from John Wiley & Sons, Inc.)

Table 9.2 Three-dimensional ultrasound criteria for classification of congenital uterine anomalies

Uterine morphology	Fundal contour	External contour
Normal	Straight or convex	Uniformly convex or with indentation <10 mm
Arcuate	Concave fundal indentation with central point of indentation at obtuse angle (>90°)	Uniformly convex or with indentation <10 mm
Partial septate	Presence of septum (does not extend to cervix) with central point of septum at an acute angle (<90 %)	Uniformly convex or with indentation <10 mm
Complete septate	Presence of septum that completely divides cavity from fundus to cervix	Uniformly convex or with indentation <10 mm
Bicornuate	Two well-formed uterine cornua	Fundal indentation >10 mm dividing the two cornua
Unicornuate uterus	Single well-formed uterine cavity with a single interstitial portion of fallopian tube and concave fundal contour	Fundal indentation >10 mm dividing the two cornua if a rudimentary horn is present

Adapted from Refs. [19, 61]

anomalies and can assess the often subtle differences between septate and bicornuate uteri [17, 18, 27, 28, 59, 61]. However, distortion by leiomyomas may make uterine assessment more challenging [7, 18, 59]. This modality is less expensive and less time consuming than surgery or pelvic MRI, is less invasive than surgery, and may be better tolerated [17, 18, 52]. Although the American Fertility Society classification for uterine anomalies (Fig. 9.1) does not provide dimensions or measurements to enable differentiation of uterine anomalies based on ultrasound findings, a modification of the AFS criteria based on 3DUS landmarks has been utilized to facilitate the diagnosis of uterine anomalies (Table 9.2, Fig. 9.3) [11, 16, 18, 19, 48, 61].

When compared to HSG and 2DUS, 3DUS demonstrates high sensitivity and specificity

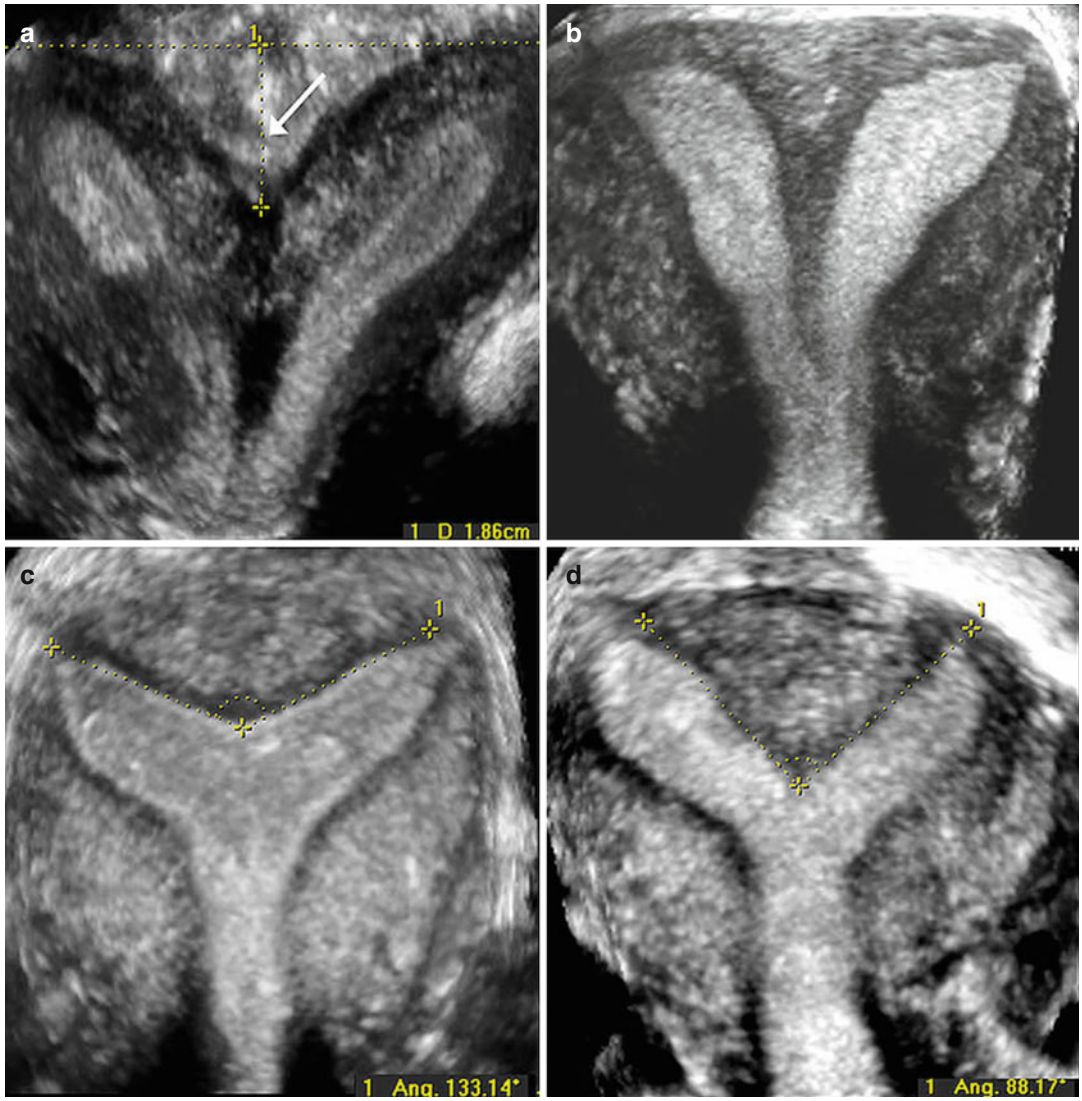

Fig. 9.3 Three-dimensional rendered coronal ultrasound images demonstrating ultrasound criteria for classification of congenital uterine anomalies. (**a**) Bicornuate uterus: two divergent cornua are noted, divided by a sagittal cleft >10 mm (*arrow*). (**b**) Complete septate uterus: a normal external uterine contour is present, and a septum divides the endometrial cavity and extends to the cervix. (**c**) Arcuate uterus: a normal external uterine contour is identified with a concave fundal indentation of the endometrial cavity at an obtuse angle. (**d**) Partial septate uterus: a normal external uterine contour is present, the septum does not extend to the cervix, and the central point of the fundal indentation demonstrates an acute angle (Reprinted Ghi et al. [48]. With permission from Elsevier)

for the identification of a normal uterus (98 and 100 %), arcuate uterus (100 and 100 %), or major uterine anomaly (100 and 100 %) [59]. In comparison, 2DUS has lower sensitivity and specificity for the diagnosis of a normal uterus (88 and 94 %) or arcuate uterus (67 and 94 %), but is similarly accurate with major uterine anomalies (100 and 95 %). Hence, 2DUS may be best utilized as a screening test for uterine anomalies, with 3DUS as the definitive diagnostic test [59].

Several studies investigated the accuracy of 3DUS for the evaluation and diagnosis of uterine anomalies and confirmed the radiologic findings at surgery (laparoscopy and/or hysteroscopy).

In one study, 3DUS assessment of the uterine fundus correlated 91.6 % with laparoscopic findings, and evaluation of the uterine cavity correlated 100 % with hysterosalpingography [62]. Wu et al. compared 3DUS with laparoscopy for the detection of uterine anomalies, and 3DUS demonstrated 100 % sensitivity and specificity and correctly diagnosed 92 % (11/12) of septate uteri and 100 % (3/3) of bicornuate uteri [28]. A study of 3,850 infertile women who underwent uterine evaluation with 3DUS and hysteroscopy identified 689 (17.9 %) with septate uteri, and 3DUS demonstrated 99.27 % sensitivity and 100 % specificity for diagnosing a septate uterus [7]. Another recent study investigated 254 nulliparous women with recurrent pregnancy loss, and 3DUS findings were confirmed by office hysteroscopy (for normal uteri) or laparoscopy/hysteroscopy if a uterine anomaly was identified [48]. Fifty-four subjects (19 %) were diagnosed with a uterine anomaly, and 3DUS correctly identified 52 (92.3 %) of the anomalies; two partial septate uteri were misclassified as bicornuate and arcuate. When 3DUS and 2DUS were compared for the diagnosis of uterine anomalies during different phases of the menstrual cycle, both modalities had higher sensitivity and specificity during the luteal phase, but 3DUS demonstrated greater sensitivity and specificity in both the follicular and luteal phases, and the diagnostic accuracy of 3DUS was comparable to HSG, hysteroscopy, and laparoscopy [52]. Lastly, the reproducibility of the interpretation of 3DUS volumes to diagnose uterine anomalies has been established [61].

Few studies have compared the diagnosis of uterine anomalies by 3DUS versus pelvic MRI. Bermejo et al. determined that in women with uterine anomalies, 3DUS and MRI demonstrate a high degree of concordance, with a kappa index of 0.880 (95 % CI, 0.77 to 0.99) [17]. Discrepancies occurred in the diagnosis of 4 of 65 anomalies; 3DUS misclassified one bicornuate uterus as uterus didelphys, and 3 septate uteri as bicornuate uteri. In contrast, Faivre et al. investigated women with suspected septate and bicornuate uteri; all 31 uterine anomalies were confirmed by hysteroscopy and/or laparoscopy [49]. 3DUS correctly identified 31/31 uterine anomalies, and pelvic MRI correctly identified 24/31 uterine anomalies; five septate uteri were misclassified as bicornuate uteri, and 2 partial septate uteri as complete septate uteri. These discrepancies were attributed to the lack of a coronal uterine image and lack of familiarity with the evaluation of uterine anomalies.

3DUS has been demonstrated to be at least as accurate as pelvic MRI for diagnosing uterine anomalies. However, 3DUS is not a widely available imaging modality and requires a high level of practitioner skill and experience to achieve high diagnostic accuracy [17, 18, 57]. Although these studies have promising results, it must be emphasized that they were performed by practitioners with expertise in the performance and interpretation of 3DUS and in the diagnosis of uterine anomalies.

Urinary Tract Imaging

Lastly, since urinary tract anomalies are associated with Müllerian anomalies, imaging of the urinary tract needs to be considered when a uterine anomaly is identified. Upper urinary tract anomalies include renal agenesis, horseshoe or pelvic kidney, duplication of the collecting system, or an ectopic ureter [10]. Renal anomalies most commonly occur with unicornuate and didelphic uteri and with Müllerian agenesis and are infrequently identified with bicornuate, septate, and arcuate uteri [63]. If an obstructive Müllerian anomaly is identified such as a unicornuate uterus with a rudimentary uterine horn or uterus didelphys with an obstructed hemivagina, renal anomalies including renal agenesis are commonly identified ipsilateral to the obstruction. In more than 50 % of cases, renal agenesis is predictive of an obstructive Müllerian anomaly [20].

Options for urinary tract imaging include renal ultrasound, intravenous pyelogram, computed tomography (CT) scan, or magnetic resonance (MR) urogram. In women diagnosed with a Müllerian anomaly, the kidneys should be evaluated with ultrasonography, and further imaging

should be undertaken based on symptoms and the extent of the malformation [10]. Due to a higher risk of urinary tract anomalies, more detailed imaging is warranted in females with uterine anomalies that may involve a unilateral obstruction: unicornuate or uterus didelphys or Müllerian agenesis [63].

Reproductive Outcomes with Uterine Anomalies

Challenges with maintenance of pregnancy, not conception, are commonly associated with uterine anomalies; uterine anomalies do not prevent conception and normal reproductive outcomes are possible. Infertile women have a 3.4 to 8 % mean prevalence of uterine anomalies which is comparable to that of the fertile population [3–5]. A higher prevalence of uterine anomalies (12.6 to 16.7 %) is seen in women with RPL [3–5]. These data suggest that uterine anomalies have a negligible effect on fertility, and maintenance of pregnancy is the larger issue [3, 29]. Furthermore, women with uterine anomalies who undergo assisted reproductive technologies have comparable pregnancy rates to infertile women with normal uteri, but a higher rate of pregnancy loss and preterm delivery [64]. These adverse reproductive outcomes are attributed to deficient musculature and reduced cavity size, abnormal vascularity, and cervical insufficiency [63].

Depending on the population studied and the accuracy of the imaging modalities in diagnosing uterine anomalies, the arcuate [4, 5] or septate uterus [3, 11, 65] is the most common uterine anomaly. Saravelos et al. report that the arcuate uterus is the most common uterine anomaly in the general (2.4 %) and recurrent miscarriage (12.0 %) populations, but the septate uterus is most common in the infertile population (3.9 %) [4]. A more recent meta-analysis identified that the arcuate uterus is the most common anomaly (3.9 %) in the general population and its prevalence is not increased in groups at high risk for poor reproductive outcomes, while the septate uterus is the most common anomaly (3.0–15.4 %) in high-risk populations (women with infertility and a history of miscarriage) [5]. These data highlight the reproductive dysfunction associated with the septate uterus and raise questions about a possible relationship between the septate uterus and infertility.

The septate uterus contains a hypovascular fibromuscular uterine septum, and this structural abnormality as well as abnormalities in the endometrium overlying the septum may predispose this anomaly to the worst reproductive outcomes [42, 46, 66]. A compilation of studies investigating pregnancy outcome in women with an untreated septate uterus identified a 44 % abortion rate (range 23–67 %), 22 % preterm delivery rate (range 8.6–33 %), 33 % term delivery rate (range 0–68 %), and 50 % live birth rate (range 28–68.5 %) (Table 9.3) [3]. Another study compared women with septate uteri to the general population and identified an increased rate of early abortion (41.1 % versus 12.1 %) and late abortion and preterm delivery (12.6 % versus 6.9 %) [7]. Due to variability in the pregnancy outcomes reported in the included studies, these data may overstate the degree of reproductive compromise seen with this anomaly and represent a "worst case scenario" [19]. Regardless,

Table 9.3 Reproductive outcomes in women with congenital uterine anomalies. Rates are averaged and presented as a percentage

Uterine anomaly	Number of studies	Number of patients	Number of pregnancies	Abortion rate	Preterm birth rate	Term delivery rate	Live birth rate
Unicornuate	11	151	250	36.5	16.2	44.6	54.2
Didelphys	8	114	152	32.2	28.3	36.2	55.9
Bicornuate	4	261	627	36	23	40.6	55.2
Septate	4	198	499	44.3	22.4	33.1	50.1
Arcuate	3	102	241	25.7	7.5	62.7	66

Based on data from Ref. [3]

it is clear that the septate uterus may significantly impact reproductive outcomes. Fortunately, it is the most treatable uterine anomaly and can be corrected with operative hysteroscopy, a minimally invasive procedure.

Unicornuate, didelphys, and bicornuate uteri are implicated in adverse reproductive outcomes; live birth rates for women with these uterine anomalies are at least 50–55 %, and miscarriage rates are approximately 35 % (Table 9.3) [3, 63]. These rates are somewhat better than those associated with the septate uterus and, again, may represent a less optimistic statement of reproductive outcomes. Additionally, overall obstetrical outcomes may be somewhat better with the bicornuate uterus due to variability in the degree of cavity division; the rate of preterm delivery differs between partial (29 %) and complete (66 %) bicornuate uteri [67].

By definition, the arcuate uterus deviates minimally from normal uterine anatomy, thus is traditionally considered benign and not associated with an increased risk of adverse pregnancy outcomes [16, 27]. However, the arcuate uterus has been associated with a range of reproductive outcomes: live birth rates range from 48 to 82.7 % [1, 3, 38]. One concern is that when less accurate imaging techniques are utilized, a bicornuate or partial septate uterus may be misclassified as an arcuate uterus and mistakenly associated with worse reproductive outcomes [27]. Based on what is known about arcuate uterine anatomy, the more optimistic reproductive data are more believable, and surgical intervention is likely not warranted unless poor reproductive outcomes occur.

Indications for Surgical Intervention

Historically, surgery was considered the gold standard for the evaluation and diagnosis of Müllerian anomalies. However, due to the availability of advanced imaging techniques that can assess the uterine fundal contour and endometrial cavity architecture, diagnostic surgical procedures such as an exam under anesthesia, vaginoscopy, hysteroscopy, and laparoscopy are infrequently necessary when diagnosing uterine anomalies.

Surgical intervention is indicated for women with obstructive anomalies, pelvic pain, endometriosis, and poor obstetric outcomes such as RPL, second trimester loss, or preterm delivery. In women with RPL and preterm delivery, it is important to rule out extrauterine causes of these obstetric issues [8, 21]. Although certain uterine anomalies such as the septate uterus are amenable to surgical correction, the unicornuate uterus is never considered operable (although rudimentary horns may warrant surgical intervention), and bicornuate and didelphys uteri are considered operable in select circumstances [21, 63, 65, 68]. Abdominal metroplasty can be performed to unify a bicornuate uterus or uterus didelphys but is only performed in select patients with poor obstetric outcomes [21, 65, 68]. The goals of surgery include treatment of pelvic pain and endometriosis, restoration of pelvic anatomy, and preservation of fertility.

Hysteroscopic metroplasty to correct a partial or complete septate uterus can improve reproductive outcomes and is indicated in women with recurrent pregnancy loss or second trimester pregnancy loss [3, 41]. After the hysteroscopic procedure, the risk of pregnancy loss or other adverse perinatal outcomes is dramatically decreased; live birth and miscarriage rates are improved to approximately 80 and 15 %, respectively [3, 7, 29, 41]. For surgical treatment of a uterine septum, the hysteroscopic approach is preferred due to its safety, simplicity, and excellent postoperative results [41, 65], and laparoscopy can be utilized to assess the fundal contour and guide the extent of septum resection but is not mandatory [29, 41].

While hysteroscopic metroplasty for women with RPL significantly improves the live birth rate, in women with unexplained infertility, surgery achieves modest improvements in pregnancy and live birth rates [41, 65, 69, 70]. Furthermore, a recent study identified that women with unexplained infertility and a septate uterus who underwent hysteroscopic metroplasty had significantly improved rates of conception (38.6 % vs. 20.4 %) and live birth (34.1 % vs. 18.9 %) compared to

women with unexplained infertility and a normal uterus [71]. These data lend support to the concern about implantation issues with a septate uterus. The risks of pregnancy loss and possible infertility are of concern when a septate uterus is identified in a woman with infertility or in a woman of advanced reproductive age with desired fertility. In these women, prophylactic metroplasty may prevent miscarriage or other obstetric complications and may improve fertility. Surgical intervention is commonly recommended to optimize pregnancy outcomes in women with prolonged infertility, in women over age 35, and in women pursuing infertility treatment with assisted reproductive technologies [1, 21, 29, 43, 65, 71–74]. However, surgical intervention for a septate uterus identified in an asymptomatic woman is controversial; a thorough discussion of the potential benefits and risks of prophylactic intervention is indicated.

In patients with a unicornuate uterus, excision of a communicating or noncommunicating functional rudimentary uterine horn and the attached fallopian tube is recommended to prevent a horn or tubal gestation [20, 65]. Due to the high risk of pregnancy complications with a functional uterine horn, surgical excision is recommended even in asymptomatic women. Additionally, this intervention treats pelvic pain associated with hematometra, hematosalpinx, retrograde menstruation, and endometriosis [20, 65]. If the uterine horn does not contain endometrium and the woman is asymptomatic, surgical excision is not required.

Lastly, the benefit of surgical correction for an arcuate uterus is unclear. This uterine configuration is typically considered a variant of normal, and reproductive outcomes are generally good. One study states that women with an arcuate uterus may benefit from hysteroscopic metroplasty since preterm birth decreased from 33.9 to 7.2 % after surgery; however, an "arcuate uterus" was defined as a small uterine septum measuring 1.3–1.5 cm in length, which could be considered a partial septate uterus [75]. Regardless, the data provide evidence that hysteroscopic metroplasty for a small partial uterine septum or prominent arcuate uterus is indicated in women with a history of preterm birth.

Conclusion

Maintaining a high suspicion for uterine anomalies is important because they affect 3–8 % of fertile and infertile women and 12–16 % of women with recurrent miscarriage and have a variety of presentations in gynecology and obstetrics. It is critical to obtain detailed uterine assessment during office 2DUS and to know when further imaging is warranted. Although a range of imaging modalities is available, 2DUS is a reasonable "screening test" for uterine anomalies, and 3DUS is emerging as the appropriate "diagnostic test." 3DUS is a noninvasive imaging technique that can screen low-risk and high-risk women with desired fertility and accurately identify those with uterine anomalies that may impact pregnancy outcomes [27]. However, complex Müllerian anomalies beyond uterine anomalies may require additional imaging such as pelvic MRI for the full definition of the anomaly. The availability of diagnostic imaging that accurately and reliably differentiates and diagnoses uterine anomalies enables the identification of women at risk of pregnancy complications, allows timely and appropriate surgical intervention, and helps guide future pregnancy management [27, 60]. To optimize patient outcomes, accurate diagnosis of uterine anomalies is essential.

References

1. Raga F, Bauset C, Remohi J, Bonilla-Musoles F, Simon C, Pellicer A. Reproductive impact of congenital müllerian anomalies. Hum Reprod. 1997; 12:2277–81.
2. Simon C, Martinez L, Pardo F, Tortajada M, Pellicer A. Müllerian defects in women with normal reproductive outcome. Fertil Steril. 1991;56: 1192–3.
3. Grimbizis GF, Camus M, Tarlatzis BC, Bontis JN, Devroey P. Clinical implications of uterine malformations and hysteroscopic treatment results. Hum Reprod Update. 2001;7:161–74.
4. Saravelos SH, Cocksedge KA, Li TC. Prevalence and diagnosis of congenital uterine anomalies in women with reproductive failure: a critical appraisal. Hum Reprod Update. 2008;14:415–29.

5. Chan YY, Jayaprakasan K, Zamora J, Thornton JG, Raine-Fenning N, Coomarasamy A. The prevalence of congenital uterine anomalies in unselected and high-risk populations: a systematic review. Hum Reprod Update. 2011;17:761–71.
6. Nahum GG. Uterine anomalies: how common are they, and what is their distribution among subtypes? J Reprod Med. 1998;43:877–87.
7. Kupesic S, Kurjac A, Skenderovic S, Bjelos D. Screening for uterine abnormalities by three-dimensional ultrasound improves perinatal outcomes. J Perinat Med. 2002;30:9–17.
8. Propst AM, Hill JA. Anatomic factors associated with recurrent pregnancy loss. Semin Reprod Med. 2000;18:341–50.
9. Hammoud AO, Gibson M, Mathew Peterson C, Kerber RA, Mineau GP, Hatasaka H. Quantification of the familial contribution to Müllerian anomalies. Obstet Gynecol. 2008;111:378–84.
10. Oppelt P, von Have M, Paulsen M, Strissel PL, Strick R, Brucker S, et al. Female genital malformations and their associated abnormalities. Fertil Steril. 2007;87: 335–42.
11. Troiano RN, McCarthy SM. Müllerian duct anomalies: imaging and clinical issues. Radiology. 2004; 233:19–34.
12. Chang AS, Siegel CL, Moley KH, Ratts VS, Odem RR. Septate uterus with cervical duplication and longitudinal vaginal septum: a report of five new cases. Fertil Steril. 2004;81:1133–6.
13. Pavone ME, King JA, Vlahos N. Septate uterus with cervical duplication and a longitudinal vaginal septum: a müllerian anomaly without a classification. Fertil Steril. 2006;85:e9–10.
14. Haddad B, Louis-Sylvestre C, Poitout P, Paniel BJ. Longitudinal vaginal septum: a retrospective study of 202 cases. Eur J Obstet Gynecol Reprod Biol. 1997; 74:197–9.
15. Ergun A, Pabuccu R, Atay V, Kücük T, Duru NK, Güngör S. Three sisters with septate uteri: another reference to bidirectional theory. Hum Reprod. 1997;12:140–2.
16. The American Fertility Society classification of adnexal adhesions, distal tubal occlusion, tubal occlusion secondary to tubal ligation, tubal pregnancies, müllerian anomalies and intrauterine adhesions. Fertil Steril. 1988;49:944–55.
17. Bermejo C, Ten Martinez P, Cantarero R, Diaz D, Perez Pedregosa J, Barron E, et al. Three-dimensional ultrasound in the diagnosis of Müllerian duct anomalies and concordance with magnetic resonance imaging. Ultrasound Obstet Gynecol. 2010;35:593–601.
18. Deutch TD, Abuhamad AZ. The role of 3-dimensional ultrasonography and magnetic resonance imaging in the diagnosis of müllerian duct anomalies: a review of the literature. J Ultrasound Med. 2008;27: 413–23.
19. Woelfer B, Salim R, Banerjee S, Elson J, Regan L, Jurkovic D. Reproductive outcomes in women with congenital uterine anomalies detected by three-dimensional ultrasound screening. Obstet Gynecol. 2001;98:1099–103.
20. Jayasinghe Y, Rane A, Stalewski H, Grover S. The presentation and early diagnosis of the rudimentary uterine horn. Obstet Gynecol. 2005;105:1456–67.
21. Lin PC, Bhatnagar KP, Nettleton GS, Nakajima ST. Female genital anomalies affecting reproduction. Fertil Steril. 2002;78:899–915.
22. Fedele L, Zamberletti D, Vercellini P, Dorta M, Candiani GB. Reproductive performance of women with unicornuate uterus. Fertil Steril. 1987;47:416–9.
23. Vercellini P, Daguati R, Somigliana E, Vigano P, Lanzani A, Fedele L. Asymmetric lateral distribution of obstructed hemivagina and renal agenesis in women with uterus didelphys: institutional case series and a systematic literature review. Fertil Steril. 2007;87:719–24.
24. Smith NA, Laufer MR. Obstructed hemivagina and ipsilateral renal anomaly (OHVIRA) syndrome: management and follow-up. Fertil Steril. 2007;87:918–22.
25. Fedele L, Ferrazzi E, Dorta M, Vercellini P, Candiani GB. Ultrasonography in the differential diagnosis of 'double' uteri. Fertil Steril. 1988;50:361–4.
26. Candiani GB, Ferrazzi E, Fedele L, Vercellini P, Dorta M. Sonographic evaluation of uterine morphology: a new scanning technique. Acta Eur Fertil. 1986;17:345–8.
27. Salim R, Jurkovic D. Assessing congenital uterine anomalies: the role of three-dimensional ultrasonography. Best Pract Res Clin Obstet Gynaecol. 2004; 18:29–36.
28. Wu MH, Hsu CC, Huang KE. Detection of congenital müllerian duct anomalies using three-dimensional ultrasound. J Clin Ultrasound. 1997;25:487–92.
29. Fedele L, Bianchi S, Frontino G. Septums and synechiae: approaches to surgical correction. Clin Obstet Gynecol. 2006;49:767–88.
30. Nawroth F, Rahimi G, Nawroth C, Foth D, Ludwig M, Schmidt T. Is there an association between septate uterus and endometriosis? Hum Reprod. 2006;21:542–4.
31. Evans TN, Poland ML, Boving RL. Vaginal malformations. Am J Obstet Gynecol. 1981;141:910–20.
32. Fedele L, Bianchi S, Frontino G, Ciappina N, Fontana E, Borruto F. Laparoscopic findings and pelvic anatomy in Mayer-Rokitansky-Küster-Hauser syndrome. Obstet Gynecol. 2007;109:1111–5.
33. Oppelt P, Renner SP, Kellermann A, Brucker S, Hauser GA, Ludwig KS, et al. Clinical aspects of Mayer-Rokitansky-Küster-Hauser syndrome: recommendations for clinical diagnosis and staging. Hum Reprod. 2006;21:792–7.
34. Pittock ST, Babovic-Vuksanovic D, Lteif A. Mayer-Rokitansky-Küster-Hauser anomaly and its associated malformations. Am J Med Genet. 2005;135A:314–6.
35. Braun P, Grau FV, Pons RM, Enguix DP. Is hysterosalpingography able to diagnose all uterine malformations correctly? A retrospective study. Eur J Radiol. 2005;53:274–9.
36. Mazouni C, Girard G, Deter R, Haumonte JB, Blanc B, Bretelle F. Diagnosis of müllerian anomalies in adults: evaluation of practice. Fertil Steril. 2008;89: 219–22.
37. Sanfilippo JS, Wakim NG, Schikler KN, Yussman MA. Endometriosis in association with uterine anomaly. Am J Obstet Gynecol. 1986;154:39–43.

38. Acien P. Reproductive performance of women with uterine malformations. Hum Reprod. 1993;8:122–6.
39. Ludmir J, Samuels P, Brooks S, Mennuti MT. Pregnancy outcome of patients with uncorrected uterine anomalies managed in a high-risk obstetric setting. Obstet Gynecol. 1990;75:906–10.
40. Acien P. Incidence of müllerian defects in fertile and infertile women. Hum Reprod. 1997;12:1372–6.
41. Homer HA, Li TC, Cooke ID. The septate uterus: a review of management and reproductive outcome. Fertil Steril. 2000;73:1–14.
42. Fedele L, Bianchi S, Marchini M, Franchi D, Tozzi L, Dorta M. Ultrastructural aspects of endometrium in infertile women with septate uterus. Fertil Steril. 1996;65:750–2.
43. Fedele L, Bianchi S. Hysteroscopic metroplasty for septate uterus. Obstet Gynecol Clin North Am. 1995;22:473–89.
44. Andrews MC, Jones Jr HW. Impaired reproductive performance of the unicornuate uterus: intrauterine growth retardation, infertility, and recurrent abortion in five cases. Am J Obstet Gynecol. 1982;144:173–6.
45. Moutos DM, Damewood MD, Schlaff WD, Rock JA. A comparison of the reproductive outcome between women with a unicornuate uterus and women with a didelphic uterus. Fertil Steril. 1992;58:88–93.
46. Candiani GB, Fedele L, Zamberletti D, De Virgiliis D, Carinelli S. Endometrial patterns in malformed uteri. Acta Eur Fertil. 1983;14:311–8.
47. Golan A, Langer R, Wexler S, Segev E, Niv D, David MP. Cervical cerclage: its role in the pregnant anomalous uterus. Int J Fertil. 1990;35:164–70.
48. Ghi T, Casadio P, Kuleva M, Perrone AM, Savelli L, Giunchi S, et al. Accuracy of three-dimensional ultrasound in diagnosis and classification of congenital uterine anomalies. Fertil Steril. 2009;92:808–13.
49. Faivre E, Fernandez H, Deffieux X, Gerviase A, Frydman R, Levaillant JM. Accuracy of three-dimensional ultrasonography in differential diagnosis of septate and bicornuate uterus compared with office hysteroscopy and pelvic magnetic resonance imaging. J Minim Invasive Gynecol. 2012;19:101–6.
50. Reuter KL, Daly DC, Cohen SM. Septate versus bicornuate uteri: errors in imaging diagnosis. Radiology. 1989;172:749–52.
51. Nicolini U, Bellotti M, Bonazzi B, Zamberletti D, Candiani GB. Can ultrasound be used to screen uterine malformations? Fertil Steril. 1987;47:89–93.
52. Caliskan E, Ozkan S, Cakiroglu Y, Sarisoy HT, Corakci A, Ozeren S. Diagnostic accuracy of real-time 3D sonography in the diagnosis of congenital müllerian anomalies in high-risk patients with respect to the phase of the menstrual cycle. J Clin Ultrasound. 2010;38:123–7.
53. Goldberg JM, Falcone T, Attaran M. Sonohysterographic evaluation of uterine abnormalities noted on hysterosalpingography. Hum Reprod. 1997;12:2151–3.
54. Troiano RN. Magnetic resonance imaging of müllerian duct anomalies of the uterus. Top Magn Reson Imaging. 2003;14:269–79.
55. Pellerito JS, McCarthy SM, Doyle MB, Glickman MG, DeCherney AH. Diagnosis of uterine anomalies: relative accuracy of MR imaging, endovaginal sonography, and hysterosalpingography. Radiology. 1992;183:795–800.
56. Letterie GS, Haggerty M, Lindee G. A comparison of pelvic ultrasound and magnetic resonance imaging as diagnostic studies for müllerian tract abnormalities. Int J Fertil Menopausal Stud. 1995;40:34–8.
57. Fedele L, Dorta M, Brioschi D, Massari C, Candiani GB. Magnetic resonance evaluation of double uteri. Obstet Gynecol. 1989;74:844–7.
58. Carrington BM, Hricak H, Nuruddin RN, Secaf E, Laros Jr RK, Hill EC. Müllerian duct anomalies: MR imaging evaluation. Radiology. 1990;176:715–20.
59. Jurkovic D, Geipel A, Gruboeck K, Jauniaux E, Natucci M, Campbell S. Three-dimensional ultrasound for the assessment of uterine anatomy and detection of congenital anomalies: a comparison with hysterosalpingography and two-dimensional sonography. Ultrasound Obstet Gynecol. 1995;5:233–7.
60. Raine-Fenning N, Fleischer AC. Clarifying the role of three-dimensional transvaginal sonography in reproductive medicine: an evidence-based appraisal. J Exp Clin Assist Reprod. 2005;2:10.
61. Salim R, Woelfer B, Backow M, Regan L, Jurkovic D. Reproducibility of three-dimensional ultrasound diagnosis of congenital uterine anomalies. Ultrasound Obstet Gynecol. 2003;21:578–82.
62. Raga F, Bonilla-Musoles F, Blanes J, Osborne NG. Congenital müllerian anomalies: diagnostic accuracy of three-dimensional ultrasound. Fertil Steril. 1996;65:523–8.
63. Reichman DE, Laufer MR. Congenital uterine anomalies affecting reproduction. Best Pract Res Clin Obstet Gynaecol. 2010;24:193–208.
64. Marcus S, al-Shawaf T, Brinsden P. The obstetric outcome of in vitro fertilization and embryo transfer in women with congenital uterine malformation. Am J Obstet Gynecol. 1996;175:85–9.
65. Taylor E, Gomel V. The uterus and fertility. Fertil Steril. 2008;89:1–16.
66. Dabirashrafi H, Bahadori M, Mohammad K, Alavi M, Moghadami-Tabrizi N, Zandinejad K, et al. Septate uterus: new idea on the histologic features of the septum in this abnormal uterus. Am J Obstet Gynecol. 1995;172:105–7.
67. Heinonen PK, Saarikoski S, Pystynen P. Reproductive performance of women with uterine anomalies: an evaluation of 182 cases. Acta Obstet Gynecol Scand. 1982;61:157–62.
68. Jacobsen LJ, DeCherney A. Results of conventional and hysteroscopic surgery. Hum Reprod. 1997;12:1376–81.

69. Pabuccu R, Gomel V. Reproductive outcome after hysteroscopic metroplasty in women with septate uterus and otherwise unexplained infertility. Fertil Steril. 2004;81:1675–8.
70. Fedele L, Arcaini L, Parazzini F, Vercellini P, Di Nola G. Reproductive prognosis after hysteroscopic metroplasty in 102 women: life-table analysis. Fertil Steril. 1993;59:768–72.
71. Mollo A, De Franciscis P, Colacurci N, Cobellis L, Perino A, Venezia R, et al. Hysteroscopic resection of the septum improves the pregnancy rate of women with unexplained infertility: a prospective controlled trial. Fertil Steril. 2009;91:2628–31.
72. Rackow BW, Arici A. Reproductive performance of women with müllerian anomalies. Curr Opin Obstet Gynecol. 2007;19:229–37.
73. Choe JK, Baggish MS. Hysteroscopic treatment of septate uterus with neodymium-YAG laser. Fertil Steril. 1992;57:81–4.
74. Daly DC, Maier D, Soto-Albors C. Hysteroscopic metroplasty: six years' experience. Obstet Gynecol. 1989;73:201–5.
75. Tomazevic T, Ban-Frangez H, Ribic-Pucelj M, Premru-Srsen T, Verdenik I. Small uterine septum is an important risk variable for preterm birth. Eur J Obstet Gynecol Reprod Biol. 2007;135:154–7.

Uterine Fibroids

10

Bradley S. Hurst

Background

The identification of uterine fibroids during evaluation for infertility or in preparation for assisted reproductive technology can present a perplexing problem for patients and their providers, especially when fibroids appear to be asymptomatic. The concern is well deserved, since unnecessary surgery for fibroids exposes the patient to risks, has a high potential to result in adhesion formation, may require future cesarean delivery, and may reduce fertility if adhesions compromise the tubo-ovarian relationship or distort the uterine cavity. However, failure to perform surgery for fibroids could impair spontaneous conception or compromise outcomes of fertility treatments or increase the risk of miscarriage and pregnancy-related complications. The goal of this chapter will be to provide rational treatment options for women with uterine fibroids based on the best available data.

A uterine fibroid is a monoclonal growth of fibrovascular cells that arise from the myometrium. Estrogen and progesterone receptors are present in fibroids, and both hormones stimulate fibroid proliferation. Fibroids are surrounded by a dense vascular pseudocapsule, and larger masses usually have a greater vascular supply [1]. Factors within the pseudocapsule stimulate fibroid growth, including a local overexpression of aromatase, which converts androgens to estrogens [2]. Estrogen stimulates growth factors in the pseudocapsule, including EGF, IGF-1, bFGF, GH, TGF-β, PDGF, endothelin A, and VEGF [3, 4]. All of these factors promote fibroid growth.

The prevalence of fibroids peaks during the fourth decade because of the cumulative effects of estrogen, progesterone, and growth factors on myoma growth during the reproductive years [5]. Fibroids are more numerous and larger in African-Americans. Ultrasound studies have found a cumulative incidence of fibroids in approximately 80 % of African-American women by age 50 [6]. However, fibroids are common in all ethnicities, including a cumulative incidence of 70 % in Caucasian women. There is great interest in identifying dietary and environmental factors for fibroids, but no clear link has been found [7].

The fibroid deforms the surrounding tissues as it grows. A fibroid that develops in the myometrial wall is considered an "intramural" myoma (Fig. 10.1). A fibroid that protrudes into the endometrial mucosa is a "submucous" myoma. Fibroids that protrude the serosal surface of the uterus are called "subserosal" myomas (Fig. 10.2). Other terms sometimes used to describe the location of fibroids include "sessile," a type of submucous myoma that is located in the myometrium, but also distorts the endometrium (Fig. 10.3). A "pedunculated" fibroid is located primarily outside of the uterus, connected to the

B.S. Hurst, MD
Department of Obstetrics and Gynecology,
Carolinas Healthcare System, 1025 Morehead
Medical Drive, Suite 500, Charlotte, NC 28204, USA
e-mail: brad.hurst@carolinashealthcare.org

L.A. Stadtmauer, I. Tur-Kaspa (eds.), *Ultrasound Imaging in Reproductive Medicine*,
DOI 10.1007/978-1-4614-9182-8_10,

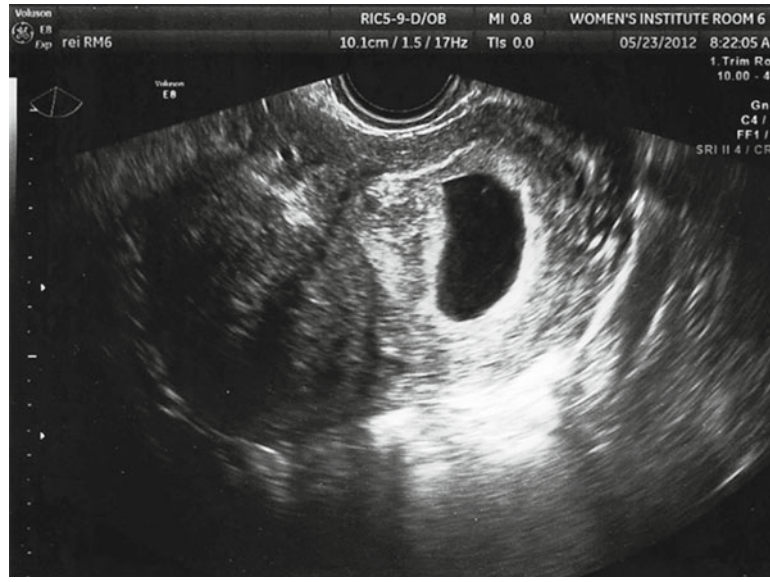

Fig. 10.1 Saline infusion sonohysterography with intramural fibroid

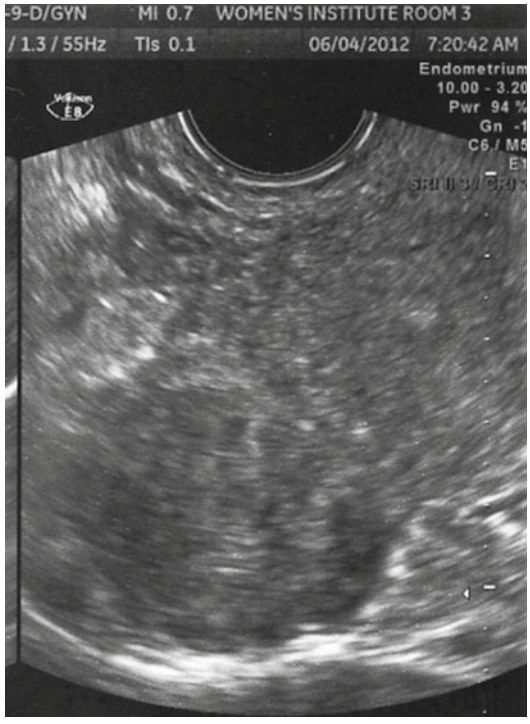

Fig. 10.2 Transvaginal ultrasound demonstrating subserosal fibroid

uterus by a fibrovascular stalk (Fig. 10.4). In this chapter, the terms fibroid, myoma, and leiomyoma are used interchangeably.

Symptoms attributed to fibroids are determined by the size and the location of the masses. Most intramural, subserosal, and pedunculated fibroids are asymptomatic. However, large fibroids may cause bulk symptoms such as abdominal pressure, bloating, or distention. A myoma that presses against the bladder may cause urinary frequency, urgency, or nocturia. A fibroid that compresses the rectum may cause constipation, diarrhea, or alternating symptoms. Infarction of a fibroid may cause severe acute pain, and the inflammation caused by degenerating myoma may cause adhesions. Fibroids located in the posterior cul de sac may cause dyspareunia. Occasionally, fibroids are associated with chronic, intermittent, or cyclic pain.

Submucous myomas often cause abnormal uterine bleeding. Symptoms of submucous fibroids include menorrhagia, dysmenorrhea, clotting, and intermenstrual bleeding [8]. When bleeding is severe, anemia may occur. With the high prevalence of fibroids and the multitude of symptoms that may be attributed to fibroids, it is not surprising that fibroids are the leading indication for hysterectomy. However, other treatment options must be considered for women who are interested in childbearing.

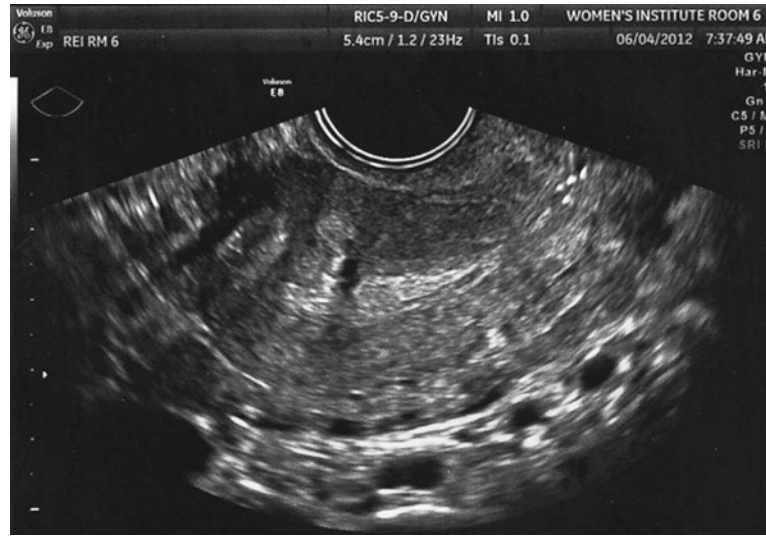

Fig. 10.3 Transvaginal ultrasound demonstrating several uterine fibroids, including one submucous myoma with deflection of the endometrial cavity

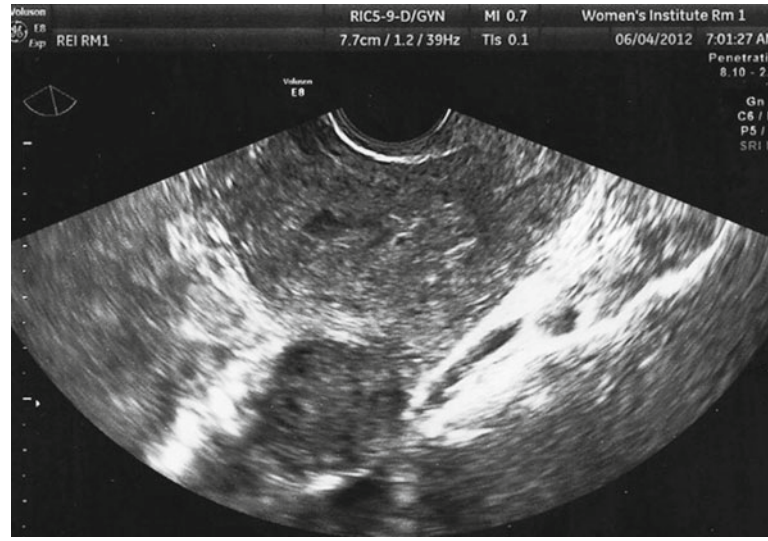

Fig. 10.4 Transvaginal ultrasound demonstrating pedunculated fibroid

Fibroids and Fertility

It is difficult to determine the direct impact of fibroids on fertility, since the incidence of uterine fibroids increases with age, fertility declines with age, and many women with fibroids conceive spontaneously.

The location of fibroids is important in determining the impact on fertility. In some circumstances, fibroids impair fertility by mechanically distorting the uterine cavity, altering the endometrium, and impairing embryo implantation and growth. Other obvious causes of fibroid-related infertility may include mechanical obstruction of the tubal ostia.

Submucous myomas directly impair fertility and cause adverse reproductive outcomes by several potential mechanisms [9]. These fibroids alter the vascular supply and development of the endometrium with intramural myomas or alter growth factors and inflammatory substances that may impair implantation or fetal growth. The mechanical distortion of the endometrial cavity almost certainly has a direct effect on fertility. In general, greater endometrial distortion

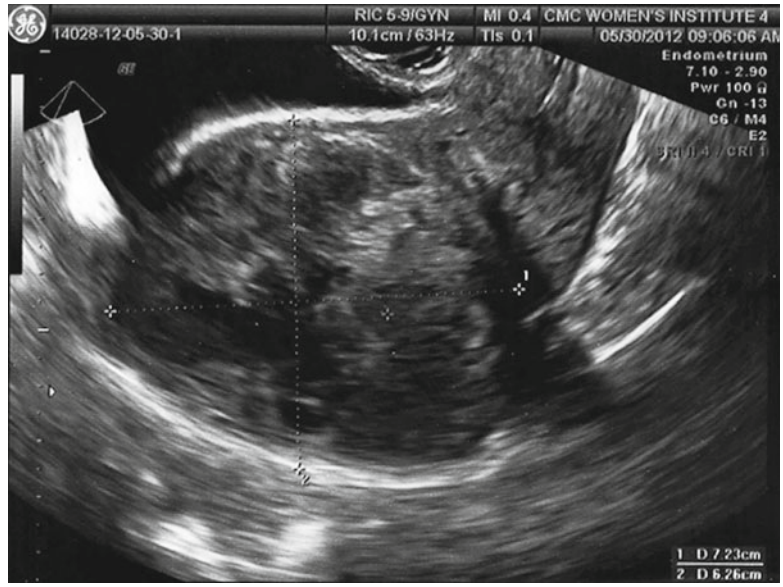

Fig. 10.5 Transvaginal ultrasound demonstrating multiple intramural fibroids; the entire endometrium is difficult to visualize

more clearly results in compromised fertility. Myomectomy improves fertility in these cases.

There is increasing data that suggests that intramural fibroids reduce fertility, especially when intramural myomas are 4 cm or larger, and myomectomy appears to restore fertility [10]. Some studies have found that fibroids between 2 and 4 cm may also compromise fertility [11]. However, the data is far from conclusive. A recent meta-analysis found a nonsignificant trend of slightly lower pregnancy rates in women with intramural myomas and a nonsignificant trend of improved pregnancy rates after myomectomy in women during assisted reproduction procedures [12]. At this time, there is no clearly proven benefit of myomectomy to enhance fertility for women with intramural myomas [13, 14]. Subserosal fibroids do not appear to affect fertility [15].

Many women have multiple fibroids, and the different size, location, number, and relative relationship to the endometrium increases the difficulty in establishing the effect of fibroids on fertility, since it is likely that no two individuals are directly comparable (Fig. 10.5). As such, the relative usefulness of myomectomy in these situations cannot be established with certainty.

Fibroids and IVF

Studies of the impact of fibroids in IVF cycles is helpful to establish the impact, since many factors impacting fertility are either controlled, such as male infertility, or directly evaluated, such as the impact of age on cycle outcome. Submucosal fibroids clearly reduce IVF pregnancy and birth rates [16, 17]. Furthermore, hysteroscopic myomectomy significantly improves pregnancy rates, with outcomes comparable to women with a normal uterine cavity [18].

The effect of medium and large intramural myomas on IVF outcomes is unclear, and most studies have shown little clinical effect. One retrospective study showed that IVF live birth rates were not improved by myomectomy: IVF "ongoing" pregnancy rates were 17 % after myomectomy ($n=47$), 21 % with untreated fibroids ($n=11$) and 19 % in normal controls [17]. However, 50 % of women with fibroids experienced a spontaneous abortion, compared to 34 % after myomectomy, possibly suggesting that fibroids compromise pregnancy outcomes. Another study of 46 IVF with intramural and subserosal fibroids showed that IVF outcomes were similar to controls, but fibroid size was not assessed [19]. Other investigators found that

myomas, 73 % of which were subserosal, had no effect on conception in 39 women [20]. A large recent study found that asymptomatic women with subserosal or intramural fibroids smaller than 5 cm did not compromise IVF pregnancy or birth rates, as long as there was no endometrial distortion [21]. One hundred nineteen women with asymptomatic intramural or subserosal fibroids were matched to controls by age and number of previous IVF cycles. The outcome was not changed when the group was limited to those with intramural myomas.

Contrary to these reports, some studies have shown that intramural fibroids impair IVF outcomes. A retrospective study found a significant decrease in IVF live birth rates in women under age 40 years with intramural fibroids (49 and 58 %, respectively) [22]. In 2005, a meta-analysis showed a significantly lower implantation rate with intramural fibroids compared to controls, 16.4 % vs. 27.7 %, respectively (OR 0.62, 0.48–0.8), and a significantly lower birth rate per embryo transfer with fibroids compared to controls, 31.2 and. 40.9 % (OR 0.69, 0.50–0.95) [23]. In a retrospective study of 91 IVF cycles in women with intramural or subserosal fibroids, Stovall et al. found a significantly lower pregnancy rate with fibroids (37 %) compared to matched controls (53 %) [24]. The fibroids' size ranged from 8 to 54 mm, with a mean diameter of 29 mm, and 95 % were intramural. The Implantation rate was 14 % with fibroids, significantly lower than the 20 % implantation rate in controls without fibroids. Another study found that women with intramural fibroids had significantly lower pregnancy rates compared to women without fibroids, 16 and 34 %, respectively, $p < 0.05$ [16]. Implantation rates were more than 50 % lower with intramural fibroids compared to the controls ($p < 0.005$), even though the mean diameter of the fibroids was 24 mm. A meta-analysis assessed 19 observational studies comprising 6,087 IVF cycles and found a significantly lower IVF live birth (RR = 0.79, 95 % CI: 0.70–0.88, $p < 0.0001$) and clinical pregnancy rate (RR = 0.85, 95 % CI: 0.77–0.94, $p = 0.002$) in women with intramural fibroids compared to those without fibroids [25]. The authors concluded that non-cavity-distorting intramural fibroids are associated with adverse pregnancy outcomes in women undergoing IVF. Finally, a study by Oliveira et al. found a significantly lower pregnancy rate with IVF only when intramural fibroids were 4 cm or larger [10].

Egg donation provides an opportunity to study the effect of implantation while minimizing the effect of confounding factors of maternal age and male fertility. There is evidence that egg donation outcomes are lower in African-American women compared to other populations, although the populations are too small to conclude that fibroids are the primary explanation for this effect [26]. It is possible that uterine fibroids could provide a possible explanation for this observation.

Uterine fibroids may increase the difficulty of the oocyte retrieval or embryo transfer and either may lower IVF outcomes. A fibroid may raise the ovary out of the pelvis, especially large masses. If this occurs, it may be necessary to perform laparoscopic oocyte retrieval or ultrasound-directed transabdominal retrieval. A fibroid may increase the difficulty of the embryo transfer in one of several ways: distorting the position of the cervix in a way that it is difficult or impossible to expose the cervix with a speculum, by markedly altering the endocervical course or causing endocervical stenosis (Fig. 10.6). Finally, a large fibroid may make visualization of embryo transfer difficult or impossible when an abdominal ultrasound-guided procedure is performed. This can be critical, especially for uterine fibroids, since increasing difficulty or tortuosity of the endocervix makes it difficult to visualize the transfer catheter to confirm optimal placement.

Myomas and Obstetrical Outcomes

While the impact of fibroids on fertility is still debated, obstetrical outcomes appear to be compromised by uterine fibroids [9]. A population-based retrospective study by Sheiner et al. [27] found that women with fibroids had a 3.5-fold increased incidence of intrauterine growth restriction (6.8 % vs. 1.9 %), a fourfold increase in placental abruption (2.8 % vs. 0.7 %), a fivefold

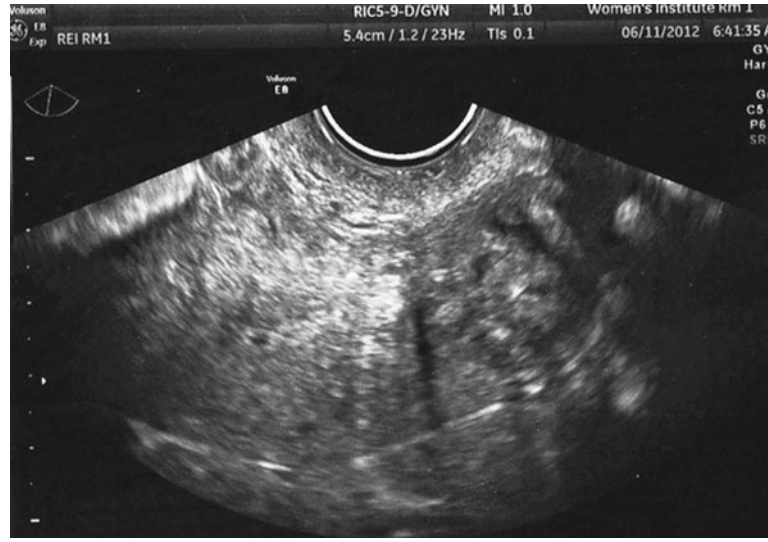

Fig. 10.6 Transvaginal ultrasound demonstrating large fibroid in the lower uterus and cervix

higher incidence of transverse lie or breech presentation (16.9 % vs. 2.4 %), a five times higher cesarean section rate (57.7 % vs. 10.8 %), 70 % higher risk of premature rupture of membranes (9.6 % vs. 5.5 %), and were three times more likely to receive transfusion (4.2 % vs. 1.4 %). All of these outcomes were significant, with $p<0.001$. Adjusting for maternal age, parity, gestational age, and malpresentation, pregnancies with fibroids still had a 6.7-times higher risk of cesarean delivery, with 95 % CI 5.5–8.1, $p<0.01$). Placental abruption and preterm deliveries remained significantly more common with fibroids. The size and locations of the fibroids were not assessed in this study, but other investigators have found that fibroids adjacent to the placenta increase the risk of bleeding and premature rupture of membranes [28].

A retrospective study in 2012 supports the hypothesis that fibroids have a detrimental impact on pregnancy, especially when the fibroids are large [29]. The mean gestation age at delivery for women with fibroids larger than 5 cm was 36.5 weeks, significantly earlier than women with smaller fibroids or no fibroids. Other significant effects included shortened cervix, premature preterm rupture of membranes, preterm delivery, blood loss during delivery, and the need for postpartum transfusion. Considering these and other publications, authors of a literature review concluded that pregnancy outcomes are compromised in women who have intramural fibroids [30].

Uterine fibroids tend to enlarge during pregnancy, regardless of size and maternal age [31]. Approximately 70 % of fibroids grow by a volume of 10 % or more between the first and second, and second and third trimesters. As a fibroid grows, masses located near the cavity have the potential to compress the cavity and cause a detrimental effect.

It would appear that myomectomy could be justified in some circumstances to reduce the risk of adverse pregnancy outcomes [32]. Unfortunately, the benefit of myomectomy for intramural fibroids has not been definitively proven. The most compelling evidence for intramural myomas appears to be cases with large fibroids, 4 cm or larger, and tumors close to the uterine cavity. It is important to clarify this issue since myomectomy for intramural fibroids has a risk of morbidity and adhesion formation, and surgery should not be considered unless the benefits outweigh the risks.

In spite of the limited data, myoma size, location, and number are key factors when discussing the outcomes after myomectomy, and these are considered separately in this discussion. However, these factors are not separable for an individual patient, and the surgeon must weigh

the cumulative impact of all three factors when deciding to perform how and when to perform a myomectomy.

Diagnosis of Uterine Fibroids

A focused history and physical examination may provide suspicion of uterine fibroids. Symptoms related to fibroids may include menorrhagia, dysmenorrhea, menstrual clotting, intermenstrual bleeding, pelvic pain, pressure, progressive constipation or alternating constipation and diarrhea, abdominal distention, or urinary frequency. However, other conditions can cause any of these symptoms, and fibroids are often asymptomatic. On examination, the uterus is often enlarged and irregular with uterine fibroids due to the distortion from the individual masses. A rectovaginal examination may be helpful to identify posterior fibroids. However, other conditions such as adenomyosis can cause uterine enlargement, and a clinically significant fibroid may be present, even if the examination is normal. Diagnostic testing with ultrasound is appropriate for any women with infertility and is considered an important component of the infertility evaluation.

Ultrasound

Transvaginal ultrasound provides better image quality than abdominal ultrasound, but both methods might be necessary in the uterus that is markedly enlarged with uterine fibroids. Since overlying bowel may limit the visualization of the uterus, abdominal ultrasound is performed with the bladder full enough to provide a "window" for the uterus. Vaginal ultrasound studies are performed with an empty bladder for patient comfort.

Careful examination of the endometrium and myometrium is needed to assess anatomic abnormalities. A submucous myoma is easily identified when the endometrium has a preovulatory "triple stripe" pattern. If there is no endometrial distortion or deflection of trilaminar endometrium, a submucous fibroid is unlikely. In the early follicular phase and after ovulation, when the endometrium is more homogeneous, endometrial distortion is more difficult to assess and saline infusion sonohysterography should be performed if a submucous fibroid is suspected [33].

Uterine fibroids may appear to have several variations in appearance using ultrasound, depending on the characteristics of the mass. For example, a calcified myoma has a bright echogenic pattern and distortion or "artifact" beyond the mass (Fig. 10.5). Although calcified fibroids are easily identified, distortion that occurs beyond the mass may "hide" the endometrium or other fibroids. Uterine fibroids are sometimes visible as "hypoechogenic" oval masses in the myometrium. Less often, a fibroid may have the same echogenic pattern as the surrounding myometrium and be identified by finding a deflection of the endometrial or the serosal surface of the uterus. Subtle or uncertain findings should be cautiously interpreted, since normal physiologic contractions of the myometrium can be confused with an intramural fibroid. If an uncertain abnormality is suspected, the sonographer should reassess the area of interest after a few minutes to allow a contracted area to change. Another method that may be helpful is the use of color Doppler. Since the fibroid is surrounded by a rich vascular supply, a myoma will usually demonstrate a "ring of fire" [34]. In some cases, 3-D ultrasound may also provide additional anatomic insight regarding the position of the myoma.

Fibroids must be differentiated from adenomyosis, especially when surgery is considered, since resection of adenomyosis and repair of the defect can be difficult [33]. Adenomyosis may have several appearances by ultrasound, making the diagnosis uncertain in some cases. To add to the confusion, hormonal changes might cause variations in the appearance of an area of adenomyosis throughout the cycle, since the response of adenomyosis is similar to the normal endometrial response. Adenomyosis may appear hyperechoic, hypoechoic, or the signal may be mixed. Adenomyosis can enlarge or shrink throughout a menstrual cycle, depending on the hormonal response. In some cases, adenomyosis forms a nodular myometrial

mass which is readily identified by ultrasound. Adenomyosis can also be a diffuse condition affecting a large segment of the myometrium, with the only ultrasound finding being a subtle uterine enlargement. Sometimes, adenomyosis and uterine fibroids have a remarkably similar appearance with ultrasound, and some women have both conditions. Color Doppler studies are helpful to distinguish uterine fibroids from adenomyosis, since vascular flow is peripheral with fibroids, and more homogeneously affects adenomyosis lesions.

Saline Infusion Sonohysterography

Saline infusion sonohysterography (SIS) is a routine procedure performed in preparation for IVF in many centers. SIS is also helpful when a submucous or sessile myoma is suspected based on clinical history or ultrasound examination.

Saline infusion sonography is performed by filling the uterus with saline while assessing the uterine cavity by transvaginal ultrasound. If evaluation of tubal patency is needed, a bubble/saline infusion system (FemView, Femasys, Suwanee, Georgia) may be beneficial [35].

Magnetic Resonance Imaging

Magnetic resonance imaging (MRI) is a highly sensitive method to define the size, number, and location of fibroids. While the expense of the test limits the widespread utilization, in some circumstances when myomectomy is planned, MRI can help determine whether abdominal or laparoscopic myomectomy is the more appropriate route. MRI can also be useful to visualize an extremely large uterus, whereas the field of visualization is limited with ultrasound. MRI is beneficial to visualize the uterus when calcifications make adequate assessment difficult with transvaginal or abdominal ultrasound. Finally, MRI can help differentiate fibroids and adenomyosis [36].

Management of Uterine Fibroids

Observation

Observation is reasonable for infertile women who are asymptomatic, especially with intramural fibroids smaller than 4 cm. Furthermore, observation is appropriate for symptomatic infertile women with subserosal or pedunculated fibroids, as long as the severity of symptoms does not warrant surgery.

There is no evidence that medical therapy of uterine fibroids enhances fertility. However, medical therapies can help prepare the endometrium to provide optimal visualization of hysteroscopy and to correct anemia before surgery.

Medical therapies for fibroids have included hormonal contraception and GnRH agonists. Except for the use of the levonorgestrel IUD to reduce bleeding in women with small submucosal fibroids [37], there is limited evidence for efficacy in controlling excessive bleeding, especially when fibroids distort the uterine cavity [38]. Pre-hysteroscopy GNRH agonists can be used to decrease preoperative menorrhagia, to allow for recovery of anemia, and to thin the endometrium in preparation for hysteroscopic myomectomy, although preoperative GNRH agonists can increase the difficulty in enucleating fibroids during myomectomy, increasing the difficulty of the procedure [39]. The high cost, hypoestrogenic side effects, and limited efficacy limit the long-term use of GnRH agonists for infertile women with uterine fibroids.

Surgery

Indications for myomectomy for infertile women with uterine fibroids include (1) abnormal uterine bleeding not responding to conservative treatments, (2) high level of suspicion of pelvic malignancy, (3) growth after menopause, (4) infertility when there is distortion of the endometrial cavity or tubal obstruction, (5) recurrent pregnancy loss (with distortion of the endometrial cavity), (6) pain or pressure symptoms that interfere with quality of life), (7) urinary tract symptoms

(frequency and/or obstruction), and (8) iron deficiency anemia secondary to chronic blood loss [40]. However, in women with otherwise unexplained infertility, myomectomy may improve pregnancy outcomes [39, 41]. Therefore, surgery should be recommended for infertile women with submucous myomas and considered for women with a myoma, 4 cm or larger, or intramural myomas within a few millimeters of the endometrial cavity in women with otherwise unexplained infertility when appropriate fertility treatments have been unsuccessful.

Myomectomy is usually the best option for young women who desire preservation of the uterus. The type of myomectomy, hysteroscopic, open, or laparoscopic, is chosen based on patient symptoms, location, size and number of fibroids, and the skill and experience of the surgeon. Considerations to the route of surgery must include selection of the approach that provides greatest improvement in the prognosis, a high safety profile. The decision should be made with the knowledge of the length of patient recovery and cost of the procedure, but these should not be the deciding factors for choosing the surgical route.

An appropriate preoperative evaluation is essential to prepare for surgery. In many cases, ultrasound establishes the fibroid size and location. SIS is beneficial to determine the relationship of a submucous myoma to the myometrium for women with a submucosal myoma. MRI should be considered if an atypical ultrasound appearance is identified, if the ultrasound is not conclusive, or if adenomyosis is suspected.

Hysteroscopic Myomectomy

Hysteroscopic myomectomy is the most appropriate approach when a submucous myoma has been identified, before initiating fertility treatment. Hysteroscopic myomectomy is appropriate for symptomatic submucous myomas and for infertile women with asymptomatic submucous myomas.

Reproductive outcomes are improved following hysteroscopic myomectomy [9]. Hysteroscopic myomectomy lowers the incidence of first trimester losses and improves the term live birth rate [42]. In women with menorrhagia caused by a submucous myoma who desire fertility preservation, hysteroscopic myomectomy compares favorably to hysterectomy [43].

For optimal visualization during hysteroscopy, the procedure is either performed in the follicular phase of the cycle to ensure a thin endometrial lining or after pretreatment with a GNRH agonist or hormonal contraception for 1 or 2 months before surgery. Hysteroscopic myomectomy can be performed concurrently with abdominal or laparoscopic myomectomy to reduce bulk symptoms.

During hysteroscopic myomectomy, the uterine cavity is filled with distention media and the fibroid is resected with monopolar or bipolar cautery with the resectoscope. A bipolar instrument allows the use of saline for distention. It is important to closely monitor fluid deficits during any hysteroscopic procedure as dangerous electrolyte imbalances can occur. Typically hysteroscopic resection of myomas is appropriate for tumors 6 cm or less, while larger masses may require a 2-step surgery [44].

The hysteroscopic morcellator is a new tool being used which breaks the myoma into small chips and evacuates the fragments into a tissue trap. This method appears to be safe and effective [45], although intraoperative bleeding may be more problematic with this approach. In order to minimize bleeding during hysteroscopic myomectomy, the myoma base may be injected with dilute vasopressin.

During hysteroscopic myomectomy of a sessile myoma located partially within the myometrial wall, there tends to be a progressive herniation of the intramural component of the myoma into the uterine cavity [46]. Movement of the fibroid into the cavity may allow for more complete resection of the fibroid than would be expected based on the percentage of the fibroid in the cavity as seen during SIS. However, continued resection into the myometrium may result in uterine perforation and could cause injury to structures adjacent to the uterus, including bowel and bladder. The use of concurrent abdominal ultrasound can provide additional safety during

complex hysteroscopic procedures, allowing for better identification of the relationship of the surgical site and the myometrium [33].

Abdominal Myomectomy

Although Washington Atlee reported his experience performing successful abdominal myomectomies in 1845 [47], the mortality rates were high until Victor Bonney mastered the techniques of this procedure, after being inspired by his childless wife's emotionally devastating hysterectomy for a submucous leiomyoma in 1908. Bonney introduced many surgical techniques still used today, including uterine artery compression with his "Bonney clamp" to reduce bleeding and elevation of the uterus to improve exposure during myomectomy. He described an approach to obliterate the dead space from the myoma bed by under-sewing the deeper tissue layers. In this career, Bonney performed more than 700 myomectomies. His mortality rate was 1.1 %, remarkably low in an era before blood transfusions and antibiotics. By the 1930s, Bonney advocated myomectomy for any woman wishing to have children under the age of 41.

Abdominal myomectomy is typically performed through a Pfannenstiel incision, although a Maylard incision or vertical incision may be helpful for women with massive fibroids. The fibroid pseudocapsule is injected with an agent to reduce intraoperative bleeding. A Cochrane review found several interventions that reduce blood loss, including a pericervical tourniquet, vasopressin, gelatin-thrombin mix, tranexamic acid, and misoprostol, whereas bupivacaine with epinephrine was less effective, and oxytocin was ineffective [48]. The surgeon should use a systematic approach and remove as many fibroids as possible through a single incision, with careful dissection of the fibroid from the surrounding pseudocapsule [1]. Morbidity of abdominal myomectomy is comparable to abdominal hysterectomy [49].

Long-term abdominal myomectomy outcomes are usually good and patient satisfaction is high [50, 51], but adhesions or recurrent fibroids may compromise the results in some individuals. Myomectomy often reduces menorrhagia and improves fertility in women with excessive bleeding or infertility primarily caused by endometrial distortion from submucous myomas or large intramural myomas. Slightly more than 50 % of women conceive after open myomectomy [52]. Adhesions form in more than 90 % of abdominal myomectomies, with the incidence highest (94 %) with posterior incisions and lower (56 %) with fundal or anterior uterine incisions [53]. When severe, adhesions can result in bowel obstruction and require additional intervention. Adhesion barriers are recommended to minimize the extent of adhesions, and a Cochrane review concluded that Interceed is the most effective adhesion barrier for myomectomy [54]. Growth of new fibroids is not uncommon after myomectomy, but additional surgery is required in a minority of patients.

Laparoscopic Myomectomy

Laparoscopic myomectomy provides several advantages compared to laparotomy: postoperative pain is reduced, recovery time is shorter, postoperative febrile morbidity is less common, intraoperative blood loss is reduced, and adhesion formation is less with laparoscopic myomectomy are the clear advantages seen in the minimally invasive approach. Recurrence risks and pregnancy outcomes are comparable after resection of myomas from abdominal versus laparoscopic route [39].

Appropriate patient selection is important when considering laparoscopic myomectomy. Optimal candidates have less than four fibroids and fibroid diameters less than 8–10 cm. Skilled surgeons may sometimes exceed these arbitrary limits, although operating time is longer with more extensive procedures [55].

The pregnancy and obstetrical outcomes of laparoscopic myomectomy are good when optimal surgical techniques are used to perform the procedure. The importance of gentle dissection of the fibroid from the pseudocapsule, with preservation of the pseudocapsule, has been demonstrated, as 74 % of infertile women who

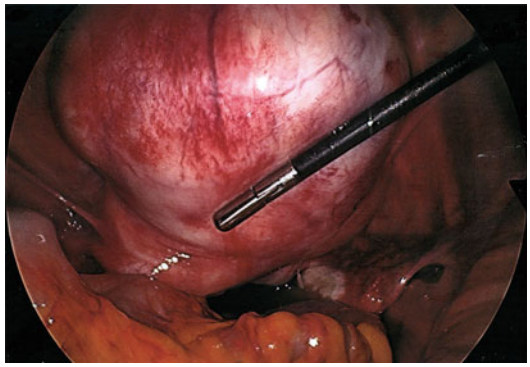

Fig. 10.7 Large fibroid demonstrated during laparoscopy with prominent vessels

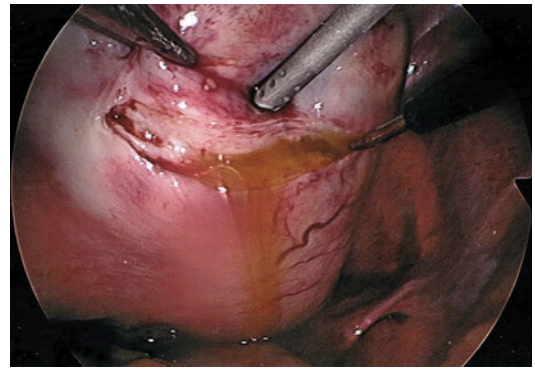

Fig. 10.8 Incision into the same fibroid showing degenerative changes and liquefaction during laparoscopic myomectomy

underwent intracapsular subserous and intramural myomectomy preserving the myoma pseudocapsule eventually conceived [41]. Many of these women were allowed to deliver vaginally, and there were no cases of uterine dehiscence.

Although many techniques of laparoscopic myomectomy have been described, we use modifications of techniques described in 2005 [39]. Four ports are used. In cases with large fibroids, the laparoscope is placed in the left upper quadrant at "Palmer's point," a 5 mm port is placed to the right of the umbilicus and another in the right lower quadrant, and an 11 mm port is placed in the left lower quadrant to prevent instrument collision. Injection of the pseudocapsule with a dilute solution of vasopressin limits intraoperative blood loss (Fig. 10.7). When a small fibroid near the endometrial cavity cannot be visualized directly by laparoscopy, intracorporeal or transvaginal ultrasound may be helpful to identify and remove the mass. A Harmonic scalpel hook provides the ability to cut into the uterus to expose the fibroid and the pseudocapsule and limit bleeding (Fig. 10.8). The fibroid is removed based on the principles of traction and counter traction, with care taken to preserve the pseudocapsule (Fig. 10.9). The myomectomy site must be closed to avoid dead space, and a barbed running suture placed in layers is effective to prevent slippage and loosening of suture during repair (Fig. 10.10) [56]. An absorbable adhesion barrier is used to limit adhesion formation at the incision sites.

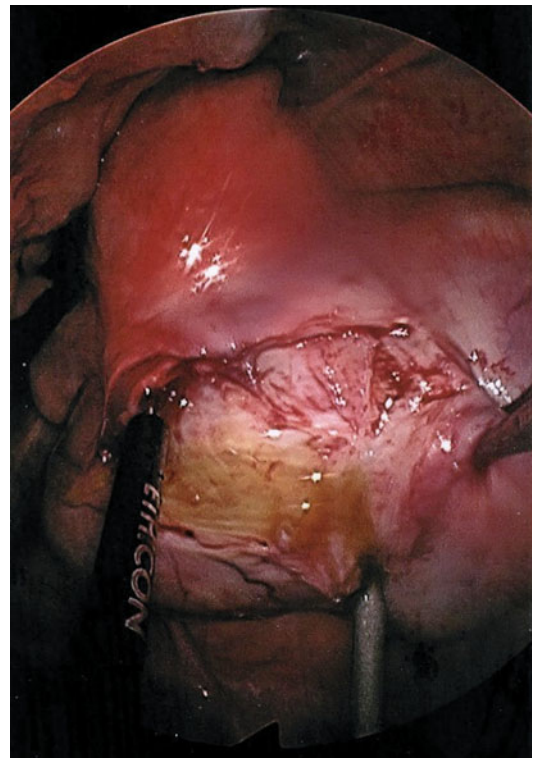

Fig. 10.9 Fibroid enucleation of the same fibroid from its surrounding pseudocapsule

While there is a steep learning curve associated with complex laparoscopic myomectomy, robotic-assisted laparoscopy may allow for laparoscopic myomectomy to be more widely utilized. Robotic-laparoscopic myomectomy has a shorter learning curve and does not increase

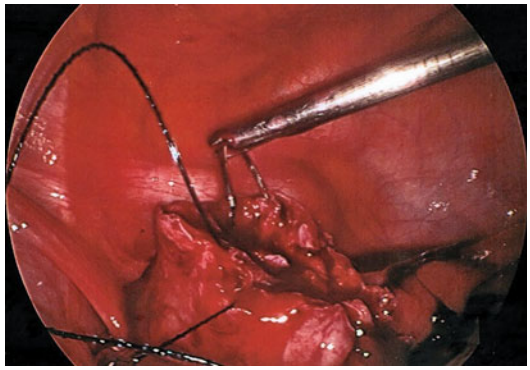

Fig. 10.10 Repair of myomectomy site from same procedure as Figs. 10.7, 10.8, and 10.9 with barbed suture

morbidity. Advantages of robotic surgery include improved dexterity and three-dimensional view. Operative times for robotic myomectomy are longer and the costs are higher compared to open myomectomy [57] and laparoscopic myomectomy. However, disadvantages of robotic surgery include the loss of tactile sensation during surgery and increased cost [58]. Alternately, laparoscopic myomectomy with the use of single-port surgery presents a steep learning curve, but has proposed benefits such as fewer surgical scars [59].

It is important to note that myomectomy increases the risk of uterine rupture during pregnancy or labor. While this risk is small, approximately 0.5–0.7 %, uterine rupture is an obstetrical emergency and can have catastrophic consequences for mother and fetus [60]. For this reason, Cesarean delivery is often recommended for women who conceive after myomectomy. In order to allow for uterine healing, a 3-month interval between myomectomy and attempts to conceive is often recommended.

Uterine Artery Embolization

Uterine artery embolization (UAE) is a reasonable alternative to hysterectomy with improved bleeding, pain, and improved quality of life [50]. However, myomectomy is preferred when future fertility is desired. One study found more pregnancy complications after UAE such as spontaneous abortion, preterm delivery, malpresentation, abnormal placentation, and postpartum hemorrhage compared to laparoscopic myomectomy [61]. This finding is logical, since fibroids are smaller but persist after UAE, and UAE alters uterine perfusion.

MRgFUS

Magnetic resonance-guided focused ultrasound surgery (MRgFUS) (InSightec, Haifa, Israel) is a noninvasive treatment for fibroids that uses MRI to deliver focused ultrasound energy to heat target tissue. MRgFUS was approved by the FDA in 2004 after studies showed significant improvement in quality of life scores [62]. Three years after treatment, fibroid volume is 32 % less [63]. MRgFUS-related complications include skin and sciatic nerve injury, and there is a small risk of bowel and bladder injury.

Less than half of women are eligible for MRgFUS due to excessive fibroid size, high cost of the procedure, and exclusion of women who desire fertility [64]. The procedure requires several hours of dedicated MRI time [65]. MRgFUS is not recommended when future pregnancy is desired, but by 2010 there were 54 pregnancies reported in 51 women MRgFUS, resulting in a 41 % live birth rate, a 20 % ongoing pregnancies, a 28 % spontaneous abortion rate, and an 11 % pregnancy termination rate [62]. As of February 2012, the ExAblate system is available in only 15 centers in 11 states, which makes this approach inaccessible or impractical for many women [66].

Conclusion

As women delay childbearing, uterine fibroids are increasingly identified during an infertility evaluation. Identification of the size, number, and location of fibroids is determined by ultrasound. Submucosal fibroids reduce fertility and compromise pregnancy, and outcomes are improved after hysteroscopic myomectomy. Women with untreated intramural fibroids have a higher incidence of maternal and fetal pregnancy-related complications, and there is

increasing evidence that fertility and pregnancy outcomes are improved following myomectomy. Laparoscopic or abdominal myomectomy is appropriate for women with symptomatic fibroids who desire fertility. Intracorporeal ultrasound may be useful when a fibroid deviates the endometrial cavity but cannot be identified by visual inspection of the uterus during myomectomy. Approximately 50 % of women conceive after myomectomy, and IVF outcomes may improve. When fibroids are too extensive to perform myomectomy or when a hysterectomy is required, preservation of the ovaries may allow consideration of a gestational carrier pregnancy.

References

1. Tinelli A, Malvasi A, Rahimi S, Negro R, Cavallotti C, Vergara D, Vittori G, Mettler L. Myoma pseudocapsule: a distinct endocrino-anatomical entity in gynecological surgery. Gynecol Endocrinol. 2009;25:661–7.
2. Ishikawa H, Reierstad S, Demura M, Rademaker AW, Kasai T, Inoue M, Usui H, Shozu M, Bulun SE. High aromatase expression in uterine leiomyoma tissues of African-American women. J Clin Endocrinol Metab. 2009;94:1752–6.
3. Ciarmela P, Islam MS, Reis FM, Gray PC, Bloise E, Petraglia F, Vale W, Castellucci M. Growth factors and myometrium: biological effects in uterine fibroid and possible clinical implications. Hum Reprod Update. 2011;17:772–90.
4. Malvasi A, Tinelli A, Cavallotti C, Morroni M, Tsin DA, Nezhat C, Stark M, Mettler L. Distribution of substance P (SP) and vasoactive intestinal peptide (VIP) in pseudocapsules of uterine fibroids. Peptides. 2011;32:327–32.
5. Practice Committee of American Society for Reproductive Medicine in collaboration with Society of Reproductive Surgeons. Myomas and reproductive function. Fertil Steril. 2008;90:S125–30.
6. Baird DD, Dunson DB, Hill MC, Cousins D, Schectman JM. High cumulative incidence of uterine leiomyoma in black and white women: ultrasound evidence. Am J Obstet Gynecol. 2003;188:100–7.
7. Laughlin SK, Schroeder JC, Baird DD. New directions in the epidemiology of uterine fibroids. Semin Reprod Med. 2010;28:204–17.
8. American Association of Gynecologic Laparoscopists (AAGL): Advancing Minimally Invasive Gynecology Worldwide. AAGL practice report: practice guidelines for the diagnosis and management of submucous leiomyomas. J Minim Invasive Gynecol. 2012;19:152–71.
9. Olive DL, Pritts EA. Fibroids and reproduction. Semin Reprod Med. 2010;28:218–27.
10. Oliveira FG, Abdelmassih VG, Diamond MP, Dozortsev D, Melo NR, Abdelmassih R. Impact of subserosal and intramural uterine fibroids that do not distort the endometrial cavity on the outcome of in vitro fertilization-intracytoplasmic sperm injection. Fertil Steril. 2004;81:582–7.
11. Hart R, Khalaf Y, Yeong CT, Seed P, Taylor A, Braude P. A prospective controlled study of the effect of intramural uterine fibroids on the outcome of assisted conception. Hum Reprod. 2001;16:2411–7.
12. Metwally M, Farquhar CM, Li TC. Is another meta-analysis on the effects of intramural fibroids on reproductive outcomes needed? Reprod Biomed Online. 2011;23:2–14.
13. Olive DL. The surgical treatment of fibroids for infertility. Semin Reprod Med. 2011;29:113–23.
14. Pritts EA, Parker WH, Olive DL. Fibroids and infertility: an updated systematic review of the evidence. Fertil Steril. 2009;91:1215–23.
15. Kroon B, Johnson N, Chapman M, Yazdani A, Hart R, Australasian CREI Consensus Expert Panel on Trial evidence (ACCEPT) group. Australasian CREI Consensus Expert Panel on Trial evidence. Aust N Z J Obstet Gynaecol. 2011;51:289–95.
16. Eldar-Geva T, Meagher S, Healy DL, MacLachlan V, Breheny S, Wood C. Effect of intramural, subserosal, and submucosal uterine fibroids on the outcome of assisted reproductive technology treatment. Fertil Steril. 1998;70:687–91.
17. Seoud MA, Patterson R, Muasher SJ, Coddington 3rd CC. Effects of myomas or prior myomectomy on in vitro fertilization (IVF) performance. J Assist Reprod Genet. 1992;9:217–21.
18. Narayan R, Rajat R, Goswamy K. Treatment of submucous fibroids, and outcome of assisted conception. J Am Assoc Gynecol Laparosc. 1994;1:307–11.
19. Farhi J, Ashkenazi J, Feldberg D, Dicker D, Orvieto R, Ben Rafael Z. Effect of uterine leiomyomata on the results of in-vitro fertilization treatment. Hum Reprod. 1995;10:2576–8.
20. Ramzy AM, Sattar M, Amin Y, Mansour RT, Serour GI, Aboulghar MA. Uterine myomata and outcome of assisted reproduction. Hum Reprod. 1998;13:198–202.
21. Somigliana E, De Benedictis S, Vercellini P, Nicolosi AE, Benaglia L, Scarduelli C, Ragni G, Fedele L. Fibroids not encroaching the endometrial cavity and IVF success rate: a prospective study. Hum Reprod. 2011;26:834–9.
22. Surrey ES, Lietz AK, Schoolcraft WB. Impact of intramural leiomyomata in patients with a normal endometrial cavity on in vitro fertilization-embryo transfer cycle outcome. Fertil Steril. 2001;75:405–10.
23. Benecke C, Kruger TF, Siebert TI, Van der Merwe JP, Steyn DW. Effect of fibroids on fertility in patients undergoing assisted reproduction. A structured literature review. Gynecol Obstet Invest. 2005;59:225–30.

24. Stovall DW, Parrish SB, Van Voorhis BJ, Hahn SJ, Sparks AE, Syrop CH. Uterine leiomyomas reduce the efficacy of assisted reproduction cycles: results of a matched follow-up study. Hum Reprod. 1998;13: 192–7.
25. Sunkara SK, Khairy M, El-Toukhy T, Khalaf Y, Coomarasamy A. The effect of intramural fibroids without uterine cavity involvement on the outcome of IVF treatment: a systematic review and meta-analysis. Hum Reprod. 2010;25:418–29.
26. Bodri D, Guillen JJ, Lopez M, Vernaeve V, Coll O. Racial disparity in oocyte donation outcome: a multiethnic, matched cohort study. Hum Reprod. 2010;25: 436–42.
27. Sheiner E, Bashiri A, Levy A, Hershkovitz R, Katz M, Mazor M. Obstetric characteristics and perinatal outcome of pregnancies with uterine leiomyomas. J Reprod Med. 2004;49:182–6.
28. Muram D, Gillieson M, Walters JH. Myomas of the uterus in pregnancy: ultrasonographic follow-up. Am J Obstet Gynecol. 1980;138:16–9.
29. Shavell VI, Thakur M, Sawant A, Kruger ML, Jones TB, Singh M, Puscheck EE, Diamond MP. Adverse obstetric outcomes associated with sonographically identified large uterine fibroids. Fertil Steril. 2012;97: 107–10.
30. Klatsky PC, Tran ND, Caughey AB, Fujimoto VY. Fibroids and reproductive outcomes: a systematic literature review from conception to delivery. Am J Obstet Gynecol. 2008;198:357–66.
31. De Vivo A, Mancuso A, Giacobbe A, Savasta LM, De Dominici R, Dugo N, Dugo C, Vaiarelli A. Uterine myomas during pregnancy: a longitudinal sonographic study. Ultrasound Obstet Gynecol. 2011;37: 361–5.
32. Campo S, Campo V, Gambadauro P. Reproductive outcome before and after laparoscopic or abdominal myomectomy for subserous or intramural myomas. Eur J Obstet Gynecol Reprod Biol. 2003;110:215–9.
33. Hurst BS. Anatomic abnormal uterine bleeding due to anatomic causes. In: Marshburn PB, Hurst BS, editors. Disorders of menstruation. West Sussex: Wiley-Blackwell; 2011. p. 86–107.
34. Tinelli A, Malvasi A, Hurst BS, Tsin DA, Davila F, Dominguez G, Dell'edera D, Cavallotti C, Negro R, Gustapane S, Teigland CM, Mettler L. Surgical management of neurovascular bundle in uterine fibroid pseudocapsule. JSLS. 2012;16:119–29.
35. Saunders RD, Shwayder JM, Nakajima ST. Current methods of tubal patency assessment. Fertil Steril. 2011;95:2171–9.
36. Rajan DK, Margau R, Kroll RR, Simons ME, Tan KT, Jaskolka JD, Kachura JR, Sniderman KW, Beecroft JR, Haider M. Clinical utility of ultrasound versus magnetic resonance imaging for deciding to proceed with uterine artery embolization for presumed symptomatic fibroids. Clin Radiol. 2011;66:57–62.
37. Soysal S, Soysal ME. The efficacy of levonorgestrel-releasing intrauterine device in selected cases of myoma-related menorrhagia: a prospective controlled trial. Gynecol Obstet Invest. 2005;59:29–35.
38. Matteson KA, Anderson BL, Pinto SB, Lopes V, Schulkin J, Clark MA. Practice patterns and attitudes about treating abnormal uterine bleeding: a national survey of obstetricians and gynecologists. Am J Obstet Gynecol. 2011;205:321.e1–8.
39. Hurst BS, Matthews ML, Marshburn PB. Laparoscopic myomectomy for symptomatic uterine myomas. Fertil Steril. 2005;83:1–23.
40. Wallach EE, Vlahos NF. Uterine myomas: an overview of development, clinical features, and management. Obstet Gynecol. 2004;104:393–406.
41. Tinelli A, Hurst BS, Hudelist G, Tsin DA, Stark M, Mettler L, Guido M, Malvasi A. Laparoscopic myomectomy focusing on the myoma pseudocapsule: technical and outcome reports. Hum Reprod. 2012;27: 427–35.
42. Roy KK, Singla S, Baruah J, Sharma JB, Kumar S, Singh N. Reproductive outcome following hysteroscopic myomectomy in patients with infertility and recurrent abortions. Arch Gynecol Obstet. 2010;282: 553–60.
43. Shokeir T, El-Shafei M, Yousef H, Allam AF, Sadek E. Submucous myomas and their implications in the pregnancy rates of patients with otherwise unexplained primary infertility undergoing hysteroscopic myomectomy: a randomized matched control study. Fertil Steril. 2010;94:724–9.
44. Camanni M, Bonino L, Delpiano EM, Ferrero B, Migliaretti G, Deltetto F. Hysteroscopic management of large symptomatic submucous uterine myomas. J Minim Invasive Gynecol. 2010;17:59–65.
45. Hamerlynck TW, Dietz V, Schoot BC. Clinical implementation of the hysteroscopic morcellator for removal of intrauterine myomas and polyps. A retrospective descriptive study. Gynecol Surg. 2011;8: 193–6.
46. Casadio P, Youssef AM, Spagnolo E, Rizzo MA, Talamo MR, De Angelis D, Marra E, Ghi T, Savelli L, Farina A, Pelusi G, Mazzon I. Should the myometrial free margin still be considered a limiting factor for hysteroscopic resection of submucous fibroids? A possible answer to an old question. Fertil Steril. 2011;95:1764–8.
47. Chamberlain G. The master of myomectomy. J R Soc Med. 2003;96:302–4.
48. Kongnyuy EJ, Wiysonge CS. Interventions to reduce haemorrhage during myomectomy for fibroids. Cochrane Database Syst Rev. 2011;11, CD005355.
49. LaMorte AI, Lalwani S, Diamond MP. Morbidity associated with abdominal myomectomy. Obstet Gynecol. 1993;82:897–900.
50. Manyonda IT, Bratby M, Horst JS, Banu N, Gorti M, Belli AM. Uterine artery embolization versus myomectomy: impact on quality of life–results of the FUME (Fibroids of the Uterus: Myomectomy versus Embolization) Trial. Cardiovasc Intervent Radiol. 2012;35:530–6.

51. Dilek S, Ertunc D, Tok EC, Cimen R, Doruk A. The effect of myomectomy on health-related quality of life of women with myoma uteri. J Obstet Gynaecol Res. 2010;36:364–9.
52. Malzoni M, Tinelli R, Cosentino F, Iuzzolino D, Surico D, Reich H. Laparoscopy versus minilaparotomy in women with symptomatic uterine myomas: short-term and fertility results. Fertil Steril. 2010;93:2368–73.
53. Anonymous. An expanded polytetrafluoroethylene barrier (Gore-Tex surgical membrane) reduces post-myomectomy adhesion formation. The Myomectomy Adhesion Multicenter Study Group. Fertil Steril. 1995;63:491–3.
54. Ahmad G, Duffy JM, Farquhar C, Vail A, Vandekerckhove P, Watson A, Wiseman D. Barrier agents for adhesion prevention after gynaecological surgery. Cochrane Database Syst Rev. 2008;2, CD000475.
55. Sizzi O, Rossetti A, Malzoni M, Minelli L, La Grotta F, Soranna L, Panunzi S, Spagnolo R, Imperato F, Landi S, Fiaccamento A, Stola E. Italian multicenter study on complications of laparoscopic myomectomy. J Minim Invasive Gynecol. 2007;14:453–62.
56. Modi R. Laparoscopic myomectomy with aquadissection and barbed sutures. J Gynec Endosc Surg. 2011;2:47–52.
57. Mansour FW, Kives S, Urbach DR, Lefebvre G. Robotically assisted laparoscopic myomectomy: a Canadian experience. J Obstet Gynaecol Can. 2012;34:353–8.
58. Nezhat C, Lavie O, Hsu S, Watson J, Barnett O, Lemyre M. Robotic-assisted laparoscopic myomectomy compared with standard laparoscopic myomectomy–a retrospective matched control study. Fertil Steril. 2009;91:556–9.
59. Jung YW, Kim YT, Lee DW, Hwang YI, Nam EJ, Kim JH, Kim SW. The feasibility of scarless single-port transumbilical total laparoscopic hysterectomy: initial clinical experience. Surg Endosc. 2010;24:1686–92.
60. Landon MB, Lynch CD. Optimal timing and mode of delivery after cesarean with previous classical incision or myomectomy: a review of the data. Semin Perinatol. 2011;35:257–61.
61. Usadi RS, Marshburn PB. The impact of uterine artery embolization on fertility and pregnancy outcome. Curr Opin Obstet Gynecol. 2007;19:279–83.
62. Rabinovici J, David M, Fukunishi H, Morita Y, Gostout BS, Stewart EA, MRgFUS Study Group. Pregnancy outcome after magnetic resonance-guided focused ultrasound surgery (MRgFUS) for conservative treatment of uterine fibroids. Fertil Steril. 2010;93:199–209.
63. Kim HS, Baik JH, Pham LD, Jacobs MA. MR-guided high-intensity focused ultrasound treatment for symptomatic uterine leiomyomata: long-term outcomes. Acad Radiol. 2011;18:970–6.
64. Behera MA, Leong M, Johnson L, Brown H. Eligibility and accessibility of magnetic resonance-guided focused ultrasound (MRgFUS) for the treatment of uterine leiomyomas. Fertil Steril. 2010;94:1864–8.
65. Hesley GK, Gorny KR, Henrichsen TL, Woodrum DA, Brown DL. A clinical review of focused ultrasound ablation with magnetic resonance guidance: an option for treating uterine fibroids. Ultrasound Q. 2008;24:131–9.
66. Comerford KP, Hurst BS. Alternatives to hysterectomy for symptomatic uterine leiomyomata. Female Patient. 2012;37(8):29–38.

Endometrial Polyps

11

Silvina M. Bocca

Introduction

Endometrial polyps are localized overgrowths of endometrial glands and stroma around a vascular core that protrude from the surface of the endometrium into the uterine cavity. They can be hyperplastic (similar to endometrial hyperplasia), atrophic (cystically dilated atrophic glands), or functional (undergo cyclical changes). Single or multiple polyps (20 % of the times, Fig. 11.1) can occur that range from a few millimeters to several centimeters in size. They can be sessile or pedunculated (Fig. 11.2). They are found in the uterine fundus (Fig. 11.3), midwall (Figs. 11.1 and 11.2), cornua (Fig. 11.4), and cervix.

Endometrial polyps are rare among women younger than 20 years of age. The incidence rises steadily with increasing age, peaks in the fifth decade of life, and gradually declines after menopause. The prevalence of polyps can range from 10 to 24 % among women undergoing endometrial biopsy or hysterectomy [1] to 8 to 36 % in postmenopausal women on tamoxifen therapy [2]. Polyps in these women may be large (>2 cm), multiple, or show molecular alterations [2–5]. Also women with Lynch syndrome may have an increased incidence of endometrial polyps compared to the general population [6]. There are several theories on the molecular mechanisms playing a role in the development of endometrial polyps: monoclonal endometrial hyperplasia [7], gene mutations [8], overexpression of endometrial aromatase [9, 10], and, like in leiomyomas, cytogenetic rearrangements and rearrangements in the HMG family of transcription factors [3, 11, 12].

Although endometrial polyps are responsible for approximately one-fourth of cases of abnormal genital bleeding (menorrhagia, postmenopausal bleeding, prolapse through the cervical os, and breakthrough bleeding during hormonal therapy) in both premenopausal and postmenopausal women [1], many polyps are asymptomatic [13].

The natural course of polyps is variable. A prospective study [14] to evaluate this performed two saline infusion sonograms 2.5 years apart on 64 initially asymptomatic women (mean age 44 years). Seven women had polyps on the first examination. Four of these women had spontaneous regression of their polyps at the second scan, while seven women developed new polyps over the 2.5-year interval. Polyps larger than 1 cm were least likely to regress, and hormone use did not appear to affect the natural history of the polyps. In rare cases, endometrial polyps continue to recur multiple times after removal. There are no data regarding management of this clinical situation. If polyps continue to recur, one option is an empiric trial of progestin treatment (oral progestin such as medroxyprogesterone acetate

S.M. Bocca, MD, PhD
Department of Obstetrics and Gynecology,
The Jones Institute for Reproductive Medicine,
601 Colley Ave, Norfolk, VA 23507, USA
e-mail: boccas@ems.edu

L.A. Stadtmauer, I. Tur-Kaspa (eds.), *Ultrasound Imaging in Reproductive Medicine*,
DOI 10.1007/978-1-4614-9182-8_11, © Springer Science+Business Media New York 2014

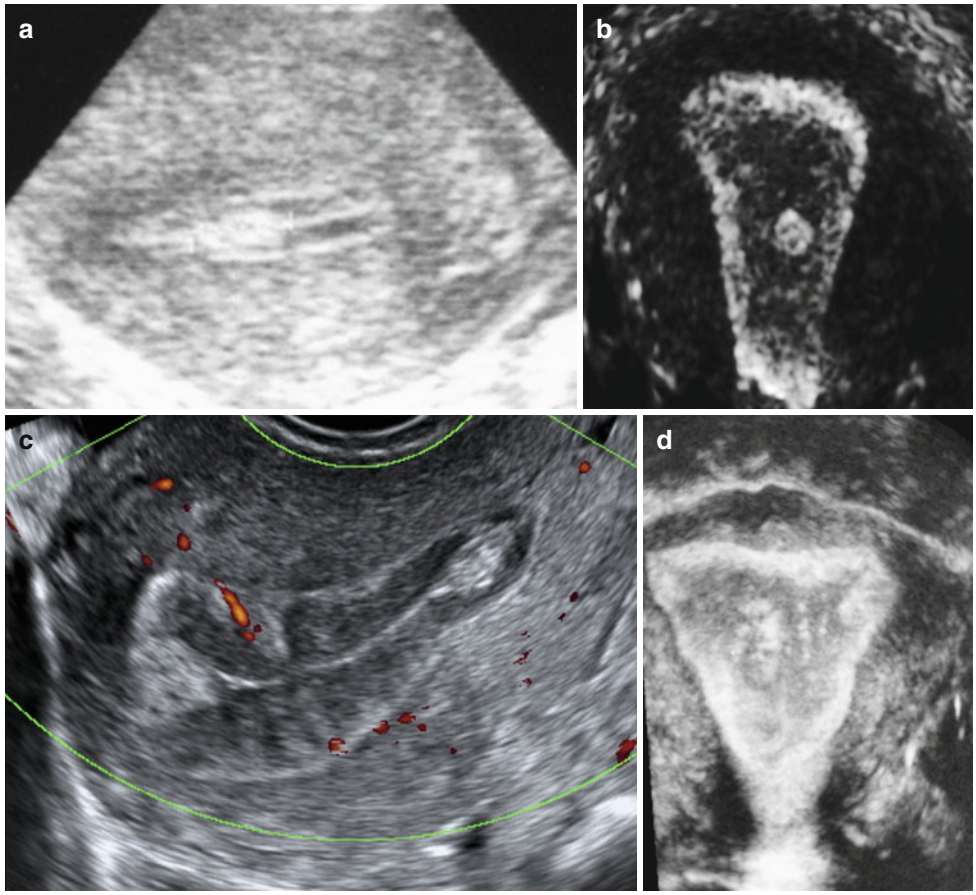

Fig. 11.1 Endometrial polyps. A single polyp located in a lateral wall at midcorpus, shown in two dimensional transvaginal ultrasonographic view (**a**) and in 3D imaging (**b**). Multiple polyps and submucosal fibroids (by Pathology) shown by 2D US (**c**) and by 3D US (**d**)

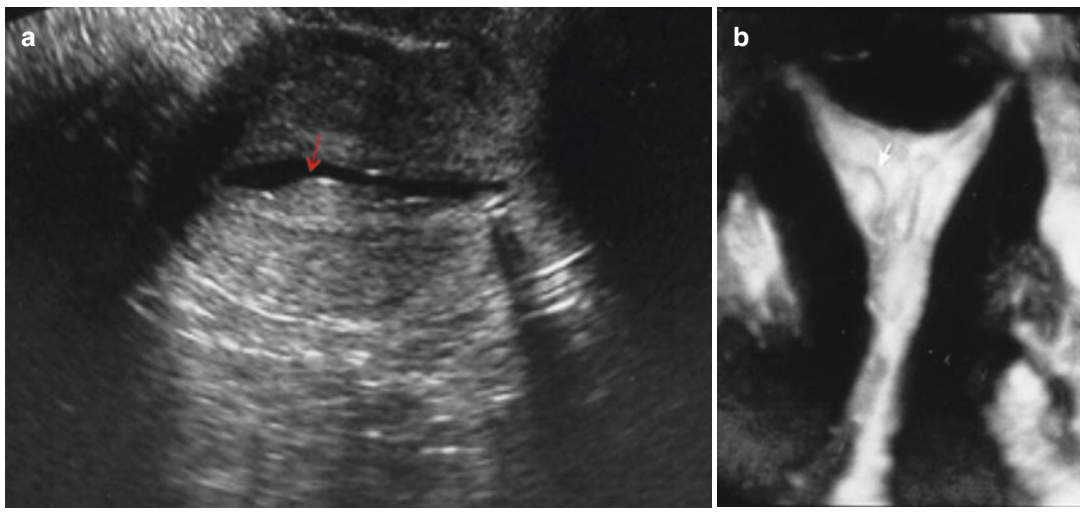

Fig. 11.2 (**a**) Sessile polyps (*arrow*) shown in a transverse 2D view of the uterus distended by saline infusion. (**b**) Coronal view (3D) of the uterus showing a pedunculated polyp (*arrow*)

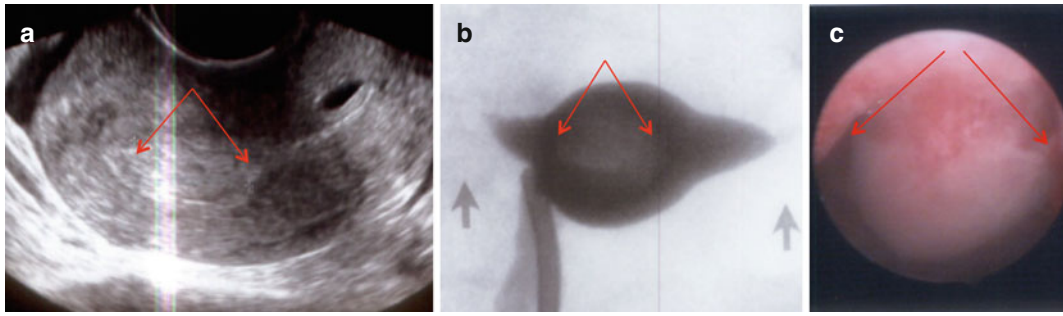

Fig. 11.3 Large polyp (*arrows*) occupying the entire fundal area shown in a sagittal 2D view (**a**), in an HSG view (**b**) giving a globular appearance of the uterus, and in a hysteroscopic view (**c**)

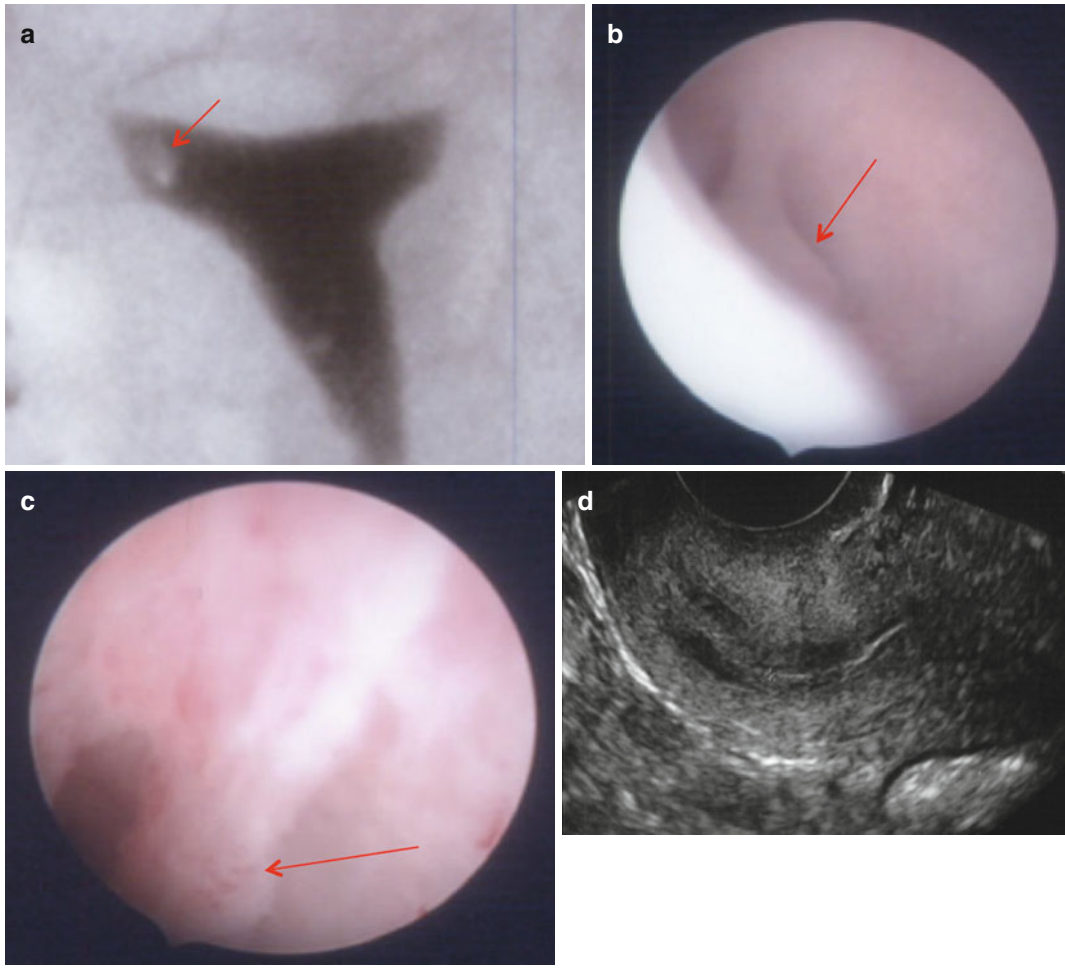

Fig. 11.4 Cornual polyps (*arrows*) clearly seen in HSG (**a**) and hysteroscopy (**b**, **c**) but not visualized in 2D US (**d**)

10 mg daily for 3–6 months, a levonorgestrel-releasing device), and another option is endometrial ablation for women who have completed their childbearing.

The great majority of endometrial polyps are benign, but malignancy occurs in some women. A systematic review of 17 observational studies including over 10,000 women reported that the

incidence of malignant or premalignant (simple hyperplasia and atypia, endometrial polyps with complex hyperplasia and atypia) polyps was significantly higher in postmenopausal compared with premenopausal women (5.4 versus 1.7 %; RR 3.86; 95 % CI 2.905.1) and those with bleeding compared to those without bleeding (4.2 % versus 2.2 %, RR 2.0; 95 % CI 1.2–3.1) [15]. Data were inconsistent regarding whether large polyp size was associated with malignancy. Malignant transformation appears to occur more frequently in women on tamoxifen (3–11 %) than in other women [2] regardless of polyp size or duration of tamoxifen therapy. The benefit of using progestagens for treatment of endometrial hyperplasia as well as to reduce the occurrence of de novo endometrial polyps in women treated with tamoxifen has been demonstrated by Chan et al. [16].

For patients with cervical polyps, Stamatellos et al. [17] reported that 25 % of them will also have concomitant endometrial polyps, making hysteroscopy a worthwhile process for their treatment, in contrast to insufficient D&C or blind endometrial biopsies.

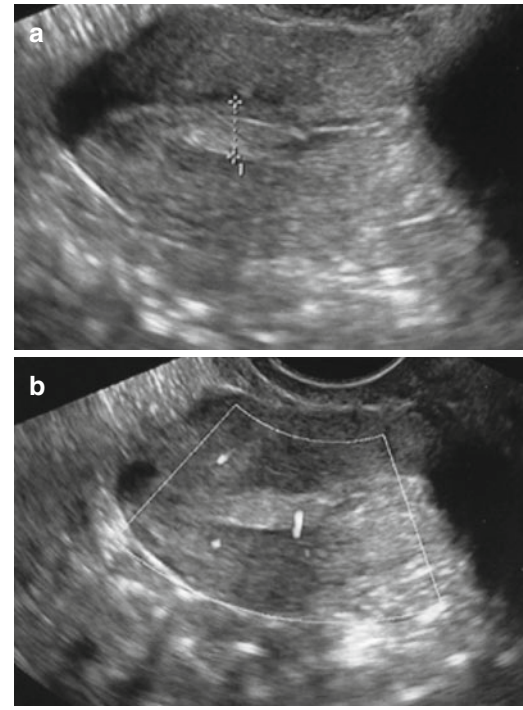

Fig. 11.5 Transvaginal ultrasonographic view of an endometrial polyp (**a**, *cursor*) appearing as an echogenic ovoid structure containing a feeding vessel visualized by Doppler (**b**)

Diagnosis

Abnormal uterine bleeding occurs in 9–14 % of women between menarche and menopause, significantly impacting quality of life and imposing financial burden. The American College of Obstetrics and Gynecology (ACOG) [18] recommends endometrial tissue assessment to rule out cancer in adolescents and in women younger than 35 years or older with suspected anovulatory bleeding and women unresponsive to medical therapy. Neither ultrasonography nor hysteroscopy can reliably distinguish between benign and malignant polyps [19, 20].

Transvaginal ultrasound (TVUS) is the initial imaging of choice, with MRI reserved for indeterminate cases or where sampling is difficult [21]. On US, endometrial polyps appear as ovoid echogenic masses that project into the endometrial lumen with Doppler US showing a feeding vessel (Figs. 11.1 and 11.5). The following guidelines have been proposed in 2012 by the American Association of Gynecologic Laparoscopists (AAGL) [22] for the diagnosis of endometrial polyps: (1) TVUS provides reliable information for the detection of endometrial polyps and should be the investigation of choice where available; (2) the addition of color or power Doppler increases the capacity of TVUS to diagnose endometrial polyps; (3) adding intrauterine contrast sonography (with or without 3D imaging) improves the diagnostic capacity for endometrial polyps; (4) blind dilatation and curettage or biopsy should not be used for diagnosis of endometrial polyps.

Transvaginal Ultrasonography

Salim et al. [23] performed a review of the literature on the diagnosis and management of endometrial polyps. On TVUS, an endometrial polyp

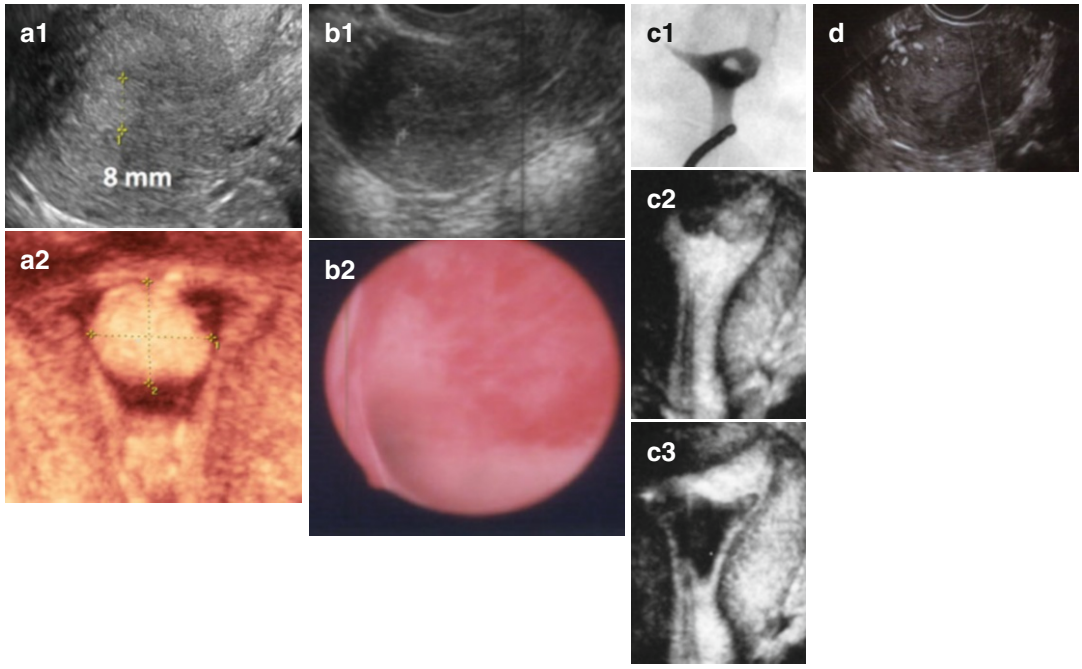

Fig. 11.6 Examples of different endometrial pathologies presenting as endometrial thickening in TVUS. (**a**) Endometrial polyp (**a1** 2D US, **a2** 3D SIS); (**b**) complex hyperplasia without atypia (**b1** 2D US, **b2** flat lesions in hysteroscopy); (**c**) retained products of conception (**c1** HSG, **c2** 3D US, **c3** 3D SIS); (**d**) trophoblastic disease (multivessel signal)

typically appears as a hyperechoic lesion with regular contours within the uterine lumen surrounded by a thin hyperechoic halo [24], occasionally cystic spaces corresponding to dilated glands filled with proteinaceous fluid may be seen within the polyp [25], or the polyp may appear as a nonspecific endometrial thickening or focal mass within the endometrial cavity [26]. None of these findings can reliably distinguish among polyps, submucous fibroids, adenomyosis, and neoplastic change.

In premenopausal women, the TVUS examination should be performed early in the proliferative phase when the endometrium is at its thinnest (4–8 mm) [27, 28] to minimize false-positive and negative findings [29]. Endometrial thickness is associated with risk of endometrial cancer in menopausal women but not in premenopausal women [30, 31]. Endometrial thickening (Fig. 11.6) is a nonspecific finding of endometrial hyperplasia as well as other causes such as polyp, endometrial cancer, trophoblastic disease (Fig. 11.6), retained products of conception (Fig. 11.6), or submucosal leiomyoma (Fig. 11.1) [21]. If structural abnormalities are suspected on ultrasound examination, then these abnormalities can be further evaluated by saline infusion sonography or hysteroscopy. In a retrospective review of multiple studies, Salim and his group [23] report that for TVUS the sensitivity varies between 19 and 96 %, specificity of 53 and 100 %, positive predictive value (PPV) of 75 and 100 %, and negative predictive value (NPV) of 87 and 97 %, when compared with hysteroscopy with guided biopsy. The ranges were tighter in a single-large prospective study evaluating the causes of menorrhagia: 86 % sensitivity, 94 % specificity, 91 % PPV, and 90 % NPV [32].

There are limited data to support color-flow or power Doppler aiding in the differentiation of hyperplasia and malignancy in polyps [33–35]. Color-flow Doppler scanning identifies a single feeding vessel (Fig. 11.5) [11]. The use of power Doppler sonography with identification of a single-vessel pattern improves diagnostic sensitivity to 89 % and specificity to 87 % for an endometrial polyp [36], in

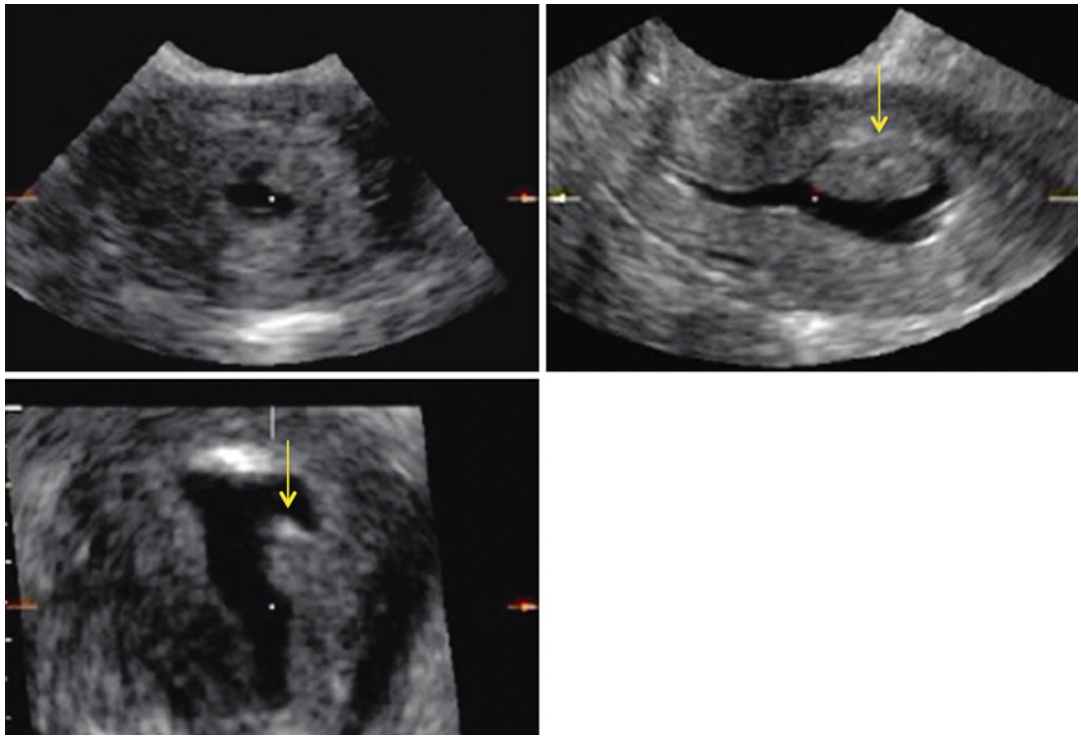

Fig. 11.7 3D-rendered view of the uterus during sonohysterography. The *arrow* points to an endometrial polyp in the left midcorpus

comparison to the multivessel (Fig. 11.6) or scattered pattern seen in malignant lesions or endometrial hyperplasia [34]. At this time, sonographic examination either with or without color-flow or power Doppler sonography is not a substitute for pathologic evaluation after surgical removal.

Sonohysterography

The use of saline infusion sonography (SIS), sonohysterography, or hydrosonogram involves injection of sterile saline into the endometrial cavity followed by a transvaginal ultrasound examination (Figs. 11.2 and 11.7). This technique increases sonographic contrast of the endometrial cavity, enabling delineation of the size, number, and location of polyps that could have been missed on gray-scale TVUS, and is likely to improve diagnostic accuracy [37, 38]. With SIS, polyps appear as echogenic, smooth, intracavitary masses with either broad bases or thin stalks outlined by fluid [26]. Differentiating endometrial polyps from submucosal fibroids can be difficult (Fig. 11.1), but examination of lesion echotexture and identification of overlying echogenic endometrium are useful features to distinguish the two [39]. SIS has relatively minor disadvantages: it cannot provide definitive diagnosis of endometrial disease [40], a longer learning curve compared with non-contrast TVUS [41], and patient discomfort caused by fluid leakage or pain with the use of a balloon catheter [42]. Bingol et al. [43] selected a total of 346 patients for operative hysteroscopy, following SIS after TVUS. SIS seems to be superior to TVS, for uterine pathologies, with respect to hysteroscopy as the gold standard.

Kamel et al. [44] reported on 106 women with menometrorrhagia where sonohysterography was significantly more accurate than ultrasound alone in making a diagnosis, with a higher sensitivity (93 % versus 65 %) and specificity (94 % versus 76 %) than transvaginal ultrasonography.

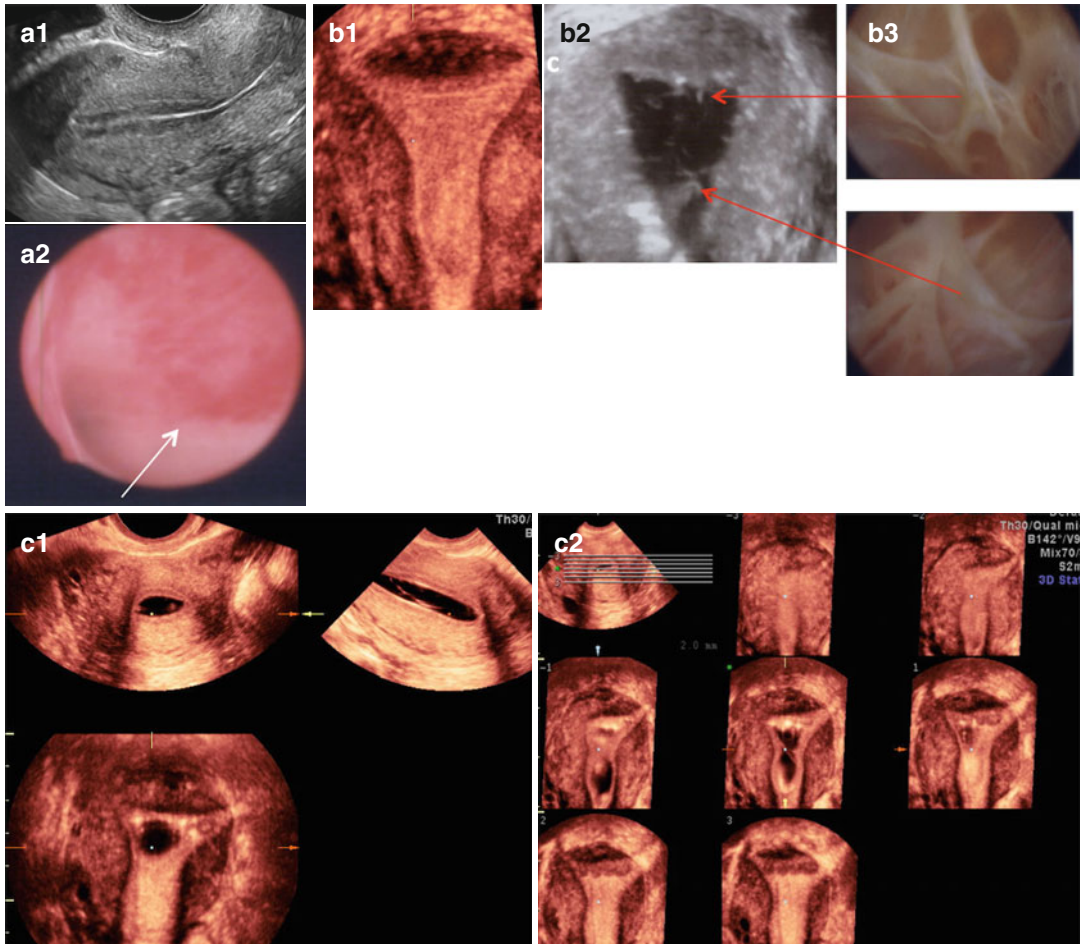

Fig. 11.8 Intrauterine lesions that may not be easily detected by TVUS. (**a1**) Apparently normal 2D sagittal view of the uterus. (**a2**) Same uterus as in (a1), containing flat hyperemic lesions visualized directly by hysteroscopy (benign polyp on Pathology). (**b1**) Apparently normal 3D coronal view of the uterus. (**b2**) Thin, though multiple, bands of synechiae seen on 3D SIS and hysteroscopy (**b3**). (**c1**) Synechiae not clearly visualized on 3D-SIS but more clearly identified upon evaluation of the multiplanar views (**c2**) of the uterus

Three-Dimensional TVUS and Three-Dimensional SIS

Three-dimensional ultrasonography (3D US) is a noninvasive imaging technique with the ability to generate multiplanar reconstructed images (Fig. 11.8) through the uterus and its external contours. Coronal views of the uterus allow more accurate visualization between the endometrium and myometrium at the fundus and cornual angles, providing superior diagnostic accuracy in detecting endometrial polyps compared to 2D TVUS (Figs. 11.1, 11.2, and 11.7).

In a study of 3,850 consecutive, Kupesic et al. [45] reported 3D US to have sensitivity of 100 %, specificity of 99 %, PPV of 99 %, and NPV of 100 % in diagnosing endometrial polyps when compared to hysteroscopy with biopsy. Adding saline solution contrast into the endometrial cavity to perform 3D SIS may provide additional information in the diagnosis of endometrial polyps (Figs. 11.6 and 11.7). However, studies report only slightly higher specificity (88–99 %) and PPV (97–100 %) for endometrial polyps than those of 3D US, with sensitivity of 92–95 % and NPV of 97 % [46, 47].

Three-dimensional sonography is simple, quick, and noninvasive for detecting most congenital and acquired uterine anomalies. We demonstrated that physicians who learn the Z technique [48] are able to retrieve the mid-coronal plane of the uterus faster and improve its image quality in volume sonography. In a prospective blinded study to evaluate the costs, accuracy, risks, and benefits of 3D TV sonography compared to hysterosalpingography [49], we enrolled 101 women aged 26–44 years with evidence of uterine anomalies (congenital and acquired). We concluded that 3D TV sonography provides visualization and evaluation of the uterine cavity with similar or better accuracy than standard hysterosalpingography (HSG) in the office setting, without radiation exposure, with lower cost and morbidity. Despite the multiple advantages of performing 3D US, including having diagnostic accuracy comparable to MRI or combined laparoscopy and hysteroscopy, it is still not widely available and accepted as a diagnostic tool, and multiple insurance carriers deny its reimbursement.

Other Imaging Modalities

Hysterosalpingography may define an endometrial polyp as pedunculated (Fig. 11.4), or as a nonspecific filing defects within the endometrial cavity (Figs. 11.3 and 11.6), with high sensitivity (98 %) but low specificity (34.6 %) compared with hysteroscopy [50]. It has the advantage of allowing for assessment of tubal patency in infertile women, but due to the disadvantages of using ionizing radiation, iodinated contrast materials, and patient discomfort, routine use of HSG for diagnosis of an endometrial polyp cannot be recommended.

T2-weighted MRI and computed tomography scanning are very high-cost, limited availability techniques with limited advantages when compared with TVUS, even with contrast enhancement [51]. Appearance on MR is not diagnostic, and endometrial polyp, secretory endometrium, stage IA endometrial cancer, and endometrial hyperplasia can demonstrate similar findings.

Hysteroscopy is an outpatient surgical procedure usually requiring local or intravenous anesthesia that provides direct visualization of the endometrial cavity (Figs. 11.3, 11.4, 11.6, 11.8, and 11.9), thereby allowing targeted biopsy or excision of lesions identified during the procedure [52]. Although considered the gold standard for the diagnosis of abnormal uterine bleeding, hysteroscopy requires advanced training and is more costly and invasive than imaging modalities for endometrial assessment [27]. Grimbizis et al. [53] studied a total of 105 consecutive women presenting in an outpatient clinic with symptoms of menorrhagia, postmenopausal bleeding, and infertility. They found diagnostic hysteroscopy to be the most accurate diagnostic technique on any endometrial pathology compared with TVUS and SIS, whereas there was no statistically significant difference in the diagnostic performances of SIS and TVUS.

False-Positive, False-Negative, and Artifacts

There is not a single imaging technique that can accurately diagnose all possible intrauterine pathologies. Ultrasonography may not distinguish very small polyps, flat endometrial anomalies (Figs. 11.6 and 11.8), cornual polyps (Fig. 11.4), or thin bands of synechiae (Figs. 11.8 and 11.9) even when combined with saline infusion sonography [54].

To the contrary, there could be transient endometrial changes detected by ultrasonography as a possible structural defect, such as an intrauterine blood clot (Fig. 11.6) or presence of mucus especially in hyperestrogenic states such as during controlled ovarian hyperstimulation for IVF (Fig. 11.10) that may spontaneously resolve. Our group [55] reported on early postoperative intrauterine changes by 3D US in patients undergoing hysteroscopic correction of various uterine anomalies. Postoperative changes 1 month after hysteroscopy were detected by 3D US in 20 % (6/30) of these patients. The changes detected consisted of intrauterine cystic loculations (Fig. 11.10) in three patients and endometrial

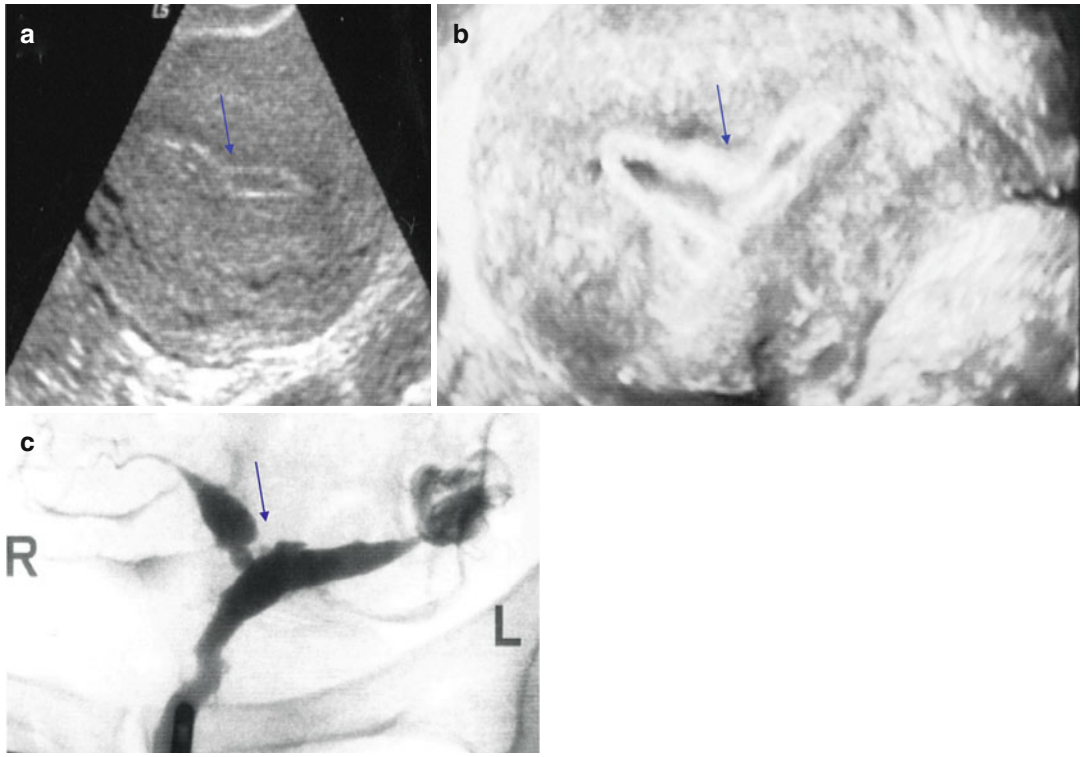

Fig. 11.9 Nonspecific endometrial US findings. An area of endometrial constrictions is shown by 2D US (**a**), by 3D SIS (**b**), and by HSG (**c**). *Arrows* point to the area of narrowing representing synechiae

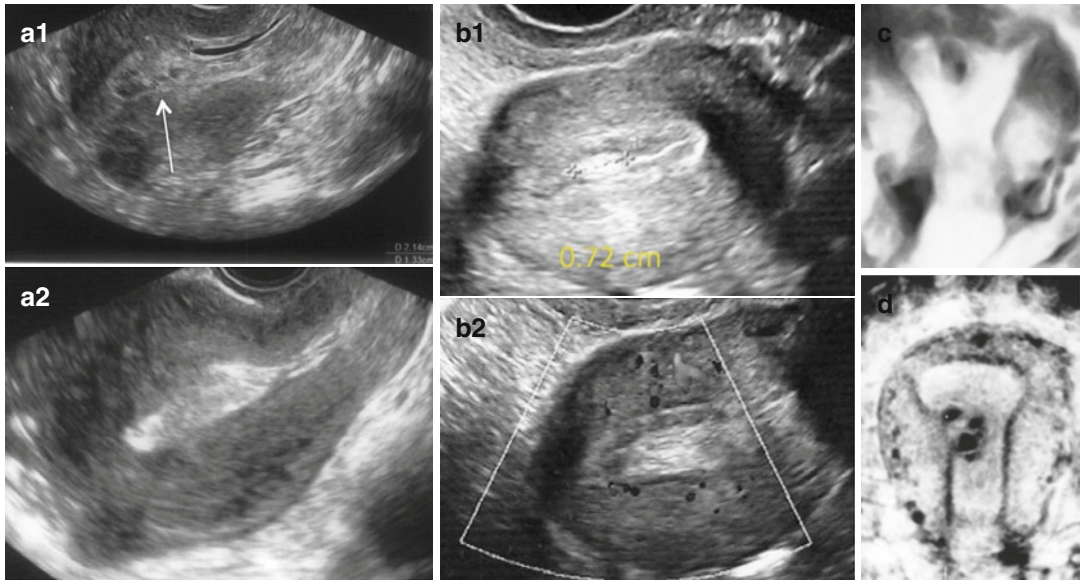

Fig. 11.10 Transient endometrial changes detected as morphological anomalies by US. Endometrial clots and fluid seen on menstrual day 4 (**a1**) that spontaneously disappeared 1 day later (**a2**). (**b1**) Endometrial mucus seen during ovarian stimulation for IVF. Notice lack of internal blood flow in the hyperechoic mucus accumulation (**b2**). Monoloculated (**c**) and multiloculated (**d**) cystic lesions observed by 3D US a few weeks after hysteroscopy that spontaneously resolved within 2 months post op

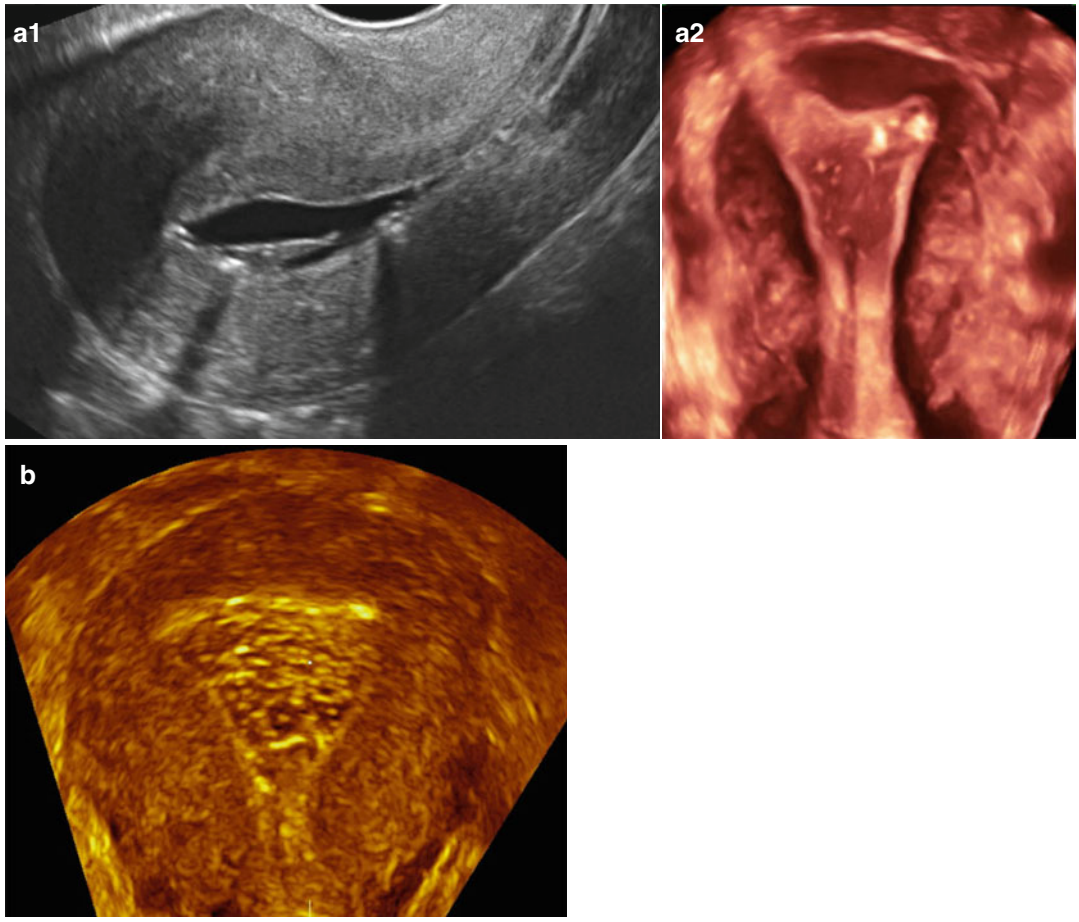

Fig. 11.11 Artifacts created during SIS giving the false impression of intracavitary pathology. Endometrial tunneling created by the catheter used resembling a polyp in a 2D sagittal view (**a1**) and in a 3D coronal view (**a2**). Air bubbles injected during SIS may resemble trophoblastic disease (**b**, 3D coronal view)

irregularities/possible mucus accumulations in the other 3. These loculations and irregularities were sometimes larger and even more complex in nature than the original lesions and always coincided with the resection site. These changes resolved spontaneously after the second postoperative month and did not interfere with embryo implantation or cause pregnancy loss in patients attempting to conceive during the study period.

Grimbizis et al. [53] reported that diagnostic hysteroscopy, on the other hand, can misdiagnose normal endometrium for small endometrial polyps or, to the contrary, can misdiagnosed a case of endometrial cancer as an endometrial polyp. As it is well known, TVS, SIS, or diagnostic hysteroscopy cannot replace biopsy in cases where endometrial cancer is suspected. Also, some artifacts can be unintentionally created during SIS that could mimic intrauterine pathology such as catheter tunneling of the endometrium which could be mistaken for a polyp (Fig. 11.11) or injection of air bubbles which could be mistaken for a trophoblastic disease (Fig. 11.11).

Impact of Polyps on Fertility

It is controversial whether endometrial polyps contribute to infertility or miscarriages [56], and because there is no uterine abnormality that is always associated with poor reproductive performance, automatic surgical correction is not

indicated when a uterine abnormality is found [57]. However, surgical correction should be considered when a submucous fibroid, endometrial polyp, septate uterus, or uterine synechiae are discovered in the setting of failure to conceive or recurrent pregnancy loss, since there may be a causal association.

Normal endometrial thickness, structure, and texture are crucial for uterine receptivity, and any structural pathology in the uterine cavity may lead to subfertility or implantation failure [58]. Doldi et al. [59] reported endometrial polyps to be the most common of the intrauterine lesions interfering with the endometrial cavity. The exact mechanism by which endometrial polyps cause infertility is not known, but some proposed mechanisms are induction of an inflammatory process similar to an intrauterine device [60], mechanical interference with sperm and embryo transport, impairment of embryo implantation, or altered endometrial receptivity such as abnormalities in the expression of molecular markers such as HOXA 10 and HOXA 11 [61]. Regardless of the mechanism of endometrial disturbance, uterine polyps have been associated with decreased pregnancy rates both in natural conceptions [62–64] and in intrauterine insemination (IUI) cycles [65].

There are no data from randomized trials to guide therapy of asymptomatic polyps, unless there are risks for hyperplasia or carcinoma. For symptomatic patients, polypectomy results in the improvement of symptoms in 75 % of patients in studies with follow-up intervals of 2–52 months [66]. Lieng et al. [67] reported on 150 women in a randomized clinical trial with an endometrial polyp allocated to hysteroscopic removal or observation. Although there was no improvement in the volume of menstrual loss, a significant improvement in other symptoms such as intermenstrual bleeding was significantly improved by removal at follow-up. Hysteroscopically guided polypectomy (with grasping forceps, suction curette, microscissors, a small electrosurgical look, i.e., resectoscope, mechanical morcellation, or a bipolar electric probe [68–70]) is the most effective method of removal since small polyps and other structural abnormalities can be missed by blind curettage [68, 71, 72].

In a retrospective study from 2000 to 2005, Stamatellos et al. [73] reported on 83 subjects with endometrial polyps and no other cause for their infertility subjected to hysteroscopic polypectomy. The mean size of the endometrial polyps was 1.9 +/− 1.4 cm. Following polypectomy, menstrual pattern was normalized in 91.6 % of patients. Spontaneous pregnancy and delivery at term rates, in the total population of the study, increased after the procedure and were 61.4 and 54.2 % respectively. There was no statistical difference in fertility rates between patients having polyps ≤1 cm and patients having >1 cm polyps or multiple polyps. Spontaneous abortion rate in the first trimester of pregnancy was 6 %, and there was no statistical difference between patients with small or bigger/multiple polyps. They concluded that hysteroscopic polypectomy appeared to improve fertility and increase pregnancy rates in previous infertile women with no other reason to explain their infertility, irrespective of the size or number of the polyps.

Polyps and Assisted Reproductive Technology

Most of the data for polypectomy in subfertile patients suggests that removal improves fertility, with reported pregnancy rates varying between 43 and 90 % [23, 62, 68, 74]. Perez-Medina et al. [65] reported that both spontaneous pregnancy rates and those associated with assisted reproductive technology increased after polypectomy. Polyps were detected in 452 of 2,800 (16.1 %) consecutive patients scheduled for IUI, and after hysteroscopic removal of endometrial polyps, there was a 63 % cumulative pregnancy rate compared with 28 % in the control group (relative risk (RR) 2.3, 95 % confidence interval (CI) 1.6–3.2). Interestingly, 65 % of all pregnancies in the polypectomy group occurred before the first IUI cycle was started, resulting in a spontaneous pregnancy rate of 29 % in the polypectomy group versus 3 % in the control group (RR 10, 95 % CI 3–30). The pregnancy rate after surgery at the uterotubal junction was significantly higher than that of other locations [75]. Increased cumulative preg-

nancy rates (76 % pregnancy rate in 1 year among 25 infertile patients) after hysteroscopic polypectomy were also reported by Spiewankiewicz et al. [74] and by Varasteh et al. [63] (78 % cumulative pregnancy rate after hysteroscopic polypectomy in cases of female infertility). Doubling of the pregnancy rates was reported by Bosteels et al. [76] in a systematic review of the literature for patients undergoing IUI who had hysteroscopic removal of endometrial polyps with a mean diameter of 16 mm detected by ultrasound when compared with diagnostic hysteroscopy and polyp biopsy (RR 2.3, 95 % CI 1.6–3.2). Given these data and additional evidence that cavitary distortion by submucosal and possibly intramural fibroids decreases successful pregnancies, most practitioners routinely remove polyps prior to an IVF cycle.

The appearance of polyps before or during IVF or intracytoplasmic sperm injection (ICSI) cycles is a very challenging situation, and the diversity of management options can be confusing: (1) cycle cancelation and polypectomy; (2) embryo freezing, removal of the endometrial polyp, and embryo transfer after a few months; (3) ignoring the polyp and continuing treatment; and lastly, (4) hysteroscopic polypectomy during the IVF/ICSI cycle before oocyte retrieval without cycle cancelation [77, 78]. There is lack of good evidence on the impact of subtle intrauterine pathologies on IVF outcome [79]. Hysteroscopic removal of endometrial polyps appears to improve spontaneous pregnancy rates in women with otherwise unexplained infertility [63, 73, 80]. However, no statistical difference in spontaneous fertility rates has been noted between patients undergoing hysteroscopic removal of polyps <1 cm in diameter and >1 cm in diameter or multiple polyps [72]. In a recent study, excision of polyps located at the uterotubal junction (Fig. 11.4) [65] was associated with a significantly higher pregnancy rate compared with localization to posterior, anterior, or lateral uterine walls [75].

There is conflict surrounding the size of polyp needed to be removed to achieve an improvement in ART. Some authors [56, 81, 82] reported that removal of polyps <2 cm has no impact on the outcome of fertility treatment, while others [74] suggested that restoration of fertility was not dependent on the size of lesion removed or that there was no significant difference in the reproductive outcome for patients with polyps ≤2.5 or >2.5 cm [68]. Even though Lass et al. [56] and Check et al. [83] reported no effect of endometrial polyps <2 cm discovered before or during IVF/ICSI on implantation rates, they also noted an increase, but not statistically significant, in miscarriage rates, making the recommendations for hysterosocpic polypectomy immediately following oocyte retrieval and freezing all embryos for embryo transfer in a subsequent cycle.

Bulent Tiras' group [58] presented probably the largest retrospective study on the impact of endometrial polyps on pregnancy rates in 8,359 ICSI patients. The study included all fresh ICSI cycles performed in the Anatolia IVF Center between 2005 and 2009. All patients diagnosed with an endometrial polyp by TVUS before the ICSI cycle underwent hysteroscopic polyp resection. Localization of the polyp (upper, middle, or lower third of the uterine cavity) or polyp size (4–14 mm) did not seem to affect pregnancy rates. They concluded that endometrial polyps <1.4 cm found during ovarian stimulation did not affect pregnancy rates, miscarriage rates, and live birth rates in ICSI cycles and that patients with an endometrial polyp detected before ICSI treatment and resected by hysteroscopy had similar pregnancy rates compared with patients with no endometrial polyps.

However, the observation from non-controlled trials that pregnancy rates are higher after removal of tubocornual polyps than after removal of polyps situated in other intrauterine locations suggests that tubocornual polyps may have a different effect on reproductive function regardless of their size [75, 80, 84]. Besides, polyps in the istmocervical part of the uterus may preferentially interfere with sperm transport. These two different mechanisms could explain the differences in conception rates after hysteroscopic removal of polyps in different locations.

Recently, two studies suggested that hysteroscopic polypectomy before oocyte retrieval without cycle cancelation in IVF cycles might be possible [77, 78]. Madani et al. [78] reported on

nine patients who were diagnosed with endometrial polyps <1.5 cm by TVUS while undergoing ART cycles and who underwent hysteroscopic polypectomy during ovarian stimulation in the standard treatment cycles. The interval between polyp resection and embryo transfer was 2–16 days. Four patients achieved pregnancy (two twins, two singletons), four patients were unsuccessful, and one pregnancy was a blighted ovum. Their trial proposes that hysteroscopic polypectomy during ovarian stimulation may be a harmless procedure. However, their series is too small to be conclusive, with nine patients in one study and six patients in the other.

Hysteroscopic polypectomy just before embryo transfer should be evaluated in detail, as recent studies fail to prove any deleterious effect of endometrial polyps <1.5 cm on pregnancy rates and pregnancy outcomes in ICSI cycles. In conclusion, further studies are required to identify the most appropriate management of endometrial polyps found during IVF stimulation.

Intrauterine Lesions in Patients with Recurrent Implantation Failure

Bozdag [85] emphasizes that recurrent implantation failure (RIF) may be due to unrecognized uterine pathology which varies, based on hysteroscopic findings, between 18 and 50 % and 40 and 43 % in patients undergoing IVF with or without RIF, respectively, and that endometrial polyps may be associated with increased miscarriage rate [86–92].

Doldi et al. [59] found 40 % of 300 patients scheduled to undergo IVF, with normal HSG within the previous year and normal US within the previous 2 months, had subtle intracavitary uterine pathologies: endometrial polyps in 78 (65 %), endometrial hyperplasia in 20 (17 %), endometrial hypotrophia in 16 (13 %), and others (endometritis, adhesions) in 6 (5 %). In another study, despite normal HSG, an abnormality was also noted in 43 % (12/28) of the patients at hysteroscopy before IVF [93] including small uterine septa, small submucous fibroids, uterine hypoplasia, and cervical ridges.

In a prospective observational study, hysteroscopic findings in 55 patients undergoing IVF who repeatedly failed to conceive despite transfer of two good quality embryos were assessed [90]. All patients had a normal uterine cavity on HSG performed within 1 year. In 25 patients (45 %) an abnormality was noted at hysteroscopy: polyps ($n=10$), endometritis ($n=7$), adhesions ($n=6$), and submucous fibroid ($n=2$). Significantly higher pregnancy (50 % versus 20 %) and implantation (19 % versus 6 %) rates were obtained after hysteroscopic surgical correction of the abnormality.

The role of hysteroscopy in RIF was assessed in two randomized controlled trials [91, 92]. A total of 421 patients with normal HSGs, who had two or more failed IVF cycles, were prospectively randomized to no-office hysteroscopy (Group I) and office hysteroscopy (Group II). Office hysteroscopy was normal in 73 % of patients (Group IIa). An abnormality was noted at hysteroscopy in 27 % of patients (Group IIb), including endometrial polyps ($n=33$), filmy and mild adhesions ($n=18$), and cervical adhesions ($n=5$). All intrauterine pathologies were corrected at the time of hysteroscopy. After correction of uterine anomaly, the clinical pregnancy rates significantly increased (22 % for Group I, 33 % for Group IIa, and 30 % for Group IIb) with similar miscarriage rates in all groups.

In summary, due to the high incidence of pathologic findings in infertile patients and the improvement in pregnancy rates after treatment, it seems prudent to perform a diagnostic hysteroscopy before the first IVF-ET in all patients, thereby reducing the failures and then the cost of IVF.

Conclusion

Endometrial polyps are a common gynecologic disease that increases with age and are rarely associated with malignancy. They are found in 10 % of women with abnormal uterine bleeding, in 36 % of women taking tamoxifen, and in up to 50 % of women with recurrent implantation failure despite normal screening with TVUS and HSG.

Traditional gray-scale TVUS (2D or 3D) is a reliable modality for diagnosing polyps, with diagnostic improvement by use of contrast materials. Polyps can easily be detected by office TVUS, but ultimately, the choice of diagnostic method depends on the patient's medical condition, body mass index, the facilities available, comparative costs, and the physician's experience with these modalities.

Hysteroscopy is the preferred method for polyp resection since it is safe and effective and allows for histological evaluation of the lesion. For patients with infertility and presence of polyps, removal of disease is likely to be helpful to subsequent pregnancy.

References

1. Van Bogaert LJ. Clinicopathologic findings in endometrial polyps. Obstet Gynecol. 1988;71:771–3.
2. Cohen I. Endometrial pathologies associated with postmenopausal tamoxifen treatment. Gynecol Oncol. 2004;94:256–66.
3. Dal Cin P, Timmerman D, Van den Berghe I, et al. Genomic changes in endometrial polyps associated with tamoxifen show no evidence for its action as an external carcinogen. Cancer Res. 1998;58: 2278–81.
4. Althuis MD, Sexton M, Langenberg P, et al. Surveillance for uterine abnormalities in tamoxifen-treated breast carcinoma survivors: a community based study. Cancer. 2000;89:800–10.
5. McGurgan P, Taylor LJ, Duffy SR, O'Donovan PJ. Does tamoxifen therapy affect the hormone receptor expression and cell proliferation indices of endometrial polyps? An immunohistochemical comparison of endometrial polyps from postmenopausal women exposed and not exposed to tamoxifen. Maturitas. 2006;54:252–9.
6. Lecuru F, Metzger U, Scarabin C, et al. Hysteroscopic findings in women at risk of HNPCC. Results of a prospective observational study. Fam Cancer. 2007;6: 295–9.
7. Jovanovic AS, Boynton KA, Mutter GL. Uteri of women with endometrial carcinoma contain a histopathological spectrum of monoclonal putative precancers, some with microsatellite instability. Cancer Res. 1996;56:1917–21.
8. Dal Cin P, Vanni R, Marras S, et al. Four cytogenetic subgroups can be identified in endometrial polyps. Cancer Res. 1995;55:1565–8.
9. Maia Jr H, Pimentel K, Silva TM, et al. Aromatase and cyclooxygenase-2 expression in endometrial polyps during the menstrual cycle. Gynecol Endocrinol. 2006;22:219–24.
10. Pal L, Nicklaus AL, Kim M, et al. Heterogeneity in endometrial expression of aromatase in polyp-bearing uteri. Hum Reprod. 2008;23:80–4.
11. Timmerman D, Verguts J, Konstantinovic ML, et al. The pedicle artery sign based on sonography with color Doppler imaging can replace second-stage tests in women with abnormal vaginal bleeding. Ultrasound Obstet Gynecol. 2003;22:166–71.
12. Vanni R, Dal Cin P, Marras S, et al. Endometrial polyp: another benign tumor characterized by 12q13-q15 changes. Cancer Genet Cytogenet. 1993;68: 32–3.
13. Hassa H, Tekin B, Senses T, et al. Are the site, diameter, and number of endometrial polyps related with symptomatology? Am J Obstet Gynecol. 2006;194:718–21.
14. DeWaay DJ, Syrop CH, Nygaard IE, et al. Natural history of uterine polyps and leiomyomata. Obstet Gynecol. 2002;100:3–7.
15. Lee SC, Kaunitz AM, Sanchez-Ramos L, Rhatigan RM. The oncogenic potential of endometrial polyps: a systematic review and meta-analysis. Obstet Gynecol. 2010;166:1197–205.
16. Chan SS, Tam WH, Yeo W, et al. A randomized controlled trial of prophylactic levonorgestrel intrauterine system in tamoxifen-treated women. BJOG. 2007; 114:1510–5.
17. Stamatellos I, Stamatopoulos P, Bontis J. The role of hysteroscopy in the current management of the cervical polyps. Arch Gynecol Obstet. 2007;276:299–303.
18. ACOG Committee on Practice Bulletins-Gynecology; American College of Obstetricians and Gynecologists. ACOG practice bulletin: management of ovulatory bleeding. Int J Gynaecol Obstet. 2001;72(3):263–71.
19. Ben-Arie A, Goldchmit C, Laviv Y, et al. The malignant potential of endometrial polyps. Eur J Obstet Gynecol Reprod Biol. 2004;115:206–10.
20. Shushan A, Revel A, Rojansky N. How often are endometrial polyps malignant? Gynecol Obstet Invest. 2004;58:212–5.
21. Griffin Y, Sudigali V, Jacques A. Radiology of benign disorders of menstruation. Semin Ultrasound CT MR. 2010;31(5):414–32.
22. American Association of Gynecologic Laparoscopists. AAGL practice report: practice guidelines for the diagnosis and management of endometrial polyps. J Minim Invasive Gynecol. 2012;19:3–10.
23. Salim S, Won H, Nesbitt-Hawes E, Campbell N, Abbott J. Diagnosis and management of endometrial polyps: a critical review of the literature. J Minim Invasive Gynecol. 2011;18(5):569–81.
24. Pérez-Medina T, Martinez O, Folgueira G, Bajo J. Which endometrial polyps should be resected? J Am Assoc Gynecol Laparosc. 1999;6:71–4.
25. Hulka CA, Hall DA, McCarthy K, Simeone JF. Endometrial polyps, hyperplasia, and carcinoma in postmenopausal women: differentiation with endovaginal sonography. Radiology. 1994;191:755–8.
26. Schorge J, Schaffer J, Halvorson L, Hoffman B, Bradshaw K, Cunningham F. Abnormal uterine bleeding. In: Schorge JO, Schaffer JI, Halvorson LM, Hoffman BL, Bradshaw KD, Cunningham FG,

editors. Williams gynecology. New York: McGraw-Hill Professional; 2008. p. 174–96.
27. Goldstein SR, Zeltser I, Horan CK, Snyder JR, Schwartz LB. Ultrasonography-based triage for perimenopausal patients with abnormal uterine bleeding. Am J Obstet Gynecol. 1997;177:102–8.
28. Goldstein SR, Monteagudo A, Popiolek D, Mayberry P, Timor-Tritsch I. Evaluation of endometrial polyps. Am J Obstet Gynecol. 2002;186:669–74.
29. Nalaboff KM, Pellerito JS, Ben-Levi E. Imaging the endometrium: disease and normal variants. Radiographics. 2001;17:145–9.
30. Dijkhuizen FP, Brolmann HA, Potters AE, et al. The accuracy of transvaginal ultrasonography in the diagnosis of endometrial abnormalities. Obstet Gynecol. 1996;87:345–9.
31. Breitkopf DM, Fredrickson RA, Snyder RR. Detection of benign endometrial masses by endometrial stripe measurement in premenopausal women. Obstet Gynecol. 2004;104:120–5.
32. Vercellini P, Cortesi I, Oldani S, Moschetta M, De Giorgi O, Crosignani PG. The role of transvaginal ultrasonography and outpatient diagnostic hysteroscopy in the evaluation of patients with menorrhagia. Hum Reprod. 1997;12:1768–71.
33. Vuento MH, Pirhonen JP, Makinen JI, Tyrkko JE, Laippala PJ, Gronroos M, et al. Screening for endometrial cancer in asymptomatic postmenopausal women with conventional and colour Doppler sonography. Br J Obstet Gynaecol. 1999;106:14–20.
34. Alcazar JL, Castillo G, Minguez JA, Galan MJ. Endometrial blood flow mapping using transvaginal power Doppler sonography in women with postmenopausal bleeding and thickened endometrium. Ultrasound Obstet Gynecol. 2003;21:583–8.
35. de Kroon C. Power Doppler area in the diagnosis of endometrial cancer. Int J Gynecol Cancer. 2010;20:1160–5.
36. Jakab A, Ovari L, Juhasz B, Birinyi L, Bacsko G, Toth Z. Detection of feeding artery improves the ultrasound diagnosis of endometrial polyps in asymptomatic patients. Eur J Obstet Gynecol Reprod Biol. 2005;119:103–7.
37. Jansen FW, de Kroon CD, van Dongen H, Grooters C, Louwe L, Trimbos-Kemper T. Diagnostic hysteroscopy and saline infusion sonography: prediction of intrauterine polyps and myomas. J Minim Invasive Gynecol. 2006;13:320–4.
38. Schwarzler P, Concin H, Bosch H, et al. An evaluation of sono-hysterography and diagnostic hysteroscopy for the assessment of intrauterine pathology. Ultrasound Obstet Gynecol. 1998;11:337–42.
39. Richenberg J. Ultrasound of the uterus. In: Callen O, editor. Ultrasonography in obstetrics and gynecology. Philadelphia: WB Saunders; 2000. p. 837.
40. Bernard JP, Rizk E, Camatte S, Robin F, Taurelle R, Lecuru F. Saline contrast sonohysterography in the preoperative assessment of benign intrauterine disorders. Ultrasound Obstet Gynecol. 2001;17:145–9.
41. Syrop CH, Sahakian V. Transvaginal sonographic detection of endometrial polyps with fluid contrast augmentation. Obstet Gynecol. 1992;79:1041–3.
42. Exalto N, Stappers C, van Raamsdonk LAM, Emanuel MH. Gel instillation sonohysterography: first experience with a new technique. Fertil Steril. 2007;87:152–5.
43. Bingol B, Gunenc Z, Gedikbasi A, Guner H, Tasdemir S, TIras B. Comparison of diagnostic accuracy of saline infusion sonohysterography, transvaginal sonography and hysteroscopy. J Obstet Gynaecol. 2011;31(1):54–8.
44. Kamel HS, Darwish AM, Mohamed SA. Comparison of transvaginal ultrasonography and vaginal sonohysterography in the detection of endometrial polyps. Acta Obstet Gynecol Scand. 2000;79:60–4.
45. Kupesic S, Kurjak A, Skenderovic S, Bjelos D. Screening for uterine abnormalities by three-dimensional ultrasound improves perinatal outcome. J Perinat Med. 2002;30:9–17.
46. La Torre R, De Felice C, De Angelis C, Coacci F, Mastrone M, Cosmi EV. Transvaginal sonographic evaluation of endometrial polyps: a comparison with two dimensional and three dimensional contrast sonography. Clin Exp Obstet Gynecol. 1999;26:171–3.
47. Makris N, Skartados N, Kalmanatis K, Mantzaris G, Papadimitriou A, Antsaklis AN. Evaluation of abnormal uterine bleeding by transvaginal 3-D hysterosonography and diagnostic hysteroscopy. Eur J Gynaecol Oncol. 2007;28:39–42.
48. Abuhamad AZ, Singleton S, Zhao Y, Bocca S. The Z technique: an easy approach to the display of the midcoronal plane of the uterus in volume sonography. J Ultrasound Med. 2006;25(5):607–12.
49. Bocca SM, Oehninger S, Stadtmauer L, Agard J, Duran EH, Sarhan A, Horton S, Abuhamad AZ. A study of the cost, accuracy, and benefits of 3-dimensional sonography compared with hysterosalpingography in women with uterine abnormalities. J Ultrasound Med. 2012;31(1):81–5.
50. Preutthipan S, Linasmita V. A prospective comparative study between hysterosalpingography and hysteroscopy in the detection of intrauterine pathology in patients with infertility. J Obstet Gynaecol Res. 2003;29:33–7.
51. Grossman J, Ricci ZJ, Rozenblit A, Freeman K, Mazzariol F, Stein MW. Efficacy of contrast-enhanced CT in assessing the endometrium. AJR Am J Roentgenol. 2008;191:664–9.
52. Bradley LD. Diagnosis of abnormal uterine bleeding with biopsy or hysteroscopy. Menopause. 2011;18:425–33.
53. Grimbizis G, Tsolakidis D, Mikos T, Anagnostou E, Asimakopoulos E, Stamatopoulos P, Tarlatzis B. A prospective comparison of transvaginal ultrasound, saline infusion sonohysterography, and diagnostic hysteroscopy in the evaluation of endometrial pathology. Fertil Steril. 2010;94:2720–5.
54. Markovitch O, Tepper R, Aviram R, Fishman A, Shapira J, Cohen I. The value of sonohysterography

in the prediction of endometrial pathologies in asymptomatic postmenopausal breast cancer tamoxifen-treated patients. Gynecol Oncol. 2004;94:754–9.
55. Bocca SM, Oehninger S, Abuhamad AZ. Detection of transient postoperative changes in the endometrial cavity by 3-dimensional ultrasonography after hysteroscopic correction of various uterine anomalies. J Ultrasound Med. 2008;27(3):461–5.
56. Lass A, Williams G, Abusheikha N, Brinsden P. The effect of endometrial polyps on outcomes of in vitro fertilization (IVF) cycles. J Assist Reprod Genet. 1999;16:410–5.
57. Heinonen PK, Saarikoski S, Pystynen P. Reproductive performance of women with uterine anomalies. An evaluation of 182 cases. Acta Obstet Gynecol Scand. 1982;61:157–62.
58. Tiras B, Korucuoglu U, Polat M, Zeyneloglu H, Saltik A, Yarali H. Management of endometrial polyps diagnosed before or during ICSI cycles. Reprod Biomed Online. 2012;24:123–8.
59. Doldi N, Persico P, Di Sebastiano F, Marsiglio E, De Santis L, Rabellotti E, et al. Pathologic findings in hysteroscopy before IVF-ET. Gynecol Endocrinol. 2005;21:235–7.
60. Ben-Nagi J, Miell J, Yazbek J, Holland T, Jurkovic D. The effect of hysteroscopic polypectomy on the concentrations of endometrial implantation factors in uterine flushings. Reprod Biomed Online. 2009;19: 737–44.
61. Rackow BW, Jorgensen E, Taylor HS. Endometrial polyps affect uterine receptivity. Fertil Steril. 2011; 95(8):2690–2.
62. Valle RF. Therapeutic hysteroscopy in infertility. Int J Fertil. 1984;29:143–8.
63. Varasteh NN, Neuwirth RS, Levin B, Keltz MD. Pregnancy rates after hysteroscopic polypectomy and myomectomy in infertile women. Obstet Gynecol. 1999;94:168–71.
64. Wang Y, Han M, Li C, Sun A, Guo X, Zhang Y. The value of hysteroscopy in the diagnosis of infertility and habitual abortion. Chin Med Sci J. 1992;7:226–9.
65. Perez-Medina T, Bajo-Arenas J, Salazar F, Redondo T, Sanfrutos L, Alvarez P, et al. Endometrial polyps and their implication in the pregnancy rates of patients undergoing intrauterine insemination: a prospective, randomized study. Hum Reprod. 2005;20:1632–5.
66. Nathani F, Clark TJ. Uterine polypectomy in the management of abnormal uterine bleeding: a systematic review. J Minim Invasive Gynecol. 2006;13:260.
67. Lieng M, Istre O, Sandvik L, Engh V, Qvigstad E. Clinical effectiveness of transcervical polyp resection in women with endometrial polyps: randomized controlled trial. J Minim Invasive Gynecol. 2010;17:351–7.
68. Preutthipan S, Herabutya Y. Hysteroscopic polypectomy in 240 premenopausal and postmenopausal women. Fertil Steril. 2005;83:705–9.
69. Muzii L, Bellati F, Pernice M, et al. Resectoscopic versus bipolar electrode excision of endometrial polyps: a randomized study. Fertil Steril. 2007;87: 909–17.
70. Emanuel MH, Wamsteker K. The intra uterine morcellator: a new hysteroscopic operating technique to remove intrauterine polyps and myomas. J Minim Invasive Gynecol. 2005;12:62–6.
71. Brooks PG, Serden SP. Hysteroscopic findings after unsuccessful dilatation and curettage for abnormal uterine bleeding. Am J Obstet Gynecol. 1988;158:1354–7.
72. Gimpelson RJ, Rappold HO. A comparative study between panoramic hysteroscopy with directed biopsies and dilation and curettage. A review of 276 cases. Am J Obstet Gynecol. 1988;158:489–92.
73. Stamatellos I, Apostolides A, Stamatopoulos P, Bontis J. Pregnancy rates after hysteroscopic polypectomy depending on the size or number of polyps. Arch Gynecol Obstet. 2008;277:395–9.
74. Spiewankiewicz B, Stelmachow J, Sawicki W, Cendrowski K, Wypych P, Swiderska K. The effectiveness of hysteroscopic polypectomy in cases of female infertility. Clin Exp Obstet Gynecol. 2003;30:23–5.
75. Yanaihara A, Yorimitsu T, Motoyama H, Watanabe H, Kawamura T. Location of endometrial polyp and pregnancy rate in infertility patients. Fertil Steril. 2008;90:180–2.
76. Bosteels J, Weyers S, Puttemans P, Panayotidis C, Van Herendael B, Gomel V, Mol B, Mathieu C, D'Hooghe T. The effectiveness of hysteroscopy in improving pregnancy rates in subfertile women without other gynaecological symptoms: a systematic review. Hum Reprod. 2010;16:1–11.
77. Batioglu S, Kaymak O. Does hysteroscopic polypectomy without cycle cancellation affect IVF? Reprod Biomed Online. 2005;10:767–9.
78. Madani T, Ghaffari F, Kiani K, Hosseini F. Hysteroscopic polypectomy without cycle cancellation in IVF cycles. Reprod Biomed Online. 2009;18:412–5.
79. Cohen MJ, Rosenzweig TS, Revel A. Uterine abnormalities and embryo implantation: clinical opinion altered by peer debate. Reprod Biomed Online. 2007;14:555–8.
80. Shokeir TA, Shalan HM, El-Shafei MM. Significance of endometrial polyps detected hysteroscopically in eumenorrheic infertile women. J Obstet Gynaecol Res. 2004;30:84–9.
81. Hereter L, Carreras O, Pasciial M. Repercusion de la presencia de polipos endometriales en un ciclo de FIV [Spanish]. Prog Obstet Ginecol. 1998;41:5–7.
82. Isikoglu M, Berkkanoglu M, Senturk Z, Coetzee K, Ozgur K. Endometrial polyps smaller than 1.5 cm do not affect ICSI outcome. Reprod Biomed Online. 2006;12:199–204.
83. Check JH, Bostick-Smith CA, Choe JK, Amui J, Brasile D. Matched controlled study to evaluate the effect of endometrial polyps on pregnancy and implantation rates following in vitro fertilization-embryo transfer (IVF-ET). Clin Exp Obstet Gynecol. 2011;38:206–8.
84. Lee A, Ying YK, Novy MJ. Hysteroscopy, hysterosalpingography and tubal ostial polyps in infertility patients. J Reprod Med Obstet Gynecol. 1997;42: 337–41.

85. Bozdag G. What is the role of office hysteroscopy in women with failed IVF cycles? Reprod Biomed Online. 2008;17:410–5.
86. Goldenberg M, Bider D, Ben-Rafael Z, et al. Hysteroscopy in a program of in-vitro fertilization. J In Vitro Fert Embryo Transf. 1991;8:336–8.
87. Kirsop R, Porter R, Torode H, et al. The role of hysteroscopy in patients having failed IVF/GIFT transfer cycles. Aust N Z J Obstet Gynaecol. 1991;31:263–4.
88. Dicker D, Ashkenazi J, Feldberg D, et al. The value of repeat hysteroscopic evaluation in patients with failed in-vitro fertilization transfer cycles. Fertil Steril. 1992;58:833–5.
89. La Sala GB, Montanari R, Dessanti L, et al. The role of diagnostic hysteroscopy and endometrial biopsy in assisted reproductive technologies. Fertil Steril. 1998; 70:378–80.
90. Oliveira FG, Abdelmassih VB, Diamond MP, et al. Uterine cavity findings and hysteroscopic interventions in patients undergoing in-vitro fertilization-embryo transfer who repeatedly cannot conceive. Fertil Steril. 2003;80:1371–5.
91. Demirol A, Gurgan T. Effect of treatment of intrauterine pathologies with office hysteroscopy in patients with recurrent IVF failure. Reprod Biomed Online. 2004;8:590–4.
92. Rama Raju GA, Shashi Kumari G, Krishna KM, et al. Assessment of uterine cavity by hysteroscopy in assisted reproduction programme and its influence on pregnancy outcome. Arch Gynecol Obstet. 2006; 274:160–4.
93. Shamma FN, Lee G, Gutmann JN, et al. The role of office hysteroscopy in in-vitro fertilization. Fertil Steril. 1992;58:1237–9.

Intrauterine Adhesions

12

Gautam N. Allahbadia

Introduction

Ever since the first description of intrauterine adhesions (IUA) by Joseph Asherman in 1948, this intrauterine pathology has been recognized as a significant gynecological complication, diagnosed with increased frequency [1, 2]. Commonly referred to as Asherman's syndrome and intrauterine synechiae, these lesions cover a spectrum that ranges from minor and insignificant to severe cohesive adhesions that affect menstrual function and fertility [3]. Pathology shows fibrous connective tissue bands with or without glandular tissue, although this may range from filmy to dense [1]. Adhesions may be classified into grades I to IV depending on the consistency and severity. Seven classification systems are described, with no universal acceptance of any one system and no validation of any of them [4].

Incidence

Intrauterine adhesions are the most frequent complications after hysteroscopic surgery in women of reproductive age, the prevalence of IUA after hysteroscopic surgery being correlated with intrauterine pathology (myoma, polyp, or adhesions) [5].

G.N. Allahbadia, MD, DNB, FNAMS
Rotunda-The Center for Human Reproduction,
36 Turner Road, 201 Second Floor, B Wing,
Bandra (W), Mumbai, Maharashtra 4400 050, India
e-mail: drallah@gmail.com

The true incidence of IUA is unknown, with most cases occurring within close temporal proximity to a pregnancy, usually within 4 months and usually, while the woman is in a hypoestrogenized state [1]. Westendorp et al. [6] reported intrauterine adhesions in 40 % of patients at ambulatory hysteroscopy, performed 3 months after secondary removal of placental remnants more than 24 h after delivery or a repeat curettage for incomplete abortions [6]. Salzani et al. [7] reported IUA on hysteroscopy performed 3 to 12 months after curettage following abortion in 37.6 % of the women, which were mostly mucous and grade I (56.1 %) [7]. Khanna and Agrawal [8] reported intrauterine adhesions in 34.8 % of the women at hysteroscopy of whom, 68.8 % were positive for tubercular bacilli [8]. The number of previous abortions and curettage procedures did not correlate with the presence of IUA [7].

Manifestation

Intrauterine adhesions may be manifested by amenorrhea accompanied with cyclic pelvic pain caused by outflow obstruction or hypomenorrhea, with up to a fourth of the patients having painless menses of normal flow and duration [1, 2], frequently associated with infertility [1].

Causes

Intrauterine adhesions or synechiae evolve after trauma to the endometrium from surgical procedures usually secondary to curettage of a recently

L.A. Stadtmauer, I. Tur-Kaspa (eds.), *Ultrasound Imaging in Reproductive Medicine*,
DOI 10.1007/978-1-4614-9182-8_12,

pregnant uterus in the context of missed abortion or pregnancy-related hemorrhage [1–3], following hysteroscopic myomectomy (10 %) and transmural myomectomies, especially when combined with uterine ischemia [9]. Previous curettage on a gravid uterus has been reported as the possible cause of Asherman's syndrome in the majority (64 %) of patients [10]. In a prospective, randomized, controlled trial in 82 women, Tam et al. [11] reported that conservative management and medical evacuation for spontaneous abortion are both acceptable alternatives to standard surgical evacuation, which resulted in a prevalence of 7.7 % filmy IUA at hysteroscopic diagnosis of IUA, 6 months after initial treatment [11].

Dawood et al. [12] evaluated the predisposing factors and treatment outcomes of different stages of intrauterine adhesions over a 7-year period in 65 patients. They identified stage I intrauterine adhesions in 36.9 %, stage II in 46.2 %, and stage III in 16.9 % of patients, the main reasons for referral being infertility (stage I 75 %, stage II 73.3 %, stage III 27.3 %) and amenorrhea (stage I 25 %, stage II 23.3 %, stage III 72.7 %). The main predisposing factor was dilatation and curettage, with 40 patients reporting IUA related to early pregnancy curettage; 45 % had stage I adhesions, 42.5 % had stage II, and 12.5 % had stage III in contrast with 10 patients who had peripartum curettage, in whom 60 % developed stage III adhesions ($p=0.004$) [12].

Genital tuberculosis has been reported as an important and common cause of Asherman's syndrome in India, causing oligomenorrhea or amenorrhoea with infertility. Sharma et al. [13] studied 28 women with positive evidence of genital tuberculosis on endometrial biopsy (histopathology or culture) or positive polymerase chain reaction (PCR) on endometrial aspirate or positive findings of tuberculosis on laparoscopy or hysteroscopy who underwent hysteroscopy with or without laparoscopy for suspected Asherman's syndrome. They reported various grades of adhesions (grade I in 17.8 %, grade II in 28.5 %, grade III in 28.5 %, and grade IV in 17.5 %) at hysteroscopy in all women, bilateral (28.5 %) or unilateral (21.3 %) blocked ostia, or inability to see the ostia (28.5 %). Only four women (14.3 %) had open ostia. On laparoscopy performed on 18 women, there were varying grades of adhesions in 16 (88.8 %) women, with beading (33.3 %), tubercles (33.3 %), caseation (11.1 %), and tuboovarian masses (11.1 %) [13].

Risk Factors

In women with menstrual disorders, a statistically significant 12-fold increased risk for Asherman's syndrome grades I–IV was found, previous abortion, as well as infection during surgery being associated with a mildly but nonsignificant increased risk [6]. Myomectomy for multiple, apposing fibroids is reported to have a higher incidence of IUA [9]. Uterine arteries embolization also carries a risk of intracavitary adhesions. Poujade et al. [14] reported a significant risk of uterine synechiae after placement of uterine compression sutures [(Hackethal technique) that transverse the uterine cavity for controlling postpartum hemorrhage (PPH)], with the development of uterine synechiae on explorative hysteroscopy or HSG in 26.7 % of women [14].

Effects

In addition to abnormal menses, infertility and recurrent spontaneous abortion are common complaints of IUA, and the accompanying retrograde menstruation may lead to endometriosis [2, 15]. Adhesions are a significant source of impaired organ functioning, decreased fertility, bowel obstruction, difficult reoperation, and possibly, pain with consequent financial sequelae [16].

Diagnosis

History and a high index of suspicion contribute significantly to the diagnosis of IUA. Several confirmatory tests, such as hysteroscopy, ultrasound-guided techniques-3D hysterosonography (3D HS), 2-dimensional (2D) and 3-dimensional (3D) transvaginal ultrasonography (TVS), hydrosonography, minimal invasive saline contrast

hysterosonography (SCHS), saline infusion hysterography (SIS), sonohysterosalpingography], radiographic techniques [hysterosalpingography (HSG)], and rarely magnetic resonance imaging have been used for the diagnosis of IUA. However, hysteroscopy has been documented as the gold standard for the diagnosis and treatment of IUA, and the several comparative studies evaluating these techniques have used hysteroscopy as the reference standard to evaluate the efficiency of a particular technique against the other. Hysteroscopy may be recommended in patients who develop menstrual disorders, either after secondary intervention for placental remnants after delivery or after a repeat curettage [6].

The Role of Ultrasound in the Diagnosis

Several ultrasound techniques, such as transvaginal color Doppler sonography (TCDS), sonohysterosalpingography (SHSG), and three-dimensional sonography (3DS), are capable of providing diagnostic information that, in some cases, is equivalent to the information afforded by established techniques that require exposure to radiation, such as hysterosalpingography (HSG), or that are more invasive, such as hysteroscopy or diagnostic laparoscopy [17], tissue biopsies, and dilation and curettage (D&C). The role of ultrasonography for the diagnosis of IUA has been studied by several authors with mixed opinions, and all these studies used hysteroscopy as the most reliable reference standard.

El-Mazny et al. [18] reported abnormal hysteroscopic findings, including IUA, in 33.1 % of patients with reported normal uterine findings on HSG who were scheduled for assisted reproductive techniques (ART) [in vitro fertilization (IVF)/intracytoplasmic sperm injection (ICSI)] investigations [1].

Transvaginal sonography (TVS) has been reported to be specific (100 %), but not sensitive (41.7 %) compared with outpatient hysteroscopy, which leads the authors to suggest that outpatient hysteroscopy should be part of the infertility workup before ART even in patients with normal HSG and/or TVS and especially in patients with prior failed ART cycles who reported a significantly higher incidence of abnormal hysteroscopic findings. The procedure was acceptable in almost all patients with no reported complications [18].

Fedele et al. [19] performed transvaginal US before hysteroscopy as part of the routine diagnostic workup in 77 women who had repeated spontaneous abortions. They were able to correctly identify uterine adhesions (minimal in ten instances and moderate in one) with TVS in 90.0 % (10/11) of the women in whom this finding was subsequently confirmed at hysteroscopy. The sensitivity, specificity, PPV, and NPV of transvaginal US were 91, 100, 100, and 98.5 %, respectively. Hysteroscopic findings were considered the reference. They concluded that TVS, which is a noninvasive and relatively inexpensive procedure, seems to be effective in screening for uterine adhesions in a population at risk [19].

Narayan and Goswamy [20] correlated preoperative TVS (performed on days 7, 14, and 21 in spontaneous ovulatory cycles) with hysteroscopic findings (performed in the subsequent cycle) in 200 patients being investigated for infertility. A total of 182 patients were diagnosed correctly to have an abnormality by TVS giving a false-positive rate of 5.5 %. The sensitivity and PPV of TVS in detecting endometrial pathology were 98.9 and 94.3 %, respectively, with a PPV of 98.5 % for the detection of intrauterine adhesions and a strong correlation between findings from transvaginal sonography and hysteroscopy. The authors concluded that TVS may be used to detect intrauterine pathology and identify patients in whom hysteroscopy and hysteroscopic surgery are indicated [20]. With further advance in ultrasound technology, Knopman and Copperman [21] assessed the value of 3-dimensional (3D) ultrasound in the management of patients with suspected Asherman's syndrome in a case series of 54 infertile patients who presented with suspected Asherman's syndrome. Intrauterine adhesions (IUAs) were demonstrated on 3D ultrasound and HSG in all cases and confirmed by hysteroscopy. They reported 100 % sensitivity with 3D ultrasound for correctly

grading the extent of IUAs compared to only 66.7 % for HSG. In 61.1 % of cases in which HSG results were inconsistent with hysteroscopy, lower uterine segment outflow obstruction was present, and HSG misclassified findings as severe Asherman's with complete cavity obstruction. With a postoperative conception rate of 90 %, the authors concluded that 3D ultrasound provides a more accurate depiction of adhesions and extent of cavity damage than HSG in patients with suspected Asherman's syndrome, particularly when differentiating severe IUAs from lower uterine segment outflow obstruction. Therefore, grading systems utilizing HSG to classify severity of disease should be revised to include 3D ultrasound findings [21].

Sonohysterography, a simple ultrasound (US) procedure technique, involves placement of a 5-F catheter into the endometrial canal with subsequent instillation of sterile saline solution under US guidance. Saline infusion offers a good contrast, enabling improved visualization and distinction between diffuse and focal abnormalities. Sonohysterography has been shown to be a safe, simple, and cost-effective outpatient method for evaluating the potentially abnormal endometrium using transvaginal ultrasound (US) in an outpatient setting and to plan the next step in case management [22]. Besides the cost-related issues, it has been indicated as a well-tolerated technique with a short learning curve in the diagnosis of abnormal uterine bleeding (premenopausal and postmenopausal), bleeding while using tamoxifen, suspected congenital uterine abnormality, and Asherman's syndrome [23]. According to Badu-Peprah et al. [24] sonohysterography is an affordable and feasible diagnostic modality in developing nations for evaluating the endometrial cavity that should be used more often where equipment and skill permit [24], thereby obviating the need for laparoscopy and hysteroscopy in the majority of cases [25]. In a very recent study, Kowalczyk et al. [26] reported real-time 3D sonohysterography (SIS 3D) to be a minimally invasive advance to conventional 2D sonohysterography (sensitivity 72 % and specificity 96 %) that enables a three-dimensional image of the uterine cavity and enables examination of endometrial lesions with a sensitivity and specificity of 83 and 99 %, respectively and a diagnostic precision similar to the results achieved by hysteroscopy [26].

In a prospective study on 65 infertile women 19 to 43 years of age, Soares et al. [27] compared the diagnostic accuracy of sonohysterography (SHG) in uterine cavity diseases in infertile patients with that of HSG and TVS, using hysteroscopy as the gold standard. Sonohysterography and HSG had a sensitivity of 75 % in the detection of intrauterine adhesions and respective PPVs of 42.9 and 50 %, while TVS showed a sensitivity and PPV of 0 % for this diagnosis. The authors concluded that, while sonohysterography was in general the most accurate test with a markedly superior diagnostic accuracy for polypoid lesions and endometrial hyperplasia (EH), with total agreement with the gold standard, however, in diagnosis of intrauterine adhesions, SHG had limited accuracy, similar to that obtained by HSG, with a high false-positive diagnosis rate [27]. Makris et al. [28] compared 3D hysterosonography (3D HS) and diagnostic hysteroscopy in 242 women with abnormal uterine bleeding. They reported a similar specificity (99.4 %), but a higher sensitivity for hysteroscopy compared to 3D HS (98.7 % vs. 93.5 %, respectively). The PPV and NPV of 3D HS were 98.6 and 97 %, respectively, compared to 98.7 and 99.4 % for hysteroscopy, respectively. The two techniques were in agreement for eight cases of adhesions and in 165 cases of normal endometrium [28].

de Kroon et al. [23] evaluated the accuracy of minimal invasive saline contrast hysterosonography (SCHS) in the diagnosis of uterine pathology. They reported that this technique can detect intracavity abnormalities (with a prevalence of 54 %) with a sensitivity, specificity, PPV, and NPV of 94, 89, 91, and 92 %, respectively, and in combination with endometrial sampling, whenever indicated, it might be able to replace diagnostic hysteroscopy as the gold standard in the evaluation of the uterine cavity in 84 % of the diagnostic hysteroscopies as SCHS is two to nine times cheaper than diagnostic hysteroscopy. However, SCHS fails more frequently in postmenopausal women than premenopausal women (12.5 % vs. 4.7 %; $p=0.03$), and the

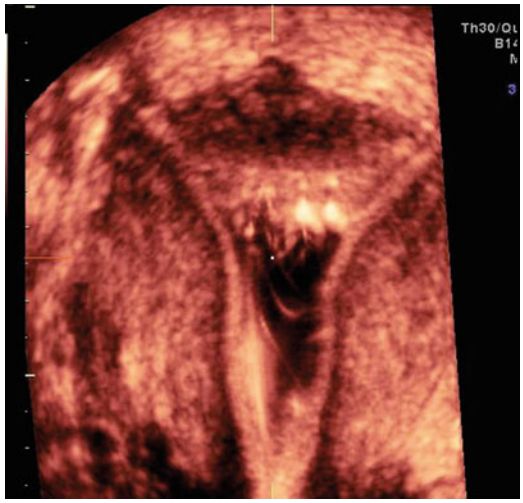

Fig. 12.1 Saline sonogram showing intrauterine adhesions

chance of a non-conclusive SCHS is 7.6 %, being higher if the uterine volume is greater than 600 cm^3 (relative risk, 2.63; 95 %-CI, 1.05–6.60) and if two or more myomas are present: (RR, 2.65; 95 %-CI, 1.16–6.10) [23].

Yucebilgin et al. [29] reported a sensitivity, specificity, positive, and negative predictive values of 85, 75, 75, and 84 %, respectively, for hydrosonography in the detection of structural endometrial cavity lesions were 45 (85 %) of 53 women, who were supposed to have normal findings on hydrosonography, were confirmed by hysteroscopy. They, however, suggested that hydrosonography may be a useful tool in the evaluation of intrauterine cavity structural pathologies in infertile patients with the exception of intrauterine adhesions [29].

Alborzi et al. [30] compared the diagnostic accuracy of hysterosalpingography and sonohysterosalpingography in detecting tubal and uterine abnormalities with surgical findings as the gold standard. They reported a sensitivity, specificity, positive predictive value, and negative predictive value of 78.2, 93.1, 82.7, and 91 %, respectively, for the detection of total tubal and uterine pathologies compared to 76.3, 81.8, 90.9, and 59.2 %, respectively, for HSG. They concluded that sonohysterosalpingography is a safe, easy, and promising procedure and more accurate than hysterosalpingography for detecting intrauterine adhesions and various forms of uterine anomalies [30].

There have been reports of MRI appearances in four cases of Asherman's syndrome in which the diagnosis was confirmed by hysteroscopy. However, the full range of MRI appearances in Asherman's syndrome has not been established and there has been only one case reported in the literature [31]. Figure 12.1 shows intrauterine adhesions using a multiplanar view after sonohysterography.

Management of IUA

Diagnosis and treatment of intrauterine adhesions are integral to the optimization of fertility outcomes [15]. Surgical management of IUA presents a challenge to the hysteroscopic surgeon. Though the appropriate management is controversial [3], and more often than not, guided by the clinician's choice, skill, and operative setting, hysteroscopic adhesiolysis with antibiotic prophylaxis followed by the use of postoperative adjuvants such as systemic estrogens and intrauterine devices or systems designed to impede the development of adhesions is the treatment of choice with favorable results in terms of pregnancy and live birth rates [3, 15, 32, 33]. Clinicians should maintain a level of suspicion of intrauterine adhesions and should investigate by hysteroscopy if necessary [32]. Non-hysteroscopic techniques are also beginning to be developed, but whether they will replace the current "gold" standard of hysteroscopy remains to be seen [34]. The success of treatment regarding term deliveries and rate of abortions depends on the severity of the adhesions, and pregnancy, when achieved, may be complicated by premature labor, placenta previa, and placenta accreta [33].

Hysteroscopic Surgery

Technological progress in optic fibers and instrumentation has made it possible to video endoscope and determine the fibrous nature of the lesions

and its precise localization and control endocavitary surgeries such as hysteroscopic adhesiolysis for uterine synechiae [35]. Though sonohysterography and hysterosalpingography are useful as screening tests of intrauterine adhesions [15], hysteroscopy has been considered the mainstay of diagnosis, classification, and treatment of the intrauterine adhesions, with medical treatments having no role in management [1, 2, 4, 15, 32, 36]. Diagnostic and therapeutic hysteroscopy is a simple, feasible, safe, reproducible, effective, quick, well-tolerated, and low-cost surgical procedure that is highly successful in an outpatient setting, offering a see-and-treat approach in majority of the subjects with intrauterine adhesions [37, 38]. Hysteroscopy has also become accepted as the optimum route of surgery, the aim being to restore the size and shape of the uterine cavity, normal endometrial function, and fertility [15, 16]. Lysis of intrauterine adhesions, for the treatment of infertility and recurrent pregnancy loss, results in improved fecundability and decreased pregnancy loss. Though adhesiolysis for pain relief appears efficacious in certain subsets of women, unfortunately, even when lysed, adhesions have a great propensity to reform [16]. According to Bettocchi et al. [38] there is no consensus on the effectiveness of hysteroscopic surgery in improving the prognosis of subfertile women. However, office hysteroscopy is a powerful tool for the diagnosis, and treatment of intrauterine benign pathologies and in patients with at least two failed cycles of assisted reproductive technology, diagnostic hysteroscopy and, if necessary, operative hysteroscopy is mandatory to improve reproductive outcome [38]. A descriptive study (Canadian Task Force classification II-2) concluded that hysteroscopic adhesiolysis is an effective and safe option even for postmenopausal women with intrauterine lesions adhesions on hysteroscopy or ultrasound. It allows the correct diagnosis to be made, reduces the need for major and unnecessary surgery, and is therapeutic in most patients [39].

Treatment can range from simple cervical dilatation in the case of cervical stenosis, but an intact uterine cavity, to extensive adhesiolysis of dense intrauterine adhesions using scissors, electro- or laser energy, or a combination of blunt and sharp dissection [32, 34]. Various techniques for adhesiolysis and for prevention of scar reformation have been advocated. According to March, [2] the use of miniature scissors for adhesiolysis and the placement of a balloon stent inside the uterus immediately after surgery appear to be the most efficacious [2]. Patients with more severe adhesions, in whom the uterine fundus is completely obscured, and those with a greatly narrowed fibrotic cavity present the greatest therapeutic challenge. Several techniques have been described for these difficult cases, but the outcome is far worse than in patients with mild, endometrial-type adhesions [4, 34]. A significantly obliterated cavity may require multiple hysteroscopic adhesiolysis to achieve a satisfactory anatomical and functional result [15, 36], while laparoscopic or ultrasound guidance may aid in the hysteroscopic lysis of dense scar tissue and difficult entry into the cervix [1].

Treatment Outcome

Treatment outcomes are difficult to assess as there is no universally agreed upon classification system [1]. Anatomic, but most of all functional prognosis, is directly correlated to the severity of adhesions, and the number of surgical procedures required to complete treatment [40].

Restoration of menstruation is highly successful (more than 90 %), and pregnancy rates around 50–60 % with live birth rates around 40–50 % can be achieved [32]. The risk of complications for those that achieve pregnancy is significant with a significant risk for placenta accreta and subsequent blood loss, transfusion, and hysterectomy [12]. In perhaps the largest study, involving 6,680 hysteroscopies with hysteroscopic adhesiolysis in 75 patients, 94.6 % functional restoration and 93.3 % anatomic resolution, with pregnancy rates ranging from 28.7 to 53.6 %, were achieved. At 2-month follow-up, the uterine cavity was completely regular in 70 cases, while in four cases, a second surgical treatment was necessary [41].

Using a standard technique with a loop electrode and glycine 1.5 % as distension medium, Dawood et al. [12] reported an improvement in

the rate of amenorrhea from 32.3 % before adhesiolysis to 9.2 % after the procedure with an overall pregnancy rate of 51.2 % and the live birth rate 32.6 % among women who wished to conceive. Severe intrauterine adhesions were managed with the assistance of abdominal ultrasound to ensure that the uterine cavity was not breached, and the rates of pregnancy and term pregnancy among this selected group of women were similar regardless of the severity of adhesions [12].

Yu et al. [42] evaluated the outcome of hysteroscopic adhesiolysis with electrode needle or loop under direct vision in 85 women with Asherman's syndrome who presented with a history of infertility or recurrent pregnancy loss. After hysteroscopic adhesiolysis, the chances of conception among the 18.2 % of women who remained amenorrheic were significantly lower than those who continued to have menses (50 %). The conception rate in women who had reformation of intrauterine adhesions at second look hysteroscopy (11.8 %) was significantly lower than that of women who had a normal cavity (59.1 %), suggesting that the outcome of hysteroscopic adhesiolysis for Asherman's syndrome is significantly affected by recurrence of intrauterine adhesions [42].

Hysteroscopic adhesiolysis with monopolar or bipolar energy can be performed safely and effectively for severe stage 3 and 4 adhesions with a 97 % restoration of menses, 43.8 % PR, and 32.8 % LBR. The pregnancy rate was significantly higher in patients ≤35 years compared to patients older than 35 years (66.6 % vs. 23.5 %, respectively; $p=0.01$), suggesting that age is the main predictive factor of success: the pregnancies were at risk of abnormal placentation [43]. The impact of age on the outcome of hysteroscopic adhesiolysis is in agreement with a previous study by Capella-Allouc et al. [44] that reported a pregnancy rate of 42.8 %, live birth rate of 32.1 %, the pregnancy rate being much higher in patients ≤35 years compared to patients older than 35 years (62.5 % vs.16.6 %, respectively; $p=0.01$) following hysteroscopic adhesiolysis in 31 patients with severe Asherman's syndrome. However, these pregnancies were at risk for hemorrhage with abnormal placentation [44].

Roy et al. [10] reported an overall conception rate of 40.4 %, live birth rate of 86.1 % and a miscarriage rate of 11.1 % in a mean conception time after surgery of 12.8 months following hysteroscopic adhesiolysis with the monopolar electrode knife in 89 infertile patients with Asherman's syndrome. The cumulative pregnancy rate showed that 97.2 % of patients conceived within 24 months. The conception rate was higher (58 %) in mild Asherman's syndrome compared to 30 % conception rate in moderate and 33.3 % conception rate in severe cases. There was a significantly higher likelihood of conception (44.3 %) in those who continued to have improved menstrual pattern compared to only 10 % likelihood of conception in those who continued to have amenorrhea after adhesiolysis. A second-look office hysteroscopy, performed after 2 months, showed reformation of adhesions in12 patients that needed a repeat adhesiolysis with no conception in these patients. The authors concluded that hysteroscopic adhesiolysis for Asherman's syndrome is a safe and effective method of choice for restoring menstrual function and fertility [10].

Shokeir et al. [45] attempted to analyze the adhesion grade in multiple hysteroscopic-guided biopsies from IUA following the initial hysteroscopic adhesiolysis at a follow-up diagnostic hysteroscopy, performed early (2–4 weeks) after the initial operation or late, about 12 months (8–16 months). They observed that at follow-up hysteroscopy, 25 % of both groups had no significant adhesions. Grade I adhesions (thin, filmy) occurred in 60 % of the early hysteroscopy patients and in only 12 % of the late group ($P<0.05$). Grade II adhesions were present in 10 % of the early group and in up to 41 % in the late group ($P<0.05$), whereas grade III adhesions were present in only 5 % of the early hysteroscopy group, but in 22 % of the late one ($P<0.05$). Correlation between hysteroscopic and histologic findings were good in most of cases in both groups. The follow-up to determine the subsequent reproductive outcome revealed similar conception rates in both groups. The authors suggested that the IUA that might be formed immediately following hysteroscopic reproductive surgery is histologically different from those

appearing a longer time after the original operation. Routine early follow-up hysteroscopy can influence the prognosis resulting from the original surgery [45].

Having excluded hormonal imbalances, premature ovarian failure, and congenital uterine abnormalities Yasmin et al. [46] reported thick fibrous adhesions in 45 % of patients, flimsy adhesions in 40 %, and muscular adhesions in 15 % at hysteroscopy, with 65 % adhesions in the body of uterus, 25 % at the site of internal os, and 1 % had adhesions in the cervical canal as well as the body of the uterus. Following diagnostic hysteroscopy and resection of adhesions in 20 patients (median age 26 years), presenting with scanty menses and secondary infertility (65 %), secondary amenorrhoea (20 %), or with primary infertility alone (15 %), they reported a restoration of menses in 95 % of the patients and conception in 10 % of the patients. Though the patient number was small, the authors suggested that hysteroscopy is an effective procedure for not only diagnosing Asherman's syndrome, but is equally effective for treating it [46].

Hysteroscopic adhesiolysis in women with Asherman's syndrome and poor reproductive performance (previous spontaneous abortions or a premature delivery) contributes significantly to a successful reproductive outcome. Whereas pregnancy outcome prior to the hysteroscopic adhesiolysis was 18.3 % term deliveries, 3.3 % premature deliveries, 62.4 % first-trimester abortions, and 16.0 % late abortions, after hysteroscopic adhesiolysis, the pregnancy outcome was 68.6 % term deliveries, 9.3 % premature deliveries, 17.4 % first-trimester abortions, and 4.7 % late abortions. The operative success rate, measured by delivering a healthy newborn, improved from 18.3 % preoperatively to 64 % postoperatively in women with two previous unsuccessful pregnancies [47], whereas in women with three or more unsuccessful pregnancies, the success rate improved from 18.3 to 75 %. Successful outcome of adhesiolysis was observed in 61.9 % of mild (stage I) and in 70.6 % of moderate to severe cases (stages II and III) of intrauterine adhesions [47].

Blunt adhesiolysis with a flexible hysteroscope, following primary treatment of intrauterine adhesions with sharp adhesiolysis has been suggested as an effective technique for the maintenance of cavity patency with an improvement in menstrual flow in 95 % of the patients, relief of dysmenorrhea in 92 %, 92 % improvement in disease staging over the treatment interval, and a pregnancy rate of 46 %. Initially, 50 % had severe adhesions, 46 % had moderate, and 4 % had minimal disease according to the March criteria [48].

Colacurci et al. [49] analyzed the reproductive outcome in 53 women undergoing hysteroscopic lysis of intrauterine adhesions, according to their localization and severity. Hysteroscopic surgery restored an acceptable menstrual cycle in almost all the patients affected by intrauterine isolated adhesions in 52 % of women with complex incomplete adhesions, and in none of the patients with an entirely obliterated cavity. In isolated, isthmic, central, or marginal synechiae, a pregnancy rate of 73.3 % was observed with a pregnancy rate to term, respectively, of 63.3 % and of 86.3 %, while in case of complex but not complete adhesions, the pregnancy rate was 25 % with only two term pregnancies. There were no pregnancies in three cases of complex synechiae. The authors concluded that the basic parameter to define the functional and reproductive prognosis of the hysteroscopic lysis of intrauterine adhesions is not the menstrual profile or the histological characteristic of the lesions, but rather their extension [49].

Hysteroscopy and hysteroscopic surgery have been the gold standard of diagnosis and treatment, respectively, for patients with Asherman's syndrome who presented with amenorrhea or hypomenorrhea, infertility, or recurrent pregnancy loss. However, according to most authors, despite the advances in hysteroscopic surgery, the treatment of moderate to severe Asherman's syndrome still presents a challenge [40, 50]. Furthermore, pregnancy after treatment remains high risk with complications including spontaneous abortion, preterm delivery, intrauterine growth restriction, placenta accreta or previa, or even uterine rupture, that necessitate close antenatal surveillance and monitoring for women who conceive after treatment [50]. According to Piketty et al. [40] despite the infrequent but well-

known complications during surgery and the less frequent but often severe obstetrical complications, the benefit gained by the recovery of fertility (either spontaneous or not) remains superior to the risks of the surgical management [40].

Role of Ultrasonography in the Treatment

Serial intrauterine device-guided hysteroscopic adhesiolysis of intrauterine synechiae, especially for early intervention, may prevent complications during the treatment of severe intrauterine adhesions and may present a secure and effective alternative for constructive clinical outcomes with spontaneous pregnancy rates of 47.2 and 30 % and live birth rates of 28 and 20 % in patients who did and did not undergo early intervention of office hysteroscopy, 1 week after insertion of the IUD at hysteroscopic adhesiolysis, respectively [51]. Following echo-controlled hysteroscopic surgical cure of complex and/or recurrent uterine synechiae in 11 patients, Salat-Baroux et al. [35] concluded that intraoperative echography allowed hysteroscopic adhesiolysis of intrauterine adhesions at a controlled and equivalent distance from the uterine walls, enabling better treatment of the uterine cornua since the operator is informed when to limit progression to avoid massive fluid infusion into the abdominal cavity and perforation of the uterus. The intraoperative echographic control was validated in the operating theater radiographically. With this technique normal cavities with bilateral tube permeability were obtained in 72.72 % of the patients and normal cycles in 90.9 % of the patients [35]. Following hysteroscopic lysis under ultrasound control for significant intrauterine synechiae, Bellingham [52] reported normal menstruation in 61 % of the patients and live births in 80 % of the patients, of whom 50 % had had severe adhesions. They reported that ultrasound control is ideally essential if the adhesions are extensive [52]. However, in both these studies, the number of patients was very small to effectively document the role of ultrasound in the treatment of IUA.

Coccia et al. [53] described a new therapeutic procedure called pressure lavage under ultrasound guidance (PLUG) for selected cases of IUA. This technique is based on sonohysterography to monitor the effects of intrauterine injections of saline solution on the continuous accumulation of saline in the uterine cavity for the mechanical disruption of IUA. In an open clinical investigation with no control group, they reported satisfactory lysis of adhesions and restoration of menses in 71.4 % of the patients with mild IUA with a pregnancy rate of 66.63 % following the use of the PLUG technique. A second-look hysteroscopy after 1 month showed the persistence of filmy adhesions in two patients with moderate IUA that were removed successfully during hysteroscopy. The authors suggested that PLUG is a safe and ideal in-office procedure that allows complete lysis in mild IUA cases avoiding the need for therapeutic, and possibly, follow-up hysteroscopy, and may represent a useful initial step in moderate IUA cases reducing the need for operative hysteroscopy [53]. In a recent study, Taniguchi and Suginami [54] also suggested that sonohysterographic (SHG) lysis for recurrent adhesions following hysteroscopic lysis may be a treatment option for recurrent adhesions in infertile patients, with improved menstrual cycles and restored tubal patency [54].

Tiras et al. [55] demonstrated the value of laparoscopic intracorporeal ultrasound (LIU)-guided hysteroscopic adhesiolysis in a patient with amenorrhea and infertility with total intrauterine synechiae. Adequate intrauterine adhesiolysis was performed by a resectoscope with a wire loop, suggesting that complex intrauterine procedures can be easily performed by the guidance of endoscopic ultrasonography to avoid the possibility of inadvertent uterine perforation [55].

Schlaff and Hurst [56] evaluated the predictive value of preoperative endometrial sonography in the diagnosis and surgical treatment of women with amenorrhea due to severe Asherman's syndrome, characterized by complete obstruction of the cavity at hysterosalpingogram. They suggested that an endometrial pattern, demonstrating a well-developed endometrial stripe on transvaginal sonography is highly predictive of a positive surgical and clinical outcome in women with

severe Asherman's syndrome with resumption of normal menses and normalization of the cavity after hysteroscopy in contrast to women with minimal endometrium who had no cavity identified and derived no benefit from surgery [56]. However, this study was limited to just seven patients and hence, substantial evidence in this direction is lacking.

Radiographic Methods

In a small but significant study, Karande et al. [57] demonstrated that in-office lysis of intrauterine adhesions, under fluoroscopic control, using a specially designed catheter (gynecoradiologic control) can be carried out safely in the majority of patients, using minimally invasive techniques. They could successfully lyse adhesions in 76 % (13/17) of the patients (9 mild, 3 moderate, and 1 severe), while in remaining 4 patients (2 moderate and 2 severe), lysis was only partially successful. Nine procedures were performed with the catheter's balloon tip and four with hysteroscopic scissors. Procedure complications resulting in the abandoning of the procedure included patient discomfort before attempting the use of scissors ($n=1$), extravasation of dye into the myometrium making visualization difficult ($n=1$), and thick, fibrotic adhesions that were resistant to scissors ($n=2$). They opined that the potential cost savings with this technique in comparison with endoscopic procedures, which require utilization of expensive operating room time, are especially relevant in a cost-conscious managed care environment and only failures of in-office procedures would reach the operating room. [57] The fluoroscopic approach to adhesions was further evaluated a decade later by Chason et al. [58] who used hysteroplasty with fluoroscopic cannulation and balloon uterine dilation to treat intrauterine adhesions and cervical stenosis and lower uterine defects in select cases. They concluded that while the treatment of intrauterine adhesions resulted in an improved pregnancy outcome, albeit in a case study, the effect of lower uterine segment-filling defects from cesarean deliveries on pregnancy outcome in assisted reproductive technology cycles warrants further investigation [58]. In a 5-year retrospective, uncontrolled cohort study, Thomson et al. [59] conducted fluoroscopically-guided hysteroscopic synechiolysis for Asherman's syndrome in 30 patients (13 % AFS grade I, 43 % AFS grade II, and 43 % AFS grade III), 60 % of whom were amenorrheic. They reported a 96 % restoration of regular menses with a 53 % pregnancy rate among patients who attempted to conceive and concluded that hysteroscopic synechiolysis, performed by injecting radiographic contrast medium and visualized under image-intensifier control, followed by cyclic high-dose estrogen therapy to stimulate endometrial proliferation, appears to be an effective treatment for Asherman's syndrome. Repeat procedures were performed monthly until the endometrial cavity was re-established [59].

Prevention of IUA

One of the most important features of treatment for intrauterine synechiae is the prevention of recurrence [4]. Follow-up studies to assure resolution of the scarring are mandatory before the patient attempts to conceive as is careful monitoring of pregnancies for cervical incompetence, placenta accreta, and intrauterine growth retardation [2]. The best available evidence demonstrates that the newly developed adhesion barriers, such as hyaluronic acid, show promise for preventing new adhesions [4, 15]. Postoperative mechanical distention of the endometrial cavity with the use of intrauterine contraceptive devices and postoperative hormonal treatment with estrogen +/− progestogen to facilitate endometrial regrowth are important in the prevention of recurrence [15, 32].

With regard to primary adhesion formation, a recent study by Rein et al. [60] demonstrated that selective hysteroscopic resection (HR) of residual trophoblastic tissue after first- or second-trimester miscarriage or term delivery significantly reduces the incidence of intrauterine adhesions and increases pregnancy rates compared to ultrasound-guided evacuation with

a curette (D&E). They reported mild adhesion in 4.2 % of the patients after selective HR compared to an incidence of 30.8 % after D&E, of which 17.9 % were mild, 7.7 % single dense adhesions, and 2.6 % with extensive endometrial fibrosis. Conception rates were significantly higher in the HR patients compared to curetted patients (68.8 % vs. 59.9 %, respectively; $p < 0.05$) and 78.1 % vs. 66.6 %, respectively; $p < 0.05$ in patients younger than 35 years of age with a significantly ($p < .05$) shorter time to conception (11.5 months vs. 14.5 months) [60]. Operative hysteroscopy for selective curettage of residual trophoblastic tissue instead of nonselective conventional curettage may prevent intrauterine adhesions [36].

Mechanical Barriers

The efficiency of barrier agents' postoperative hysteroscopic adhesiolysis to prevent the recurrence of adhesions has been addressed in a few clinical trials. Barrier agents have been grouped under mechanical agents (intrauterine device-IUCD, Foley catheter), fluid agents [Seprafilm, Hyalobarrier, auto-cross-linked hyaluronic acid (ACP) gel], postoperative systemic treatment (cyclic estrogen-progesterone therapy), and the latest tissue barriers (fresh or dries amnion grafts).

Several comparative studies, evaluating the efficacy of various barrier agents, have been conducted. Orhue et al. [61] compared two adjunctive treatments following intrauterine adhesiolysis—the intrauterine contraceptive device (IUCD) and the Foley catheter. In a 4-year initial period, patients with intrauterine adhesions were treated with the insertion of an IUCD after adhesiolysis. In the next 4 years, a pediatric Foley catheter balloon was used after adhesiolysis instead of the IUCD. They reported a significantly higher restoration of normal menstruation (81.4 % vs. 62.7 %, $p < 0.05$), less frequent persistent posttreatment amenorrhea and hypomenorrhea (18.6 % vs. 37.3 %; $P < 0.03$), a higher conception rate (33.9 % vs. 22.5 %), and a significantly lesser need for repeated treatment in the Foley catheter group compared to the IUCD group, respectively. They concluded that the Foley catheter is a safer and more effective adjunctive method of treatment of IUA compared with the IUCD [61].

Fluid Barriers

The application of auto-cross-linked hyaluronic acid (ACP) gel has been reported to significantly reduce the incidence and severity of de novo formation of intrauterine adhesions after hysteroscopic surgery, with a significant decrease in adhesion severity on staging of adhesions [62].

Tissue Barriers

The role of amnion grafts as barrier agents to prevent recurrence of adhesions has currently gained a lot of attention. In a pilot study involving 25 patients with moderate or severe intrauterine adhesions, Amer et al. [63] reported that hysteroscopic adhesiolysis followed by intrauterine application of a fresh amnion graft over an inflated balloon of a Foley catheter for 2 weeks seems to be a promising procedure for decreasing recurrence of adhesions and encouraging endometrial regeneration. They reported failure to achieve normal menstrual flow in 16.7 % of the patients with moderate versus 23.1 % of the patients with severe adhesions and observed adhesion reformation at follow-up hysteroscopy in 48 % of the patients, all with severe adhesions. However, randomized comparative studies are needed to validate its benefits, including reproductive outcome [63].

In a more recent pilot prospective randomized comparative study (Canadian Task Force classification I), Ameret et al. [64] estimated the efficacy of inserting fresh and dried amnion graft after hysteroscopic lysis of severe intrauterine adhesions in decreasing its recurrence and encouraging endometrial regeneration in 45 patients. Hysteroscopic lysis of intrauterine adhesions was followed by insertion of an intrauterine balloon only (group 1) or either fresh amnion graft (group 2) or dried amnion graft (group 3) for

2 weeks. Diagnostic hysteroscopy, performed at 2 to 4 months postoperatively, revealed significant improvement in adhesion grade with the amnion graft versus intrauterine balloon alone ($p=0.003$) and significant improvement with fresh compared to dried amnion graft ($p=0.01$). Restoration of normal menstruation (46.7 % in group 3, 35.7 % in group 2, 28.6 % in group 1) and the conception rate (80 % after amnion graft and 20 % without amnion) was higher in patients with the graft compared to the balloon. The overall conception rate was 23.3 % with a miscarriage rate of 60 %. The authors concluded that hysteroscopic lysis of severe intrauterine adhesions with grafting of either fresh or dried amnion is a promising adjunctive procedure for decreasing recurrence of adhesions and encouraging endometrial regeneration [64].

Prevention strategies, including bipolar resection, barrier gel, or postoperative estradiol, might be useful, but stronger evidence is needed and there is a need for other randomized controlled trials to fully justify the use of adhesion barriers for clinical use [5, 9]. In view of the current knowledge, Gambadauro et al. [9] recommend a prevention strategy based on a combination of surgical trauma minimization and identification of high-risk cases, with early hysteroscopic diagnosis and lysis possibly representing the best means of secondary prevention and treatment of postoperative intrauterine adhesions [9]. Considering the decreased pregnancy outcome in patient with recurrence of adhesions, further research in Asherman's syndrome should be directed toward reduction of adhesion reformation with a view to improving outcome [42].

Recent Advances

In an effort to treat injured endometrium nonresponsive to conventional treatment for Asherman's syndrome (IUCD) with cyclical hormonal therapy for 6 months, Nagori et al. [65] demonstrated that placement of endometrial angiogenic stem cells in the endometrial cavity under ultrasound guidance after curettage followed by cyclical hormonal therapy can regenerate injured endometrium. These cells could be isolated from adult autologous stem cells isolated from a patient's own bone marrow using immunomagnetic isolation [65]. Gargett and Healy [66] also reported regeneration of thin endometrium refractory to estrogen stimulation following intrauterine administration of bone marrow stem/progenitor cells sufficiently to support a pregnancy in a case study. However, whether its local endometrial damage is induced by concurrent curettage that stimulated endogenous endometrial stem/progenitor cells into action, or both, is open to question [66].

Conclusion

Intrauterine adhesions are a significant gynecological complication that require prompt and accurate diagnosis and treatment. Despite its invasiveness, cost issues and the technical skill required, hysteroscopy is recognized as the gold standard for the diagnosis, classification, and treatment of adhesions with an encouraging restoration of fertility in terms of menstruation, pregnancy rates, and live birth rates in patients with mild, moderate, and severe IUA, including postmenopausal women. Moreover, it offers a see-and-treat approach in majority of the patients where therapy is required, thus obviating the need for a second intervention. Though ultrasonography is gradually gaining acceptance in the diagnosis of IUA, particularly in economically compromised settings, with the purpose of avoiding costly invasive techniques, it has limited accuracy and sensitivity in the diagnosis of IUA compared to hysteroscopy. The addition of 3D ultrasound is reported to have improved accuracy in the diagnosis, but consistent large-scale studies are lacking. However, with regard to treatment, ultrasound may have a significant role in controlling hysteroscopic surgery, especially in patients with complex severe adhesions, to avoid inadvertent uterine perforation. More large-scale randomized trials will be required before ultrasonography can be established as a more functionally effective alternative to hysteroscopy in the diagnosis and treatment of IUA.

References

1. Berman JM. Intrauterine adhesions. Semin Reprod Med. 2008;26(4):349–55.
2. March CM. Asherman's syndrome. Semin Reprod Med. 2011;29(2):83–94.
3. Fedele L, Bianchi S, Frontino G. Septums and synechiae: approaches to surgical correction. Clin Obstet Gynecol. 2006;49(4):767–88.
4. Deans R, Abbott J. Review of intrauterine adhesions. J Minim Invasive Gynecol. 2010;17(5):555–69.
5. Revaux A, Ducarme G, Luton D. Prevention of intrauterine adhesions after hysteroscopic surgery. [Article in French]. Gynecol Obstet Fertil. 2008;36(3):311–7.
6. Westendorp IC, Ankum WM, Mol BW, Vonk J. Prevalence of Asherman's syndrome after secondary removal of placental remnants or a repeat curettage for incomplete abortion. Hum Reprod. 1998;13(12): 3347–50.
7. Salzani A, Yela DA, Gabiatti JR, Bedone AJ, Monteiro IM. Prevalence of uterine synechia after abortion evacuation curettage. Sao Paulo Med J. 2007;125(5):261–4.
8. Khanna A, Agrawal A. Markers of genital tuberculosis in infertility. Singapore Med J. 2011;52(12):864–7.
9. Gambadauro P, Gudmundsson J, Torrejón R. Intrauterine adhesions following conservative treatment of uterine fibroids. Obstet Gynecol Int. 2012;2012:853269.
10. Roy KK, Baruah J, Sharma JB, Kumar S, Kachawa G, Singh N. Reproductive outcome following hysteroscopic adhesiolysis in patients with infertility due to Asherman's syndrome. Arch Gynecol Obstet. 2010; 281(2):355–61.
11. Tam WH, Lau WC, Cheung LP, Yuen PM, Chung TK. Intrauterine adhesions after conservative and surgical management of spontaneous abortion. J Am Assoc Gynecol Laparosc. 2002;9(2):182–5.
12. Dawood A, Al-Talib A, Tulandi T. Predisposing factors and treatment outcome of different stages of intrauterine adhesions. J Obstet Gynaecol Can. 2010;32(8):767–70.
13. Sharma JB, Roy KK, Pushparaj M, Gupta N, Jain SK, Malhotra N, Mittal S. Genital tuberculosis: an important cause of Asherman's syndrome in India. Arch Gynecol Obstet. 2008;277(1):37–41.
14. Poujade O, Grossetti A, Mougel L, Ceccaldi PF, Ducarme G, Luton D. Risk of synechiae following uterine compression sutures in the management of major postpartum haemorrhage. BJOG. 2011;118(4):433–9.
15. Kodaman PH, Arici A. Intra-uterine adhesions and fertility outcome: how to optimize success? Curr Opin Obstet Gynecol. 2007;19(3):207–14.
16. Diamond MP, Freeman ML. Clinical implications of postsurgical adhesions. Hum Reprod Update. 2001; 7(6):567–76.
17. Bonilla-Musoles F, De Velasco LA, Osborn NG, MacHado LE, Flores DP, MacHado FR, Bonilla Jr F. Two-dimensional and three-dimensional ultrasound differential diagnosis of endometrial hyperplasia and endometrial adenocarcinoma. J Gynecol Surg. 2003; 19(3):105–20.
18. El-Mazny A, Abou-Salem N, El-Sherbiny W, Saber W. Outpatient hysteroscopy: a routine investigation before assisted reproductive techniques? Fertil Steril. 2011;95(1):272–6.
19. Fedele L, Bianchi S, Dorta M, Vignali M. Intrauterine adhesions: detection with transvaginal US. Radiology. 1996;199(3):757–9.
20. Narayan R, Goswamy RK. Transvaginal sonography of the uterine cavity with hysteroscopic correlation in the investigation of infertility. Ultrasound Obstet Gynecol. 1993;3(2):129–33.
21. Knopman J, Copperman AB. Value of 3D ultrasound in the management of suspected Asherman's syndrome. J Reprod Med. 2007;52(11):1016–22.
22. Jorizzo JH, Riccio GJ, Chen MYM, Carr JJ. Sonohysterography: the next step in the evaluation of the abnormal endometrium. Radiographics. 1999; 19:S117–30.
23. de Kroon CD, Jansen FW, Trimbos JB. Efficiency of saline contrast hysterosonography for evaluating the uterine cavity. [Article in Dutch]. Ned Tijdschr Geneeskd. 2003;147(32):1539–44.
24. Badu-Peprah A, Odoi AT, Dassah ET, Amo-Wiafe Y. Sonohysterography: time to step up its use in gynaecologic imaging in West Africa. Afr J Reprod Health. 2011;15(3):133–9.
25. Onah HE, Ezike HA, Mgbor SO. Saline sonohysterosalpingographic findings in infertile Nigerian women. J Obstet Gynaecol. 2006;26(8):788–90.
26. Kowalczyk D, Guzikowski W, Więcek J, Sioma-Markowska U. Clinical value of real time 3D sonohysterography and 2D sonohysterography in comparison to hysteroscopy with subsequent histopathological examination in perimenopausal women with abnormal uterine bleeding. Neuro Endocrinol Lett. 2012;33(2):212–6.
27. Soares SR, Barbosa dos Reis MM, Camargos AF. Diagnostic accuracy of sonohysterography, transvaginal sonography, and hysterosalpingography in patients with uterine cavity diseases. Fertil Steril. 2000;73(2): 406–11.
28. Makris N, Skartados N, Kalmantis K, Mantzaris G, Papadimitriou A, Antsaklis A. Evaluation of abnormal uterine bleeding by transvaginal 3-D hysterosonography and diagnostic hysteroscopy. Eur J Gynaecol Oncol. 2007;28(1):39–42.
29. Yucebilgin MS, Aktan E, Bozkurt K, Kazandi M, Akercan F, Mgoyi L, Terek MC. Comparison of hydrosonography and diagnostic hysteroscopy in the evaluation of infertile patients. Clin Exp Obstet Gynecol. 2004;31(1):56–8.
30. Alborzi S, Dehbashi S, Khodaee R. Sonohysterosalpingographic screening for infertile patients. Int J Gynaecol Obstet. 2003;82(1):57–62.
31. Bacelar AC, Wilcock D, Powell M, Worthington BS. The value of MRI in the assessment of traumatic intra-uterine adhesions (Asherman's syndrome). Clin Radiol. 1995;50(2):80–3.
32. Thomson AJ, Abbott JA, Deans R, Kingston A, Vancaillie TG. The management of intrauterine

synechiae. Curr Opin Obstet Gynecol. 2009;21(4): 335–41.
33. Schenker JG. Etiology of and therapeutic approach to synechia uteri. Eur J Obstet Gynecol Reprod Biol. 1996;65(1):109–13.
34. Magos A. Hysteroscopic treatment of Asherman's syndrome. Reprod Biomed Online. 2002;4 Suppl 3:46–51.
35. Salat-Baroux J, Pambou O, Guyot B. Hysteroscopic cure under ultrasonic control of complex and/or recurrent uterine synechiae. [Article in French]. Presse Med. 1995;24(17):811–4.
36. Heinonen PK. Intrauterine adhesions – Asherman's syndrome. [Article in Finnish]. Duodecim. 2010; 126(21):2486–91.
37. Gulumser C, Narvekar N, Pathak M, Palmer E, Parker S, Saridogan E. See-and-treat outpatient hysteroscopy: an analysis of 1109 examinations. Reprod Biomed Online. 2010;20(3):423–9.
38. Bettocchi S, Achilarre MT, Ceci O, Luigi S. Fertility-enhancing hysteroscopic surgery. Semin Reprod Med. 2011;29(2):75–82.
39. Shushan A, Protopapas A, Hart R, Magos AL. Diagnostic and therapeutic advantages of hysteroscopic surgery in management of intrauterine lesions in postmenopausal women. J Am Assoc Gynecol Laparosc. 2001;8(1):87–91.
40. Piketty M, Lesavre M, Prat-Ellenberg L, Benifla JL. Surgical management of intrauterine adhesions: is benefice bigger than risk? [Article in French]. Gynecol Obstet Fertil. 2010;38(9):547–9.
41. Pace S, Stentella P, Catania R, Palazzetti PL, Frega A. Endoscopic treatment of intrauterine adhesions. Clin Exp Obstet Gynecol. 2003;30(1):26–8.
42. Yu D, Li TC, Xia E, Huang X, Liu Y, Peng X. Factors affecting reproductive outcome of hysteroscopic adhesiolysis for Asherman's syndrome. Fertil Steril. 2008;89(3):715–22.
43. Fernandez H, Al-Najjar F, Chauveaud-Lambling A, Frydman R, Gervaise A. Fertility after treatment of Asherman's syndrome stage 3 and 4. J Minim Invasive Gynecol. 2006;13(5):398–402.
44. Capella-Allouc S, Morsad F, Rongières-Bertrand C, Taylor S, Fernandez H. Hysteroscopic treatment of severe Asherman's syndrome and subsequent fertility. Hum Reprod. 1999;14(5):1230–3.
45. Shokeir TA, Fawzy M, Tatongy M. The nature of intrauterine adhesions following reproductive hysteroscopic surgery as determined by early and late follow-up hysteroscopy: clinical implications. Arch Gynecol Obstet. 2008;277(5):423–7.
46. Yasmin H, Nasir A, Noorani KJ. Hysteroscopic management of Ashermans syndrome. J Pak Med Assoc. 2007;57(11):553–5.
47. Katz Z, Ben-Arie A, Lurie S, Manor M, Insler V. Reproductive outcome following hysteroscopic adhesiolysis in Asherman's syndrome. Int J Fertil Menopausal Stud. 1996;41(5):462–5.
48. Robinson JK, Colimon LM, Isaacson KB. Postoperative adhesiolysis therapy for intrauterine adhesions (Asherman's syndrome). Fertil Steril. 2008; 90(2):409–14.
49. Colacurci N, Fortunato N, Nasto R, Mele D, Errico G, De Franciscis P, Zarcone R. Reproductive outcome of hysteroscopic lysis of intrauterine adhesions. [Article in Italian]. Minerva Ginecol. 1997;49(7–8):325–7.
50. Yu D, Wong YM, Cheong Y, Xia E, Li TC. Asherman syndrome – one century later. Fertil Steril. 2008; 89(4):759–79.
51. Pabuccu R, Onalan G, Kaya C, Selam B, Ceyhan T, Ornek T, Kuzudisli E. Efficiency and pregnancy outcome of serial intrauterine device-guided hysteroscopic adhesiolysis of intrauterine synechiae. Fertil Steril. 2008;90(5):1973–7.
52. Bellingham FR. Intrauterine adhesions: hysteroscopic lysis and adjunctive methods. Aust N Z J Obstet Gynaecol. 1996;36(2):171–4.
53. Coccia ME, Becattini C, Bracco GL, Pampaloni F, Bargelli G, Scarselli G. Pressure lavage under ultrasound guidance: a new approach for outpatient treatment of intrauterine adhesions. Fertil Steril. 2001; 75(3):601–6.
54. Taniguchi F, Suginami H. Pregnancy and delivery following sonohysterographic lysis to treat recurrence after hysteroscopic lysis of severe intrauterine adhesions: a case report. Clin Exp Obstet Gynecol. 2008; 35(3):215–7.
55. Tiras MB, Oktem M, Noyan V. Laparoscopic intracorporeal ultrasound guidance during hysteroscopic adhesiolysis. Eur J Obstet Gynecol Reprod Biol. 2003;108(1):80–4.
56. Schlaff WD, Hurst BS. Preoperative sonographic measurement of endometrial pattern predicts outcome of surgical repair in patients with severe Asherman's syndrome. Fertil Steril. 1995;63(2):410–3.
57. Karande V, Levrant S, Hoxsey R, Rinehart J, Gleicher N. Lysis of intrauterine adhesions using gynecoradiologic techniques. Fertil Steril. 1997;68(4):658–62.
58. Chason RJ, Levens ED, Yauger BJ, Payson MD, Cho K, Larsen FW. Balloon fluoroscopy as treatment for intrauterine adhesions: a novel approach. Fertil Steril. 2008;90(5):2005.e15–7.e15.
59. Thomson AJ, Abbott JA, Kingston A, Lenart M, Vancaillie TG. Fluoroscopically guided synechiolysis for patients with Asherman's syndrome: menstrual and fertility outcomes. Fertil Steril. 2007;87(2): 405–10.
60. Rein DT, Schmidt T, Hess AP, Volkmer A, Schöndorf T, Breidenbach M. Hysteroscopic management of residual trophoblastic tissue is superior to ultrasound-guided curettage. J Minim Invasive Gynecol. 2011;18(6):774–8.
61. Orhue AA, Aziken ME, Igbefoh JO. A comparison of two adjunctive treatments for intrauterine adhesions following lysis. Int J Gynaecol Obstet. 2003;82(1): 49–56.
62. Guida M, Acunzo G, Di Spiezio Sardo A, Bifulco G, Piccoli R, Pellicano M, Cerrota G, Cirillo D, Nappi C. Effectiveness of auto-crosslinked hyaluronic acid gel in the prevention of intrauterine adhesions after hys-

teroscopic surgery: a prospective, randomized, controlled study. Hum Reprod. 2004;19(6):1461–4.
63. Amer MI, Abd-El-Maeboud KH. Amnion graft following hysteroscopic lysis of intrauterine adhesions. J Obstet Gynaecol Res. 2006;32(6):559–66.
64. Amer MI, Abd-El-Maeboud KH, Abdelfatah I, Salama FA, Abdallah AS. Human amnion as a temporary biologic barrier after hysteroscopic lysis of severe intrauterine adhesions: pilot study. J Minim Invasive Gynecol. 2010;17(5):605–11.
65. Nagori CB, Panchal SY, Patel H. Endometrial regeneration using autologous adult stem cells followed by conception by in vitro fertilization in a patient of severe Asherman's syndrome. J Hum Reprod Sci. 2011;4(1):43–8.
66. Gargett CE, Healy DL. Generating receptive endometrium in Asherman's syndrome. J Hum Reprod Sci. 2011;4(1):49–52.

Sonohysterography in Reproductive Medicine

13

Ilan Tur-Kaspa and Laurel A. Stadtmauer

Introduction

The existing practice guidelines, indications, and contraindications and the optimal technique for Sonohysterography (SHG) are reviewed. This will include a discussion on how to make the procedure pain free for women by using flexible catheters and gentle movements, inflating the balloon inside the cervix rather than inside the uterine cavity, and injecting the saline slowly. The main focus will be on diagnosis of intrauterine abnormalities through SHG rather than their treatment thereafter. We conclude that SHG is a safe, accurate, cost-effective, and easy-to-perform procedure, for patients as well as for physicians, to evaluate intrauterine pathology and can be used as the primary diagnostic tool for the evaluation of infertility and before ART.

I. Tur-Kaspa, MD (✉)
Institute for Human Reproduction (IHR),
Department of Obstetrics and Gynecology,
The University of Chicago, 409 W. Huron St.,
Chicago, IL 60654, USA
e-mail: drtk@infertilityihr.com

L.A. Stadtmauer, MD, PhD
Department of Obstetrics and Gynecology,
Eastern Virginia Medical School, Jones Institute for Reproductive Medicine, 601 Colley Avenue,
Norfolk, VA 23507, USA
e-mail: stadtmla@evms.edu

SHG vs. Hysteroscopy

Sonohysterography (SHG) was first described in 1986 by Randolph et al. [1]. Randolph et al. instilled saline into the uterus to provide contrast during transabdominal US and compared the SHG findings in 61 women to hysterosalpingography (HSG) and laparoscopy/hysteroscopy. They concluded that real-time US with fluid installation provides an accurate alternative to HSG in screening for uterine abnormalities and tubal patency. Syrop and Sahakian were the first to describe transvaginal SHG in 1992, followed by Parsons and Lense in 1993 [2, 3].

For a long time hysteroscopy with direct visualization of the intrauterine cavity was considered the gold standard for diagnosing uterine abnormalities [4–13]. The percentage of intracavitary abnormalities in women screened by SHG or hysteroscopy for infertility range from 11 to 45 %, with polyps range between 6 and 25 % [5, 14]. In the last 15 years, accumulating evidence-based data, including randomized control trials, systematic reviews, and meta-analyses, has demonstrated that SHG has comparable sensitivity, specificity, and accuracy in diagnosing intrauterine abnormalities as hysteroscopy [7–13, 15–21]. Therefore, SHG and other ultrasonography techniques may be used as effectively as hysteroscopy for diagnosing intracavitary abnormalities [8, 10, 11]. Pre-IVF SHG was shown to be effective at limiting cycle cancellations caused by endometrial polyps [22], and it was shown to be highly valuable as the first line of office-based

L.A. Stadtmauer, I. Tur-Kaspa (eds.), *Ultrasound Imaging in Reproductive Medicine*,
DOI 10.1007/978-1-4614-9182-8_13,

diagnostic tool for patients with recurrent IVF implantation failure [23]. These data may explain why most of the high-performing IVF programs in the US use SHG for the evaluation of uterine cavity before ART [24].

In addition, cost analysis comparing SHG vs. hysteroscopy screening prior to IVF showed that using SHG is more cost-effective. While hysteroscopic screening is cost-effective [25], Kim and Rone [26] have shown that SHG is more cost-effective than hysteroscopy. They calculated the average cost per patient ($n=229$) of SHG screening and hysteroscopy in the subset of patients who had significant and/or correctable abnormalities ($n=35$, 15.3 %). The cost per patient using SHG screening with additional hysteroscopy as needed was $645. If hysteroscopy would have been used to screen the same group of patients instead of SHG, the cost per patient would have been $1281.

Practice Guidelines for SHG

The American Institute of Ultrasound in Medicine (AIUM) has published in March 2008 [27] a practice guideline for ultrasonography in reproductive medicine. In the same year, the American College of Obstetrics and Gynecology (ACOG) published a technology assessment on SHG, in collaboration with AIUM; the Society for Reproductive Endocrinology and Infertility (SREI), an affiliate of the American Society for Reproductive Medicine (ASRM); and the American College of Radiology (updated in 2012) [28]. The reader is highly encouraged to review these guidelines. They describe the technique, the indications and contraindications, and the qualifications and responsibilities of the physician performing the SHG. The authors of this chapter have found it easy to adhere and to comply with the above guidelines in their practices and have incorporated them into this review.

Indication and Contraindication

The AIUM and ACOG guidelines [27, 28] describe the indications and contraindications for SHG. The most common indication for SHG is pre- and postmenopausal abnormal uterine bleeding [29, 30]. Screening of the uterine cavity prior to ART and for the evaluation of infertility and habitual abortions is the second most common indication. SHG may be performed for the evaluation of congenital or acquired (fibroids, polyps, and synechiae) uterine anomalies and preoperative and postoperative evaluations of the uterine cavities. SHG may also be performed for further diagnosis of any suboptimal imaging of the endometrium and when focal or diffuse endometrial thickening or abnormalities are seen on a regular TVUS.

The two main contraindications for SHG is pregnancy and pelvic infection or unexplained pelvic tenderness. Abnormal uterine bleeding (AUB) is not a contraindication, though it may make the interpretation of the findings more challenging [20]. Tur-Kaspa et al. [14] have prospectively analyzed SHG of 409 consecutive patients with AUB and have found 37.2 % of intracavitary abnormalities, mainly polyps and submucosal fibroids. Goldstein [30] has suggested "ultrasound first" as an approach to women with postmenopausal bleeding. SHG may be used for triage by identifying patients with no disease vs. those with focal or global abnormalities. Furthermore, patient acceptability and diagnostic capability of SHG is high, and it reduces demand for hysteroscopy [29]. SHG-guided endometrial biopsy provided an accurate pathological diagnosis in 89 % of patients compared to 52 % with blind endometrial sampling [29, 31].

SHG Procedure [14, 27, 28, 32]

Menstrual dating should be documented and pregnancy should be ruled out before performing SHG. The best timing for performing SHG is after the menstrual flow and prior to ovulation, in cycle days 5–10. This is when the endometrial lining is most symmetrical and precludes the chance for an early pregnancy. During the luteal phase, the lining is thickened and more echogenic and may be associated with a higher false-positive rate of polyps. Using birth control pills may assist in scheduling this test at any day of the menstrual cycle.

Patients should be informed of alternative procedures and the possible risks and complications of SHG (mainly discomfort, low risk of infection, and bleeding) and then sign a consent form. Pretreatment antibiotic is not recommended routinely unless the patient has a history of gynecological infections or tubal factor infertility [33]. Several RCTs, using different analgesics, have failed to demonstrate benefits of using any drug to significantly reduce pain during or after SHG [34–36]. Unless indicated, no analgesics or sedatives are routinely needed before, during, or after SHG, since it may be considered as a pain-free procedure [14, 37].

Prior to SHG, TVUS is performed with routine evaluation and measurement of the uterus, endometrium, and ovaries. The presence of fluid in the cul-de-sac should be noted, and any pelvic abnormal findings such as hydrosalpinges should be documented. If a patient had a baseline TVUS on day 3 of her period and returns for SHG a few days later, then a quick scan for the evaluation of the uterine cavity and of fluid in the cul-de-sac may be performed after the insertion of the catheter before the injection of the saline.

A speculum is placed in the vagina to visualize the cervix. After cleansing the external os with betadine or equivalent solution, the SHG catheter is inserted into the cervical canal. The SHG catheter should be prefilled with saline in order to avoid infusing air bubbles into the uterine cavity. There are many catheter options, including HSG/SHG curved catheters, intrauterine insemination catheters, and balloon SHG/HSG catheters. Any rigid catheter, which requires grasping the cervix with a tenaculum, may induce significant pain for the patient. If a balloon catheter is used, it is preferred to inflate the balloon intracervically rather than intrauterine, and the appropriate position of the catheter may be confirmed by pulling it slightly. An RCT recently showed a significantly less fluid used for SHG and significantly less pain felt by patients when the balloon was inflated inside the cervix rather than in the lower uterine segment [38]. Furthermore, by inflating the balloon intracervically, one may avoid balloon hyperinflation inside the uterine cavity, which may displace and obscure a pathological finding, such as endometrial polyp. Next, the speculum is removed and the TVUS probe is inserted into the vagina. Physiological saline solution is then slowly injected to distend the endometrial lumen under direct real-time visualization. Injecting the fluid slowly is mandatory to avoid abrupt uterine distension and pain. Documentation should include images of the endometrial cavity, including the lower segment and the upper cervical canal in at least two planes, longitudinal and transverse (Fig. 13.1). The reader is encouraged to read the official guidelines set by ACOG and AIUM [27, 28].

SHG for Congenital Uterine Anomalies

SHG is a cost-effective method available in an outpatient setting which is highly accurate in identifying uterine anomalies, especially septate and bicornuate uterus [44]. Mullerian anomalies are congenital defects in the development of the uterus and the upper vagina. The ability of 2D US to distinguish between different types of uterine anomalies is limited and operator dependent. The finding of a uterine anomaly may affect the management of the infertile and/or pregnant woman and the pregnancy outcome. In a recent meta-analysis [39], including 94 observational studies comprising 89,861 women, the prevalence of uterine anomalies diagnosed by optimal tests was 5.5 % (95 % CI, 3.5–8.5) in unselected population, 8.0 % (95% CI, 5.3–12) in infertile women, 13.3 % (95 % CI, 8.9–20.0) in women with a history of miscarriage, and 24.5 % (95 % CI, 18.3–32.8) in women with miscarriage and infertility.

Congenital uterine anomalies are associated with poor reproductive outcome [40]. All uterine anomalies are associated with an increase incidence of fetal malpresentations at delivery. Unification defects do not reduce fertility but some defect, in particular bicornuate uteri, are associated with aberrant outcomes throughout the course of pregnancy. Canalization defects appear to reduce the chance of clinical pregnancy and to increase risk of preterm delivery. These are more

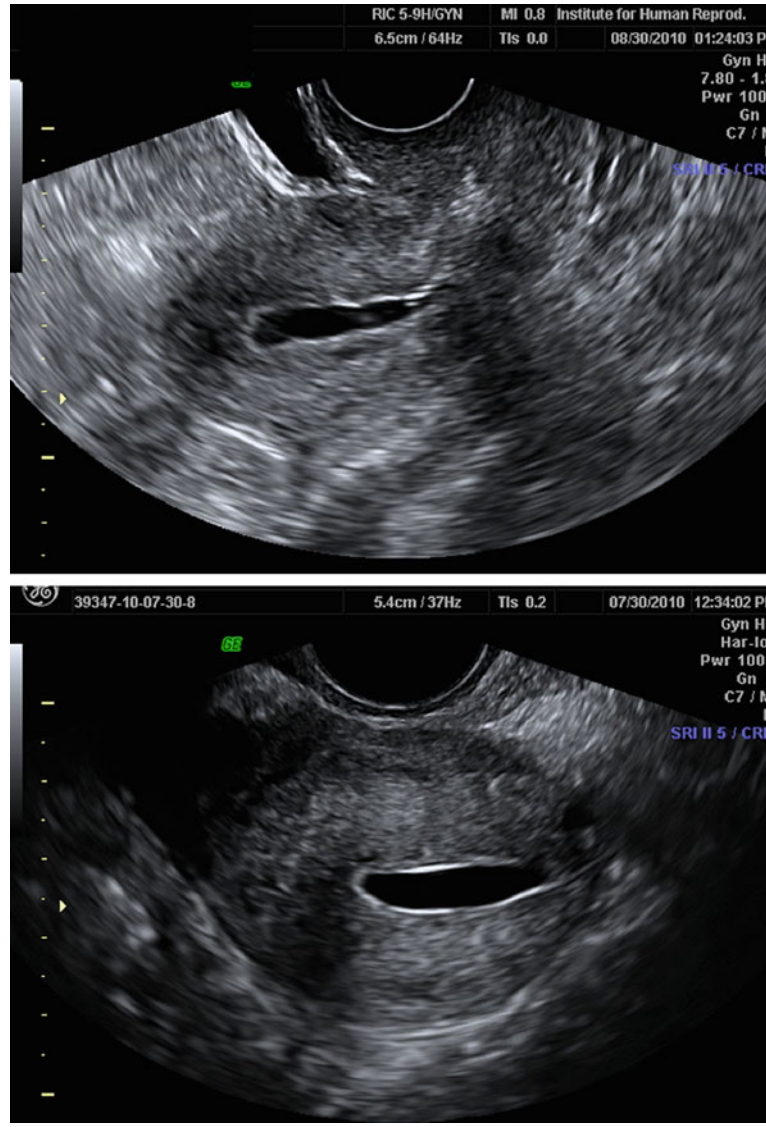

Fig. 13.1 2D longitudinal (*upper image*) and transverse (*lower image*) images of the uterus showing adequate distention of the endometrial canal with saline during SHG

profound in cases of septate uteri. Arcuate uteri, while previously considered to have no reproductive sequelae, are specifically associated with poor outcomes in late pregnancy, i.e., second-trimester miscarriage and malpresentation [40].

Uterine anomalies are defined by the criteria outlined by the American Society of Reproductive Medicine [41]. The visualization of the uterine fundus at the coronal plane is necessary for classifying uterine shape. SHG has been shown to have superior diagnostic ability with compared with HSG and 2D US for the evaluation of uterine malformation. Tur-Kaspa et al. [14] studied prospectively the prevalence of uterine anomalies diagnosed by SHG in 600 consecutive infertile patients compared to 409 patients with AUB. While the prevalence of septate uterus was 3 % in each group, arcuate uterus was significantly more common among the infertile patients (15 % vs. 6 %, respectively). All other anomalies had <1 % frequency in either group. Tur-Kaspa et al. [14], as well as others [7–11], concluded that SHG is an excellent method for the evaluation of congenital uterine anomalies. 3D SHG may be needed in some cases to assist in the final diagnosis.

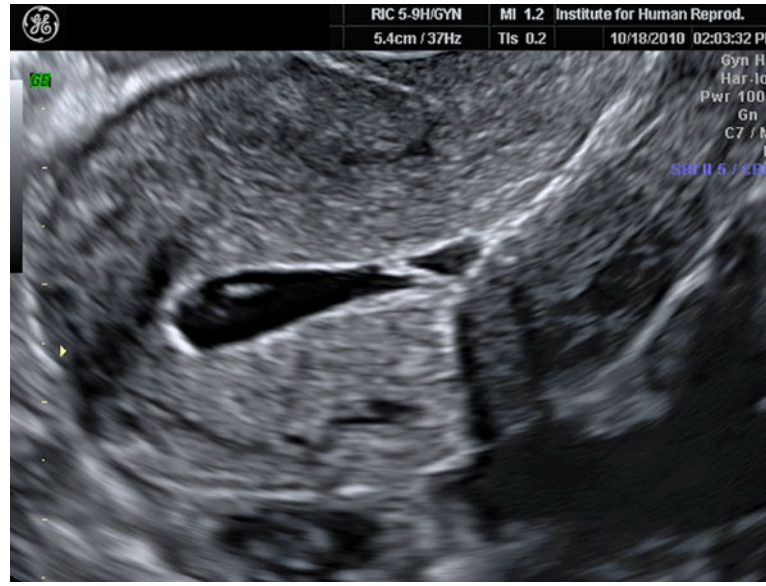

Fig. 13.2 2D longitudinal image of SHG demonstrating intrauterine adhesion at the lower uterine segment, connecting the anterior and the posterior walls of the uterus

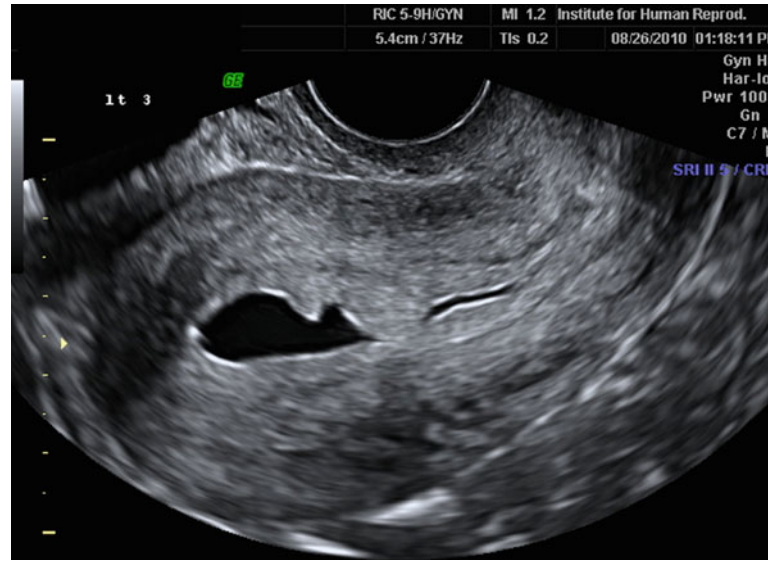

Fig. 13.3 2D longitudinal image of SHG demonstrating two polyps protruding into the uterine cavity

SHG for Acquired Uterine Abnormalities

SHG can serve as a first-line test for the evaluation of acquired intrauterine abnormalities such as adhesions (Fig. 13.2), polyps (Fig. 13.3), and fibroids. Tur-Kaspa et al. [14] have documented that intracavitary abnormalities are significantly more frequent among patients with AUB than with infertility. Polyps were the most common abnormal finding among patients with AUB or infertile women (30 and 13 %, respectively) [14].

Submucosal fibroids were found in 9 % of the AUB group and 3 % among infertile women [14]. Submucosal fibroids have been shown by meta-analysis to significantly lower pregnancy rates in ART and should be removed by operative hysteroscopy [4, 6]. Besides infertility, the submucosal fibroids may cause bleeding and miscarriages. The European Society of Hysteroscopy has developed

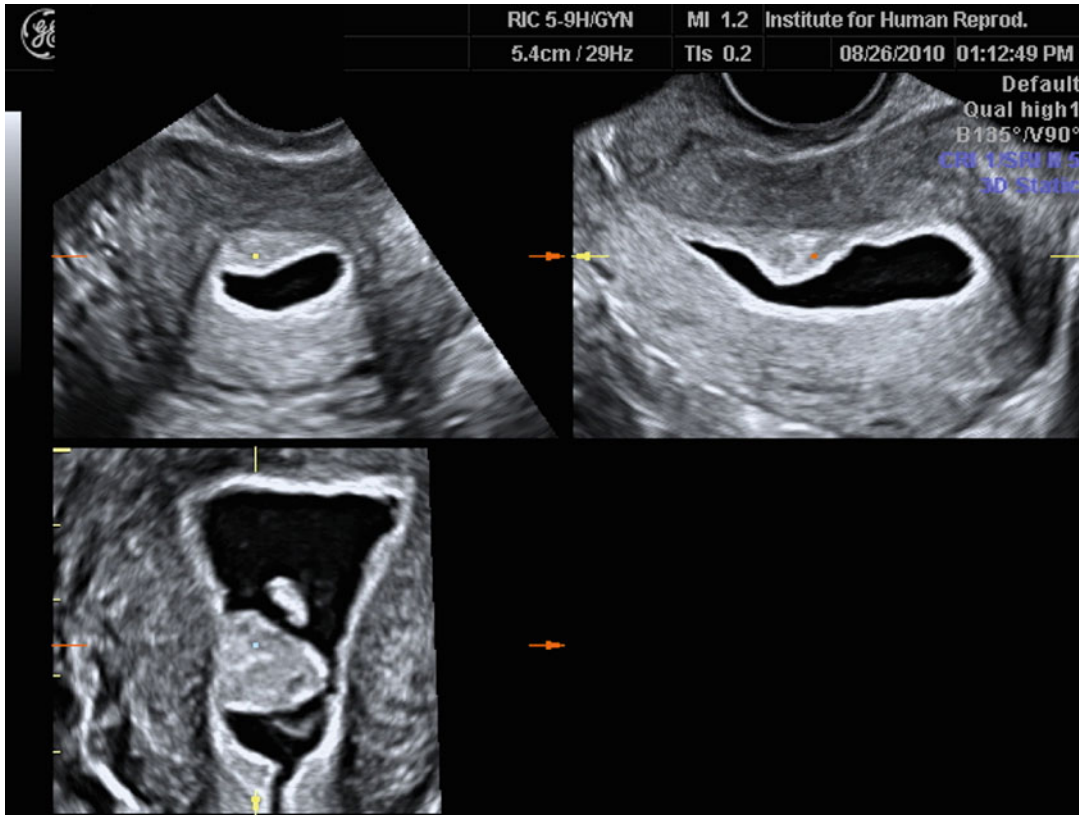

Fig. 13.4 3D SHG images of a uterine polyp. They are able to show the size and location of the stalk of the polyp more accurately in preparation for operative hysteroscopy and for consulting the patient

a classification system for fibroids which can also assist in the surgical approach. A Type 0 submucosal fibroid has no myometrial invasion, while a T1 has <50 % extension and T2 has more than 50 % extension into the myometrium. The TO and T1 are appropriate for the hysteroscopic approach, while the T2 may require more than one procedure or be removed laparoscopically.

2D vs. 3D SHG

When the option of having a 3D SHG scan is available, it may shorten the procedure and the volume of the saline used [42]. 3D SHG vs. 2D SHG is more accurate for diagnosing congenital uterine anomalies. For acquired uterine anomalies, in experienced hands, 3D will not improve the accuracy, but may assist it for better imaging (Figs. 13.4 and 13.5) [43, 44]. For the evaluation of postmenopausal bleeding, 2D and 3D SHG have similar diagnostic accuracy as hysteroscopy with higher patient acceptability of SHG [45, 46].

A 3D US, in comparison to a 2D US, allows for the visualization of the entire uterine cavity in the coronal view; it can detect the exact placement of uterine fibroids, polyps, and synechiae in the cavity, as well as the mean diameter of different tissues. A 3D US examination comprises approximately four steps: (1) data acquisition, (2) volume calculation, (3) image animation, and (4) data storage and transfer. The scans can be obtained either by freehand, by manual movement through the region of interest (ROI), or, automatically, by sweeping through the ROI. 3D US needs post-processing of the received data. Data can be stored and visualized in various displays such as multiplanar with navigation through the planes or surface rendering mode.

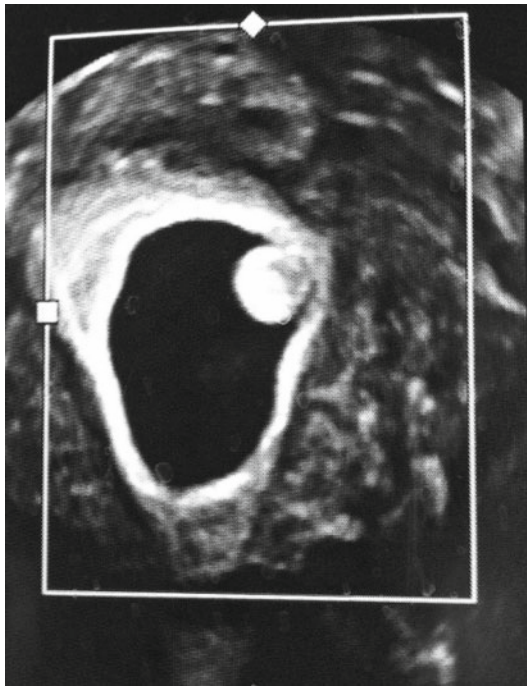

Fig. 13.5 3D SHG image of a corneal uterine polyp providing excellent information for the practitioner and patient on the size and location of the polyp

For more details on 3D US technique, the reader may refer to Chap. 2.

A saline infusion enhances the contrast in a 3D US and can facilitate the accurate diagnosis of congenital uterine anomalies, especially the arcuate uterus (Fig. 13.6) compared with the septate uterus (Fig. 13.7) and the bicornuate uterus. The serosal edge and the fundal indentation can be clearly seen. Through TUI tomographic imaging, a series of images can visualize the leiomyomata protruding into the uterine cavity vs. deviating the endometrial cavity.

3D adds value to 2D SHG by improving with visualization of the uterine fundus [47]. Others suggest that when the SHG is performed by an experienced examiner, 3D does not add additional value to the 2D SHG [48]. It is the opinion of the authors that adding a 3D US to a 2D SHG will allow the exam to be completed faster with the same or better accuracy. Still in most cases, 2D SHG is adequate for diagnosing abnormal intracavitary finding.

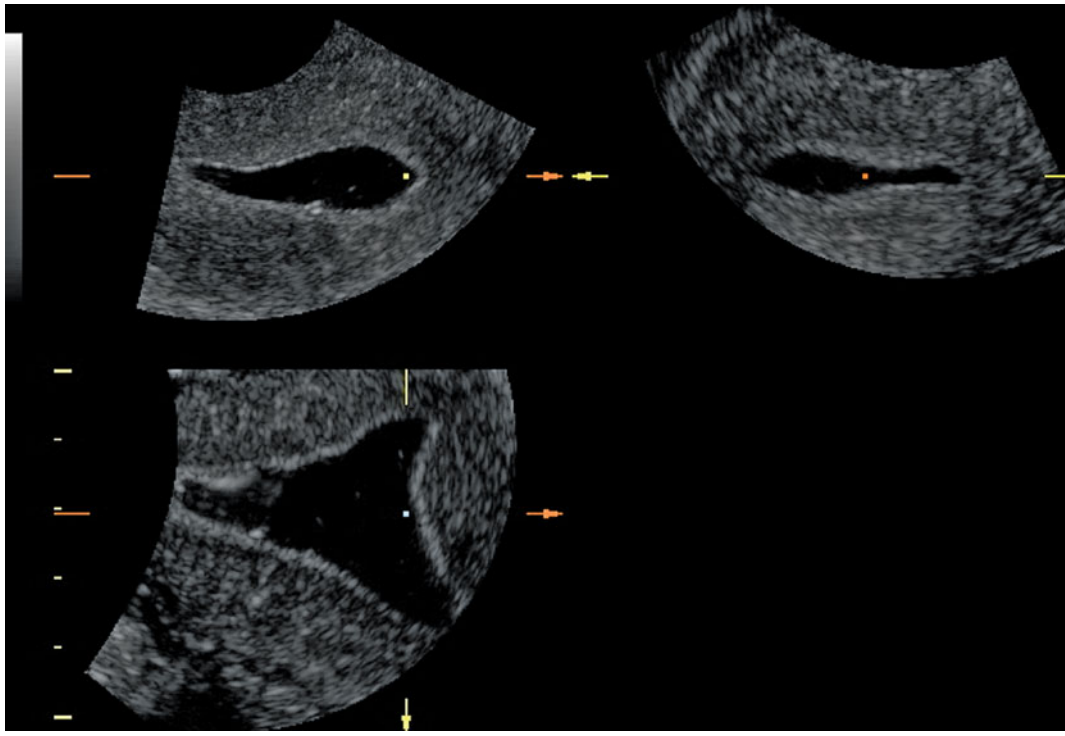

Fig. 13.6 3D SHG demonstrating an arcuate uterus. The visualization of the fundal area at the coronal plane and the ability to measure the depth of the anomaly can easily define arcuate uterus and rule out a septum

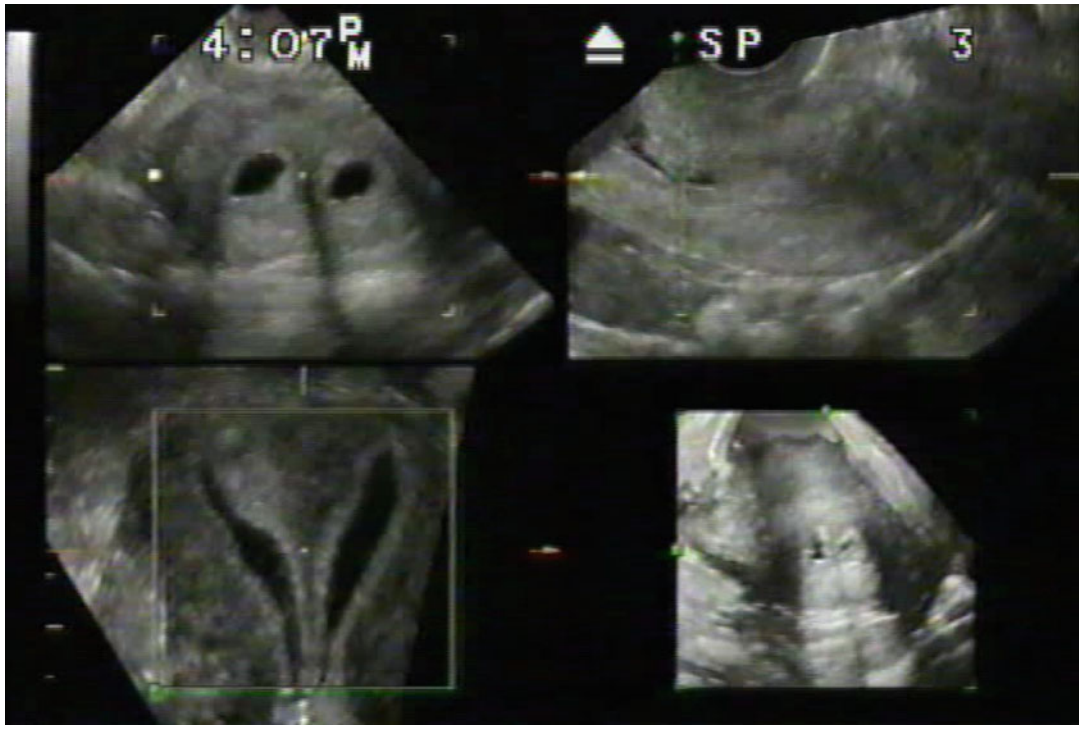

Fig. 13.7 3D SHG demonstrating a completely septated uterus. The 3D reconstruction at the coronal plane leaves no space for imagination, providing definite diagnosis and assisting in planning the surgical treatment needed as well as consulting with the patient

Gel Instillation SHG

Gel SHG uses hydroxyethylcellulose gel instead of saline as its medium. This is done in order to try to simplify the technique of artificial uterine cavity distension for SHG [49]. The gel provides a more stable filling of the uterine cavity, allowing a high-quality ultrasonographic visualization of intrauterine pathology by 2D and 3D US [50–55]. Still, most centers will use saline for SHG.

No Pain with SHG

Tur-Kaspa [37] has recently summarized data supporting that SHG, as well as HSG and HysteroContrastSonography (HyCoSy), should be considered pain-free procedures. Hysterosalpingography (HSG) has a long-standing reputation of being a painful procedure. The use of modern thin catheters and nonionic media that significantly reduced pain during and after HSG [56–60] was unable to affect significantly HSG's "reputation." SHG and HyCoSy, the modern ultrasound-based procedures that are currently used instead of HSG for the evaluation of the uterine cavity and/or the fallopian tubes, "inherited" this high level of fear of pain. It is possible that this stigma discourages patients and makes them believe that the procedure should be painful when it does not have to be. Several recent randomized controlled trials (RCT) have failed to demonstrate a significant benefit of various pharmacological strategies available to reduce pain during these procedures, suggesting that the pain is more psychological than physical [34–36]. It is the author's opinion, based on evidence data and the experience of performing thousands of these tests, that they can be pain free for women.

One of the primary ways to make SHG a pain-free procedure is using gentle movements with a thin flexible catheter. Using a rigid catheter,

which requires grasping the cervix with a tenaculum, will promote pain. If a balloon catheter is used, it is preferred to inflate the balloon intracervically rather than intrauterine, and the appropriate position of the catheter may be confirmed by pulling it slightly. An RCT recently showed a significantly less fluid used for SHG and significantly less pain felt by patients when the balloon was inflated inside the cervix rather than in the lower uterine segment [38]. Warming the saline solutions to body temperature before instillation is another way of reducing patients' discomfort. It is crucial to introduce the saline solution *slowly* into the cavity to prevent abrupt overdistention of the uterus, which would induce immediate pain. While women naturally may feel embarrassed, stressed, and discomfort, as with any medical and gynecological examinations, there should be no more fear of pain from procedures such as SHG, HyCoSy, and HSG [37].

Conclusions

SHG is a simple, cost-effective, safe, and easy-to-perform procedure for the evaluation of congenital and acquired uterine abnormalities. Published guidelines by AIUM and ACOG are easy to implement in routine gynecological and reproductive medicine practice. While using thin flexible catheters, placing them inside the cervix, and injecting the saline slowly, this procedure can be pain free. SHG can serve as a first-line test for screening and evaluation of the uterine cavity for the diagnosis of infertility and before ART.

References

1. Randolph JR, Ying YK, Maier DB, Schmidt CL, Riddick DH. Comparison of real-time ultrasonography, hysterosalpingography, and laparoscopy/hysteroscopy in the evaluation of uterine abnormalities and tubal patency. Fertil Steril. 1986;46:828–32.
2. Syrop C, Sahakian V. Transvaginal sonographic detection of endometrial polyps with fluid contrast augmentation. Obstet Gynecol. 1992;79:1041–3.
3. Parsons A, Lense J. Sonohysterography for endometrial abnormalities: preliminary results. J Clin Ultrasound. 1993;21:87–9.
4. Bozdag G, Aksan G, Esinler I, Yarali H. What is the role of office hysteroscopy in women with failed IVF cycles? Reprod Biomed Online. 2008;17:410–5.
5. Fatemi HM, Kasius JC, Timmermans A, van Disseldorp J, Fauser BC, Devroey P, Broekmans FJ. Prevalence of unsuspected uterine cavity abnormalities diagnosed by office hysteroscopy prior to in vitro fertilization. Hum Reprod. 2010;25(8):1959–65.
6. Bosteels J, Kasius J, Weyers S, Broekmans FJ, Mol BW, D'Hooghe TM. Hysteroscopy for treating subfertility associated with suspected major uterine cavity abnormalities. Cochrane Database Syst Rev. 2013;(1):CD009461. doi:10.1002/14651858.CD009461.pub2.
7. van Dongen H, de Kroon CD, Jacobi CE, Trimbos JB, Jansen FW. Diagnostic hysteroscopy in abnormal uterine bleeding: a systematic review and meta-analysis. BJOG. 2007;114(6):664–75.
8. Saunders RD, Shwayder JM, Nakajima ST. Current methods of tubal patency assessment. Fertil Steril. 2011;95:2171–9.
9. Taylor E, Gomel V. The uterus and fertility. Fertil Steril. 2008;89:1–16.
10. Van Voorhis BJ. Ultrasound assessment of the uterus and fallopian tube in infertile women. Semin Reprod Med. 2008;26:232–40.
11. Devroey P, Fauser BCJM, Diedrich K, and on behalf of the Evian Annual Reproduction (EVAR) Workshop Group 2008. Approaches to improve the diagnosis and management of infertility. Hum Reprod Update. 2009;15:391–408.
12. Grimbizis GF, Tsolakidis D, Mikos T, Anagnostou E, Asimakopoulos E, Stamatopoulos P, et al. A prospective comparison of transvaginal ultrasound, saline infusion sonohysterography, and diagnostic hysteroscopy in the evaluation of endometrial pathology. Fertil Steril. 2010;94:2720–5.
13. Brown SE, Coddington CC, Schnorr J, Toner JP, Gibbons W, Oehninger S. Evaluation of outpatient hysteroscopy, saline infusion hysterosonography, and hysterosalpingography in infertile women: a prospective, randomized study. Fertil Steril. 2000;74(5):1029–34.
14. Tur-Kaspa I, Gal M, Hartman M, Hartman J, Hartman A. A prospective evaluation of uterine abnormalities by saline infusion sonohysterography (SIS) in 1009 women with infertility or abnormal uterine bleeding. Fertil Steril. 2006;86:1731–5.
15. Ayida G, Chamberlain P, Barlow D, et al. Uterine cavity assessment prior to in vitro fertilization: comparison of transvaginal scanning, saline contrast hysterosonography and hysteroscopy. Ultrasound Obstet Gynecol. 1997;10(1):59–62.
16. Loverro G, Nappi L, Vicino M, et al. Uterine cavity assessment in infertile women: comparison of transvaginal sonography and hysteroscopy. Eur J Obstet Gynecol Reprod Biol. 2001;100(1):67–71.
17. de Kroon CD, de Bock GH, Dieben SW, Jansen FW. Saline contrast hysterosonography in abnormal uterine bleeding: a systematic review and meta-analysis. BJOG. 2003;110:938–47.

18. Ragni G, Diaferia D, Vegetti W, Colombo M, Arnoldi M, Crosignani PG. Effectiveness of sonohysterography in infertile patient work-up: a comparison with transvaginal ultrasonography and hysteroscopy. Gynecol Obstet Invest. 2005;59:184–8.
19. Bingol B, Gunenc Z, Gedikbasi A, Guner H, Tasdemir S, Tiras B. Comparison of diagnostic accuracy of saline infusion sonohysterography, transvaginal sonography and hysteroscopy. J Obstet Gynaecol. 2011;31(1):54–8.
20. van Hanegem N, Breijer MC, Khan KS, Clark TJ, Burger MP, Mol BW, et al. Diagnostic evaluation of the endometrium in postmenopausal bleeding: an evidence-based approach. Maturitas. 2011;68(2):155–64.
21. Yang T, Pandya A, Marcal L, Bude RO, Platt JF, Bedi DG, Elsayes KM. Sonohysterography: principles, technique and role in diagnosis of endometrial pathology. World J Radiol. 2013;5(3):81–7.
22. Yauger BJ, Feinberg EC, Levens ED, Gustofson RL, Larsen FW, DeCherney AH. Pre-cycle saline infusion sonography minimizes assisted reproductive technologies cycle cancellation due to endometrial polyps. Fertil Steril. 2008;90:1324–6.
23. Shokeir T, Abdelshaheed M. Sonohysterography as a first-line evaluation for uterine abnormalities in women with recurrent failed in vitro fertilization-embryo transfer. Fertil Steril. 2009;91:1321–2.
24. Van Voorhis BJ, et al. What do consistently high-performing in vitro fertilization programs in the U.S. do? Fertil Steril. 2010;94(4):1346–9.
25. Kasius JC, Eijkemans RJ, Mol BW, Fauser BC, Fatemi HM, Broekmans FJ. Cost-effectiveness of hysteroscopy screening for infertile women. Reprod Biomed Online. 2013;26(6):619–26.
26. Kim AH, Rone HM. Cost of sonohysterographic (SHG) versus hysteroscopic (HS) screening prior to in vitro fertilization (IVF). Fertil Steril. 2006;86 (3 Suppl):S52–3.O-124.
27. AIUM practice guideline for ultrasonography in reproductive medicine. J Ultrasound Med. 2009;28(1): 128–37.
28. ACOG technology assessment no. 8: sonohysterography. Obstet Gynecol. 2012;119(6):1325 (update of ACOG Technology Assessment in Obstetrics and Gynecology no. 5: sonohysterography. Obstet Gynecol. 2008;112(6):1467–9).
29. Choudry A, Shukr I, Khan S, Hafeez H, Jamal S, Anwer A. Acceptability and accuracy of saline infusion sonohysterography in women with postmenopausal bleeding. J Coll Physicians Surg Pak. 2010;20(9):571–5.
30. Goldstein SR. Modern evaluation of the endometrium. Obstet Gynecol. 2010;116(1):168–76.
31. Moschos E, Ashfaq R, McIntire DD, Liriano B, Twickler DM. Saline-infusion sonography endometrial sampling compared with endometrial biopsy in diagnosing endometrial pathology. Obstet Gynecol. 2009;113(4):881–7.
32. Allison SJ, Horrow MM, Kim HY, Lev-Toaff AS. Saline-infused sonohysterography: tips for achieving greater success. Radiographics. 2011;31(7):1991–2004.
33. ACOG Practice Bulletin. Antibiotic prophylaxis for gynecologic procedures. No. 104, May 2009. Obstet Gynecol. 2009;113:1180–9.
34. Ahmad G, Duffy J, Watson AJ. Pain relief in hysterosalpingography. Cochrane Database Syst Rev. 2007;(2):CD006106.
35. Ahmad G, Attarbashi S, O'Flynn H, Watson AJ. Pain relief in office gynaecology: a systematic review and meta-analysis. Eur J Obstet Gynecol Reprod Biol. 2011;155:3–13.
36. Moro F, Selvaggi L, Sagnella F, Morciano A, Martinez D, Gangale MF, Ciardulli A, Palla C, Uras ML, De Feo E, Boccia S, Tropea A, Lanzone A, Apa R. Could antispasmodic drug reduce pain during Sonosalpingohysterography (SSHG) in infertile patients? A randomized double-blinded clinical trial. Ultrasound Obstet Gynecol. 2012;39(3):260–5.
37. Tur-Kaspa I. Fear no pain: uterine cavity and tubal patency assessment tests should be pain free. Ultrasound Obstet Gynecol. 2012;39(3):247–51.
38. Spieldoch RL, Winter TC, Schouweiler C, Ansay S, Evans MD, Lindheim SR. Optimal catheter placement during sonohysterography: a randomized controlled trial comparing cervical to uterine placement. Obstet Gynecol. 2008;111(1):15–21.
39. Chan YY, Jayaprakasan K, Zamora J, Thornton JG, Raine-Fenning N, Coomarasamy A. The prevalence of congenital uterine anomalies in unselected and high-risk populations: a systematic review. Hum Reprod Update. 2011;17(6):761–71.
40. Chan YY, Jayaprakasan K, Tan A, Thornton JG, Coomarasamy A, Raine-Fenning NJ. Reproductive outcomes in women with congenital uterine anomalies: a systematic review. Ultrasound Obstet Gynecol. 2011;38(4):371–82.
41. The American Fertility Society classification of adnexal adhesions, distal tubal occlusion, tubal occlusion secondary to tubal ligation, tubal pregnancies, Mullerian anomalies and intrauterine adhesions. Fertil Steril. 1988;49:944–55.
42. Tur-Kaspa I, Segal S, Zohav E. The ART of imaging: three-dimensional (3D) ultrasound and ART. In: Revelli A, Tur-Kaspa I, Holte JG, Massobrio M, editors. Biotechnology of human reproduction. New York: The Parthenon Publishing Group; 2003. p. 363–73.
43. Mora-Guanche P, Sparacino L, García-Guzman R, Bennett RA, Hernández J, Palumbo A. Three-dimensional sonohysterography (SHG) has improved diagnostic accuracy for intrauterine pathology compared to two-dimensional SHG: a prospective pilot study in infertility patients. Fertil Steril. 2009;92(Suppl):S119.
44. Ludwin A, Pityński K, Ludwin I, Banas T, Knafel A. Two- and three-dimensional ultrasonography and sonohysterography versus hysteroscopy with laparoscopy in the differential diagnosis of septate, bicornuate, and arcuate uteri. J Minim Invasive Gynecol. 2013;20(1):90–9.
45. Katsetos C, Radhakrishnan S, Koumousidis A, Kontoyannis M, Sanoulis V, Spaliaras D, et al.

Comparison of transvaginal 3D sonohysterography with outpatient hysteroscopy in the evaluation of abnormal uterine bleeding. Clin Exp Obstet Gynecol. 2013;40(1):74–7.
46. Adel M, Kandil M, Abo-Elnasr M, Sanad Z, Farag H. Three-dimensional sonohysterography may replace hysteroscopy for women with perimenopausal bleeding. Climacteric. 2013. doi:10.3109/13697137.2013.801014.
47. Hartman MR, Hartman JD, Oprea C, Hartman BD, Hartman A. 3D ultrasound vs 3D sonohysterography in the diagnosis of uterine anomalies: a prospective blinded study of 600 consecutive infertility patients. Fertil Steril. 2008;90(Suppl):S20.
48. Opolskiene G, Sladkevicius P, Valentin L. Two- and three-dimensional saline contrast sonohysterography: interobserver agreement, agreement with hysteroscopy and diagnosis of endometrial malignancy. Ultrasound Obstet Gynecol. 2009;33(5):574–82.
49. Exalto N, Stappers C, van Raamsdonk LA, Emanuel MH. Gel instillation sonohysterography: first experience with a new technique. Fertil Steril. 2007;87(1):152–5.
50. Marasinghe JP, Senanayake HM. Gel instillation sonohysterography: first experience with a new technique. Fertil Steril. 2007;88(2):536–7.
51. Van den Bosch T, Betsas G, Van Schoubroeck D, Daemen A, Vandenbroucke V, Cornelis A, De Moor B, Deprest J, Timmerman D. Gel infusion sonography in the evaluation of the uterine cavity. Ultrasound Obstet Gynecol. 2009;34(6):711–4.
52. Bij de Vaate AJ, Brölmann HA, van der Slikke JW, Emanuel MH, Huirne JA. Gel instillation sonohysterography (GIS) and saline contrast sonohysterography (SCSH): comparison of two diagnostic techniques. Ultrasound Obstet Gynecol. 2010;35(4):486–9.
53. Bij de Vaate AJ, Brölmann HA, van der Voet LF, van der Slikke JW, Veersema S, Huirne JA. Ultrasound evaluation of the Cesarean scar: relation between a niche and postmenstrual spotting. Ultrasound Obstet Gynecol. 2011;37(1):93–9.
54. Van Den Bosch T, Van Schoubroeck D, Luts J, Bignardi T, Condous G, Epstein E, Leone FP, Testa AC, Valentin L, Van Huffel S, Bourne T, Timmerman D. Effect of gel-instillation sonography on Doppler ultrasound findings in endometrial polyps. Ultrasound Obstet Gynecol. 2011;38(3):355–9.
55. Van den Bosch T, Van Schoubroeck D, Daemen A, Domali E, Vandenbroucke V, De Moor B, Deprest J, Timmerman D. Lidocaine does not reduce pain perception during gel instillation sonography or subsequent office hysteroscopy: results of a randomized trial. Gynecol Obstet Invest. 2011;71(4):236–9.
56. Golan A, Tur-Kaspa I. The management of the infertile patient with proximal tubal occlusion. Hum Reprod. 1996;11:1833–4.
57. Tur-Kaspa I, Seidman DS, Soriano D, Greenberg I, Dor J, Bider D. Hysterosalpingography with a balloon catheter versus a metal cannula: a prospective, randomized, blinded comparative study. Hum Reprod. 1998;13(1):75–7.
58. Tur-Kaspa I, Moscovici O, Meltzer S, Peled R, Rabinson J, Segal S. Transcervical tubal catheterization (TTC) is the treatment of choice for infertile women with proximal tubal obstruction – an experience with 1010 fallopian tubes. Fertil Steril. 2002;78 Suppl 1:S90.
59. Ricci G, Guastalla P, Ammar L, Cervi G, Guarnieri S, Sartore A. Balloon catheter vs. cervical vacuum cup for hysterosalpingography: a prospective, randomized, single-blinded study. Fertil Steril. 2007;87(6):1458–67.
60. Anserini P, Delfino F, Ferraiolo A, Remorgida V, Menoni S, De Caro G. Strategies to minimize discomfort during diagnostic hysterosalpingography with disposable balloon catheters: a randomized placebo-controlled study with oral nonsteroidal premedication. Fertil Steril. 2008;90(3):844–8.

Evaluation of Tubal Patency (HyCoSy, Doppler)

14

Dimuthu Vinayagam and Kamal Ojha

Subfertility affects 1 in 10 couples worldwide. Tubal pathology is thought to be a contributor in up to 40 % [1–3] of cases of subfertility, making tubal pathology the leading female cause. Assessment of the fallopian tubes forms an important and integral part of the fertility workup. Tubal patency will determine subsequent treatment as well as assisted conception options. If tubal assessment does reveal tubal blockage, then the couple may be referred for in vitro fertilisation or tubal surgery. If the tubes are patent, then alternative causes and consequent treatment options will be investigated. The question of "are the tubes patent" is one of the most important clinical questions that must be answered when performing a subfertility workup.

Any ideal modality of tubal assessment will be sensitive, specific, safe, widely available, inexpensive and diagnostically accurate. Laparoscopy and dye testing is the accepted gold standard for assessment of tubal pathology. However, this is an invasive and expensive procedure. Hysterosalpingography (HSG) was classically the first-line investigation used in the assessment of tubal pathology [4]. HSG involves a radiological examination of the uterus and fallopian tubes using X-rays and contrast media. Advances in ultrasonography have resulted in the development of techniques using ultrasound to diagnose tubal pathology. Hysterosalpingo-contrast-sonography (HyCoSy) is the name given to a technique that combines the use of ultrasound and contrast media to delineate tubal pathology. HyCoSy can be combined with 3D imaging as well as advanced computer software to enhance diagnostic imaging. Contrast media employed include air, saline, albumin with micro air bubbles and galactose with micro air bubbles. The supplementary use of colour flow Doppler has also been employed as a reliable and accurate alternative modality.

In this chapter, we aim to provide an outline of the currently employed methods used in the evaluation of tubal patency.

Laparoscopy and Dye Test (Chromopertubation)

Laparoscopy (+/– hysteroscopy) and dye testing is the gold standard method for evaluation of tubal patency. This is especially true of high-risk women who have a history of endometriosis, previous pelvic infection or abdominal surgery. Laparoscopy allows direct visualisation and concurrent treatment for various pelvic and tubal pathologies such as endometriomas, pelvic endometriosis and peritubal adhesions. Methylene blue dye is introduced via the cervix, and if tubal patency is present, bilateral spill of dye can be directly visualised from each fimbrial end. This is

D. Vinayagam, MB BS, BSc
K. Ojha, MRCOG (✉)
Obstetrics and Gynecology, St. George's Hospital, Blackshaw Road, Tooting, London, SW17 OQT, UK
e-mail: dvinayagam@doctors.org.uk; kamal.ohja@stgeorges.nhs.ui

L.A. Stadtmauer, I. Tur-Kaspa (eds.), *Ultrasound Imaging in Reproductive Medicine*,
DOI 10.1007/978-1-4614-9182-8_14, © Springer Science+Business Media New York 2014

captured either on still photographs or on video. Although laparoscopy is now a routine operation, it is still associated with risks. These include bleeding, infection, vascular damage as well as visceral injuries to other organs (bowel and bladder). Should complications at laparoscopy occur, then a laparotomy may be required. The use of a general anaesthetic poses risks, and the possibility of subsequent venous thromboembolism must not be overlooked. Facilities to perform laparoscopy may not be readily available in all fertility clinic settings.

Laparoscopy is an expensive and invasive procedure when used in this context, and appropriately trained clinical and auxiliary staff are required to perform this.

Although this procedure is the gold standard method for evaluating tubal patency, it shouldn't be the first-line screening method employed on a large scale. Patients should be appropriately selected for this procedure. One possible way of risk assessing women would be to perform the inexpensive chlamydia antibody titre (CAT) blood test, and if positive, these women should be offered laparoscopy as the possibility of encountering pelvic pathology is higher in this group of patients [2]. This is already occurring in some parts of Europe where CAT testing is used as a first-line test in subfertility workup, and those above a fixed cut-off level have post-infectious pelvic disease excluded by means of laparoscopy and chromopertubation, rather than having HSG [5, 6]. In patients who are CAT positive, HSG should be omitted in order to avoid the potential of infectious complications [7]. Patients with a high-risk history (e.g. known endometriosis and previous pelvic surgery) should have their pelvis assessed by means of a laparoscopy and dye test [8].

Hysterosalpingography (HSG)

HSG is an outpatient X-ray examination of the uterine cavity and fallopian tubes using contrast media. This procedure is performed in the follicular phase of the menstrual cycle so as to not disrupt an early pregnancy. A cannula (often metal) is inserted transcervically, and a radio-opaque dye (e.g. Urografin) is passed through the cannula. X-ray images are then obtained and patency is confirmed by visualising the bilateral peritoneal spillage of the dye. Following the procedure, patients should be advised about pelvic pain, which will be similar to dysmenorrhoea. Prophylactic antibiotics are also usually prescribed.

In comparison to laparoscopy, HSG is more cost-effective, can be performed in a low-resource setting and does not require as much operator expertise. In addition, HSG can delineate uterine cavity abnormalities as well as tubal blockage. The passage of dye through the tubes can sometimes inadvertently cure the blockage and therefore HSG can, on occasions, be therapeutic. A meta-analyses of over 4,000 subjects concluded that HSG has a sensitivity of 53 % and a specificity of 87 % for any tubal pathology and 46 and 95 % for bilateral tubal pathology [6, 9]. Both oil-soluble and water-soluble contrast media have been employed in HSG. Oil-soluble media are associated with risk of oil emboli as well as inducing inflammatory reactions within the diseased fallopian tubes. The more commonly used water-soluble agents have been shown to result in increased bleeding post HSG; however, they do produce superior radiographic images. A randomised controlled trial did not show any statistically significant difference in the live birth rates following oil- or water-soluble contrast media [10].

Disadvantages of HSG include the radiation exposure to the pelvis. The mean dose-area product (DAP) for HSG is 2.05 Gy cm^2 versus 0.09 Gy cm^2 for a chest X-ray [11]. The use of iodine-based contrast media can result in hypersensitivity reactions and should be avoided in patients known to be sensitive to iodine-containing compounds. HSG requires the services of the radiology department for interpretation of the images produced. The procedure is associated with patient discomfort during and after the procedure. The use of thinner, non-metal cervical catheters may reduce the discomfort experienced by the patient. A study comparing HSG using a rigid, metal cannula with a balloon catheter

demonstrated less patient-reported pain, less fluoroscopic time, smaller amounts of contrast medium and easier operation using the balloon catheters [12].

Some operators advise patients to take simple analgesia prior to attending for the procedure, although there is a paucity of evidence that this actually provides any significant relief.

Hysterosalpingo-Contrast-Sonography (HyCoSy)

Hysterosalpingo-contrast-sonography is an outpatient transvaginal ultrasound procedure that visualises the uterine cavity and observes spill from the fimbrial ends of the fallopian tubes.

The technique of HyCoSy was founded upon two independent observations. The initial observation, published over 30 years ago, was that saline could be injected into the uterine cavity to delineate endometrial structures using a transvaginal ultrasound probe [13]. The same investigators noted that saline would then be present in the pouch of Douglas, indicating spill of saline had occurred through patent fallopian tubes.

Normal fallopian tubes are rarely visualised on ultrasound; however, diseased tubes (e.g. hydrosalpinx) are more readily apparent due to the presence of fluid. The notion that a fluid-filled intrauterine cavity/fallopian tubes could enhance visual diagnosis leads to the idea that injecting fluid into the uterus could be used to detect both intrauterine anomalies and tubal patency at ultrasound. Although saline was the first fluid agent to be used, its use was reported with varying degrees of success. There were limitations in observing the flow through the entire tube as well as unpredictable and not easily reproducible results. Air has also been described as a contrast agent that can be used at HyCoSy. Although it has obvious cost benefits, visualisation of the tubal course may be more challenging. This, in part, may be due to the similar echogenicities of air and the surrounding structures (e.g. bowel gas) (Fig. 14.1).

In the mid-1980s, an ultrasound contrast agent named Echovist® was being trialled for use in echocardiography. Due to its echogenic properties, Echovist® revolutionised the visualisation of the fallopian tubes using HyCoSy. Echovist® consists of galactose particles suspended in an aqueous galactase solution. Echovist is no longer available, and SonoVue®, a second-generation agent, is now commonly used. The SonoVue® kit consists of a lyophilised powder which is mixed vigorously with normal saline to form the injectable contrast media. SonoVue consists of microbubbles of sulphur hexafluoride. The interface between the sulphur hexafluoride bubble and aqueous medium acts as a reflector of the ultrasound beam, thus enhancing blood echogenicity and increasing contrast between the blood and the surrounding tissues (Fig. 14.2).

The contrast agent produces a hyperechoic appearance on transvaginal ultrasonography. The contrast media are detected first in the uterine cavity, proximal and then distal fallopian tubes

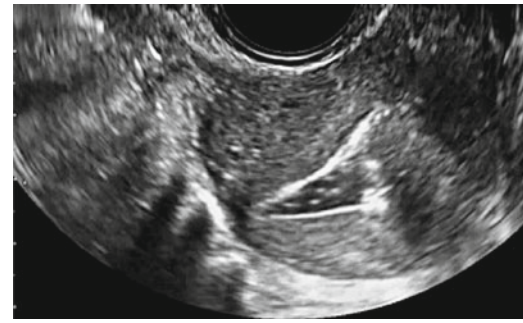

Fig. 14.1 HyCoSy with water and air: this image demonstrates air echogenic areas with a background of echo-free areas. The air bubbles are seen to move through the tube to demonstrate patency

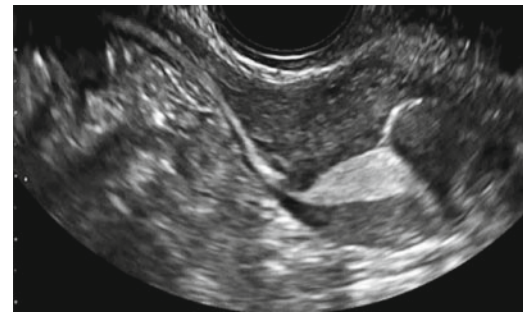

Fig. 14.2 HyCoSy with SonoVue® dye showing dye in the uterine cavity and the right tube

(if they are patent). Tubal patency is demonstrated by visualising intratubal flow for 5–10 s using B-mode scanning and until peritoneal spill is detected around the ovaries [14].

Below we outline a suggested technique for performing the procedure. There are variations to this technique, as well as inclusion and exclusion of steps that may not be routinely performed by other operators.

As HyCoSy is often performed as an outpatient procedure, it is imperative that clinicians performing this procedure remember the basics of good bedside manner, effective communication and making the patient feel at ease. Most patients will be apprehensive about the possible findings but also the anticipated discomfort. Operators performing HyCoSy should be proficient in transvaginal ultrasonography and placement of transcervical catheters and possess the relevant clinical experience and skills to perform this investigation.

It is good practice to issue patients with an information leaflet (some time before the procedure) outlining the procedure so that they have some idea of what to expect when they attend. Leaflets can also inform patients of what to do pre-procedure and expect post-procedure and whom to contact in the event of any complications.

Some operators will perform a urinary beta-HCG test to exclude pregnancy prior to commencing the procedure, although as HyCoSy is performed in the follicular phase of the cycle, this isn't done routinely.

The Technique

1. After gaining verbal consent and a brief description of the procedure, the patient is placed into the dorsal lithotomy position.
2. A warmed, sterile and well-lubricated Cusco's (bivalve) speculum (of the appropriate size for the patient) is then carefully and slowly inserted into the vagina in order to visualise the cervix. Occasionally, the cervix may not be easily identified, and gently changing the angle of direction of the speculum may help with this.

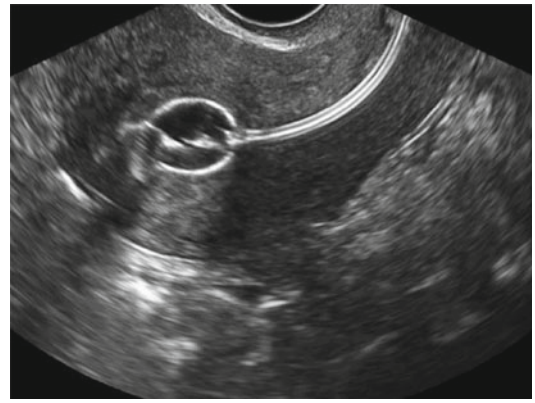

Fig. 14.3 HyCoSy catheter in cavity – ideally the catheter should be in the cervical canal. Occasionally, it is placed in the cavity to prevent displacement during the procedure

3. Once the cervix is identified, it is cleaned with an aseptic solution.
4. The authors recommend the use of a flexible balloon catheter and not the previously used metal cannulae. Foleys catheters have also been employed at this stage. The insertion of the catheter does not routinely require the use of a tenaculum; however, if tenaculum use is required, then the authors suggest a paracervical block with 1 % lignocaine prior to grasping the cervix or only blocking the anterior lip when the tenaculum is applied.
5. If a balloon catheter is used, then the authors recommend intracervical, as opposed to intrauterine, balloon dilatation. It has been demonstrated that this causes less pain, and less contrast media are required in this way too [15]. The balloon can be inflated with air or sterile water. This also allows visualisation of the lower end of the uterine catheter. If the catheter is found to be placed in the uterine cavity under ultrasound guidance, this can be withdrawn into the cervical canal. Figure 14.3 shows the balloon in the uterine cavity – this is occasionally done if the catheter does not appear to be well fixated in the cervical canal (and therefore prevents it from falling out).
6. Once the catheter is in situ and secure, the speculum (and tenaculum if applied) can be

gently removed, ensuring the catheter is not dislodged. The patient is then forewarned that the transvaginal ultrasound probe will be inserted.

7. At this stage, the authors perform a conventional B-mode transvaginal scan to assess the uterus, ovaries and pouch of Douglas. The correct placement of the catheter balloon can also be checked at this point. Alternatively, a conventional scan can be performed after step 1(before the catheter is introduced).
8. After warning the patient, the contrast medium can be injected slowly and steadily. It is important to remember that the uterus is pressure sensitive, and as such, excessive rates and/or volumes of injecting will result in unnecessary patient discomfort. Beware that blocked fallopian tubes may increase the pain experienced by the patient. The authors suggest using no more than 10 ml of contrast media. If the balloon has been inflated correctly, there should be no leakage, and evaluation of the uterus and both tubes should be possible using less than 10 ml. In the author's experience, 2–5 ml is sufficient for demonstrating tubal patency.
9. Tubal patency is assessed by demonstrating flow along the entire length of the tube or by streaming at the cornual end for at least 10 s with spill into the pouch of Douglas [16].
10. A detailed examination of the uterus is performed by scanning slowly and systematically from the cervix to fundus. Any relevant lesions (e.g. submucous leiomyoma) can be closely analysed and relevant images produced.
11. Each tube is followed, in turn, until spill is visualised adjacent to the ovary.
12. Strict criteria must be adhered to in order to ensure that the fallopian tube is followed in its entirety, before it is considered to be patent. Any delay in tubal fill and/or spill must be appropriately documented. Any apparent distortion of the tubal diameter or tubal course must also be documented and preferable supplemented with the use of images/videography.
13. This could be followed by assessment of the uterine cavity with normal saline to exclude endometrial polyp or submucous fibroids.

HyCoSy (and HSG) has the significant advantage over laparoscopy of being outpatient-based (office) investigations without a need for general anaesthesia. There is no risk of visceral or vascular injuries. Patients do not need to be fasted for either procedure, and both the patient and her partner can be present whilst the investigation is being performed.

Unlike HSG, HyCoSy does not involve the use of ionising radiation and iodine-based contrast media or the use of radiology services – it can be performed by a gynaecologist/specialist in reproductive medicine, obviating the need for a radiologist. As an ultrasound-based investigation, other pelvic structures can be assessed simultaneously. HSG may preclude the need for laparoscopy in some cases, thereby improving patient satisfaction and preventing the need for invasive investigations.

HyCoSy has been shown to be at least as effective as hysterosalpingography at detecting tubal blockage. When compared with the gold standard of laparoscopy and dye testing, reported rates for sensitivity and specificity are 80 and 84 %, respectively [17]. The use of HyCoSy is superior to hysterosalpingography in detecting intrauterine anomalies such as leiomyoma, polyps, septae and hydrosalpinx.

Two-dimensional transvaginal HyCoSy as described above, although in many ways superior to HSG, does have its limitations. Due to the tortuous course of the fallopian tubes, the entire tube will not be visualised in one scanning plane. Visualisation of the tubal course can be further limited by tubal spasms. As a result, the false-positive rate for tubal occlusion is 5–10 % [18]. Due to the echogenicity of bowel, distal spill from the tubes may be difficult to distinguish from surrounding bowel and therefore relies on a certain level of operator expertise. Interpretation can therefore be slightly more challenging as compared to hysterosalpingography. As the procedure does rely on the technical ability of the clinician performing the procedure, there can be considerable inter- and intra-observer variability.

Three-Dimensional Coded Contrast Imaging (3D CCI) During HyCoSy

Coded contrast imaging (CCI) comprises of dedicated computer software, designed to enhance the view of the fallopian tubes whilst filtering out signals from other tissues. The image which is produced is based on ultrasound signals produced by the contrast media and not by surrounding tissues.

Coded contrast imaging enhances the use of contrast media by means of low acoustic pressure, thereby enhancing visualisation of the fallopian tube by enabling the clinician to differentiate between the harmonic response of the contrast medium and signals from other surrounding organs such as bowel [18]. The software is able to filter out ultrasound signals produced by the organs and thereby display an image which is solely based on harmonic signals produced by the contrast media.

This technology has been applied in other fields including studying the microvasculature of the liver, breast lesions as well has myocardial perfusion function.

In order to further enhance the technology, second-generation contrast media are used. The first-generation contrast media (Echovist®) contain microbubbles that have rigid membranes and are therefore unable to respond with harmonic signals at low acoustic pressures. However, second-generation agents, such as SonoVue®, provide a substantial harmonic response at low acoustic pressure. The use of a second-generation contrast medium with CCI technology enables the operator to view the hyperechoic fluid firstly in the uterus and then the proximal tube and lastly spill into the abdominal cavity. Due to the detectable differences between the harmonic response between the contrast media and that of the surrounding tissue, there is a clear distinction between the contrast media and the surrounding structures.

The use of 3D imaging (without CCI) using saline-air contrast has been reported; however, the resulting image may not necessarily be clear enough to make a conclusion regarding tubal patency. However, when 3-dimensional imaging is combined with CCI, the tubal course and structure can be studied in much greater detail.

Software packages that provide the volume acquisition images are available, and when this is combined with 3D CCI, then a 3D image with the uterus and tubes, showing the tubal course in its entirety and tubal spill (if patent), is seen as a hyperechoic image in a completely anechoic pelvis (i.e. no other structures are seen).

Volume acquisition performed during HyCoSy is a static procedure and as such requires less challenging probe movements and therefore requires less operator experience and expertise as compared to conventional 2D TVS HyCoSy [18]. As 3D CCI visualises both fallopian tubes, less contrast media are required – this is beneficial both to the patient and also from a cost perspective. Another advantage of 3D CCI at HyCoSy is that the images can be stored (similar to Doppler imaging and HSG) and viewed by clinical colleagues, unlike conventional 2D HyCoSy which is a dynamic procedure that only the operator can interpret. However, 3D imaging requires greater funding and therefore is not accessible in resource poor settings. A recent study [19] comparing 3D HyCoSy in 150 tubes to laparoscopy and dye testing demonstrated a sensitivity and specificity of 93.5 and 86.3 %, respectively. The authors reported a positive predictive value of 87.8 % and negative predictive value of 92.6 %. These values compare favourably with previously reported sensitivities and specificities of 2D HyCoSy.

Although more work is required to assess the diagnostic accuracy and feasibility of 3D CCI HyCoSy, it appears that this novel method of evaluating tubal patency will become widespread in the future and an integral part of the subfertility workup (Fig. 14.4).

Blood-Flow and Doppler Imaging

Blood flow and Doppler are additional modalities that can be employed in conjunction with HyCoSy.

Blood flow is a relatively new technique which has been employed in other medical

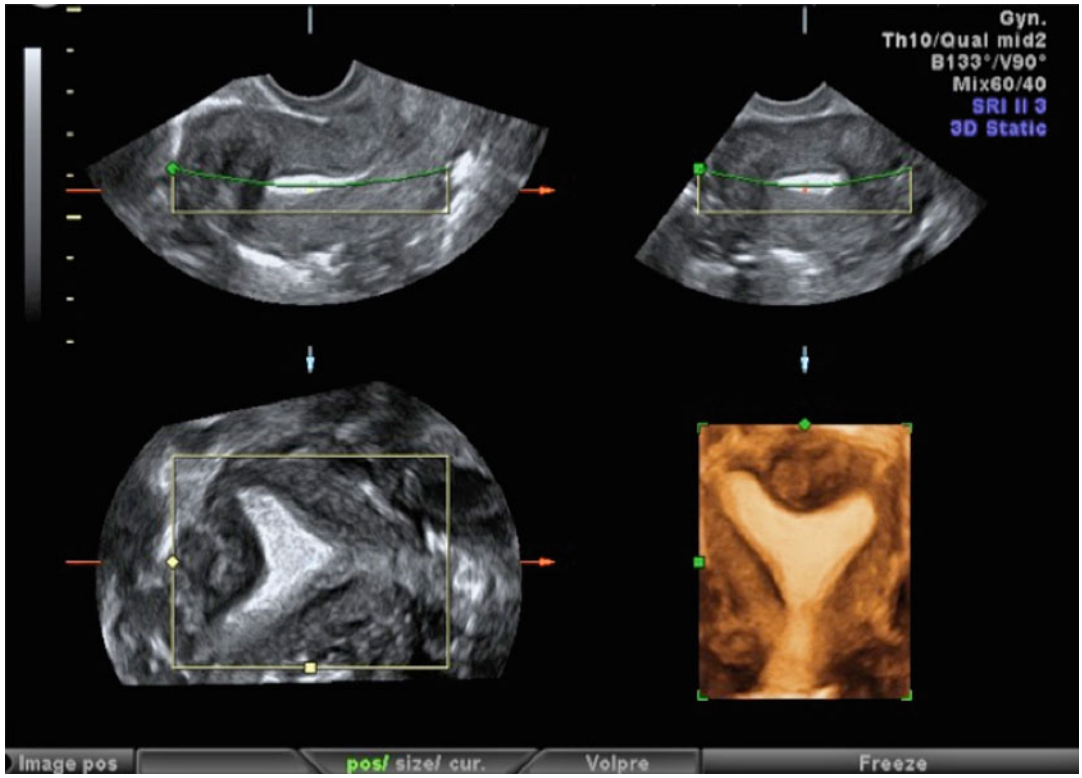

Fig. 14.4 3D HyCoSy with Echovist dye showing the cavity

specialities such as vascular studies. Blood flow is an ultrasound technique developed to analyse blood flow. It does not employ the Doppler principle; rather, the reflected amplitudes of scattering particles (e.g. erythrocytes) are imaged by subtraction modes of two or four image vectors along one line. Therefore, moving particles are imaged and stationary structures (such as vessel walls) can be subtracted. Blood-flow data can then be combined with B-mode information to enable a better amplitude visualisation of flow. With this technique, water can be used, and tubal patency is demonstrated with blood-flow technique.

Although the application of blood flow is not yet an established method of assessment for tubal patency, increased experience and knowledge of it is likely to lead to more widespread use of this modality in the assessment of tubal function (Fig. 14.5).

Colour-coded Doppler imaging can be used as an adjunct to greyscale imaging in order to visualise the flow of media through the tubes. Doppler imaging has been shown to be valuable in cases where HyCoSy has been inconclusive [20]. When 3-dimensional power Doppler imaging (3D-PDI) is employed in conjunction with

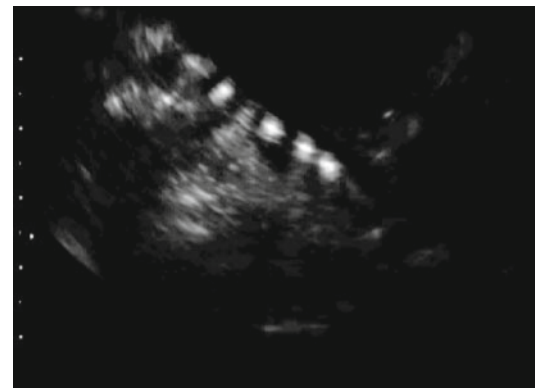

Fig. 14.5 HyCoSy with B-flow technique: this is a form of inversion mode where movement of fluid is captured in greyscale and the rest of the image appears dark. The *grey images* below the tube represent the bowel peristalsis

HyCoSy, it allows visualisation of contrast media throughout the entire tubal length. The use of 3D-PDI has clear advantages over the use of HyCoSy alone. It has been shown that visualisation of distal tubal spill occurs twice as often when 3D-PDI is employed [21]. As the procedure does rely on the technical ability of the clinician performing the procedure and, in the case of 3D-PDI, time for analysis, this has not been routinely implemented in clinical practice.

Conclusion

Being one of the commonest causes of subfertility, tubal patency is an essential component of the subfertility workup. In this chapter, we have provided an overview of the gold standard technique of chromopertubation and classical methods such as the hysterosalpingogram and then covered the use of ultrasound in slightly more detail. We hope we have provided the reader with a good understanding of these newer techniques involving ultrasound as well as a foundation for a technique that we employ. The methods we have outlined above are by no means exclusive, and the readers are encouraged to develop their own techniques when carrying out the procedures discussed. As the boundaries of investigative medicine continue to be expanded, there will be further development of the above employed methods as well as newer modalities. What is certain is that ultrasound does and will continue to play a pivotal role in the armamentarium we have at our disposal in the investigation of our patients.

References

1. Steinkeler JA, Woodfield CA, Lazarus E, Hillstrom MM. Female infertility: a systematic approach to radiologic imaging and diagnosis. Radiographics. 2009;29:1353–70.
2. Lim CP, Hasafa Z, Bhattacharya S, Maheswari A. Should a hysterosalpingogram be a first-line investigation to diagnose female tubal subfertility in the modern subfertility workup? Hum Reprod. 2011; 26(5):967–71.
3. Watrelot A, Hamilton J, Grudzinskas JG. Advances in the assessment of the uterus and fallopian tube function. Best Pract Res Clin Obstet Gynaecol. 2003;17(2):187–209.
4. Lanzani C, Savasi V, Leone FP, Ratti M, Ferrazzi E. Two-dimensional HyCoSy with contrast tuned imaging technology and a second-generation contrast media for the assessment of tubal patency in an infertility program. Fertil Steril. 2009;92:1158–61.
5. Coppus SFPJ, Opmeer BC, Logan S, Van der Veen F, Bhattacharya S, Mol BWJ. The predictive value of medical history taking and Chlamydia IgG ELISA antibody testing (CAT) in the selection of subfertile women for diagnostic laparoscopy: a clinical prediction model approach. Hum Reprod. 2007;22:1353–8.
6. Swart P, et al. The accuracy of hysterosalpingography in the diagnosis of tubal pathology: a meta-analysis. Fertil Steril. 1995;64(3):486–91.
7. den Hartog JE, Lardenoije CM, Severens JL, Land JA, Evers JL, Kessels AG. Screening strategies for tubal factor subfertility. Hum Reprod. 2008;23:1840–8.
8. National Collaboratry Centre for Women's and Children's Health. Fertility: Assessment and Treatment for People with Fertility Problems. Commissioned by the National Institute for Clinical Excellence (NICE). London: RCOG Press 2004. ISBN 1-900364-97-2.
9. Broeze KA, Opmeer BC, Van Geloven N, Coppus SFPJ, Collins JA, den Hartog JE, et al. Are patient characteristics associated with the accuracy of hysterosalpingography in diagnosing tubal pathology? An individual patient data meta-analysis. Hum Reprod. 2011;17:293–300.
10. Spring DB, et al. Potential therapeutic effects of contrast materials in hysterosalpingography: a prospective randomised controlled trial. Radiology. 2000;214:53–7.
11. Hart D, Hillier MC, Wall BF. HPA-RPD-029-doses to patients from radiographic and fluoroscopic X-ray imaging procedures in the UK – 2005. Review. 2009;2010:95.
12. Tur-Kaspa I, Seidman DS, Soriano D, Greenberg I, Dor J, Bider D. Hysterosalpingography with a balloon catheter versus a metal cannula: a prospective, randomized, blinded comparative study. Hum Reprod. 1998;13:75–7.
13. Nanini R, Chelo E, Branconi F, Tantini C, Scarselli GF. Dynamic echohysteroscopy: a new diagnostic technique in the study of female infertility. Acta Eur Fertil. 1981;12:165–71.
14. Campbell S, Bourne T, Tan S, Collins W. Hysterosalpingo-contrast-sonography (HyCoSy) and its future role within the investigation of infertility in Europe. Ultrasound Obstet Gynecol. 1994;4:245–53.
15. Spieldoch RL, Winter TC, Schouweiler C, Ansay S, Evans MD, Lindheim SR. Optimal catheter placement during sonohysterography: a randomized controlled trial comparing cervical to uterine placement. Obstet Gynecol. 2008;111:15–21.
16. Ayida G, Chamberlain P, Barlow D, Koninckx P, Golding S, Kennedy S. Is routine diagnostic laparoscopy for infertility still justified? A pilot-study

assessing the use of hysterosalpingo-contrast sonography and magnetic resonance imaging. Hum Reprod. 1997;12(7):1436–9.
17. Tanawattanacharoen S, Suwajanakorn S, Uerpairojkit B, Boonkasemsanti W, Virutamesan P. Transvaginal hysterosalpingo-contrast sonography (HyCoSy) compared with chromolaparoscopy. J Obstet Gynaecol Res. 2000;26:71–5.
18. Exacoustos C, Di Giovanni A, Szabolcs B, Binder-Reisinger H, Gabardi C, Arduini D. Automated sonographic tubal patency evaluation with three-dimensional coded contrast imaging (CCI) during hysterosalpingo-contrast sonography (HyCoSy). Ultrasound Obstet Gynecol. 2009;34:609–12.
19. Zhou L, Zhang X, Chen X, Liao L, Pan R, Zhou N, Di N. Value of three-dimensional hysterosalpingo-contrast sonography with SonoVue in the assessment of tubal patency. Ultrasound Obstet Gynecol. 2012;40(1):93–8.
20. Kalogirou D, Antoniou G, Botsis G, Kassanos D, Vitoratos N, Zioris C. Is colour Doppler necessary in the evaluation of tubal patency by hystero-contrast-sonography. Clin Exp Obstet Gynecol. 1997;24(2):101–3.
21. Sladkevicius P, Ojha K, Campbell S, Nargund G. Three-dimensional power Doppler imaging in the assessment of fallopian tube patency. Ultrasound Obstet Gynecol. 2000;16(7):644–7.

Hydrosalpinx

15

Dale W. Stovall and Mark W. Austin

Introduction

The fallopian tubes derive their name from the sixteenth-century Italian anatomist, Gabriel Fallopius. The fallopian tubes originate embryologically from the most cephalad portion of the Mullerian ducts. In the developing embryo, this occurs at 6–8 weeks' gestation. The fallopian tubes serve as the site for oocyte pickup, sperm transport, fertilization, early embryonic development, and transport of the embryo to the uterine cavity. However, as the fallopian tubes are indirectly connected to the lower genital tract, they are vulnerable to sexually transmitted infections. Furthermore, at the distal end of the fallopian tubes are the fimbriae; these are delicate structures that are particularly susceptible to injury following infection, abdominal or pelvic surgery, and subsequent healing. Damage to the fallopian tubes can result in tubal occlusion, which is most common at the distal end of the tube. Distal tubal occlusion is commonly followed by the formation of a collection of fluid inside the tube. When a fallopian tube becomes filled with fluid, it is called a hydrosalpinx. The diameter and length of a hydrosalpinx can vary widely from patient to patient depending upon many variables. In any event, the fluid within a hydrosalpinx functions as an acoustic window that allows for ultrasonic visualization of the tube without additional administration of contrast media.

Occluded fallopian tubes serve as barriers to conception. Initially, infertility specialists developed surgical techniques to repair damaged fallopian tubes. As the success of these procedures was unsatisfactory, assisted reproductive techniques (ART) were developed to specifically bypass the various reproductive processes that occur within the fallopian tubes. However, the presence of hydrosalpinges has subsequently been shown to be associated with a reduction in ART success rates. These findings lead to clinical trials that have evaluated the effect of various methods of treatment of hydrosalpinges on ART success rates. This chapter will review the anatomy of the fallopian tube, the prevalence and etiology of hydrosalpinges, the assessment of hydrosalpinges, and the reproductive impact of this condition.

Anatomy of the Fallopian Tube

Similar to the uterus, the fallopian tubes are composed of an outer serosal surface, a middle muscularis layer, and an internal lumen that is lined with both secretory and ciliated epithelial cells. As both the uterus and the fallopian tubes are formed from the Mullerian ducts, they are contiguous organs with a connecting lumen. The fallopian tubes range in size from 10 to 13 cm in length and 0.5 to 1.2 cm in diameter. Anatomically,

D.W. Stovall, MD (✉) • M.W. Austin, MD
Department of Obstetrics and Gynecology,
Riverside Regional Medical Center,
Annex Building, 2nd Floor, 500 J Clyde Morris Boulevard,
Newport News, VA 23601, USA
e-mail: dale.stovall@rivhs.com; mark.austin@rivhs.com

L.A. Stadtmauer, I. Tur-Kaspa (eds.), *Ultrasound Imaging in Reproductive Medicine*,
DOI 10.1007/978-1-4614-9182-8_15,

the fallopian tube can be divided into distinct segments. The most proximal portion of the fallopian tube, which is connected to the lateral surface of the fundus of the uterus, is called the interstitial segment. This segment of tube primarily functions as the tubal lumen's entry into the uterine cavity. For all practical purposes, this segment of the fallopian tube is contained within the wall of the uterus. As the uterus contains several smooth muscle layers, this portion of the fallopian tubes' lumen is surrounded by a thick smooth muscle lining. The opening of the interstitial segment into the uterus is called the tubal ostea, and it can be seen from inside the uterine cavity via hysteroscopy. Moving distally from the uterus, the next tubal segment is called the isthmic portion of the fallopian tube. It is approximately 2 cm in length. This segment is completely clear from the serosal and muscular layers of the uterus and contains the second thickest muscular layer of the tube. However, the lumen of the isthmic portion of the fallopian tube, like that of the interstitial segment, is very narrow. The next segment of the tube is called the ampullary segment. The ampula is approximately 7 mm in length and has a relatively thin muscularis layer and a wide internal lumen as compared to isthmic portion of the tube. The mucosal lining of the ampullary portion of the tube contains more pronounced mucosal folds also known as rugal folds. The next tubal segment is known as the infundibulum. It is approximately 1 cm in length and is the widest portion of the fallopian tube. Extending off the end of the tube are feather-like projections known as the fimbriae. These projections are thought to assist in oocyte pickup after ovulation. A long projection of the fimbria, the fimbria ovarica, is commonly connected to the ovarian surface to maintain the fimbria in close proximity to the ovarian surface.

Tubal Function

The fallopian tube is an integral part of the reproductive process. Beyond reproduction, however, the fallopian tubes serve no further physiologic function. After ovulation, the oocyte is picked up by the fimbriated end of the fallopian tube. Assisted by tubal contractions and the tubal epithelial lining, the oocyte migrates to the ampullary portion of the tube. There, the oocyte is fertilized. For spermatozoa to reach the ovulated oocyte, they must travel from the vagina, through the cervical os, into the uterus, through the small tubal ostea, and finally to the ampullary segment of the tube. Once fertilized, the embryo migrates through the fallopian tube in the opposite direction of the aforementioned spermatozoa into the intrauterine cavity where it subsequently implants. The secretory cells within the fallopian tube secrete electrolytes, calcium, glucose, and protein that serve as nutrients for the spermatozoa, oocyte, and the developing embryo. The fluid within the fallopian tube also assists in the transport of both gametes and embryos.

Definition, Prevalence, and Etiology

Injury to the distal end of the fallopian tube can result in either a hydrosalpinx or fimbrial phimosis. Hydrosalpinges are fallopian tubes that are completely occluded at their distal end and are dilated with fluid. In this case, the secretions from within the fallopian tube accumulate within the tube, distending primarily the ampullary portion of the fallopian tube. This occurs despite the fact that the proximal portion of the tube remains patent. Fimbrial phimosis results from a partial obstruction of the distal end of the fallopian tube. In this case the distal end of the fallopian tube is still patent, but there is agglutination of the fimbria and adhesive bands that surround the terminal end of the tube yielding a narrow phimotic tubal opening.

The incidence and prevalence of hydrosalpinges is unknown. However, it is known that approximately 25–35 % of female factor infertility is caused by tubal disease. Furthermore, more than half of the cases of tubal disease arise from salpingitis [1]. Salpingitis is part of the more general process known as pelvic inflammatory disease or PID. PID is an acute infection of the upper genital tract which includes the uterus, fallopian tubes, and ovaries. The two most common

organisms associated with salpingitis are Chlamydia trachomatis and Neisseria gonorrhoeae [2]. In general, the longer salpingitis is allowed to go untreated, and the greater the number of infections, the greater the damage to the fallopian tube and the greater the likelihood of developing a hydrosalpinx. Therefore, patients with a history of pelvic inflammatory disease are at risk for distal tubal occlusion and hydrosalpinx. Other risk factors for tubal occlusion and hydrosalpinx include a history of endometriosis, ectopic pregnancy, and prior pelvic surgery. For patients with no risk factors, a negative chlamydia antibody test indicates that there is less than a 15 % likelihood of tubal pathology [3].

Signs and Symptoms

The natural history of hydrosalpinges is not well studied. In other words, it is not well known how rapidly they develop from a given insult or how commonly they resolve or recur. Furthermore, no selected population of patients has been screened by ultrasound or any other imaging method to determine the incidence of the disease. Therefore, the percentage of women with a hydrosalpinx who are symptomatic is unknown. Clearly, some women with hydrosalpinges do suffer from intermittent or constant lower abdominal pain and a bothersome vaginal discharge. However, it is possible that the majority either are asymptomatic or have infertility as their only clinical problem associated with their hydrosalpinges.

Effects on Pregnancy

Complete bilateral distal tubal occlusion produces sterility. However, even the presence of a unilateral hydrosalpinx can have a significant effect on fertility. In this regard, one must realize that there are numerous causes for infertility, and therefore, it is very likely that patients with a unilateral hydrosalpinx and infertility are likely to be a very heterogeneous group. This heterogeneity may involve not only multiple causes for infertility (e.g., endometriosis, PCOS, and male factor infertility) but heterogeneity in regard to the contents within their hydrosalpinx, the condition of their contralateral tube, and adhesions within the pelvis. It has been well documented that the fluid within a hydrosalpinx may contain microorganisms, debris, toxins, cytokines, and prostaglandins. Furthermore, it is known that even though a fallopian tube may be completely occluded distally and contain a significant collection of fluid within its ampullary region, its proximal end may still be patent, allowing for drainage of fluid into the uterine cavity. Thus, tubal fluid contents may come into direct contact with the endometrium, gametes, and embryos.

To better assess these contents and to determine their effects on fertility, Beyer et al. studied the contents of tubal fluid from infertile women with hydrosalpinges and the effects of this fluid on murine embryonic development. They found that as compared to values for normal human tubal fluid, fluid from hydrosalpinges tended to be normal with respect to components such as sodium, chloride, and bicarbonate and with respect to pH and osmolarity. However, they found that hydrosalpinx was relatively low in regard to the concentrations of potassium, calcium, phosphate, glucose, and protein. Although there was some variability within the biochemical components of the hydrosalpinx fluid, murine embryonic development was inhibited by this fluid [4]. These investigators concluded, however, that it was likely a lipophilic embryotoxic factor(s) and not the differences in the biochemical components found between "normal" and hydrosalpinx-derived tubal fluid that was responsible for the reduction in embryonic development. To date, the embryotoxic effects of hydrosalpinx fluid have not been documented in human embryos.

Other studies have evaluated the effects of hydrosalpinges on endometrial receptivity. Meyer et al. prospectively studied the endometrium of 103 women with hydrosalpinges for three integrin markers of endometrial receptivity and compared those results to 55 infertile and 44 fertile controls. They also looked at the effects of tubal occlusion or resection on endometrial receptivity markers. These investigators found that women with hydrosalpinges expressed significantly less

αvβ1 integrin as compared to controls. Based on these data, they concluded that hydrosalpinges may have a direct impact on endometrial receptivity [5]. Subsequently, these investigators demonstrated a restoration of αvβ1 integrin following surgical treatment for hydrosalpinx. In addition, other investigators have found potential defects in embryo implantation that are associated with hydrosalpinges. In this regard, the expression of HOXA10, a transcription factor for embryo implantation, was shown to be decreased in women with hydrosalpinges and the expression of this transcript was restored after salpingectomy [6]. Finally, the effects of hydrosalpinx fluid on sperm motility and velocity have been studied. These investigators found that sperm motility and velocities remained unchanged after a 5-h incubation period with various concentrations of hydrosalpinx fluid but that the percentage of motile spermatozoa were significantly reduced after 24 h of incubation [7]. Therefore, it appears that there are several possible etiologies for the negative effects of hydrosalpinx-derived fluid on reproduction beyond simple tubal occlusion. Whether unilateral salpingectomy is appropriate for women with infertility who have a unilateral hydrosalpinx and are undergoing infertility therapy with induction of ovulation with or without insemination has not been well studied.

Imaging

Hysterosalpingogram (HSG)

Hysterosalpingography is a well-established method used for imaging of the intrauterine cavity and the fallopian tubes. The technique utilized is oft published and well known [8]. Briefly, the procedure is performed between menstrual cycle days 5 and 12, that is, after the cessation of menses, but before ovulation and thus the possibility of pregnancy. An NSAID such as ibuprofen is commonly prescribed to be taken approximately 1 h before the procedure to ameliorate cramping. A prophylactic antibiotic such as doxycycline may be given to those patients with a history of PID or evidence of same at the time of the procedure. The patient is placed in the dorsal lithotomy position on the examination table in the fluoroscopy suite, and a bimanual pelvic examination is performed. In the absence of any evidence of acute pelvic or cervical infection, the procedure can commence. The patient's perineum is draped with sterile cloth or paper, the uterine cervix is visualized using a sterile speculum, and the cervix is cleaned with an iodine solution. If the Jarcho cannula is to be used, the cervix is grasped with a tenaculum. The cannula is filled with an iodinated, radio-opaque, water-soluble contrast medium, taking care to expel any trapped air. The prefilled cannula is placed into the cervical os and held in place by a spring-loaded mechanism. If a balloon HSG catheter is used, one may be able to dispense with the tenaculum; however, the filled balloon may cause discomfort to the patient as well. A randomized trial failed to demonstrate the efficacy of the intrauterine instillation of 2 % lidocaine prior to HSG for the relief of pain [9]. Typically, a scout film is taken prior to the instillation of dye to look for pelvic calcifications. Contrast media are slowly injected under fluoroscopic control, and an image is taken during this filling phase to look for intrauterine cavity filling defects. A second image is taken when the uterus appears to be distended, and a third documents the dye filling the fallopian tubes. Lastly, an image of the contrast media spilling from the tubes and flowing freely in the pelvis is obtained. At the conclusion of the procedure, the cannula or catheter is withdrawn, the tenaculum is removed, and the speculum is withdrawn.

Normal tubes appear thin, with a smooth contour. Rugae are often visible. Hydrosalpinges appear enlarged and irregular, with absent rugae, and contrast medium is most often not visible spilling from the tubes into the pelvis. In a meta-analysis of studies that evaluated HSG and laparoscopy findings independently, the authors calculated a point estimate of 0.65 for sensitivity and 0.83 for specificity [10]. The authors concluded that although HSG is of limited use for detecting tubal patency because of its low sensitivity, its high specificity made it a useful test for detecting tubal obstruction. Of more relevance, Mol et al. studied the reproducibility and accuracy of hysterosalpingography in diagnosing

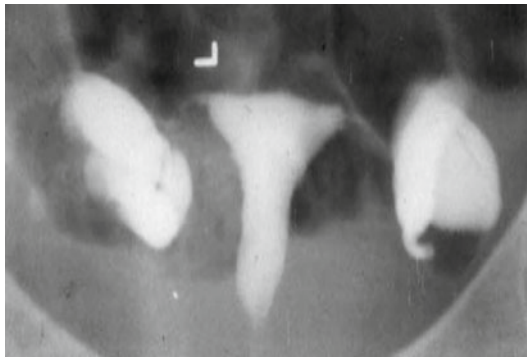

Fig. 15.1 Hysterosalpingogram image of a patient with bilateral hydrosalpinges

hydrosalpinges. The authors found the inter- and intraobserver reproducibility of the interpretation of hydrosalpinx to be only "substantial" (k 0.64 and 0.68). Compared with findings at diagnostic laparoscopy, for hydrosalpinx, the likelihood ratio of a positive test was 5.8 (4.4–7.6). However, the likelihood ratio of a negative test was 0.64 (0.54–0.76). The authors concluded that HSG is a useful test to detect hydrosalpinx, but an imperfect test to rule out hydrosalpinx [11]. Obviously, in the presence of proximal tubal occlusion, HSG will fail to reveal the presence of hydrosalpinx. Figure 15.1 shows a HSG of bilateral hydrosalpinges.

Ultrasound Appearance

Using standard transabdominal or transvaginal ultrasonography, the appearance of a hydrosalpinx is that of a hypoechoic cystic adnexal mass. Patel et al. evaluated the utility of four specific sonographic findings in diagnosing hydrosalpinges: incomplete septation, short linear projection, tubular shape, and presence of a waist [12]. The authors calculated the likelihood ratio for each finding. The presence of a "waist" in a cystic collection refers to diametrically opposed indentations in the wall of the collection. The waist sign in combination with tubular shape was found in 12 of 26 hydrosalpinges and no other masses (likelihood ratio of between 18.9 and infinity). Small round projections combined with tubular

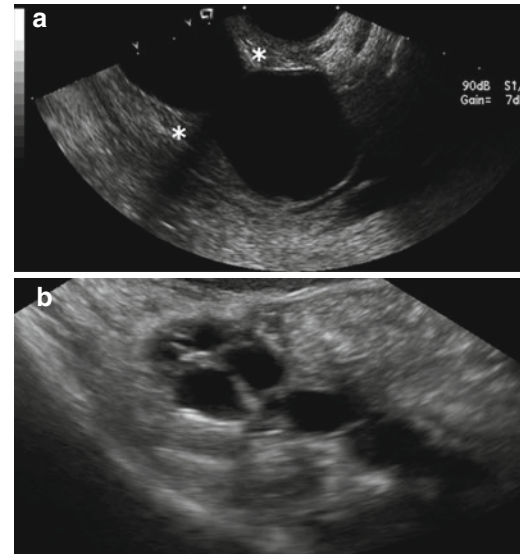

Fig. 15.2 (**a**) "Waist sign" of a hydrosalpinx, marked by the *asterisks*, as seen with 2-D ultrasound. (**b**) "Beads on a string" sign of a hydrosalpinx demonstrated by 2-D ultrasound

shape was found in 14 hydrosalpinges and one other mass (likelihood ratio of 22.1). The authors concluded that when these combinations are identified in a cystic adnexal mass that does not have solid-appearing areas or features characteristic of hemorrhagic cysts, endometriomas, or dermoid cysts, one can make the diagnosis of hydrosalpinx with a high level of confidence. Waist sign (Fig. 15.2a) and beads on a string (Fig. 15.2b) are classic features of a hydrosalpinx on ultrasound.

Color Doppler Sonography

Color Doppler sonography is used to assess blood flow in a given organ and assesses directional flow as well. The utility of color Doppler to improve the evaluation of hydrosalpinges has been studied. In this regard, the addition of color Doppler does not seem to increase the accuracy of standard 2-D transvaginal ultrasonography in detecting hydrosalpinges. More specifically, Guerriero et al. prospectively evaluated 239 consecutive premenopausal, nonpregnant women who shortly thereafter underwent sur-

gery for adnexal masses, with transvaginal B-mode ultrasonography with and without color Doppler, and CA-125 measurements. The sensitivity, specificity, and positive and negative predictive values were calculated and found to be identical for each category, with color Doppler and CA-125 levels adding nothing to the diagnostic accuracy of 2-D transvaginal ultrasonography alone [13].

Contrast Medium

As a fluid contrast medium can serve as an acoustic window for ultrasonography, one might expect that adding contrast to enhance ultrasound images would be advantageous in the assessment of the fallopian tubes. As previously discussed in this text, this technique is very useful in the basic infertility evaluation to assess tubal patency. In regard to hydrosalpinges, however, there are no studies that directly address the utility of sonographic contrast in the diagnosis of hydrosalpinx, per se. In a study comparing HSG and transvaginal 2-D ultrasonography with an air/saline mixture as the contrast medium in the evaluation of tubal patency, both had the same high concordance with laparoscopy, 86.7 and 86.7 %, respectively [14]. Strandell et al. compared transvaginal sonography utilizing a commercially available contrast agent (Echovist®) and HSG to the gold standard laparoscopic evaluation and found similarly high concordance rates (83 and 80 %, respectively) [15]. Therefore, it appears that transvaginal ultrasound in combination with a contrast medium is a very good method of assessing tubal patency. However, to determine if a patient has a hydrosalpinx, an ultrasound without contrast must first be performed. Otherwise, one might misdiagnose a patient with a hydrosalpinx who instead has distal tubal occlusion alone and no fluid collection within the fallopian tube. In other words, if contrast medium is used initially to evaluate the fallopian tubes either by HSG or via ultrasound, an "iatrogenic" hydrosalpinx may be misdiagnosed as a true hydrosalpinx.

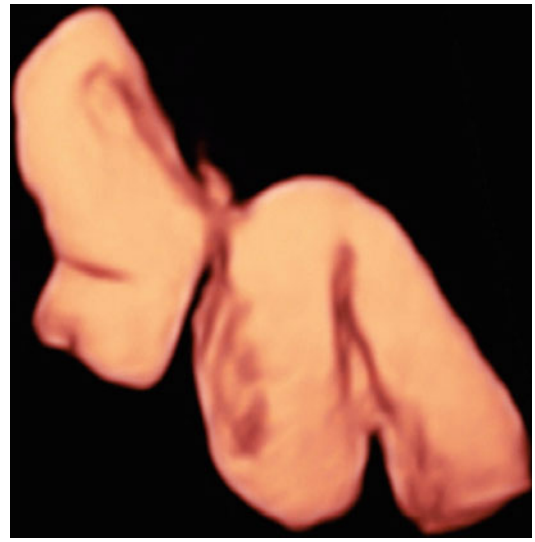

Fig. 15.3 3-D ultrasound inversion rendering image used to identify a hydrosalpinx

Three-Dimensional (3-D) Ultrasound

Three-dimensional ultrasonography may be helpful in the identification of hydrosalpinges. In one study, 21 consecutive patients scheduled to have laparoscopy were recruited to undergo the 3-D HyCoSy 2 days before the scheduled laparoscopy. Echovist® (Schering AG, Berlin, Germany), the ultrasound contrast medium, was injected into the uterine cavity via a Foley catheter. The flow of the medium in the fallopian tube was captured by using three-dimensional power Doppler mode and was stored for later analysis. The sensitivity of 3-D HyCoSy for detecting tubal patency was 100 % with a specificity of 67 %. The positive and negative predictive values were 89 and 100 %, respectively; the concordance rate was 91 % [16]. Finally, Timor-Tritsch et al. reported using 3-D ultrasound inversion rendering to diagnose hydrosalpinges (Fig. 15.3). Fifty-two patients with fluid-filled adnexal masses suspected of being abnormal fallopian tubes were scanned by two-dimensional and 3-D transvaginal ultrasound. The acquired volumes were then "inverted" to display a cast-like appearance of the fluid-filled structures. The authors concluded that the rendered images increased their confidence in diagnosing hydrosalpinges [17]. Therefore, it appears that

3-D ultrasonography is a useful tool for the diagnosis of hydrosalpinges and may be utilized initially, or in addition to 2-D ultrasound imaging when the results from 2-D images are equivocal.

Utility of Tubal Surgery

In regard to tubal surgery, patients with a good prognosis are those who have no more than limited filmy adnexal adhesions, mildly dilated tubes (<3 cm) with thin and pliable walls, and a lush endosalpinx with preservation of the mucosal folds [18]. The mean cumulative pregnancy rates reported after terminal salpingostomy overall is approximately 30 %, with an ectopic pregnancy rate of 5 %. However, in poor prognosis patients with large hydrosalpinges, thick non-pliable walls, and loss of luminal rugae, the cumulative pregnancy rate may be as low as zero. In comparison, the pregnancy rates following terminal salpingostomy in good prognosis patients who are younger and have a more conserved tubal anatomy may be as high as 80 % [19, 20]. Unfortunately, it is difficult to determine the presence of rugal folds with ultrasonography. This is better evaluated via hysterosalpingogram. Nevertheless, an increased tubal diameter is associated with a greater destruction of tubal rugae and a more rigid tube. Therefore, ultrasonography is a reasonable tool for the assessment of patients for tubal surgery with a hydrosalpinx. However, pregnancy rates with IVF exceed the chances for pregnancy with tubal surgery except for the patients with the best prognosis after surgery.

Assisted Reproduction

Hydrosalpinges have been shown to have an adverse effect on both pregnancy and delivery rates in women undergoing IVF. Similar to women with a unilateral hydrosalpinx and a contralateral patent tube who are trying to conceive without IVF, women with either unilateral or bilateral hydrosalpinges who are undergoing IVF may experience drainage of hydrosalpinx fluid into their uterine cavities with adverse reproductive consequences. In fact, this phenomenon has been widely studied. A meta-analysis of 6713 IVF cycles compared the pregnancy outcomes of women with and without a hydrosalpinx. This study found that the presence of a hydrosalpinx was associated with approximately a 50 % reduction in pregnancy rates and a two-fold increase in the risk for spontaneous abortion [21]. Another large study of women with tubal disease who either did or did not have a hydrosalpinx revealed similar results [22]. Therefore, it seems clear that the presence of a hydrosalpinx has a significant negative impact on both pregnancy and live birth rates after IVF.

Numerous procedural methods used to treat unilateral or bilateral hydrosalpinges either before an anticipated IVF cycle or during an ongoing IVF cycle have been studied. Included are laparoscopic salpingectomy, proximal tubal occlusion via either laparoscopy or hysteroscopy, salpingostomy, and ultrasound-guided needle aspiration. A Cochrane review, using data from several randomized trials, evaluated the utility of laparoscopic salpingectomy, laparoscopic proximal tubal occlusion, and ultrasound-guided aspiration of hydrosalpinges on pregnancy rates with IVF [23]. These data revealed that ongoing pregnancy rates were increased by an odds ratio (OR) of 2.14 (95 % CI, 1.23–3.73) after laparoscopic salpingectomy, that clinical pregnancy rates were increased by an OR of 4.66 (95 % CI, 2.47–10.01) after proximal tubal occlusion, and that the clinical pregnancy rates were not significantly increased (OR = 1.97, 95 % CI, 0.62–6.29) after ultrasound-guided aspiration. Two small reports have evaluated the use of hysteroscopic-guided proximal tubal occlusion using the Essure® device [24, 25]. Although these data are very promising, the technique cannot be recommended at this time. However, it may be an option for patients who are not candidates for laparoscopy secondary to known extensive pelvic adhesion disease. Other data regarding the effectiveness of laparoscopic salpingectomy on IVF pregnancy rates has demonstrated that the effectiveness of this procedure is greatest with

the resection of larger hydrosalpinges (i.e., those that are visible by ultrasound). When the removal of these larger hydrosalpinges were specifically evaluated, a pregnancy rate hazards ratio of 3.8 (95 % CI, 1.5–9.2) was found. Therefore, it appears that the assessment of hydrosalpinges by ultrasound may help clinicians to determine which patients may benefit the most from salpingectomy.

Other types of treatments for hydrosalpinges prior to IVF include salpingostomy and antibiotic therapy. Each of these therapies has specific advantages. Salpingostomy allows one to drain the hydrosalpinx fluid and to preserve the fallopian tube. Therefore, this procedure may not only improve pregnancy rates with IVF, but may also improve fertility without the assistance of IVF. Of course, fallopian tubes treated in this manner may re-accumulate with fluid making the procedure somewhat less desirable in patients who are only planning to undergo IVF. Furthermore, although one study has shown this procedure to increase pregnancy rates with IVF to a similar level as that seen after salpingectomy, more data are needed to determine its true effectiveness [26]. In addition, there are data to demonstrate that the administration of doxycycline both before and after oocyte retrieval may increase pregnancy rates specifically in women with tubal occlusion. However, these data are very preliminary, whether or not antibiotic therapy is truly efficacious for the improvement of pregnancy with IVF in women with hydrosalpinges is not known. In conclusion, it appears that either salpingectomy or proximal tubal occlusion yields the best pregnancy rates with IVF in women with hydrosalpinges and that the patients who may benefit most from this procedure are those whose hydrosalpinges are large enough to be seen by ultrasound. If a patient is not a surgical candidate, it makes sense to use pre- and post-oocyte retrieval doxycycline therapy as an alternative. Hysteroscopic proximal tubal occlusion with a sterilization device is another option, but further study is needed before this procedure can be recommended prior to IVF.

Conclusions

The fallopian tubes serve several important steps in the reproductive process including oocyte pickup, gamete transportation, fertilization, and early embryonic development and transfer. However, the fallopian tubes are vulnerable to damage from both infectious and inflammatory processes. When the distal end of a fallopian tube is completely blocked and the tube fills with fluid, it is referred to as a hydrosalpinx. Using specific criteria, hydrosalpinges can be readily diagnosed via ultrasound imaging. The presence of a hydrosalpinx(s) has a significant effect on one's chances for pregnancy. Bilateral hydrosalpinges result in sterility. In good prognostic cases, surgical intervention can significantly improve the chances for successful intrauterine pregnancy. However, most individuals with bilateral hydrosalpinges must undergo IVF-ET to conceive. Furthermore, the presence of a hydrosalpinx(s) that is visible via ultrasound clearly reduces the chances for pregnancy from IVF. Treatment of a hydrosalpinx(s) prior to IVF by either salpingectomy or proximal tubal occlusion has been proven to increase the chance for pregnancy with IVF.

References

1. Honore GM, Holden AE, Schenken RS. Pathophysiology and management of proximal tubal blockage. Fertil Steril. 1999;5:785–95.
2. CDC. Centers for disease control and prevention. Sexually transmitted diseases (STDs). 2010 STD treatment guidelines. 2011. http://www.cdc.gov/std/treatment/2010/default.htm. Accessed 03 July 2011.
3. den Hartog JE, Morre SA, Land JA. Chlamydia trachomatis-associated tubal factor subfertility: immunogenetic aspects and serological screening. Hum Reprod Update. 2006;12(6):719–30.
4. Beyler SA, James KP, Fritz MA, Meyer WR. Hydrosalpingeal fluid inhibits in-vitro embryonic development in a murine model. Hum Reprod. 1997;12(12):2724–8.
5. Meyer WR, Castelbaum AJ, Somkuti S, Sagoskin AW, Doyle M, Harris JE, Lessey BA. Hydrosalpinges

adversely affect markers of endometrial receptivity. Hum Reprod. 1997;12(7):1393–8.
6. Daftary GS, Kayisli U, Seli E, Bukulmez O, Arici A, Taylor HS. Salpingectomy increases peri-implantation endometrial HOXA10 expression in women with hydrosalpinx. Fertil Steril. 2007;87(2):367–72.
7. Ng EH, Ajonuma LC, Lau EY, Yeung WS, Ho PC. Adverse effects of hydrosalpinx fluid on sperm motility and survival. Hum Reprod. 2000;15(4):772–7.
8. Baramki T. Hysterosalpingography. Fertil Steril. 2005;83:1595–606.
9. Frishman GN. The use of intrauterine lidocaine to minimize pain during hysterosalpingography: a randomized trial. Obstet Gynecol. 2004;103:1261–6.
10. Swart P. The accuracy of hysterosalpingography in the diagnosis of tubal pathology: a meta-analysis. Fertil Steril. 1995;64(3):486–91.
11. Mol BWJ. Reproducibility of the interpretation of hysterosalpingography in the diagnosis of tubal pathology. Hum Reprod. 1996;11:1204–8.
12. Patel MD. Likelihood ratio of sonographic findings in discriminating hydrosalpinx from other adnexal masses. AJR Am J Roentgenol. 2006;186:1033–8.
13. Guerriero S. Transvaginal ultrasonography associated with color Doppler energy it the diagnosis of hydrosalpinx. Hum Reprod. 2000;15:1568–72.
14. Exacoustos C. Hysterosalpingo-contrast sonography compared with hysterosalpingography and laparoscopic dye perturbation to evaluate tubal patency. J Am Assoc Gynecol Laparosc. 2003;10(3):367–72.
15. Strandell A. The assessment of endometrial pathology and tubal patency: a comparison between the use of ultrasonography and X-ray hysterosalpingography for the investigation of infertility patients. Ultrasound Obstet Gynecol. 1999;14:200–4.
16. Chan CC. Comparison of three-dimensional hysterosalpingo-contrast-sonography and diagnostic laparoscopy with chromopertubation in the assessment of tubal patency for the investigation of subfertility. Acta Obstet Gynecol Scand. 2005;84(9):909–13.
17. Timor-Tritsch IE. Three-dimensional ultrasound inversion rendering technique facilitates the diagnosis of hydrosalpinx. J Clin Ultrasound. 2010;38(7):372–6.
18. American Fertility Society. The American Fertility Society classifications of adnexal adhesions, distal tubal occlusion, tubal occlusion secondary to tubal ligation, tubal pregnancies, Mullerian anomalies and intrauterine adhesions. Fertil Steril. 1988;49:944–55.
19. Schlaff WD, Hassiakos DK, Damewood MD, Rock JA. Neosalpingostomy for distal tubal obstruction: prognostic factors and impact of surgical technique. Fertil Steril. 1990;54:984–90.
20. Rock JA, Katayama KP, Martin EJ, et al. Factors influencing the success of salpingostomy techniques for distal fimbrial obstruction. Obstet Gynecol. 1978;52:591–6.
21. Zeyneloglu HB, Arici A, Olive DL. Adverse effects of hydrosalpinx on pregnancy rates after in vitro fertilization-embryo transfer. Fertil Steril. 1998;70:492–9.
22. Camus E, Poncelet C, Aucouturier JS, et al. Hydrosalpinx and fertilization in vitro-embryo transfer abstention or salpingectomy? Abstention, salpingectomy, or salpingostomy? Gynecol Obstet Fertil. 2000;29:466–73.
23. Johnson N, van Voorst S, Sowter MC, et al. Surgical treatment for tubal disease in women due to undergo in vitro fertilization. Cochrane Database Syst Rev. 2010;(3):CD002125.
24. Mijatovic V, Veersema S, Emanuel MH, et al. Essure hysteroscopic tubal occlusion device for the treatment of hydrosalpinx prior to in vitro fertilization-embryo transfer in patients with a contraindication for laparoscopy. Fertil Steril. 2010;93:1338–42.
25. Galen DI, Khan N, Richter KS. Essure multicenter off-label treatment for hydrosalpinx before in vitro fertilization. J Minim Invasive Gynecol. 2011;18:338–42.
26. Murray DL, Sagoskin AW, Widra EA, Levy MJ. The adverse effect of hydrosalpinges on in vitro fertilization pregnancy rates and the benefit of surgical correction. Fertil Steril. 1998;69:41–5.

16 Virtual Hysterosalpingography: A New Diagnostic Technique for the Study of the Female Reproductive Tract

Patricia Carrascosa and Carlos E. Sueldo

General Concepts

Virtual hysterosalpingography (VHSG) is a new noninvasive diagnostic technique that evolved from our prior experience with virtual colonoscopy studies [1]; it allows the evaluation of the entire gynecologic tract in a single study, including the cervix, uterus [2], and fallopian tubes [3]. The use of MDCT allows the capture of an axial volumetric acquisition in only a few seconds. This can be post-processed in different planes without loss of definition, permitting the evaluation of the anatomy or pathology in any plane with similar quality. This concept is known as isotropic images, where tridimensional and bidimensional images have the same resolution than axial images.

The CT scanners should have at least 64 rows of detectors [4] in order to acquire the images in less than 5 s. The VHSG provides information not only about the gynecologic tract but also of the intrapelvic structures revealing associated findings.

The patient preparation for the study and the timing in the menstrual cycle is similar to a conventional HSG; also it has the same contraindications (pregnancy, pelvic infections, etc.). After exposing the ectocervix with a vaginal speculum and applying iodine to the cervix, we place a plastic catheter size 10 F through the ectocervix and instill 15 ml of a diluted iodine solution (at 70 % in Physiosol) with a pump running at 0.3 ml/s. The purpose of using the pump is to achieve steady pressure and speed, to diminish the patient's discomfort, and to assure an optimal uterine distention. The image acquisition begins 30 s after starting the instillation and is completed after 5 s; MDCT with 256 or 320 rows of detectors complete the study in only 1.5 s, making VHSG a real-time study with easy visualization of the contrast as it passes into the peritoneum (Figs. 16.1 and 16.2).

Technical parameters in the CT equipment with either 64 [5] or 256 rows are shown in Table 16.1.

Once the images are acquired, they are transferred to the workstation for different reconstructions: multiplanar reconstruction (MPR), maximal intensity projection (MIP), volume rendering (VR), and endoscopic views.

Multiplanar reconstructions (coronal, sagittal, and oblique) allow for the evaluation of the cervix, uterus, and fallopian tubes, as well as extrauterine structures, while the curved MPR evaluates all the female structures in a single plane (Fig. 16.3).

Maximal intensity projection (MIP) images provide excellent definition of the fallopian tubes in a tridimensional format with grey tones,

P. Carrascosa, MD
Maipu Diagnostics, Buenos Aires, Argentina

C.E. Sueldo, MD (✉)
Department of Obstetrics and Gynecology (REI Division),
University of California San Francisco-Fresno,
722 Medical Center Dr. East Suite 105,
Clovis, CA 93611, USA
e-mail: drsueldo@hotmail.com

L.A. Stadtmauer, I. Tur-Kaspa (eds.), *Ultrasound Imaging in Reproductive Medicine*,
DOI 10.1007/978-1-4614-9182-8_16,

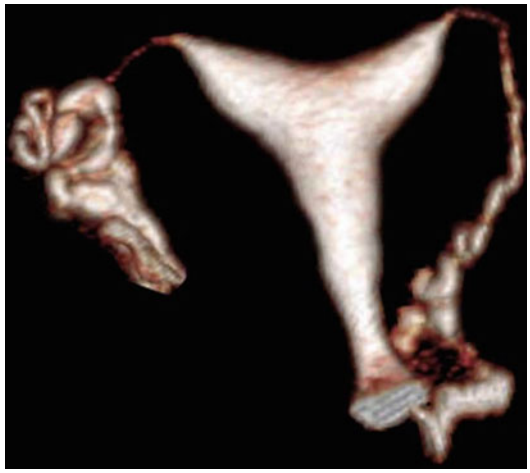

Fig. 16.1 VHSG (volume rendering projection)

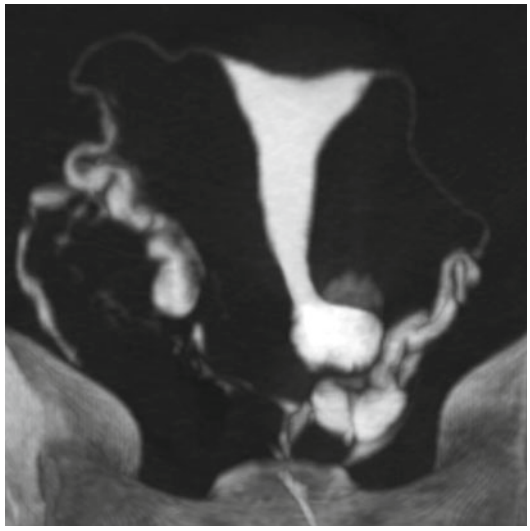

Fig. 16.2 VHSG (maximum intensity projection)

detecting the presence of hydrosalpinx and tubal obstructions (Fig. 16.2).

Volume rendering reconstructions provide tridimensional views of the reproductive tract, with a window that recognizes the endoluminal contrast. These reconstructions detect a large spectrum of uterine and tubal pathology such as cervical stenosis, polyps, and tubal disease (Figs. 16.4, 16.5, and16.6).

Virtual endoscopy algorithm of reprocessing images confirms the findings encountered with the previous methods and provides intraluminal

Table 16.1 Technical parameters in CT equipment with 64 vs 256 rows

Technical parameters	64 rows	256 rows
Slice thickness	0.9	0.625
Reconstruction interval	0.45	0.3
KV	100	80
mAs	100–150	100–150
Scan time acquisition	5 s	1.5 s
Radiation dose (mSv)	0.9	0.3

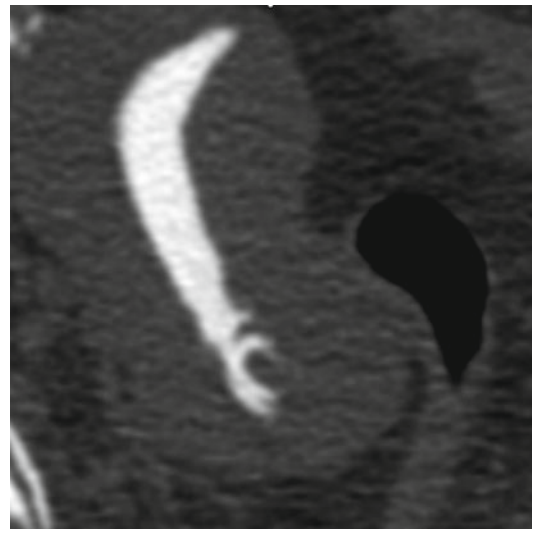

Fig. 16.3 VHSG (multiplanar reconstruction of an endocervical polyp)

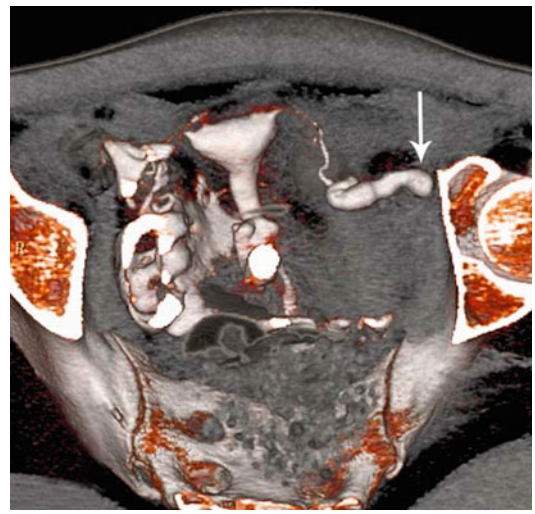

Fig. 16.4 VHSG (volume rendering in tubal disease)

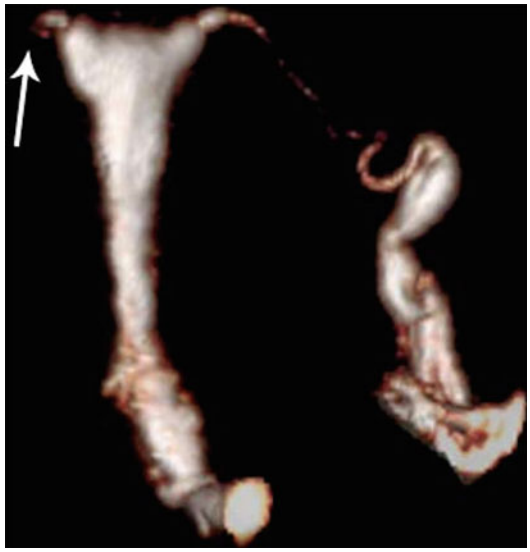

Fig. 16.5 VHSG (volume rendering in tubal disease)

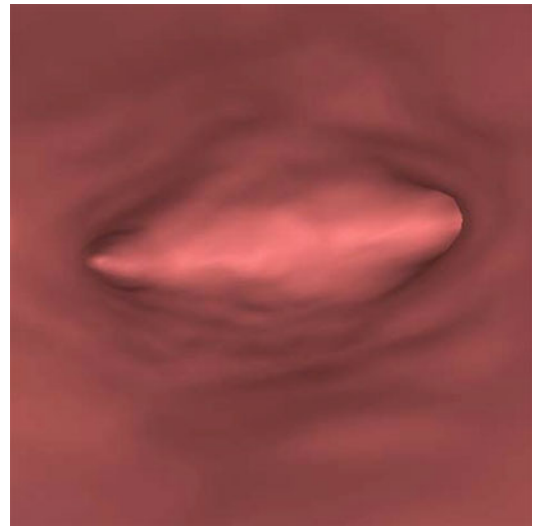

Fig. 16.7 Normal uterine cavity (endoscopy view)

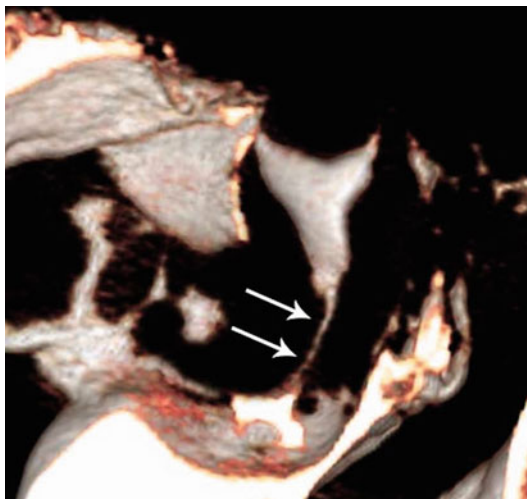

Fig. 16.6 Cervical stricture

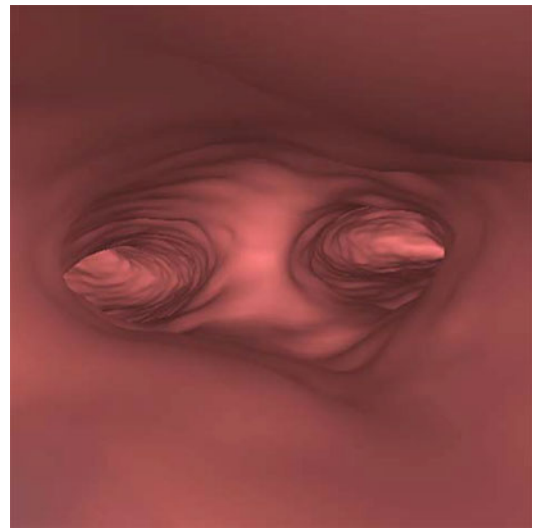

Fig. 16.8 Abnormal uterine cavity (endoscopy view)

information similar to a conventional hysteroscopy and falloposcopy (Figs. 16.7 and 16.8).

The rate of complications with VHSG in our experience is extremely low; in over 7,000 VHSG studies performed since 2006, we did not find any cases of infection, bleeding, or other significant complications requiring hospitalization. In a few cases we observed intravascular passage of contrast, of which only one patient had an allergic reaction requiring medical treatment that improved all symptoms in a very short time.

In known cases of allergy to iodine, we use gadolinium [6], a nonallergenic paramagnetic contrast with a much higher cost (3×) than the iodine contrast and therefore should not be used routinely. We recently performed a comparative study between iodine and gadolinium

($n = 50$ patients, with 25 in each group) which gave the following results: gadolinium was slightly better tolerated than iodine in terms of discomfort, the density of the intraluminal images was not as intense with gadolinium, and however the overall quality of the studies was fairly similar. In addition, the amounts of radiation exposure (0.9 mSv) for both contrasts used in this particular study were also similar.

The VHSG study [7, 8] is well tolerated by our patients, and they all completed a questionnaire post-procedure to evaluate the degree of discomfort experienced, categorized from grade 0 (no discomfort) to grade IV (very severe discomfort). Over 60 % of the patients had grade 0, 20 % grade I, 16 % grade II, 1.5 % grade III, and 0.5 % grade IV. Interestingly, those patients that previously had a conventional HSG revealed much better acceptance of VHSG compared to those patients that never had a conventional HSG.

Radiation During VHSG: The obvious comparison of the amount of radiation during a VHSG study is with a conventional HSG, which itself varies a great deal depending upon the time of fluoroscopy employed and the number of films taken per study. If, for example, an HSG with 2 min of fluoroscopy and 6 films obtained was performed, it would result in a radiation exposure of 5 mSv. On the other hand, a VHSG with a 256-row multidetector CT using our latest protocols and technical parameters will produce an exposure of only 0.3–0.4 mSv. It is important to emphasize that this remarkable drop in radiation exposure with the use of the latest CT models is accomplished without compromising the quality of the studies performed.

Clinical Experience with Virtual Hysterosalpingography in Reproductive Medicine

Cervical Pathology in Infertility

The cervical anomalies may include different types of pathology, like cervical stenosis, synechiae, wall irregularities, polypoid lesions, and diverticula. The pathology present may alter uterine access in infertile patients during certain procedures such as uterine studies, intrauterine inseminations, and embryo transfers, as well as the possibility of causing cervical bleeding during those procedures, interfering with the optimization of results.

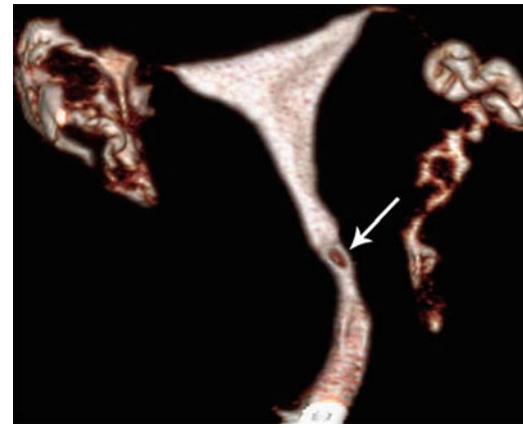

Fig. 16.9 Cervical synechiae

The etiology of *stenotic cervices* may be congenital, postsurgical, or postinfections; VHSG is an ideal diagnostic instrument for cervical pathology as it does not require traction with a tenaculum, and it does not leave blind sectors after image reconstruction; the MPR, MIP, and VR are useful in diagnosing cervical stenosis allowing one to navigate through the cervical lumen clearly identifying the defects (Fig. 16.6).

Cervical synechiae are bands of fibrous tissue localized inside the cervix, partially or completely occupying the lumen; the synechiae are easily identified by VHSG as elevated endocervical images showing soft tissue densities coming from the wall toward the center of the cervix (Fig. 16.9).

Cervical polyps are elevated lesions which vary in size and number, although the majority of patients have only a single polyp. They may result from an abnormal response to the presence of elevated estrogens, chronic inflammation, etc. and can present either asymptomatically or with vaginal bleeding during intercourse or any other cervical manipulation. They are rarely malignant, but after removal they should always be sent to pathology. They are seen by VHSG as

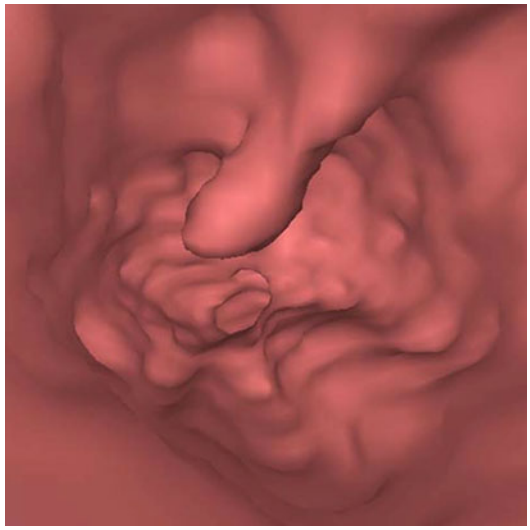

Fig. 16.10 Endocervical polyp

partially or totally obstructing the lumen; the MPRs show the soft tissue images and the virtual endoscopy the endoluminal view of the polyp (Fig. 16.10).

The *cervical diverticula* are herniations of the cervical wall that can be seen by VHSG through tridimensional and endoscopic views, where one can clearly detect the neck of the diverticulum inside the lumen. It is unclear if diverticula play a role in human infertility.

Pathology of the Endometrial Cavity in Infertility

There are different pathologies that can affect the endometrial cavity and also can be detected by VHSG [9]. Most of them have tremendous importance in reproductive medicine, as they can compromise sperm transport, embryo implantation, or embryo growth, potentially increasing the rate of spontaneous miscarriages. In one of our VHSG studies, we evaluated in a prospective manner the diagnostic accuracy and potential clinical value in the detection of cervical and uterine pathology in 69 patients, in comparison to conventional diagnostic hysteroscopy (done by clinicians blinded to the VHSG findings). Virtual HSG showed a diagnostic sensitivity of 96 %, a specificity of 86 %, a positive predictive value of 90 %, and a negative predictive value of 95.6 %.

Congenital anomalies of the Müllerian duct, such as septate or bicornuate uterus, can be diagnosed by VHSG [10]. An accurate diagnosis is important in order to properly advise patients about the best treatment to be implemented. The MRI is considered the study of choice due to its tissue resolution and its ability to outline the outer margins of the uterine wall. Recently, we demonstrated the value of VHSG in the differential diagnosis of these uterine anomalies, as one can easily outline the external surface of the uterine fundus. VHSG with volume rendering reconstruction allows the visualization of the endometrial cavity plus the adjacent flat or minimally indented myometrium consistent with a septated uterus. On the other hand, when the indentation in the uterine fundus is deeper than 15 mm, creating the presence of two separate horns, the diagnosis of bicornuate uterus is made (Fig. 16.11a); in uterine malformations, the endoscopic view is unable to differentiate between septate and bicornuate uteri (Fig. 16.11b).

Uterine synechiae consist of fibrous bands that bind the uterine walls to one another; they represent scars usually caused by trauma from an aggressive curettage postabortion or postpartum; their presence may be localized in a small sector of the cavity or extensively spread out in a diffuse manner, obliterating large sectors of the uterine cavity. They can cause infertility or repeated pregnancy losses. VHSG is an excellent diagnostic tool as MPR shows irregularly elevated lesions with soft tissue density, while volume rendering reconstructions show filling defects where the synechiae are localized (Fig. 16.12).

Endometrial polyps constitute focal elevations of the endometrium and contain glands, fibrous stroma, and blood vessels; they are fairly common (11–24 %) among infertile patients. Their role in causing infertility is controversial, but there is some consensus that those polyps larger than 1 cm should be removed, especially when present in IVF candidates. VHSG has various modalities of image reconstruction (bidimensional, tridimensional, and endoscopic) that allow the visualization and identification of the

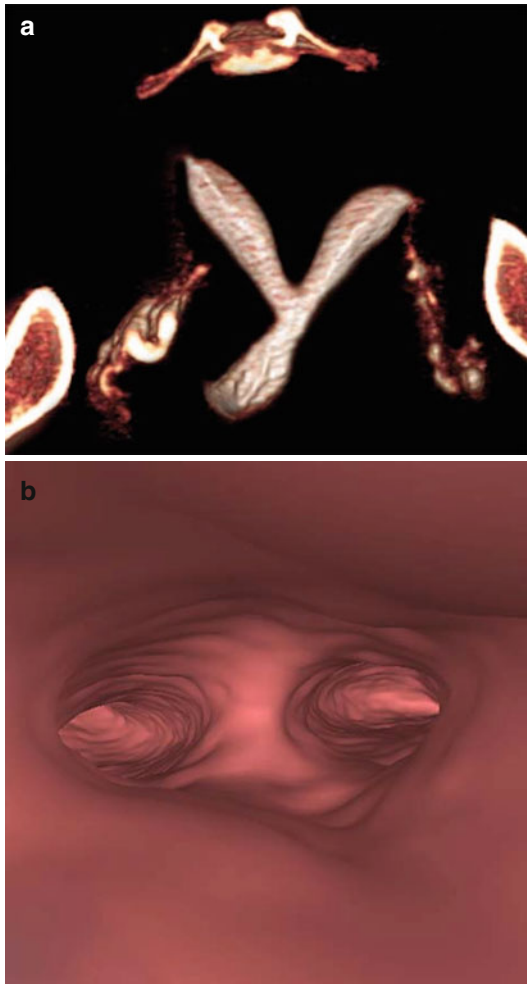

Fig. 16.11 Uterine malformation: (**a**) volume rendering and (**b**) endoscopic views

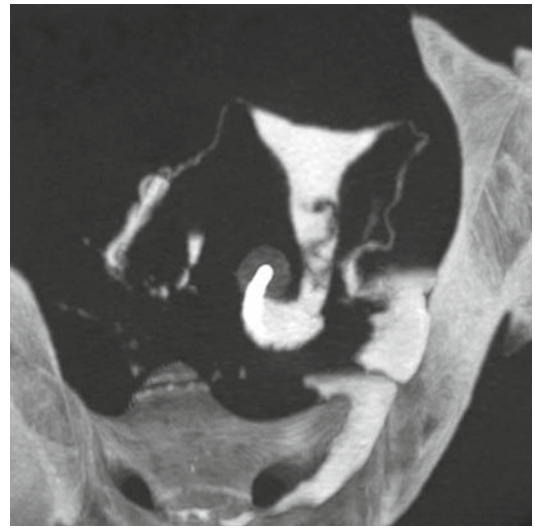

Fig. 16.12 Endometrial synechiae

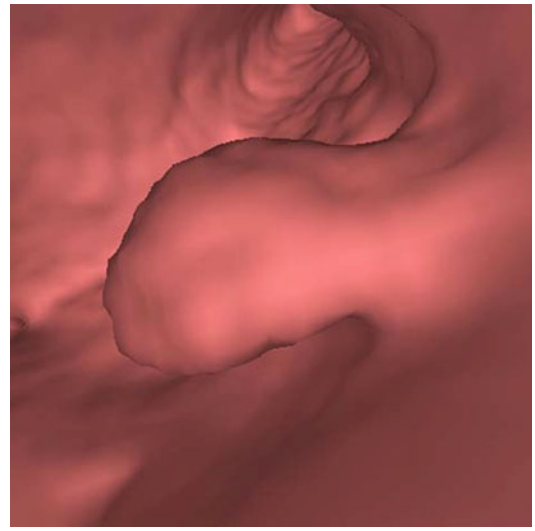

Fig. 16.13 Endometrial polyp

intrauterine lesions; the MPRs show the polyps as elevated lesions from the wall that move toward the cavity with a soft tissue density. The virtual endoscopic images show the polyps with endoluminal views, allowing the assessment of polyp size and shape (Fig. 16.13).

Submucous myomas are generally benign tumors from the smooth muscle, single or multiple, with a variable size, number, and location. They may be a cause of infertility when they are submucous in location, as they may interfere with sperm transport and/or embryo implantation and they may also cause repeated miscarriages. The identification of the tumors is important as it can help plan the best surgical approach for their

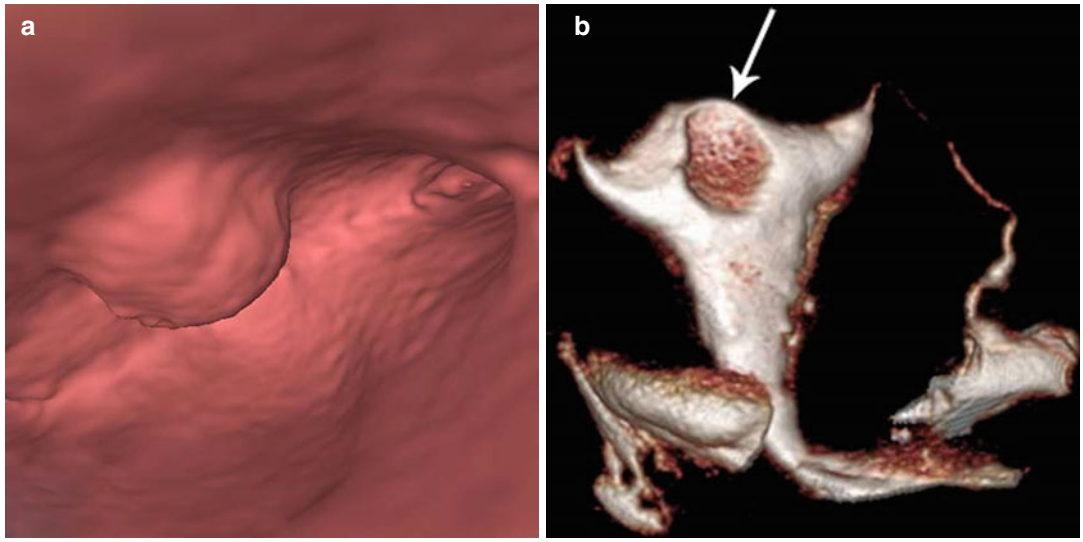

Fig. 16.14 Submucous myoma seen by (**a**) endoscopic and (**b**) volume rendering views

removal and the possible success of the procedure. The use of VHSG permits the identification of submucous myomas and determines the size and at times the percentage of intramural extension. We determined that the sensitivity and specificity of VHSG for the detection of submucous myomas are 91.7 and 100 %, respectively. The volume rendering and endoscopic views clearly distinguish the endometrial-myometrial line and localize the myoma and its relation with the endometrial cavity (Fig. 16.14a, b).

Evaluation of the Fallopian Tubes

Hysterosalpingography (HSG) has been the traditional method of evaluation of the fallopian tubes for the last several decades; tubal patency is clearly established as the dye injected passes through the fimbriated ends and disperses around the peritoneal cavity near the adnexa. The diagnosis of tubal obstruction when a hydrosalpinx is present is fairly certain; on the other hand the lack of passage of dye into the fallopian tube may represent a cornual spasm, a mucus plug, or insufficient amount (or pressure) of the contrast injected transcervically to complete the study. Recently, the introduction of VHSG, as a new diagnostic modality based on computer tomography, appears to be a step forward in the diagnosis of fallopian tube pathology. Initially in our experience with this technique, using older CT equipment, we were not able to clearly visualize the fallopian tubes. More recently, the use of 256-row MDCT allows the study to be completed in only 1.5 s, capturing the images in real time while the filling material is still present in the tubes or as it escapes through the fimbriated ends. Through the filling of the fallopian tubes, one is able to obtain volumetric images of high resolution, which allows high image quality and virtual endoscopic navigation, similar to the visualization of the inner tubal lumen as described by conventional falloposcopy. Also, the projection of volume rendering (VR) provides excellent definition of the fallopian tubes, detecting the presence of hydrosalpinx (Fig. 16.15), tubal obstructions (Fig. 16.5), etc. making VHSG a valuable diagnostic tool for the assessment of tubal pathology.

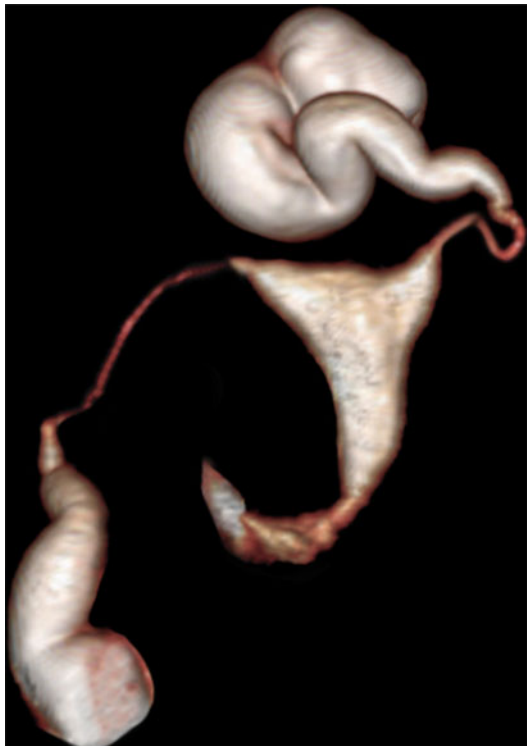

Fig. 16.15 Bilateral hydrosalpinges

Conclusions

VHSG should be considered a new and improved diagnostic technique for the evaluation of the female reproductive tract over other existing diagnostic modalities, as it provides high-quality images of the cervix, uterine cavity, and fallopian tubes. The versatility of the image reconstructions allows for accurate visualization and diagnosis of diverse pathologic processes in the female reproductive tract, many of them of high significance in infertility. The study is completed in a short amount of time, well tolerated, and with minimal radiation exposure as compared to conventional HSG. The cost-benefit ratio, which varies from country to country, is an important consideration that should be determined on an individual basis; yet we are confident that VHSG has a bright future given its many diagnostic advantages.

References

1. Carrascosa P, Capunay C, Sangster D, Carrascosa J. Virtual colonoscopy: experience in 500 patients. Acta Gastroenterol Latinoam. 2003;33(3):145–9.
2. Carrascosa P, Capunay C, Baronio M, Lopez EM, Borghi M, Sueldo C, Papier S. Virtual hysteroscopy by multidetector computed tomography. Abdom Imaging. 2008;33(4):381–7.
3. Carrascosa P, Baronio M, Capunay C, Lopez E, Borghi M, Sueldo C, Papier S. Multidetector CT virtual hysterosalpingography in the investigation of the uterus and fallopian tubes. Eur J Radiol. 2008;67(3):531–35.
4. Carrascosa P, Baronio M, Capunay C, Lopez EM, Sueldo C, Papier S. Clinical use of 64-row multislice CT hysterosalpingography in the evaluation of female factor infertility. Fertil Steril. 2008;90(5):1953–58.
5. Carrascosa P, Capunay C, Vallejos J, Baronio M, Lopez EM, Borghi M, Sueldo C, Papier S. 64 Row multidetector CT virtual HSG. Abdom Imaging. 2009;34(1):121–33.
6. Carrascosa P, Capunay C, Vallejos J, Baronio M. Gadolinium vs iodine virtual HSG: an alternative for patients allergic to iodine 64 row multidetector CT virtual HSG. Fertil Steril. 2008;90:S157.
7. Carrascosa P, Capunay C, Vallejos J, Lopez EM, Carrascosa J. Virtual HSG: a new multidetector CT technique for evaluating the female reproductive system. Radiographics. 2010;30(3):643–61.
8. Celik O, Karkas H, Hascalik S, Tagluk M. Virtual hysterosalpingography and hysteroscopy: assessment of uterine cavity and fallopian tubes using 64-detector CT data sets. Fertil Steril. 2010;93(7):2383–84.
9. Carrascosa P, Capunay C, Vallejos J, Baronio M, Carrascosa J. Virtual hysterosalpingography: experience with over 1000 consecutive patients. Abdom Imaging. 2011;36(1):1–14.
10. Carrascosa P, Sueldo C, Capunay C, Baronio M, Papier S. Virtual HSG in the diagnosis of bicornuate vs septate uterus. Fertil Steril. 2011;96(5):1190–92.

Ultrasound in Male Infertility

17

Landon W. Trost, David D. Casalino,
and Robert E. Brannigan

Abbreviations

CBAVD	Congenital bilateral absence of the vas deferens
EDO	Ejaculatory duct obstruction
MAGI	Male accessory gland infection
SV	Seminal vesicle
TESE	Testicular sperm extraction
TRUS	Transrectal ultrasonography
TURED	Transurethral resection of ejaculatory duct

Introduction

Infertility remains a significant issue both for the individual couple as well as from a public health standpoint. Although the exact prevalence is unknown, with varied results reported by region, definition, and methodology utilized, infertility is reported to affect 14–20 % of couples with a male-factor contributory in 56–75 % of cases [1–9]. Infertility is commonly defined as the inability of a couple to achieve pregnancy following at least 12 months of unprotected intercourse. Couples presenting with infertility are frequently evaluated concomitantly to assess for the presence of correctable male and female factors with several guidelines/algorithms available to assist treating clinicians [10–14].

In addition to obtaining a history, physical examination, semen analysis, and laboratory assessments, ultrasonography has a role in both the evaluation and treatment of male-factor infertility. Although significant variability exists in the actual utilization, ultrasound may be employed in the initial assessment, as a confirmatory/adjunctive test to physical examination; as a predictor of underlying fertility and operative outcomes, in the treatment of certain causes of infertility; and in the acquisition of sperm for assisted reproductive techniques (ARTs). Given the noninvasive nature and ready availability of ultrasound, it is frequently selected as a first-line modality among imaging options.

Overview of Genitourinary Ultrasonography

The use of ultrasound for evaluation of male-factor infertility predominantly consists of scrotal and transrectal ultrasonography with occasional use of retroperitoneal imaging in select cases.

L.W. Trost, MD
Department of Urology, Mayo Clinic,
200 First Street SW, Rochester, MN 55905, USA
e-mail: trost.landon@mayo.edu

D.D. Casalino, MD (✉)
Department of Radiology, Northwestern University,
Feinberg School of Medicine, 676 N. St. Clair St.,
Ste. 800, Chicago, IL 60611, USA
e-mail: dcasalino@nmff.org

R.E. Brannigan, MD
Department of Urology, Northwestern University,
Feinberg School of Medicine,
675 N. Saint Clair Street,
Galter Suite 20-150, Chicago, IL 60611, USA
e-mail: r-brannigan@northwestern.edu

L.A. Stadtmauer, I. Tur-Kaspa (eds.), *Ultrasound Imaging in Reproductive Medicine*,
DOI 10.1007/978-1-4614-9182-8_17,

Prior to imaging, patients are positioned so as to maximize image quality and patient comfort. For scrotal ultrasonography, patients are placed in a semi-recumbent versus supine position with the penis retracted cephalad. A warm probe is applied to minimize contraction of the dartos muscle. For transrectal ultrasonography, the patient is most commonly positioned in the lateral decubitus position with the knees drawn to the chest. Alternatively, the patient may be placed in dorsolithotomy or prone jackknife depending on the clinical context of the procedure. Evaluation of the retroperitoneum is performed in a sloppy lateral to full flank position, with the highest-frequency transducer utilized which will permit sufficient depth of penetration.

Similar to other applications of ultrasonography, imaging is achieved through transmission of ultrasonic waves from the transducer, which are subsequently reflected and represented graphically on a monitor. Structures with increased density or points of transition between structures of varying densities reflect a greater portion of sound waves and are visualized as brighter when compared to those of lower density. Structures which do not permit passage of ultrasound waves such as calcifications result in complete reflectivity which is perceived as a bright image with an absence of signal distal to the calcification. This "shadowing" is clearly demonstrated with larger calcifications and may be imperceptible in smaller applications such as with testicular microlithiasis.

The selection of the probe utilized depends on the desired application including organ visualized and depth of penetration required (Fig. 17.1). In general, increasing frequencies are associated with improved tissue resolution and decreasing depths of penetration. Given the relatively short skin-to-organ distance with scrotal and transrectal ultrasonography, the majority of probes utilized range from 7.5 to 14 MHz.

In addition to increasing ultrasound frequency, various forms of Doppler may be utilized to enhance the diagnostic value of the imaging obtained. Power (i.e., color flow) Doppler refers to a form of pulse wave Doppler in which returning echoes are assigned a color (red if moving towards the probe, blue if moving away) so as to differentiate images with velocity (vascular structures) from nonmotile tissue. Duplex Doppler includes the combination of both spectral (flow velocity represented graphically on an *X*/*Y* axis) and flow color imaging and is particularly useful to assess the intensity of vascular flow and to assign resistive indices (Fig. 17.2). Additional techniques including elastosonography are under ongoing investigations to determine their clinical utility in routine practice.

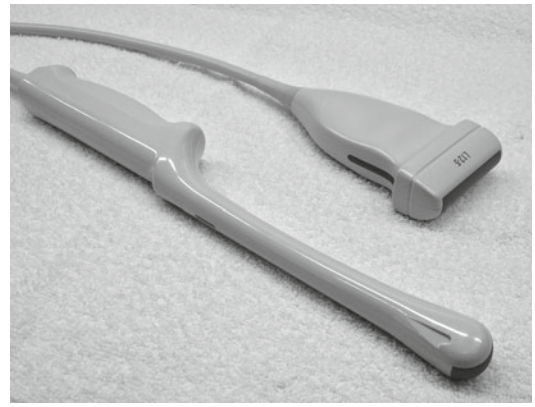

Fig. 17.1 Ultrasound probes: photo shows a high-frequency, linear array transducer above and a curved array endocavitary transducer below

To further discuss the role of ultrasound in the diagnosis and management of male-factor infertility, the current chapter is outlined to review normal and abnormal findings on scrotal and transrectal ultrasonography associated with infertility. When available, standard measurements and anatomic variants are reported. See Table 17.1 for a summary of ultrasound findings associated with male infertility. Brief mention is given to the management of various infertility causes when they relate to pre- and posttreatment ultrasound findings and to the use of ultrasonography with assisted reproductive techniques.

Scrotal Ultrasonography

Ultrasound is an optimal imaging modality for the primary evaluation of scrotal pathology. In addition to providing real-time assessments

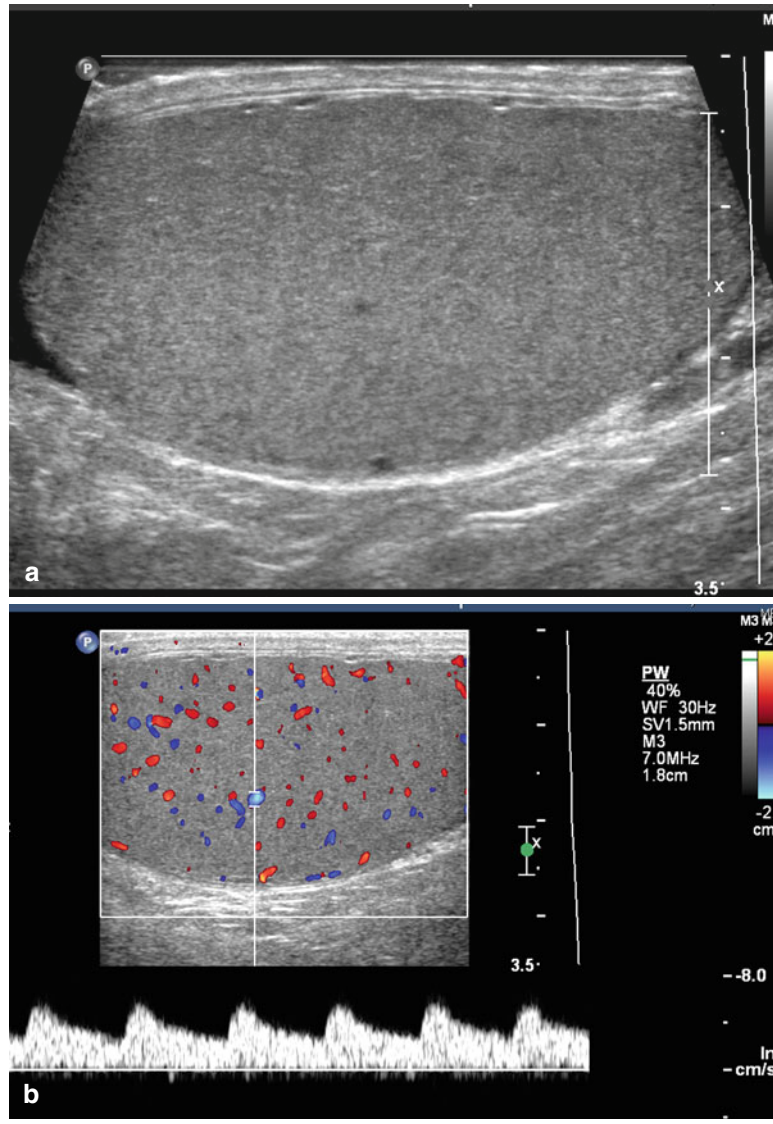

Figs. 17.2 Normal testis: longitudinal sonogram (**a**) shows the testis to have a homogeneous echogenicity and echotexture. Longitudinal color Doppler sonogram (**b**) with duplex shows a normal blood flow pattern and normal intratesticular artery velocity tracing

including patient assistance in localization of findings (e.g., pain), advancements in technology permit increasing resolution of underlying structures, assessments of vascular flow, and tissue characteristics (elastosonography). As the scrotum typically does not consist of gas-containing or large calcified structures, a complete visualization of anatomy is available in multiple planes of imaging.

The role for scrotal ultrasonography in the evaluation of the infertile male has been previously established. Scrotal abnormalities have been reported to occur in 38–65 % of infertile men, approximately 60–70 % of which were not found clinically on physical examination alone [15, 16]. In reporting scrotal ultrasound findings in 545 infertile males with a mean age of 36 years, Sakamoto and colleagues identified left varicoceles in 313 (57.4 %), testicular microlithiasis in 30 (5.5 %), epididymal cysts in 21 (3.9 %), right varicoceles in 4 (0.8 %), testicular cysts in 3 (0.6 %), and a testicular tumor, intrascrotal hemangioma, and hydrocele of the spermatic cord in 1 (0.2 %) patient each [16]. When compared to normospermic men, males with infertility have been confirmed to have significantly increased

Table 17.1 Ultrasound findings associated with male infertility

Structure	US findings	Associations with infertility
Scrotal ultrasound		
Epididymis	Normal caput diameter 7–8 mm	
Cysts	Hypo-/anechoic, well circumscribed, commonly located at head	Simple cysts (no sperm) and spermatoceles (sperm present) not associated with infertility
Infections	Enlarged, thickened, decreased echogenicity	MAGI associated with decreased motility, increased sperm DNA fragmentation, abnormal sperm morphology
Masses	Presence of vascularity, varied echotexture	Most commonly adenomatoid tumors; others include cystadenomas, mesotheliomas, sarcomas
Obstruction	Epididymal enlargement, prominence of rete testis, hypoechoic appearance	Normal-volume ejaculate with oligo-/azoospermia
Testicles		
Cysts	Hypo-/anechoic, well circumscribed, thin wall	Increased incidence, no known impact on fertility
Hydroceles	Fluid located between tunica albuginea and vaginalis	Increased incidence, no known impact on fertility
Infections	Early – decreased echogenicity, increased heterogeneity, enlargement Late – atrophy, increased echogenicity	Associated with subsequent infertility, particularly with postpubertal mumps
Masses	Presence of vascularity, varied echotexture	Increased incidence of benign and malignant masses
Microlithiasis	Increased small focal echogenicity, absence of shadowing	Increased incidence, associated with carcinoma in situ, no known impact on fertility
Torsion	Early – hyperemia, increased size Late – absence of flow, "whirlpool" sign	Unilateral testicular loss associated with decreased sperm density, increased FSH/LH
Trauma	May visualize seminiferous tubules, hematomas	May lead to secondary infertility, antisperm antibodies
Testicular cord		
Masses	Presence of vascularity, varied echotexture	Adenomatoid tumor most common, no known impact on fertility
Varicocele	Internal spermatic vein ≥3 mm	Decreased sperm count, motility, abnormal morphology, decreased sperm function, varicocele grade inversely associated with sperm density
Vas deferens	CBAVD[a] with dilated efferent ducts, prominent epididymal heads, and rete testes	CBAVD found in patients with cystic fibrosis, absence/anomalies of SVs, renal agenesis/anomalies
Transrectal ultrasound		
Prostate		
Cysts	May be located peripherally, midline, paramedian, hypo-/anechoic, thin wall	May result in obstruction, rare malignant processes
Seminal vesicles		
EDO[a]	Dilated ejaculatory duct and SVs, may have calcifications	Low-volume ejaculate, oligo-/azoospermia, decreased fructose and semen pH, requires confirmatory aspiration demonstrating sperm

CBAVD congenital bilateral absence of the vas deferens, *EDO* ejaculatory duct obstruction, *MAGI* male accessory gland infections, *SV* seminal vesicles

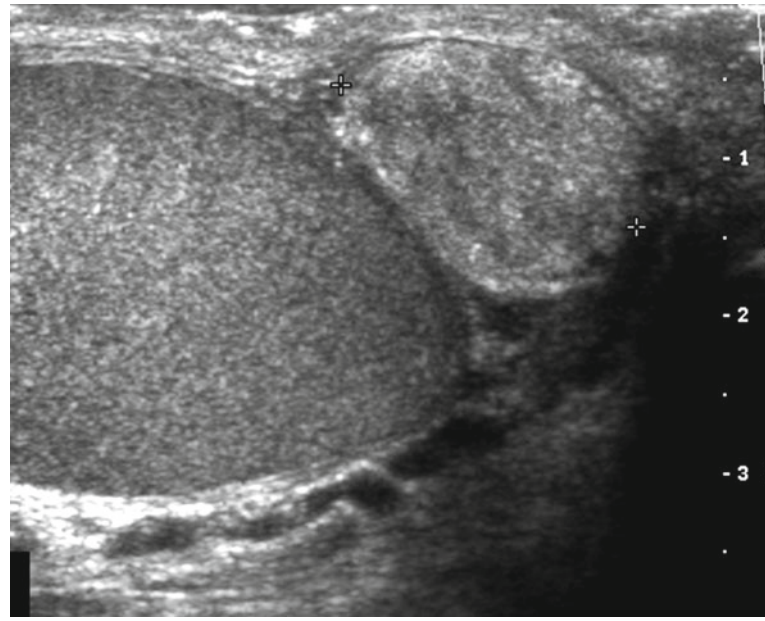

Fig. 17.3 Solid epididymal mass: longitudinal sonogram shows a normal right testis and a solid, heterogeneous mass (between calipers) of the epididymal tail that proved to be an adenomatoid tumor

rates of scrotal findings including varicocele (35.5 % vs. 16 %), hydrocele (16.7 % vs. 8.7 %), testicular microlithiasis (9.8 % vs. 2 %), epididymal enlargement (9 % vs. 2.6 %), and epididymal cysts (7.7 % vs. 2 %) [17].

Color flow Doppler adds further value to scrotal ultrasonography as it provides real-time assessments with increased sensitivity to testicular blood flow. This is particularly useful in cases of testicular ischemia, trauma, differentiation of testicular/paratesticular lesions, and infectious processes. Elastosonography, which further assesses tissue firmness, has also been reported to improve characterization of testicular lesions <1 cm [18].

Given the high rate of intrascrotal findings in infertile men, particularly the increased risk of significant pathology such as testicular tumors, scrotal ultrasound is becoming increasingly utilized in the assessment of males presenting with infertility.

Paratesticular Structures

Epididymis

Ultrasound evaluation of the epididymis is performed to assess for the presence of infectious findings, masses or lesions, or evidence of epididymal obstruction. Measurements of the epididymis are obtained at the caput with a normal epididymis measuring 7–8 mm in diameter, with increasing diameter associated with infectious processes [19]. Epididymitis as a clinical diagnosis may be confirmed with ultrasound findings, which include an enlarged or thickened epididymis with decreased echogenicity.

Infectious processes associated with infertility are more broadly categorized as male accessory gland infections (MAGI), which include infections of the epididymis, seminal vesicles, prostate, or bladder. Organisms commonly identified include Chlamydia, Mycoplasma, and E. coli, although organisms such as tuberculosis have also been directly associated with infertility [20]. Although relatively limited data exist and vary by region, the prevalence of MAGI and infertility have been reported to occur in up to 12 % of cases [21]. Several studies have identified abnormal semen parameters in patients with MAGI including decreased motility, increased abnormal forms, and a higher rate of DNA fragmentation [22, 23]. Despite these findings, the etiologic role of MAGI with male-factor infertility remains unclear, as reports have failed to demonstrate consistent findings [24, 25].

Epididymal masses may be further defined as being solid versus cystic. Solid masses are most commonly benign adenomatoid tumors with additional lesions encountered including cystadenoma, mesothelioma, or sarcomas (Fig. 17.3).

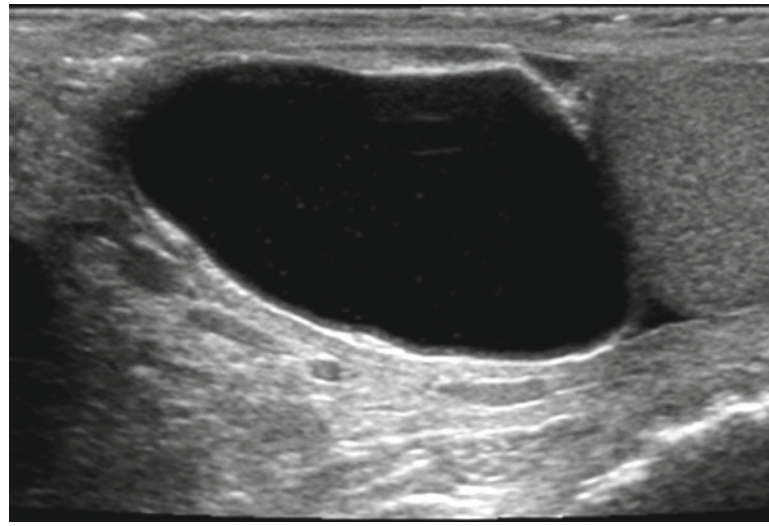

Fig. 17.4 Cystic epididymal mass: longitudinal sonogram shows a large cystic mass of the epididymal head, along the superior aspect of the testis. Spermatocele is likely a diagnosis, particularly given the few low-level echoes within the mass

Cysts of the epididymis are benign lesions commonly located at the head of the epididymis and may represent simple cysts (no sperm in fluid) or spermatoceles (sperm in fluid) (Fig. 17.4). Although epididymal cysts are found more commonly among men with infertility than those without, they have not been shown to result in epididymal obstruction or infertility [17]. In performing surgical resection of spermatoceles and hydroceles, epididymal injury has been reported to occur in 17 and 6 % of cases, respectively [26]. A more recent report by Kauffman and colleagues describing a microsurgical technique of spermatocelectomy demonstrated no changes in sperm count among patients with pre- and postoperative semen analyses, suggesting the absence of iatrogenic epididymal obstruction [27].

In addition to identifying paratesticular masses and infectious processes, improvements in ultrasound resolution have led to its utility in diagnosing epididymal obstruction. Clinical and laboratory findings of epididymal obstruction include normal volume ejaculate with oligo- or azoospermia. Imaging findings may demonstrate epididymal enlargement with prominence of the rete testis and a hypoechoic appearance. Epididymal findings have further been described to help delineate between congenital and acquired causes of obstructive azoospermia. In a report of 211 infertile males undergoing scrotal ultrasonography for obstructive azoospermia, men with a congenital etiology were found to have higher rates of ectasia in the epididymal head with tapering and absence of the epididymal body and tail [28]. Acquired azoospermia, in contrast, exhibited increased rates of epididymal body and tail duct ectasia and an epididymal inflammatory mass.

Varicocele

Varicoceles are reported to occur in approximately 15–25 and 35–60 % of fertile and infertile males, respectively, and remain the most common, reversible cause of male-factor infertility [16, 17, 29]. Clinical varicoceles are more common on the left and are graded on a scale of I–III with grade I varicoceles palpable in the standing position with Valsalva maneuver, grade II palpable in the standing position without Valsalva maneuver, and grade III in the standing position grossly visible. Intratesticular varicoceles identified on ultrasonography are relatively uncommon and are likely of minimal significance for male-factor infertility [30].

Ultrasonography is able to detect varicoceles with a 97 % sensitivity and 94 % specificity [31] (Fig. 17.5). When using the commonly accepted definition of internal spermatic veins measuring ≥3 mm in diameter, ultrasound has been demonstrated to have 53 % sensitivity and 91 % specificity in identifying varicoceles when compared to physical examination [32].

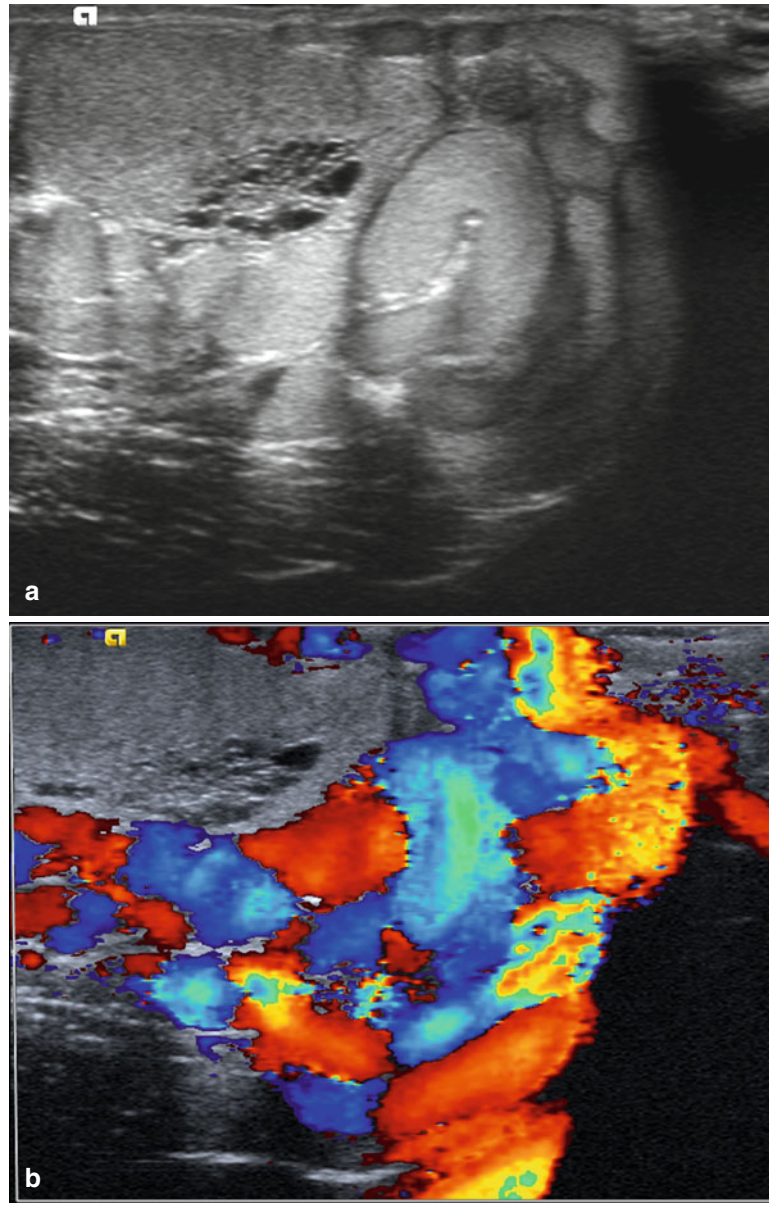

Fig. 17.5 Varicocele: longitudinal sonogram (**a**) shows multiple serpiginous, dilated scrotal veins. Longitudinal color Doppler sonogram (**b**) during Valsalva maneuver shows prominent color flow within the vessels

The presence of a varicocele is associated with infertility and impaired semen characteristics including decreased sperm count, motility, and abnormal morphology [33]. In addition, the grade of the varicocele present has been shown to be inversely associated with sperm density [34]. Among infertile patients with a palpable varicocele, only 33.3 % were found to have normozoospermia, highlighting the significant impact on semen characteristics [34]. Similarly, the presence of a varicocele is associated with impaired sperm function with up to 45 % of infertile males with varicoceles demonstrating an abnormal acrosome reaction [35].

Although there is controversy regarding the optimal treatment of males with clinical and subclinical (detected on imaging alone) varicoceles, correction of a palpable varicocele has been consistently shown to improve semen parameters and may prevent progressive decline [36–41].

While the treatment of subclinical varicoceles has not been shown to improve semen characteristics, their presence may be associated with impaired spermatogenesis [42].

A further role for scrotal ultrasonography in the evaluation of patients with clinical varicoceles is the ability to assess and compare testicular volumes. Men presenting with a left clinically palpable varicocele have been shown to have increased rates of ipsilateral testicular atrophy, while subclinical varicoceles have not been associated with discrepant testicular volumes [43]. These findings are significant as adolescents with testicular volume differentials >10 % have been shown to have significantly lower sperm concentrations when compared to those with <10 % differential. This finding was even more pronounced among those with a >20 % differential volume.

Beyond its initial diagnostic role with varicoceles, ultrasonography has further prognostic value in determining paternity success following varicocelectomy. Patients with testicular atrophy were shown to have decreased paternity (11 %) compared to those with normal testicular volumes (30 %) [44]. Similarly, those with clinically apparent varicoceles, bilateral varicoceles, shunt-type varicoceles (both retrograde and antegrade reflux demonstrated on ultrasound), or a permanent degree of varicocele were associated with decreased paternity [44].

An additional study evaluating the impact of preoperative parameters on surgical outcomes demonstrated significant improvements following microsurgical varicocelectomy in sperm concentration, motility, and morphology in patients with testicular vein measurements (taken at the inferior pole of the testis) >2.5 mm compared to veins measuring <2.5 mm [45]. Reflux identified at the inferior pole was similarly associated with improved sperm characteristics compared to those with reflux only identified in the suprates-ticular venous channels.

Following surgical repair, ultrasound has been reported as a reliable tool in follow-up assessments to document decreased venous diameter at rest and with Valsalva maneuver, although this is of questionable clinical relevance [46].

Vas Deferens

Congenital bilateral absence of the vas deferens (CBAVD) is identified in 1–2 % of infertile males and in approximately 10 % of males with azoospermia [47, 48]. It is found in essentially all patients with cystic fibrosis and is associated with genitourinary abnormalities including absence of the vasal ampulla and seminal vesicles (SV) [49, 50]. Unilateral absence of the vas deferens is associated with both absence (90 % of ipsilateral and 20 % of contralateral) of the SVs as well as SV anomalies including hypoplasia, cysts, and calcifications [49, 51].

Patients found to have an absence of the vas deferens either unilaterally or bilaterally on physical examination can be considered for a confirmatory scrotal ultrasound. Ultrasound findings include absence of the body or tail of the epididymides as well as dilated efferent ducts with associated prominent epididymal heads and rete testis [50, 52, 53]. In the absence of cystic fibrosis, patients with unilateral or bilateral absence of the vas deferens should undergo imaging of the retroperitoneum, as up to 21 or 85 % of patients, respectively, have been reported to have upper tract abnormalities (renal agenesis, renal ectopia, horseshoe kidney) [54, 55].

Testicular Ultrasound

Testicular ultrasonography provides significant information regarding potential etiologies for infertility, identification of prognostic findings, and as a screening modality for associated lesions. Testicular volume assessment may be obtained through various methodologies, with Lambert's formula (volume [mL] = length × width × AP depth [cm] × 0.71) most commonly utilized [56, 57].

Testicular volume is directly associated with semen parameters including total sperm counts, sperm density, and motility. As seminiferous tubules comprise 70–80 % of testicular volume and are responsible for spermatogenesis, a reduced testicular volume has been correlated with global gonadal dysfunction, as indicated by elevated FSH and LH levels [43, 58–62]. Sakamoto and colleagues noted significant

oligospermia in patients with testicular volumes <10 mL (normal 15–20 mL), including length <3.5 cm, depth <1.75 cm, and width <2.5 cm with direct correlations noted with sperm density, total sperm count, motility, and FSH and LH levels [62]. Diminished testicular volume may be secondary to several etiologies including varicoceles, current or previous cryptorchidism, postpubertal mumps, Klinefelter's syndrome, or hormonal abnormalities, among others.

In addition to estimating testicular volume, Doppler ultrasound may be utilized to identify and assess testicular microcirculation. As spermatogenesis is dependent upon microcirculatory perfusion, diminished testicular blood flow as visualized on ultrasound directly correlates with elevated FSH levels and decreased sperm quality [63–65]. Resistive indices may be obtained to further quantify testicular tissue perfusion and are commonly obtained at the level of the testicular artery and via intratesticular branches near the rete testis. Intratesticular branch resistive indices less than 0.6 have been suggested as a threshold level of normal tissue perfusion, with elevated levels indicative of impaired microcirculation [66, 67].

Testicular ultrasound may assist in differentiating between obstructive and nonobstructive etiologies for infertility. Moon and colleagues demonstrated a reduced median testicular volume in patients with nonobstructive (8.3 mL, range 1.2–16.4) versus obstructive (11.6 mL, range 7.7–25.8) azoospermia [68]. Similarly, patients with azoospermia secondary to obstruction were shown to have dilation of the mediastinum testis, epididymis, and intrascrotal portion of the vas deferens. The sensitivity, specificity, and accuracy for differentiating obstructive versus nonobstructive azoospermia were noted to be 82.1, 100, and 87.5 %, respectively. Further findings which suggest a nonobstructive etiology include reduced or absent testicular vessels, with isolated regions of visualized blood flow potentially indicative of residual spermatogenic production [69].

Cryptorchidism

Cryptorchidism is estimated to occur in approximately 2–5 % of boys born at term and is associated with impaired future fertility [70]. Although there is ongoing debate as to the optimal time for orchiopexy, there is increasing consensus that earlier repair (at 6–12 months of age) results in improved long-term fertility potential [71].

In evaluating future paternity in males previously undergoing orchiopexy for undescended testes, Lee and colleagues observed successful paternity within 12 months in 90 and 65 % of patients with prior unilateral or bilateral cryptorchidism, respectively [72]. This was compared against control subjects who demonstrated a 93 % rate of successful paternity. The author concluded that patients with unilateral cryptorchidism have equal rates of paternity to controls, while patients with repaired bilateral cryptorchidism continue to have impairments in paternity lifelong. Further findings indicated that although patients with unilateral cryptorchidism demonstrated equal rates of paternity, they exhibited elevated levels of FSH, decreased inhibin B, and preserved levels of LH/testosterone compared to controls, suggesting subclinical impairments in spermatogenesis.

To further evaluate the effect of timing of orchiopexy on paternity outcomes among azoospermic patients undergoing IVF, Wiser and colleagues found no difference in rates of sperm retrieval, fertilization, implantation, pregnancy, or live birth rates among men with a history of unilateral (2 patients) or bilateral (40 patients) orchiopexy at ≤10 years of age versus >10 years [73]. Despite the late repairs performed, 60 % of patients were found to have sperm at the time of testicular sperm extraction (TESE).

The role for ultrasonography is likely limited in the initial evaluation of patients presenting with cryptorchidism (Fig. 17.6). Tasian and colleagues performed a meta-analysis to review the diagnostic performance of ultrasonography among patients with non-palpable cryptorchidism with results demonstrating a sensitivity of 45 % and specificity of 78 % in localizing nonpalpable testes [74]. These findings increased or decreased in the probability of actually finding an intra-abdominal testicle based on imaging from 55 to 64 % and 49 %, respectively. Given these low rates of precision, the authors indicated

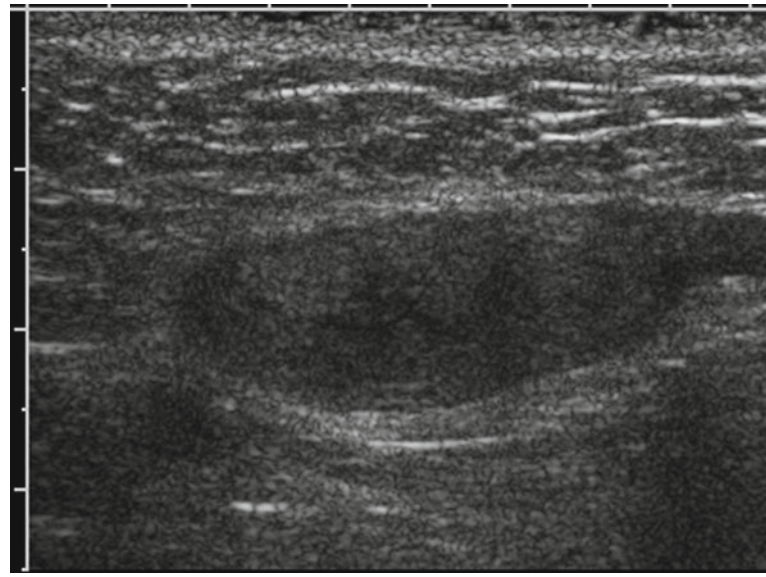

Fig. 17.6 Undescended testis: longitudinal sonogram shows a small, hypoechoic testis in the inguinal canal

that abdominal-scrotal ultrasonography did not reliably assist in the management decision tree for patients with non-palpable testes and was therefore of limited utility. Older patients presenting with non-palpable testes may more reliably undergo MRI in lieu of ultrasound to further assist in localization of intra-abdominal testes.

Although there is likely limited utility for ultrasound during the initial evaluation of undescended testes, patients with a history of cryptorchidism have a known two- to eightfold increased risk of testicular cancer, with 5–10 % of men with testicular cancer having a prior history of cryptorchidism [70, 75]. This finding has led some authors to advocate for the routine use of scrotal ultrasonography as a screening tool for testicular malignancy among patients presenting with infertility, particularly those with a history of cryptorchidism [76–78].

Cysts, Hydrocele, Infectious Processes

Testicular ultrasonography is an excellent modality for identifying benign testicular structures including cysts, hydroceles, and infectious processes. Intratesticular cysts are identified as hypoechoic/anechoic regions, can represent cystic dilation of the rete testes, and may be a result of postinfectious or posttraumatic epididymal obstruction [79, 80]. Testicular cysts have been reported to occur in 1.2 % of infertile men and are of unclear significance [81].

Scrotal hydroceles represent accumulation of fluid within the tunica vaginalis and are commonly the result of prior trauma, inflammatory, or infectious processes. Although there is a known increased prevalence of hydroceles in infertile males (17 % vs. 9 %), it is unclear if treatment of the hydrocele results in improved semen parameters or fertility [17]. Epididymal injury has been reported to occur in up to 6 % of patients undergoing hydrocelectomy, and this injury may result in impaired fertility, including azoospermia [26, 82]. A long-term follow-up study of children undergoing inguinal hernia repairs demonstrated a 5 % infertility rate, with 15 % of patients previously undergoing hydrocelectomy at the time of herniorrhaphy [83]. To our knowledge, no study has thus far examined the impact of hydrocelectomy on semen parameters in infertile males.

Infectious processes of the testicles visualized on ultrasonography may frequently demonstrate decreased echogenicity, increased heterogeneity, hypervascularity, and testicular enlargement (Fig. 17.7). Similar to MAGI, orchitis may be secondary to infectious (E. coli, Chlamydia, Mycobacterium, mumps, among others) or non-infectious etiologies. Although there remains

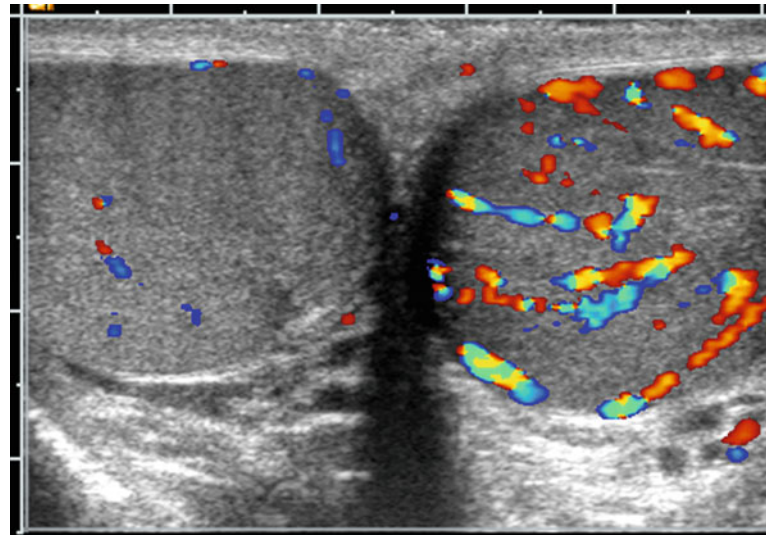

Fig. 17.7 Orchitis: transverse color Doppler sonogram shows both testes with abnormally increased blood flow in the symptomatic left testis

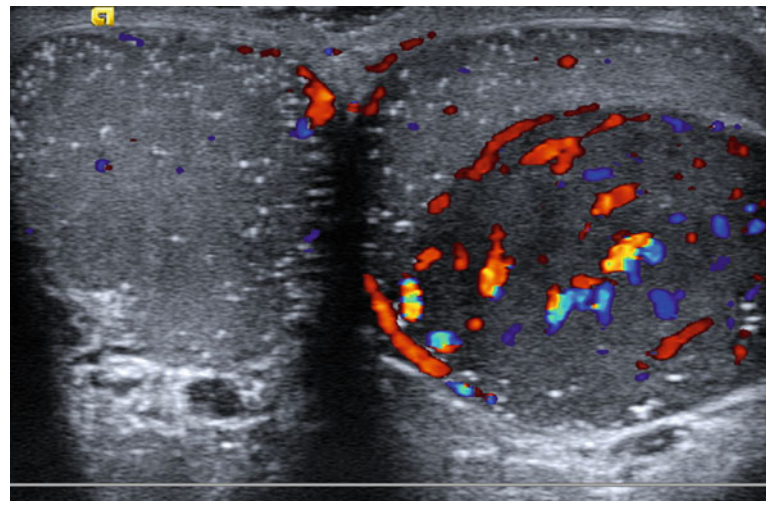

Fig. 17.8 Testicular tumor: transverse color Doppler sonogram shows a large, well-circumscribed hypoechoic mass with prominent blood flow in the left testis and both testes with numerous tiny hyperechoic foci, characteristic of microlithiasis. The mass proved to be a seminoma

limited epidemiological data on the impact of orchitis on overall infertility, previous reports have demonstrated oligospermia and azoospermia occurring at follow-up among 15–33 % and 8–27 % of males with unilateral epididymo-orchitis, respectively [84, 85]. Subsequent pathologic analysis of patients with prior epididymo-orchitis has demonstrated scarring of the seminiferous tubules involving both the ipsilateral and contralateral testicles with chronic inflammatory changes noted [84].

Mumps orchitis is the most common complication of pubertal and postpubertal mumps and is reported to occur in 5–37 % of patients with mumps, with 16–65 % occurring bilaterally [86]. Among patients with a history of mumps orchitis, approximately 50 % will demonstrate some degree of testicular atrophy with one study demonstrating complete atrophy of seminiferous tubules in 38 % of biopsies obtained [24, 87, 88]. These findings may be persistent, even in the setting of appropriate acute phase treatment [88].

Testicular Masses

Males presenting with infertility are at increased risk for both immediate and subsequent development of testicular malignancy (Fig. 17.8). The reported incidence of testicular malignancy in

infertile males ranges from 0.2 to 1 % and is estimated to be 20–100-fold more common than in the general population [15, 19, 77, 89–92]. Men with abnormal semen parameters are also at an increased risk of testicular malignancy with an incidence ratio of 1.6 [93]. Additionally, infertile men continue to be at risk for malignancy following sterility with one report of subsequent development of testicular cancer occurring 14 years after initial evaluation [78]. These findings have led some authors to advocate for the routine use of ultrasound during the initial infertility evaluation [76, 77].

The increasing utilization and improved resolution of scrotal ultrasonography have additionally resulted in an increased rate of detection of testicular lesions with series reporting incidental testicular masses in 1–6 % of infertile patients [77, 91, 94, 95]. When the criteria for an incidental testicular lesion are broadened to include hypoechoic/hyperechoic regions, 34 % (49/145) of azoospermic patients are found to have focal abnormalities, with only one of the 49 cases subsequently found to represent malignancy [92].

This increased rate of detection has also led to an altered ratio of benign versus malignant lesions [96]. Carmignani and colleagues reported on a series of patients undergoing scrotal ultrasonography for infertility evaluations as well as multiple causes (varicoceles, testicular pain) with benign pathology found at surgical excision in 75–80 % of incidentally discovered testicular lesions [91, 94]. Other groups have reported higher ratios of malignancies occurring in 50 % (2/4)–71 % (7/9) of incidental lesions, albeit these series were comprised of relatively small numbers [77, 89]. When benign findings are reported on frozen section with later determination of malignancy on final pathology, subsequent orchiectomy specimens were found to have no residual malignancy detected [89].

Given the higher rate of incidental, benign lesions, close observation with repeat physical examinations and ultrasonography has been proposed for non-palpable testicular lesions, particularly those <1 cm [97]. Despite the increasing rate of detection of benign testicular lesions, the decision as to perform radical excision, testicular sparing surgery, or active surveillance remains an area of active debate.

Of interest, testicular ultrasound findings following sperm retrievals including PESA, TESA, and TESE demonstrate focal abnormalities which persist in 77 and 54 % of patients at 5 days and 6 months, respectively [98]. These findings are not to be misinterpreted as concerning for malignancy in this otherwise at-risk population.

Microlithiasis

Microlithiasis is identified on testicular ultrasonography as hyperechoic regions measuring 3 mm or smaller without definitive shadowing present (Fig. 17.9). Among asymptomatic patients undergoing screening scrotal sonography, testicular microlithiasis is reported in 2.4–6 % of individuals with a higher frequency of testicular microlithiasis present in infertile males (10 % vs. 2 % in controls) [99–101]. Despite the known association between testicular microlithiasis and infertility, Yee and colleagues reported no differences noted in semen analyses between infertile males with microlithiasis versus those without microlithiasis [100].

Microlithiasis has additionally been associated with a relative risk of testicular malignancy of 21.6, with testicular tumors occurring in approximately 6 % of patients with microlithiasis [102, 103]. Patients with microlithiasis and unilateral testicular germ cell tumors have an increased incidence of carcinoma in situ in the contralateral testicle, with some authors recommending routine biopsy of the contralateral testicle [104, 105]. However, subsequent surveillance of patients with isolated testicular microlithiasis followed over a period of 7 years has not been shown to develop malignancy [104].

Given the increased incidence of testicular microlithiasis with malignancy and indeterminate clinical relevance of carcinoma in situ, routine surveillance is commonly recommended with repeat self-testicular exams with or without serial scrotal ultrasonography [102, 103].

Testicular Torsion/Trauma

Scrotal ultrasonography is an excellent imaging modality for the rapid assessment and triage of testicular injuries. In the case of testicular trauma, ultrasonography provides visualization of the tunica albuginea and assessment of rupture of

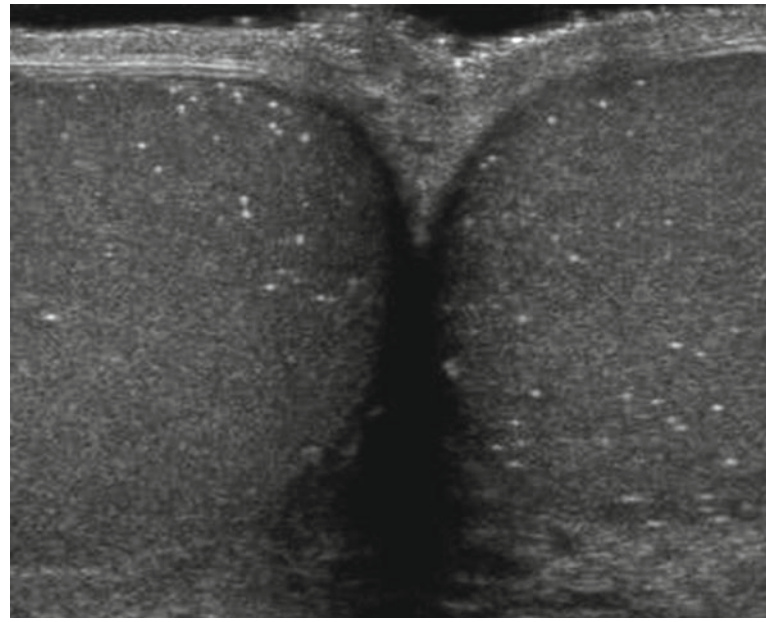

Fig. 17.9 Microlithiasis: transverse sonogram shows multiple diffuse hyperechoic foci with no acoustic shadowing in both testes

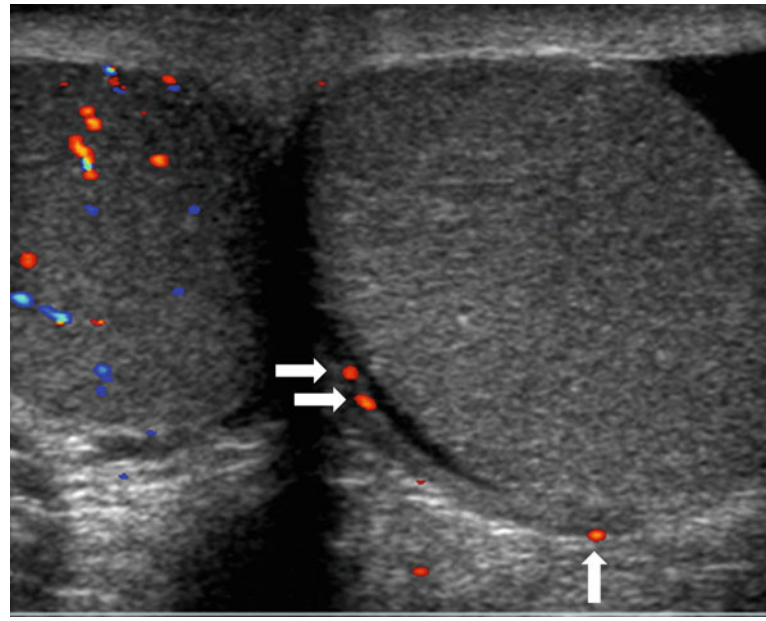

Fig. 17.10 Torsion: transverse color Doppler sonogram shows absence of blood flow in the symptomatic left testis, which is slightly enlarged and surrounded by a small hydrocele. Note normal color flow in the left extratesticular soft tissues (*arrows*)

seminiferous tubules, scrotal and testicular hematomas, and incidental testicular lesions [106]. In patients with an acute scrotum, Doppler ultrasonography is able to differentiate between infectious processes and testicular torsion [107]. Epididymitis and/or orchitis may present with various imaging findings including diffuse hypoechogenicity, enlarged epididymis/testicle, increased heterogeneity, increased Doppler flow, or straightened spermatic cord. In contrast, early or partial testicular torsion may present with venous congestion and preserved arterial inflow. Complete torsion is characterized by the absence of testicular blood flow, frequently with a proximal "whirlpool" sign (Fig. 17.10). Given the occasional difficulty in identifying early ischemic injuries, alternative imaging techniques including pulse inversion ultrasound may eventually

offer a superior assessment in cases of acute ischemia [108].

Multiple studies have examined hormonal and semen profiles following unilateral testicular loss. In patients undergoing orchiectomy secondary to testicular trauma, impaired hormonal and semen characteristics were identified including decreased sperm density and elevated FSH/LH compared to fertile controls [109]. Studies comparing outcomes following orchiectomy versus orchiopexy for acute testicular torsion have reported varied results. Arap and colleagues reported decreased sperm counts and morphology with preserved hormonal levels in patients undergoing either orchiectomy or orchiopexy while a second study noted decreased inhibin B levels in both groups, indicating possible persistent subclinical gonadal dysfunction [110, 111]. Other studies demonstrate decreased inhibin B levels, elevated FSH, and impaired sperm density in patients undergoing orchiectomy compared to orchiopexy [112, 113].

Transrectal Ultrasonography

Transrectal ultrasonography (TRUS) is frequently utilized during the evaluation of male infertility in cases of low-volume ejaculate, azoospermia on semen analysis, or palpable asymmetry on digital rectal exam in order to rule out ejaculatory duct obstruction or to evaluate for the presence/absence of seminal vesicles. TRUS identifies pathologic findings (hypoplastic/atrophic SVs, vasal agenesis, among others) in 75 % of azoospermic males, compared to no pathology in 65 % of non-azoospermic males [114].

TRUS is frequently performed with a 6.5–7.5 MHz probe with the bladder partially filled. Patients are placed in the lateral decubitus and knee-to-chest position and may alternatively be placed in the prone jackknife or dorsolithotomy positions depending on the surgical scenario.

Prostate

Transrectal ultrasonography is an excellent modality to assess obstructive etiologies of infertility including prostatic cysts and ejaculatory duct obstruction (EDO) and may be used as an adjunctive measure in cases of suspected prostatic infections or abscesses. Infertile males with EDO or prostatic cysts may present with varied accompanying symptoms including perineal pain, low-volume ejaculate, hematospermia, painful ejaculation, or epididymal tenderness, among others [6, 23, 24].

Cysts

Prostatic cysts are frequently identified in cases of obstructive azoospermia/severe low-volume oligospermia and may be further classified based on location including peripheral/parenchymal, midline, or paramedian. Midline cysts are typically of a Mullerian embryologic origin and usually do not contain sperm, while paramedian cysts are typically of Wolffian duct origin and may contain sperm upon aspiration [115, 116]. Midline cysts may further be differentiated into utricular cysts which are typically 15 mm in diameter or true Mullerian cysts which may be larger and extend posteriorly beyond the prostatic base (Fig. 17.11). Peripheral cysts may be acquired following infectious processes or rarely may represent benign or malignant processes including multilocular cystadenoma/cystadenocarcinoma [117, 118].

Ejaculatory Duct Obstruction

The ejaculatory duct is minimally visualized on ultrasonography in the absence of obstruction and enters the urethra at the level of the verumontanum with standard lengths of approximately 4–8 mm and a lumen of 2 mm. In contrast, ejaculatory duct obstruction (EDO) is often well demonstrated in the sagittal view and is commonly associated with dilation of the ejaculatory duct, seminal vesicles, and occasional ejaculatory ductal calcifications.

Ejaculatory duct obstruction may occur secondary to congenital processes including compression by prostatic cysts or ejaculatory duct atresia/stenosis or may be acquired from infections (UTI, sexually transmitted diseases, tuberculosis), inflammatory conditions, traumatic strictures, or stone formation or following prior surgical procedures (transurethral resection of

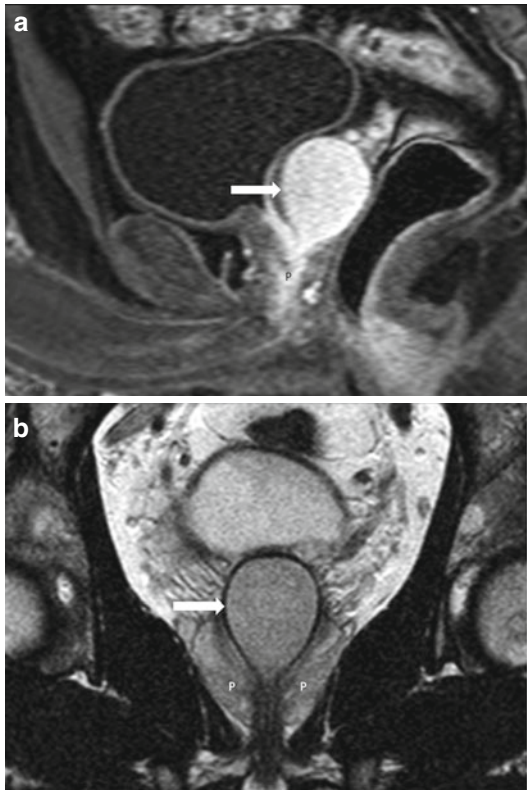

Fig. 17.11 Mullerian duct cyst: sagittal T1-weighted, post-contrast (**a**), and coronal T2-weighted (**b**) MR images show a midline, large Mullerian duct cyst (*arrows*) arising from the verumontanum and extending above the prostate (*p*). The cyst does not enhance but has high signal intensity on the T1-weighted image because of hemorrhagic or proteinaceous content

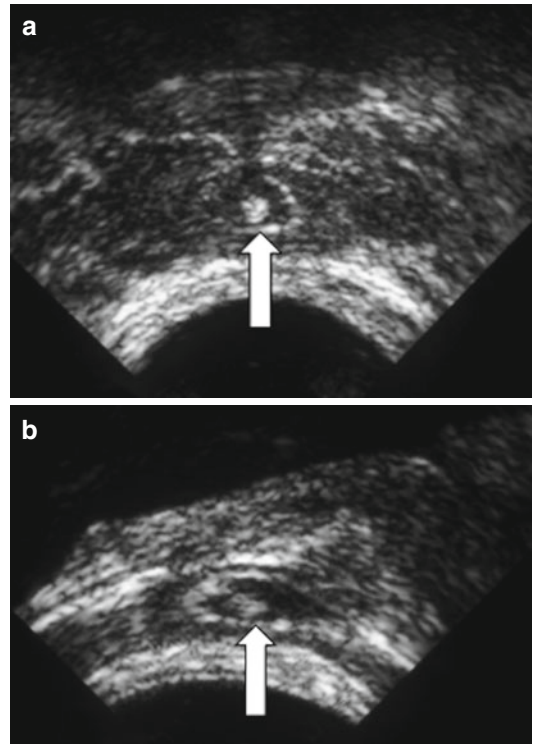

Fig. 17.12 Stone in dilated ejaculatory duct: transverse (**a**) and longitudinal (**b**) transrectal sonograms show a very small hyperechogenic stone (*arrows*) in the dilated right ejaculatory duct

the prostate, exstrophy repair, colorectal surgery) [119–122] (Fig. 17.12). Partial EDO may result from any of the above etiologies and has a variable presentation including low volume with varied sperm densities/total sperm on semen analysis and dilation of one or both of the SVs [123, 124].

Although TRUS findings may suggest EDO, confirmatory tests are commonly required given the relatively low specificity of TRUS alone. In males with azoospermia/severe oligospermia suspected of having EDO, TRUS with concurrent SV aspiration demonstrating the presence of sperm (common definition requiring three or more per high power field) confirmed obstruction in 49.1 % of cases [114, 125–127]. Similarly, Purohit and colleagues compared adjunctive testing including chromotubation, SV aspiration, and seminal vesiculography with confirmation of EDO in 52, 48, and 36 % of cases, respectively [128]. An additional measure which is less commonly utilized includes ejaculatory ductal manometry which identifies higher opening pressures in men with EDO compared to fertile controls [129].

The treatment of EDO is frequently performed in combination with TRUS to confirm treatment success and assist in localization or extent of obstruction where indicated. Isolated cysts resulting in compression of the ejaculatory duct may be treated with aspiration alone when not in communication with the ejaculatory system or with transurethral resection of the ejaculatory duct (TURED) when communication exists [120, 130]. Results of TURED for complete EDO demonstrate improved semen quality in 50–92 % of patients with complete EDO with subsequent spontaneous (without need for ART) paternity rates of 13–29 % [131–135]. An alternative therapy for the treatment of EDO

includes ejaculatory ductal dilation utilizing seminal vesicoscopy, with one study demonstrating equal efficacy and fewer complications compared to TURED [136].

Calcifications of the prostate are commonly visualized on transrectal ultrasonography and are of unlikely significance in regards to infertility. Increasing calcifications are associated with age and are present in 23 % of asymptomatic males aged 20–29 versus 83 % in males 60–69 years old [137].

Seminal Vesicles

The SVs are clearly visualized on TRUS cephalad to the prostate and posterior to the bladder and may result in decreases to semen volume, pH, and fructose concentration when abnormalities are present. Although there is variability in reported standard SV lengths, normal, hypoplastic, and atrophic are commonly classified as occurring at >24, 17–24, and <17 mm, respectively, without significant change following ejaculation [137–139]

Dilation of the SVs resulting from mechanical obstruction, particularly when >15 mm, is most commonly associated with EDO as described previously. Dilation may also be seen in patients with adult polycystic disease and infertility, ipsilateral upper urinary tract agenesis (Zinner syndrome), or diabetes mellitus and is felt to be secondary in these cases to SV hypotonicity rather than anatomic obstruction [140–142].

Absence of the SVs is associated with cystic fibrosis and unilateral/bilateral absence of the vas deferens as well as renal anomalies including renal agenesis, ectopia, and horseshoe, among others [49, 51, 54, 55]. Infections of the seminal vesicles may also be visualized on ultrasound and have been reported to impact fertility with improved semen parameters following antibiotic therapy [143].

Assisted Reproductive Techniques

In addition to the initial evaluation of the infertile male, ultrasound has been increasingly utilized in the performance of sperm retrieval for use in ARTs. Several studies have examined the use of power Doppler at the time of TESE to identify regions with increased sperm density to improve the likelihood of sperm retrieval.

Herwig and colleagues reported on the use of a laser Doppler scanner to determine perfusion rates and noted higher sperm quality and quantity based on underlying tissue perfusion. In patients with at least 70 tissue perfusion units (TPU), 72.3 % of biopsies identified progressive sperm compared to 13.3 % among those with ten or fewer TPUs [65, 144]. A similar study performed in patients with nonobstructive azoospermia demonstrated successful sperm extractions in 38 and 14 % of patients with subjective good versus poor vascularity, respectively [145]. A more recent Cochrane review evaluating the efficacy of various techniques for sperm aspiration demonstrated no statistically significant improvement in ultrasound-guided testicular sperm aspiration versus aspirations performed without ultrasound [146]. It is not clear, however, how these techniques compare to the results reported by Herwig and colleagues, and therefore the role for ultrasound at the time of sperm extraction remains unclear.

Further techniques to enhance extraction of sperm at the time of TESE are being developed with Ramkumar and colleagues recently reporting their initial experience with microdissection probe-TESE (MP-TESE) [147]. The procedure utilizes a microfabricated silicon microprobe with an ultrasonic horn actuator and strain gauges to detect tissue interface boundaries between seminiferous tubules. This reportedly improves size discrimination of seminiferous tubules with the average diameter of sperm containing tubules noted to be 41.2 +/− 1.6 μm per report. Although this technology reports intriguing findings, it has yet to be validated by other groups and remains experimental at the present time.

Conclusion

Ultrasonography, including adjunctive techniques of power and duplex Doppler, is increasingly utilized in the evaluation and management of male-factor infertility. Scrotal and transrectal ultrasonographies provide

both anatomic and functional information to assist in identifying underlying etiologies for infertility including infectious processes and varicoceles as well as differentiating between obstructive (EDO, epididymal obstruction, absence of the vas deferens) and nonobstructive causes. Ultrasonography may additionally detect associated findings including testicular/paratesticular lesions, upper tract renal anomalies, testicular microlithiasis, hydroceles, and cysts. Although ultrasound currently has a limited role with ARTs, an emerging body of investigative literature suggests that its use at the time of TESE may enhance the yield of sperm obtained and therefore improve overall outcomes. As ultrasound technology continues to improve, it will likely play an increasingly prominent role in the evaluation and treatment of male-factor infertility.

References

1. Brugh 3rd VM, Matschke HM, Lipshultz LI. Male factor infertility. Endocrinol Metab Clin North Am. 2003;32:689.
2. Jaffe SB, Jewelewicz R. The basic infertility investigation. Fertil Steril. 1991;56:599.
3. Bablok L, Dziadecki W, Szymusik I, et al. Patterns of infertility in Poland – multicenter study. Neuro Endocrinol Lett. 2012;32:799.
4. Chiamchanya C, Su-angkawatin W. Study of the causes and the results of treatment in infertile couples at Thammasat Hospital between 1999–2004. J Med Assoc Thai. 2008;91:805.
5. Sundby J. Methodological considerations in the study of frequency, risk factors and outcome of reduced fertility. Scand J Soc Med. 1989;17:135.
6. Wilkes S, Chinn DJ, Murdoch A, et al. Epidemiology and management of infertility: a population-based study in UK primary care. Fam Pract. 2009;26:269.
7. Hull MG, Glazener CM, Kelly NJ, et al. Population study of causes, treatment, and outcome of infertility. BMJ. 1985;291:1693.
8. Milardi D, Grande G, Sacchini D, et al. Male fertility and reduction in semen parameters: a single tertiary-care center experience. Int J Endocrinol. 2012;2012:649149.
9. Thonneau P, Marchand S, Tallec A, et al. Incidence and main causes of infertility in a resident population (1,850,000) of three French regions (1988–1989). Human Reprod. 1991;6:811.
10. Male Infertility Best Practice Policy Committee of the American Urological Association; Practice Committee of the American Society for Reproductive Medicine. Report on optimal evaluation of the infertile male. Fertil Steril. 2006;86(5 Suppl 1):S202–9.
11. Male Infertility Best Practice Policy Committee of the American Urological Association; Practice Committee of the American Society for Reproductive Medicine. Report on evaluation of the azoospermic male. Fertil Steril. 2006;86(5 Suppl 1):S210–5.
12. Practice Committee of the American Society for Reproductive Medicine. Report on management of obstructive azoospermia. Fertil Steril. 2006;86 (5 Suppl 1):S259–63.
13. American Society for Reproductive Medicine. Report on varicocele and infertility. Fertil Steril. 2008;90: S247–249.
14. Dohle GR, Colpi GM, Hargreave TB, et al. EAU guidelines on male infertility. Eur Urol. 2005;48:703.
15. Pierik FH, Dohle GR, van Muiswinkel JM, et al. Is routine scrotal ultrasound advantageous in infertile men? J Urol. 1999;162:1618.
16. Sakamoto H, Saito K, Shichizyo T, et al. Color Doppler ultrasonography as a routine clinical examination in male infertility. Int J Urol. 2006;13:1073.
17. Qublan HS, Al-Okoor K, Al-Ghoweri AS, et al. Sonographic spectrum of scrotal abnormalities in infertile men. J Clin Ultrasound. 2007;35:437.
18. Grasso M, Blanco S, Raber M, et al. Elastosonography of the testis: preliminary experience. Arch Ital Urol Androl. 2010;82:160.
19. Nashan D, Behre HM, Grunert JH, et al. Diagnostic value of scrotal sonography in infertile men: report on 658 cases. Andrologia. 1990;22:387.
20. Wise GJ, Marella VK. Genitourinary manifestations of tuberculosis. Urol Clin North Am. 2003;30:111.
21. Everaert K, Mahmoud A, Depuydt C, et al. Chronic prostatitis and male accessory gland infection – is there an impact on male infertility (diagnosis and therapy)? Andrologia. 2003;35:325.
22. La Vignera S, Condorelli R, D'Agata R, et al. Semen alterations and flow-cytometry evaluation in patients with male accessory gland infections (MAGI). J Endocrinol Invest. 2012;35(2):219–23.
23. Lotti F, Corona G, Mancini M, et al. Ultrasonographic and clinical correlates of seminal plasma interleukin-8 levels in patients attending an andrology clinic for infertility. Int J Androl. 2011;34:600.
24. Weidner W, Krause W, Ludwig M. Relevance of male accessory gland infection for subsequent fertility with special focus on prostatitis. Hum Reprod Update. 1999;5:421.
25. Huwe P, Diemer T, Ludwig M, et al. Influence of different uropathogenic microorganisms on human sperm motility parameters in an in vitro experiment. Andrologia. 1998;30 Suppl 1:55.
26. Zahalsky MP, Berman AJ, Nagler HM. Evaluating the risk of epididymal injury during hydrocelectomy and spermatocelectomy. J Urol. 2004;171:2291.
27. Kauffman EC, Kim HH, Tanrikut C, et al. Microsurgical spermatocelectomy: technique and outcomes of a novel surgical approach. J Urol. 2011;185:238.

28. Wang ZQ, Li FH, Du J, et al. Ultrasonographic features of epididymides in obstructive azoospermia. Zhonghua Nan Ke Xue. 2010;16:984.
29. Cocuzza M, Athayde KS, Alvarenga C, et al. Grade 3 varicocele in fertile men: a different entity. J Urol. 2012;187(4):1363–8.
30. Vasilios S, Charalampos L, Elias P, et al. Ultrasound findings of an intratesticular varicocele. Report of a new case and review of the literature. Int Urol Nephrol. 2006;38:115.
31. Trum JW, Gubler FM, Laan R, et al. The value of palpation, varicoscreen contact thermography and colour Doppler ultrasound in the diagnosis of varicocele. Hum Reprod. 1996;11:1232.
32. Chiou RK, Anderson JC, Wobig RK, et al. Color Doppler ultrasound criteria to diagnose varicoceles: correlation of a new scoring system with physical examination. Urology. 1997;50:953.
33. MacLeod J. Seminal cytology in the presence of varicocele. Fertil Steril. 1965;16:735.
34. Al-Ali BM, Marszalek M, Shamloul R, et al. Clinical parameters and semen analysis in 716 Austrian patients with varicocele. Urology. 2010;75:1069.
35. Glazier DB, Marmar JL, Diamond SM, et al. A modified acrosome induction test. Arch Androl. 2000;44:59.
36. Dohle GR, Colpi GM, Hargreave TB, et al. EAU guidelines on male infertility. Eur Urol. 2005;48:703.
37. Zheng YQ, Gao X, Li ZJ, et al. Efficacy of bilateral and left varicocelectomy in infertile men with left clinical and right subclinical varicoceles: a comparative study. Urology. 2009;73:1236.
38. Marmar JL, Agarwal A, Prabakaran S, et al. Reassessing the value of varicocelectomy as a treatment for male subfertility with a new meta-analysis. Fertil Steril. 2007;88:639.
39. Agarwal A, Deepinder F, Cocuzza M, et al. Efficacy of varicocelectomy in improving semen parameters: new meta-analytical approach. Urology. 2007;70:532.
40. Zorba UO, Sanli OM, Tezer M, et al. Effect of infertility duration on postvaricocelectomy sperm counts and pregnancy rates. Urology. 2009;73:767.
41. Romeo C, Santoro G. Varicocele and infertility: why a prevention? J Endocrinol Invest. 2009;32:559.
42. Kondoh N, Meguro N, Matsumiya K, et al. Significance of subclinical varicocele detected by scrotal sonography in male infertility: a preliminary report. J Urol. 1993;150:1158.
43. Sakamoto H, Ogawa Y, Yoshida H. Relationship between testicular volume and varicocele in patients with infertility. Urology. 2008;71:104.
44. Donkol RH, Salem T. Paternity after varicocelectomy: preoperative sonographic parameters of success. J Ultrasound Med. 2007;26:593.
45. Hussein AF. The role of color Doppler ultrasound in prediction of the outcome of microsurgical subinguinal varicocelectomy. J Urol. 2006;176:2141.
46. El-Haggar S, Nassef S, Gadalla A, et al. Ultrasonographic parameters of the spermatic veins at the inguinal and scrotal levels in varicocele diagnosis and post-operative repair. Andrologia. 2012;44(3):210–3.
47. Jequier AM, Ansell ID, Bullimore NJ. Congenital absence of the vasa deferentia presenting with infertility. J Androl. 1985;6:15.
48. Bromage SJ, Falconer DA, Lieberman BA, et al. Sperm retrieval rates in subgroups of primary azoospermic males. Eur Urol. 2007;51:534.
49. Raviv G, Mor Y, Levron J, et al. Role of transrectal ultrasonography in the evaluation of azoospermic men with low-volume ejaculate. J Ultrasound Med. 2006;25:825.
50. Cornud F, Amar E, Hamida K, et al. Imaging in male hypofertility and impotence. BJU Int. 2000;86 Suppl 1:153.
51. Hall S, Oates RD. Unilateral absence of the scrotal vas deferens associated with contralateral mesonephric duct anomalies resulting in infertility: laboratory, physical and radiographic findings, and therapeutic alternatives. J Urol. 1993;150:1161.
52. Sakamoto H, Yajima T, Suzuki K, et al. Cystic fibrosis transmembrane conductance regulator (CFTR) gene mutation associated with a congenital bilateral absence of vas deferens. Int J Urol. 2008;15:270.
53. Cornud F, Belin X, Delafontaine D, et al. Imaging of obstructive azoospermia. Eur Radiol. 1997;7:1079.
54. Donohue RE, Fauver HE. Unilateral absence of the vas deferens. A useful clinical sign. JAMA. 1989; 261:1180.
55. Augarten A, Yahav Y, Kerem BS, et al. Congenital bilateral absence of vas deferens in the absence of cystic fibrosis. Lancet. 1994;344:1473.
56. Sakamoto H, Saito K, Oohta M, et al. Testicular volume measurement: comparison of ultrasonography, orchidometry, and water displacement. Urology. 2007;69:152.
57. Sakamoto H, Saito K, Ogawa Y, et al. Testicular volume measurements using Prader orchidometer versus ultrasonography in patients with infertility. Urology. 2007;69:158.
58. Lenz S, Thomsen JK, Giwercman A, et al. Ultrasonic texture and volume of testicles in infertile men. Hum Reprod. 1994;9:878.
59. Bujan L, Mieusset R, Mansat A, et al. Testicular size in infertile men: relationship to semen characteristics and hormonal blood levels. Br J Urol. 1989;64:632.
60. Sakamoto H, Ogawa Y, Yoshida H. Relationship between testicular volume and testicular function: comparison of the Prader orchidometric and ultrasonographic measurements in patients with infertility. Asian J Androl. 2008;10:319.
61. Arai T, Kitahara S, Horiuchi S, et al. Relationship of testicular volume to semen profiles and serum hormone concentrations in infertile Japanese males. Int J Fertil Womens Med. 1998;43:40.
62. Sakamoto H, Yajima T, Nagata M, et al. Relationship between testicular size by ultrasonography and testicular function: measurement of testicular length, width, and depth in patients with infertility. Int J Urol. 2008;15:529.
63. Battaglia C, Pasini A, Mancini F, et al. Role of intratesticular ultrasonographic and Doppler flow analyses

in evaluating gonadal status in male survivors of childhood malignancy. Fertil Steril. 2005;83:1867.
64. Tarhan S, Gumus B, Gunduz I, et al. Effect of varicocele on testicular artery blood flow in men – color Doppler investigation. Scand J Urol Nephrol. 2003;37:38.
65. Herwig R, Tosun K, Schuster A, et al. Tissue perfusion-controlled guided biopsies are essential for the outcome of testicular sperm extraction. Fertil Steril. 2007;87:1071.
66. Schurich M, Aigner F, Frauscher F, et al. The role of ultrasound in assessment of male fertility. Eur J Obstet Gynecol Reprod Biol. 2009;144 Suppl 1:S192.
67. Unsal A, Turgut AT, Taskin F, et al. Resistance and pulsatility index increase in capsular branches of testicular artery: indicator of impaired testicular microcirculation in varicocele? J Clin Ultrasound. 2007;35:191.
68. Moon MH, Kim SH, Cho JY, et al. Scrotal US for evaluation of infertile men with azoospermia. Radiology. 2006;239:168.
69. Foresta C, Garolla A, Bettella A, et al. Doppler ultrasound of the testis in azoospermic subjects as a parameter of testicular function. Hum Reprod. 1998;13:3090.
70. Toppari J, Kaleva M. Maldescendus testis. Horm Res. 1999;51:261.
71. Ritzen EM, Bergh A, Bjerknes R, et al. Nordic consensus on treatment of undescended testes. Acta Paediatr. 2007;96:638.
72. Lee PA. Fertility after cryptorchidism: epidemiology and other outcome studies. Urology. 2005;66:427.
73. Wiser A, Raviv G, Weissenberg R, et al. Does age at orchidopexy impact on the results of testicular sperm extraction? Reprod Biomed Online. 2009;19:778.
74. Tasian GE, Copp HL. Diagnostic performance of ultrasound in nonpalpable cryptorchidism: a systematic review and meta-analysis. Pediatrics. 2011;127:119.
75. Dieckmann KP, Pichlmeier U. Clinical epidemiology of testicular germ cell tumors. World J Urol. 2004;22:2.
76. Onur MR, Firdolas F, Onur R, et al. Scrotal ultrasonography: should it be used in routine evaluation of infertile men? Andrologia. 2008;40:58.
77. Phillips N, Jequier AM. Early testicular cancer: a problem in an infertility clinic. Reprod Biomed Online. 2007;15:520.
78. Kanto S, Takahashi K, Maehara I, et al. Incidental testicular cancers that subsequently developed in oligozoospermic and azoospermic patients: report of three cases. Fertil Steril. 2007;88:1374.
79. Older RA, Watson LR. Tubular ectasia of the rete testis: a benign condition with a sonographic appearance that may be misinterpreted as malignant. J Urol. 1994;152:477.
80. Colangelo SM, Fried K, Hyacinthe LM, et al. Tubular ectasia of the rete testis: an ultrasound diagnosis. Urology. 1995;45:532.
81. Jequier AM, Phillips N. Cystic dilatation of the rete testis: a hidden diagnosis among infertile men. Reprod Biomed Online. 2009;18:190.
82. Ross LS, Flom LS. Azoospermia: a complication of hydrocele repair in a fertile population. J Urol. 1991; 146:852.
83. Zendejas B, Zarroug AE, Erben YM, et al. Impact of childhood inguinal hernia repair in adulthood: 50 years of follow-up. J Am Coll Surg. 2010;211:762.
84. Osegbe DN. Testicular function after unilateral bacterial epididymo-orchitis. Eur Urol. 1991;19:204.
85. Weidner W, Garbe C, Weissbach L, et al. Initial therapy of acute unilateral epididymitis using ofloxacin. II. Andrological findings. Urologe A. 1990;29:277.
86. Beard CM, Benson Jr RC, Kelalis PP, et al. The incidence and outcome of mumps orchitis in Rochester, Minnesota, 1935 to 1974. Mayo Clin Proc. 1977;52:3.
87. Mikuz G, Damjanov I. Inflammation of the testis, epididymis, peritesticular membranes, and scrotum. Pathol Annu. 1982;17(Pt 1):101.
88. Yeniyol CO, Sorguc S, Minareci S, et al. Role of interferon-alpha-2B in prevention of testicular atrophy with unilateral mumps orchitis. Urology. 2000;55:931.
89. Powell TM, Tarter TH. Management of nonpalpable incidental testicular masses. J Urol. 2006;176:96.
90. Raman JD, Nobert CF, Goldstein M. Increased incidence of testicular cancer in men presenting with infertility and abnormal semen analysis. J Urol. 2005; 174:1819.
91. Carmignani L, Gadda F, Mancini M, et al. Detection of testicular ultrasonographic lesions in severe male infertility. J Urol. 2004;172:1045.
92. Eifler Jr JB, King P, Schlegel PN. Incidental testicular lesions found during infertility evaluation are usually benign and may be managed conservatively. J Urol. 2008;180:261.
93. Jacobsen R, Bostofte E, Engholm G, et al. Risk of testicular cancer in men with abnormal semen characteristics: cohort study. BMJ. 2000;321:789.
94. Carmignani L, Gadda F, Gazzano G, et al. High incidence of benign testicular neoplasms diagnosed by ultrasound. J Urol. 2003;170:1783.
95. Hopps CV, Goldstein M. Ultrasound guided needle localization and microsurgical exploration for incidental nonpalpable testicular tumors. J Urol. 2002;168:1084.
96. Leonhartsberger N, Ramoner R, Aigner F, et al. Increased incidence of Leydig cell tumours of the testis in the era of improved imaging techniques. BJU Int. 2011;108:1603.
97. Toren PJ, Roberts M, Lecker I, et al. Small incidentally discovered testicular masses in infertile men – is active surveillance the new standard of care? J Urol. 2010;183:1373.
98. Ron-El R, Strauss S, Friedler S, et al. Serial sonography and colour flow Doppler imaging following testicular and epididymal sperm extraction. Hum Reprod. 1998;13:3390.
99. Serter S, Gumus B, Unlu M, et al. Prevalence of testicular microlithiasis in an asymptomatic population. Scand J Urol Nephrol. 2006;40:212.
100. Yee WS, Kim YS, Kim SJ, et al. Testicular microlithiasis: prevalence and clinical significance in a

population referred for scrotal ultrasonography. Korean J Urol. 2011;52:172.
101. Aizenstein RI, DiDomenico D, Wilbur AC, et al. Testicular microlithiasis: association with male infertility. J Clin Ultrasound. 1998;26:195.
102. Cast JE, Nelson WM, Early AS, et al. Testicular microlithiasis: prevalence and tumor risk in a population referred for scrotal sonography. AJR Am J Roentgenol. 2000;175:1703.
103. Lam DL, Gerscovich EO, Kuo MC, et al. Testicular microlithiasis: our experience of 10 years. J Ultrasound Med. 2007;26:867.
104. Sakamoto H, Shichizyou T, Saito K, et al. Testicular microlithiasis identified ultrasonographically in Japanese adult patients: prevalence and associated conditions. Urology. 2006;68:636.
105. Meissner A, Mamoulakis C, de la Rosette JJ, et al. Clinical update on testicular microlithiasis. Curr Opin Urol. 2009;19:615.
106. Bhatt S, Dogra VS. Role of US in testicular and scrotal trauma. Radiographics. 2008;28:1617.
107. Vijayaraghavan SB. Sonographic differential diagnosis of acute scrotum: real-time whirlpool sign, a key sign of torsion. J Ultrasound Med. 2006;25:563.
108. Paltiel HJ, Kalish LA, Susaeta RA, et al. Pulse-inversion US imaging of testicular ischemia: quantitative and qualitative analyses in a rabbit model. Radiology. 2006;239:718.
109. Lin WW, Kim ED, Quesada ET, et al. Unilateral testicular injury from external trauma: evaluation of semen quality and endocrine parameters. J Urol. 1998;159:841.
110. Arap MA, Vicentini FC, Cocuzza M, et al. Late hormonal levels, semen parameters, and presence of antisperm antibodies in patients treated for testicular torsion. J Androl. 2007;28:528.
111. Romeo C, Impellizzeri P, Arrigo T, et al. Late hormonal function after testicular torsion. J Pediatr Surg. 2010;45:411.
112. Anderson MJ, Dunn JK, Lipshultz LI, et al. Semen quality and endocrine parameters after acute testicular torsion. J Urol. 1992;147:1545.
113. Taskinen S, Taskinen M, Rintala R. Testicular torsion: orchiectomy or orchiopexy? J Pediatr Urol. 2008;4:210.
114. Engin G, Kadioglu A, Orhan I, et al. Transrectal US and endorectal MR imaging in partial and complete obstruction of the seminal duct system. A comparative study. Acta Radiol. 2000;41:288.
115. Parsons RB, Fisher AM, Bar-Chama N, et al. MR imaging in male infertility. Radiographics. 1997;17:627.
116. Jarow JP. Transrectal ultrasonography of infertile men. Fertil Steril. 1993;60:1035.
117. Tuziak T, Spiess PE, Abrahams NA, et al. Multilocular cystadenoma and cystadenocarcinoma of the prostate. Urol Oncol. 2007;25:19.
118. Park JP, Cho NH, Oh YT, et al. Giant multilocular prostatic cystadenoma presenting with obstructive aspermia. Yonsei Med J. 2007;48:554.
119. Goluboff ET, Stifelman MD, Fisch H. Ejaculatory duct obstruction in the infertile male. Urology. 1995;45:925.
120. Donkol RH. Imaging in male-factor obstructive infertility. World J Radiol. 2010;2:172.
121. Philip J, Manikandan R, Lamb GH, et al. Ejaculatory-duct calculus causing secondary obstruction and infertility. Fertil Steril. 2007;88:706 e9.
122. Pryor JP, Hendry WF. Ejaculatory duct obstruction in subfertile males: analysis of 87 patients. Fertil Steril. 1991;56:725.
123. Nagler HM, Rotman M, Zoltan E, et al. The natural history of partial ejaculatory duct obstruction. J Urol. 2002;167:253.
124. Ruiz Rubio JL, Fernandez Gonzalez I, Quijano Barroso P, et al. The value of transrectal ultrasonography in the diagnosis and treatment of partial obstruction of the seminal duct system. J Urol. 1995;153:435.
125. Engin G, Celtik M, Sanli O, et al. Comparison of transrectal ultrasonography and transrectal ultrasonography-guided seminal vesicle aspiration in the diagnosis of the ejaculatory duct obstruction. Fertil Steril. 2009;92:964.
126. Orhan I, Onur R, Cayan S, et al. Seminal vesicle sperm aspiration in the diagnosis of ejaculatory duct obstruction. BJU Int. 1999;84:1050.
127. Jarow JP. Seminal vesicle aspiration of fertile men. J Urol. 1996;156:1005.
128. Purohit RS, Wu DS, Shinohara K, et al. A prospective comparison of 3 diagnostic methods to evaluate ejaculatory duct obstruction. J Urol. 2004;171:232.
129. Eisenberg ML, Walsh TJ, Garcia MM, et al. Ejaculatory duct manometry in normal men and in patients with ejaculatory duct obstruction. J Urol. 2008;180:255.
130. Stricker HJ, Kunin JR, Faerber GJ. Congenital prostatic cyst causing ejaculatory duct obstruction: management by transrectal cyst aspiration. J Urol. 1993;149:1141.
131. Heshmat S, Lo KC. Evaluation and treatment of ejaculatory duct obstruction in infertile men. Can J Urol. 2006;13 Suppl 1:18.
132. Schroeder-Printzen I, Ludwig M, Kohn F, et al. Surgical therapy in infertile men with ejaculatory duct obstruction: technique and outcome of a standardized surgical approach. Hum Reprod. 2000;15:1364.
133. Meacham RB, Hellerstein DK, Lipshultz LI. Evaluation and treatment of ejaculatory duct obstruction in the infertile male. Fertil Steril. 1993;59:393.
134. Kadioglu A, Cayan S, Tefekli A, et al. Does response to treatment of ejaculatory duct obstruction in infertile men vary with pathology? Fertil Steril. 2001;76:138.
135. Yurdakul T, Gokce G, Kilic O, et al. Transurethral resection of ejaculatory ducts in the treatment of complete ejaculatory duct obstruction. Int Urol Nephrol. 2008;40:369.
136. Xu B, Niu X, Wang Z, et al. Novel methods for the diagnosis and treatment of ejaculatory duct obstruction. BJU Int. 2011;108:263.

137. Zackrisson B, Hugosson J, Aus G. Transrectal ultrasound anatomy of the prostate and seminal vesicles in healthy men. Scand J Urol Nephrol. 2000;34:175.
138. Hernandez AD, Urry RL, Smith Jr JA. Ultrasonographic characteristics of the seminal vesicles after ejaculation. J Urol. 1990;144:1380.
139. Tanahashi Y, Watanabe H, Igari D, et al. Volume estimation of the seminal vesicles by means of transrectal ultrasonotomography: a preliminary report. Br J Urol. 1975;47:695.
140. Manno M, Marchesan E, Tomei F, et al. Polycystic kidney disease and infertility: case report and literature review. Arch Ital Urol Androl. 2005;77:25.
141. Pace G, Galatioto GP, Guala L, et al. Ejaculatory duct obstruction caused by a right giant seminal vesicle with an ipsilateral upper urinary tract agenesia: an embryologic malformation. Fertil Steril. 2008;89:390.
142. La Vignera S, Vicari E, Condorelli R, et al. Ultrasound characterization of the seminal vesicles in infertile patients with type 2 diabetes mellitus. Eur J Radiol. 2011;80:e64.
143. Andrade-Rocha FT. Unusual presentation of seminal vesiculitis in an infertile man. Can J Urol. 2007;14:3750.
144. Herwig R, Tosun K, Pinggera GM, et al. Tissue perfusion essential for spermatogenesis and outcome of testicular sperm extraction (TESE) for assisted reproduction. J Assist Reprod Genet. 2004;21:175.
145. Tunc L, Alkibay T, Kupeli B, et al. Power Doppler ultrasound mapping in nonobstructive azoospermic patients prior to testicular sperm extraction. Arch Androl. 2005;51:277.
146. Van Peperstraten A, Proctor M L, Johnson NP, et al. Techniques for surgical retrieval of sperm prior to intra-cytoplasmic sperm injection (ICSI) for azoospermia. Cochrane Database Syst Rev. 2008;(2):CD002807.
147. Ramkumar A, Lal A, Paduch DA, et al. Ultrasonically actuated silicon-microprobe-based testicular tubule metrology. Conf Proc IEEE Eng Med Biol Soc. 2010;2010:6469.

Part III

Ultrasound in Infertility Treatment

Ultrasound in Follicle Monitoring for Ovulation Induction/IUI

18

Josef Blankstein, Shumal Malepati, and Joel Brasch

Abbreviations

AFC	Antral follicle count
AIUM	American Institute of Ultrasound in Medicine
AMH	Anti-Mullerian hormone
AVC	Automatic volume calculation
CC	Clomiphene citrate
COS	Controlled ovarian stimulation
EFG	Early follicular stage
EFP	Early follicular phase
FI	Flow index
FSH	Serum follicle-stimulating hormone
GC	Granulosa
hCG	Human chorionic gonadotropin
HPO	Hypothalamic-pituitary-ovarian
IUI	Intrauterine insemination
IVF	In vitro fertilization
IVF-ET	Ovulation induction in in vitro fertilization programs
LH	Luteinizing hormone
OHSS	Ovarian hyperstimulation syndrome
PCOS	Polycystic ovary syndrome
PFBF	Perifollicular blood flow
TC	Theca cells
uLH	Urinary LH testing
VFI	Vascularization flow index
VI	Vascularization index

J. Blankstein, MD, ARDMS (✉)
Department of Obstetrics and Gynecology,
Rosalind Franklin University of Medicine and Science,
Mount Sinai Hospital, 15th St at California Ave,
Chicago, IL 60608, USA
e-mail: josef.blankstein@sinai.org

S. Malepati, MD
Department of Obstetrics and Gynecology,
Mount Sinai Hospital, Chicago, IL, USA
e-mail: shumal_malepati@yahoo.co.in

J. Brasch, MD
Department of Obstetrics and Gynecology,
Rosalind Franklin University of Medicine and Science,
The Chicago Medical School, Chicago, IL, USA
e-mail: joel.brasch@chicago-ivf.com

Ovulation induction refers to the treatment in which ovulation is achieved by medication such as Clomid and gonadotropins to enhance fertility. Transvaginal ultrasonography has become the norm in infertility centers to provide noninvasive access to the dynamic processes such as ovarian follicular development, ovulation, and endometrial response to hormonal stimulation [1–3].

Recent advances in reproductive endocrinology have led to greater understanding of the basic regulatory mechanisms governing the reproductive process. It is fitting to introduce our topic by outlining the major morphological changes of the menstrual cycle that can be visualized by ultrasound.

Follicular Selection: Morphological and Ultrasound Observations

In the beginning of each ovarian or menstrual cycle, many follicles may start developing; however, only one is selected to continue

L.A. Stadtmauer, I. Tur-Kaspa (eds.), *Ultrasound Imaging in Reproductive Medicine*,
DOI 10.1007/978-1-4614-9182-8_18, © Springer Science+Business Media New York 2014

development while the remainders undergo atresia. While oocyte recruitment and development is predominately dependent upon genetic endowment, follicular growth, in contrast, is a gonadotropin and sex steroid regulated phenomena, likely a postreceptor-modulated increase in hormone sensitivity.

The early follicular phase of the ovarian cycle is characterized by relatively elevated levels of FSH and low levels of LH, estrogens, and progesterone. During this early cycle phase, the growth of a number of follicles, referred to as a cohort of follicles, is initiated. It has been demonstrated that this oocyte selection process involves two main processes. First, a number of follicles are recruited, and second, a number of growing follicles are selected out of the recruited group to continue towards maturation. Studies supporting the "dominant follicle theory" support that new follicular growth is arrested in the presence of a single dominant follicle. Provision of more gonadotropins in stimulated or induced cycles by clomiphene citrate or human menopausal gonadotropins or both will violate the normal monoovular quota. Moreover, the responsiveness of other follicles to human menopausal gonadotropin (hMG) therapy was found to be suppressed in the presence of the overt dominant follicle, while the same dose of hMG early in the follicular cycle increased the number of follicles recruited and/or selected for maturation (Fig. 18.1).

In the normal ovulatory cycle, the dominant follicle steadily increases in size, while the accompanying smaller follicles are not observed to show a similar increase. Thus, while one or more follicles will grow to full maturity and ovulate, others are destined to atresia and degeneration. This follicular atresia appears to involve genetically programmed cell death within the oocyte – a nuclear cell death referred to as apoptosis.

Ovarian secretion of estradiol (E_2) and estrone, from the granulosa cells, promotes follicular maturation by increasing follicular sensitivity to gonadotropin stimulation. This is accepted to be a gonadotropin receptor-mediated process.

The temporal relationship between hormonal profile and follicular development with respect to ovulation is summarized in Fig. 18.2.

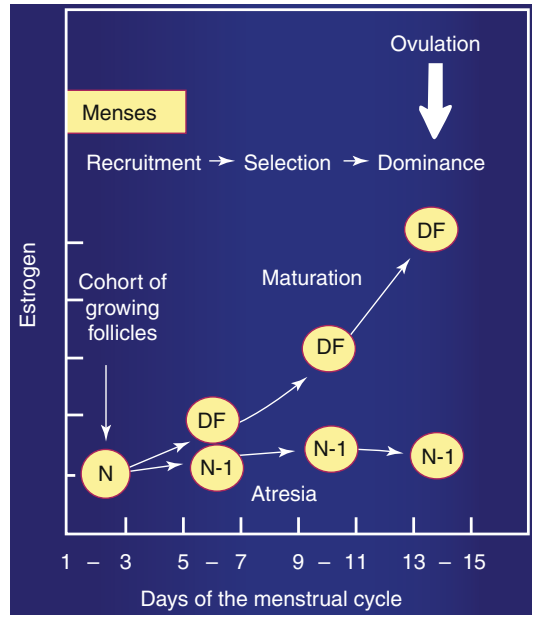

Fig. 18.1 Cyclic ovarian changes: time course for recruitment, selection, and ovulation of the dominant ovarian follicle, with onset at atresia among other follicles of the cohort (Adapted from Hodgen [40])

The dominant follicle is selected due to its responsiveness to elevated circulatory FSH levels. It is not uncommon to observe two, or more, follicles developing to approximately 10 mm, with one achieving dominance and growing, while the others regress. LH reinitiates meiosis of the oocyte, and typically, ovulation occurs within 36 h of its "surge."

Small follicles can be visualized easily as echo-free, smooth-walled, structures and usually lie towards the periphery of the more echogenic ovarian tissue. As the follicle matures, more fluid is released and accumulates into its center. The granulosa cell mass, lining the inner of the follicle, increases. Microscopically the oocyte itself, which is less than one-tenth of 1 mm, is surrounded by a cluster of granulosa cells. This complex surrounding the oocyte is termed the cumulus oophorus. It measures approximately 1 mm and can occasionally be depicted by transvaginal scan (TVS) adjacent to the wall of a mature follicle. Immediately prior to ovulation the cumulus separates from the wall and floats freely within the follicle's center. Today, even

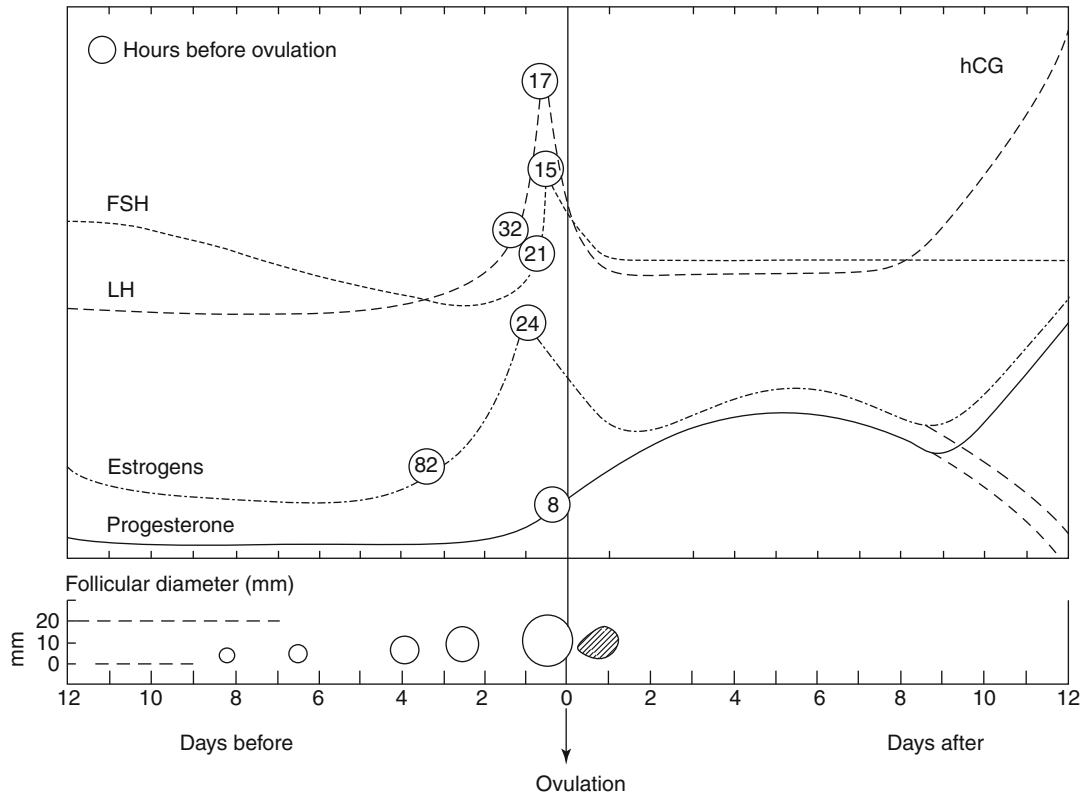

Fig. 18.2 Temporal relationships between hormonal profile and follicular development with respect to ovulation. Significant hormone levels and their preovulatory peaks are given in hours prior to ovulation (*circled numbers*) (Courtesy of Dr. Josef Blankstein)

with the enhanced resolution afforded by TVS, the attached or floating cumulus is only rarely seen. However, new technological developments, mainly high-resolution probes (40 MHz), have enabled clinical researchers to clearly visualize the antrum, the granulosa (GC), and the theca cells (TC) in a preovulatory follicle (Fig. 18.3).

Monitoring ovarian response to ovulation induction can be achieved by ultrasonography alone. The dimensions of the growing follicles are plotted from around day 8 of stimulation together with a measurement of endometrial thickness. The mean follicular growth rate is 1.4 mm/day in spontaneous menstrual cycle and 1.7 mm during ovarian stimulation cycles [4].

Mature follicles, those containing a mature oocyte, typically measure from 17 to 25 mm in average inner dimension. The optimal follicular size before triggering ovulation in intrauterine insemination cycles with clomiphene citrate or letrozole was found to be in the 23–28 mm range. The optimal size of the leading follicle was not statistically significantly different between cycles using letrozole or clomiphene citrate and was closely related to the endometrial thickness [5]. Intrafollicular echoes may be observed with mature follicles, probably arising from clusters of granulosa cells that shear off the wall near the time of ovulation. After ovulation, the follicular wall becomes irregular as the follicle becomes "deflated." The fresh corpus luteum usually appears as a hypoechoic structure with an irregular internal wall and may contain some internal free-floating or fixed echoes that correspond to hemorrhage. As the corpus luteum develops 4–8 days after ovulation, it appears as an echogenic structure of approximately 15 mm in size. Its wall is thickened due

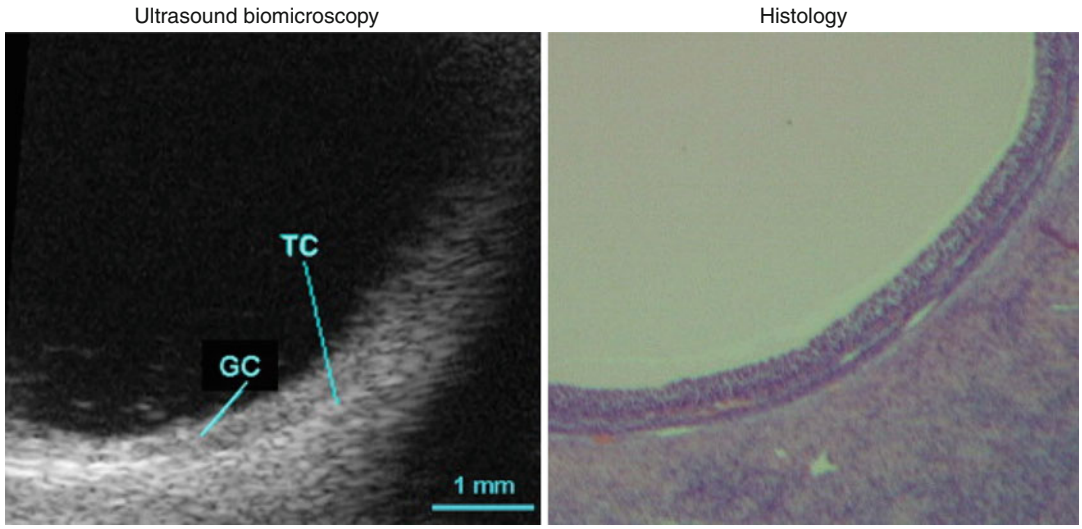

Fig. 18.3 Antrum, granulosa (*GC*), and the theca cells (*TC*) in a preovulatory follicle (Reprinted from Palleres et al. [41]. With permission from Elsevier)

to the process of luteinization. TVS shows the neovascularity within the wall that is associated with formation of the corpus luteum. In addition to delineation of changes in follicle size and structure, TVS can depict the presence of intraperitoneal fluid. It is normal to have approximately 1–3 mL of intraperitoneal fluid in the cul-de-sac throughout the cycle. When ovulation occurs, there typically is between 4 and 5 mL within the cul-de-sac. The intraperitoneal fluid resulting from ovulation may be located outside of the posterior cul-de-sac, surrounding bowel loops in the lower abdomen, and upper pelvis or in the anterior cul-de-sac superior to the uterine fundus (Fig. 18.4).

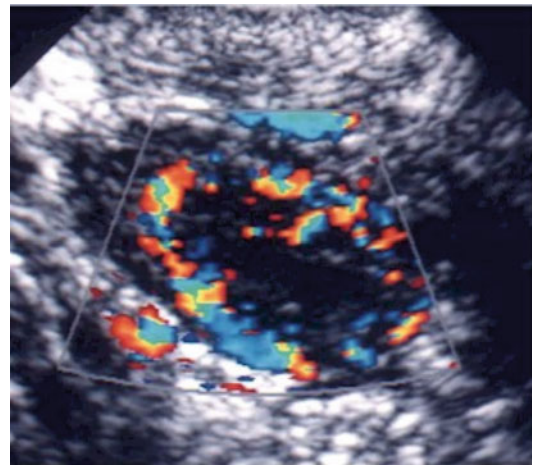

Fig. 18.4 Corpus luteum ultrasound study. (1) Note the irregular cystic mass with crenulated borders and low-level echoes. (2) Doppler findings of a hypervascular corpus luteum with low resistance index

The Role of Doppler in Reproduction

The formation of new blood vessels is taking place in the ovary during folliculogenesis and corpus luteum formation, as well in the endometrium mainly during the follicular phase. It was already recognized as early as in 1926 that neovascularization may be of prime importance in the growth and selection of ovulatory follicles, in addition to the subsequent development and function of the corpus luteum. Studies of ovarian vascular morphology showed that the capillary network of preovulatory follicles was more extensive than that of other follicles, consequently proposing that initiation and maintenance of follicular growth depends on development of the follicular microvasculature.

A study done by Shrestha et al. [6] to determine whether ovarian perifollicular blood flow (PFBF) in the early follicular phase (EFP) is

associated with treatment outcome of IVF showed high-grade ovarian PFBF in the EFP during IVF to be associated with a higher clinical pregnancy rate. Coulam et al. [7] correlated peak systolic velocity (PSV) of individual follicles with oocyte recovery, fertilization rate, and embryo quality in women undergoing in vitro fertilization (IVF) and embryo transfer. They assessed the role of quantitative and qualitative indices of follicular vascularity in predicting pregnancy after IVF and embryo transfer. Women who had PSV ≥10 cm/s in at least one follicle on the day of hCG administration more often became pregnant than those with PSV <10 cm/s ($P=0.05$). Nargund et al. [8] demonstrated that there was a 70 % chance of producing a grade I or II embryo if the follicular blood velocity was >10 cm/s, compared with 14 % if the PSV was <10 cm/s. This study concluded that there is a physiological relationship between follicular blood velocity, oocyte recovery, and the production of a high-grade preimplantation embryo, which may form the basis of a useful clinical test. Jayaprakasan et al. [9] on the other hand concluded that ovarian vascularity as measured by 3D ultrasound is not decreased in women who demonstrate poor ovarian response to controlled ovarian stimulation as part of assisted reproduction treatment.

Perifollicular vascular perfusion appears to be an important factor in determining the outcome of stimulated cycles, and may have clinical implications in assisted reproduction therapy. As there were low pregnancy rates and oocyte retrieval in the group of women with uniformly low-grade vascularity, the identification of these cycles would be valuable in terms of counseling with regard to the potential outcome in that cycle. Ideally, the identification of these women (who may also be "low recruiters") earlier in the cycle would be helpful. This could allow the cancellation of treatment after careful counseling, on the basis of perifollicular vascular perfusion, and could be cost-effective, both financially and emotionally. However, further longitudinal data would be needed before this form of prospective management of treatment cycles could be applied clinically. The risk of multiple pregnancies and their implications on the health service is also well recognized. Since there were higher multiple pregnancy rates in stimulated intrauterine insemination (IUI) cycles with uniformly high-grade follicular vascularity, perhaps these cycles in particular should be considered for follicle reduction or even cancellation. This may potentially reduce the number of developmentally competent oocytes that have a higher capability of producing more viable embryos for implantation [10].

In a recent prospective study by Ivanovsky et al. [11], vascular impedance was calculated using the uterine artery and arcuate artery pulsatility resistance and velocity on the day of hCG administration. It was found that optimal uterine receptivity can be accomplished by reduced vascular resistance and increased blood flow. Obviously more studies are needed to confirm their results.

The relationship between endometrial and subendometrial blood flow and pregnancy after intrauterine insemination was examined in a prospective study. The main outcome measured were vascularization index (VI), flow index (FI), and vascularization flow index (VFI) of the endometrium as well as those of the subendometrial region. These measurements were analyzed in relation to IUI outcome, pregnant versus nonpregnant. It was found that the pregnant group had higher endometrium VI, FI, and VFI scores than the nonpregnant group. The subendometrial region VI, FI, and VFI scores did not differ between the groups [12] (Fig. 18.5).

Ovulation Induction and Intrauterine Insemination (IUI)

In conjunction with ovulation induction, IUI is a way to potentially overcome various fertility problems such as oligospermia, i.e., low sperm count, low sperm motility, cervical factor infertility (cervical mucus inactivates sperm motility), sexual dysfunction, and unexplained infertility.

By placing sperm directly into the uterine cavity, the greatest barrier, the mucus in the cervix, is bypassed; therefore, more sperm reaches the egg,

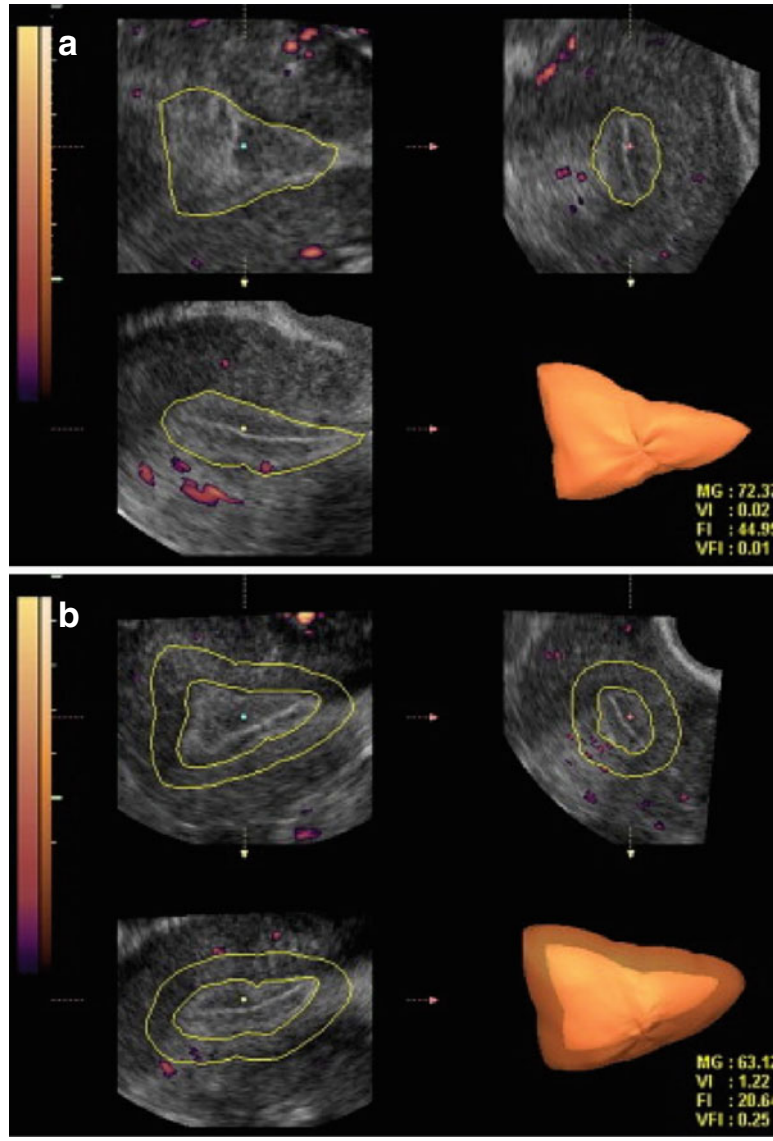

Fig. 18.5 Three-dimensional power Doppler images generated using VOCAL software. (**a**) Endometrial. (**b**) Subendometrial blood flow parameters on the day of IUI (see text) (Reprinted from Kim et al. [12]. With permission from Elsevier)

creating a better chance of fertilization for the egg. IUI is usually combined with ovulation induction. Optimal timing of insemination is achieved either by the detection of a luteinizing hormone (LH) surge through urinary LH testing (uLH) or by ultrasound monitoring of follicular growth followed by the administration of human chorionic gonadotropin (hCG). In most centers, when the leading follicle reached >18 mm diameter, 10,000 IU hCG was given to trigger ovulation and IUI is timed 36 + or – 2 h later. While IUI is a natural starting point for many treatment schemes, unfortunately this therapy may be complicated by premature luteinization and hyperstimulation.

Premature Luteinization: Premature LH surge will luteinize the follicle which is too small and not ready to ovulate. Cantineau et al. [13] studied the prevalence of premature LH surges in an IUI program. It has been concluded that 24 % of IUI cycles suffer from premature LH surge and this can result in IUI procedure cancellation. Obviously, this represents economic and psychological stress for the patients.

Manzi et al. [14] showed that patients who underwent controlled ovarian stimulation (COS)/IUI treatment and had premature LH surge demonstrated much better pregnancy rates in the subsequent cycle when a GnRH analogue was added, thus avoiding premature LH surge.

GnRH agonist has been, in the past, the standard of care in reducing the incidence of premature LH surge by reversibly blocking pituitary gonadotropin secretion in IUI-stimulated cycles [15]. These drugs are nowadays completely abandoned in IUI cycles because of their stimulatory effect, with consequent higher incidence of multiple pregnancy and OHSS and the long pretreatment period required.

An alternative to GnRH agonists, GnRH antagonists have been proposed to prevent premature LH surge [16]. These drugs do not produce flare-up effect, reducing synchronous follicular pool recruitment. Moreover, the potential advantage of a GnRH antagonist is that pituitary gonadotropin secretion is suppressed immediately after the start of the therapy. Therefore, co-treatment with GnRH antagonists can be restricted to the time in the cycle where there is a risk of premature LH rise.

Multiple Pregnancies

Another concern with controlled ovarian stimulation COS/IUI cycles is the risk of multiple pregnancies. The problem with multiple gestations is that they are associated with major maternal and fetal risks (see Table 18.3).

This past decade has shown increasing medical, societal, and regulatory attention to controlling multiple gestations in all areas of assisted reproduction. Improved outcome-based medical procedures, such as lower gonadotropin dosages, single embryo IVF transfer, and increased utilization of cryopreservation of embryos, have all contributed to the reduction in multiple gestations from ART procedures. Regulatory pressure to lower multiple gestations has come in the form of multiple agencies publishing embryo transfer number guidelines and a national ART tracking database through SART (Society for Assisted Reproductive Technologies). In the USA such regulations remain voluntary, while in many other countries, such guidelines are legislated and strictly enforced.

Low-dose stimulation and careful follicular monitoring may help to reduce the risk of multiple pregnancies. The risk of multiple pregnancies after IUI is dependent on the type of stimulation (clomiphene citrate vs. gonadotropins) and on the size and number of follicles. Dickey et al. [17] reported a positive correlation of multiple pregnancies with the number of follicles 12 and 15 mm or larger. Offering oocyte aspiration of excess follicles in an effort to reduce multiple gestations has been proposed by many researchers, and this method has shown to reduce the risk of multiple pregnancies.

Stoop et al. [18] concluded that aspiration of excess oocytes in stimulated IUI cycles reduced cancellation rates and further reduced multiple pregnancy rates. Additional studies are needed to better define the criteria and methods for oocyte aspiration of preovulatory follicles prior to hCG administration.

Polycystic Ovarian Syndrome (PCOS)

A significant disorder of concern to the reproductive endocrinologist is the polycystic ovary syndrome (PCOS). This is a common cause of anovulation with multiple etiologies. This disorder affects 5–10 % of women. PCOS patients respond well to ovulation induction (see below); however, one has to remember that those patients are prone to develop hyperstimulation and multiple gestations.

For years, PCOS has been one of the most controversial entities in gynecologic endocrinology. Despite a vast amount of clinical and laboratory data that have been accumulated since the initial report of Stein and Leventhal in 1935, our knowledge of the endocrine metabolism underlying the disease is still fragmentary. The PCOS is a disorder of multiple etiologies involving a self-perpetuating imbalance between various interdependent endocrine and peripheral structures. In dealing with patients who exhibit symptoms of

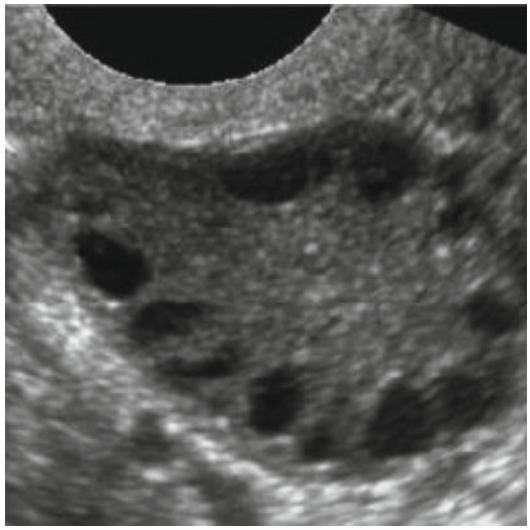

Fig. 18.6 PCOS ultrasound study (note the peripheral small cysts "string of pearls")

the PCOS, we cannot escape the suspicion that we are facing a whole series of interrelated disorders leading to manifestations often classified under this single title (Fig. 18.6).

The Classical Picture of PCOS

The PCO syndrome is characterized by a variety of symptoms, all of which are not necessarily present in every patient. These include (1) a broad spectrum of menstrual abnormalities, (2) signs of hyperandrogenism, (3) infertility, and (4) bilateral polycystic ovaries. Menstrual disorders observed include secondary amenorrhea (rarely primary amenorrhea may occur) and oligomenorrhea.

Grossly, the polycystic ovary appears enlarged, sometimes twice the normal size, and is characterized by a shiny, oyster-grey color and small, embedded, bluish cysts (2–6 mm in diameter). Microscopically, the ovarian capsule is thick (approximately 144–595 u wide as opposed to 100 u in normal ovaries) and fibrous and contains numerous primordial follicles. In the substance of the ovary, there are follicles in all stages of development and atresia, and multiple cystic follicles are lined with one to three layers of granulosa cells. Luteinized follicles are present and occasionally corpora lutea have been reported. The walls of the atretic follicles often display hyperplasia of the theca interna cells.

Ultrasound Diagnosis

The criteria for ultrasound diagnosis of PCO have recently been revised in the light of improved ultrasound technology and better understanding of the condition [19]. The diagnosis can be supported when one or more of the following features are demonstrated:

- 12 or more follicles (2–9 mm diameter) are present in an ovary (either peripheral or diffusely arranged).
- Ovarian volume is over 10 cm^3 (when no follicles measuring over 10 mm in diameter).

Only a single ovary need be affected to make a diagnosis. If a large follicle is present (over 10 mm), then the volume should be calculated on a repeat scan when the ovary is quiescent to prevent overestimation of ovarian volume.

Remember that imaging findings alone should not diagnose PCOS in an asymptomatic patient. In this situation further supporting evidence in terms of clinical examination and blood tests should be obtained before a firm diagnosis is made. Oftentimes, without clear ultrasonographic or endocrine finding consistent with PCO, the practitioner can still diagnose "suspect PCO" based upon the ovarian response pattern to exogenous gonadotropins, i.e., greater than expected estradiol response and fewer than expected mature follicles – oftentimes, scores of small (less than 10 mm) immature follicles.

Induction of Ovulation

In patients whose infertility can be attributed to an ovulation abnormality, ovulation induction is indicated. Ovulation induction is also used in in vitro fertilization programs (IVF-ET) to increase the number of oocytes aspirated, which in turn increases the number of fertilized conceptus that may be transferred, thereby increasing the chance

of pregnancy. Commonly used ovulation induction medications include clomiphene citrate, human menopausal gonadotropin, purified FSH, and recombinant gonadotropins. Although all of these medications result in the development of multiple follicles, they act via different mechanisms.

Transvaginal sonography has a vital role in monitoring the follicular growth rate in women receiving ovulation induction medications.

In an elegant prospective study, Baerwold et al. [4] compared the growth rate of ovarian follicles during natural cycle and ovarian stimulation cycles using standardized techniques.

While the growth rate in natural cycles was 1.42 mm per day, the growth in stimulated cycles was significantly greater, i.e., 1.7 mm per day. Continued research on the effect of greater follicular growth rates and shorter intervals to ovulation is being conducted (Fig. 18.7).

The baseline scan of the pelvis is mandatory to rule out ovarian or uterine pathology and assess the ovarian reserve: moreover one needs to rule out the presence of ovarian cysts [3].

The objectives of a baseline scan are:

A. *To rule out ovarian or uterine pathology* requiring attention prior to beginning infertility treatment (see Table 18.1)

A common adnexal finding, endometrosis [20], can be seen in over 30 % of women with clinically defined infertility. Endometriosis is defined as the extrauterine presence of endo-

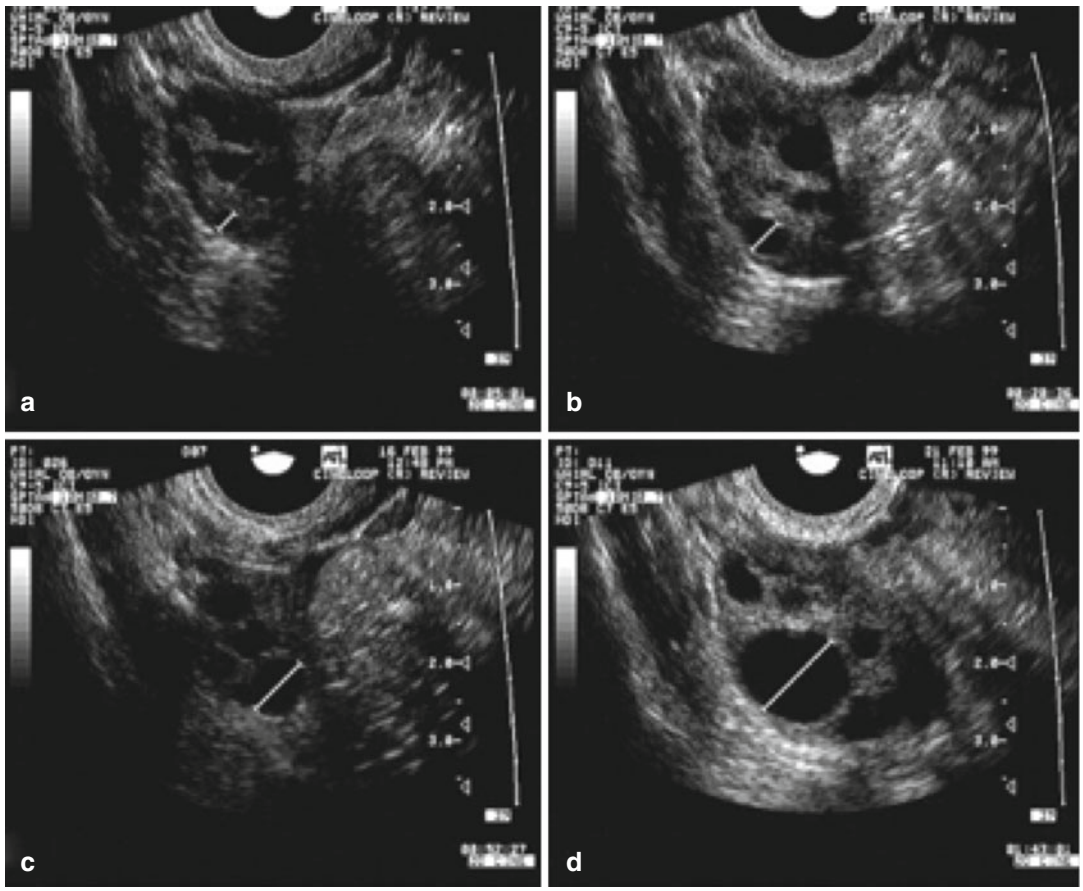

Fig. 18.7 Serial transvaginal ultrasonographic images of the right ovary of a research participant on days 1 (**a**), 4 (**b**), 7 (**c**), 11 (**d**), 16 (**e**), and 17 (**f**) of a spontaneous menstrual cycle. The same ovarian follicle is identified throughout the growth phase in (a–e). The corresponding corpus luteum on the day of ovulation is shown in (e) (Reprinted from Baerwald et al. [4]. With permission from Elsevier)

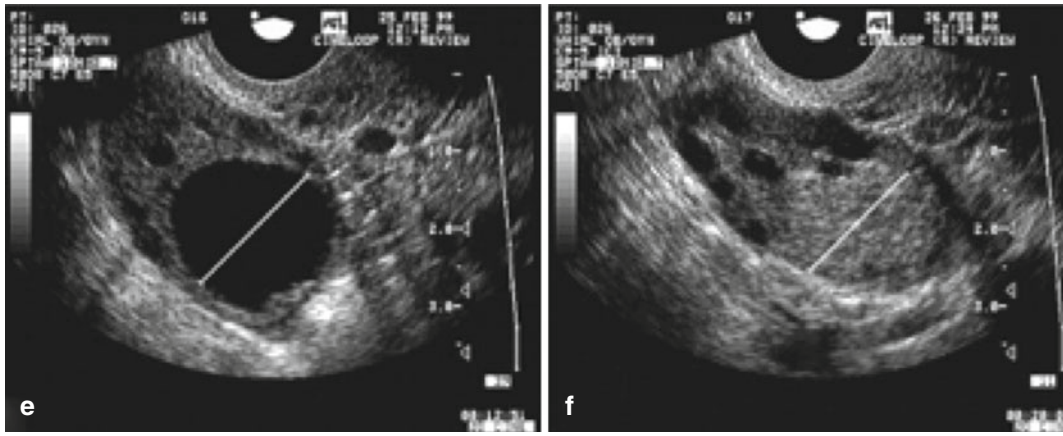

Fig. 18.7 (continued)

Table 18.1 Common adnexal masses

Cystic masses	Follicular cyst, corpus/luteum cyst, hydrosalpinx, dermoid cyst, endometrioma/hemorrhagic cyst
Solid masses	Fibroma, dysgerminoma, teratoma, carcinoid subserosal fibroid
Complex masses	Dermoid cyst, cyst adenoma, granulosa

metrial tissue and is likely due to retrograde menstruation and/or immunologic variations or deficiencies within the peritoneal cavity.

In mild cases small lesions are often located on the ovarian and peritubular surfaces. Cases of minimal endometriosis are not amenable to ultrasonographic diagnosis. However, in more moderate cases, one can visualize an endometrioma, i.e., a cystic structure which is lined with endometrial epithelium which can involve one or both ovaries, uterosacral ligaments, etc.

Endometrioma may appear as an ovarian cyst with an echo-dense appearance of blood within a cyst; the appearance may range from anechoic to solid, depending on the amount and organization of the blood within the cystic structure; commonly one can visualize low-level echoes evenly distributed throughout the cyst (Fig. 18.8).

It is important for the physicians to familiarize the ultrasonographic picture of the endometrioma in order to avoid aspirating the cyst because of an increased risk of infection, compared with aspiration of a simple cyst.

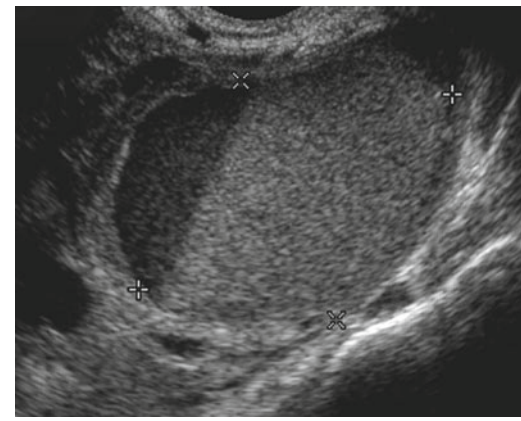

Fig. 18.8 Endometrioma ultrasound study (note the homogenous, low-level echoes, "ground glass" appearance)

Since ovarian teratomas are the most common ovarian neoplasm especially in reproductive-age women [21], one may encounter them during a baseline scan; the ultrasonographic findings will depend on which elements are present: ectoderm, mesoderm, etc. Very often one can appreciate an echogenic mass with acoustic shadowing. The presence of ectodermal elements gives irregular and variable internal echogenicity (Fig. 18.9).

B. *Check ovarian reserve*: which will help identify the ideal treatment protocol

Markers of ovarian reserve are associated with ovarian aging as they decline with chronologic age and hence may predict stages of reproductive aging including the menopause

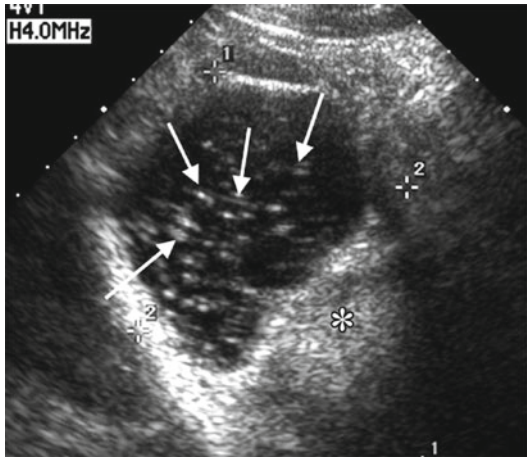

Fig. 18.9 Teratoma ultrasound study (note the echogenic linear speckles). (*asterisk*) shows echogenic mass, (*arrows*) shows echogenic linear speckles

transition. Assessment of ovarian reserve includes measurement of serum follicle-stimulating hormone (FSH), anti-Mullerian hormone (AMH), and inhibin B. Ultrasound determination of antral follicle count (AFC), ovarian vascularity, and ovarian volume also can have a role. In infertile women, ovarian reserve markers can be used to predict low and high oocyte yield and treatment failure in women undergoing in vitro fertilization [22].

Small antral follicles (<6.0 mm) measured using 3D ultrasound and AMH show little intra-cycle variation and perhaps should be evaluated in prediction of ovarian reserve independent of menstrual cycle [23].

In our clinic a baseline scan involves antral follicle count and evaluation of ovarian volume. The number of antral follicles of at least 2 mm in diameter can be detected using ultrasound imaging; generally follicles that are greater than 2 mm in diameter are highly responsive to gonadotropins; however, some follicles in this size range may be in the early stages of atresia. Antral follicle count is performed on day 2–4 of a natural cycle or following pituitary downregulation. Prospective studies assessing antral follicle count demonstrate that lower counts (less than four follicles) are associated with significantly decreased pregnancy rates and increased cycle cancellation rates [24].

Low AFC did predict a higher cancellation rate. Antral follicle count did not predict implantation rate, pregnancy rate, or live birth rate per cycle start. Antral follicle count may be helpful in determining stimulation protocol, as it is the most reliable determinant of oocytes retrieved per starting FSH dose. Antral follicle count predicts ovarian response, not embryo quality or pregnancy [13].

Ovarian volume is measured using the following formula: volume (cm^3) = length × width × anterior posterior diameter × 0.53. In a prospective cross-sectional study, it has been shown that ovarian volume, number of follicles, and total follicular volume decreased significantly with age [25].

It has been shown that ovarian volume is inversely correlated with age. Significant decrease in ovarian volume is observed in women older than 35 years of age. The prognostic practicality of measuring early follicular ovarian volume is limited because clinically meaningful changes are only manifest at the physiologic extremes [26]. However, one has to note that ovarian volumes less than 3 cc are associated with a significant decrease in clinical pregnancy rates.

C. *Ovarian cyst/hydrosalpinx*

It is important to identify cysts and/or hydrosalpinx prior to stimulation since these situations could later be misinterpreted as developing follicle. Moreover, basal ovarian cyst significantly reduces ovulating events in patients treated with clomiphene citrate [27]. Thus, the recommendation is to do a routine ultrasound screening in those patients with a history of prior cysts, as they are more likely to have a recurrent cyst and those not ovulating on clomiphene citrate.

Upon detection of an ovarian cyst, a conservative approach is generally effective. One can wait for a spontaneous menstrual bleed which indicates that endogenous ovarian hormone levels returned to base level; if the cyst is not resolving and hormone levels of E_2 are high, then cyst aspiration prior to stimulation remains a viable option.

Upon detection of suspect hydrosalpinx, confirmatory hysterosalpingogram and/or laparoscopy is indicated. Significant international data supports the observation that hydrosalpinx lowers the success rate for IVF and related ART procedures. It is thought that the mechanism of action involves the retrograde flow of inflammatory fluid into the uterine cavity and resultant inhibition of embryo implantation.

Selection of Patients

The ovulatory treatment options are based on WHO classification with patients separated into 3 main groups (see Table 18.2):

Group I: Hypothalamic-pituitary failure included women with primary or secondary amenorrhea, low levels of endogenous gonadotropins, and lack of endogenous estrogen activity. The treatment of choice for this group of patients is gonadotropic therapy.

Group II: Hypothalamic-pituitary dysfunction included patients with anovulation associated with a variety of menstrual disorders whose serum gonadotropin levels were within the normal range and who had evidence of endogenous estrogen activity.

The treatment of choice for patients belonging to Group II is a chlorotrianisene analogue, such as clomiphene citrate.

Group III: Includes patients with high FSH levels and the only viable option for them is ovum donation.

Table 18.2 Anovulation treatment options (based on WHO classifications)

Group I	Option I	Option II
Low FSH	GnRH (pulsatile) Gonadotropins Bromocriptine	 Gonadotropins, bromocriptine, and clomiphene citrate
Group II Normal FSH	Clomiphene citrate	Gonadotropins Surgical approach
Group III High FSH	Ovum donation	

The above classification is based on hormone levels of FSH and estrogens; however, some conclusions can be drawn following a baseline ultrasound evaluation of the endometrium. In cases where the endometrium is thick (7–14 mm), one can conclude that the patient had sufficient ovarian estrogen secretion and normal FSH level (i.e., Group II).

If on the other hand the endometrium is thin, the patient has low estrogen level, and in this case, a single FSH level will differentiate between Group I (low FSH) and Group III (high FSH).

Technical Tips on How to Scan the Ovaries and Follicular Growth

Ovaries: The ovaries are located posterior to the broad ligament and anteromedial to the internal iliac vessels which are easily located and can be used as a land mark for ovarian localization; moving laterally from the endometrial canal will produce the image of the ovary adjacent to the iliac vessels.

The pelvic organs may be scanned either transabdominally or transvaginally. In most infertility units, transvaginal ultrasound has become the routine method since it improves spatial resolution; however, it has a smaller field of view. During the transvaginal approach, only a few centimeters separate the probe from the ovaries.

The best way to locate the ovaries is to scan along the lateral margin of the uterus in transverse plane from the fundus to the cervix. In cases where you cannot locate the ovaries, look for them adjacent to the iliac vessels, which are usually easily identified, or try to follow the fallopian tube laterally.

In cases when the ovary is high in the pelvis, a transabdominal scan is also necessary; in these situations begin with the abdominal transducer perpendicular at the midline just superior to the symphysis pubis. Once you locate the long axis of the uterus, move the transducer lateral until the ovary is located. Again remember that the internal iliac vessels are located immediately posterior to the ovary.

Follicle: The spatial resolution of transvaginal scans is 2–3 mm, so small follicles can be visualized easily as echo-free structures which usually lie towards the periphery of the more echogenic ovarian tissue. Since the follicles may be flattened in one plane or have their shape altered due to pressure, the internal diameter of the follicle should be measured in three planes and the mean value calculated. The intra-observer standard deviation of transabdominal follicular measurement was reported in one study to be 0.6 mm, and the inter-observer standard deviation is 1.2 mm, irrespective of the follicular diameter. Thus, the 95 % confidence limits for any particular measurement should be 2.4 mm [3, 28], and one would expect transvaginal measurements to confer even greater accuracy [16].

Follicles can be confused with blood vessels (hypogastric vein), and they can be differentiated by rotating the transducers. If the structure is a vessel, it will appear tubular following rotation.

A baseline scan should always be done to identify cystic structures which could later be misinterpreted as follicles.

Sono AVC (*Automatic Volume Calculation*): Recently a new software program (GE) with 3D data set, which can automatically estimate the diameter and volume of each follicle, has been developed; this ultrasound program will automatically identify the ovarian follicle and the volume for each follicle (Fig. 18.10).

Raine-Fenning et al. [29] compared automatic volume measurement of each follicle to manual measurements from 2D and 3D ultrasound; Sono AVC provided measurements that were more accurate than manual measurements, and obviously the time taken for measurements was significantly shorter.

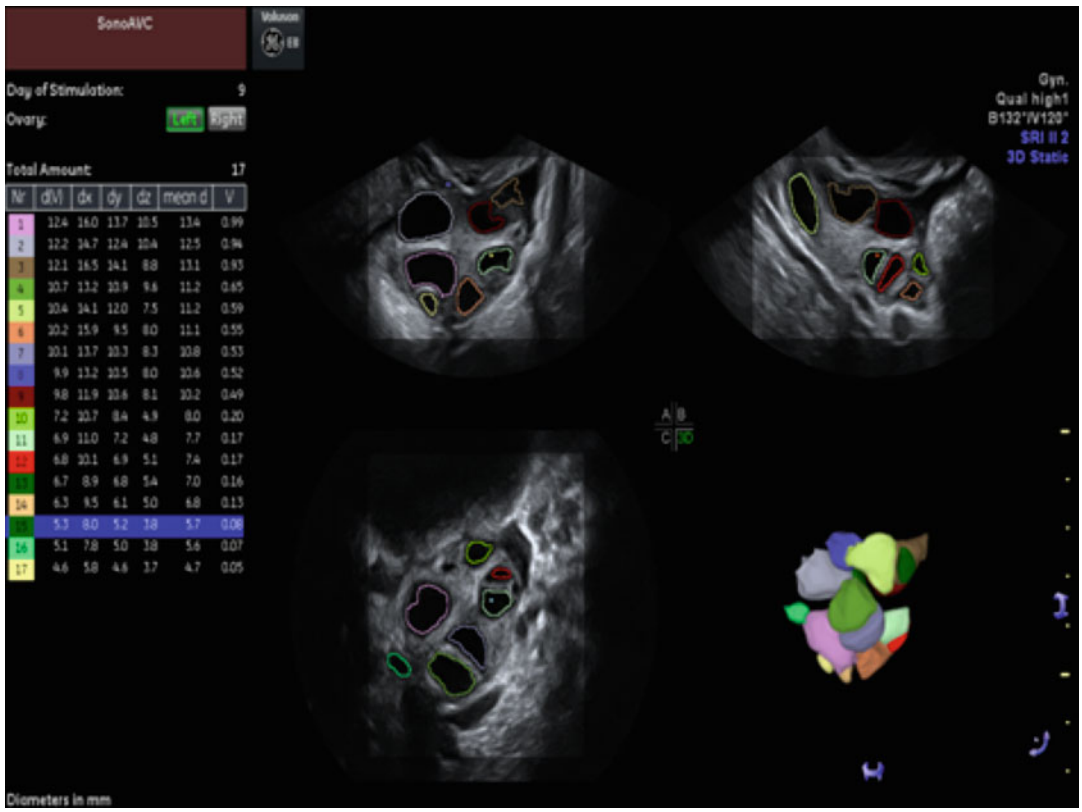

Fig. 18.10 Sono AVC ultrasound study: automatic estimation of diameter and volume. Each volume is separately color coded (see text)

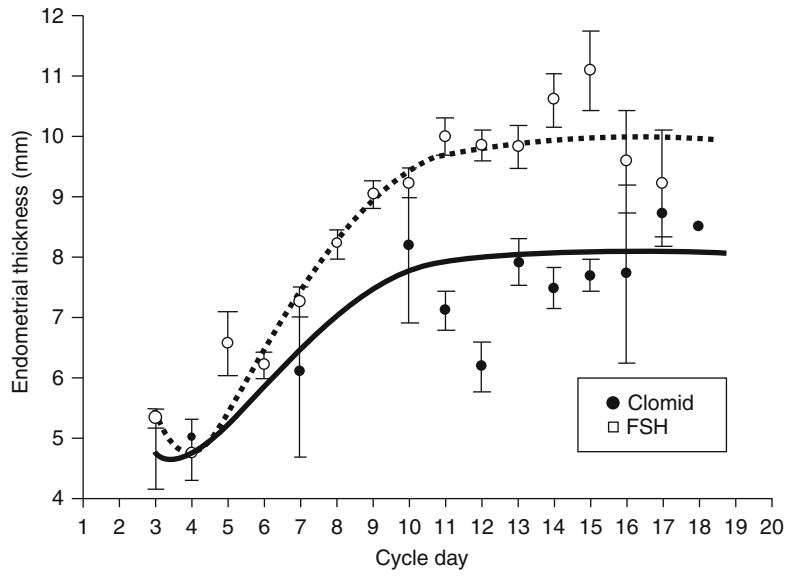

Fig. 18.11 The impact of ovulation induction treatment on endometrial thickness (Clomid *black*; FSH *white*) (Reprinted from Bromer et al. [42]. With permission from Elsevier)

Clomiphene Citrate

Clomiphene citrate (CC) is a nonsteroidal triphenylethylene compound currently used as the first choice of treatment for induction of ovulation in anovulatory or oligo-ovulatory women.

Mode of Action: The stereoscopic configuration of CC is sufficiently similar to that of ß-estradiol to complete with it for available estrogen receptor sites in all estrogen-dependent target cells such as the hypothalamus, pituitary, ovary, uterus, and cervical glands.

The mode of action of CC in the induction of ovulation may be tentatively described as follows. "Blinded" by CC molecules occupying the estrogen receptor sites, the hypothalamus and pituitary are unable to correctly perceive true serum estrogen levels. A false message of insufficient estrogen concentration is registered and acted upon, resulting in exaggerated FSH and LH secretion. The occupation of hypothalamic estrogen receptors by CC is a short duration, time-limited process. A fair chance exists that by the time ovarian follicles that are stimulated by the CC-induced gonadotropin elevation reach the preovulatory stage, the hypothalamus is already free of CC influence and ready to perceive the correct steroid signal. From this moment forward, the events are regulated and controlled by the endogenous feedback mechanisms within the hypothalamic-pituitary-ovarian (HPO) axis.

Considering its mode of action, an antiestrogen such as CC should be effective in patients having a hypothalamus capable of releasing pulsatile GnRH, a pituitary gland capable of responding to GnRH, and an ovary containing normal primordial follicles. Clomiphene citrate is most effective when used in patients with hypothalamic-pituitary dysfunction. These patients lack the proper regulation within the HPO axis, but they have some endogenous GnRH secretion and estradiol production. These anovulatory women probably have irregularities in the pulsatile secretion of GnRH, even though they do have fluctuating, detectable levels of gonadotropins and estrogens.

Antiestrogenic Effects on the Cervix and Endometrium

The antiestrogenic effect of CC may exert an adverse effect on the uterus and the cervix (Fig. 18.11). This detrimental effect, caused by the drug's competition for estrogen receptors is claimed to be one factor responsible for the

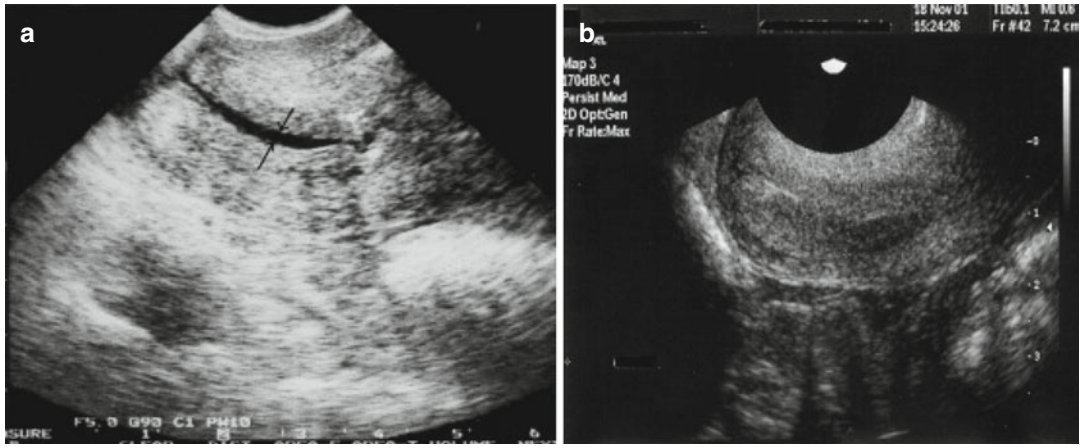

Fig. 18.12 (**a**) Cervical canal measurement near ovulation and (**b**) after ovulation (Reprinted from Wolman et al. [31]. With permission from Elsevier)

discrepancy between the ovulation rate (85 %) and the pregnancy rate (43 %) of women receiving CC treatment. Jirge and Patil [30] have demonstrated in a prospective crossover study that the number of follicles at the assumed time of ovulation is significantly higher in patients treated with clomiphene citrate; moreover, the endometrial thickness on the same day was significantly smaller (7.6 mm vs. 8.5 mm). Most investigators report decreased secretion of mucus from the cervical glands caused by antiestrogenic agents such as CC. The antiestrogenic effect on the cervical mucus, when present, is expressed by a decreased amount of mucus, which occurs despite the relatively high levels of estrogen in the circulation. Wollman et al. [31] demonstrated that the cervical mucus can be visualized in many patients around the time of ovulation using pelvic ultrasound (see Fig. 18.5). In many patients given CC, the cervical mucus does not exhibit any depressed effects. To understand this phenomenon, we must remember that the antiestrogenic effect on the hypothalamus will result in elevated circulating FSH and LH levels. The elevated gonadotropin levels may cause multifollicular development, which in turn enhances estrogen production. The elevated estrogen levels, five to ten times higher than in normal cycles, sometimes mask the antiestrogenic effect of CC and tamoxifen citrate in the cervix and uterus (Fig. 18.12).

Treatment Schema and Monitoring of Clomiphene Citrate Therapy

Clomiphene citrate is administered orally in 50-mg tablets. Therapy should be initiated with 50 mg of CC over a period of 5 days, usually starting on the fifth day after the first appearance of spontaneous or progestin-induced menstrual bleeding. Clomiphene citrate dosage is typically increased in subsequent months until ovulatory cycles become evident. Clomiphene-citrate-induced ovarian cysts often resolve spontaneously and typically do not require intervention.

In addition to the baseline scan, we advocate cycle monitoring via ultrasonographic evaluation of follicular size, endometrial thickness, and cervical mucus observation. Ultrasound monitoring of patients undergoing ovulation induction cycles will ensure adequate follicular recruitment and identify those patients not responding or have delayed endometrial thickening. In cases where there is concern that cervical mucus is insufficient, often due to the antiestrogenic effect of Clomid, intrauterine insemination (bypassing the cervix) is probably the best solution. Whenever the endogenous feedback mechanism responsible for the preovulatory LH surge is not properly activated, the midcycle LH peak may consequently be inadequate, ill-timed, or entirely absent. In such instances hCG should be

administered to induce ovulation. Optimal timing for hCG ovulation trigger injections includes ultrasonographic measurement of mean follicular diameter ranging 19–20 mm. Ovulation will occur 34–36 h following hCG injection, so the IUI is often performed 34 h later. Recently Paltnik et al. [5] have shown that higher pregnancy rates were achieved when the leading follicle was in the 23–28 mm range.

Universal agreement is lacking as to when to introduce ultrasonographic cycle monitoring versus less complicated or costly alternatives. However, we agree with the predominant opinion that the additional ultrasound expense is justified by the prevention of protracted periods of ineffective therapy [32]; moreover it has been shown that a significant number of women (14 %) developed 3 or more follicles, despite receiving low doses of clomiphene citrate [33].

Gonadotropins

Principles of Gonadotrophic Therapy: In order to optimally stimulate follicular maturation, both FSH and LH are required. While FSH content of the pharmacologic preparation is essential for follicular development, final maturation of the follicles and subsequent ovulation are brought about by a pituitary release and circulatory surge of LH. Thus two gonadotropins are required for induction of ovulation: one providing the required amount of FSH and another providing LH or LH-like material (hCG) of sufficient quantity to provoke ovulation and corpus luteum formation. Well accepted ovulation induction protocols include alterations in the precise ratio of FSH to LH.

Selection of Patients: Ideal candidates for ovulation induction with gonadotropins are patients who have low endogenous gonadotropin secretion and are amenorrheic or anovulatory (Group I—WHO). This treatment can also be given to patients with hypothalamic-pituitary dysfunction (Group II), including anovulatory patients associated with a variety of menstrual disorders. The treatment of choice for patients belonging to Group II is a clomiphene citrate alone or in conjunction with estrogen and/or hCG. Patients who fail to ovulate or conceive within a reasonable time are considered "clomiphene failures" and can be considered for hMG therapy.

Monitoring of Therapy: Gonadotropins are given daily by injection in order to stimulate follicular development; ovulation is actually induced by hCG. The daily dose of gonadotropins given in a particular cycle depends upon the ovarian response of the patient in that particular cycle. The response is reflected by a growth of follicles accompanied by biochemical changes mainly with respect to increased synthesis and secretion of steroidal hormones. The follicular enlargement can be visualized by ultrasonographic measurement, while estrogen secretion values can be estimated directly by blood measurement.

Ultrasonographic monitoring of treatment cycles serves to assess the effective dose required to evoke an ovarian response, the length of time required for follicular maturation, and the appropriate time for induction of ovulation. Furthermore, such monitoring should aim to prevent ovarian hyperstimulation syndrome (OHSS), or at least lead to early detection. For these purposes, a combination of ultrasonography and estrogen determination was advocated. Given that exogenous gonadotropic stimulation usually induces the development and growth of several follicles, ultrasonographic monitoring is particularly advisable for these treatment cycles.

Sonographic visualization may thus discriminate between single and multiple follicular growths, and their measurement may aid in the interpretation of the meaning of the estrogen levels. Evidence is accumulating that follicles of diameters greater than 18–19 mm should be "ovulated." Thus, sonography can be a more precise indicator for the determination of the optimal ovulatory timing. Gonadotropin treatment is often started on the fifth day of spontaneous or induced bleeding. It is safe to start with low doses of gonadotropins with close ultrasonic

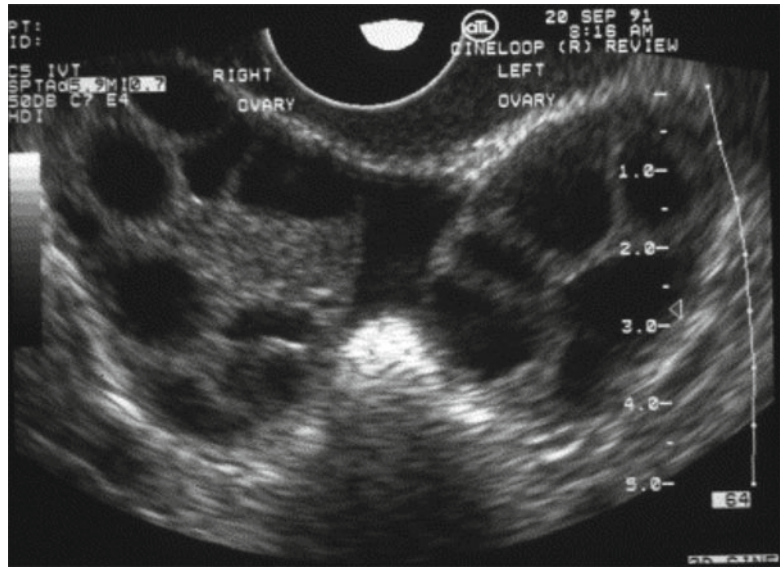

Fig. 18.13 Multiple follicles – ultrasound study

monitoring to ensure appropriate follicular growth and development (Fig. 18.13).

Follicular development should be monitored with frequent ultrasound studies. Ultrasound plays a critical role in assessing response to gonadotropins and timing of hCG administration. A baseline ultrasound scan is suggested in the early follicular phase to determine the presence or absence of persistent follicles. Scanning should become more frequent when the follicle reaches 14 mm or greater. When a follicle 18 mm or greater is identified, hMG is discontinued, and hCG is administered 24 h later to cause ovum release. Usually 10,000 units of hCG, injection, are given to trigger ovulation.

While in the past it was emphasized that ultrasound scanning should be complimentary to estradiol data, Shoham et al. [34, 35] have raised the question of whether it is possible to run a successful ovulation induction program based solely on ultrasound monitoring. In their prospective study, monitoring of ovulation induction was performed using serial ultrasound measurements and correlated with the patient's E_2 concentrations that became available at the end of each cycle. Twenty hypogonadotropic and 29 ultrasonically diagnosed polycystic ovary patients received treatment with gonadotropins. The results of this study demonstrated that transvaginal ultrasound findings including (a) follicular growth, (b) uterine measurements, and (c) endometrial thickness all strongly correlated with serum E_2 concentrations ($P<0.0001$). Shoam et al. concluded that serial ultrasound examinations used alone (eliminating determination of serum E_2 levels) have proven to be an effective monitoring approach for ovulation induction cycles.

Wiser et al. [36] studied two groups of patients undergoing their first IVF treatment. The ultrasound-only group (study group) was monitored by US for follicle size and endometrial thickness without blood tests. In this group, only one blood test was taken before human chorionic gonadotropin (hCG) injection to ensure a safe level of estradiol (E(2)) regarding ovarian hyperstimulation syndrome (OHSS) risk. The control group was monitored by ultrasound plus serum estradiol and progesterone concentration at each visit. No differences were found between the groups. The conclusion of the study was that ultrasound as a single monitoring tool for IVF cycles is reliable, safe, and patient friendly and reduces treatment expenses.

Clomiphene Citrate and hMG

The rationale of clomiphene citrate followed by hMG is the utilization of the former to increase FSH in the initial phase (recruitment and selection) and maintain adequate FSH levels by administration of hMG during follicular growth phase.

It has been shown that by using the combined clomiphene citrate/hMG protocol in normogonadotropic patients, they could reduce the necessary hMG requirement by 50 %. Abdelazim and Makhlouf [37] compared sequential clomiphene citrate/hMG regimen to hMG regimen for ovulation induction in clomiphene citrate-resistant women. They found that the sequential CC/hMG regimen is as effective as hMG regimen for ovulation induction, produces satisfactory pregnancy results, and reduces treatment cost.

The clomiphene citrate/hMG treatment scheme is as follows: on the fifth through the ninth days after induced or spontaneous bleeding, the normogonadotropic patient receives 100 mg of clomiphene citrate daily. From the eighth day onwards, hMG is administered. The patient is carefully monitored by estrogen determination and ultrasound visualization of the growing follicle(s). This will help to determine if and when the ovulatory dose of hCG should be administered and to prevent hyperstimulation and multiple pregnancies.

The Help of Ultrasound: Assessing Complications

Multiple Pregnancies: The major adverse effects of induction of ovulation are multiple pregnancies and OHSS.

Five to eight percent of clomiphene-induced pregnancies and 15–25 % of all pregnancies following gonadotropin-induced ovulation are multiple gestations.

While almost all of the multiple gestations conceived on clomiphene will be twins, 30 % of multiple gestations following gonadotropin therapy will be triplets.

Poorly monitored ovulation induction is probably the major cause of the multiple pregnancy epidemics. Table 18.3 summarizes the clinical complication associated with twin pregnancies. It is important to diagnose multiple pregnancies early, in the first trimester, so women who conceive with high-order multiple pregnancies may consider multiple pregnancy reduction.

Table 18.3 Complications associated with twin pregnancy

Maternal complications	Fetal complications
Anemia	Premature delivery
Preeclampsia/eclampsia	Difficult delivery
Pre-/postpartum hemorrhage	Prolapse of an umbilical cord
	Hypoxia of second twin

In cases of twin pregnancy, it is recommended by the AIUM to document amnionicity and chorionicity in the early first trimester, so one can prepare for high-risk situations such as a monochorionic twin gestation.

In many countries, triggering of ovulation with hCG is only done if there are no more than two mature follicles around the assumed time of ovulation.

Adhering to strict guidelines involving ultrasound monitoring will definitely reduce the incidence of multiples.

Ovarian hyperstimulation is the most serious complication which in extreme situations is potentially life threatening and the reader is referred to Chap. 23.

It is important to understand the risk factors that can be identified in high-risk patients before ovulation is being induced. The presence of polycystic ovaries put the patient at increased risk; we have shown that a decrease in the fraction of the mature follicles and an increase in the fraction of the very small follicles around the assumed time of ovulation correlated with an augmented risk for the development of severe stimulation of the ovaries. Our data suggest [38] that ultrasonography is of good predictive value in the occurrence of clinically moderate to severe OHS in women treated by hMG and hCG. Even with estrogen levels within accepted normal limits, it is suggested that hMG/hCG administration should be interrupted in the presence of 11 or more preovulatory follicles, especially if most of them are immature (<9 mm).

Final Remarks

Ultrasound is the most powerful tool to monitor normal and stimulated cycles; predictions of the assumed time of ovulation allow optimal timing of various procedures such as insemination and ovum aspiration.

In stimulated cycles sonographic detection of too many follicles allows withholding hCG induction thus preventing hyperstimulation.

In the past ovulation function was monitored by estradiol estimation; since the development of sophisticated ultrasonographic techniques, monitoring of ovarian follicular growth by ultrasound became a routine addition to estradiol measurement in most clinics.

Accumulating data based on the Cochrane database [39] indicate that there is no evidence from randomized trials to support cycle monitoring by ultrasound plus serum estradiol as more efficacious than cycle monitoring by ultrasound only on outcomes of live birth and pregnancy rates.

As far as OHSS, randomized trial with a sufficiently large sample is needed. Until such a trial is considered, ultrasound plus serum estradiol may need to be retained as a precautionary good practice point in patients prone to develop hyperstimulation.

References

1. Aboulghar MM. Chapter 20: Ultrasound monitoring for ovulation induction: pitfalls and problems. In: Ovarian stimulation. Cambridge: Cambridge University Press; 2009. Online publication. ISBN 9780511762390.
2. Pierson RA, Olatunbosun OA, et al. Transvaginal ultrasonography and the evaluation of female infertility. In: Sciarra JJ, editor. Gynecology and obstetrics, vol. 5. Saskatoon: University of Saskatchewan; 2004. p. 1–12.
3. Blankstein J, Arora S, Brasch J. Ultrasound to monitor ovulation induction. In: Rizk B, Puschek E, editors. Ultrasonography in gynecology. Cambridge University Press. [In press].
4. Baerwald A, Walker R, Pierson R. Growth rate of ovarian follicles during natural menstrual cycles, oral contraceptives cycles and ovarian stimulation cycles. Fertil Steril. 2009;91(2):440–9.
5. Palatnik A, Strawn E, Szabo A, Robb P. What is the optimal follicular size before triggering ovulation in intrauterine insemination cycles with clomiphene citrate or letrozole? Fertil Steril. 2012;97(5):1089–94. e1–3.
6. Shrestha SM, Costello MF, Sjoblom P, McNally G, Bennett M, Steigrad SJ, Hughes GJ. Doppler ultrasound assessment of follicular vascularity in the early follicular phase and its relationship with outcome of in-vitro fertilization. J Assist Reprod Genet. 2006;23(4):161–9. Epub 2006 Apr 22.
7. Coulam CB, Goodman C, Rinehart JS. Colour Doppler indices of follicular blood flow as predictors of pregnancy after in vitro fertilization and embryo transfer. Hum Reprod. 1999;14(8):1979–82.
8. Nargund G, Bourne T, Doyle P, Parsons J, Cheng W, Campbell S, Collins W. Associations between ultrasound indices of follicular blood flow, oocyte recovery and preimplantation embryo quality. Hum Reprod. 1996;11(1):109–13.
9. Jayaprakasan K, Al-Hasie H, Jayaprakasan R, Campbell B, Hopkisson J, Johnson I, Raine-Fenning N. The three-dimensional ultrasonographic ovarian vascularity of women developing poor ovarian response during assisted reproduction treatment and its predictive value. Fertil Steril. 2009;92(6):1862–9. Epub 2008 Oct 29.
10. Bhal PS, Pugh ND, Gregory L, O'Brien S, Shaw RW. Peri-follicular vascularity as a potential variable affecting outcome in stimulated intrauterine insemination treatment cycles: a study using transvaginal power Doppler. Hum Reprod. 2001;16(8):1682–9.
11. Ivanovski M, Damcevski N, Radevska B, Doicev G. Assessment of uterine and arcuate artery blood flow by transvaginal color Doppler ultrasound on the day of human chorionic gonadotropin administration as predictors of pregnancy in an in vitro fertilization program. Akush Ginekol (Sofiia). 2012;51(2):55–60.
12. Kim A, Han JE, Yoon TK, Lyu SW, Seok H, Won HJ. Relationship between endometrial and subendometrial blood flow measured by three-dimensional power Doppler ultrasound and pregnancy after intrauterine insemination. Fertil Steril. 2010;94(2):747–52.
13. Cantineau AE, Cohlen BJ, Dutch IUI Study Group. The prevalence and influence of luteinizing hormone surges in stimulated cycles combined with intrauterine insemination during a prospective cohort study. Fertil Steril. 2007;88(1):107–12. Epub 2007 Apr 18.
14. Manzi DS, Dumez S, Scott LB, Nulsen JC. Selective use of leuprolide acetate in women undergoing superovulation with intrauterine insemination results in significant improvement in pregnancy outcome. Fertil Steril. 1995;63(4):866–73.
15. Allegra A, Marino A, Coffaro F, Scaglione P, Sammartano F, Rizza G, Volpes A. GnRH agonist-induced inhibition of the premature LH surge increases pregnancy rates in IUI-stimulated cycles. A prospective randomized trial. Hum Reprod. 2007; 22(1):101–8.
16. Kolibianakis EM, Zikopoulos K, Schiettecatte J, Smitz J, Tournaye H, Camus M, Van Steirteghem AC,

Devroey P. Profound LH suppression after GnRH antagonist administration is associated with a significantly higher ongoing pregnancy rate in IVF. Hum Reprod. 2004;19(11):2490–6.
17. Dickey RP, Olar TT, Taylor SN, Curol DN, Rye PH, Matulich EM. Relationship of follicle number, serum estradiol, and other factors to birth rate and multiparity in human menopausal gonadotropin-induced intrauterine insemination cycles. Fertil Steril. 1991;56(1):89–92.
18. Stoop D, Van Landuyt L, Paquay R, Fatemi H, Blockeel C, De Vos M, Camus M, Van den Abbeel E, Devroey P. Offering excess oocyte aspiration and vitrification to patients undergoing stimulated artificial insemination cycles can reduce the multiple pregnancy risk and accumulate oocytes for later use. Hum Reprod. 2010;25(5):1213–8.
19. Rotterdam Eshre/ASRM-sponsored PCOS consensus workshop group. Revised 2003 consensus on diagnostic criteria and long-term health risks related to polycystic ovary syndrome. Fertil Steril. 2004;81(1):19–25.
20. Kinkel K, Frei KA, Balleyguier G, et al. Diagnosis of endometriosis with imaging: a review. Eur Radiol. 2006;16:285.
21. de Silva KS, Kanumakala S, Grover SR, et al. Ovarian lesions in children and adolescents-an 11 year review. J Pediatr Endocrinol Metab. 2004;17:951.
22. La Marca A, Argento C, Sighinolfi G, Grisendi V, Carbone M, D'Ippolito G, Artenisio AC, Stabile G, Volpe A. Possibilities and limits of ovarian reserve testing in ART. Curr Pharm Biotechnol. 2012;13(3):398–408.
23. Deb S, Campbell BK, Clewes JS, Pincott-Allen C, Raine-Fenning NJ. The intra-cycle variation in the number of antral follicles stratified by size and in the endocrine markers of ovarian reserve in women with normal ovulatory menstrual cycles. Ultrasound Obstet Gynecol. 2012;41(2):216–22.
24. Frattearelli JL, Levi AJ, Miller BT, Segars JH. A prospective assessment of predictive value of basal antral follicles in in-vitro fertilization cycles. Fertil Steril. 2003;80:350–5.
25. Jokubkiene L, Sladkevicius P, Valentin L. Number of antral follicles, ovarian volume, and vascular indices in asymptomatic women 20 to 39 years old as assessed by 3-dimensional sonography – a prospective cross-sectional study. J Ultrasound Med. 2012;31:1635–49.
26. Hendriks DJ, Ben-Willem JM, Laszlo FJ, Egbert R, Broekmans FJM. Antral follicle count in the prediction of poor ovarian response and pregnancy after in vitro fertilization: a meta-analysis and comparison with basal follicle-stimulating hormone level. Fertil Steril. 2005;83(2):291–301.
27. Csokmay JM, Frattarelli JL. Basal ovarian cysts and clomiphene citrate ovulation induction cycles. Obstet Gynecol. 2006;107(6):1292–6.
28. Eissa MK, Hudson K, Docker MF, Sawers RS, Newton JR. Ultrasound follicular diameter measurement: and assessment of inter-observer and intra-observer variation. Fertil Steril. 1985;44:751–4.
29. Raine-Fenning NJ, Jayaprakasan K, Chamberlain S, Devlin L, Priddle H, Johnson I. Automated measurements of follicle diameter: a chance to standardize? Fertil Steril. 2009;91(4 Suppl):1469–72.
30. Jirge PR, Patil RS. Comparison of endocrine and ultrasound profiles during ovulation induction with clomiphene citrate and letrozole in ovulatory volunteer women. Fertil Steril. 2010;93(1):174–83.
31. Wolman I, Birenbaum-Gal T, Jaffa AJ. Cervical mucus status can be accurately estimated by transvaginal ultrasound during fertility evaluation. Fertil Steril. 2009;92(3):1165–7.
32. Homburg R. Clomiphene citrate – end of an era? Hum Reprod. 2005;20(8):2043–51.
33. Coughlan C, Fitzgerald J, Milne P, Wingfield M. Is it safe to prescribe clomiphene citrate without ultrasound monitoring facilities? J Obstet Gynaecol. 2010;30(4):393–6.
34. Shoham Z, DiCarlos C, Patel A, Conway GS, Jacobs HS. Is it possible to run a successful ovulation induction program based solely on ultrasound monitoring? The importance of endometrial measurements. Fertil Steril. 1992;56:836–41.
35. Shoham Z. Ultrasound is the only monitoring modality necessary for ovulation induction. OBGyn.net. 2011. http://hcp.obgyn.net/fetal-monitoring/content/article/1760982/1911450. Last accessed on 30 May 2013.
36. Wiser A, Gonen O, Ghetler Y, Shavit T, Berkowitz A, Shulman A. Monitoring stimulated cycles during in vitro fertilization treatment with ultrasound only-preliminary results. Gynecol Endocrinol. 2012;28(6):429–31.
37. Abdelazim IA, Makhlouf HH. Sequential clomiphene citrate/hMG versus hMG for ovulation induction in clomiphene citrate-resistant women. Arch Gynecol Obstet. 2013;287(3):591–7.
38. Blankstein J, Shalev J, Saadone T, Kukia EE, et al. Ovarian hyperstimulation syndrome; prediction by number and size of preovulatory follicles. Fertil Steril. 1987;47(4):597–602.
39. Kwan I, Bhattacharya S, et al. (Systemic review) Cochrane Menstrual Disorders and Sub-fertility Group (MDSG). Cochrane Database Syst Rev. 2008:(4).
40. Hodgen GD. Ovarian physiology and in vitro fertilization. In: Collins RC, editor. Ovulation induction. New York: Springer; 1991. p. 22–40.
41. Palleres P, Lealier C, Gonzales-Bulnes A. Progress toward "in vitro virtual histology" of ovarian follicle and corpora lutea by ultrasound. Fertil Steril. 2009;91(2):624–6.
42. Bromer JG, Aldad TS, Taylor HS. Defining the proliferative phase endometrial defect. Fertil Steril. 2009;91(3):698–704.

2D Ultrasound in Follicle Monitoring for ART

19

Mette Toftager and David P. Cohen

Abbreviations

2D	Two dimensional
3D	Three dimensional
AFC	Antral follicle count
ART	Assisted reproductive technologies
CI	Confidence interval
CL	Corpus luteum
ET	Embryo transfer
FI	Flow index
FSH	Follicle-stimulating hormone
GnRH	Gonadotropin-releasing hormone
GV	Germinal vesicle
hCG	Human chorionic gonadotropin
ICSI	Intracytoplasmic sperm injection
IVF	In vitro fertilization
LH	Luteinizing hormone
MII	Mature metaphase II
OHSS	Ovarian hyperstimulation syndrome
PI	Pulsatility index
PR	Pregnancy rates
PSV	Peak systolic velocity
RI	Resistance index
S/D	Systole/diastole ratio
VI	Vascularization index

M. Toftager, MD
Department of Gynecology and Obstetrics,
Section of Infertility, Hvidovre University Hospital,
Kettegaard Alle 30, Hvidovre 2650, Denmark
e-mail: mette.toftager@gmail.com

D.P. Cohen, MD (✉)
Department of Obstetrics and Gynecology/
Section of Reproductive Endocrinology,
University of Chicago Medical Center,
5841 S. Maryland Avenue – MC 2050,
Chicago, IL 60637, USA
e-mail: dcohen@babies.bsd.uchicago.edu

Introduction

Ultrasound imaging may be the most powerful instrument in the tool chest the reproductive endocrinologist has to improve success rates with assisted reproductive technologies (ART). This modality, improving yearly, permits noninvasive access to view ovarian responses to gonadotropin stimulation. Ultrasound examination of follicle maturation was first performed in 1978 by Hackeloer and showed a linear correlation between follicle size and serum estradiol levels [1]. In the early 1980s, additional studies confirmed the relationship between serum estrogen level and the number of follicles, the diameter of the follicles, and ovarian size. An increase in uterine size during stimulation was also described [2].

The introduction of transvaginal ultrasound in 1983 for follicle monitoring during ovulation induction has dramatically improved both the safety and success of ART. Transvaginal ultrasound imaging is thought to be imperative for the safe use of gonadotropins, to optimize treatment, to reduce the risk of multiple pregnancies, and to avoid potentially life-threatening side effects, such as ovarian hyperstimulation syndrome. Currently, the use of 2D ultrasound for assessing follicular development during gonadotropin stimulation for ART is essentially universal.

L.A. Stadtmauer, I. Tur-Kaspa (eds.), *Ultrasound Imaging in Reproductive Medicine*,
DOI 10.1007/978-1-4614-9182-8_19,

In addition 2D ultrasound with power Doppler has made it possible to study ovarian and endometrial blood flow. By monitoring perifollicular blood flow, the physician can identify follicles with oocytes that may have a better chance of pregnancy (see Chap. 5).

Why Monitor the Follicular Phase?

During in vitro fertilization (IVF), gonadotropins cause growth of the cohort of ovarian follicles, and monitoring at various stages is essential in order to optimize and individualize IVF treatments. Ultrasound monitoring during the follicular phase has many useful attributes.

It can identify the quiescent ovary and avoid initiating ovulation induction if there is any ovarian abnormality. For example, it may be that a follicular cyst remains from a recent ovulatory cycle or there may be an as yet identified ovarian pathologic cyst or adnexal mass that needs to be addressed. Next, a baseline count of antral follicles provides a hint into the probable success of the cycle, predicting ovarian response to identify the optimal starting dose of gonadotropin and decide upon the type of stimulation protocol. Third is to verify pituitary downregulation; before gonadotropin stimulation is started (when GnRH analogs are used to suppress ovulation), it is imperative to determine whether the initially suggested gonadotropin stimulation dosing is ideal or needs to be adjusted. Fourth, evaluating the ease with which the ovaries will be accessible for transvaginal needle aspiration is crucial, and this information is easily obtained again, just prior to initiating gonadotropin stimulation. Fifth, ultrasound scanning conveniently estimates follicle size and number to predict how many oocytes will be mature and ready to aspirate after gonadotropin stimulation is complete. Sixth is avoiding ovarian hyperstimulation syndrome (OHSS). When OHSS is evolving, free fluid is identified in the peritoneal cavity and clearly recognized with 2D ultrasound imaging. Finally, ultrasound monitoring is critical to determine the optimal time to provoke ovulation; most clinicians agree that given only one modality to monitor ovulation induction, they would select ultrasound first.

At the beginning of an ovarian cycle, in preparation to monitor follicular growth and development (with or without added ovulation induction medications), the 2D ultrasound assessment of the antral follicle count (AFC) is simple, minimally invasive, and a beneficial information. Ben-Haroush et al. [3] assessed the correlation between AFC and IVF cycle success. In their study of 115 women, 33 % achieved a pregnancy, and AFC was significantly higher in the successful IVF group. Furthermore, and perhaps more interestingly, the subgroup of women with high AFC values of smaller follicles (2–5 mm) did best compared to those with larger follicles (5–10 mm). A subsequent study by the same authors [4] documented better outcomes after IVF among women with higher AFC values, and higher AFC values correlated positively with age, ovarian volume, number of oocytes retrieved, and the number of highest quality embryos.

Normal Folliculogenesis

Before reviewing the details of the parameters of follicular growth studied with 2D ultrasound imaging, it is helpful to summarize normal folliculogenesis, in order to be able to correlate imaging findings with physiologic expectations. Follicles grow in two stages: the gonadotropin-independent and gonadotropin-dependent stages. Primordial follicles consist of an oocyte with a thin layer of granulosa and stromal cells and cannot be seen on ultrasound. By the time follicles develop a fluid antrum, they are ultrasonographically identifiable, and they have reached the gonadotropin-dependent stage of the 3-month maturation process. These antral follicles measure between 2 and 10 mm and represent the pool of follicles that may be recruited in the ensuing follicular phase. In a natural cycle, one is ultimately selected for ovulation, and that selection process occurs during the latter half of the follicular phase of the ovarian cycle when the endogenous pituitary follicle-stimulating hormone (FSH) level is falling in response to the increasing ovarian estradiol production. Falling FSH promotes a selection process in which each of the follicular

microenvironments competes for the diminishing FSH needed to stimulate granulosa cells in the follicle to produce aromatase. Aromatase, in turn, is necessary to convert testosterone and androstenedione produced in the peripheral theca cells into estradiol and estrone, respectively. Failure of this conversion leads to an elevated androgen to estrogen ratio, which leads to follicular atresia. From this cursory review of the anatomy and physiology of oocyte maturation, it is easy to see how ovulation-inducing agents that either indirectly increase endogenous FSH (e.g., clomiphene citrate) or directly add FSH to the system diminish the competition between the follicles and permit the development of multiple dominant follicles [5, 6].

Monitoring Follicular Maturation

Methods for Monitoring

It is difficult to predict the optimal number of growing ovarian follicles in an IVF cycle, since there is considerable variation in ovarian response among women undergoing ovulation induction therapy. The ovarian response depends on age, ovarian reserve, how the hypothalamic-ovarian axis is manipulated exogenously (the stimulation protocol), FSH dose, cause of infertility, ethnicity, etc.

Follicular maturation in IVF cycles can be monitored clinically in different ways, either by:

- Serum estradiol value alone
- 2D ultrasound alone
- 3D ultrasound alone
- Serum estradiol and ultrasound combined
- Supplemental power Doppler imaging

There are numerous studies on the use of these different methods for monitoring follicular maturation. Traditional monitoring of an IVF treatment cycle includes a combination of regular ultrasonography and serum estradiol concentrations and has long been accepted as the gold standard. However, the need for estradiol monitoring remains controversial [7]. Ultrasound provides more accurate measurement of follicle number and size than can be obtained by serum estradiol alone. Whether serum estradiol or ultrasound is superior to the other is questionable, but it has been shown that ultrasound imaging of follicular growth and endometrial thickness is sufficient to monitor follicular maturation [8, 9].

Which approach, when to adjust the gonadotropin dose up or down, and how often monitoring should be done is dependent on the individual clinician, the experience, and the routine at each individual clinic. Some monitoring methods are very complex, whereas other methods are rather simple; however, the outcomes of IVF cycles seem to be the same, regardless of the chosen method [10].

When viewed on ultrasound, follicles appear as echo-free structures within the more echogenic ovarian tissue. By convention, follicle size in 2D is estimated by calculating the mean of the maximum follicular internal diameter in two perpendicular planes [11]. Alternatively, the follicle size can be estimated in three dimensions, the x, y, and z planes. Using this technique, it is possible to calculate volumes for each follicle. Most recently, 3-dimensional software programs that distinguish the echogenicity of the well-circumscribed, sharp-edged, echolucent follicular fluid from the surrounding greater echogenicity of the ovarian cortical parenchyma have automated this process and permitted follicular volume calculations from data derived from 2D-derived images. The technician can now simply sweep through the ovarian tissue, and the stored image data is analyzed, reducing the time needed to separately measure each follicle's multiple axes. Particularly in busy practices performing dozens of follicular monitoring scans daily, this is a valuable asset.

Standard Ultrasound Monitoring Program

Follicular growth can be directly monitored with 2D ultrasound, since the follicular diameter increases during the gonadotropin-sensitive stage of development. Most practices measure the follicles at baseline (Fig. 19.1), prior to initiating gonadotropin stimulation and then again after approximately 5 days of gonadotropin stimulation, and then every 24–48 h depending

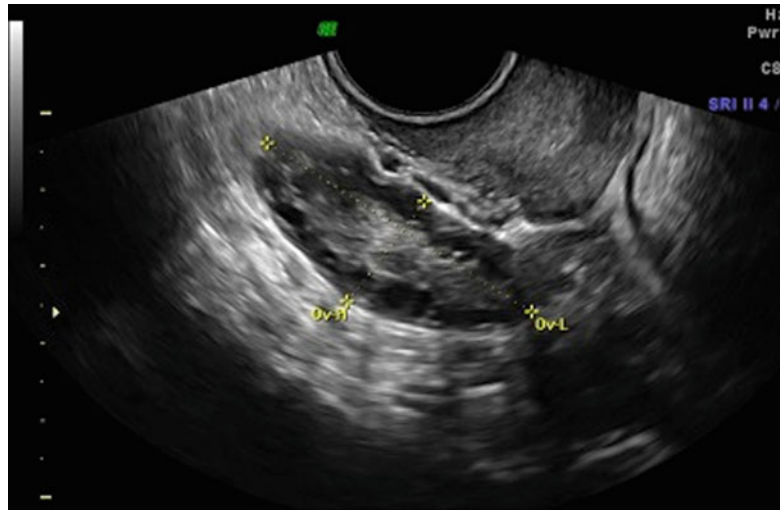

Fig. 19.1 Baseline, prior to initiating gonadotropin stimulation. Ovary with antral follicles

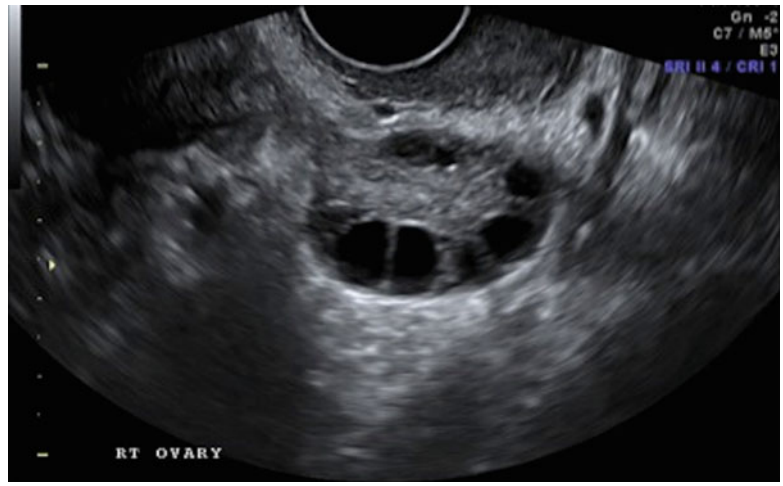

Fig. 19.2 Stimulation day 5, showing recruited follicles measuring 10–12 mm

on the rate of development (Figs. 19.2, 19.3, 19.4, and 19.5). Once the mature follicle measures 18–21 mm, the practitioner can trigger ovulation with human chorionic gonadotropin (hCG, a luteinizing hormone (LH) surrogate) (Fig. 19.6), and confirmation of ovulation can be demonstrated with ultrasound as well. The sudden change from an intact follicle, made up of concentric layers of theca cells surrounding granulosa cells enclosing the follicular fluid and the oocyte, is suddenly lost at ovulation. Physiologically it is at this moment that both testosterone-secreting theca cells and estradiol-secreting granulosa cells convert intracellular steroid production to preferentially favor progesterone production. This is accompanied by a dramatic loss of the concentric architecture of the preovulatory follicle and an increase in blood supply, presumably designed to channel progesterone from the corpus luteum to the endometrium. A very specific, nearly pathognomonic "ring of fire" ultrasound finding is easily discerned around each corpus luteum at this time (Fig. 19.7). Doppler technology added to the 2D image enables observation of this flow pattern so it is nearly impossible to mistake. Combining the classic echogenicity of the corpus luteum with the Doppler low impedance flow characteristics surrounding the corpus luteum confirms the structure [5].

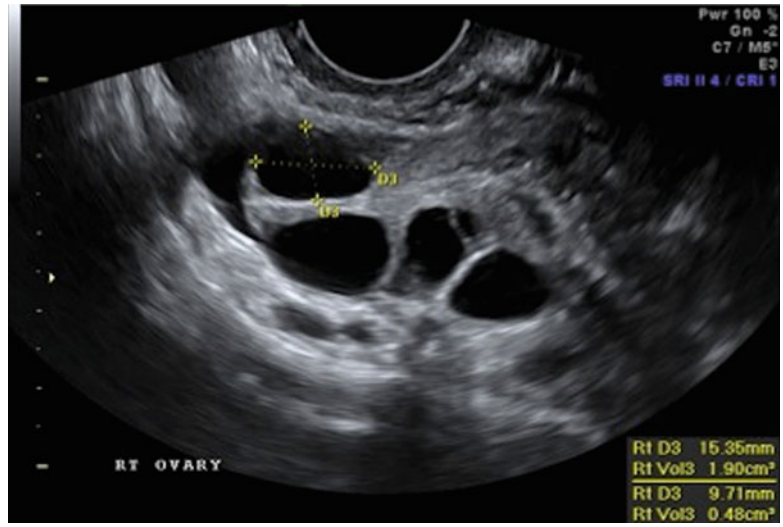

Fig. 19.3 Stimulation day 7, showing ovary with leading follicle >12 mm

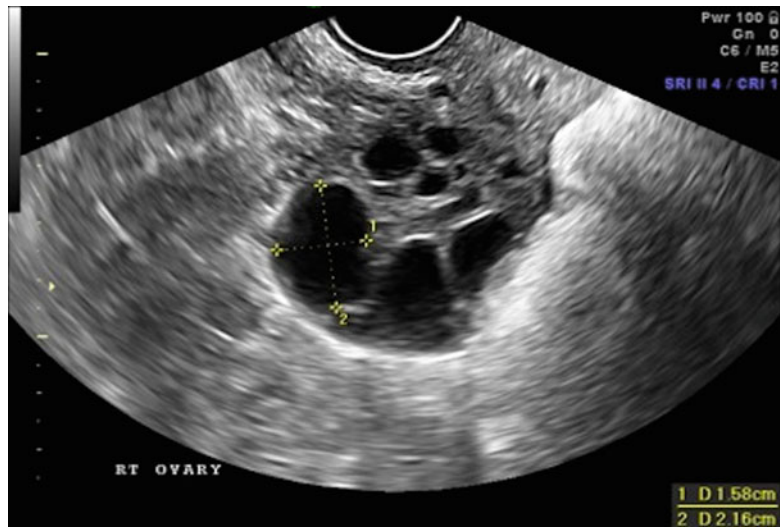

Fig. 19.4 Stimulation day 9, showing ovary with growing follicles

Follicular Size and Volume

During ovulation induction it is realistic to recruit five to ten ovarian follicles in each ovary; however, the number, rate of growth of each follicle, and the number of stimulation days can vary greatly.

After 6–7 days of gonadotropin stimulation, follicles measuring more than 10 mm are expected.

Once a dominant follicle measures greater than 12 mm, follicular growth of 2 mm (1–3 mm) per day is expected [12]. Growth continues until follicular maturation at 18–21 mm, and at that point the oocyte inside is ready to ovulate, that is, complete meiosis, and be released in preparation for fertilization.

Criteria Used for Triggering Ovulation

The criteria used for triggering ovulation-inducing final oocyte maturation vary between protocols, but all aim to produce mature oocytes to be fertilized; it is important to keep in mind that mature

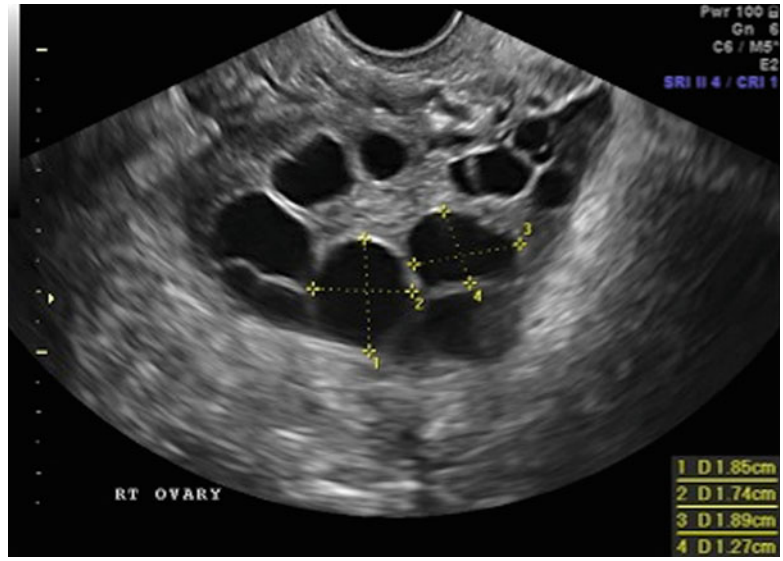

Fig. 19.5 Stimulation day 11, 2–3 follicles measuring 17–18 mm

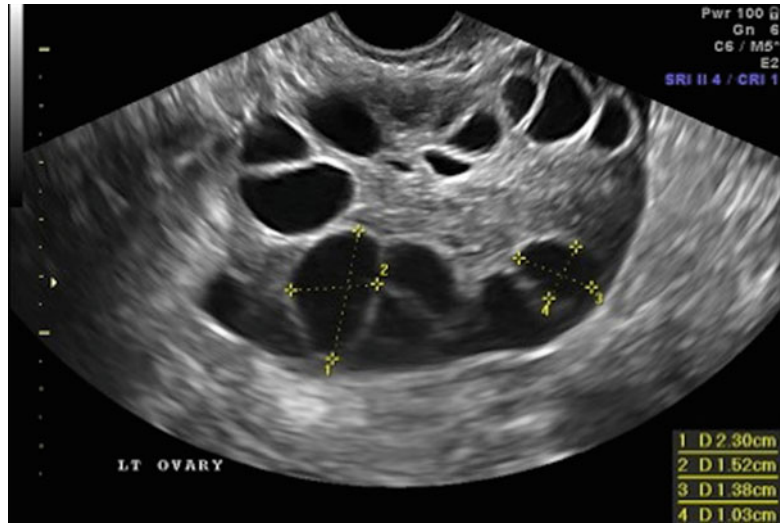

Fig. 19.6 Day of ovulation induction. Leading follicles measuring more than 18 mm

oocytes are those that have completed meiosis I, extruded the first polar body, and rearrested in metaphase of meiosis II. Most commonly hCG is administered to mimic the endogenous LH surge to provoke meiotic re-initiation from the oocyte's prophase I resting state. As noted, protocols vary and are often altered, but most commonly ovulation is provoked when ≥3 follicles ≥17 mm are identified on ultrasound. Another approach many clinicians employ is to trigger final oocyte maturation when ≥3 follicles is observed, each with a maximum diameter of 18 mm, or, finally, when ≥1 follicle of ≥18 mm and three follicles of ≥15 mm are identified. More complex criteria have taken into consideration serum estradiol levels; hCG is administered when the leading follicle reaches 18–20 mm and the coincident serum estradiol level suggests satisfactory follicular development. In addition, induction of final oocyte maturation has been performed in the presence of at least one follicle ≥20 mm and a serum estradiol level ≥1,200 pg/ml. Finally, hCG has been administered in the presence of at least one follicle ≥20 mm or a serum estradiol level

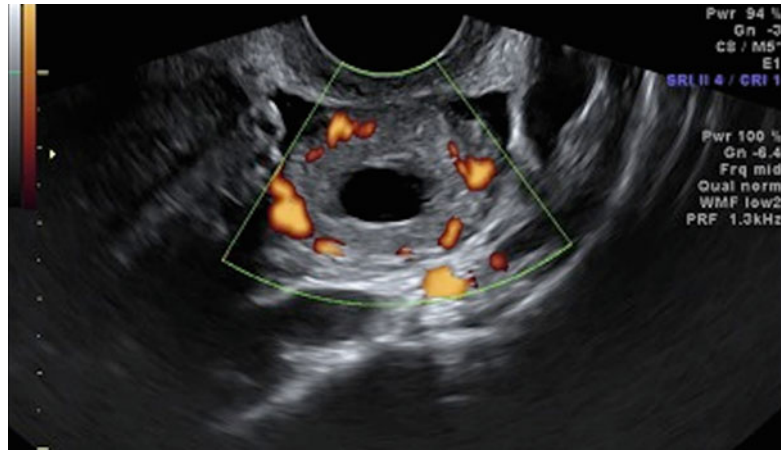

Fig. 19.7 Corpus luteum cyst – "ring of fire"

≥1,200 pg/ml [13]. There are no data to suggest that any one protocol is significantly superior to any other, and protocols will vary based on individual physician preferences and patient responses to stimulation.

In summary, for timing of hCG administration, the number of adequate size follicles (12–24 mm) appears to be more important than the size of the leading follicle [14]. It has been shown that when hCG is administered in the presence of a leading follicle >20 mm, the fertilization rate is greater and the embryo implantation rate higher than when hCG is given with a leading follicle of smaller size [15].

How to Predict Retrieval of Mature Oocytes?

Follicular size and the volume of follicular fluid have always been recognized as possible predictors of oocyte quality, specifically, oocytes that will be fertilized and result in embryos that implant and result in a live-born infant. In one study, embryo quality, defined as decreased embryo fragmentation and increased cleavage rate, and the implantation rate was higher, and clinical and ongoing pregnancy rates tended to be higher when hCG was administered after a larger follicle size was observed [16]. The follicular volume together with follicle number are the only two independent predictors of the number of oocytes that will be retrieved, the fertilization rate, and the number and morphological quality of the embryos developed [17].

Attempts to find a universally accepted threshold of a worth-to-be-punctured follicle size, however, has been disappointing due to conflicting outcomes. What is accepted is that a large follicle is more likely to lead to the retrieval of a mature oocyte than a smaller follicle. The correlation between the follicle size and the likelihood of retrieving a mature oocyte may be the observable physical manifestation of the idea that larger follicles have completed the maturation process and released the oocyte-cumulus cell mass as a free-floating structure in the antral fluid just before follicle rupture [18]. According to Teissier [19], 14 mm diameter should be considered the threshold follicle size to get an acceptable chance of finding meiotically competent oocytes at retrieval, both in normal and polycystic ovaries. For IVF patients, Bergh et al. found oocytes in follicles with a mean diameter >16 mm to have a significantly higher fertilization rate (71.4 %) compared to oocytes from smaller follicles (58.1 %). Interestingly, in that same study, the authors note that once an oocyte is fertilized, embryo cleavage rates were similar (95.4 and 93.9, respectively), but pregnancy rates for the two groups were dramatically different, 47 and 15 %, respectively. For intracytoplasmic sperm injection (ICSI) patients, the fertilization rate was 72.0 and 71.1 % for oocytes from large and small follicles, respectively; the corresponding cleavage rate was 93.0 and 91.1 %, and the

pregnancy rate for the two groups was 41 and 42 % [20]. Follicles measuring 11–15 mm were observed to have a 50 % chance of yielding a mature oocyte [21].

Mature metaphase II (MII) oocytes are more frequently retrieved from 16 to 22 mm diameter (2–5 ml volume) follicles, and MII oocytes tend to develop the best morphologically scored embryos. On the contrary, follicles with a mean diameter above 22 mm result in lower recovery of mature, fertilizable oocytes as they often contain postmature eggs, postulated to result from the development of intrafollicular atresia and degenerative phenomena [22].

Other investigators have also observed a correlation between oocyte fitness and ultrasound-measured size prior to retrieval. A higher proportion of immature germinal vesicle (GV) stage oocytes, for example, are found in smaller follicles, particularly follicles below 12 mm of mean diameter. This is not a universal finding, however, since even small follicles can generate mature MII oocytes [20, 23]. Wittmaack et al. [14] found the optimal follicle volume to be >1 ml, which corresponds to ≥12 mm, and the maximum volume to be 6–7 ml, corresponding to a 24 mm follicle. They observed a higher oocyte recovery rate, higher fertilization rate, and higher cleavage rate for follicles in this interval. Oocytes from larger follicles are reported to allow higher fertilization rates and generate better embryos.

Conversely, in a prospective study including 9,933 follicles from 535 IVF cycles, it was observed that oocytes from follicles with volume <1 ml (<12 mm diameter) had a significantly lower fertilization rate than oocytes from larger follicles, but when fertilized they yielded embryos of comparable quality; in fact, no significant differences in the implantation, clinical pregnancy, or live birth rates per cycle were detectable from embryos derived from oocytes measured in small or large follicles [24].

In these studies, however, it was not possible to identify a clear relationship between follicle size and morphological quality of the in vitro-produced embryos. This may be due to the fact that follicles with a volume within a certain interval contain oocytes that lead to embryos of comparable morphologic scores and/or to the fact that the male gamete contributes to embryo quality as well and needs to be considered along with the oocyte.

Importantly, follicular size, volume, morphology, or vascularity does not provide enough information to ascertain oocyte quality when quality is defined as the conception of a euploid child. The best approximation of quality, however, is that a follicle with at least a diameter of 14 mm, more than 0.6 ml volume, and well-developed vascularity houses an oocyte more likely to be successfully fertilized.

Monitoring of Endometrial Proliferation

During the proliferative phase of the menstrual cycle, many factors have been studied and identified to contribute to a successful pregnancy among patients undergoing assisted reproduction. The aim of 2D monitoring of the follicular phase in ART is not solely to monitor follicular development, but also to monitor endometrial development. Predicting the probability of pregnancy by assessing the degree of endometrial development on sonography has been the objective of numerous studies.

Endometrial thickness and pattern, in response to estrogen secretion by the ovarian follicles, varies throughout the menstrual cycle. The endometrium is thin immediately after menstruation (2–5 mm), thickens during the proliferative phase, is trilaminar before ovulation, and is thick and echogenic in the secretory phase of the cycle. A small amount of endometrial fluid (0.5–1.0 mm film in the middle of the cavity), thought to be mucus, can be seen before ovulation, is considered normal, and rapidly disappears. However, significant endometrial fluid at the time of an embryo transfer (ET), often visible in the presence of hydrosalpinges, is associated with a poorer prognosis. When this observation is made, freezing of all the embryos is frequently considered to provide time to optimize management.

With respect to endometrial differentiation, sonography predictors that are often studied

include endometrial blood flow, endometrial echo pattern, and endometrial thickness.

The thickened endometrium provides the critical site for embryo attachment. Controversies exist, however, regarding the clinical significance of observed variations in endometrial thickness in relation to pregnancy rates (PR) during IVF. Some studies reported no correlation between endometrial thickness and PR, while others suggest a positive correlation between endometrial thickness and PR, reporting significantly greater endometrial thicknesses occur in successful IVF cycles compared to unsuccessful cycles. Possible reasons for this observed discordancy in results may be attributed to different treatment protocols and/or the different etiologies of infertility. All studies, however, seem to agree that a "thin" endometrium is detrimental to the implantation and development of a pregnancy [25]. Patients with a thin endometrium present the clinician with a dilemma, therefore, whether to continue the cycle despite a possibly reduced chance of pregnancy or to cancel the cycle and cryopreserve the embryos [26]. Most recently a meta-analysis from 2011 found a significant difference in mean endometrial thickness on the day of hCG administration between IVF patients achieving pregnancy versus those failing to achieve a pregnancy; a difference of 0.4 mm (95 % CI 0.22–0.58) and an odds ratio for pregnancy of 1.40 (95 % CI 1.24–1.58) were reported [27].

The use of endometrial blood flow in predicting endometrial receptivity has also been studied. Presence of both endometrial and subendometrial blood flow correlates with higher implantation and pregnancy rates, and the absence of endometrial and subendometrial blood flow is associated with a thinner endometrium and is associated with higher uterine artery resistance [28, 29].

Studies indicate that echogenic patterns of the endometrium reflect histologic processes that are believed to be involved in the establishment of receptivity as well. This may explain the reported association between premature hyperechogenic patterns of the endometrium and poor implantation rates [30]. Check et al. demonstrated a trend for higher pregnancy rates in controlled ovarian stimulation cycles with triple-line isoechogenic patterns observed in the late follicular phase [31].

Although there may be a relationship between endometrial differentiation and pregnancy, implantation potential is probably more complex than a few ultrasound measurements can determine. De Geyter concludes that pregnancy rates of assisted reproductive procedures are influenced only marginally by the degree of endometrial proliferation, and treatment should not be canceled because of inadequate endometrial thickness [26, 32]. At this point there is no consensus to resolve this question.

Monitoring with 2D Versus 3D

Three-dimensional follicular volume measurements have a stronger correlation with the number of mature oocytes retrieved than 2D measurements. As 3D technology improves, this parameter may replace 2D measurements in the optimal timing of hCG before oocyte retrieval [21].

Most recently 3D power Doppler angiography has been introduced for the study of perifollicular blood flow, and this technique enables the study of all the ovarian and follicular blood vessels. It can be used to calculate both the vascularization index (VI) and the flow index (FI) from the whole ovary [33].

Monitoring with Power Doppler (In Relation to 2D)

Under physiological gonadotropin stimulation, granulosa cells produce angiogenesis factors which contribute to the increasing vascularization needed for follicle development, ovulation, and optimal function of the corpus luteum (CL). Around the dominant follicle, neovascularization can be detected by Doppler ultrasound both during spontaneous ovulation and during ovulation induction. This phenomenon allows measurement of the increased perifollicular blood fluxes, and the associated decreased vascular resistance

indexes, around the preovulatory follicle. A rapid increase in blood flow velocity has been reported to occur at the time of the LH surge in the perifollicular and ovarian stromal blood vessels and has been associated with a sign of follicle maturity and approaching ovulation [34, 35].

Nargund et al. studied this correlation and suggested that a perifollicular flow >10 cm/s can enhance selection of oocytes and ultimately increase pregnancy rates [36].

High-grade ovarian perifollicular blood perfusion in the early follicular phase during IVF is associated with both high-grade perifollicular blood perfusion in the late follicular phase and a higher clinical pregnancy rate [37].

Jadaon et al. measured four Doppler indices in women prior to IVF treatment: peak systolic velocity (PSV), pulsatility index (PI), resistance index (RI), and systole/diastole ratio (S/D). They found a positive correlation between the number of ≥14 mm follicles on the day of hCG and PSV. The number of follicles ≥14 mm and retrieved oocytes had a significant negative correlation with RI and S/D ratio. As well, the number of fertilized oocytes had a significant negative correlation with S/D ratio. Absence of a Doppler signal in one or both ovaries was significantly higher in the women with a poor response (31 %) as compared to women with a normal response (16 %) [38]. PSV of individual follicles among women undergoing IVF has been shown to correlate with oocyte recovery, fertilization rate, developmental potential of the oocyte, and the quality of the preimplantation embryo [39].

It has been suggested that the Doppler blood flow analysis of the growing follicles could be used in IVF to select the best oocytes that lead to embryos with better implantation potential. However, it is questionable if power Doppler is an option in busy practices running IVF cycles. Controlled ovarian hyperstimulation generates multiple follicles overlapping one another in normal responders, and it may be difficult to assign a specific flow to an isolated follicle versus the neighboring one with 2D Doppler. This may imply that power Doppler is better to use on low responders, women closer to menopause, or women with a history of multiple failed IVF cycles.

Conclusion

2D ultrasound monitoring of follicular development and maturation during controlled ovarian stimulation is an integral component of most clinical practices. It is not always necessary, particularly when using oral agents to stimulate ovulation, but it is now a standard of care during any ovulation induction therapy in advance of an intrauterine insemination or in vitro fertilization procedure. It provides the information needed to permit the safe use of these medications and to avoid the acute risks of hyperstimulation syndrome and the longer-term sequelae associated with multiple gestation pregnancies. The accuracy and ease of use of this technical tool was unchallenged; it only remains to be determined what the positive and negative predictive values of the data it generates will be. Regardless of the final outcomes and interpretations of the studies still underway to find those answers it will remain a tool, it will not replace the physician's required judgment of the entire clinical presentation.

References

1. Hackeloer BJ, Robinson HP. Ultrasound examination of the growing ovarian follicle and of the corpus luteum during the normal physiologie menstrual cycle (author's transl). Geburtshilfe Frauenheilkd. 1978; 38(3):163–8.
2. Ylostalo P, Lingren PG, Nillius SJ. Ultrasonic measurement of ovarian follicles, ovarian and uterine size during induction of ovulation with human gonadotrophins. Acta Endocrinol (Copenh). 1981;98(4): 592–8.
3. Ben-Haroush A, Farhi J, Zahalka Y, Sapir O, Meizner I, Fisch B. Small antral follicle count (2–5 mm) and ovarian volume for prediction of pregnancy in in vitro fertilization cycles. Gynecol Endocrinol. 2011;27(10): 748–52.
4. Ben-Haroush A, Farhi J, Zahalka Y, Sapir O, Meizner I, Fisch B. Correlations between antral follicle count and ultrasonographic ovarian parameters and clinical variables and outcomes in IVF cycles. Gynecol Endocrinol. 2012;28(6):432–5.
5. Jokubkiene L, Sladkevicius P, Rovas L, Valentin L. Assessment of changes in volume and vascularity of the ovaries during the normal menstrual cycle using three-dimensional power Doppler ultrasound. Hum Reprod. 2006;21(10):2661–8.

6. Verberg MF, Macklon NS, Nargund G, Frydman R, Devroey P, Broekmans FJ, et al. Mild ovarian stimulation for IVF. Hum Reprod Update. 2009;15(1):13–29.
7. Thomas K, Searle T, Quinn A, Wood S, Lewis-Jones I, Kingsland C. The value of routine estradiol monitoring in assisted conception cycles. Acta Obstet Gynecol Scand. 2002;81(6):551–4.
8. Wiser A, Gonen O, Ghetler Y, Shavit T, Berkovitz A, Shulman A. Monitoring stimulated cycles during in vitro fertilization treatment with ultrasound only–preliminary results. Gynecol Endocrinol. 2012;28(6): 429–31.
9. Kwan I, Bhattacharya S, McNeil A, van Rumste MM. Monitoring of stimulated cycles in assisted reproduction (IVF and ICSI). Cochrane Database Syst Rev. 2008;(2):CD005289.
10. Wikland M, Hillensjö T. Monitoring ovarian response in IVF cycles. In: Gardner D, Weissman A, Howles C, Shoham Z, editors. Textbook of assisted reproductive techniques. 4th ed. London: Informa Healthcare; 2012. p. 560.
11. Penzias AS, Emmi AM, Dubey AK, Layman LC, DeCherney AH, Reindollar RH. Ultrasound prediction of follicle volume: is the mean diameter reflective? Fertil Steril. 1994;62(6):1274–6.
12. Tur-Kaspa I, Stadtmauer L. Ultrasonography in assisted reproduction. In: Gardner DK, Weismann A, Howles CM, Shoham Z, editors. Textbook of assisted reproductive techniques. 4th ed. London: Informa Healthcare; 2012. p. 225–42.
13. Kolibianakis EM, Albano C, Camus M, Tournaye H, Van Steirteghem AC, Devroey P. Prolongation of the follicular phase in in vitro fertilization results in a lower ongoing pregnancy rate in cycles stimulated with recombinant follicle-stimulating hormone and gonadotropin-releasing hormone antagonists. Fertil Steril. 2004;82(1):102–7.
14. Wittmaack FM, Kreger DO, Blasco L, Tureck RW, Mastroianni Jr L, Lessey BA. Effect of follicular size on oocyte retrieval, fertilization, cleavage, and embryo quality in in vitro fertilization cycles: a 6-year data collection. Fertil Steril. 1994;62(6):1205–10.
15. Miller KF, Goldberg JM, Falcone T. Follicle size and implantation of embryos from in vitro fertilization. Obstet Gynecol. 1996;88(4 Pt 1):583–6.
16. Haning Jr RV, Austin CW, Kuzma DL, Shapiro SS, Zweibel WJ. Ultrasound evaluation of estrogen monitoring for induction of ovulation with menotropins. Fertil Steril. 1982;37(5):627–32.
17. Merce LT, Bau S, Barco MJ, Troyano J, Gay R, Sotos F, et al. Assessment of the ovarian volume, number and volume of follicles and ovarian vascularity by three-dimensional ultrasonography and power Doppler angiography on the HCG day to predict the outcome in IVF/ICSI cycles. Hum Reprod. 2006;21(5):1218–26.
18. Suchanek E, Simunic V, Juretic D, Grizelj V. Follicular fluid contents of hyaluronic acid, follicle-stimulating hormone and steroids relative to the success of in vitro fertilization of human oocytes. Fertil Steril. 1994; 62(2):347–52.
19. Teissier MP, Chable H, Paulhac S, Aubard Y. Comparison of follicle steroidogenesis from normal and polycystic ovaries in women undergoing IVF: relationship between steroid concentrations, follicle size, oocyte quality and fecundability. Hum Reprod. 2000; 15(12):2471–7.
20. Bergh C, Broden H, Lundin K, Hamberger L. Comparison of fertilization, cleavage and pregnancy rates of oocytes from large and small follicles. Hum Reprod. 1998;13(7):1912–5.
21. Shmorgun D, Hughes E, Mohide P, Roberts R. Prospective cohort study of three- versus two-dimensional ultrasound for prediction of oocyte maturity. Fertil Steril. 2010;93(4):1333–7.
22. Ectors FJ, Vanderzwalmen P, Van HJ, Nijs M, Verhaegen G, Delvigne A, et al. Relationship of human follicular diameter with oocyte fertilization and development after in-vitro fertilization or intracytoplasmic sperm injection. Hum Reprod. 1997;12(9):2002–5.
23. Inaudi P, Germond M, Senn A, De GP. Timing of hCG administration in cycles stimulated for in vitro fertilization: specific impact of heterogeneous follicle sizes and steroid concentrations in plasma and follicle fluid on decision procedures. Gynecol Endocrinol. 1995;9(3): 201–8.
24. Salha O, Nugent D, Dada T, Kaufmann S, Levett S, Jenner L, et al. The relationship between follicular fluid aspirate volume and oocyte maturity in in-vitro fertilization cycles. Hum Reprod. 1998;13(7):1901–6.
25. Detti L, Yelian FD, Kruger ML, Diamond MP, Puscheck EE. Endometrial thickness dynamics and morphologic characteristics during pituitary down-regulation with antagonists in assisted reproductive technology cycles. J Ultrasound Med. 2008;27(11): 1591–6.
26. De GC, Schmitter M, De GM, Nieschlag E, Holzgreve W, Schneider HP. Prospective evaluation of the ultrasound appearance of the endometrium in a cohort of 1,186 infertile women. Fertil Steril. 2000;73(1): 106–13.
27. Momeni M, Rahbar MH, Kovanci E. A meta-analysis of the relationship between endometrial thickness and outcome of in vitro fertilization cycles. J Hum Reprod Sci. 2011;4(3):130–7.
28. Wang L, Qiao J, Li R, Zhen X, Liu Z. Role of endometrial blood flow assessment with color Doppler energy in predicting pregnancy outcome of IVF-ET cycles. Reprod Biol Endocrinol. 2010;8:122.
29. Chien LW, Au HK, Chen PL, Xiao J, Tzeng CR. Assessment of uterine receptivity by the endometrial-subendometrial blood flow distribution pattern in women undergoing in vitro fertilization-embryo transfer. Fertil Steril. 2002;78(2):245–51.
30. Fanchin R. Assessing uterine receptivity in 2001: ultrasonographic glances at the new millennium. Ann N Y Acad Sci. 2001;943:185–202.
31. Check JH, Choe JK, Amui J, Brasile D, Jamison T. Evaluation of the importance of late follicular phase endometrial echo patterns and pregnancy outcome following embryo transfer by evaluating infertile

donor/recipient pairs. Clin Exp Obstet Gynecol. 2011; 38(4):318–9.
32. Check JH. The importance of sonographic endometrial parameters in influencing success following embryo transfer in the modern era and therapeutic options–part 1: the importance of late proliferative phase endometrial thickness. Clin Exp Obstet Gynecol. 2011;38(3):197–200.
33. Jarvela IY, Sladkevicius P, Tekay AH, Campbell S, Nargund G. Intraobserver and interobserver variability of ovarian volume, gray-scale and color flow indices obtained using transvaginal three-dimensional power Doppler ultrasonography. Ultrasound Obstet Gynecol. 2003;21(3):277–82.
34. Ardaens Y, Gougeon A, Lefebvre C, Thomas P, Leroy M, Leroy JL, et al. Contribution of ovarian and uterine color Doppler in medically assisted reproduction techniques (ART). Gynecol Obstet Fertil. 2002;30(9):663–72.
35. Lovrec VG, Vlaisavljevic V, Reljic M. Dependence of the in-vitro fertilization capacity of the oocyte on perifollicular flow in the preovulatory period of unstimulated cycles. Wien Klin Wochenschr. 2001; 113 Suppl 3:21–6.
36. Nargund G, Doyle PE, Bourne TH, Parsons JH, Cheng WC, Campbell S, et al. Ultrasound derived indices of follicular blood flow before HCG administration and the prediction of oocyte recovery and preimplantation embryo quality. Hum Reprod. 1996;11(11):2512–7.
37. Shrestha SM, Costello MF, Sjoblom P, McNally G, Bennett M, Steigrad SJ, et al. Power Doppler ultrasound assessment of follicular vascularity in the early follicular phase and its relationship with outcome of in vitro fertilization. J Assist Reprod Genet. 2006; 23(4):161–9.
38. Jadaon JE, Ben-Ami M, Haddad S, Radin O, Bar-Ami S, Younis JS. Prospective evaluation of early follicular ovarian stromal blood flow in infertile women undergoing IVF-ET treatment. Gynecol Endocrinol. 2012;28(5):356–9.
39. Coulam CB, Goodman C, Rinehart JS. Colour Doppler indices of follicular blood flow as predictors of pregnancy after in-vitro fertilization and embryo transfer. Hum Reprod. 1999;14(8):1979–82.

3D Ultrasound for Follicle Monitoring in ART

20

Maximilian Murtinger and Nicolas Herbert Zech

Introduction

There are many factors that influence the success of assisted reproduction technology (ART). These include medical indications, health status, hormone levels, the stimulation protocol, the preparation of the endometrium for implantation, and gamete quality. For most of the aforementioned factors, ultrasound (US) is becoming increasingly important for use in reproductive medicine. US is essential for the evaluation of women for infertility factors and subsequent therapy scheduling. It is also used for the determination of endometrial thickness (Fig. 20.1) and US measurements allow and facilitate the evaluation of uterine morphology. US can reveal uterine malformations such as a uterine septum or bicornuate uterus. Moreover, US can identify pathologic conditions such as hydrosalpinx, cysts, polyps, and fibroid tumors. It can also be helpful for the diagnosis of intrauterine adhesions or fibrosis (Asherman's syndrome) or just to confirm that no abnormalities of the reproductive system are present.

An important strategy to facilitate ART success is to increase the number of mature oocytes at the time of ovum pickup (OPU). Therefore, follicular maturation and timing of oocyte development and retrieval must be geared to maximize the mature oocyte yield, thus providing the best chance of an in vitro fertilization (IVF) success. US monitoring plays a crucial role in this process, even in the event of unanticipated difficulties encountered during embryo transfer. Following ART and successful implantation, US is necessary to monitor the course of pregnancy: (1) to confirm fetal heartbeat, (2) to detect fetal growth restriction, and (3) to detect fetal abnormalities such as anencephaly, spina bifida, or cardiac defects.

Regarding the course and outcome, there are major differences between a natural cycle and a hormonally induced, controlled ovarian hyperstimulation (COH) with multifollicular growth with ART. Usually, in a natural menstrual cycle, an average of 10 follicles compete for dominance; however, ultimately only one follicle prevails and only one oocyte becomes mature; the other follicles degenerate. Within COH, the preconditions and course differ completely from a natural cycle.

Although the stimulation protocols might vary, IVF is usually based on the administration of gonadotropins, which are glycoprotein hormones such as follicle-stimulating hormone (FSH), luteinizing hormone (LH), and chorionic gonadotropin. Basically, three different protocols of stimulation are used with major or minor modifications (gonadotropin-releasing hormone (GnRH) agonist (long or short protocol) and GnRH antagonist protocol). The most commonly used stimulation protocol is the long protocol; it

M. Murtinger, MD
IVF Centers Prof. Zech,
Römerstrasse 2, Bregenz 6900, Austria
e-mail: m.murtinger@ivf.at

N.H. Zech, MD (✉)
Department of Obstetrics and Gynecology,
Medical University Graz,
Römerstrasse 2, 6900 Bregenz, Austria
e-mail: n.zech@ivf.at

L.A. Stadtmauer, I. Tur-Kaspa (eds.), *Ultrasound Imaging in Reproductive Medicine*,
DOI 10.1007/978-1-4614-9182-8_20,

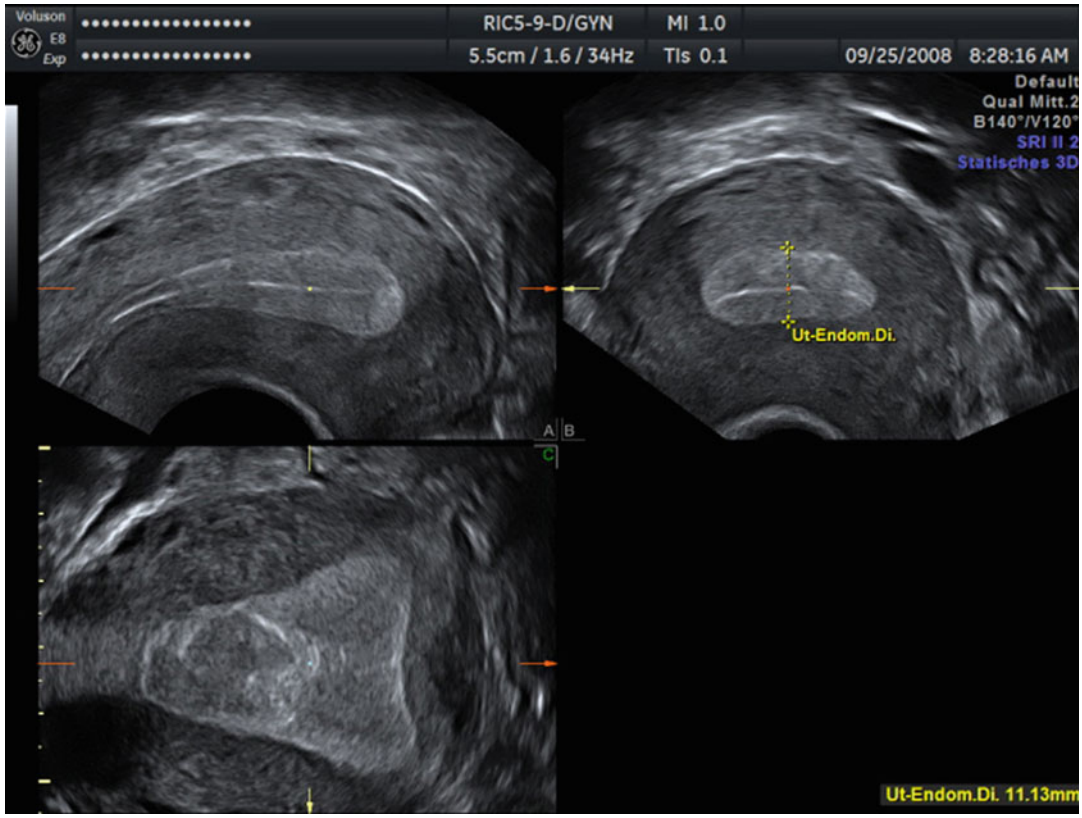

Fig. 20.1 Measurement of endometrial thickness

was first described almost 30 years ago in 1984 [1]. Even though several infertility clinics apply generally the two other protocols, short and antagonist protocols were designed for distinct medical indications such as low responders or patients at high risk for ovarian hyperstimulation syndrome (OHSS) syndrome [2, 3].

Before initiating follicular growth using the long protocol, the first step after the medical examination is the downregulation of the pituitary gland by supraphysiological doses of GnRH agonists. These pharmaceutical peptides (i.e., triptorelin, ganirelix, cetrorelix, and buserelin) prevent a premature LH surge. Indeed, in almost one-fourth of all cycles, such an LH surge occurs only when gonadotropins are used [4]. Provided the menstrual cycle is regular, the initiation of GnRH agonists in the long protocol is normally between days 18 and 22 of the menstrual cycle. GNRH agonists are usually administered via a subcutaneous injection. These agonists do not quickly dissociate from the GnRH receptor and block the GnRH function by reversibly binding to the GnRH receptor of the pituitary gland (also known as competitive inhibition). As a result, the release of FSH and LH from the pituitary gland is suppressed.

This physiological state, also called downregulation, is usually confirmed by two main criteria: (1) the determination of blood hormone levels (serum estradiol <200 pmol/l) by a clinical laboratory and (2) transvaginal ultrasound (TVUS) by a physician. The pituitary downregulation should be confirmed by a hypoestrogenic state, and additionally, the endometrial thickness (ETS) should be <5 mm. Measurement of the ETS diameter performed by 3D TVUS can be a highly predictive method to determine the state of hypoestrogenism [5]. It should also be noted that an endometrial morphology examination is also necessary to

determine whether the embryos can be transferred in a fresh cycle or it is advisable to cryopreserve them in order to perform a transfer in a subsequent cryo-cycle (this will be further discussed later in this chapter). Examinations of the endometrial volume and the endometrial morphology are crucial to estimate the implantation success, the risk of spontaneous abortion, or other risks.

In a subsequent step, ovarian stimulation is performed by FSH (i.e., Puregon®, Gonal-F®, Altermon®, or Bravelle®) or combinations of LH and FSH (i.e., Pergoveris®, Merional®, or Menopur®); these are administered by subcutaneous or intramuscular injections. The administration of such high, ultra-physiological doses of human FSH triggers the stimulation, growth, and retrieval of multiple follicles, thus increasing the number of mature oocytes [6]. The retrieval of good quality oocytes increases the likelihood of a high fertilization rate and an adequate number of high-quality embryos. Before initiating ovarian stimulation, an US is a prerequisite for planning the IVF therapy in detail; it can estimate the ovarian reserve, which can be done most accurately by an antral follicle count.

To date, as previously mentioned, there are many applications of US for gynecology and reproductive biology; furthermore, a variety of US equipment and techniques are available to perform US scans. However, as a matter of principle, US techniques can be differentiated by 2- or 3-dimensional techniques. Very recently, 4D US has emerged. With 4D US, only 3D data can be acquired in real-time mode.

Conventional 2D US instruments are based on cross-sectional scans, where only a single focus is visualized. In contrast, 3D US is based on a series of 2D images, received either by manual or automatic systems; the 3D image is then calculated and generated. In 3D mode, several scans are assembled into a 3-dimensional structure; therefore, the limitation of 3D US quality depends on the quality of the initial 2D imaging. Thus, it must be kept in mind that when the original 2D quality is low, there might be a loss of spatial resolution in the reconstructed 3D image also.

A 3D US examination comprises four steps: (1) data acquisition, (2) volume calculation, (3) image animation, and (4) data storage and transfer. In regard to the mode of data acquisition, US scans can be obtained either freehand, by manual movement through the region of interest (ROI), or automatically, by sweeping through the ROI. It is indisputable that the former modality is more subjective and is more susceptible to inter- and intraobserver reliability, while the latter is more standardized and accurate. However, it should be noted that 3D US needs post-processing of the received data. Data can be stored and visualized in various displays such as multi-planar with navigation through the planes or surface rendering mode. The 3D US technique allows for an easy volume calculation of the examined objects, which is one of its greatest fortitudes in contrast to 2D imaging; furthermore, the determination of the mean diameter of the analyzed object can be determined. Additionally, post-processing software allows the presentation of 3-dimensional structures of the examined object in the so-called inversion mode [7]. According to differences in density of tissues or structures, there are differences in ultrasound reflection and scattering, which is also referred as echogenicity. Normally, the degree of echogenicity can be visualized by a gray scale. Minor echogenicity is represented by black voxels, while regions of high echogenicity are pictured by white voxels. The gray-scale voxels of volume data sets can be inverted; this sometimes allows a better illustration of anechoic structures such as cysts. Inversion mode can be used for a better determination of tissue boundaries and efficient volume calculation. Some software programs also picture the captured objects in different colors and, therefore, enable a clear overview. This is needed when many objects are scanned and counted (i.e., follicles).

One of the major advantages of US is that it is a noninvasive, painless, and harmless procedure. In contrast to X-ray, US scans are not hazardous either to the patients or to the follicles; furthermore, US radiation does not impair the developmental potential of implanted embryos [8, 9]. Portable magnetic resonance tomography (MRT) instruments are now available; however, the advantage of US over other imaging techniques such as MRT is that US equipment is less expensive and easier to operate. Examination with MRT

is more time-consuming than US; furthermore, it requires contrast agents. Moreover, regarding imaging and velocity, 3D Doppler sonography is the only established imaging method for ART that can display liquid flow such as blood circulation; this is accomplished by calculating the frequency shift within the analyzed sample volume. Due to these various options, Doppler sonography is applicable to a broad field of diagnostic applications.

Interestingly, the principle of 3D US is not a new innovation; the technique itself has been in existence for almost three decades [10]. This fact might be quite astonishing; however, it must be kept in mind that in the past its application was limited because of the restricted calculation and memory capacity of computer systems at that time. With the tremendous acceleration of technical advancements in this field, instruments also became available at an affordable price for medical applications. Fast computers now enable 3D ultrasound picture construction, and the Digital Imaging and Communications in Medicine (DICOM) specification has facilitated the full integration of ultrasound into the picture archiving and communication system (PACS).

Use of 3D Ultrasound of the Female Reproductive System Before and During IVF in Regard to Endometrial Receptivity

On occasion, ultrasound can help determine factors involved in female infertility. Three-dimensional TVUS allows evaluation of the pelvic organs, and it is useful for the detection of pelvic pathologies such as myomata, polyps, or cysts, which can have detrimental effects on a patient's health, fertility, and pregnancy outcome. US aids in the identification of malformations of the uterus such as unicornuate uterus, bicornuate uterus, or uterine septae. Patients with these malformations require intense pregnancy surveillance because pregnancy loss, premature birth, and other complications are more common [11–14]. Furthermore, approximately about one-fourth of patients with recurrent pregnancy loss may have uterine anomalies [15]. The use of 3D ultrasound techniques is superior to other modalities for the detection of uterine malformations. The correct diagnosis of malformations is crucial for deciding whether to correct them i.e., by hysteroscopy or to refrain from surgical intervention.

Although 3D US can confirm the status of a woman's reproductive system, the medical literature contains only a handful of studies in this regard. A prospective study encompassing 284 women demonstrated the reliability of 3D US for the detection of Müllerian anomalies [16]. The accuracy was verified by endoscopy, and the authors noted that the scan could be performed in a brief period of time. Their findings confirmed previous studies by other investigators [17, 18]. Furthermore, the high intra- and interobserver reliability for 3D sonography has been reported [15]. In view of this, it must be kept in mind that 2D US of the pelvic organs cannot achieve this degree of accuracy. Rosendahl et al. demonstrated this feature by comparing the true ovarian volume and the volume determined by 2D US; they reported a discrepancy of approximately 30 % [19].

Ultrasound not only allows the imaging of the major organs but also the detection of small histological abnormalities. For example, a recent study evaluated 275 consecutive women undergoing an IVF cycle in which TVUS was applied; it showed that the clinical and ongoing pregnancy rates drastically decreased when women had adenomyosis [20]. The authors pointed out that the diagnosis of adenomyosis could be promptly made with high-resolution transvaginal ultrasound. The finding that adenomyosis can impair pregnancy is also supported by a former retrospective study of 748 IVF patients who underwent a TVUS to identify possible pelvic pathology before starting IVF therapy with the GnRH antagonist protocol. The investigators found that the clinical pregnancy rate was reduced by 50 % in patients with adenomyosis, compared to women without the condition [21]. Nevertheless, these authors correctly stated that "there is no consensus regarding the impact of adenomyosis on implantation potential." This finding is quite remarkable because the worldwide IVF success rates are still unsatisfactorily low and

assisted reproduction facilities are still facing the challenge of pregnancy rate improvement. This situation might be explained by the fact that US advancements, especially the 3D techniques, have only recently appeared; thus, IVF pregnancy rates may increase in the near future.

The endometrium is the innermost glandular layer of the uterus and the location for embryo implantation. Morphology and thickness (volume) of the endometrium can be visualized by US. This technique is widely used because pathological alternations of the endometrium can drastically impair female fertility. Endometrial polyps might affect embryo implantation (depending on their size, position, and number). Therefore, detection of these polyps is relevant for IVF success. Either subsequent removal by polypectomy or the application of IVF cryo-cycles is the method of choice. Nevertheless, to date only limited data is available, and only a few studies have demonstrated the superiority of 3D techniques in the diagnosis of endometrial polyps compared to 2D US [22]. A study of 103 patients with postmenopausal bleeding revealed the advantages of 3D techniques for the diagnosis of endometrial pathologies [23]. Therefore, the application of 3D US allows a conceivably better discrimination between benign and malignant endometrial pathologies with less false-positive results; furthermore, endometrial volume calculation with 3D US was found to be superior to 2D US for the measurement of endometrial thickness. The advantage of 3D US to discriminate between different uterine anomalies was also demonstrated by two other studies [17, 18].

In addition to correctly diagnosing endometrial pathology, a second crucial point is that follicular maturation needs to be synchronized with endometrial receptivity in order to achieve and sustain a pregnancy. Endometrial morphology, thickness, and perfusion are subjected to hormonal alterations, which are reflected by a shift in morphology and function. Beginning in the 1990s, the relationship between serum estradiol levels and endometrial thickness during downregulation has been demonstrated by multiple studies; however, the first study of the new 3D US that imaged the endometrium was published by Yaman et al. [5]. They first examined endometrial volume by 3D ultrasound in the case of pituitary downregulation. They found that 3D measurements of the endometrial volume were highly accurate; however, the authors reported no additional benefits of the endometrial volume measurement. The endometrial receptivity for embryo implantation is characterized by certain morphological and biochemical alternations and is also called the "window of implantation." These alternations include an increase in the proliferation and thickness of the endometrium.

According to the application of high, supraphysiological hormone dosages during stimulation, it is sometimes difficult to simultaneously achieve both perfect development of multiple follicles and optimal endometrium buildup. Therefore, characteristics of the human endometrium, including thickness (volume), morphology, endometrial blood flow, and vascularization, can be readily and noninvasively monitored by US monitoring. Nevertheless, a direct correlation between endometrium buildup and implantation rates as well as pregnancy rates is still to be confirmed. Although endometrial patterns have been reported to correlate with endometrial stages for the past 15 years [24], large discrepancies have been reported in regard to correlations between the foregoing and endometrial thickness necessary for successful implantation. Some studies have reported correlations between endometrial thickness, endometrial morphology, and pregnancy outcome; however, others do not address those factors [25, 26].

Currently, there is still no consensus regarding the endometrial thickness and endometrial volume necessary for successful implantation. However, most physicians agree that a certain degree of buildup is crucial. Several studies have suggested that pregnancy rates dramatically decrease when the endometrial thickness is <5–7 mm or the endometrial volume is <2.5 or 1 ml, respectively [5, 27–30].

In a 2001 study, it was reported that implantation is unlikely when the endometrial thickness is <5 mm [31]. Other investigators report no correlation of endometrial thickness and patterns to implantation rates [32]. The reason for these

discrepancies might be based on the application of different stimulation protocols, the various sonographic instruments and techniques (primarily 2D US) employed, and especially on the different patient subgroups analyzed. Therefore, the outcome cannot be directly compared. It must be noted, however, that there are application limitations of 2D US for this procedure. Measuring the endometrial volume by this technique yields limited accuracy and requires significant time. Even for endometrial thickness, there is currently no general consensus of a cutoff value [30]. However, some authors have proposed a minimum of 5–8 mm. Despite this situation, there might be a higher consensus to recommend embryo cryopreservation in cases of thin and non-trilaminar endometrium because the likelihood of implantation is low with this finding.

One study directly compared 2D and 3D US applications in US scans of the endometrium [30]; in addition, several studies have reported the advantages of 3D US in analyzing the endometrium. The major advantage of 3D US over 2D US is that it is a simple method of measuring the endometrial volume. The morphology of the endometrium can be readily determined when it appears as trilaminar (with a central echogenic line, inner hypoechoic regions, and hyperechogenic outer walls) or non-trilaminar (as a homogenous layer). Additionally the advantage of 3D US for calculation of the endometrial volume is its low deviation of inter- and intraobserver reliability [33, 34]. However, these parameters might not in themselves be adequate for the prediction of successful implantation [35, 36]; thus, other factors that can influence the success rate have to be considered.

US Monitoring of Polycystic Ovary Syndrome (PCOS) Patients

Polycystic ovary syndrome (PCOS) is one of the most common endocrine disorders impairing female fertility; it has been reported to occur in about 20 % of the general female population and in up to 50 % of women undergoing IVF therapy [37–39].

A number of symptoms have been associated with PCOS that are subject to controversy; however, four defined criteria have broad acceptance as symptomatic of the disease: (1) chronic irregular ovulation or anovulation (therefore oligomenorrhea, might be an early clinical symptom for PCOS), (2) hyperandrogenism diagnosed clinically (expressed by alopecia, hirsutism, and/or acne) or by laboratory findings (serum testosterone >1.4 nmol/l), and (3) the exclusion of other endocrine disorders. The fourth criterion can only be defined by ultrasound examination. Polycystic ovaries are defined as those which contain ten or more cysts with a maximum diameter of 10 mm arranged either peripherally around a dense core of stroma and/or scattered throughout an increased amount of stroma [40]. Moreover, PCOS patients are more likely to have larger ovarian volumes (>10 cm^3) and ovarian stroma with increased volume and increased numbers of antral follicles (12 or more follicles, according to the Rotterdam criteria) [41]. Therefore, US scans play a crucial role in diagnosing this disease. The new automated 3D US techniques facilitate the exclusion of a false-positive PCOS diagnosis and reflect pathophysiological changes in these patients in a more accurate manner. An early detection of PCOS is highly recommended for women undergoing IVF treatment, due to the elevated risk for OHSS. Unfortunately, because 3D ultrasound is a relatively new imaging modality, the Rotterdam criteria only take 2D US sonography into account.

At present, only a few studies have evaluated the use of 3D US for PCOS patients [42]; furthermore, to date, only one study has addressed automated 3D US (SONO-AVC) [43]. In a retrospective cohort study, Allemand et al. analyzed 29 normoandrogenic, ovulatory women with tubal or male factor infertility and 10 PCOS women with chronic anovulation and clinical or biochemical hyperandrogenism [42]. Mean follicle number/ovary (FNPO) as well as the maximal number of follicles in a single sonographic plane (FSSP) was determined by 3D TVUS; simultaneously, the ovarian volume was determined by 2D TVUS. Interestingly, the authors postulated a considerably higher threshold of antral follicles (20 or more) for PCOS patients, which is a considerably higher threshold than that of the Rotterdam criteria. The authors explained this

discrepancy by the identification of more follicles by 3D US. The weakness of this study is the small number of patients, the missing direct comparison to 2D US, and the low sensitivity (true positive rate) using receiver operating characteristics (ROCs). According to most publications dealing with 3D US in PCOS patients, there is a broad agreement about increased ovarian volume of polycystic ovaries [43–48]. Nevertheless there is still disagreement regarding ovarian vascularity, stromal changes, and cutoff values for antral follicles [41, 44, 48, 49].

In most PCOS studies where 3D techniques were applied, the numbers of analyzed patients were low; therefore, further studies are necessary. However, it should be noted that a major advantage of 3D US imaging of female pelvic organs when a hydrosalpinx or cyst is noted is the aforementioned inversion mode. Such structures might not be displayed by a single slice; however, they may be recognized at full scale by viewing multiple planes. In 2006, Benaceraf [50] noted that the transformation of voxels within a volume to echogenic structures and voxels of solid structures to radiolucent images is one method that can facilitate the acquisition of the total volume of a hydrosalpinx or cyst without being hampered by the gray-scale portion of the image.

Ultrasound in Estimation of the Ovarian Reserve

Before initiating an ART cycle, it is crucial to estimate the ovarian response to stimulation. The latest time for this estimation should be the cycle prior controlled ovarian hyperstimulation (COH) cycle; moreover, it is the last possible opportunity to determine any pelvic organ abnormalities before stimulation.

The ovaries contain several subtypes of follicles: the primordial follicles (≤0.05 mm diameter), primary follicles, secondary follicles, pre-antral follicles, and antral follicles (>2 mm diameter). However, only a small number of ovarian follicles are highly responsive to FSH [51]. The number of these so-called antral (or Graafian) follicles represents the "for stimulation selectable follicles." The antral follicle count (AFC) reflects the ovarian reserve and is predictive of the IVF outcome in regard to the number of yielded oocytes in response to hormonal stimulation [45, 52, 53]. This allows the classification from very low (≤6) to high responding patients (≥12 up to 30), the calculation of risks for ovarian hyperstimulation syndrome or polycystic ovaries (PCO), and, most importantly, the adaption of gonadotropin dosage during the stimulation schedule [41, 54–57]. Inappropriate stimulation with subsequent excessive response increases the risk of OHSS; however, inadequate stimulation might result in cancellation of an IVF cycle. It should also be noted that antral follicles of different sizes respond differently to gonadotropin stimulation. Furthermore, follicles that are >9 mm are more likely to become atretic (apoptosis-induced degeneration and the following reabsorption process) [58]. The accurate assessment of the ovarian reserve is therefore a prerequisite for planning the optimal therapy for each patient and an individualized management protocol. Various clinical, endocrinologic, and other parameters (i.e., estradiol, the basal FSH, the declining levels of anti-Müllerian hormone (AMH), or inhibin B levels) have been suggested as predictive indicators for ovarian reserve and COH response [59–64]; however, their validity is extremely limited, and hormonal assays are currently expensive [65, 66]. Additionally, there are several markers that significantly correlate with the ovarian reserve such as age or ovarian volume; however, these markers are less predictive [67, 68]. It is widely accepted that age is strongly associated with ovarian reserve; however, there is a high variability even among women of the same age [69].

The estimation of antral follicle count and antral follicle size performed by TVUS is currently the most reliable method and gives the best correlation with retrieved oocytes [64, 68, 70, 71]; moreover, it is easy to perform and is noninvasive. Therefore, the AFC determined by ultrasound, notably by 3D techniques, is the best predictor for poor ovarian response, OHSS, oocytes collected, and live birth rates [72].

It should be noted that it is imperative to distinguish between the total antral follicle count (TAFC), including follicles >6 mm in diameter and the number of small antral follicles which better reflects the ovarian reserve [73] and predicts the COH response [74].

AFC can even be obtained on day 2 of the menstrual cycle [71]; however, the best time for estimation of antral follicles is the middle to late phase of folliculogenesis. Currently, the AFC is determined by 2D as well as 3D US, with predominance of the 2-dimensional techniques. In regard to 3D ultrasound, we must distinguish between manual and automatic systems (such as Voluson e in combination with SONO-AVC software); this will be discussed later in this chapter. Nevertheless, there is the question regarding the reliability of AFC determined by different US techniques as well as which current methods are the best. Of note, only a handful of studies compare the accuracy of ultrasound in regard to AFC and inter- /intraobserver reliability. Broekmans et al. described the value of AFC determined by AVC needed for the improvement of standardization and presented a tutorial on clinical and technical requirements [52].

Standard AFC assessment was, and still is, performed primarily with 2D US imaging. Although this modality might be sufficient in some cases, there might be some uncertainties and disadvantages. One disadvantage of 2D involves inter- and intraobserver reproducibility. Scheffer et al. [75] compared healthy volunteers with proven fertility to patients visiting an infertility clinic. For each patient, 2D or 3D TVS was conducted for AFC (2–10 mm), and interobserver reliability was calculated. Both techniques were adequate when only a few follicles were present; however, when higher AFCs occurred, the reproducibility decreased with the 2D technique. In addition to this report, studies by the group of Raine-Fenning [76–80] demonstrated an improvement of interobserver/intraobserver reliability by the application of 3D methods (in particular by automated systems, such as SONO-AVC). One of the disadvantages of manual 3D US AVC is the greater examination time that occurred in a study comprising 55 women [78]. Nevertheless, this finding was contradicted by the same researchers in a second study, in which they measured the examination time instead of including time for post-processing of the US scans [79].

Interestingly, in several studies the TAFC was found to differ between 2D and 3D techniques [78, 79]. This might be explained by the fact that when the follicle number increases, the accuracy of 2D techniques decreases because of losing track of counted follicles and multiple counting of the same follicles [81, 82]. In conclusion AFC is highly predictive for the ovarian reserve and strongly associated with the serum AMH level [74]. The estimation of the ovarian response by US is simple and noninvasive; thus, it is an advisable procedure. The reliability of this method is probably increased with 3D instruments.

Follicle Tracking During Controlled Ovarian Hyperstimulation

The consistent aim of controlled ovarian hyperstimulation during an IVF is to obtain the maximum number of mature and good quality oocytes. This increases the chance for having an adequate number of high-quality embryos, which rises the likelihood of achieving a viable pregnancy. Therefore, oocyte maturity is a critical factor. The cytoplasmic as well as nuclear maturity, defined as oocytes that have completed their first meiotic division and reside in metaphase II (MII), is required for a high fertilization rate and optimal embryo development. According to the classical IVF protocols, GnRH analogues and hCG are administered to trigger the ovulation process when the dominant follicle reaches a diameter between 18 and 20 mm or the follicle volume has reached 3–4 ml [83]. The timing for hCG administration is the most critical step of an IVF cycle. During COH, follicle growth occurs at different rates; thus, follicles of varying sizes are present. Therefore, the best method to obtain a maximal yield of MII oocytes is to obtain a maximal number of follicles of large diameter or volume. Nevertheless it should be also considered that in the case of an extended stimulation period, follicles might become atretic and oocyte quality

might be markedly compromised. In addition, a possible danger of OHSS and chromosomal abnormalities in the oocytes due to excessive hormonal stimulation is discussed. Currently, follicle growth is monitored with serial ultrasound examinations at regular intervals. In these examinations, the total number of follicles in each ovary is counted, and each follicle is measured by ultrasound. Thus, it is likely that these regular examination intervals can result in a maximal error rate for intra- and interobserver reliability.

Ovarian size, follicle growth rate, and follicular volume were considered to be important indicators of oocyte maturity and regarded to be measurements of therapy success [84]. This was not always the case. A main stimulator of follicle growth is 17β-estradiol (E2); it was and currently is used as indicator of follicle growth during COH. Quigley et al. [85] reported that they administered hCG on the sixth day of E2 rise. They stated that "the use of E2-rise days proved to be a simple, successful technique for the timing of hCG administration in an IVF treatment program." This viewpoint was also assumed by other researchers [86]. Nevertheless, follicle growth and oocyte maturation are regulated by protein and peptide hormones, growth factors, steroids, and many other factors; thus, these factors must be take into account when performing IVF. Moreover, one must keep in mind that only the overall E2 value can be measured. However, this quantitative hormone determination does not take into account the E2 production of the individual follicles.

Casper et al. [87] pointed out the problems occurring with a spontaneous LH surge during mid-cycle and the possibility of ovulation, thus demonstrating the incalculability of follicle maturation monitoring by E2. In 1985, Nilsson et al. [88] postulated that ultrasound scanning should be the sole index of monitoring follicle maturity. Actually, growth rate and follicular volume are the only applicable factors, because the estimation of hormonal levels for follicular maturation such as the serum E2 value alone for prediction of follicular maturity was reported to be unsatisfactory [89]. US technology is the best modality to determine an accurate strategy of ovulation and to determine the date of OPU.

Human chorionic gonadotropin mimics the endogenous LH surge and induces the nuclear maturation and the germinal vesicle breakdown. For decades, it has been used as the universal trigger of final oocyte maturation. Therefore, the state of follicular maturity reflects the developmental potential of oocytes and embryos as well as the ART outcome.

The induction of multiple follicle maturation requires the determination of the best time point for hCG administration to induce final oocyte maturation. This time point was and still is determined by US. In a retrospective study of 2,429 oocytes from 215 patients, the fertilization rate of all oocytes showed a positive linear correlation with increasing follicle diameter regardless of the morphological type of oocyte-cumulus-corona complex [90].

Although 3D US systems had been developed and patented at the end of the 1980s [91], there is still a broad debate on the benefits of 3D US in follicle monitoring during COH. Moreover, there are still no uniform standards for follicle monitoring via US in ART. The conventional two-dimensional (2D) transvaginal ultrasound (US) techniques are used in many centers; however, they completely neglect the third follicular diameter (z-diameter). Therefore, the follicular volume is calculated by the formula for spherical volume $V=(4/3)r^3\pi$. Some observers rely on a single "best" estimate, while others use one or more planes. Although this might hold more or less true for follicles of a natural cycle, the induction of multiple follicular growth during hormonal stimulation results in undesirable side effects. Of note, especially when multiple follicles are present, the follicles almost never exhibit a spherical shape, which can result in an overestimation of the mean follicular diameter. Almost two decades ago, it was demonstrated by a prospective clinical trial that the mean diameter estimated by 2D US reflects the follicle volume if the follicles have a round or polygonal shape. In contrast, for elliptical follicles, the volumes could not be predicted and were over- or underestimated; this was shown by a prospective clinical study comprised of 14 patients and 96 follicles [84]. This was also observed in a prospective

clinical study of Kyei-Mensah and colleagues [92], where they demonstrated that the follicle volume measured by 3D US reflects a more accurate follicular volume than 2D measurements. With 3D US, they found discrepancies of up to 1 ml of the true volume. In contrast, with 2D US an overestimation of 3.5 ml or underestimation of 2.5 ml of the true volume was observed; thus, 2D US is inferior to 3D for follicular volume measurement. According to our own observations, the follicle size is typically underestimated for small follicles and overestimated for the larger ones. The total number of follicles cannot be determined the classical 2D US. In cases of ovarian hyperstimulation syndrome, the stimulation response is likely to be high, which means an antral follicle count >30. In these cases, it is often difficult to ensure that every follicle is accounted for and often the qualification regarding the follicle size and quantification is unreliable.

Additionally, follicular asynchrony occurs, which means that the stimulated follicles are a heterogeneous group of varying size with different degrees of maturity. This might be one reason that E2 values are not predictable as they do not, as aforementioned, reflect the individual follicles but overall follicle maturity [93]. Even though there might be broad agreement that follicle size and oocyte maturity correlate with the IVF outcome, there is a considerable dissent when to trigger final oocyte maturation prior to oocyte pickup and what size the leading or the three biggest follicles should be when hCG is administered. This might be due to the small number of studies. Moreover, the available data is conflicting. Although several studies have suggested that human oocytes derived from larger follicles have greater potential than oocytes originating from smaller follicles, the correlation of oocyte competence with follicular size following COH has not been fully evaluated [94]. Therefore, the crucial question is: At which follicle diameter hCG should be administered? An even more confusing question is: Should ovulation triggered when one follicle or a cohort of follicles exceeds the critical diameter?

Scott et al. [95] analyzed 412 follicles and postulated that to receive the best possible outcome of follicular aspiration in terms of mature oocytes, aspiration should be performed when the FD is ≥15 mm. Ectors et al. [96] reported that an optimal fertilization rate occurred when the FD was between 16 and 23 mm.

In the past, hCG administration for triggering ovulation was estimated on the basis of the size of the dominant follicle: when its diameter was 17–20 mm [92]. Although this method is still widely used in the IVF clinics around the world, clinicians are currently employing this concept less frequently. An alternative viewpoint is to wait until a few follicles reach a critical diameter rather than just one dominant follicle reaching a certain size. A prospective study encompassing 2,934 oocytes from 235 cycles showed that the lead follicular group (>18 mm FD) had the highest capacity for fertilization [94]. According to our preliminary observations using the 3D data set, the critical value for an adequate fertilization rate is considerably lower. Nevertheless, more studies concerning this topic are necessary to draw final conclusions.

The next pivotal question is whether the follicle volume is a more representative criterion for maturity than the FD. In 2009, Yalcin, Yavas, and Minna Selub [93] stated that "ovarian follicular volume and follicular surface area are better indicators of follicular growth and maturation, respectively than is the follicular diameter alone." For these statements, the authors gave the following reasons: First, testosterone, the precursor of E2, is produced by the theca interna cells, which are located on the follicle's surface. It is quite obvious that the measurement of the follicle diameter has limited reliability when the evaluated object is not spherical. Thus, volume measurement appears to be a more appropriate technique [97]. In a study of 30 patients under the long stimulation protocol, Amer et al. [98] compared the use of 2D to 3D US (TVUS vs. Combison 530 US System, Kretz Technology, Zipf, Austria) before follicle aspiration; they reported a higher accuracy of 3D US in regard to follicle volume (a discrepancy <1 ml above or below the true volume). In contrast, 2D US was found to have a standard deviation of 3.5 ml above or 2.5 ml below the true volume. Moreover,

3D US was reported to be superior for the identification of the cumulus oophorus complex [98]. Nevertheless, it must be kept in mind that 3D US only differs in capturing volume while 2D produces slices.

From the 3D ultrasound data set, the exact volume of a clearly defined object is calculated. The basic principle of volume calculation is based on the combination of shape information from different image planes. The automatic systems significantly facilitate volume calculation.

New Applications of 3D US

The application of 3D US technologies in medicine is rapidly evolving. Promising new applications in ultrasound technology have been developed during recent years and have been successfully introduced in the field of IVF. These new applications facilitate ultrasound examinations by automatic measurements and calculation; thus, they markedly increase the reproducibility of the results. Several new software programs support this: VOCAL, STIC, TUI, VCI, and SONO-AVC. One of the most frequently employed applications is the sonography-based automated volume calculation (SONO-AVC; GE Medical Systems, Zipf, Austria). The application of SONO-AVC for IVF was first described by Raine-Fenning et al. in 2007 [99]. Furthermore, SONO-AVC is not only used in ART but also in pregnancy and for examinations of the bladder [100, 101].

Nevertheless, SONO-AVC is a software especially designed for the automatic detection of multifollicular growth and to overcome the aforementioned problems of follicle observation by 2D US. This software allows not only the display of single follicles in 3D but also automatically calculates the number and volume of hypoechoic structures in a 3D echo-derived data set; furthermore, it provides estimations regarding the absolute dimensions of follicles. The only necessary requirement is adjustment of the ROI box over the entire ovary to include only the information which is needed for calculation. Measurements are based on calculation of the largest diameters in three orthogonal planes: the mean follicle diameter, the follicular volume, and the volume-based diameter of the follicle [82]. Thus, the volume is calculated via the voxel count within hypoechoic structures. The true volume can be measured, and SONO-AVC calculates the follicle diameter by rendering the follicle as a perfect sphere. This results in the visualization of sono-anatomic details, which could not previously be recognized. A major advantage of this sono-anatomic rendering is that individual structures are color-coded (Figs. 20.2, 20.3, and 20.4) allowing the exact count, which is needed for the determination of factors such as ovarian reserve.

Several studies have demonstrated the advantages and validity of SONO-AVC in vitro and in vivo. In this report, we focus only on studies and reviews concerning the application of SONO-AVC related to assisted reproduction. Most importantly, 3D SONO-AVC yields high reliability for volume and diameter calculations.

In a 2008 study by Raine-Fenning et al. [76], which comprised 51 women undergoing controlled ovarian stimulation, 200 follicles were analyzed. Measurements were performed in six different ways, including manual 2D US, manual 3D US, and automatic measurements with SONO-AVC. Ultrasound data were analyzed by a single observer, and diameters of each follicle were estimated. The true volumes were determined by manual measurement of the follicle aspirate. The true diameter was estimated by the sphere formula. The researchers concluded that the automatic system provides more accurate measurements of follicle diameter than manual measurements. SONO-AVC perfectly reflects not only the true follicular diameter but also follicular volume. Most studies addressing these topics confirmed a high accuracy [102–107], and most importantly, this accuracy was also maintained with follicles of different size [108]. Additionally, using the automatic system, the measurement time was significantly curtailed [109]. The time-saving feature of the SONO-AVC was also reported and acknowledged by numerous other studies [77, 103, 110]. The time-saving aspect was also highlighted by Sherbahn and Deutch in 2009 [110]. By comparing two groups of patients,

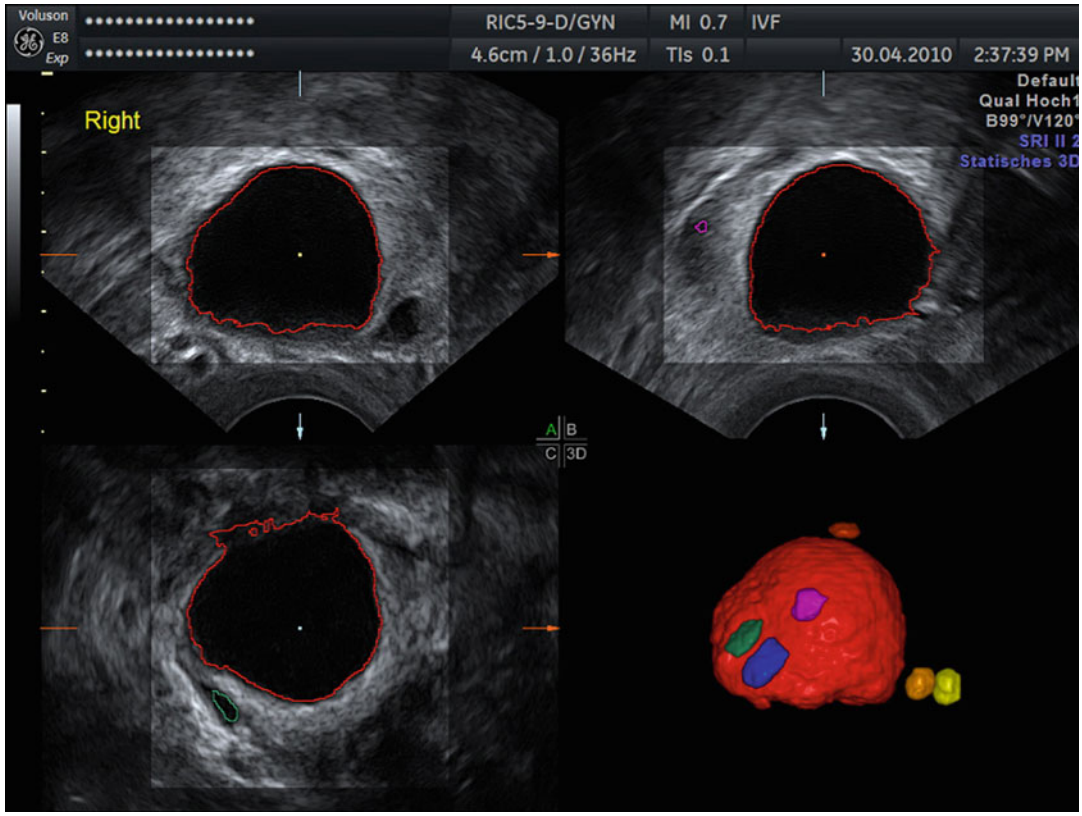

Fig. 20.2 Imaging of a cyst as a scan and in 3D reconstruction. US scans of a cyst performed with E8 Voluson and 3D imaging by SONO-AVC software

either using SONO-AVC or traditional 2D-US, they reported that less time was required for performing the scans, data analysis, and chart recording.

Raine-Fenning et al. [76] described the superiority of another 3D imaging software product, 3D VOCAL™ (Virtual Organ Computer-aided AnaLysis, Kretz Technik, Zipf, Austria), for volumes, which had been estimated from 2D US measurements. The basic principle of 3D VOCAL is the combination of 3D ultrasound tissue presented as voxels and the geometric information regarding surfaces in a 3D data set. The main advantage of VOCAL is the surface characterization. This software enables the determination of volumes by the virtual plane rotation around a fixed axis, calculating the contours of each 2D plane.

Another useful application of SONO-AVC might be for hCG administration. In a study comprised of 40 IVF patients between 25 and 35 years of age, Murtinger et al. compared the outcome of follicle monitoring and the calculated day of hCG administration in regard to the number of mature oocyte retrieved, mature oocytes per oocytes recovered, embryo development to day 5, and pregnancy rate. For 20 patients, follicle monitoring was proceed by 2D US; hCG was administered when a cohort of follicles reached a diameter between 16 and 24 mm. For the other 20 patients, the day of hCG administration was estimated by the same criteria; however, follicle diameter was processed by 3D US, and subsequent volume was calculated by the SONO-AVC software. In this group, more oocytes were retrieved, and significantly more oocytes were found to have been fertilized on day one [109]. Rodriguez-Fuentes et al. [107] elucidated a correlation between follicular volume (determined by SONO-AVC), day of hCG

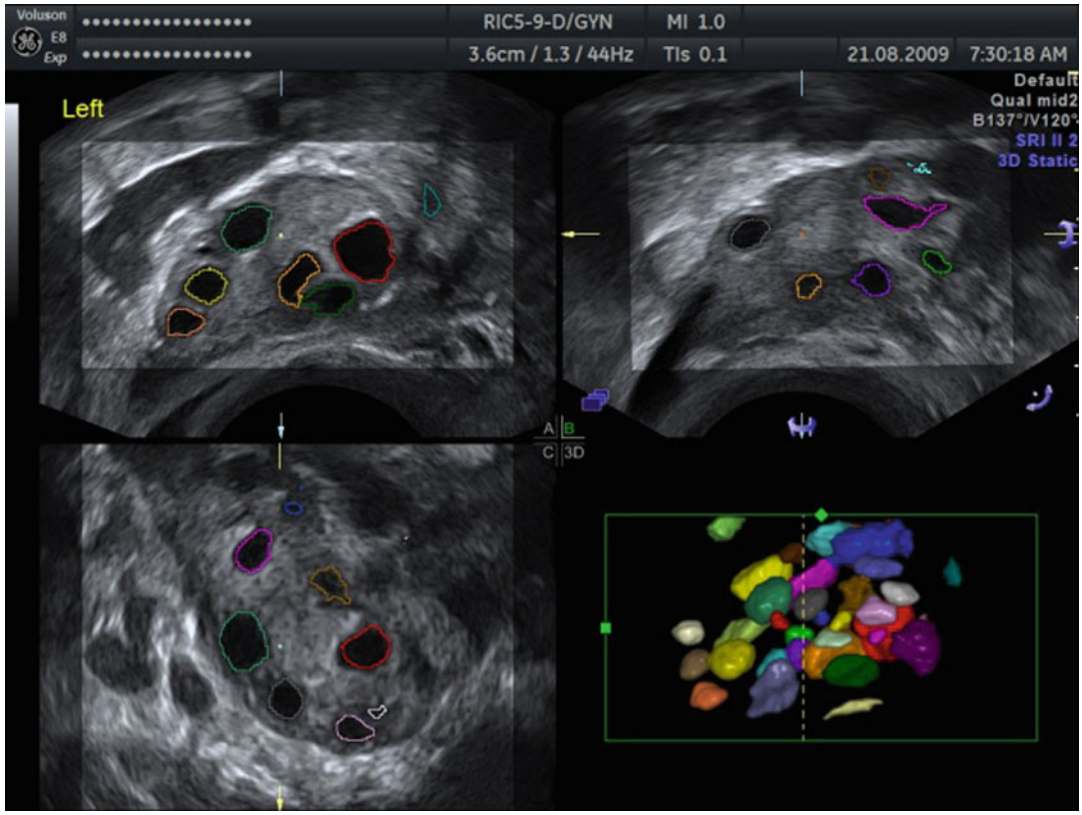

Fig. 20.3 Antral follicle count performed by 3D US SONO-AVC. Automatically identified antral follicles by E8 Voluson in combination with SONO-AVC software. Follicle boundaries are marked by different colors. Lower right: color-encoded 3-dimensional reconstruction of follicles enables the accurate determination of the number of follicles

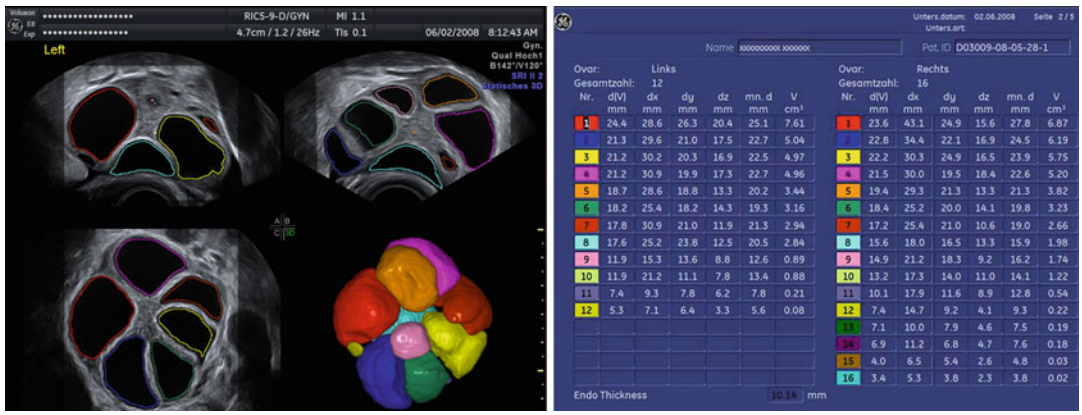

Fig. 20.4 Representation of a stimulated ovary generated via 3D TVUS scanning plus SONO-AVC software 1 day before OPU. Follicle boundaries are marked by colors. *Lower right*: color-encoded 3-dimensional reconstruction of follicles. *Left*: detailed SONO-AVC report. Each *colored line* corresponds to a follicle. The lines are coded with the same colors as the corresponding follicles; dx, dy, and dz diameters; mean diameter; and volumes are automatically provided

administration, and retrieval of mature oocytes. They postulated that there is a higher likelihood of obtaining mature oocytes when the follicular volume is ≥0.6 ml. In contrast to these results, in a randomized study, no difference in the COH outcome in terms of mature oocytes, fertilized oocytes, embryo development, and pregnancy rate were observed by Raine-Fenning et al. [111]. However, it should be noted that they used diameter rather than volume-based criteria for determining the timing of hCG injection. However, due to the paucity of studies concerning SONO-AVC and timing of final follicle maturation, there is a need for larger studies. The time-saving aspects of these new techniques might decrease patient anxiety, physician stress, and facilitate a smooth work outflow. SONO-AVC allows automated volume calculation without the need for separate measurement of each follicle. To date, studies addressing AFC estimation by SONO-AVC are limited. In a study comprised of 55 patients under age 40 years, Deb et al. [79] estimated the TAFC by SONO-AVC and compared the results to these obtained by 2D and manual 3D techniques. Antral follicle volumes were analyzed automatically by SONO-AVC or manual via longitudinal or transversal planes. The initial automated count was recorded and post-processed. The median AFC by SONO-AVC was significantly less than 2D, and SONO-AVC measurements took longer than 2D. In contrast, in a subsequent study in 2010 conducted by the same investigators [79], the required measurement time using SONO-AVC was less than that of 2D US. The first study was not performed in real time and included the time for post-processing; however, the second study focused on real-time count.

Moreover, SONO-AVC was demonstrated to be time-saving, compared to manual applications [103, 109]. However, as the manufacturers noted, the focus for the automatic detection is mainly on follicles ≥12 mm diameter. In regard to antral follicle imaging, the algorithm is not adequate for optimal imaging regarding the true size and volume [112]. Nevertheless, it should be noted that not the exact diameter but the correct number of antral follicles is crucial. The repeated observation of fewer antral follicles in several studies might be explained by the inaccuracy of 2D when the number of follicles is high. In contrast the SONO-AVC color coding prevents counting one follicle twice. Moreover the received data still requires post-processing [82].

Optimal Outpatient Monitoring

There are several advantages of the new 3D US techniques. New software systems such as SONO-AVC allow a smooth, facilitated workflow with a shorter examination time. This provides an advantage for physicians in busy IVF centers as well as patient-friendly therapy [103]. Another problem, which can now be avoided, is the already mentioned inter- and intrapersonal variability in the processing, readout, and interpretation of ultrasound scans. When manual post-processing of US scans is required, there is a natural maximal interpersonal variability and error source when the attending physicians are from different institutions and differ in their routines, experience, handling, and knowledge.

The complexity of assisted reproductive technologies has increased markedly during recent decades due to the rise of scientific and medical data as well as the statutory requirements of the effort to improve the safety and the outcome of an IVF therapy. Therefore, it is essential that therapy planning and ART processing be conducted at highly specialized IVF units. As a result of this increasing complexity, it is likely that the number of IVF centers will decrease rather than increase. Not all centers will be able to keep pace with the increasing technical requirements and the appearance of new (and sometime cost-intensive) applications. Currently, gynecologists who practice apart from infertility clinics are involved in patient care during the IVF therapy, especially for the monitoring of follicle growth. Results are routinely communicated to the IVF clinic so that physicians there can determine how to proceed with the therapy in terms of further dosing of follicle-stimulating hormone, the adaption of hormonal stimulation, the duration of stimulation, and the time of initiating final oocyte maturation. These challenges were previously reported by Murtinger et al. in 2010 [113]. The difference in operative experience and handling, distinct ways

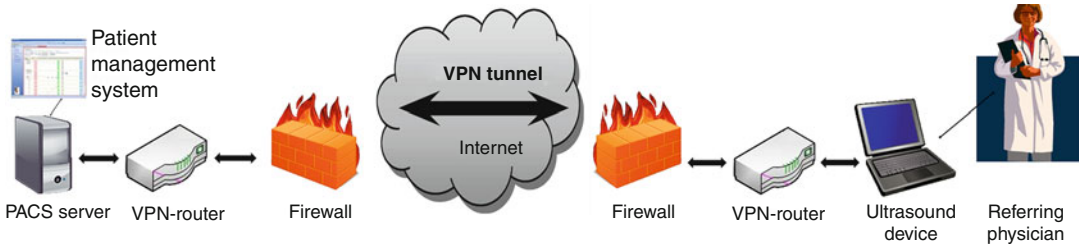

Fig. 20.5 Scheme of patient data transmission between local gynecologist and IVF center. The ultrasound device (USD) transmits the results of the medical examination (follicle volumes and endometrium measurements) to the PACS server. The USD queries work lists and patients data from the PACS server. All data transmission between USD of the referring physician and PACS server in the clinic is done by VPN (virtual private network) tunneling. All data is encrypted and safe from unauthorized access. IPsec (Internet Protocol Security) with encryption key length of approximately 2,048 bits allows the secure Internet protocol by data, authentication, and integrity validation. Data is encrypted during the communication and the encryption key changes every second

of interpretation of ultrasound scans, and the interobserver variability can lead to too early or too late hCG administration, thus negatively affecting the IVF outcome. Currently, there is an enormous need for an unobstructed interaction between the IVF centers and the referring physicians who might be separated by a distance of hundreds of kilometers. Additionally, in large IVF centers, which comprise several subunits or satellite clinics, an unobstructed data transfer must be guaranteed. In 1995, Roest et al. [114] noted, "Travelling time and inconvenience for the patients is limited since the monitoring of ovarian stimulation is carried out in their local hospital by their own gynecologist." However, this situation brings up a counter-argument that, when satellite physicians monitor ovarian stimulation for their own patients, quality assurance is necessary. Additionally, regarding patient subgroups, which are at high risk of OHSS (primarily PCOS patients), it is commonly accepted that short monitoring intervals are crucial to detect OHSS. Therefore, accurate and complete transmission of US data is crucial. The introduction of new US techniques such as Voluson I ultrasound system (GE Medical Systems, Kretztechnik, Zipf, Austria) combined with the SonoAVC® software (General Electric Company, New York, USA) now allows optimal digital data transfer. The results can be communicated via DICOM. The IVF centers now have the ability to transfer patient data via a PACS server to the ultrasound machine of the gynecologist. The firewall prevents unauthorized access to the PACS server. The ultrasonic device is connected via a DSL modem to the Internet. All communication takes place through a secured connection (virtual private network (VPN)) tunneling to ensure that non-authorized individuals cannot gain access to sensitive data. The requested ultrasound examinations and structured reports are performed by the gynecologist, and if necessary, the images are sent via DICOM standard back to the center. There, medical software such as DynaMed® (IMA Systems, Bregenz, Austria) allows the seamless integration of all processes needed for an accurate and precise workflow (Fig. 20.5). The technical advances in ultrasound will play a crucial role for more patient and practitioner-friendly therapies in the future. Two major benefits can be attained. First, the establishment of standards in the application of ultrasound in assisted reproduction. This is a prerequisite to fulfill the regulatory requirements such as those given by the EU Directive on tissue and cells (2004/23/EC) [115]. Moreover, a smooth clinical workflow can be guaranteed. In fact, the objective and standardized information exchanges and documentation allow more legal certainty in cases of legal disputes between IVF centers, physicians, and patients.

Conclusions

During the last two decades, 2D US was one of the key modes employed for IVF; however, 3D US is increasingly being employed for reproductive medicine. There are several advantages of 3D-based US instruments. Examination time is reduced because the US

scan data are stored and can be analyzed in detail at a later time. These data can be reconstructed in any plane, regardless of the original scan plane facilitating detailed analysis. 2D US is fixed on the performed scans with more or less good quality. Another advantage is that this new technique reduces the operator's influence on scan interpretation and objectivity; therefore, interobserver variability is reduced. The reliability of volume measurement is improved. The time-saving of the automated 3D systems enables a high and efficient workflow in the IVF unit, which is of benefit for the physicians as well as the patients. The new generation of 3D US instruments is portable, and data can be easily communicated and integrated within the electronically health record by supporting software. As the number of automated 3D systems introduced in the IVF field is rapidly increasing, a growing number of studies are being published, which report their benefits. With the higher sensitivity and observational possibilities of the 3D technique in combination with automated scan analysis, this technique could be of great value for the elucidation of controversial opinions in reproductive medicine such as the morphology and thickness of the endometrium necessary for implantation. Diagnosis of diseases such as PCOS can be facilitated, and follicle monitoring during ART becomes much easier and less time-consuming. There is also no doubt that this new technique will help to find distinct new US criteria for better subgroups or individual therapy in the future.

References

1. Porter RN, Smith W, Craft IL. Induction of ovulation for in-vitro fertilisation using buserelin and gonadotropins. Lancet. 1984;2:1284–5.
2. Marci R, Caserta D, Dolo V, Tatone C, Pavan A, Moscarini M. GnRH antagonist in IVF poor-responder patients: results of a randomized trial. Reprod Biomed Online. 2005;11:189–93.
3. Fridén BE, Nilsson L. Gonadotrophin-releasing hormone-antagonist luteolysis during the preceding mid-luteal phase is a feasible protocol in ovarian hyperstimulation before in vitro fertilization. Acta Obstet Gynecol Scand. 2005;84:812–26.
4. Janssens RM, Lambalk CB, Vermeiden JP, Schats R, Bernards JM, Rekers-Mombarg LT, et al. Dose-finding study of triptorelin acetate for prevention of a premature LH surge in IVF: a prospective, randomized, double-blind, placebo-controlled study. Hum Reprod. 2000;15:2333–40.
5. Yaman C, Ebner T, Sommergruber M, Hartl J, Pölz W, Tews G. Three-dimensional endometrial volume estimation as a predictor of pituitary down-regulation in an IVF-embryo transfer programme. Hum Reprod. 2000;15:1698–702.
6. Fauser BC. Follicular development and oocyte maturation in hypogonadotrophic women employing recombinant follicle-stimulating hormone: the role of oestradiol. Hum Reprod Update. 1997;3:101–8. Review.
7. Lee W, Gonçalves LF, Espinoza J, Romero R. Inversion mode: a new volume analysis tool for 3-dimensional ultrasonography. J Ultrasound Med. 2005;24:201–7.
8. Mahadevan M, Chalder K, Wiseman D, Leader A, Taylor PJ. Evidence for an absence of deleterious effects of ultrasound on human oocytes. J In Vitro Fert Embryo Transf. 1987;4:277–80.
9. Hershkovitz R, Sheiner E, Mazor M. Ultrasound in obstetrics: a review of safety. Eur J Obstet Gynecol Reprod Biol. 2002;101:15–8. Review.
10. Norton SJ, Linzer M. Ultrasonic reflectivity imaging in three dimensions: reconstruction with spherical transducer arrays. Ultrason Imaging. 1979;1:210–31.
11. Reichman D, Laufer MR, Robinson BK. Pregnancy outcomes in unicornuate uteri: a review. Fertil Steril. 2009;91:1886–94. Review.
12. Rackow BW, Arici A. Reproductive performance of women with müllerian anomalies. Curr Opin Obstet Gynecol. 2007;19:229–37. Review.
13. Airoldi J, Berghella V, Sehdev H, Ludmir J. Transvaginal ultrasonography of the cervix to predict preterm birth in women with uterine anomalies. Obstet Gynecol. 2005;106:553–6.
14. Propst AM, Hill 3rd JA. Anatomic factors associated with recurrent pregnancy loss. Semin Reprod Med. 2000;18:341–50. Review.
15. Salim R, Woelfer B, Backos M, Regan L, Jurkovic D. Reproducibility of three-dimensional ultrasound diagnosis of congenital uterine anomalies. Ultrasound Obstet Gynecol. 2003;21:578–82.
16. Ghi T, Casadio P, Kuleva M, Perrone AM, Savelli L, Giunchi S, et al. Accuracy of three-dimensional ultrasound in diagnosis and classification of congenital uterine anomalies. Fertil Steril. 2009;92:808–13.
17. Raga F, Bonilla-Musoles F, Blanes J, Osborne NG. Congenital Müllerian anomalies: diagnostic accuracy of three-dimensional ultrasound. Fertil Steril. 1996;65:523–8.
18. Wu MH, Hsu CC, Huang KE. Detection of congenital müllerian duct anomalies using three-dimensional ultrasound. J Clin Ultrasound. 1997;25:487–92.

19. Rosendahl M, Ernst E, Rasmussen PE, Andersen CY. True ovarian volume is underestimated by two-dimensional transvaginal ultrasound measurement. Fertil Steril. 2010;93:995–8.
20. Salim R, Riris S, Saab W, Abramov B, Khadum I, Serhal P. Adenomyosis reduces pregnancy rates in infertile women undergoing IVF. Reprod Biomed Online. 2012;25:273–7. doi:10.1016/j.rbmo.2012.05.003.
21. Thalluri V, Tremellen KP. Ultrasound diagnosed adenomyosis has a negative impact on successful implantation following GnRH antagonist IVF treatment. Hum Reprod. 2012;27(12):3487–92.
22. La Torre R, De Felice C, De Angelis C, Coacci F, Mastrone M, Cosmi EV. Transvaginal sonographic evaluation of endometrial polyps: a comparison with two dimensional and three dimensional contrast sonography. Clin Exp Obstet Gynecol. 1999;26:171–3.
23. Gruboeck K, Jurkovic D, Lawton F, Savvas M, Tailor A, Campbell S. The diagnostic value of endometrial thickness and volume measurements by three-dimensional ultrasound in patients with postmenopausal bleeding. Ultrasound Obstet Gynecol. 1996;8:272–6.
24. Forrest TS, Elyaderani MK, Muilenburg MI, Bewtra C, Kable WT, Sullivan P. Cyclic endometrial changes: US assessment with histologic correlation. Radiology. 1988;167:233–7.
25. Remohí J, Ardiles G, García-Velasco JA, Gaitán P, Simón C, Pellicer A. Endometrial thickness and serum oestradiol concentrations as predictors of outcome in oocyte donation. Hum Reprod. 1997;12:2271–6.
26. Schild RL, Indefrei D, Eschweiler S, Van der Ven H, Fimmers R, Hansmann M. Three-dimensional endometrial volume calculation and pregnancy rate in an in-vitro fertilization programme. Hum Reprod. 1999;14:1255–8.
27. Raga F, Bonilla-Musoles F, Casañ EM, Klein O, Bonilla F. Assessment of endometrial volume by three-dimensional ultrasound prior to embryo transfer: clues to endometrial receptivity. Hum Reprod. 1999;14:2851–4.
28. Zollner U, Zollner KP, Blissing S, Pöhls U, Steck T, Dietl J, et al. Impact of three-dimensionally measured endometrial volume on the pregnancy rate after intrauterine insemination. Zentralbl Gynakol. 2003;125:136–41.
29. Kovachev E, Ganchev Z, Cherneva S, Zokhav E, Shperberg A. Measurement of endometrial volume and endometrial thickness for assessment of endometrial receptivity in assisted reproductive techniques. Akush Ginekol (Sofiia). 2005;44:27–33.
30. Zollner U, Specketer MT, Dietl J, Zollner KP. 3D-Endometrial volume and outcome of cryopreserved embryo replacement cycles. Arch Gynecol Obstet. 2012;286(2):517–23.
31. Out HJ, David I, Ron-El R, Friedler S, Shalev E, Geslevich J, et al. A randomized, double-blind clinical trial using fixed daily doses of 100 or 200 IU of recombinant FSH in ICSI cycles. Hum Reprod. 2001;16:1104–9.
32. Corbacioğlu A, Baysal B. Effects of endometrial thickness and echogenic pattern on assisted reproductive treatment outcome. Clin Exp Obstet Gynecol. 2009;36:145–7.
33. Raine-Fenning N, Campbell B, Collier J, Brincat M, Johnson I. The reproducibility of endometrial volume acquisition and measurement with the VOCAL-imaging program. Ultrasound Obstet Gynecol. 2002;19:69–75.
34. Bordes A, Bory AM, Benchaïb M, Rudigoz RC, Salle B. Reproducibility of transvaginal three-dimensional endometrial volume measurements with virtual organ computer-aided analysis (VOCAL) during ovarian stimulation. Ultrasound Obstet Gynecol. 2002;19:76–80.
35. Momeni M, Rahbar MH, Kovanci E. A meta-analysis of the relationship between endometrial thickness and outcome of in vitro fertilization cycles. J Hum Reprod Sci. 2011;4:130–7.
36. Singh M, Chaudhry P, Asselin E. Bridging endometrial receptivity and implantation: network of hormones, cytokines, and growth factors. J Endocrinol. 2011;210:5–14. Review.
37. Jacobs HS. Polycystic ovaries and polycystic ovary syndrome. Gynecol Endocrinol. 1987;1:113–31. Review.
38. Polson DW, Adams J, Wadsworth J, Franks S. Polycystic ovaries – a common finding in normal women. Lancet. 1988;1:870–2.
39. Kousta E, White DM, Cela E, McCarthy MI, Franks S. The prevalence of polycystic ovaries in women with infertility. Hum Reprod. 1999;14:2720–3.
40. Adams J, Polson DW, Franks S. Prevalence of polycystic ovaries in women with anovulation and idiopathic hirsutism. Br Med J. (Clin Res Ed). 1986;293:355–9.
41. Rotterdam ESHRE/ASRM-Sponsored PCOS Consensus Workshop Group. Revised 2003 consensus on diagnostic criteria and long-term health risks related to polycystic ovary syndrome. Fertil Steril. 2004;81:19–25.
42. Allemand MC, Tummon IS, Phy JL, Foong SC, Dumesic DA, Session DR. Diagnosis of polycystic ovaries by three-dimensional transvaginal ultrasound. Fertil Steril. 2006;85:214–9.
43. He LR, Zhou LX, Pan RK. Zhang X [Clinical significance of counting follicles in diagnosis of polycystic ovary syndrome by the three-dimensional ultrasound imaging with sonography based automated volume calculation method]. Zhonghua Fu Chan Ke Za Zhi. 2011;46:350–4.
44. Kyei-Mensah AA, Lin Tan S, Zaidi J, Jacobs HS. Relationship of ovarian stromal volume to serum androgen concentrations in patients with polycystic ovary syndrome. Hum Reprod. 1998;13:1437–41.
45. Järvelä IY, Mason HD, Sladkevicius P, Kelly S, Ojha K, Campbell S, et al. Characterization of normal and polycystic ovaries using three-dimensional power Doppler ultrasonography. J Assist Reprod Genet. 2002;19:582–90.
46. Pan HA, Wu MH, Cheng YC, Li CH, Chang FM. Quantification of Doppler signal in polycystic ovary

syndrome using three-dimensional power Doppler ultrasonography: a possible new marker for diagnosis. Hum Reprod. 2002;17:201–6.
47. Ng EH, Chan CC, Tang OS, Yeung WS, Ho PC. The role of endometrial and subendometrial blood flows measured by three-dimensional power Doppler ultrasound in the prediction of pregnancy during IVF treatment. Hum Reprod. 2006;21:164–70.
48. Pascual MA, Graupera B, Hereter L, Tresserra F, Rodriguez I, Alcázar JL. Assessment of ovarian vascularization in the polycystic ovary by three-dimensional power Doppler ultrasonography. Gynecol Endocrinol. 2008;24:631–6.
49. Dolz M, Osborne NG, Blanes J, Raga F, Abad-Velasco L, Villalobos A, et al. Polycystic ovarian syndrome: assessment with color Doppler angiography and three-dimensional ultrasonography. J Ultrasound Med. 1999;18:303–13.
50. Benacerraf BR. Inversion mode display of 3D sonography: applications in obstetric and gynecologic imaging. AJR Am J Roentgenol. 2006;187:965–71. Review.
51. Gougeon A. Regulation of ovarian follicular development in primates: facts and hypotheses. Endocr Rev. 1996;17:121–55. Review.
52. Broekmans FJ, Kwee J, Hendriks DJ, Mol BW, Lambalk CB. A systematic review of tests predicting ovarian reserve and IVF outcome. Hum Reprod Update. 2006;12:685–718. Review.
53. Verhagen TE, Hendriks DJ, Bancsi LF, Mol BW, Broekmans FJ. The accuracy of multivariate models predicting ovarian reserve and pregnancy after in vitro fertilization: a meta-analysis. Hum Reprod Update. 2008;14:95–100.
54. Adibi A, Mardanian F, Hajiahmadi S. Comparison of Ovarian volume and Antral follicle count with Endocrine tests for prediction of responsiveness in ovulation induction protocols. Adv Biomed Res. 2012;1:71. doi: 10.4103/2277-9175.102975.
55. van der Stege JG, van der Linden PJ. Useful predictors of ovarian stimulation response in women undergoing in vitro fertilization. Gynecol Obstet Invest. 2001;52:43–6.
56. Karande VC. Managing and predicting low response to standard in vitro fertilization therapy: a review of the options. Treat Endocrinol. 2003;2:257–72. Review.
57. Danninger B, Brunner M, Obruca A, Feichtinger W. Prediction of ovarian hyperstimulation syndrome by ultrasound volumetric assessment [corrected] of baseline ovarian volume prior to stimulation. Hum Reprod. 1996;11:1597–9.
58. Palma GA, Argañaraz ME, Barrera AD, Rodler D, Mutto AÁ, Sinowatz F. Biology and biotechnology of follicle development. Scientific World Journal. 2012;2012:938138. doi:10.1100/2012/938138. Review.
59. Smotrich DB, Widra EA, Gindoff PR, Levy MJ, Hall JL, Stillman RJ. Prognostic value of day 3 estradiol on in vitro fertilization outcome. Fertil Steril. 1995; 64:1136–40.
60. Seifer DB, Scott Jr RT, Bergh PA, Abrogast LK, Friedman CI, Mack CK, et al. Women with declining ovarian reserve may demonstrate a decrease in day 3 serum inhibin B before a rise in day 3 follicle-stimulating hormone. Fertil Steril. 1999;72:63–5.
61. van Rooij IA, Broekmans FJ, te Velde ER, Fauser BC, Bancsi LF, de Jong FH, et al. Serum anti-Müllerian hormone levels: a novel measure of ovarian reserve. Hum Repod. 2002;17:3065–71.
62. de Vet A, Laven JS, de Jong FH, Themmen AP, Fauser BC. Antimüllerian hormone serum levels: a putative marker for ovarian aging. Fertil Steril. 2002;77: 357–62.
63. Fanchin R, Schonäuer LM, Righini C, Frydman N, Frydman R, Taieb J. Serum anti-Müllerian hormone dynamics during controlled ovarian hyperstimulation. Hum Reprod. 2003;18:328–32.
64. Hendriks DJ, Mol BW, Bancsi LF, Te Velde ER, Broekmans FJ. Antral follicle count in the prediction of poor ovarian response and pregnancy after in vitro fertilization: a meta-analysis and comparison with basal follicle-stimulating hormone level. Fertil Steril. 2005;83:291–301.
65. Visser JA, Themmen AP. Anti-Müllerian hormone and folliculogenesis. Mol Cell Endocrinol. 2005;234:81–6. Review.
66. Klinkert ER, Broekmans FJ, Looman CW, Habbema JD, te Velde ER. The antral follicle count is a better marker than basal follicle-stimulating hormone for the selection of older patients with acceptable pregnancy prospects after in vitro fertilization. Fertil Steril. 2005; 83:811–4.
67. Visser JA, de Jong FH, Laven JS, Themmen AP. Anti-Müllerian hormone: a new marker for ovarian function. Reproduction. 2006;131:1–9. Review.
68. Kupesic S, Kurjak A. Predictors of IVF outcome by three-dimensional ultrasound. Hum Reprod. 2002;17: 950–5.
69. Arslan M, Bocca S, Mirkin S, Barroso G, Stadtmauer L, Oehninger S. Controlled ovarian hyperstimulation protocols for in vitro fertilization: two decades of experience after the birth of Elizabeth Carr. Fertil Steril. 2005;84:555–69. Review.
70. Tomas C, Nuojua-Huttunen S, Martikainen H. Pretreatment transvaginal ultrasound examination predicts ovarian responsiveness to gonadotrophins in in-vitro fertilization. Hum Reprod. 1997;12:220–3.
71. Chang MY, Chiang CH, Chiu TH, Hsieh TT, Soong YK. The antral follicle count predicts the outcome of pregnancy in a controlled ovarian hyperstimulation/intrauterine insemination program. J Assist Reprod Genet. 1998;15:12–7.
72. Jayaprakasan K, Chan Y, Islam R, Haoula Z, Hopkisson J, Coomarasamy A, et al. Prediction of in vitro fertilization outcome at different antral follicle count thresholds in a prospective cohort of 1,012 women. Fertil Steril. 2012;98:657–63.
73. Haadsma ML, Bukman A, Groen H, Roeloffzen EM, Groenewoud ER, Heineman MJ, et al. The number of small antral follicles (2–6 mm) determines the outcome of endocrine ovarian reserve tests in a subfertile population. Hum Reprod. 2007;22:1925–31.

74. Jayaprakasan K, Deb S, Batcha M, Hopkisson J, Johnson I, Campbell B, et al. The cohort of antral follicles measuring 2–6 mm reflects the quantitative status of ovarian reserve as assessed by serum levels of anti-Müllerian hormone and response to controlled ovarian stimulation. Fertil Steril. 2010;94:1775–81.
75. Scheffer GJ, Broekmans FJ, Bancsi LF, Habbema JD, Looman CW, Te Velde ER. Quantitative transvaginal two- and three-dimensional sonography of the ovaries: reproducibility of antral follicle counts. Ultrasound Obstet Gynecol. 2002;20:270–5.
76. Raine-Fenning N, Jayaprakasan K, Clewes J, Joergner I, Bonaki SD, Chamberlain S, et al. SonoAVC: a novel method of automatic volume calculation. Ultrasound Obstet Gynecol. 2008;31:691–6.
77. Raine-Fenning N, Jayaprakasan K, Chamberlain S, Devlin L, Priddle H, Johnson I, et al. Automated measurements of follicle diameter: a chance to standardize? Fertil Steril. 2009;91:1469–72.
78. Deb S, Jayaprakasan K, Campbell BK, Clewes JS, Johnson IR, Raine-Fenning NJ. Intraobserver and interobserver reliability of automated antral follicle counts made using three-dimensional ultrasound and SonoAVC. Ultrasound Obstet Gynecol. 2009;33:477–83.
79. Deb S, Campbell BK, Clewes JS, Raine-Fenning NJ. Quantitative analysis of antral follicle number and size: a comparison of two-dimensional and automated three-dimensional ultrasound techniques. Ultrasound Obstet Gynecol. 2010;35:354–60.
80. Jayaprakasan K, Campbell BK, Clewes JS, Johnson IR, Raine-Fenning NJ. Three-dimensional ultrasound improves the interobserver reliability of antral follicle counts and facilitates increased clinical work flow. Ultrasound Obstet Gynecol. 2008;31:439–44.
81. Forman RG, Robinson J, Yudkin P, Egan D, Reynolds K, Barlow DH. What is the true follicular diameter: an assessment of the reproducibility of transvaginal ultrasound monitoring in stimulated cycles. Fertil Steril. 1991;56:89–92.
82. Ata B, Tulandi T. Ultrasound automated volume calculation in reproduction and in pregnancy. Fertil Steril. 2011;95:2163–70. Review.
83. Wittmaack FM, Kreger DO, Blasco L, Tureck RW, Mastroianni Jr L, Lessey BA. Effect of follicular size on oocyte retrieval, fertilization, cleavage, and embryo quality in in-vitro fertilization cycles: a 6-year data collection. Fertil Steril. 1994;62:1205–10.
84. Penzias AS, Emmi AM, Dubey AK, Layman LC, DeCherney AH, Reindollar RH. Ultrasound prediction of follicle volume: is the mean diameter reflective? Fertil Steril. 1994;62:1274–6.
85. Quigley MM, Sokoloski JE, Richards SI. Timing human chorionic gonadotropin administration by days of estradiol rise. Fertil Steril. 1985;44:791–5.
86. Levran D, Lopata A, Nayudu PL, Martin MJ, McBain JC, Bayly CM, et al. Analysis of the outcome of in vitro fertilization in relation to the timing of human chorionic gonadotropin administration by the duration of estradiol rise in stimulated cycles. Fertil Steril. 1985;44:335–41.
87. Casper RF, Armstrong DT, Brown SE, Daniel SA, Yuzpe AA, Erskine H. In vitro fertilization: determination of follicular maturation for timing of human chorionic gonadotropin administration. Fertil Steril. 1987;47:345–9.
88. Nilsson L, Wikland M, Hamburger L, Hillensjo T, Chari S, Sturm G, et al. Simplification of the method of in vitro fertilization: Sonographic measurements of follicular diameter as a sole index of follicular maturity. J In Vitro Fert Emryo Transf. 1985;2:17.
89. Tan SL, Balen A, el Hussein E, Mills C, Campbell S, Yovich J, et al. A prospective randomized study of the optimum timing of human chorionic gonadotropin administration after pituitary desensitization in in-vitro fertilization. Fertil Steril. 1992;57:1259–64.
90. Dubey AK, Wang HA, Duffy P, Penzias AS. The correlation between follicular measurements, oocyte morphology, and fertilization rates in an in vitro fertilization program. Fertil Steril. 1995;64:787–90.
91. Von Ramm OT, Smith SW. Three-dimensional imaging system. 1987. United States Patent 4,694,434. Available from: http://www.freepatentsonline.com/4694434.html. Last accessed 5 Dec 2012.
92. Kyei-Mensah A, Maconochie N, Zaidi J, Pittrof R, Campbell S, Tan SL. Transvaginal three-dimensional ultrasound: accuracy of follicular volume measurements. Fertil Steril. 1996;66:718–22.
93. Yavas Y, Selub MR. Ovarian follicular volume and follicular surface area are better indicators of follicular growth and maturation, respectively, than is follicular diameter. Fertil Steril. 2009;91:1299–302.
94. Rosen MP, Shen S, Dobson AT, Rinaudo PF, McCulloch CE, Cedars MI. A quantitative assessment of follicle size on oocyte developmental competence. Fertil Steril. 2008;90:684–90.
95. Scott RT, Hofmann GE, Muasher SJ, Acosta AA, Kreiner DK, Rosenwaks Z. Correlation of follicular diameter with oocyte recovery and maturity at the time of transvaginal follicular aspiration. J In Vitro Fert Embryo Transf. 1989;6:73–5.
96. Ectors FJ, Vanderzwalmen P, Van Hoeck J, Nijs M, Verhaegen G, Delvigne A, et al. Relationship of human follicular diameter with oocyte fertilization and development after in-vitro fertilization or intracytoplasmic sperm injection. Hum Reprod. 1997;12:2002–5.
97. Raine-Fenning N, Jayaprakasan K, Deb S, Clewes J, Joergner I, Dehghani Bonaki S, et al. Automated follicle tracking improves measurement reliability in patients undergoing ovarian stimulation. Reprod Biomed Online. 2009;18:658–63.
98. Amer A, Hammadeh ME, Kolkailah M, Ghandour AA. Three-dimensional versus two-dimensional ultrasound measurement of follicular volume: are they comparable? Arch Gynecol Obstet. 2003;268:155–7.
99. Raine-Fenning NJ, Jayaprakasan K, Clewes JS, Joergner I, Bonaki SD, Chamberlain S. Establishing the validity of a new technique that facilitates automated follicular volume measurement. Ultrasound Obstet Gynecol. 2007;30:393.

100. Rousian M, Verwoerd-Dikkeboom CM, Koning AH, Hop WC, van der Spek PJ, Exalto N, et al. Early pregnancy volume measurements: validation of ultrasound techniques and new perspectives. BJOG. 2009;116:278–85.
101. Raga F, Bonilla-Musoles F, Castillo JC. SonoAVC: a new tool in early diagnosis of patent urachus with bladder prolapse. Ultrasound Obstet Gynecol. 2012;39:241–2.
102. Deutch TD, Joergner I, Matson DO, Oehninger S, Bocca S, Hoenigmann D, et al. Automated assessment of ovarian follicles using a novel three-dimensional ultrasound software. Fertil Steril. 2009; 92:1562–8.
103. Ata B, Seyhan A, Reinblatt SL, Shalom-Paz E, Krishnamurthy S, Tan SL. Comparison of automated and manual follicle monitoring in an unrestricted population of 100 women undergoing controlled ovarian stimulation for IVF. Hum Reprod. 2011;26:127–33.
104. Hernández J, Sanabria V, Rodríguez-Fuentes A, García-Guzman R, Palumbo A. Comparison of automated measurements of follicular volume and manual measurements of follicular diameter to HCG administration: a prospective study in egg donors. Fertil Steril. 2009;92:47.
105. Lamazou F, Arbo E, Salama S, Grynberg M, Frydman R, Fanchin R. Reliability of automated volumetric measurement of multiple growing follicles in controlled ovarian hyperstimulation. Fertil Steril. 2010;94:2172–6.
106. Salama S, Arbo E, Lamazou F, Levaillant JM, Frydman R, Fanchin R. Reproducibility and reliability of automated volumetric measurement of single preovulatory follicles using SonoAVC. Fertil Steril. 2010;93:2069–73.
107. Rodríguez-Fuentes A, Hernández J, García-Guzman R, Chinea E, Iaconianni L, Palumbo A. Prospective evaluation of automated follicle monitoring in 58 in vitro fertilization cycles: follicular volume as a new indicator of oocyte maturity. Fertil Steril. 2010;93:616–20.
108. Raine-Fenning NJ, Jayaprakasan K, Deb S, Clewes JS, Johnson IR. Automated three-dimensional follicular measurements increase the clinical work flow in an IVF programme. Ultrasound Obstet Gynecol. 2008;32: 308–97.
109. Murtinger M, Aburumieh A, Rubner P, Eichel V, Zech MH, Zech NH. Improved monitoring of ovarian stimulation using 3D transvaginal ultrasound plus automated volume count. Reprod Biomed Online. 2009;19:695–9.
110. Sherbahn R, Deutch T. Follicle measurements using a computerized 3D ultrasound system (SonoAVC) is effective and efficient. Fertil Steril. 2009;92:118.
111. Raine-Fenning N, Deb S, Jayaprakasan K, Clewes J, Hopkisson J, Campbell B. Timing of oocyte maturation and egg collection during controlled ovarian stimulation: a randomized controlled trial evaluating manual and automated measurements of follicle diameter. Fertil Steril. 2010;94:184–8.
112. Jörger I, Scherleitner E. SonoAVC Studies on automated detection and measurements of hyperstimulated follicles utilizing a new algorithm. GE Medical Systems Ultrasound & Primary Care Diagnostics, LLC, a General Electric company, doing business as GE Healthcare. 2008. Available from: http://www.gehealthcare.com/laes/docs/SonoAVC7.pdf. Last accessed on 5 Dec 2012.
113. Murtinger M, Aburumieh A, Zech MH, Spitzer D, Zech NH. Objective follicle monitoring and accurate result communication from referring physicians in an IVF program. Ultrasound Obstet Gynecol. 2010;38:98–9.
114. Roest J, Verhoeff A, van Lent M, Huisman GJ, Zeilmaker GH. Results of decentralized in-vitro fertilization treatment with transport and satellite clinics. Hum Reprod. 1995;10:563–7.
115. EU Directive on tissue and cells (2004/23/EC). Available from: http://eur-lex.europa.eu/LexUriServ/LexUriServ.do?uri=OJ:L:2004:102:0048:0058:en:PDF. Last accessed on 5 Dec 2012.

Ultrasound-Guided Surgical Procedures

21

Donna R. Session and Jennifer F. Kawwass

Introduction

Ultrasonography plays an integral role not only in diagnostic testing but also in guiding hysteroscopic procedures, ovarian cyst and hydrosalpinx aspiration, difficult intrauterine device insertion and removal, and ART procedures such as oocyte retrieval and embryo transfer.

The use of ultrasonography at the time of intrauterine procedures provides visualization of the intrauterine contents as well as the myometrium and may decrease procedure-associated risks, particularly uterine perforation. For hysteroscopic procedures such as uterine septum, myoma, or synechiae resection, operative ultrasonographic guidance provides an alternative to laparoscopy and, as a result, shortens overall operating time, decreases cost, and eliminates the risk of laparoscopy. In addition, performing intrauterine procedures under ultrasonographic guidance may increase the likelihood of completing the procedure in a single operation.

Portions of text reprinted from Session D, Kelly A, Goudas V, et al. Ultrasonographically guided intrauterine surgery. Female Pelvic Med Reconstr Surg. 1999;5(2):91–95. With permission from John Wiley & Sons, Inc.

D.R. Session (✉) • J.F. Kawwass
Division of Reproductive Endocrinology and Infertility,
Department of Gynecology and Obstetrics,
Emory University School of Medicine,
550 Peachtree Street, Suite 1800,
Atlanta, GA 30308, USA
e-mail: dsessio@emory.edu;
jennifer.kawwass@emory.edu

Assisted reproductive technology (ART) procedures such as oocyte retrieval and embryo transfer require ultrasonographic guidance for improved outcomes. In addition, ultrasound guidance is used for aspiration of ascites resulting from ovarian hyperstimulation syndrome, a complication of ART.

Ultrasound guidance has been described in IUD placement, cervical stenosis, tubal cannulation, and suction curettage for pregnancy loss [1, 2].

Ultrasound Guidance at Time of Uterine Surgery: Uterine Septum Resection, Myoma Excision, Synechiae Lysis, Intrauterine Foreign Bodies, Hematometra

Before starting the procedure, the bladder is completely drained so that the amount of water inserted into the bladder can be accurately quantified and overdistention can be avoided. Next, the urethral catheter is flushed with water and the syringe filled with water and cleared of air. The bladder is then retrograde-filled with 200–400 cc of warm water. A 3-contrast technique has been described by Lin et al. in which saline is injected into the abdomen in addition to the bladder [3]. Shalev and Zuckerman claimed that there is little advantage to the 3-contrast method, because a clear view of the uterus and uterine cavity is obtained with the distending media used in hysteroscopy [4]. Moreover, the benefits of the 3-contrast technique may not outweigh the

L.A. Stadtmauer, I. Tur-Kaspa (eds.), *Ultrasound Imaging in Reproductive Medicine*,
DOI 10.1007/978-1-4614-9182-8_21,

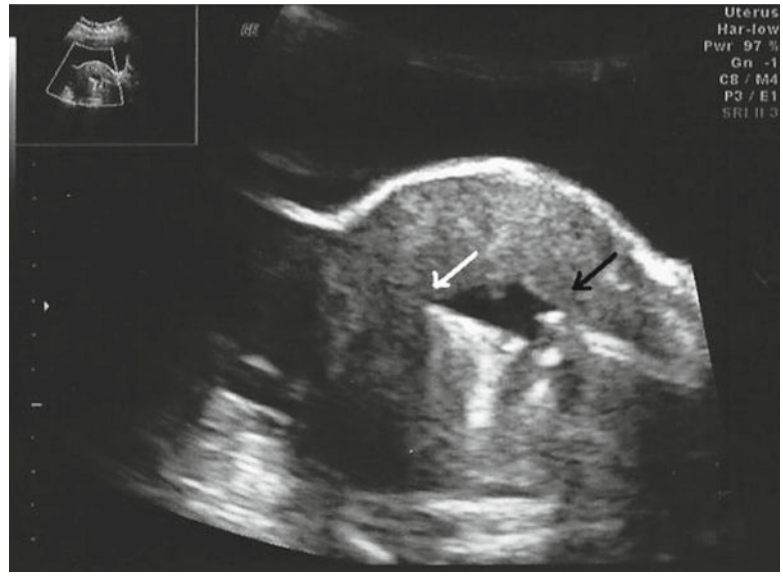

Fig. 21.1 Ultrasound guidance at time of hysteroscopy (*Black arrow* pointing at hysteroscope, *white arrow* pointing at hysteroscopic scissors)

potential risks. An abdominal ultrasound covered with a sterile sheath can be used to visualize boundaries of the uterine cavity, the instrument's location within the cavity, and the extent of resection/depth of remaining myometrium (see Fig. 21.1). The ultrasonographic operator may provide a narrative of position of the instruments and depth of the uterine wall at the operative site. Alternatively, the surgeon may view the ultrasonographic and hysteroscopic images simultaneously.

Uterine Septum

The incidence of congenital uterine anomalies is estimated to be 3–4 % of reproductive age women and 5–10 % in women with recurrent miscarriages [5, 6]. The anomalies may be asymptomatic or result in infertility, recurrent pregnancy loss, intrauterine growth retardation, or endometriosis when obstruction is present. Uterine septum, which results from incomplete resorption of the medial septum between two normally fused hemi-uteri, is not only the most common uterine anomaly but also is the malformation most highly associated with poor pregnancy outcomes [5, 7]. Case series report a spontaneous miscarriage rate ranging from 65 to 88 % in the presence of a uterine septum [8, 9]. It is hypothesized that implantation on a poorly vascularized septum may contribute to this increased risk of miscarriage. After resection, spontaneous miscarriage rates return to the baseline rate of approximately 15 %; 80 % of pregnancies post-resection result in term delivery [7, 8].

The high degree of accuracy of magnetic resonance imaging (MRI) and three-dimensional (3D) ultrasound in the diagnosis of congenital anomalies has decreased the previous need for diagnostic laparoscopy at the time of surgery to aid in characterization of the type of anomaly. Three-dimensional ultrasound has been shown to have 98 % specificity and 100 % sensitivity of accurate septum diagnosis [10]. Although diagnostic hysteroscopy/laparoscopy is still considered the gold standard, MRI and 3D ultrasound are accepted alternatives with both lower risk and cost.

Upon diagnosis, a uterine septum is treated by noninvasive outpatient hysteroscopic surgical resection which results in significant improvement in subsequent pregnancy outcomes [5, 7, 11]. Ultrasonographic guidance without the aid of hysteroscopy has also been described; 11 patients had postprocedural evaluation of the uterine cavity, 2 patients had a residual septum, and 1 patient had extensive synechiae [12]. Although the number of cases is limited, the results with ultrasonographically guided hysteroscopy appear

better than metroplasty without the use of hysteroscopy. Hysteroscopic metroplasty can be successfully performed using microscissors, laser, or electrocautery with comparable improvements in future pregnancy outcomes [7]. The procedure is complete once both ostia are visible simultaneously and when less than 1 cm of myometrium remains [13]. Discontinuing the procedure once a fundal thickness of 8–10 mm is obtained was associated with a normal intrauterine contour on hysterosalpingography [14]. Postoperative hysterosalpingography revealed incomplete resection of the septum when thicknesses of 11–16 mm were used [14].

A prospective, open study including 81 patients undergoing ultrasound-guided operative hysteroscopy for uterine septum or submucosal myoma compared outcomes to that of a historical control group of 45 patients who underwent the same procedure under laparoscopic guidance [15]. All patients in the ultrasound group were successfully treated with a single surgery, and none required conversion to laparoscopy. In contrast, four of the control group patients required additional surgery to resect residual fibroid or septum. Ultrasound guidance allowed the surgeon to accurately determine depth of remaining septum and the outer limit of uterine fundus.

Submucosal Fibroids

Uterine fibroids, the most common benign tumors in females, have a prevalence of 8–18 % in the general population and are often asymptomatic [16, 17]. Symptomatic fibroids can cause pelvic pain, menorrhagia, abdominal fullness, and occasional urinary and bowel symptoms. Fibroid size and location affect the type and degree of patient symptoms and may also have reproductive consequences including pregnancy loss and infertility.

As with uterine septa, resection of submucosal fibroids benefits from ultrasound guidance at time of hysteroscopy. The extent of uterine fibroids' effect on pregnancy rates and outcomes remains controversial. However, submucosal myomas that significantly distort or encroach on the uterine cavity may lower implantation and pregnancy rates in infertile women undergoing IVF [18]. Several recent studies evaluated the effect of fibroids on in vitro fertilization cycles; the balance of data suggests that pregnancy outcomes and implantation rates are adversely affected by submucosal myomas that enter the uterine cavity but not by subserosal or intramural fibroids that are less than 5–7 cm in size [19–22]. Resection of submucosal fibroids clearly within the uterine cavity is likely warranted in patients with dysfunctional uterine bleeding, infertility, or pregnancy loss who desire to optimize future fertility. A hysteroscopic approach is reasonable if the majority of the fibroid is within the cavity or if subtotal hysteroscopic myomectomy is deemed preferable to abdominal myomectomy. Hysteroscopic resection may be performed using a hysteroscopic morcellator or resectoscope. A resectoscope allows for the use of electrocautery at time of resection but, as a result, requires electrolyte-poor distending media such as mannitol, sorbitol, or glycine. Morcellating devices resect using a rotating blade rather than electrocautery and allow for use of isotonic distending media such as normal saline or lactated ringers which have lower risk for fluid overload and subsequent electrolyte imbalance. The avoidance of electrocautery also has a theoretical benefit of avoiding thermal damage to the myometrium and decreasing chance of future uterine rupture at time of pregnancy. Both methods incur a risk of procedure abortion secondary to bleeding. Prior to starting the hysteroscopy, injection of vasopressin into the cervical stroma can be used to help decrease myoma bleeding. If bleeding is encountered intraoperatively, conversion from morcellator to electrocautery or use of uterine balloon for tamponade and uterine compression can be used to help achieve hemostasis. Lin et al. resected six submucosal myomas under ultrasonographic guidance [23]. All cases were completed in less than 1 h. There were no traumatic complications. None of the patients required laparotomy or blood transfusion. Postoperative electrolyte values revealed no significant change from preoperative values. Menorrhagia and metrorrhagia improved. Postoperative hysteroscopy revealed no intrauterine adhesions, and the endometrium at the operative site appeared normal. Wortman and Dagget used ultrasonographic control to

remove large submucosal myomas [24]. These authors claimed that ultrasonography may help prevent perforation and obviate laparoscopy [24].

Synechiae

Asherman's syndrome, scarring of the endometrial cavity that may have resulted from preexisting infection or uterine instrumentation, may be manifested as hypomenorrhea, amenorrhea, infertility, or recurrent pregnancy loss. Hysteroscopic lysis of adhesions remains the treatment of choice. In severe cases of intrauterine adhesions, it is difficult to determine, without ultrasonography, which part of the cavity is being observed during hysteroscopy. Shalev et al. performed hysteroscopic lysis of intrauterine adhesions using ultrasound (rather than laparoscopic) guidance in 106 women with varying degrees of Asherman's syndrome. Adhesiolysis was successful in all cases; there were no complications [25]. In cases of moderate-to-severe intrauterine synechiae, ultrasonographic guidance permits the accurate localization of the instruments within the uterus and of myometrial depth. This may result in a greater chance of success in a single surgical procedure with a lower perforation rate. A recent retrospective cohort study including 159 procedures affirms a lower uterine perforation rate for ultrasound-guided (1.9 %) compared to laparoscopic (8.7 %) or blind (5.3 %) hysteroscopic uterine septum resection [17]. Cost was also significantly less for the ultrasound- rather than laparoscopic-guided resections [17].

After significant adhesiolysis, the placement of an intrauterine balloon stent to provide mechanical separation and administration of estrogen to promote endometrial proliferation have been shown to decrease postoperative synechiae formation [19, 26–28]. Initial extent of adhesions has been shown to correlate with adhesion reformation [29]. Both uterine balloons and intrauterine devices have been evaluated for postoperative Asherman's management. A 1993 study revealed significantly improved outcomes (resumption of menses, increased conception, and decreased need for reoperation) in patients for whom a uterine balloon was placed for 10 days as compared to those who received a nonhormonal copper intrauterine device for 3 months [27]. More recently, investigators are comparing the effectiveness of newer synthetic barrier methods such as Seprafilm and hyaluronic acid gel compounds [30, 31]. Preliminary results are promising; however, larger randomized studies have not yet been performed. Of note, antibiotic prophylaxis is recommended for as long as a foreign intrauterine device remains in place.

The exact regimen and dose of oral estrogen remains unclear. Accepted supplementation ranges from 4 to 6 mg daily (often dosed bi-daily) for 4–10 weeks duration.

Intrauterine Foreign Bodies

The use of ultrasonographic guidance for the retrieval of an intrauterine foreign body has been described [32]. Retained bony fragments after a therapeutic abortion were removed successfully with the use of an ultrasonographically guided resectoscope [3]. Ultrasonography allowed visualization of bone embedded in the myometrium.

Hematometra

As in the case of intrauterine foreign body, ultrasonography can direct the surgeon to the pathologic site within the uterus when this is not evident by direct hysteroscopic vision, as in hematometra. Kohlenberg et al. described five cases of hematometra following endometrial ablation [33]. Ultrasonography was used to guide the hysteroscope to the cornua where these collections were located. Similarly, Goudas and Session described a case of successful treatment of cervical stenosis and hematometra with ultrasonographically guided hysteroscopy [34].

Limitations of the Technique

Replacing laparoscopy with ultrasound at time of hysteroscopic resection of a uterine septum, myoma, or adhesive disease usually decreases potential risk while shortening operative time

and maintaining optimal surgical results [25, 35]. However, in a limited number of patients in whom abdominal pathology is suspected, laparoscopy concurrent with hysteroscopy may reveal an intra-abdominal abnormality that can be treated laparoscopically. Additionally, severe retroversion and cul-de-sac adhesions may hinder clear transabdominal ultrasound visualization. Furthermore, diathermy heat may alter tissue or distending fluid by creating microbubbles or produce electrical interference that appears as a "snowstorm" that impedes ultrasonographic imaging [33]. Nonetheless, it is still usually possible to measure myometrial depth, although hysteroscopic localization within the area may be difficult. Additionally, the majority of hysteroscopic procedures can now be performed without cautery using new hysteroscopic morcellating devices.

Summary

For uterine septa, submucosal fibroids, and uterine synechiae, ultrasound guidance helps obtain complete resection while minimizing risk of uterine perforation [24].

Ovarian Cyst and Hydrosalpinx Aspiration

Both ovarian cysts and tubal fluid can be easily aspirated while using transvaginal ultrasound guidance. A needle guide fits on the superior aspect of a standard transvaginal ultrasound allowing the sonographer/surgeon to advance the needle in a predictable, visible plane. Ultrasound color Doppler can be used to confirm an avascular path from the vagina to the ovary or tube.

Ovarian Cyst Aspiration

Large, simple ovarian cysts can form spontaneously, after previous stimulation cycles or as the result of a flare response from GnRH-agonist treatment, and have potential to cause pain or interfere with subsequent stimulation. Usually, cysts rupture or are reabsorbed within 6 months without need for intervention; a recent meta-analysis including eight randomized controlled trials found no benefit to oral contraceptive use to hasten cyst resolution [36]. However, if a cyst is causing significant pain, persists for several months, and grows large enough to pose a significant bleeding or torsion risk, or if time constraints exist for a subsequent cycle, a role remains for cyst aspiration. Cysts may be either functional (hormone-secreting) or nonfunctional. Small (<15–20 mm), nonfunctional (<50 pg/mL estradiol) cysts likely have little effect on fertility treatment; however, functional cysts can deleteriously affect number and quality of retrieved oocytes, fertilization rates, implantation rates, miscarriage rates, and cycle continuation rates [37, 38].

Small, nonfunctional cysts usually do not require intervention. Larger, functional cysts may be managed conservatively either by prolonging downregulation with GnRH agonist prior to stimulation start or by surgical aspiration. In this situation, no clear benefit to surgical aspiration exists [39]. In fact, even for larger (>15 mm), estrogen-producing (>50 pg/mL estradiol) cysts, the majority of evidence suggests no improvement in number of retrieved oocytes, embryo quality, fertilization rate, and implantation and pregnancy rates between women whose cysts were aspirated and those whose cysts were not [39–42]. The deleterious impact of functional cysts on in vitro fertilization cycles persists and, unfortunately, has not been shown to be blunted by cyst aspiration.

Occasionally, however, time pressure, inability to prolong stimulation start, or patient discomfort drive the need for surgical cyst aspiration. Aspirated fluid may be collected and sent to pathology for further cytologic evaluation. A 1992 study including 1,544 oocyte retrievals sent aspirated follicular fluid for cytologic evaluation and found no cases of malignancy [43].

Hydrosalpinx Aspiration

Evidence suggests that the presence of a hydrosalpinx may have a deleterious effect on implantation and pregnancy rates in IVF. This may

result from a direct embryo toxic effect of the hydrosalpinx fluid on inhibition of implantation or from a more direct mechanical flushing effect. Implantation rates have been improved by aspiration of hydrosalpinges during the IVF cycle following oocyte aspiration, by salpingectomy or tubal occlusion prior to the IVF cycle, and by extended antibiotic treatment during the IVF cycle [44–46]. Diagnosed hydrosalpinx is usually treated (excised or occluded) prior to initiation of IVF. However, the size of a hydrosalpinges varies during the menstrual cycle [47]. As a result, patients may not have a visible hydrosalpinx prior to stimulation but may accumulate fluid during an IVF cycle. In such situations, mixed evidence exists regarding benefit of aspiration at time of retrieval. A controlled retrospective analysis of 151 women compared implantation rates in patients with hydrosalpinx at time of retrieval and found no benefit to drainage at time of retrieval but confirmed overall reduction in implantation rates in the presence of hydrosalpinx compared to patients without tubal disease [48]. However, a smaller retrospective study ($n=34$) reported significantly improved implantation rates (14 % versus 1 % $p=.015$) with transvaginal aspiration of the hydrosalpinges at time of oocyte retrieval [45]. Possible concerns with this approach include the rapid re-accumulation of hydrosalpinx fluid and risk of pelvic infection caused by the aspiration of the hydrosalpinx. Nonetheless, aspiration of tubal fluid rather than cryopreservation of all embryos may be useful when hydrosalpinges become evident during an IVF cycle as a significant decrease in chance of pregnancy was found only when the hydrosalpinx was evident on ultrasound [49].

Oocyte Retrieval

Although initially performed laparoscopically, oocyte retrieval is now routinely performed using ultrasound guidance due decreased operative risk and a higher rate of oocytes retrieved. Ultrasound-guided aspiration was first described by Lenz in 1981 [50]. Aspiration techniques have included transabdominal, transvesical, and transurethral approaches using sterile-draped abdominal ultrasound and either a guided or freehand needle. The procedure may be performed using mineral oil rather than potentially oocyte-toxic ultrasound gel in a manner similar to amniocentesis [51]. Transvaginal aspiration, first described by Gleicher in 1983, has replaced other routes of aspiration, except when the ovary is not accessible vaginally such as in some cases of Mullerian anomalies [52, 53]. As with all surgical intervention, oocyte retrieval incurs a risk of infection, bleeding, and damage to nearby structures. Such risks are <1 % and are minimized by adequate visualization and proper surgical technique [54]. For transvaginal aspiration, the patient is placed in the dorsal lithotomy position. After sedation is obtained by either a local, regional, or intravenous route, the vagina is prepped with saline lavage or antiseptic to decrease bacterial counts. Prophylactic antibiotics may be given to reduce the occurrence of possible pelvic inflammatory disease particularly in patients with endometriosis [55]; however, peri-retrieval antibiotics have not been shown to affect clinical pregnancy rates [56]. As with cyst and hydrosalpinx aspiration, a transvaginal ultrasound probe is placed in a sterile sheath and fitted with a needle guide through which a single- or double-lumen 16–17 gauge needle is passed to sharply puncture ovarian follicles and aspirate (at 100–200 mmHg) follicular fluid and oocytes. The tip of the needle is etched to increase echogenicity.

Puncture site is determined by visual observation and use of color Doppler for avoidance of vaginal and pelvic blood vessels. The planned course of the needle can be clearly visualized with the biopsy line setting on the ultrasound machine and the probe rotated in such a manner as to avoid blood vessels (see Fig. 21.2). Absence of vasculature in the needle's course can be confirmed with color Doppler. Additionally, if an ovary is malpositioned, its location can be improved with abdominal pressure or by rotation of the surgical table.

The decision to use a single- or double-lumen needle depends on the physicians desire to flush aspirated follicles with culture media to attempt to increase oocyte yield. Flushing requires a

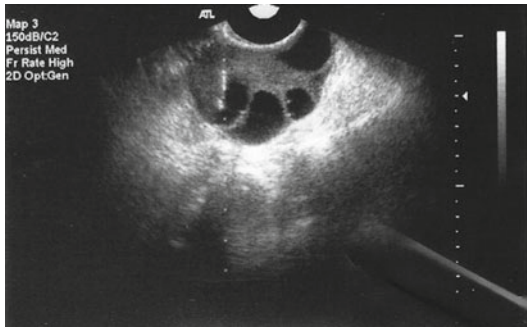

Fig. 21.2 Transvaginal oocyte retrieval (*Dotted line* denotes "needle biopsy line")

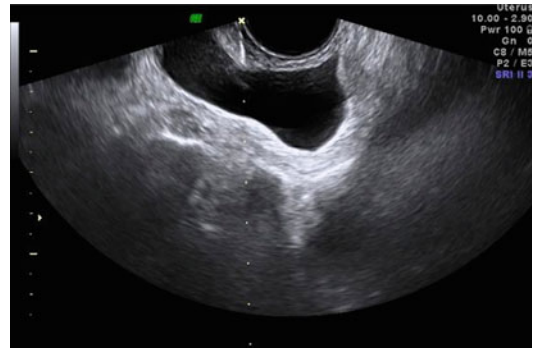

Fig. 21.3 Transvaginal aspiration of ascitic fluid in patient with ovarian hyperstimulation syndrome. Needle visualized along *dotted biopsy line*

double-lumen needle while direct aspiration can be performed using a single-lumen needle. Proponents of flushing contend that it increases oocyte yield and may be clinically significant in poor responders for whom even one additional oocyte may improve pregnancy potential. Waterstone and Parsons found a 20 % increase in oocyte yield in the first three flushes after direct aspiration in 50 patients for whom oocyte yield was quantified after direct aspiration, after 3 flushes, and after 6 flushes [57, 58]. However, a Cochrane review including four randomized trials with number of study participants ranging from 4 to 100 found no significant difference in oocyte yield or clinical pregnancy rates for flushed compared to directly aspirated follicles[58]. Flushing required statistically significant increased operative time and analgesia use [58].

After retrieval completion, assessment of hemostasis is essential. A survey of the pelvis with Doppler ultrasound before and after the retrieval should be performed to look for fluid pockets and for active sources of bleeding. If observed, focused bimanual pressure usually suffices to tamponade active bleeding. After abdominal hemostasis has been confirmed, a speculum should be placed in the vagina to inspect puncture sites. Bleeding vaginal sites also usually stop either with direct pressure, vaginal packing, application of an atraumatic clamp for focal direct pressure, or rarely with placement of a nonreactive vaginal suture.

Ovarian hyperstimulation is a complication of assisted reproductive technology (ART). Ascites results from increased vascular permeability. Paracentesis may decrease pain, shortness of breath, and oliguria [59]. Both transvaginal and transabdominal aspiration have been described under ultrasound guidance (see Fig. 21.3) [59].

Embryo Transfer

Ultrasound guidance has potential to play an integral part in IVF embryo transfer. Pregnancy rates may be affected by embryo transfer techniques in IVF. Embryo transfer techniques that have been demonstrated to have an effect on pregnancy outcome include type of catheter [60], trial transfer attempt prior to the IVF cycle [61], technique of catheter loading [62], time to withdraw catheter [63, 64], and atraumatic transfer [65]. Abdominal ultrasound guidance for embryo transfer has been evaluated by several investigators.

Embryos are loaded into a catheter with the placement marked by air bubbles. Under abdominal ultrasound guidance with a full bladder, the placement of the catheter can be confirmed and the air bubble visualized when injected into the uterus (see Fig. 21.4). Of note, the bladder should be filled to aid in visualization (to the fundus of the uterus) but not "overfilled" as excess distention, particularly for retroverted uteri, may hinder transfer ability and also result in significant patient discomfort. Embryo catheters with an echodense tip may improve visualization of the catheter [66]. However, the impact of ultrasound

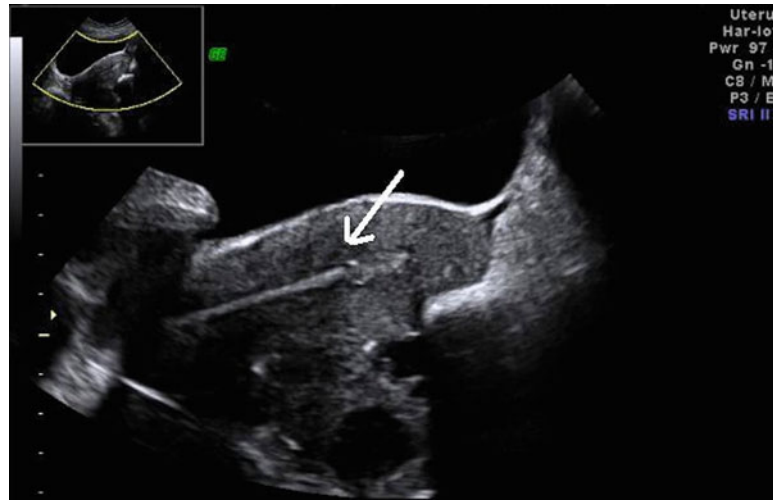

Fig. 21.4 Embryo transfer (*Arrow* denotes transfer catheter and air bubble containing embryos)

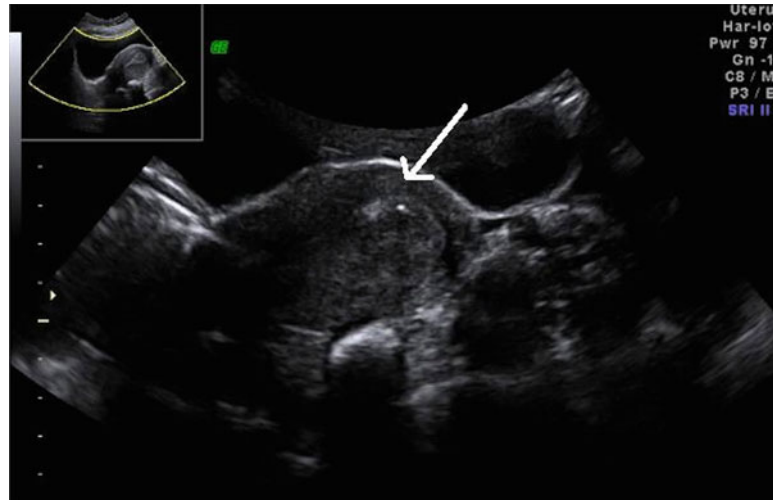

Fig. 21.5 Embryo transfer (*Arrow* denotes location of embryo-containing media)

on embryo placement was once controversial. In 1985, Strickler et al. reported ultrasound-guided embryo transfer in 16 patients. It was noted that the transfer catheter tip could be accurately positioned in the uterine cavity and ejection of the transfer media and air bubble could be documented [67] (see Fig. 21.5). Woolcott and Stranger suggest that blind tactile feedback is unreliable for ascertaining proper embryo placement [68]. They describe abnormal placement near the internal tubal ostia in 9 of 121 transfers of the embryo transfer catheter documented by ultrasound [68]. The authors suggest that ultrasound guidance may decrease ectopic pregnancy rate by avoiding transfer near the tubal ostia. Similarly, Hurley et al. found tactile feedback unreliable; they identified 19 of 94 cases of ultrasound-guided embryo transfer where the physician unknowingly misplaced the catheter (6 in the cervix, 12 in the lower uterine segment, and 1 in a false passage). However, they did not find a significant difference in implantation rate with and without ultrasound, 20.2 and 17.5 %, respectively [69]. A randomized controlled trial by Kan et al. also found no significant difference in implantation rate in the ultrasound-guided group (20.4 %) compared to the control (16.2 %) [70]. This study controlled for the pregnancy rate of the physician performing the procedure and day of the procedure (the control patient was

selected on the same day as the study patient). Although not significant, the implantation rate of difficult transfers was 54.5 % in the study group and 10.0 % in the control group [70]. This group suggested that ultrasound guidance may be useful in patients with difficult transfers. In contrast, Coroleu performed a randomized trial in 362 patients and found a significant difference in implantation rate: 25.3 % in the ultrasound-guided group compared to 18.1 % in the control group [71]. However, they failed to control for the pregnancy rate of the physician performing the procedure. In addition, the location of embryo transfer differed between the two groups. In the ultrasound-guided group, the embryos were transferred to within 1.5 cm of the fundus, while the control group had embryos transferred as close to the fundus as possible without touching. Coroleu et al. in 2002 prospectively randomized 180 consecutive patients to embryo transfer at 10 mm from the fundus, 15 mm from the fundus, and 20 mm from the fundus [72]. All groups were equal in regard to patient age, BMI, diagnosis, duration of infertility, number of embryos transferred, and the degree of difficulty with transfers. Implantation rates were 26 % if transferred 10 mm from the fundus, 31.3 % at 15 mm, and 33.3 % at 20 mm. The benefit of ultrasound guidance appears to occur by placing embryos in the thickest portion of endometrium at a distance of at least 15 mm from the fundus [72].

Additionally, it is generally well accepted that an easy, atraumatic bloodless transfer improves implantation rates [65]. Trauma and bleeding increase the likelihood of uterine contractions and increase embryo expulsion [73]. Blood on the tip of the embryo catheter has been associated with a six- to seven-fold decrease in clinical pregnancy rate [74].

A 2003 meta-analysis including eight randomized controlled trials revealed improved implantation (OR 1.39) and clinical pregnancy rates (OR 1.44) in the ultrasound compared to "clinical touch" groups [75]. The group attributes previously reported insignificance to lack of power [75]. These significant findings favoring ultrasound use were affirmed by a 2010 Cochrane review comparing ultrasound-guided versus "clinical touch" embryo transfer [76].

Although initially controversial, ultrasound guidance appears to play a beneficial role in embryo transfer. While the only disadvantages include the need for additional time, equipment, and skilled personnel, ultrasonography has the potential to aid in ideal embryo placement 15–20 mm from the fundus, to decrease uterine contractions, to increase the frequency of "easy" atraumatic transfers, and most important to improve implantation and pregnancy rates.

Intrauterine Device Placement and Removal

The intrauterine device (IUD) is one of the most effective forms of reversible contraception; the failure rate is 0.1–0.8 % in the first year of use and risk of complications such as perforation or expulsion is extremely low, 0–2 % and 2–3 %, respectively [77, 78]. Occasionally, a tortuous cervical canal may make insertion difficult. In such instances, using the aforementioned techniques to obtain visualization of the cervical path and uterine contour, transabdominal ultrasound can be used to help with difficult intrauterine device insertion. In addition, the use of misoprostol before the procedure may soften the cervix and make the procedure easier to perform [2]. Similarly, ultrasound can be used to confirm appropriate IUD placement and also can be used to help with device localization if IUD strings are not visible at time of desired removal (see Fig. 21.6). A role for ultrasound guidance has also been reported for immediate postpartum IUD placement at which time theoretical risk of uterine perforation or IUD expulsion is greater [79]. Routine transvaginal ultrasound use has not been shown to be beneficial at time of IUD insertion [80].

Conclusion

The use of ultrasonography at the time of intrauterine procedures provides visualization of the intrauterine instruments as well as the myometrium. Therefore, ultrasonographic guidance may decrease the risk of perforation and

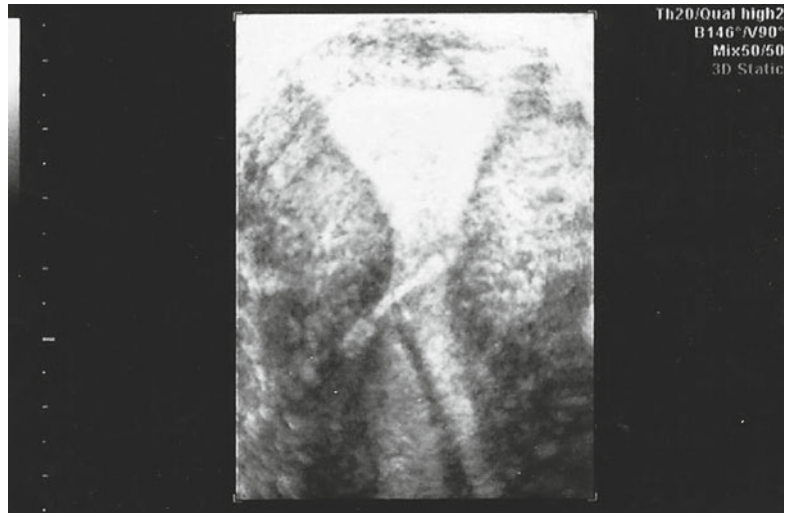

Fig. 21.6 Misplaced intrauterine device within the lower uterine segment (3D ultrasound image)

increase the chance of a successful procedure. As an alternative to laparoscopy, ultrasonographic guidance may also shorten procedure time, decrease cost, and eliminate the risk of an additional surgical procedure. Not all procedures require ultrasound guidance; however, for selected cases, ultrasonography provides valuable assistance in carrying out the surgical procedure successfully and with lower risk.

Ultrasonography also plays an integral role in assisted reproductive treatment; effective egg retrieval relies on ultrasonography and current literature suggests that ultrasound guidance at time of embryo transfer improves implantation and clinical pregnancy rates.

References

1. Session DR, et al. Ultrasound-guided fallopian tube cannulation using Albunex. Fertil Steril. 1997;67(5):972–4.
2. Christianson MS, Barker MA, Lindheim SR. Overcoming the challenging cervix: techniques to access the uterine cavity. J Low Genit Tract Dis. 2008;12(1):24–31.
3. Wu MH, Hsu CC, Lin YS. Three-dimensional ultrasound and hysteroscopy in the evaluation of intrauterine retained fetal bones. J Clin Ultrasound. 1997;25(2):93–5.
4. Shalev E, Zuckerman H. Operative hysteroscopy under real-time ultrasonography. Am J Obstet Gynecol. 1986;155(6):1360–1.
5. Grimbizis GF, et al. Clinical implications of uterine malformations and hysteroscopic treatment results. Hum Reprod Update. 2001;7(2):161–74.
6. Acien P. Incidence of Mullerian defects in fertile and infertile women. Hum Reprod. 1997;12(7):1372–6.
7. Homer HA, Li TC, Cooke ID. The septate uterus: a review of management and reproductive outcome. Fertil Steril. 2000;73(1):1–14.
8. Propst AM, Hill 3rd JA. Anatomic factors associated with recurrent pregnancy loss. Semin Reprod Med. 2000;18(4):341–50.
9. Selvaraj P, Selvaraj K. Reproductive outcome of septate uterus following hysteroscopic septum resection. J Hum Reprod Sci. 2010;3(3):143–5.
10. Kupesic S, Kurjak A. Septate uterus: detection and prediction of obstetrical complications by different forms of ultrasonography. J Ultrasound Med. 1998;17(10):631–6.
11. Daly DC, Maier D, Soto-Albors C. Hysteroscopic metroplasty: six years' experience. Obstet Gynecol. 1989;73(2):201–5.
12. Querleu D, Brasme TL, Parmentier D. Ultrasound-guided transcervical metroplasty. Fertil Steril. 1990;54(6):995–8.
13. Fedele L, et al. Residual uterine septum of less than 1 cm after hysteroscopic metroplasty does not impair reproductive outcome. Hum Reprod. 1996;11(4):727–9.
14. Dabirashrafi H, Moghadami-Tabrizi N. Establishing the accuracy of ultrasound-guided transcervical metroplasty. Fertil Steril. 1991;56(1):152–3.
15. Coccia ME, et al. Intraoperative ultrasound guidance for operative hysteroscopy. A prospective study. J Reprod Med. 2000;45(5):413–8.
16. Cook H, et al. The impact of uterine leiomyomas on reproductive outcomes. Minerva Ginecol. 2010;62(3):225–36.
17. Kresowik J, Syrop C, Van Voorhis B, Ryan G. Ultrasound is the optimal choice for guidance in difficult hysteroscopy. Ultrasound Obstet Gynecol. 2012;39:715–8.
18. Olive DL. The surgical treatment of fibroids for infertility. Semin Reprod Med. 2011;29(2):113–23.

19. Farhi J, et al. Induced regeneration of endometrium following curettage for abortion: a comparative study. Hum Reprod. 1993;8(7):1143–4.
20. Ramzy AM, et al. Uterine myomata and outcome of assisted reproduction. Hum Reprod. 1998;13(1):198–202.
21. Jun SH, et al. Uterine leiomyomas and their effect on in vitro fertilization outcome: a retrospective study. J Assist Reprod Genet. 2001;18(3):139–43.
22. Surrey ES, Lietz AK, Schoolcraft WB. Impact of intramural leiomyomata in patients with a normal endometrial cavity on in vitro fertilization-embryo transfer cycle outcome. Fertil Steril. 2001;75(2):405–10.
23. Lin CC, et al. Myomectomy through the uterine cervix using forceps under sonographic guidance. Ultrasound Obstet Gynecol. 2009;33(2):228–31.
24. Wortman M, Dagget A. Hysteroscopic myomectomy. J Am Assoc Gynecol Laparosc. 1995;3(1):39–46.
25. Shalev E, Shimoni Y, Peleg D. Ultrasound controlled operative hysteroscopy. J Am Coll Surg. 1994;179(1):70–1.
26. Myers EM, Hurst BS. Comprehensive management of severe Asherman syndrome and amenorrhea. Fertil Steril. 2012;97(1):160–4.
27. Orhue AA, Aziken ME, Igbefoh JO. A comparison of two adjunctive treatments for intrauterine adhesions following lysis. Int J Gynaecol Obstet. 2003;82(1):49–56.
28. Amer MI, Nadim EA, Karim H. The role of intrauterine balloon after operative hysteroscopy in the prevention of intrauterine adhesions; a prospective controlled study. Middle East Fertil Soc. 2005;10:135–9.
29. Pabuccu R, et al. Hysteroscopic treatment of intrauterine adhesions is safe and effective in the restoration of normal menstruation and fertility. Fertil Steril. 1997;68(6):1141–3.
30. Tsapanos VS, et al. The role of Seprafilm bioresorbable membrane in the prevention and therapy of endometrial synechiae. J Biomed Mater Res. 2002;63(1):10–4.
31. Acunzo G, et al. Effectiveness of auto-cross-linked hyaluronic acid gel in the prevention of intrauterine adhesions after hysteroscopic adhesiolysis: a prospective, randomized, controlled study. Hum Reprod. 2003;18(9):1918–21.
32. Letterie GS, Case KJ. Intraoperative ultrasound guidance for hysteroscopic retrieval of intrauterine foreign bodies. Surg Endosc. 1993;7(3):182–4.
33. Kohlenberg CF, Pardey J, Ellwood DA. Transabdominal ultrasound as an aid to advanced hysteroscopic surgery. Aust N Z J Obstet Gynaecol. 1994;34(4):462–4.
34. Goudas VT, Session DR. Hysteroscopic cervical cannulation under ultrasound guidance. A case report. J Reprod Med. 1998;43(8):696–8.
35. Dabirashrafi H, Mohamad K, Moghadami-Tabrizi N. Three-contrasts method hysteroscopy: the use of real-time ultrasonography for monitoring intrauterine operations. Fertil Steril. 1992;57(2):450–2.
36. Grimes DA, et al. Oral contraceptives for functional ovarian cysts. Cochrane Database Syst Rev. 2011;(9):CD006134.
37. Qublan HS, et al. Ovarian cyst formation following GnRH agonist administration in IVF cycles: incidence and impact. Hum Reprod. 2006;21(3):640–4.
38. Jenkins JM, et al. The detrimental influence of functional ovarian cysts during in-vitro fertilization cycles. Hum Reprod. 1992;7(6):776–80.
39. Firouzabadi RD, Sekhavat L, Javedani M. The effect of ovarian cyst aspiration on IVF treatment with GnRH. Arch Gynecol Obstet. 2010;281(3):545–9.
40. Rizk B, et al. Ovarian cyst aspiration and the outcome of in vitro fertilization. Fertil Steril. 1990;54(4):661–4.
41. Parinaud J, et al. Influence of ovarian cysts on the results of in vitro fertilization. Fertil Steril. 1992;58(6):1174–7.
42. Tarlatzis BC, et al. Follicle cyst formation after administration of different gonadotrophin-releasing hormone analogues for assisted reproduction. Hum Reprod. 1994;9(11):1983–6.
43. Greenebaum E, et al. Aspiration cytology of ovarian cysts in in vitro fertilization patients. Acta Cytol. 1992;36(1):11–8.
44. Hurst BS, et al. Hydrosalpinx treated with extended doxycycline does not compromise the success of in vitro fertilization. Fertil Steril. 2001;75(5):1017–9.
45. Van Voorhis BJ, et al. Ultrasound-guided aspiration of hydrosalpinges is associated with improved pregnancy and implantation rates after in-vitro fertilization cycles. Hum Reprod. 1998;13(3):736–9.
46. Vandromme J, et al. Hydrosalpinges in in-vitro fertilization: an unfavourable prognostic feature. Hum Reprod. 1995;10(3):576–9.
47. Osuga Y, et al. A case of hydrosalpinx associated with the menstrual cycle. Fertil Steril. 2008;90(1):199.e9-11.
48. Sowter MC, et al. Is the outcome of in-vitro fertilization and embryo transfer treatment improved by spontaneous or surgical drainage of a hydrosalpinx? Hum Reprod. 1997;12(10):2147–50.
49. de Wit W, et al. Only hydrosalpinges visible on ultrasound are associated with reduced implantation and pregnancy rates after in-vitro fertilization. Hum Reprod. 1998;13(6):1696–701.
50. Lenz S, Lauritsen JG, Kjellow M. Collection of human oocytes for in vitro fertilisation by ultrasonically guided follicular puncture. Lancet. 1981;1(8230):1163–4.
51. Barton SE, et al. Transabdominal follicular aspiration for oocyte retrieval in patients with ovaries inaccessible by transvaginal ultrasound. Fertil Steril. 2011;95(5):1773–6.
52. Gleicher N, et al. EGG retrieval for in vitro fertilisation by sonographically controlled vaginal culdocentesis. Lancet. 1983;2(8348):508–9.
53. Damario MA. Transabdominal-transperitoneal ultrasound-guided oocyte retrieval in a patient with mullerian agenesis. Fertil Steril. 2002;78(1):189–91.
54. Weinerman R, Grifo J. Consequences of superovulation and ART procedures. Semin Reprod Med. 2012;30(2):77–83.
55. Moini A, et al. Endometriosis may contribute to oocyte retrieval-induced pelvic inflammatory disease:

report of eight cases. J Assist Reprod Genet. 2005; 22(7–8):307–9.
56. Kroon B, et al. Antibiotics prior to embryo transfer in ART. Cochrane Database Syst Rev. 2012;3:CD008995.
57. Waterstone JJ, Parsons JH. A prospective study to investigate the value of flushing follicles during transvaginal ultrasound-directed follicle aspiration. Fertil Steril. 1992;57(1):221–3.
58. Wongtra-Ngan S, Vutyavanich T, Brown J. Follicular flushing during oocyte retrieval in assisted reproductive techniques. Cochrane Database Syst Rev. 2010; (9):CD004634.
59. The Practice Committee of the American Society for Reproductive Medicine. Ovarian hyperstimulation syndrome. 2008. ASRM, Birmingham.
60. Penzias AS, Harris D, Barrett CB, Alper MM, Berger MJ, Oskowitz SP. Outcome oriented research in an IVF program: transfer catheter type affects IVF outcome. Cincinnati: ASRM; 1997.
61. Mansour R, Aboulghar M, Serour G. Dummy embryo transfer: a technique that minimizes the problems of embryo transfer and improves the pregnancy rate in human in vitro fertilization. Fertil Steril. 1990;54(4): 678–81.
62. Poindexter 3rd AN, et al. Residual embryos in failed embryo transfer. Fertil Steril. 1986;46(2):262–7.
63. Leong M, et al. Ultrasound-assisted embryo transfer. J In Vitro Fert Embryo Transf. 1986;3(6):383–5.
64. Martinez F, et al. Ultrasound-guided embryo transfer: immediate withdrawal of the catheter versus a 30 second wait. Hum Reprod. 2001;16(5):871–4.
65. Matorras R, et al. Ultrasound-guided embryo transfer improves pregnancy rates and increases the frequency of easy transfers. Hum Reprod. 2002;17(7):1762–6.
66. Letterie GS, Marshall L, Angle M. A new coaxial catheter system with an echodense tip for ultrasonographically guided embryo transfer. Fertil Steril. 1999;72(2):266–8.
67. Strickler RC, et al. Ultrasound guidance for human embryo transfer. Fertil Steril. 1985;43(1):54–61.
68. Woolcott R, Stanger J. Potentially important variables identified by transvaginal ultrasound-guided embryo transfer. Hum Reprod. 1997;12(5):963–6.
69. Hurley VA, et al. Ultrasound-guided embryo transfer: a controlled trial. Fertil Steril. 1991;55(3):559–62.
70. Kan AK, et al. Embryo transfer: ultrasound-guided versus clinical touch. Hum Reprod. 1999;14(5):1259–61.
71. Coroleu B, et al. The usefulness of ultrasound guidance in frozen-thawed embryo transfer: a prospective randomized clinical trial. Hum Reprod. 2002; 17(11):2885–90.
72. Coroleu B, et al. The influence of the depth of embryo replacement into the uterine cavity on implantation rates after IVF: a controlled, ultrasound-guided study. Hum Reprod. 2002;17(2):341–6.
73. Lesny P, et al. Embryo transfer–can we learn anything new from the observation of junctional zone contractions? Hum Reprod. 1998;13(6):1540–6.
74. Goudas VT, et al. Blood on the embryo transfer catheter is associated with decreased rates of embryo implantation and clinical pregnancy with the use of in vitro fertilization-embryo transfer. Fertil Steril. 1998;70(5):878–82.
75. Buckett WM. A meta-analysis of ultrasound-guided versus clinical touch embryo transfer. Fertil Steril. 2003;80(4):1037–41.
76. Brown J, et al. Ultrasound versus 'clinical touch' for catheter guidance during embryo transfer in women. Cochrane Database Syst Rev. 2010;(1): CD006107.
77. Trussell J, Vaughan B. Contraceptive failure, method-related discontinuation and resumption of use: results from the 1995 National Survey of Family Growth. Fam Plann Perspect. 1999;31(2):64–72, 93.
78. Kaislasuo J, et al. Intrauterine contraception: incidence and factors associated with uterine perforation–a population-based study. Hum Reprod. 2012;27(9): 2658–63.
79. Hayes JL, et al. A pilot clinical trial of ultrasound-guided postplacental insertion of a levonorgestrel intrauterine device. Contraception. 2007;76(4): 292–6.
80. de Kroon CD, et al. The value of transvaginal ultrasound to monitor the position of an intrauterine device after insertion. A technology assessment study. Hum Reprod. 2003;18(11):2323–7.

Ultrasound Role in Embryo Transfers

22

Edmond Confino, Roohi Jeelani, and Ilan Tur-Kaspa

Introduction

High-resolution high-frequency transvaginal US (TVUS) has become an integral part of infertility evaluation, follicular growth monitoring during controlled ovarian hyperstimulation (COH), as well as the method of choice to achieve an efficient and rapid oocyte harvesting [1, 2]. ET is a more difficult procedure to master than oocyte retrieval [3]. Strickler et al. [4] was the first to describe in 1985 the use of US to guide an embryo transfer (ET). Since then, TVUS and mainly abdominal US have gradually been added to achieve an atraumatic, controlled, quick, and anatomically defined ET [4, 5]. Accurate knowledge of the uterine depth and cervical trajectory has always been regarded as a mandatory requirement to achieve high pregnancy rates (PR) [6]. While today US is routinely used for it, pre-IVF evaluation of the uterine and cervical anatomy was described by using HSG, and even MRI and/or CT scan (Figs. 22.1 and 22.2). The performance of "trial ET" has emerged as a rather poor predictor of the real ET [7, 8]. US availability and ease of performance has made sonohysterography (SHG) (see Chap. 13) the preferred and cost-effective visualization method of the uterus prior to ET [9, 10]. Pre-ET US measurement of the cervical uterine depth verifies the mock transfer data, but still is a poor predictor of ET success (Fig. 22.3). Recent several RCTs and meta-analyses concluded that compared to clinical touch, US guidance significantly increased clinical pregnancy rate and chance of a live birth of IVF treatment [11–14]. There is increase in easy transfer rates after ultrasound guidance. US-guided ET

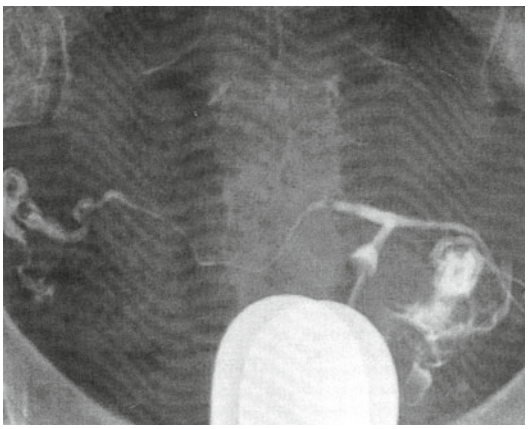

Fig. 22.1 A short, thin-lumen, T-shaped uterus. Saline 3D US may replace the radiologic hysterography in similar cases. 2D US may be difficult to measure and interpret because of thin lumen cavity

E. Confino, MD (✉)
Repro/Endo, Infertility, Feinberg School of Medicine, Northwestern University, 675 N. St. Clair St., Chicago, IL 60611, USA
e-mail: e-confino@northwestern.edu

R. Jeelani, MD
Department of Obstetrics and Gynecology, Wayne State University, Detroit, MI, USA

I. Tur-Kaspa, MD
Institute for Human Reproduction (IHR), Department of Obstetrics and Gynecology, The University of Chicago, 409 W. Huron St., Chicago, IL 60654, USA
e-mail: drtk@infertilityihr.com

L.A. Stadtmauer, I. Tur-Kaspa (eds.), *Ultrasound Imaging in Reproductive Medicine*,
DOI 10.1007/978-1-4614-9182-8_22,

does not reduce ectopic pregnancy or miscarriage rates. This chapter will review the data available today on the important role of US in ET.

Tactile ET Versus Ultrasound-Guided ET

The optimal area of embryo deposition in the uterine cavity is probably 1–1.5 cm from the fundus resulting in higher PR [15, 16]. Evidence-based data demonstrated that US-guided ET will result in easier ETs and significantly improve ART outcome [11–14]. These RCTs and meta-analysis compared the main outcomes of clinical touch ETs versus ultrasound-guided ETs: implantation, clinical pregnancies, and live birth rates. In addition, other parameters were investigated: miscarriage rate, multiple and ectopic pregnancies rate, difficult or failed transfers, the need for instrumental assistance during the transfer (e.g., stylette, tenaculum, dilatation), signs of cervical or endometrial trauma (e.g., presence of blood, mucus, or both), and percentage of retained embryos. While few studies have found no significance in ART outcomes, most RCTs and the meta-analysis concluded that ultrasound guidance improves the chances of clinical pregnancies and live birth compared to the clinical touch method. A recent analysis showed that blood on the catheter is associated with decreased implantation rates, clinical pregnancy rates, and live birth rates when compared to no blood, which is easier to attain when performing US-guided ET [17]. Furthermore, it increases the ease of transfer rate and significantly decreases the chance of a difficult transfer [18], the need for instrumental assistance, and the failure to transfer with the assigned catheter. The incidence of finding blood on the catheter tips after US-guided ET was significantly lower. Adding ultrasound had no significant effect

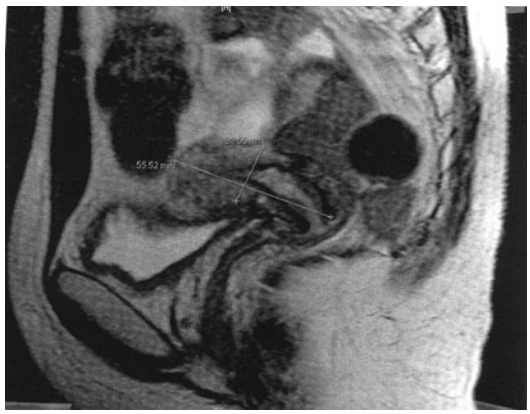

Fig. 22.2 A very anteverted 3 cm deep uterine cavity depicted on MRI. A skilled vaginal US may replace the MRI and result in a significant cost savings

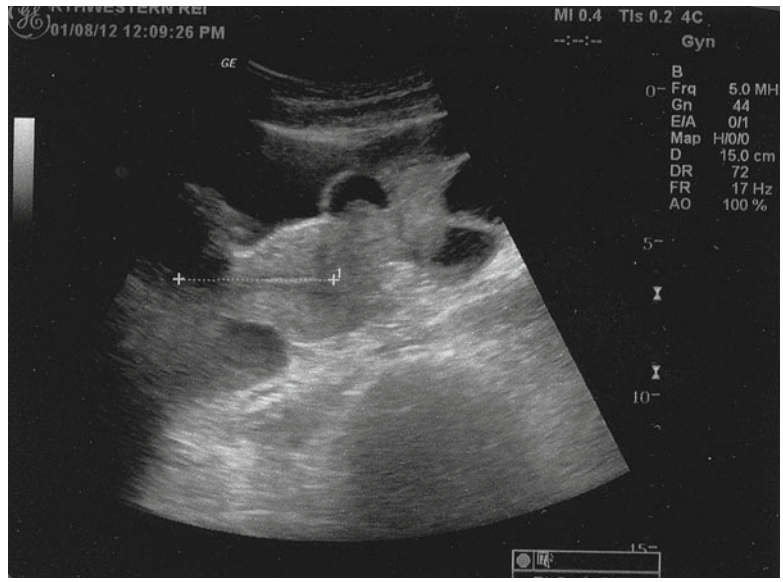

Fig. 22.3 Pre-ET vaginal US measurement of cervical-fundal distance allows accurate ET catheter placement

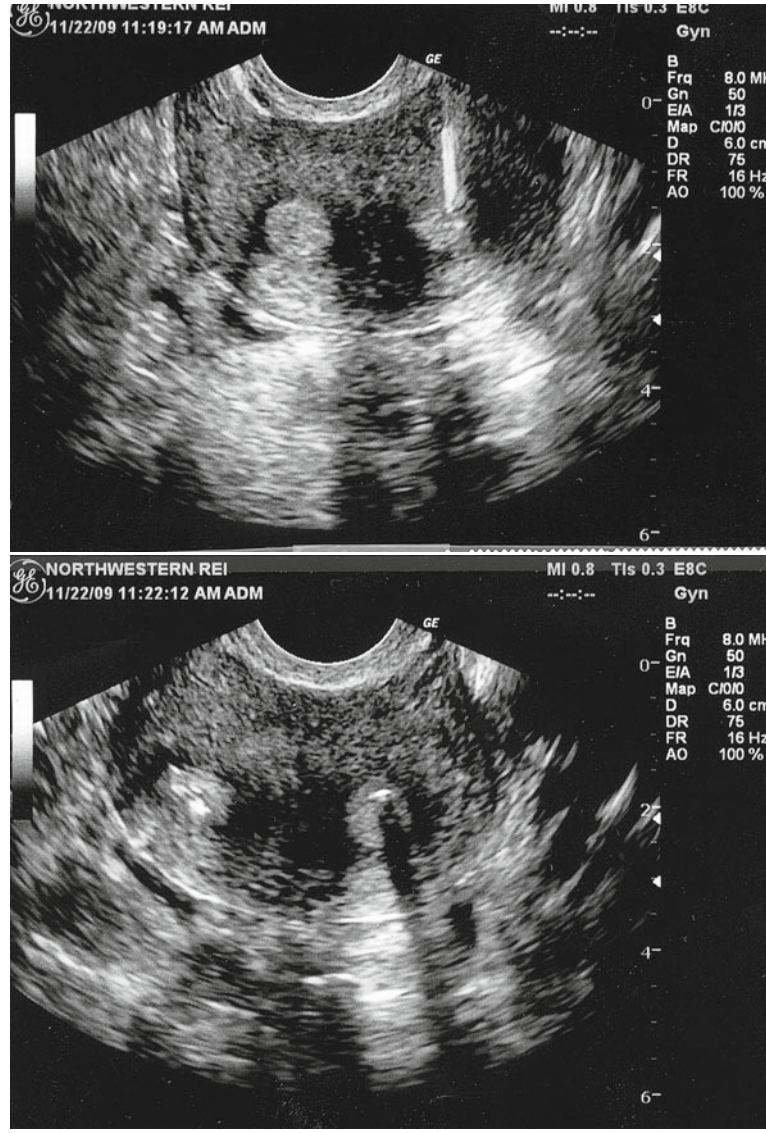

Fig. 22.4 Vaginal US-guided transmyometrial needle placement in a partially fused bicornuate uterus (*upper figure right*). Bubble markers are present in both right and left uterine horns depicting proper bilateral placement of one embryo in each uterine cavity (*lower figure*)

on finding mucus on the catheter tips, percentage of transfer with retained embryos, and the rate of multiple pregnancies, ectopic pregnancies, and spontaneous miscarriages.

Routine US use before, during, and post-ET has largely eliminated the discordance between mock ET and live ET [19]. US guidance has reduced unrecognized events such as 180° curling of the inner catheter and cervical deposition of the embryos. US prevents inadvertent embryo injection into the fallopian tube and directly into the uterine wall.

US-guided transmyometrial ET (Fig. 22.4) can be easily performed in the rare occasion when catheter access into the uterus is impossible [20, 21]. This alternative US-guided approach eliminates an unplanned laparoscopic intratubal ET. This technique is usually performed under conscious sedation using a coaxial needle outfitted with a matching ET catheter.

There are several mechanisms by which ultrasound-guided ET may improve ART outcome. The full bladder needed for transabdominal US straightens the angle between the cervix

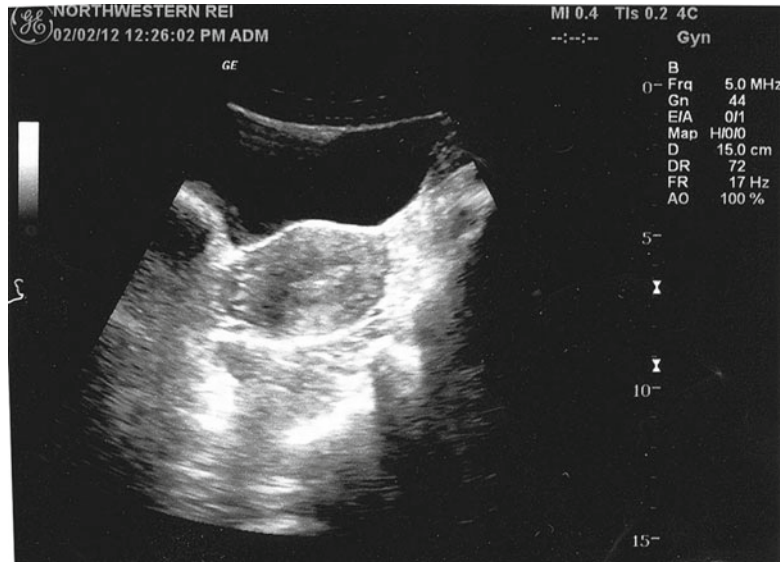

Fig. 22.5 Abdominal US with full bladder depicts two marker bubbles visualized in mid uterine cavity and confirming a perfect placement of embryos

and the uterus. Avoiding endometrial indentation and uterine contractions as well as confirming the position of the tip of the catheter at the desirable site for embryo deposition seems to be the predominant mechanism by which US guidance improves ART outcomes.

Transvaginal Versus Transabdominal Ultrasound for ET

Transabdominal ultrasound in ET has been the most commonly reported form of US guidance for ET. Typically during such an US, the patient needs to have a full bladder. The full bladder is needed for the transabdominal visualization of the endometrial canal and it will also straighten the uterocervical angle, which is one of the main benefits of a full bladder. This in turn will make the transfer easier. However, this may cause additional cramping and discomfort during the ET to the patient, which may have an impact on clinical PR and increase times, as physicians may need for the bladder to fill and distend. A transvaginal US does not cause such issues, but does come with its own difficulties. Although it may give a better visualization of the uterocervical angle and clearly delineate the catheter tip, it is technically more difficult to perform. It needs to be placed in the vagina, in addition to a speculum and catheter for ET. Several RCTs demonstrated no difference in overall pregnancy, live birth, or implantation rate when comparing a transabdominal to transvaginal US [22, 23]. While the duration of the procedure is significantly longer with the TVUS, it was associated with increased patient comfort due to the absence of bladder distension [23].

Training in Embryo Transfer

Pregnancy rates have been shown to vary between different physicians performing ET, even at the same practice [24]. US-guided intrauterine inseminations (IUIs) have been used to train fellows in reproductive medicine before allowing them to perform a live ET. Live US ET guidance minimizes the potential complication of myometrial contractions. The post-ET marker bubbles visualized on US verify mid-cavity embryo placement (Fig. 22.5). The physician, the patient, and the spouse observing the marker bubbles are instantly reassured of proper embryo placement. The extent of post-ET embryo migration in the uterus is still unclear [25, 26]. Shah et al. [27] recently demonstrated that the most important

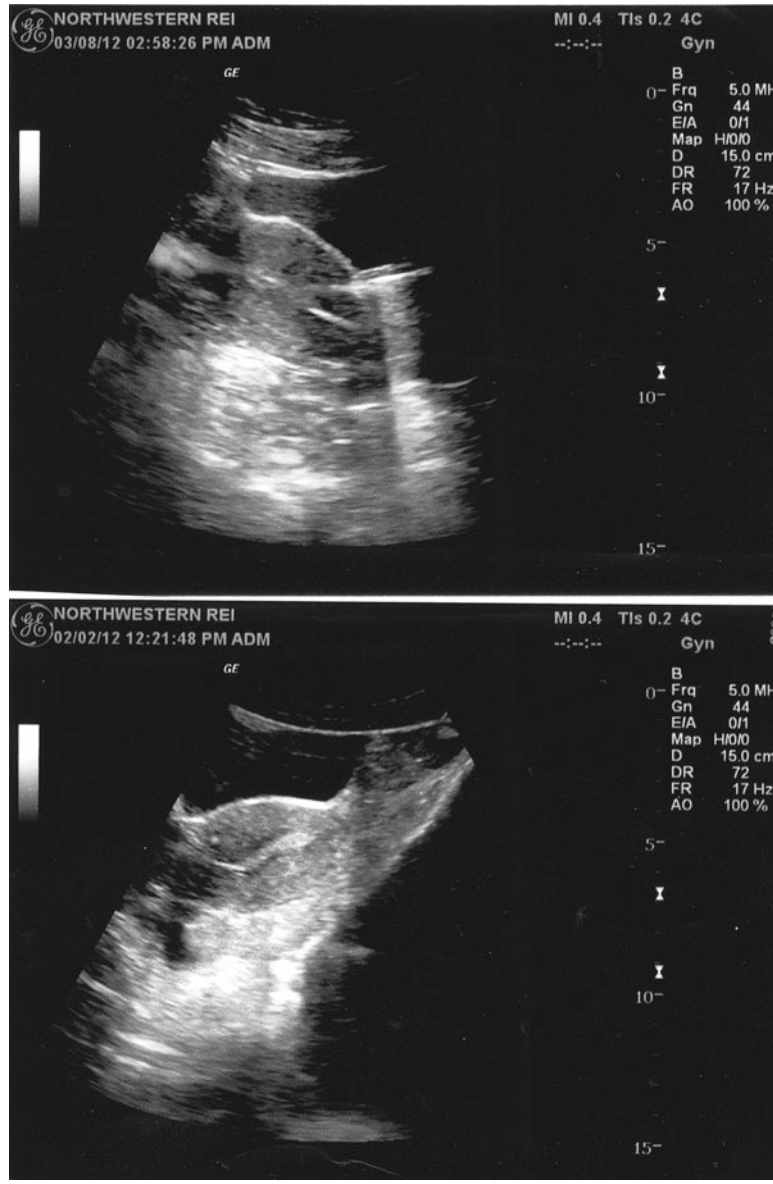

Fig. 22.6 Abdominal US depicts the external coaxial catheter wedged into the endometrium in an anteverted uterus (*lower figure*). Sliding a rehearsal inner catheter allows proper placement in the lower uterine segment (*upper figure*)

factor in obtaining high ET success rates was the actual performance of live ETs rather than practicing US-guided IUIs. Thus, how training in embryo transfer should be performed remains a controversy [3].

Coaxial catheter US-guided ET approach involves initial placement of an outer catheter in the internal uterine os (Fig. 22.6). The outer catheter protects the inner catheter from mucus exposure and eliminates the need to renegotiate a deviated or a branching cervical canal. In this instance, time is not a limiting factor because the embryos are loaded into the inner catheter while the outer catheter is already in place. US will then allow ET time to be less than 30 s (Fig. 22.7). US guidance is extremely instructive at training facilities as it can provide feedback and reassurance to physicians in training. Coaxial live US guided ET allows teaching ET without a decline in the center's PR.

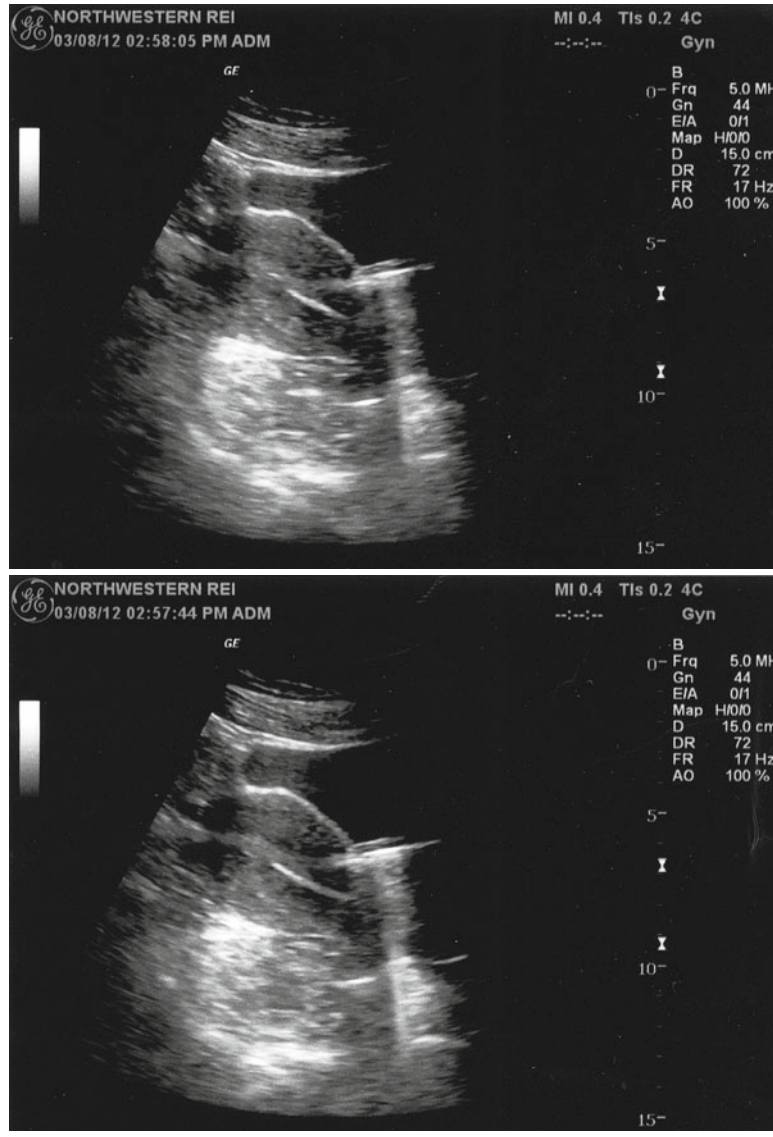

Fig. 22.7 Abdominal US demonstrates that the outer coaxial catheter is withdrawn leaving the inner soft embryo-loaded catheter at one cm from the uterine fundus (*lower figure*). Under live US observation, the embryo is injected and the marker bubble is observed in mid-cavity (*upper figure*)

Disadvantages of Ultrasound-Guided ET

When using US for ET, there is a significant increase in the time and space needed. It is obvious that US equipment and trained US personnel are needed. Cross-training of the existing IVF staff to provide US guidance eliminates the need for an additional US technician. The clinical experience of the ultrasonographer assisting US-guided ET had no effect on the clinical outcome [28]. Because of the full bladder required for transabdominal US, patients may suffer from discomfort and cramping. Emptying the bladder after ET may cause concern of losing embryos at that time. This psychological stress may be resolved with reassurance that the embryo will not "pop out" with urination.

Some physicians prefer tactile ET to minimize the need to observe the cervix and the US screen simultaneously and avoid the need for additional personnel. They also state that the use of US technique may slow the ET and require additional steps. Pre-ET vaginal ultrasound may be

performed to reassess the cervix and uterus (Fig. 22.3). Pre-ET US may measure the endometrial lining, detect the presence of fluid in the endometrial cavity, and retrace on the screen the measurement of the desired depth to achieve the ideal ET. However, a recent RCT involving single physician operator confirmed that US guidance significantly increased clinical pregnancies and live birth rates compared to the clinical touch method [29].

Conclusion

Evidence-based guidelines encourage US-guided ET. This approach will result in easier ETs and better PRs. Difficult, long, and bloody ET should be avoided. Recommendations based on expert opinions include the performance of a mock ET to identify a difficult ET, meticulous cervical mucus removal, mid uterine cavity embryo placement, a slow catheter withdrawal to avoid embryo dragging to the cervix, and a short embryo load to unload time [30, 31].

US has become an indispensable tool used to prepare the patient for the upcoming ET and monitor, guide, and verify proper embryo deposition in the uterus. Importantly, patients take great comfort in having the ability to visualize the final step of a difficult process. The use of US guidance is an integral part of a perfect ET and is only expanding to improve and may include 3D and 4D ultrasound.

References

1. Tarlatzis BC, Laufer N, Decherney AH. The use of ovarian ultrasonography in monitoring ovulation induction. J In Vitro Fert Embryo Transf. 1984;1:226–32.
2. Peluso JJ, Damien M, Nulsen JC, Luciano AA. Identification of follicles with fertilizable oocytes by sequential ultrasound measurements during follicular development. J In Vitro Fert Embryo Transf. 1990;7:304–9.
3. Bishop L, Brezina PR, Segars J. Training in embryo transfer: how should it be done? Fertil Steril. 2013;100(2):351–2.
4. Strickler RC, Christianson C, Crane JP, Curato A, Knight AB, Yang V. Ultrasound guidance for human embryo transfer. Fertil Steril. 1985;43:54–61.
5. Sallam HN, Sadek SS. Ultrasound-guided embryo transfer: a meta-analysis of randomized controlled trials. Fertil Steril. 2003;80:1042–6.
6. Matorras R, Urquijo E, Mendoza R, Corcostegui B, Exposito A, Rodriguez-Escudero FJ. Ultrasound-guided embryo transfer improves pregnancy rates and increases the frequency of easy transfers. Hum Reprod. 2002;17:1762–6.
7. Yoldemir T, Erenus M. Does the timing of mock embryo transfer trial improve implantation in intracytoplasmic sperm injection cycles? Gynecol Endocrinol. 2011;27:396–400.
8. Mansour R, Aboulghar M, Serour G. Dummy embryo transfer: a technique that minimizes the problems of embryo transfer and improves the pregnancy rate in human in vitro fertilization. Fertil Steril. 1990;54:678–81.
9. Gera PS, Allemand MC, Tatpati LL, Galanits TM, Morbeck D, Coddington CC. Role of saline infusion sonography in uterine evaluation before frozen embryo transfer cycle. Fertil Steril. 2008;89:562–6.
10. Sankpal RS, Confino E, Matzel A, Cohen LS. Investigation of the uterine cavity and fallopian tubes using three-dimensional saline sonohysterosalpingography. Int J Gynaecol Obstet. 2001;73:125–9.
11. Abou-Setta AM, Mansour RT, Al-Inany HG, Aboulghar MM, Aboulghar MA, Serour GI. Among women undergoing embryo transfer, is the probability of pregnancy and live birth improved with ultrasound guidance over clinical touch alone? A systemic review and meta-analysis of prospective randomized trials. Fertil Steril. 2007;88:333–41.
12. Brown JA, Buckingham K, Abou-Setta A, Buckett W. Ultrasound versus 'clinical touch' for catheter guidance during embryo transfer in women. Cochrane Database Syst Rev. 2007;24(1):CD006107.
13. Brown J, Buckingham K, Abou-Setta AM, Buckett W. Ultrasound versus 'clinical touch' for catheter guidance during embryo transfer in women. Cochrane Database Syst Rev. 2010;(1):CD006107.
14. Flisser E, Grifo JA. Is what we clearly see really so obvious? Ultrasonography and transcervical embryo transfer–a review. Fertil Steril. 2007;87:1–5.
15. Pope CS, Cook EK, Arny M, Novak A, Grow DR. Influence of embryo transfer depth on in vitro fertilization and embryo transfer outcomes. Fertil Steril. 2004;81:51–8.
16. Frankfurter D, Trimarchi JB, Silva CP, Keefe DL. Middle to lower uterine segment embryo transfer improves implantation and pregnancy rates compared with fundal embryo transfer. Fertil Steril. 2004;81:1273–7.
17. Tiras B, Korucuoglu U, Polat M, Saltik A, Zeyneloglu HB, Yarali H. Effect of blood and mucus on the success rates of embryo transfers. Eur J Obstet, Gynecol Reprod Biol. 2012;165:239–42.
18. Allahbadia GN, Kadam K, Gandhi G, Arora S, Valliappan JB, Joshi A, et al. Embryo transfer using the SureView catheter-beacon in the womb. Fertil Steril. 2010;93:344–50.

19. Henne MB, Milki AA. Uterine position at real embryo transfer compared with mock embryo transfer. Hum Reprod. 2004;19:570–2.
20. Kato O, Takatsuka R, Asch RH. Transvaginal-transmyometrial embryo transfer: the Towako method; experiences of 104 cases. Fertil Steril. 1993;59:51–3.
21. Groutz A, Lessing JB, Wolf Y, Azem F, Yovel I, Amit A. Comparison of transmyometrial and transcervical embryo transfer in patients with previously failed in vitro fertilization-embryo transfer cycles and/or cervical stenosis. Fertil Steril. 1997;67:1073–6.
22. Porat N, Boehnlein LM, Schouweiler CM, Kang J, Lindheim SR. Interim analysis of a randomized clinical trial comparing abdominal versus transvaginal ultrasound-guided embryo transfer. J Obstet Gynaecol Res. 2010;36:384–92.
23. Bodri D, Colodron M, Garcia D, Obradors A, Vernaeve V, Coll O. Transvaginal versus transabdominal ultrasound guidance for embryo transfer in donor oocyte recipients: a randomized clinical trial. Fertil Steril. 2011;95:2263–8, 8e1.
24. Karande VC, Morris R, Chapman C, Rinehart J, Gleicher N. Impact of the "physician factor" on pregnancy rates in a large assisted reproductive technology program: do too many cooks spoil the broth? Fertil Steril. 1999;71:1001–9.
25. Woolcott R, Stanger J. Ultrasound tracking of the movement of embryo-associated air bubbles on standing after transfer. Hum Reprod. 1998;13:2107–9.
26. Confino E, Zhang J, Risquez F. Air bubble migration is a random event post embryo transfer. J Assist Reprod Genet. 2007;24:223–6.
27. Shah DK, Missmer SA, Correia KF, Racowsky C, Ginsburg E. Efficacy of intrauterine inseminations as a training modality for performing embryo transfer in reproductive endocrinology and infertility fellowship programs. Fertil Steril. 2013;100:386–91.
28. Harris ID, Styer AK, Petrozza JC. Ultrasonographer experience does not impact outcomes following ultrasound-guided embryo transfer. Fertil Steril. 2009;92:918–22.
29. Eskandar M, Abou-Setta AM, Almushait MA, El-Amin M, Mohmad SE. Ultrasound guidance during embryo transfer: a prospective, single-operator, randomized, controlled trial. Fertil Steril. 2008;90:1187–90.
30. Ebner T, Yaman C, Moser M, Sommergruber M, Polz W, Tews G. The ineffective loading process of the embryo transfer catheter alters implantation and pregnancy rates. Fertil Steril. 2001;76:630–2.
31. Mains L, Van Voorhis BJ. Optimizing the technique of embryo transfer. Fertil Steril. 2010;94:785–90.

Ultrasound and Ovarian Hyperstimulation Syndrome

23

Laura Proud Smith

Ultrasound in the Prediction of Ovarian Hyperstimulation Syndrome

Because ovarian hyperstimulation syndrome (OHSS) is one of the most severe iatrogenic complications of in vitro fertilization (IVF), there have been many attempts to predict which patients are most at risk. Unfortunately, there are no perfectly reliable tests which universally predict the development of OHSS. Ultrasound determination of antral follicle count, counting the number of follicles developing in response to controlled ovarian hyperstimulation, sonographic evidence of polycystic ovarian syndrome, assessment of ovarian volume, and Doppler flow studies of ovarian vasculature have all been evaluated as markers to identify a higher likelihood of developing OHSS.

Among the sonographic tools used in the prediction of OHSS, quantitation of the antral follicle count (AFC) is one of the most accurate tests. Antral follicles are 2–10 mm follicles which can be identified by ultrasound in the early follicular phase. Antral follicles appear as round, sonolucent structures scattered throughout the ovary when viewed by 2D transvaginal ultrasound (Fig. 23.1). The size of the antral follicle pool is considered to reflect the total number of remaining follicles [1]. Generally, a low antral follicle count suggests a poor response to ovarian stimulation and a high antral follicle count suggests better ovarian response to gonadotropin stimulation and higher oocyte yield.

Several investigators have evaluated AFC to predict the development of OHSS. Kwee et al. evaluated 110 patients with unexplained infertility, male factor, or cervical factor infertility, counted antral follicles in all patients, and correlated the number of antral follicles with level of ovarian response to IVF [2]. They categorized ovarian response as poor, normal, and high and then calculated the AFC cutoff which most accurately identified each group. The AFC value of >14 identified hyper-responders with a sensitivity of 82 % and a specificity of 89 %. Oncal et al. also evaluated the predictive role of AFC in OHSS in 41 women identified to have moderate to severe OHSS and 41 age-matched controls who did not develop OHSS [3]. They found that AFC had a moderate accuracy to predict the development of OHSS. Using an AFC cutoff of eight, much lower than the AFC cutoff used by Kwee et al., they calculated 78 % sensitivity and 65 % specificity. In a meta-analysis done by Broer et al. investigating AFC as a predictor of ovarian hyperstimulation, five studies were identified which met criteria for inclusion [4]. Two reported on AFC alone, three reported on both anti-Mullerian hormone (AMH) and AFC, and all five were prospective cohort studies. Among the included studies, the definition of excessive

L.P. Smith, MD
Department of Reproductive Endocrinology and Infertility, Reproductive Medicine and Surgery Center of Virginia, P.L.C, 595 Martha Jefferson Drive, Suite 390, Charlottesville, VA 22902, USA
e-mail: laura.smith@rmscva.com

L.A. Stadtmauer, I. Tur-Kaspa (eds.), *Ultrasound Imaging in Reproductive Medicine*,
DOI 10.1007/978-1-4614-9182-8_23, © Springer Science+Business Media New York 2014

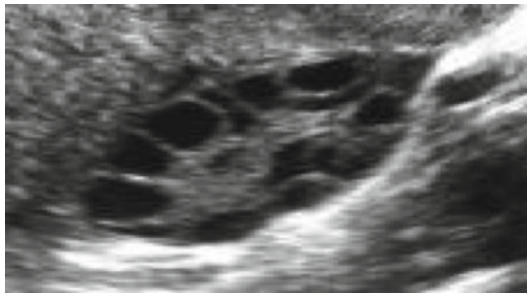

Fig. 23.1 Ovary with normal antral follicle count

ovarian response to IVF varied between ≥15 and ≥20 oocytes. Importantly, the number of oocytes retrieved was used as a surrogate for risk of OHSS; no study specifically identified the patients who met diagnostic criteria for OHSS. When these five studies of AFC were evaluated together, the sensitivity of AFC to predict ovarian hyper-response was seen to vary between 20 and 94 % depending on the AFC cutoff used, and the specificity varied between 33 and 98 %. From these values, the authors calculated a sum estimate of the sensitivity to be 82 % and a sum estimate of the specificity to be 80 %. Considering this evidence, there is a clear association between increased AFC and increased risk of OHSS. Given the sensitivity and specificity estimates of AFC in the studies to date, if the AFC is found to be greater than 14–16, caution should be executed in the initial gonadotropin dosing and choice of stimulation protocol since there is clearly increased risk of ovarian hyper-response in such patients.

When proposing the use of AFC to predict OHSS, it is important to be aware of the variability both in definition of antral follicle and operator technique in follicle counting [5]. Interestingly, some authors adhere to the definition of antral follicle as those follicles which are measured to be 2–10 mm in the early follicular phase, as above; but other authors limit that definition to only those follicles which measure 2–5 mm. The precise menstrual timing of the measurement of AFC is also important. AFC should be performed either between cycle day 2 and 4 or while on oral contraceptive pills for greatest accuracy and reproducibility.

The number of growing follicles in response to gonadotropin stimulation during ART is another sonographic test which has been proposed to predict the development of OHSS. Clearly, there is a connection between the ovarian response to stimulation and AFC, as patients with higher baseline AFC would be expected to have a more robust ovarian response to treatment. Papanikolaou et al. sought to correlate the number of follicles ≥11 mm growing in response to gonadotropin treatment during IVF with the likelihood of developing moderate or severe ovarian hyperstimulation syndrome [6]. They evaluated 1,801 patients undergoing IVF treatment over a 2-year period. Factors such as peak estradiol level and number of follicles ≥11 mm were correlated with the development of OHSS. In this cohort, 53 patients were hospitalized because of OHSS. They found that a threshold of ≥13 follicles measuring ≥11 mm was predictive of the development of OHSS with a sensitivity of 85.5 % and a specificity of 69 %. Interestingly, the number of follicles ≥11 mm was a much better predictor of OHSS than the peak serum estradiol level, which had only a 53 % sensitivity and 77 % specificity. Therefore, if it becomes apparent during an IVF cycle that there are 13 or more follicles measuring ≥11 mm, the patient and physician should both be cognizant of the increased risk of developing OHSS regardless of the serum estradiol level.

Because patients who have higher baseline AFC and higher functional ovarian response to stimulation have been found to have a greater likelihood of developing OHSS, it is important to identify such patients early in clinical care. It is well known that patients with polycystic ovarian syndrome (PCOS) have by definition a high antral follicle count and magnified response to IVF. Ultrasound assessment of ovarian morphology serves as one of the key criteria for the diagnosis of PCOS by the Rotterdam criteria [7]. The sonographic findings which meet Rotterdam diagnostic criteria are either 12 or more follicles in each ovary measuring 2–9 mm in diameter and/or increased ovarian volume >10 mL [8] (Fig. 23.2). In combination with either anovulation/oligo-ovulation or clinical/biochemical hyperandrogenism and

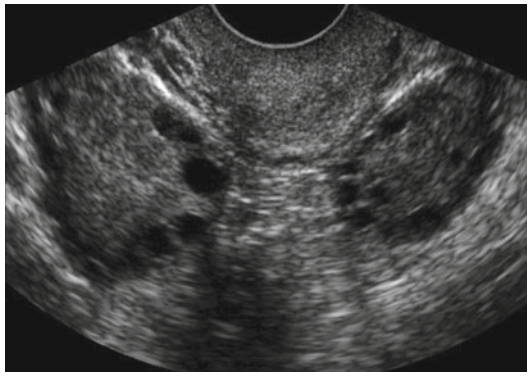

Fig. 23.2 AFC of PCOS ovary in 2D ultrasound

having excluded other endocrine conditions such as Cushing's syndrome and congenital adrenal hyperplasia, a patient could be diagnosed as having PCOS. Interestingly, even women who do not technically meet criteria for PCOS but have isolated polycystic-appearing ovaries on ultrasound have been found to have a higher risk of developing OHSS [7]. Therefore, clinical management including gonadotropin dosing and choice of stimulation protocol should incorporate knowledge of PCOS or polycystic-appearing ovaries on ultrasound in an attempt to minimize the development of OHSS in these patients.

Using patients with PCOS as a model for other patients at risk for OHSS, researchers have investigated ultrasound calculation of baseline ovarian volume alone as a predictive marker. Danninger et al. studied 101 patients undergoing IVF, all of whom had 3D volumetric assessment of ovarian volume starting on stimulation day 1 [9]. The authors then remeasured ovarian volume on the day of human chorionic gonadotropin (hCG) and correlated those findings with the development of OHSS. They found a significant correlation between the baseline ovarian volume and OHSS ($p = 0.03$) with a greater baseline ovarian volume in women who subsequently developed OHSS compared to those who did not. The authors estimated an ovarian volume cutoff of 10 mL as predictive of OHSS. Importantly, this sonographic finding was not as robust as some of the other markers already discussed. Even in the 34 patients identified to have an ovarian volume >10 mL, only 23.5 % ultimately developed OHSS. Although it is logical in the context of PCOS and the PCOS-associated risk of OHSS, the measurement of ovarian volume is not considered to be a standard marker at this time to predict OHSS.

The final ultrasound characteristics which have been used to attempt to predict the development of OHSS are Doppler flow studies of ovarian vasculature. The concept behind the assessment of ovarian vascular resistance and flow is that because OHSS involves third spacing of fluid secondary to increased vascular permeability, one might expect changes in ovarian vascular flow which may occur prior to clinical signs or symptoms of OHSS and therefore could be used to predict the development of OHSS [10]. Coupled with increased vascular permeability, there is also abnormal intraovarian angiogenesis in OHSS leading to low vascular impedance. Multiple authors have investigated sonographic characterization of ovarian vascular flow, resistance, peak systolic velocity, and pulse-wave power Doppler to try to correlate vascular chances with the likelihood of developing OHSS. In 1997, Moohan et al. evaluated 30 patients who were diagnosed with mild or severe OHSS within 2–15 days of oocyte retrieval [10]. All patients underwent transabdominal ultrasound at the time of diagnosis of OHSS with color Doppler done on low-flow setting to characterize the flow velocity waveforms within the ovarian vessels. Vascular pulsatility index, resistance index, S-D ratio, and maximal peak systolic velocity were calculated. The authors found that in patients with severe OHSS, there was markedly reduced vascular impedance with a statistically significantly higher resistance index in patients with mild OHSS compared to severe (0.49 vs. 0.41, $p < 0.005$). Surprisingly, there was no difference in maximal peak systolic velocity, but pulsatility index and S-D ratio also differed significantly between patients with mild and severe OHSS. Of importance, this study evaluated only patients diagnosed with OHSS. There was no comparison with patients who did not develop OHSS, so it is impossible to know if these differences in vascular flow could have been used to predict the development of OHSS. Other authors including

Agrawal et al. did compare patients with OHSS to controls and found a difference in ovarian stromal peak systolic velocity and time-averaged maximal velocity between patients with and without OHSS [11]. In the study by Agrawal et al. published in 1998, ovarian Doppler flow velocity was statistically significantly higher in patients with OHSS than controls, but pulsatility index and resistance index did not differ between the groups. The authors concluded that the changes in flow velocity correlated with changes in vascular endothelial growth factor (VEGF) serum and follicular fluid concentrations. More recently, Jayaprakasan et al. used three-dimensional (3D) power Doppler angiography to attempt to predict OHSS [12]. In 118 patients, of whom 18 developed moderate or severe OHSS, ovarian vascular flow indices were quantified by 3D ultrasound. Unexpectedly, there was no difference in vascularization index, flow index, or vascularization flow index between either patients with OHSS vs. controls or the subgroups of patients with moderate vs. severe OHSS. Therefore, although the pathophysiology of OHSS involves known changes in vascular permeability which logically suggest a connection between Doppler measurements of ovarian vascular flow and the development of OHSS, unfortunately no studies to date have convincingly shown that ultrasound measurement of ovarian vascular parameters can be used to predict the risk of OHSS.

In summary, ultrasound has been investigated as a tool to predict the development of OHSS through assessment of AFC, quantitation of follicular development during IVF, identification of polycystic-appearing ovaries or PCOS, determination of ovarian volume, and Doppler flow studies of ovarian vasculature. Of these potential sonographic markers, AFC is the most significant predictor of the development of OHSS and should be used to guide management. There is also evidence linking the number of developing follicles and the diagnosis of PCOS with the risk of OHSS. To date, the other ultrasound tools including ovarian volume and vascular flow analysis do not have clinical utility in the prediction of OHSS.

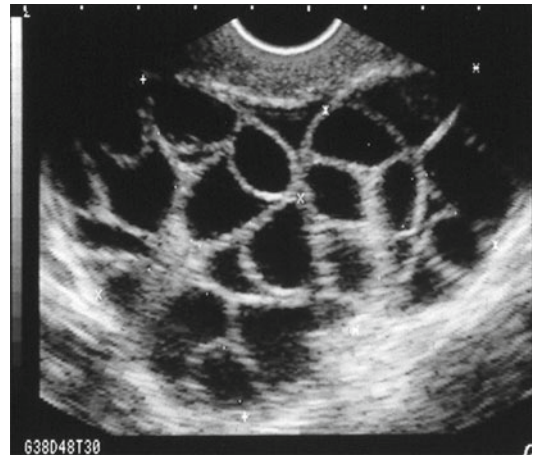

Fig. 23.3 Hyperstimulated ovary after gonadotropin therapy

Ultrasound in the Diagnosis of Ovarian Hyperstimulation Syndrome

Once OHSS is suspected on clinical grounds, the diagnosis is aided by ultrasound findings. OHSS is categorized into mild, moderate, and severe disease. The differentiation involves sonographic features including the degree of ovarian enlargement, presence and volume of abdominal ascites, presence or absence of pleural effusions, and Doppler studies showing venous thromboembolism [13].

The clinical findings of OHSS encompass a spectrum ranging from mild disease, unpleasant for the patient but not considered to be dangerous, to severe OHSS with significant consequences and risk of death. Mild OHSS is common and involves symptoms such as lower abdominal or pelvic discomfort, gastrointestinal complaints including nausea, emesis, and diarrhea, and some degree of abdominal distention [14]. The process of superovulation frequently leads to these mild manifestations of OHSS, and up to a third of IVF cycles may involve these complaints. The only sonographic characteristic of mild OHSS may be enlarged ovaries (5–12 cm) [15] (Fig. 23.3).

Moderate OHSS consists of intensified pain, nausea or emesis, enlarged ovaries seen on ultrasound, and sonographic identification of abdominal or pelvic ascites with normal serum

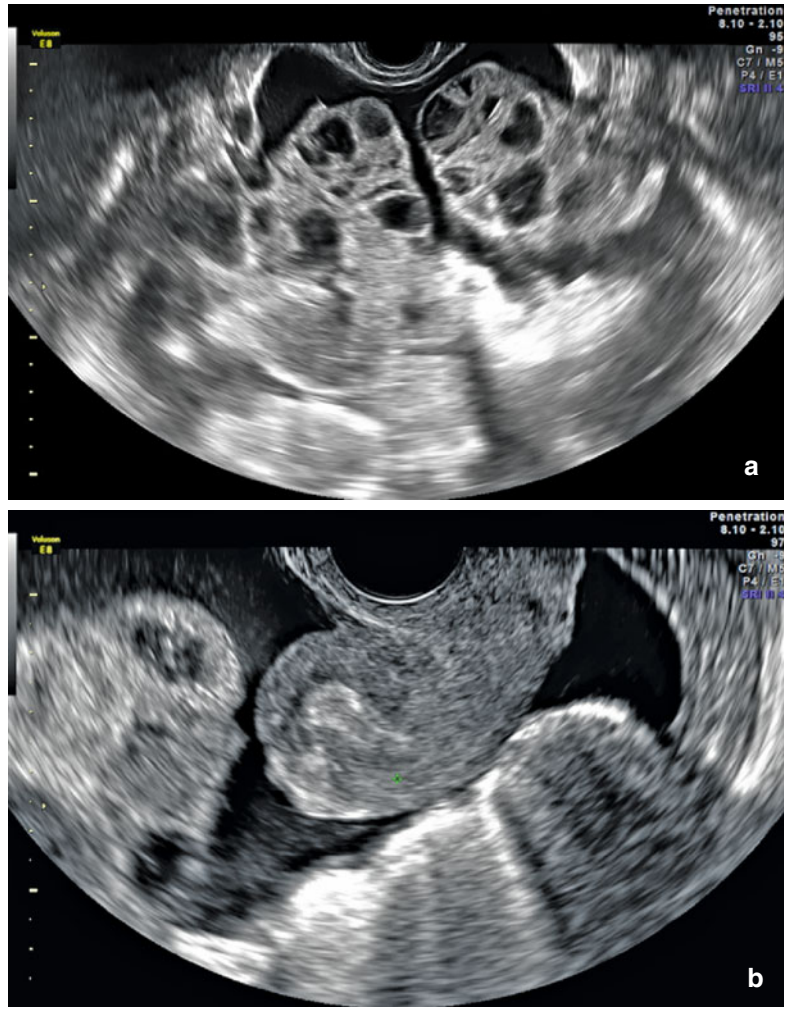

Fig. 23.4 (**a**) Ultrasound of moderate OHSS with ascites. (**b**) Ultrasound of ascites in the cul-de-sac with severe OHSS

laboratory parameters (Fig. 23.4a). Some authors have described OHSS as an abdominal compartment syndrome because the rapid accumulation of ascites can lead to increased intra-abdominal pressure [16]. Increased intra-abdominal pressure can become acute and lead to organ dysfunction. In severe forms, abdominal compartment syndrome affects respiratory function, as in the case of severe OHSS.

Given that abdominal ascites is a key characteristic of the diagnosis of moderate OHSS, it is critical that the ultrasound findings be interpreted correctly in the context of the clinical presentation. Gunabushanam et al. reported the case of a 22-year-old woman who had received fertility treatments and presented to the emergency department complaining of a 12 h history of severe lower abdominal pain [17]. Transabdominal ultrasound showed enlarged ovaries bilaterally (7×5×5 cm) with significant anechoic peritoneal free fluid felt consistent with ascites. She was diagnosed with OHSS. She then began to clinically decompensate with the development of pallor and peritoneal signs and underwent diagnostic paracentesis notable for non-clotting blood. Ultimately she was taken to the operating room for emergent laparotomy and a bleeding ovarian cyst was identified and treated. This case demonstrates the dangers of assuming the diagnosis of OHSS in all patients undergoing

fertility treatments, as other pelvic pathology can clearly lead to the accumulation of pelvic fluid. Cyst rupture can certainly lead to significant intraperitoneal bleeding with risk of death, and accurate communication between the sonographer, Radiologist, Emergency Department physician, and Reproductive Endocrinologist is critical to appropriate and timely diagnosis.

Severe OHSS is one of the most serious complications of ovarian hyperstimulation (Fig. 23.4b). The incidence of severe OHSS is estimated between 0.5 and 5 % per IVF cycle. Severe OHSS has been reported to be fatal, so the prompt diagnosis and treatment is paramount [18]. Patients with severe OHSS describe rapid weight gain, significant abdominal distention with inability to fit into usual clothes, shortness of breath, pain which can be refractory to oral medications, oliguria, and severe and unrelenting nausea or emesis with inability to tolerate oral intake. Clinical findings include all of the features of moderate OHSS plus clinical ascites, sonographic ascites, ultrasound evidence of pleural effusions, and serum laboratory abnormalities such as hemoconcentration, coagulopathy, electrolyte imbalance, and renal and hepatic dysfunction or failure [19].

Current research indicates that the fluid shifts which occur in OHSS are directly caused by increased VEGF. VEGF leads to increased vascular permeability, reduced colloid osmotic gradient, and spillage of fluid out of the vascular compartment and into the extravascular spaces [20]. These fluid shifts can be identified sonographically, and it is recommended that in the evaluation of the patient suspected to have moderate or severe OHSS, ultrasound should be used to check for abdominal ascites or pleural effusions. Generally, the volume of accumulated fluid is not subtle and can easily be identified either through abdominal or vaginal ultrasound or ultrasound of the lung bases. The third spacing of fluid into the peritoneal and pleural cavities leads to respiratory compromise, hypotension, increased intra-abdominal pressure, and renal compromise related to decreased perfusion [21].

The hemoconcentration and resultant hypercoagulability of severe OHSS can lead to venous and arterial thromboembolism both in the typical locations such as lower extremities and lungs and in sites which seem more specific to OHSS such as the subclavian and internal jugular vessels. It is unclear why thrombosis may be localized to the neck rather than the lower extremities; some have hypothesized that increased peritoneal fluid containing inflammatory mediators drains into the thoracic duct and directly into the subclavian veins, possibly locally increasing coagulation at those sites [22]. Rova et al. evaluated the risk of venous thromboembolism in all IVF cycles and particularly in the subset complicated by OHSS [21]. They found that the incidence of venous thromboembolism from the time of the IVF cycle into the first trimester of pregnancy was 0.17 % (32 out of 19,194 patients), which was a 10-fold increase over the background risk in spontaneous conceptions. Furthermore, in patients diagnosed with OHSS, the risk of venous thromboembolism was 1.4 % (19/1,272), a 100-fold increase. Given this markedly increased risk, Doppler studies to evaluate for thromboembolism are a critical part of the evaluation of the patient with suspected moderate or severe OHSS. Even if thrombosis is not identified, it is generally recommended to initiate prophylactic anticoagulation in hemoconcentrated patients with heparin or low molecular weight heparin when the hematocrit is found to be 45–50 % in order to mediate this risk [23].

Ultrasound in the Management and Treatment of Ovarian Hyperstimulation Syndrome

Timely and accurate diagnosis of OHSS facilitates proactive management and treatment. The management strategy varies in the literature, from some authors recommending immediate hospitalization upon the diagnosis of moderate or severe OHSS to others advocating active outpatient treatment. Regardless of the location, ultrasound is critical in the management and treatment of OHSS. Sonographic monitoring can determine decrease in volume of abdominal ascites which

would indicate improving disease. Ultrasound-guided transabdominal and transvaginal paracenteses have been shown to markedly improve patient symptoms of OHSS and avoid the need for hospitalization. Ultrasound-guided placement of pigtail catheters has been used in the past for continuous drainage of ascites. Thoracentesis to drain pleural effusions is also aided by ultrasound guidance [14]. By fully and accurately using ultrasound, clinicians can optimize the care of patients with this serious complication.

OHSS can be diagnosed early or late in the IVF process, either during initial ovarian stimulation with gonadotropins, around the time of the oocyte retrieval, or more commonly, 1–2 weeks following embryo transfer when the serum beta human chorionic gonadotropin (*B*hCG) begins to rise. "Early" OHSS generally presents 3–7 days after the hCG trigger shot, while "late" OHSS occurs 12–17 days after the hCG trigger [24]. When OHSS is identified early during IVF treatment, generally ultrasound is used to monitor the progression of ascites and in conjunction with clinical assessment of the patient's stability, a determination made about the safety of proceeding with embryo transfer. If the risks of embryo transfer are felt to exceed the benefits, then one of a number of strategies can be employed including cycle cancellation with withholding of the hCG trigger, decreased hCG trigger dosing, agonist trigger, and cryopreservation of all embryos [13]. The data on the effectiveness of any of these strategies is mixed. The most effective preventative technique is unquestionably outright cycle cancellation.

If the IVF cycle proceeds and embryo transfer is performed, then OHSS may develop within a few days to a few weeks of the embryo transfer. It is clear that in the case of pregnancy, OHSS is perpetuated by placental *B*hCG and can become both more severe and of longer duration than if pregnancy does not occur. When there is concern for OHSS, the first step is clear communication about symptoms between the patient and the IVF staff. Early urgent clinic visits for evaluation of the stage of OHSS are extremely important for active management. If in the course of evaluation abdominal ascites is identified, transabdominal or transvaginal paracentesis with ultrasound guidance can lead to dramatic improvement in patient symptoms.

Paracentesis is not a new treatment for OHSS. It was first described by Rabau et al. in 1967, and since that time many authors have proposed active use of both transabdominal and transvaginal ultrasound-guided paracentesis in patients with OHSS [25]. The idea for paracentesis in OHSS actually originated in the care of other patients with ascites: cirrhotic patients who underwent large-volume paracentesis when they became refractory to diuretics [26, 27]. In these cirrhotics, when at least 750 mL of ascitic fluid was removed, intra-abdominal pressure decreased, venous return improved, and renal perfusion improved. Distinct from the situation with cirrhosis, in patients with OHSS, there also appears to be a compounded therapeutic effect of the direct removal of inflammatory and vasoactive substances from the peritoneal cavity [28].

Several authors have studied the clinical consequences of paracentesis in patient with OHSS. Universally, there has been identified to be improvement in hemodynamic parameters such as uterine and renal artery perfusion [29]. These changes then lead to cardiovascular stabilization, improvement in oliguria, improved respiratory function, and dramatic relief from abdominal distention and pain. Paracentesis can be performed via a transabdominal or transvaginal approach, depending on the available equipment and the familiarity of the operator. The original reports of paracentesis described a transabdominal approach using ultrasound guidance, but more recent reports have focused on transvaginal paracentesis. Enthusiastic proponents of transvaginal paracentesis tout the ease and similarity to the technique of transvaginal oocyte retrieval, ability to perform the procedure on an outpatient basis, and improved patient pain and tolerance to the procedure [23, 30, 31]. In general, the procedure for transvaginal ultrasound-guided paracentesis starts with minimal intravenous (IV) sedation. It can be done with the injection of local anesthesia in the vaginal fornices using a spinal needle, but generally patient comfort is improved with light sedation. The vagina is cleansed with

povidone-iodine (Betadine) and then a #17 egg retrieval needle is affixed to conventional operating room suction tubing and attached to wall suction. The suction can be set at any pressure; generally 200 mmHg speeds the procedure. A vaginal ultrasound probe with a standard needle guide is then inserted and the posterior cul-de-sac with dependent ascites visualized. It is often helpful to place the patient in reverse Trendelenburg position in order to allow gravity to assist with ascites pooling. Under direct ultrasound visualization, the egg retrieval needle is advanced into the deepest pocket of ascites, taking care to avoid vital structures including the cervix, uterus, bowel, and vessels. Wall suction is activated and ascites fluid drained. Paracentesis is continued until the fluid is identified to be maximally removed. There is no particular limit to the amount of ascites which may be aspirated. Generally, we limit the volume to <5 L of fluid given the hemodynamic changes which can occur, but clinics vary in the specific parameters of drainage.

In the largest series evaluating outpatient management of severe OHSS using transvaginal paracentesis, we identified 183 patients with OHSS presenting between 1999 and 2007 [23]. During this time frame, 96 patients with OHSS underwent 146 outpatient transvaginal paracenteses. Of these patients, 36 % (35/96) required two paracenteses, 8 % (8/96) required three paracenteses, 3 % (3/96) required a fourth procedure, and one patient underwent five transvaginal paracenteses until OHSS symptoms resolved and ascitic fluid is no longer accumulated leading to clinical symptoms. The mean volume of ascites aspirated was 2,155 mL (range 500–4,500 mL). There were no procedure-related complications and no instances of pregnancy loss in this group. The use of aggressive outpatient transvaginal paracentesis not only decreased the need for hospitalization but was also associated with a decreased hospital stay in cases when hospitalization was required [23].

Other uses of ultrasound in the management of OHSS have included ultrasound-guided drainage with autotransfusion of ascitic fluid as well as transabdominal and transvaginal attempts at pigtail catheter placement for continuous drainage of ascites. In 1992, Aboulghar et al. reported three patients with OHSS who underwent transvaginal aspiration of ascites which was then autotransfused [32]. They described rapid improvements in hematologic parameters and improved clinical symptoms. Another group in Japan also described reinfusion of ascitic fluid in two patients in 1994 [33]. In that report, ascites was removed, underwent ultrafiltration, and was then reinfused, leading to resolution of the severe OHSS. Subsequent reports moved away from autotransfusion and transitioned to the placement of pigtail catheters for continuous ascites drainage. In 2003, Abuzeid et al. reported transabdominal-guided placement of an abdominal pigtail catheter which was left in place until ascitic fluid ceased to drain [34]. In that report, 26 patients with severe OHSS were identified. Half (13) underwent placement of a pigtail catheter and the other half were hospitalized without intervention. They described the placement of a 6-0 French, 2 mm pigtail catheter through the abdominal wall into the largest pocket of ascites fluid under continuous abdominal ultrasound guidance. The catheter was then attached to a drainage bag and left in place until ascites resolved. In those patients who underwent ultrasound-guided pigtail catheter placement, the catheter was left in place for an average of 12–13 days and mean amount of ascites drained was 11 L. There were no documented infections and no impact on the pregnancy rates between the two groups. The authors concluded that pigtail catheter placement was safe and effective and could be an alternative to multiple paracenteses in patients with severe OHSS. Another group tested the efficacy of transvaginal pigtail catheter placement for continuous ascites drainage [35]. They reported on one patient with severe OHSS, obesity, and generalized edema who had an extremely thick abdominal wall (15 cm) which limited ultrasound visualization of both ascites and internal organs. She therefore had an Oosterlinck drainage catheter placed vaginally and left in place for continuous drainage for a total of 4 days. A total of 17.45 L of ascites were drained over this time frame and she was ultimately discharged to home

in good condition without complications. The investigators concluded that ultrasound-guided transvaginal pigtail catheter placement was an alternative to the transabdominal approach when body habitus limits abdominal visualization.

The final way in which ultrasound may be used in the management and treatment of OHSS is to assist with thoracentesis in the case of severe OHSS with pulmonary compromise and pleural effusions. Similar to the case of abdominal ascites, protein-poor fluid can accumulate in the pleural cavity and lead to problems due to restriction of diaphragm movement, restriction of lung expansion with collapse of pulmonary parenchyma, poor ventilation, and shunting [36]. It is estimated that pleural effusions occur in about 10 % of patients with severe OHSS. Chest X-ray (CXR) is the typical imaging modality used to diagnose pleural effusions, with ultrasound used to guide needle placement for thoracentesis as in the case of paracentesis. Abramov et al. in 1999 evaluated 2,902 patients with OHSS between 1987 and 1996, 209 of whom were diagnosed with severe OHSS [36]. They characterized the pulmonary findings in these patients and the required interventions. Not surprisingly, 92.3 % (193) presented with dyspnea and 71 % had bilaterally elevated diaphragms on CXR. Almost a third (29 %) were diagnosed with pleural effusions on CXR, right lung > left lung, and 13 % underwent thoracentesis. The hypothesis for the laterality of pleural effusions which seem to favor the right lung is that in the face of massive ascites, diaphragmatic lymphatics channel the fluid to the right pleural space via the thoracic duct. Man et al. also investigated pleural effusions in four patients with severe OHSS [37]. They characterized the location and volume of the fluid drained. Interestingly, 3/4 patients presented with right-sided pleural effusions. All ultimately underwent thoracentesis secondary to pulmonary symptoms and a total of 1,200–2,000 mL was drained. Finally, isolated pleural effusions in the absence of abdominal ascites or other signs or symptoms of OHSS have been reported [38]. Mullin et al. in 2011 reported symptomatic isolated pleural effusion as a sole manifestation of OHSS. They note that isolated pleural effusions in severe OHSS occur with an incidence of 0.65 %. The two patients reported both underwent therapeutic thoracentesis with resolution of dyspnea. Therefore, in patients with OHSS and clinical evidence of pulmonary compromise, pleural effusions should be actively sought and treated. It should not be simply assumed that dyspnea is attributable to abdominal distension from ascites and compression of the lung bases since pleural effusions are found in approximately 10–30 % of patients with severe OHSS and may require treatment with thoracentesis.

In conclusion, ultrasound plays important roles in the prevention, diagnosis, and treatment of OHSS. By fully and accurately using ultrasound, clinicians can be proactive in the evaluation and management of this severe iatrogenic complication of ovulation induction. By using ultrasound to determine AFC, diagnose PCOS, and monitor follicle development during gonadotropin stimulation, clinicians may anticipate the risk of OHSS and modulate the IVF treatment plan. If clinically suspected, ultrasound is key to speedy diagnosis of OHSS into mild, moderate, or severe disease. Once OHSS is found to occur, ultrasound guidance for transabdominal or transvaginal paracentesis, sonographic monitoring for improvement in ascites, and ultrasound assistance for thoracentesis will improve patient symptoms, lessen hemodynamic, pulmonary, and renal compromise, and may avoid the need for hospitalization.

References

1. Papanikolaou EG, Humaidan P, Polyzos NP, Tarlatzis B. Identification of the high-risk patient for ovarian hyperstimulation syndrome. Semin Reprod Med. 2010;28(6):458–62.
2. Kwee J, Elting ME, Schats R, McDonnell J, Lambalk CB. Ovarian volume and antral follicle count for the prediction of low and hyper-responders with in vitro fertilization. Reprod Biol Endocrinol. 2007;5:9.
3. Ocal P, Sahmay S, Cetin M, Irez T, Guralp O, Cepni I. Serum anti-mullerian hormone and antral follicle count as predictive markers of OHSS in ART cycles. J Assist Reprod Genet. 2011;28:1197–203.
4. Broer SL, Dolleman M, Opmeer BC, Fauser BC, Mol BW, Broekmans FJM. AMH and AFC as predictors of excessive response in controlled ovarian hyperstimulation: a meta-analysis. Hum Reprod Update. 2011; 17(1):46–54.

5. Broekmans FJM, de Ziegler D, Howles CM, Gougeon A, Trew G, Oliviennes F. The antral follicle count: practical recommendations for better standardization. Fertil Steril. 2010;94:1044–51.
6. Papanikolaou EG, Pozzobon C, Kolibianakis EM, Camus M, Tournaye H, Fatemi HM, Van Steirteghem AV, Devroey P. Incidence and prediction of ovarian hyperstimulation syndrome in women undergoing gonadotropin-releasing hormone antagonist in vitro fertilization cycles. Fertil Steril. 2006;85(1):112–20.
7. Humaidan P, Quartarolo J, Papanikolaou EG. Preventing ovarian hyperstimulation syndrome: guidance for the clinician. Fertil Steril. 2010;94(2): 389–400.
8. Rotterdam ESHRE/ASRM-Sponsored PCOS Consensus Workshop Group. Revised 2003 consensus on diagnostic criteria and long-term health risks related to polycystic ovary syndrome. Fertil Steril. 2004;81(1):19–25.
9. Danninger B, Brunner M, Obruca A, Feichtinger W. Prediction of ovarian hyperstimulation syndrome of baseline ovarian volume prior to stimulation. Hum Reprod. 1996;11(8):1597–9.
10. Moohan JM, Curcio K, Leoni M, Healy D, Hurley V. Low intraovarian vascular resistance: a marker for severe ovarian hyperstimulation syndrome. Fertil Steril. 1997;67(4):728–32.
11. Agrawal R, Conway G, Sladkevicius P, Tan SL, Engmann L, Payne N, Bekir J, Campbell S, Jacobs H. Serum vascular endothelial growth factor and Doppler blood flow velocities in in vitro fertilization: relevance to ovarian hyperstimulation syndrome and polycystic ovaries. Fertil Steril. 1998;70(4):651–8.
12. Jayaprakasan K, Jayaprakasan R, Al-Hasie HA, Clewes JS, Campbell BK, Johnson IR, Raine-Fenning NJ. Can quantitative three-dimensional power Doppler angiography be used to predict ovarian hyperstimulation syndrome? Ultrasound Obstet Gynecol. 2009;33:583–91.
13. Alper MM, Smith LP, Sills ES. Ovarian hyperstimulation syndrome: current views on pathophysiology, risk factors, prevention, and management. J Exp Clin Assist Reprod. 2009;6:3.
14. Practice Committee of the American Society for Reproductive Medicine. Ovarian hyperstimulation syndrome. Fertil Steril. 2008;90(3):S188–93.
15. Whelan JG, Vlahos NF. The ovarian hyperstimulation syndrome. Fertil Steril. 2000;73(5):883–96.
16. Grossman LC, Michalakis KG, Browne H, Payson MD, Segars JH. The pathophysiology of ovarian hyperstimulation syndrome: an unrecognized compartment syndrome. Fertil Steril. 2010;94(4):1392–8.
17. Gunabushanam G, Mandal K, Lal S. Hemoperitoneum from ruptured cyst in a hyperstimulated ovary: a sonographic mimic of ovarian hyperstimulation syndrome. J Clin Ultrasound. 2007;35(5):281–3.
18. Brinsden PR, Wada I, Tan SL, Balen A, Jacobs HS. Diagnosis, prevention, and management of ovarian hyperstimulation syndrome. Br J Obstet Gynaecol. 1995;102:767–72.
19. Rizk B, Aboulghar M. Modern management of ovarian hyperstimulation syndrome. Hum Reprod. 1991;6:1082–7.
20. Tollan A, Holst N, Forsdahl F, Fadnes HO, Oian P, Maltau JM. Transcapillary fluid dynamics during ovarian stimulation for in vitro fertilization. Am J Obstet Gynecol. 1990;162:554–8.
21. Scheppach W. Abdominal compartment syndrome. Best Pract Res Clin Gastroenterol. 2009;23:25–33.
22. Rova R, Passmark H, Lindqvist PG. Venous thromboembolism in relation to in vitro fertilization: an approach to determining the incidence and increase in risk in subsequent cycles. Fertil Steril. 2012;97(1):95–100.
23. Smith LP, Hacker MR, Alper MM. Patients with severe ovarian hyperstimulation syndrome can be managed safely with aggressive outpatient transvaginal paracentesis. Fertil Steril. 2009;92:1953–9.
24. Mathur RS, Akande AV, Keay SD, Hunt LP, Jenkins JM. Distinction between early and late ovarian hyperstimulation syndrome. Fertil Steril. 2000;73(5):901–7.
25. Rabau E, David A, Serr DM, Mashiach S, Lunenfeld B. Human menopausal gonadotropin for anovulation and sterility. Am J Obstet Gynecol. 1967;98:92–8.
26. Cabrera J, Falcon L, Gorriz E, Pardo MD, Granados R, Quinones A, Maynar M. Abdominal decompression plays a major role in early post paracentesis hemodynamic changes in cirrhotic patients with tense ascites. Gut. 2001;48:384–9.
27. Forouzandeh B, Konicek F, Sheagren JN. Large-volume paracentesis in the treatment of cirrhotic patients with refractory ascites: the role of postparacentesis volume expansion. J Clin Gastroenterol. 1996;22:207–10.
28. Delbaere A, Bergmann PJ, Gervy-Decoster C, Staroukine M, Englert Y. Angiotensin II immunoreactivity is elevated in ascites during severe ovarian hyperstimulation syndrome: implications for pathophysiology and clinical management. Fertil Steril. 1994;62:731–7.
29. Chen C-D, Yang J-H, Chao K-H, Chen S-U, Ho H-N, Yang Y-S. Effects of repeated abdominal paracentesis on uterine and intraovarian haemodynamics and pregnancy outcome in severe ovarian hyperstimulation syndrome. Hum Reprod. 1998;13(8):2077–81.
30. Fluker MR, Copeland JE, Yuzpe AA. An ounce of prevention: outpatient management of the ovarian hyperstimulation syndrome. Fertil Steril. 2000;73(4): 821–4.
31. Aboulghar MA, Mansour RT, Serour GI, Amin Y. Ultrasonically guided vaginal aspiration of ascites in the treatment of ovarian hyperstimulation syndrome. Fertil Steril. 1990;53:933–5.
32. Aboulghar MA, Mansour RT, Serour GI, Riad R, Ramzi AM. Autotransfusion of the ascitic fluid in the treatment of severe ovarian hyperstimulation syndrome. Fertil Steril. 1992;58(5):1056–9.
33. Fukaya T, Chida S, Terada Y, Funayama Y, Yajima A. Treatment of severe ovarian hyperstimulation syndrome by ultrafiltration and reinfusion of ascitic fluid. Fertil Steril. 2004;61(3):561–4.

34. Abuzeid MI, Nassar Z, Massaad Z, Weiss M, Ashraf M, Fakih M. Pigtail catheter for the treatment of ascites associated with ovarian hyperstimulation syndrome. Hum Reprod. 2003;18(2):370–3.
35. Raziel A, Friedler S, Schachter M, Strassgurger D, Bukovsky I, Ron-El R. Transvaginal drainage of ascites as an alternative to abdominal paracentesis in patients with severe ovarian hyperstimulation syndrome, obesity, and generalized edema. Fertil Steril. 1998;69(4):780–3.
36. Abramov Y, Elchalal U, Schenker JG. Pulmonary manifestations of severe ovarian hyperstimulation syndrome: a multicenter study. Fertil Steril. 1999;71(4):645–51.
37. Man A, Schwarz Y, Greif J. Pleural effusion as a presenting symptom of ovarian hyperstimulation syndrome. Eur Respir J. 1997;10:2425–6.
38. Mullin CM, Fino ME, Reh A, Grifo JA, Licciardi F. Symptomatic isolated pleural effusion as an atypical presentation of ovarian hyperstimulation syndrome. Case Rep Obstet Gynecol. 2011; Epub 2011 Aug 7.

Pregnancy of Unknown Viability

24

Emily N.B. Myer, Jane Arrington,
and Steven L. Warsof

Abbreviations

β-hCG	Beta subunit of human chorionic gonadotropin
FHR	Fetal heart rate
FP	Fetal pole
GS	Gestational sac
hCG	Human chorionic gonadotropin
IPUV	Intrauterine pregnancy of unknown viability
PUL	Pregnancy of unknown location
SAB	Spontaneous abortion
YS	Yolk sac

Introduction

Bleeding in early pregnancy complicates 15 % of all conceptions and accounts for nearly 2 % of all emergency department visits [1]. Seventy to ninety percent of these pregnancies will progress normally. The remainder will either spontaneously abort or be an ectopic pregnancy. With advances in technology, the ability to detect pregnancy at earlier gestational age, either biochemically or sonographically, provides both diagnostic assistance and challenge to practitioners. One of the more clinically challenging scenarios is the patient with a positive pregnancy test who presents with uterine bleeding or pelvic pain and whose fetus cannot be located by ultrasound. An astute clinician must always have concern for a life-threatening ectopic pregnancy or miscarriage. When the situation is uncertain, the clinician must decide if the patient has signs and symptoms highly concerning for abnormal pregnancy. This is important to avoid erroneous treatments or counseling which could not only harm a viable fetus but also may lead to significant medical legal risk. The uncertainty of diagnosis and management is especially true when physicians from multiple disciplines with different skill sets converge in the emergency department. The goal of this chapter is to clarify for the practitioner the evaluation and treatment of early pregnancy of unknown viability or location.

E.N.B. Myer, MD • S.L. Warsof, MD (✉)
Department of Obstetrics and Gynecology,
Eastern Virginia Medical School,
825 Fairfax Avenue, Norfolk, VA 23507, USA
e-mail: myeren@evms.edu; warsofsl@evms.edu

J. Arrington, RDMS
Maternal Fetal Medicine, Eastern Virginia Medical School, 2075 Glenn Mitchell Dr. #500,
Virginia Beach, VA 23456, USA
e-mail: arringjn@evms.edu

Case Scenario

A 24-year-old G3 P0,1,1,LC 1 presents to the local emergency department after 2 days of right-sided abdominal pain and cramping with intermittent nausea and vomiting. She also complains of one episode of scant bleeding per vagina after intercourse.

L.A. Stadtmauer, I. Tur-Kaspa (eds.), *Ultrasound Imaging in Reproductive Medicine*,
DOI 10.1007/978-1-4614-9182-8_24,

The patient reports she is sexually active with one partner. She does not use any form of contraception. Her LMP was 6 weeks prior. Her periods are irregular. She thinks she is pregnant based on a home pregnancy test she took today.

Her medical and surgical history are benign except for a cesarean section 3 years ago at 34 weeks gestation for fetal distress and a spontaneous first trimester abortion 1 year ago. She does not smoke or drink alcohol.

On exam the patient is an obese female sitting comfortably in bed. Vital signs are stable. The abdomen is soft and mildly tender in the right lower quadrant without guarding or rebound tenderness. The external genitalia and vagina are normal. There is no blood in the vaginal vault. The cervix is closed.

Bimanual exam reveals a 6-week-size uterus with no palpable adnexal masses and mild tenderness on the right side. The remainder of the exam is normal.

What is the diagnosis and management at this point?

Early Pregnancy Complications: Vaginal Bleeding and Pelvic Pain

Bleeding per vagina and pelvic pain complicate 15–25 % of all pregnancies and are common presenting complaints to the emergency department [1]. Bleeding in early pregnancy is never normal. It is often a sign of an ectopic pregnancy or impending spontaneous abortion, but it does not always indicate a failed pregnancy. When a patient presents with bleeding in pregnancy, first ensure the patient is hemodynamically stable. Then, obtain a thorough history and physical exam and a beta subunit of human chorionic gonadotropin (β-hCG). Next a transvaginal ultrasound (TVU/S) to evaluate the pregnancy and its location should be performed as up to 18 % of those presenting with bleeding in early pregnancy will be diagnosed with an ectopic pregnancy [2]. This combination of history, exam, β-hCG, and TVU/S should resolve the diagnosis for most cases.

History and Physical Exam

Obtaining the patient's medical history, including obstetric and sexual history, contraceptive practices, and last menstrual period (LMP), is the first step in the patient encounter. Symptoms of pregnancy including a missed menstrual period, breast tenderness, nausea, and vomiting should be elicited. Physical exam is then performed and may reveal an enlarged, soft uterus. Adnexal tenderness or mass may raise suspicion of an ectopic pregnancy or other ovarian pathology. The physical exam, however, is nonspecific and has become more limited due to the obesity epidemic. This traditional clinical approach has largely been superseded by biochemical studies and ultrasound imaging.

β-hCG

Human chorionic gonadotropin (hCG) is a heterodimeric hormone produced by placental syncytiotrophoblasts early in pregnancy. It is composed of two dissimilar subunits: alpha and beta. The alpha subunit is similar to thyroid-stimulating hormone and luteinizing hormone. The beta (β) subunit is unique to hCG and is the component analyzed to confirm pregnancy [3]. β-hCG is measured by radioimmunoassay and can be detected within 8–10 days postovulation at levels as low as 25 milli-international units per milliliter (mIU/ml) [4, 5]. Thus, biochemical detection of pregnancy occurs prior to ultrasound detection.

Though early detection of pregnancy has multiple benefits, it often leads to unnecessary intervention. Historically, women with a positive pregnancy test, non-visible pregnancy on abdominal ultrasound, and any symptom concerning for ectopic pregnancy were taken for diagnostic laparoscopy. This surgical approach to diagnosis

proved to be problematic since as many as 39 % of laparoscopies were unnecessarily performed in women later confirmed to have a normal intrauterine pregnancy (IUP) [6]. Today we have a better understanding of the utility of β-hCG beyond diagnosis of pregnancy [7, 8].

In a normal intrauterine pregnancy (IUP), fetal growth and placental hormone secretion occur together. β-hCG rises in a predictable logarithmic fashion from the fourth to the tenth week of gestation, after which there is a wide biological variation (Table 24.1, Fig. 24.1) [3, 7, 9]. In 1984, Kadar defined a normal pregnancy by the rise of β-hCG. He measured β-hCG levels at 0 and 48 h in 20 women. A rise of 66 % predicted a normal intrauterine pregnancy (IUP) with 85 % accuracy [10, 11]. This became known as the "doubling time" which is now frequently used to determine the viability of a pregnancy. A common misconception is that failure of β-hCG to double in 48 h is diagnostic of an abnormal pregnancy. Subsequent studies have shown the normal rate of rise of β-hCG has a wider variance. In 2004, Barnhart followed β-hCG levels at 0 and 48 h in 300 women and defined the minimal rise as 53 % with 99 % accuracy [12]. In 2012, Morse reported the lowest rate of rise associated with a normal IUP in a series of 1,000 women is 35 % in 48 h [13]. Below this rate of rise, the pregnancy can be considered abnormal with no chance of viability [14, 15].

Table 24.1 Range of β-hCG as measured in viable pregnancies delivering at term

Embryonic week of gestation	Lower limit of β-hCG (mIU/ml)	Upper limit of β-hCG (mIU/ml)
4	12	2,548
5	330	37,290
6	440	142,230
8–12 (peak)		53,715
18–40 (plateau)		11,806

Adapted from Refs. [3, 7]

It is still true that pregnancies with a lower rate of rise of β-hCG are more likely to fail. On the other hand, a normal rise does not necessarily guarantee the pregnancy will be normal. Up to 30 % of ectopic pregnancies mimic the β-hCG trend of an IUP. Therefore, rising β-hCG alone has a poor sensitivity and specificity for diagnosing ectopic pregnancy, and visual confirmation of pregnancy location is necessary [16, 17]. Condous and Kirk have advocated the use of a β-hCG ratio as a more reliable indicator of pregnancy viability for non-visible pregnancies (see Table 24.2) [18, 19]. It is important to note that this anticipated rise only applies if β-hCG is <2,000 mIU/ml, as above this level the rise is less predictable.

To assist in the diagnosis of abnormal pregnancy, Kadar proposed the use of a "discriminatory zone," the β-hCG concentration above which the gestational sac of an intrauterine pregnancy should be identified on ultrasound. His study of 53 women found that at β-hCG

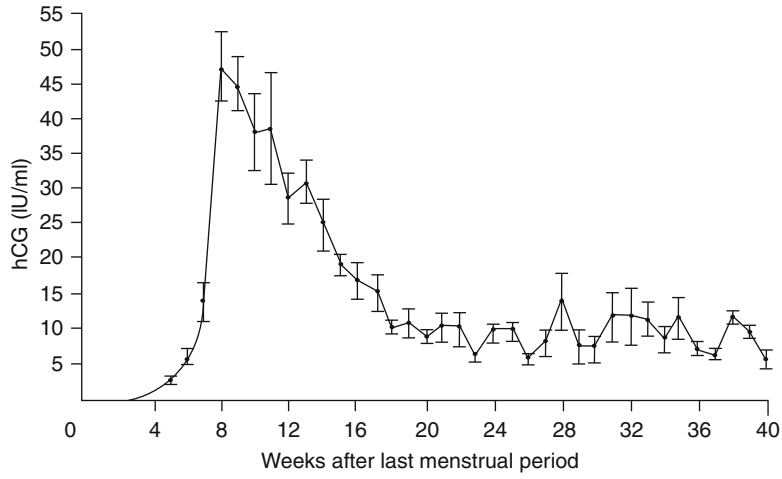

Fig. 24.1 Mean serum β-hCG levels throughout normal pregnancy: arithmetic scale used on ordinate. Bars represent SEM (Reprinted from Braunstein et al. [9]. With permission from Elsevier)

Table 24.2 β-hCG ratio as predictors of pregnancy viability (*β-hCG ratio = β-hCG at 48 h divided by β-hCG at 0 h*)

β-hCG ratio >1.66	Likely normal IUP
β-hCG ratio <0.79	Concerning for ectopic pregnancy
β-hCG ratio 0.79–1.66	Likely failed pregnancy

Adapted from Refs. [18, 19]

≥6,000–6,500 mIU/ml, a transabdominal ultrasound (TAU/S) was consistently able to detect the gestational sac, though not necessarily the fetal pole or cardiac activity, of an IUP. Below β-hCG of 6,000 mIU/ml, seeing an intrauterine gestational sac would not be anticipated [14]. With the advent of TVU/S with improved resolution due to a higher-frequency probe and less dependence of maternal body mass index for adequate visualization, the discriminatory zone has been lowered to 1,500–2,000 mIU/ml. [20–22] A more recent retrospective cohort study by Connolly reevaluated the discriminatory zone in 1,015 women presenting with vaginal bleeding, pain, or both in the first trimester of pregnancy. Using the higher-frequency 8–9-MHz TVU/S probe, the discriminatory zone for detection of the gestational sac, yolk sac, and fetal pole was 2,317, 9,975, and 35,486 mIU/ml, respectively [23]. The value for the gestational sac is higher than previously reported values. Additionally, this is the first report of a discriminatory zone for the yolk sac and fetal pole. This study also found a lower than previously reported threshold β-hCG for visualization of the gestational sac, 390 mIU/ml. The threshold values for yolk sac and fetal pole visualization were 1,094 and 1,394 mIU/ml, respectively, in viable pregnancies [23]. And as sonographic technology changes, the discriminatory zone and minimal threshold values will continue to evolve.

The American College of Radiology emphasizes that the discriminatory zone should not be taken as an absolute. Failure to visualize a pregnancy with a β-hCG above the discriminatory zone does not necessarily mean the pregnancy is abnormal. The ability to visualize a pregnancy at a very early gestation is influenced by factors such as ultrasound resolution, sonographer experience, maternal body habits, uterine orientation, and fibroids. [23] Additionally, pregnancies with structural or chromosomal anomalies, multifetal gestation, or those complicated by ovarian hyperstimulation syndrome may have a β-hCG above the discriminatory zone while being too early to visualize on ultrasound [23, 24]. Pregnancies complicated by ovarian hyperstimulation syndrome will initially have a high β-hCG due to hemoconcentration; levels then appear to plateau as post-hydration hemodilution sets in [25]. Therefore, it is important to correlate clinical age based on LMP or known date of conception with the β-hCG level and patient symptoms to avoid iatrogenic compromise of a potentially normal pregnancy.

If the β-hCG is below the discriminatory zone in an asymptomatic patient, TVU/S will rarely be diagnostic and therefore should not be ordered as its clinical utility and cost-effectiveness is low. TVU/S is clinically useful in a symptomatic patient with bleeding or pelvic pain even if the β-hCG is below the discriminatory zone as a life-threatening ectopic pregnancy or abortion may be diagnosed. An ectopic pregnancy can often be visualized below the discriminatory zone as ectopic pregnancies usually do not follow the normal β-hCG curve. Therefore, the ectopic pregnancy may be further along than suggested by the β-hCG. If the ultrasound is nondiagnostic and the patient is stable with no other symptoms, serial β-hCG levels can be obtained every 2 days until the discriminatory zone is reached or the location of the pregnancy becomes clinically apparent. This more conservative approach of waiting for a ultrasonographic diagnosis of ectopic in a stable patient rather than making ectopic a diagnosis of exclusion by empty uterus with positive β-hCG can save numerous normal pregnancies from iatrogenic termination [24]. If clinical suspicion for ectopic pregnancy is high, one can admit the patient to the hospital for serial abdominal exams and hemodynamic monitoring. Alternatively, if concerned for tubal rupture and hemoperitoneum, it is advisable to proceed directly to surgery even prior to obtaining a TVU/S as a ruptured ectopic can lead to

exsanguination as is the cause of 6 % of all pregnancy-related deaths [26].

Progesterone

Although serum progesterone and other hormones have been studied extensively in early pregnancy, they are rarely helpful and bring little management assistance in this clinical setting as compared to β-hCG and TVU/S.

Ultrasound

Sonography offers the clinician a consistent and reliable way to visualize the pelvic organs and aid in the diagnosis of early pregnancy and its complications. The American Congress of Obstetricians and Gynecologists lists indications for a first trimester ultrasound (see Table 24.3) [24].

A TVU/S uses a higher-frequency probe permitting visualization of pregnancy at an earlier gestation, as early as 4.5–5 weeks [23]. Additionally, the exam is less likely to cause iatrogenic distortion of the gestational sac as the bladder is empty and transducer pressure is not required [27]. Therefore, whenever TAU/S is not definitive, a TVU/S should be performed. The initial ultrasound should evaluate the pregnancy location and presence of a gestational sac, yolk sac, and fetal cardiac activity and measure the embryonic pole with crown rump length (CRL) to estimate gestational age. The accuracy of the ultrasound varies depending on quality of ultrasound equipment, sonographer experience, maternal body habitus, and obstructing pelvic organs such as fibroids or ovarian masses [28].

Table 24.3 The American Congress of Obstetricians and Gynecologists indications for a first trimester ultrasound

Confirmation of pregnancy, its location, and viability
Estimation of gestational age
Diagnosis of multifetal gestation
Evaluation of potential sources of vaginal bleeding and pelvic pain

Based on data from Ref. [30]

Ultrasound Characteristics of Normal Intrauterine Pregnancy

The first structure visualized in pregnancy is the gestational sac (Fig. 24.2). It can be seen as early as 4–5 weeks of gestation with an average mean sac diameter (MSD) of 2–3 mm [23]. Gestational age, in days, is estimated by adding 30 to the MSD (mm) [29]. The gestational sac diameter grows 0.2–1.0 mm/day [30, 31]. When the MSD reaches 5–13 mm, around 5–6 weeks gestation, the yolk sac should be visible (Fig. 24.3) [23]. Occasionally the embryo will be seen at this gestational age, but it may take 6–7 weeks with a MSD of 8–16 mm. Once visible, the embryo CRL grows 0.2–0.6 mm/day (Fig. 24.4) [30, 31]. By 8 weeks gestation, an embryo with a separate amniotic sac and yolk sac should be seen (Fig. 24.5) [32]. The approximate gestational age can be calculated by the following formula:

$$\mathrm{GA}\left(\text{gestational age in weeks}\right) = 6.5 + \mathrm{CRL}\left(\mathrm{cm}\right)$$

The presence of fetal cardiac activity confirms pregnancy viability (Fig. 24.6). The mean heart rate increases from 110 to 175 beats per minutes (bpm) from 5 to 9 weeks gestation. Jauniaux reported on a series of 15 studies showing a slow fetal heart rate, less than 80 bpm, is associated with increased risk of miscarriage. The greatest risk of spontaneous abortion is a gradually decreasing rather than increasing fetal heart rate [33]. Though there is some variation of normal

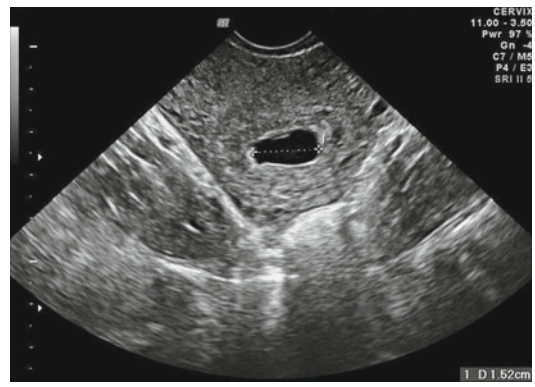

Fig. 24.2 Normal gestational sac in early pregnancy. MSD 15.2 mm

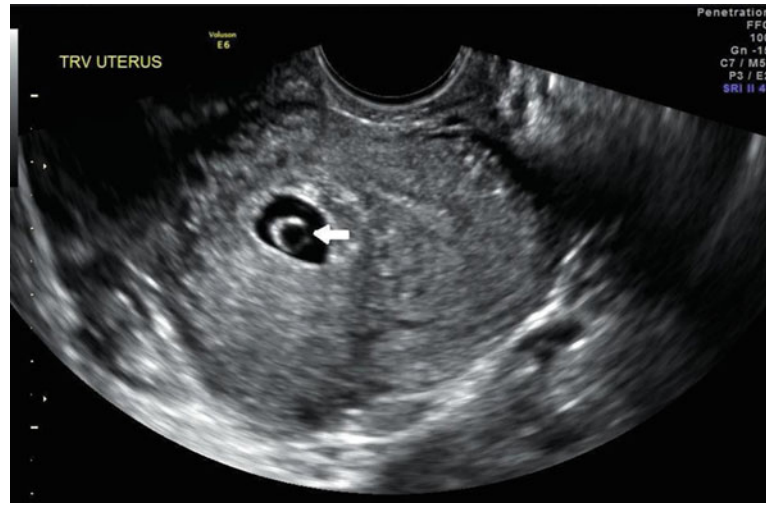

Fig. 24.3 Yolk sac (*white arrow*) within intrauterine gestational sac, fetal pole not yet visible

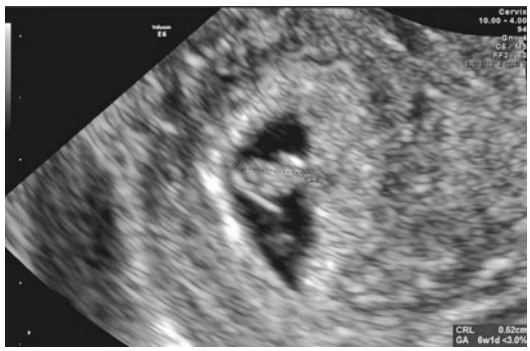

Fig. 24.4 Early fetal pole, measurable crown rump length 5.2 mm

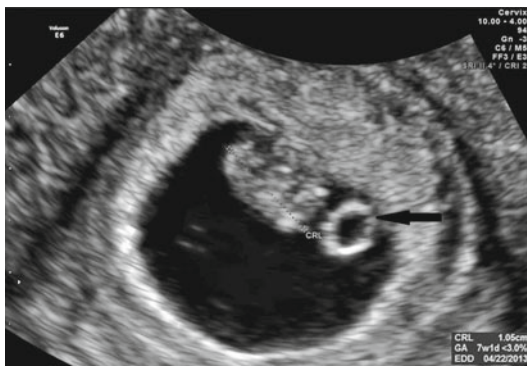

Fig. 24.5 Fetal pole (measured CRL) and yolk sac (*black arrow*)

embryonic growth, if the pre-specified criteria are not met (Table 24.4), the diagnosis of early pregnancy failure can be made with confidence.

Ultrasound Characteristics of Abnormal Pregnancy

Sonographic diagnosis of ectopic pregnancy can be difficult, and frequently the diagnosis is made by exclusion. Failure to identify an intrauterine pregnancy by TVU/S with a positive β-hCG above the discriminatory zone raises the potential for ectopic pregnancy. Characteristics of an ectopic pregnancy include either a mass in the adnexa that moves separate from the ovary or an extrauterine gestational sac which may or may not contain an embryo. Only 13 % of ectopic pregnancies have an obvious extrauterine gestational sac with a fetal pole [34]. Initial TVU/S has been reported to diagnose ectopic pregnancy with a 74 % sensitivity which increases to 94 % by the time of a follow-up scan [21]. Occasionally the pregnancy is too early to visualize the yolk sac or embryo, but there is a uterine fluid collection referred to as a decidual reaction or pseudogestational sac (Fig. 24.7). It can be differentiated from a true gestational sac associated with an IUP in that a pseudogestational sac is central rather than eccentrically located in the uterus, has an oval rather than circular shape, and lacks a thick chorionic ring [35, 36].

With a β-hCG above the discriminatory zone, estimated gestational age based on LMP of 5 weeks and absence of an intrauterine gestational sac, abnormal pregnancy is likely. This

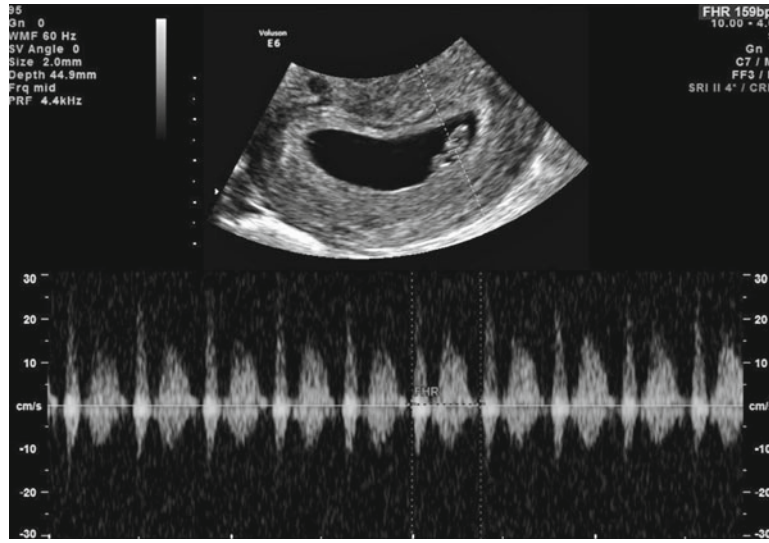

Fig. 24.6 Fetal cardiac activity noted at 6 weeks gestation, the first sign of pregnancy viability

Table 24.4 Anticipated sonographic findings in a normal intrauterine pregnancy by estimated gestational age

Weeks	Gestational sac (mean sac diameter, MSD)	Yolk sac	Embryo (crown rump length CRL)	Fetal cardiac activity
4+ 0/7 – 4+ 6/7	2–3 mm			
5+ 0/7 – 5+ 6/7	5–13 mm	Visible		
6+ 0/7 – 6+ 6/7	8–16 mm	Visible	Visible	
7+ 0/7 – 7+ 6/7	16–20 mm	Visible	Visible, CRL 16 mm	Visible
Expected growth	*0.2–1 mm/day*		*0.2–0.6 mm/day*	
Estimated gestational age in days	*MSD(mm)+30*			

Adapted from Abdallah et al. [31]. With permission from John Wiley & Sons, Inc.

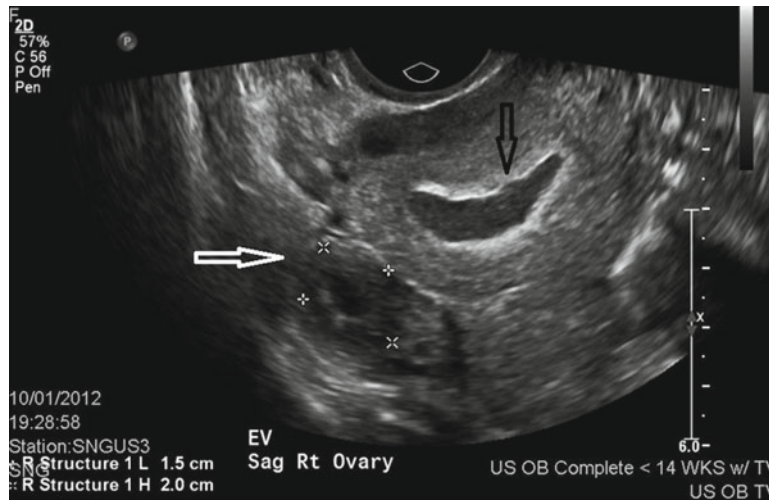

Fig. 24.7 Ectopic pregnancy. Decidual reaction with hyperechoic rim around pseudogestational sac (*black arrow*) and the ectopic in the right adnexa (*white arrow*) separate from the ovary

may be a failing or ectopic pregnancy. If the β-hCG continues to rise without visualizing an IUP, then the diagnosis is ectopic pregnancy. If an early unruptured ectopic pregnancy is diagnosed and the patient is stable and has no other contraindications, medical management with

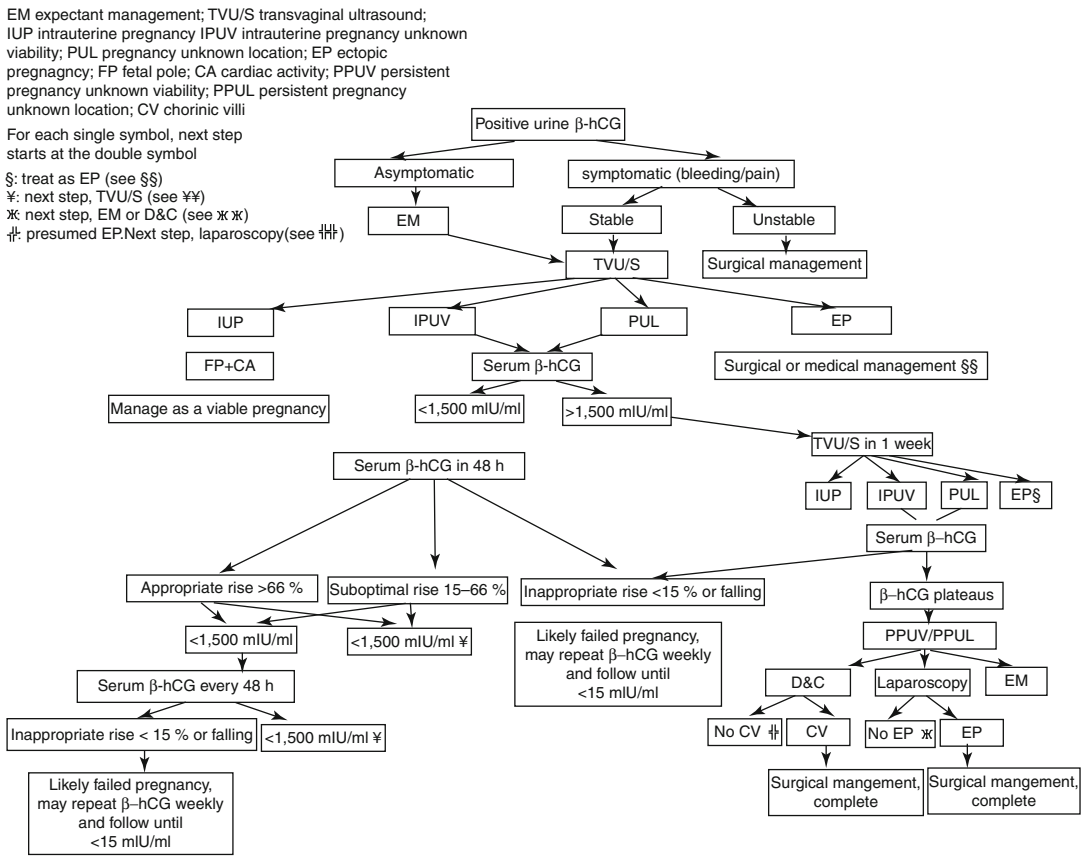

Fig. 24.8 Algorithm for management of early pregnancy

methotrexate is the preferred method of treatment as it is a fertility preserving therapy [2]. Conversely, if the β-hCG continues to fall without visualizing an IUP, then a spontaneous abortion is the likely diagnosis [37]. Therefore, it is recommended, in a stable patient, to follow the trend of the β-hCG and wait 1 week to repeat the ultrasound before any intervention to avoid iatrogenic compromise of a potentially normal pregnancy or use of a chemotherapeutic agent for a failing pregnancy (see Fig. 24.8). Occasionally the pregnancy will mimic that of both an intrauterine and an ectopic pregnancy. One must also be aware of the possibility of a heterotopic pregnancy. This is a rare situation seen in approximately 1:10,000–1:50,000 pregnancies but may be as high as 1:100 if a woman has conceived by assisted reproductive technology [38] (Fig. 24.9).

Pregnancy of Unknown Location (PUL)

One of the most difficult scenarios in early pregnancy is a pregnancy not visualized on ultrasound. This is the case for 8–31 % of women who present for examination in early pregnancy [39, 40]. The differential diagnosis for PUL includes an early intrauterine pregnancy <4.5 weeks, an early non-visualized ectopic pregnancy, or spontaneous abortion. A study of 135 women with PUL found 50 % of pregnancies resolved spontaneously as a presumed anembryonic pregnancy with resolution of β-hCG but no known passage of products of conception, 27 % were normal intrauterine pregnancies, 14 % ectopic, and 9 % miscarriages [40].

If the β-hCG is below the discriminatory zone, the American College of Radiology (ACR)

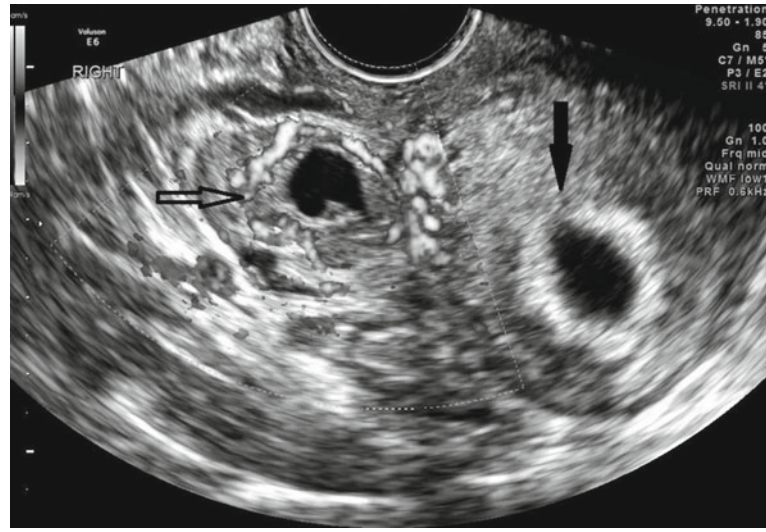

Fig. 24.9 Heterotopic pregnancy with a gestational sac in both the uterus (*solid arrow*) and adnexa (*outlined arrow*)

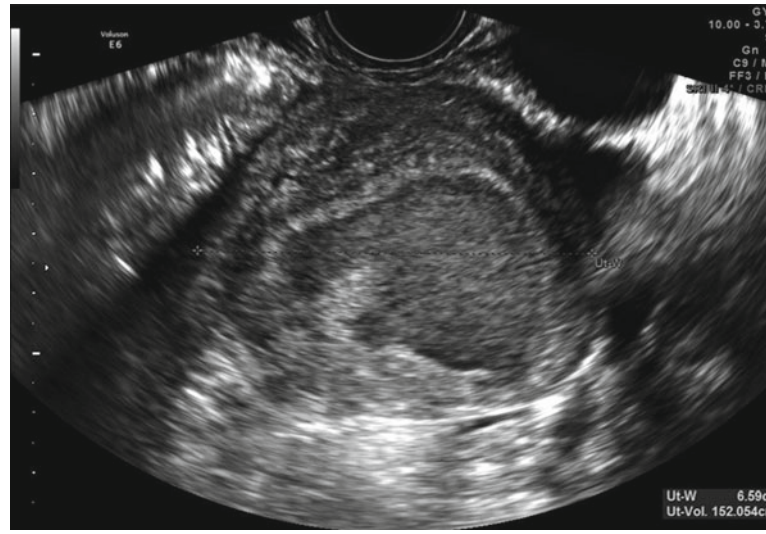

Fig. 24.10 Nonviable pregnancy. Pregnancy dated 9 weeks gestation by last menstrual period without gestational sac, yolk sac, and fetal pole. Hemorrhagic endometrium. Patient had falling β-hCG level

recommends repeating a quantitative β-hCG every 48 h until the discriminatory zone is reached [23]. Once at this level, an ultrasound should be performed to identify the pregnancy location. If the pregnancy is not visible in the uterus or adnexa, the patient is clinically asymptomatic, and the β-hCG is above the discriminatory zone, conservative management by serial β-hCGs is the best approach to avoid harm to a potentially normal pregnancy (*see* Fig. 24.8).

A falling β-hCG level suggests pregnancy loss as β-hCG should never fall during the first 12 weeks of a normal pregnancy. When embryonic demise is suspected based on an abnormal β-hCG, a repeat transvaginal ultrasound should be performed with a minimum 7 days interval between scans (Fig. 24.10) [35]. If the ultrasound continues to show an empty uterus and no adnexal mass and the patient remains asymptomatic and the β-hCG level falls, it is suggestive of a spontaneous abortion. In this case, the β-hCG should be followed until <15 mIU/ml [41].

When the β-hCG level plateaus or rises above the discriminatory zone and the pregnancy is not seen in the uterus, the diagnosis is an ectopic pregnancy or persistent pregnancy of unknown

Table 24.5 Characteristics of definitive intrauterine gestation and/or definitive viability above which absence of these features defines pregnancy failure when assessed with a transvaginal ultrasound

Organization	Estimated gestational age	Gestational sac (mean sac diameter)	Yolk sac	Fetus	B-hCG (mIU/ml)	Probe (MHz)
ACR	4.5–5	2–3 mm				
ACR SCOG		8 mm	*Visible*			9–5
ACR SCOG		8–16 mm 20 mm (*transabdominal*)		*Visible*	≥10,000	
ACOG		20 mm		*Visible*		
ACR ACOG SCOG	6.2–7			≥5 mm CRL *Cardiac activity*		M-mode

Adapted from Refs. [24, 25, 33, 46]
ACR American College of Radiology, *ACOG* American Congress of Obstetricians and Gynecologist, *SCOG* Society of Obstetricians and Gynaecologists of Canada, *RCOG* Royal College of Obstetricians and Gynecologists

location. In this difficult scenario, some recommend definitive diagnosis and treatment by dilation and curettage, laparoscopy, or methotrexate due to the risk of ectopic pregnancy. In some cases with a low β-hCG, a more conservative approach with expectant management has been shown to be safe and not associated with adverse outcomes [42, 43].

Ultrasound Characteristics of Early Pregnancy Failure and Intrauterine Pregnancy of Unknown Viability

When the ultrasound reveals an IUP but neither an embryonic pole nor fetal heart activity is identified, the pregnancy is classified as an intrauterine pregnancy of unknown viability (IPUV). Jeve et al. performed a metanalysis of sonographic features associated with early embryonic demise and found a false-negative rate of zero with:

1. MSD ≥16–17 mm with neither a yolk sac nor fetal pole
2. CRL ≥5–6 mm with absence of fetal cardiac activity [44, 45]

The reported measurements for diagnosing pregnancy failure are listed by national organization in Table 24.5. These measurements are highly reproducible, making them an accurate way to determine viability [9]. In situations where the clinical diagnosis based on ultrasound is uncertain, follow up ultrasound in 7–14 days to confirm pregnancy viability is recommended. [30]. This time frame is appropriate as approximately 90 % of incomplete abortions and 50 % of missed abortions can be expected to spontaneously abort within 2 weeks of initial presentation and ultrasound [39]. If there is any uncertainty in the diagnosis, failure to visualize a yolk sac or embryo on a repeat scan after at least 7 days is always associated with spontaneous abortion [46].

Case Scenario

The patient's serum β-hCG is 652 mIU/ml.

Though the β-hCG is below the discriminatory zone, the patient presented with pelvic pain concerning for an ectopic pregnancy or abortion. A TVU/S was ordered. The ultrasound report reads "Normal sized uterus and ovaries. No intrauterine pregnancy visualized. No ectopic pregnancy noted in right or left adnexal region but the possibility of ectopic pregnancy is not excluded, please correlate clinically."

The patient's pain improved with acetaminophen and hydration. She feels comfortable going home knowing her symptoms are attributable to her pregnancy. The patient understands

the limitation of ultrasound to see the conception at such an early stage. She is sent home with strict ectopic precautions to return for worsening bleeding or pain. She is scheduled to have a repeat β-hCG in 48 h, and if the level is above the discriminatory zone at that time, an ultrasound will be scheduled.

The repeat β-hCG level at 48 h was 1,652 mIU/ml. The β-hCG level is now above the discriminatory zone. An ultrasound is scheduled for 2 days later. The following day, however, the patient returns to the emergency department due to worsening abdominal cramping and the fact that she started having her "period."

Her vital signs are stable. Physical exam reveals mild right adnexal tenderness and a closed cervix with scant blood

A transvaginal ultrasound reveals a gestational sac noted in the uterus measuring 7 mm. There is no visible yolk sac or embryo. The left and right ovary measure within normal limits with normal blood flow to each ovary. There were no ultrasound findings of an ectopic pregnancy.

The patient is informed of the results. She is confused

What is the diagnosis and how to proceed?

At this time you can assure the patient that she is pregnant and the pregnancy is in the uterus. It is unlikely that she would have a heterotropic pregnancy as the adnexal structures are normal and this pregnancy was a natural conception. The viability of the pregnancy cannot yet be determined and would rely upon a repeat scan in about 1 week. Neither D&C, laparoscopy, nor methotrexate should be considered at this time.

The patient is discharged home with follow-up ultrasound and prenatal appointment scheduled for 1 week. The follow-up ultrasound showed a normally developing embryo with a fetal heart rate of 160 bpm.

Conclusion

Patients presenting in early pregnancy with either bleeding or pain continue to present diagnostic and management dilemmas. With the availability of medical treatment options with methotrexate as well as surgery, recognition of an ectopic pregnancy at the earliest time, especially prior to rupture, will enhance the patient's future fertility potential. The combination of quantitative β-hCG and transvaginal ultrasound of the pelvis will lead to accurate diagnosis in the majority of cases. When initial evaluation is uncertain, patience, close observation, and follow-up TVU/S and β-hCG will clarify the situation. Surgical or medical management must be delayed until a definitive diagnosis is made. Maternal awareness and participation in all aspects of her evaluation and treatment will be helpful to avoid untoward clinical or medical legal consequences.

References

1. Wittels KA, Pelletier AJ, Brown DFM, et al. United States emergency department visits for vaginal bleeding during early pregnancy, 1993–2003. Am J Obstet Gynecol. 2008;198:523.e1–6.
2. American College of Obstetricians and Gynecologists. Medical management of ectopic pregnancy. ACOG practice bulletin no. 94. Obstet Gynecol. 2008;111:1479–85.
3. Davies S, Byrn F, Cole L. Human chorionic gonadotropin testing for early pregnancy viability and complications. Clin Lab Med. 2003;23:257–64.
4. First week of development: ovulation to implantation. In: Sadler TW, editor. Langman's medical embryology. 10th ed. Baltimore: Lippincott Williams & Wilkins; 2006. p. 31–43.
5. Second week of development: bilaminar germ disc. In: Sadler TW, editor. Langman's medical embryology. 10th ed. Baltimore: Lippincott Williams & Wilkins; 2006. p. 46–53.
6. Romero R, Copel JA, Kadar N, Jeanty P, Decherney A, Hobbins J. Value of culdocentesis in the diagnosis of ectopic pregnancy. Obstet Gynecol. 1985;65(4):519–22.
7. Kletzky OA, Rossman F, Bertolli SI, Platt LD, Mishell Jr DR. Dynamics of human chorionic gonadotropin, prolactin, and growth hormone in serum and amniotic fluid throughout normal human pregnancy. Am J Obstet Gynecol. 1985;151(7):878–84.

8. Keay SD, Vatish M, Karteris E, Hillhouse EW, Randeva HS. REVIEW: the role of β-hCG in reproductive medicine. BJOG. 2004;111:1218–28. doi:10.1111/j.1471-0528.2004.00412.x.
9. Braunstein GD, Rasor J, Hanser H, et al. Serum human chorionic gonadotropin levels throughout normal pregnancy. Am J Obstet Gynecol. 1976;126:678.
10. Fritz MA, Guo SM. Doubling time of human chorionic gonadotropin (β-hCG) in early normal pregnancy: relationship to β-hCG concentration and gestational age. Fertil Steril. 1987;47(4):584.
11. Kadar N, DeVore G, Romero R. Discriminatory β-hCG zone: its use in the sonographic evaluation for ectopic pregnancy. Obstet Gynecol. 1981;58(2):156–61.
12. Barnhart KT, Sammel MD, Rinaudo PF, Zhou L, Hummel AC, Guo W. Symptomatic patients with an early viable intrauterine pregnancy: HCG curves redefined. Obstet Gynecol. 2004;104:50–5.
13. Morse C, Sammel M, Shaunik A, Allen-Taylor L, Oberfoell N, Tackacs P, Chung K, Barnhart K. Performance of human chorionic gonadotropin curves in women at risk for ectopic pregnancy: exceptions to the rules. Fertil Steril. 2012;97(1):101–6.
14. Romero R, Kadar N, Jeanty P, Copel J, Chervenak F, DeCherney A, Hobbins J. Diagnosis of ectopic pregnancy: value of human chorionic gonadotropin zone. Obstet Gynecol. 1985;66(3):357–60.
15. Barnhart KT, Katz I, Hummel A, Gracia CR. Presumed diagnosis of ectopic pregnancy. Obstet Gynecol. 2002;100(3):505–10.
16. Silva C, Sammel MD, Zhou L, Gracia C, Hummel AC, Barnhart K. Human chorionic gonadotropin profile for women with ectopic pregnancy. Obstet Gynecol. 2006;107(3):605–10.
17. Shepherd R, Patton P, Novy M, Burry K. Serial β-hCG measurements in the early detection of ectopic pregnancy. Obstet Gynecol. 1990;75(3):417–20.
18. Condous G, Kirk E, Van Calster B, Van Huffel S, Timmerman D, Bourne T. Failing pregnancies of unknown location: a prospective evaluation of the human chorionic gonadotrophin ratio. BJOG. 2006;113:521–7.
19. Reid S, Condous G. Is there a need to definitively diagnose the location of a pregnancy of unknown location? The case for "no". Fertil Steril. 2012;98(5):1085–90.
20. Cacciatore B, Stenman U, Ylostalo P. Diagnosis of ectopic pregnancy by vaginal ultrasonography in combination with a discriminatory serum β-hCG level of 1000 IU/1 (IRP). BJOG. 1990;97:904–8.
21. Condous G, Kirk E, Lu S, VanHuffel S, Gevaert O, DeMoor B, DeSmet F, Timmerman D, Bourne T. Diagnostic accuracy of varying discriminatory zones for the prediction of ectopic pregnancy in women with a pregnancy of unknown location. Ultrasound Obstet Gynecol. 2005;26(7):770–5.
22. Mol B, Hajeniius PJ, Engelsbel S, Ankum W, VanderVeen F, Hemrika D, Bossuyt P. Serum human chorionic gonadotropin measurement in the diagnosis of ectopic pregnancy when transvaginal sonography is inconclusive. Fertil Steril. 1998;70(5):972–81.
23. Connolly AM, Ryan DH, Stuebe AM, Wolfe HM. Reevaluation of discriminatory and threshold levels for serum β-hCG in early pregnancy. Obstet Gynecol. 2013;121(1):65–70.
24. American College of Radiology. ACR appropriateness criteria for first trimester bleeding. 2012. http://www.acr.org/~/media/ACR/Documents/AppCriteria/Diagnostic/SecondAndThirdTrimesterBleeding.pdf. Last accessed on 4 Dec 2012.
25. AIUM practice guideline for the performance of obstetric ultrasound. 2007. http://www.aium.org/resources/guidelines/obstetric.pdf. Last accessed on 4 Dec 2012.
26. Seeber B. What serial hCG can tell you, and cannot tell you, about an early pregnancy. Fertil Steril. 2012;98(5):1074–7.
27. Hoover KW, Tao G, Kent CK. Trends in the diagnosis and treatment of ectopic pregnancy in the United States. Obstet Gynecol. 2010;115:495–502.
28. Pexsters A, Luts J, Van Schoubroeck D, Bottomley C, Van Calster B, Van Huffel S, Abdallah Y, D'Hooghe T, Lees C, Timmerman D, Bourne T. Clinical implications of intra- and interobserver reproducibility of transvaginal sonographic measurement of gestational sac and crown–rump length at 6–9 weeks' gestation. Ultrasound Obstet Gynecol. 2011;38:510–5.
29. Goldstein S, Snyder JR, Watson C, Danon M. Very early pregnancy detection with endovaginal ultrasound. Obstet Gynecol. 1988;72(2):200–4.
30. American College of Obstetricians and Gynecologists. Ultrasonography in pregnancy. ACOG practice bulletin no. 101. Obstet Gynecol. 2009;113:451–61.
31. Abdallah Y, Daemen A, Guha S, Syed S, Naji O, Pexsters A, Kirk E, Stalder C, Gould D, Ahmed S, Bottomley C, Timmerman D, Bourne T. Gestational sac and embryonic growth are not useful as criteria to define miscarriage: a multicenter observational study. Ultrasound Obstet Gynecol. 2011;38:503–9.
32. Abdallah Y, Daemen A, Kirk E, Pexsters A, Naji O, Stalder C, Gould D, Ahmed S, Guha S, Syed S, Bottomley C, Timmerman D, Bourne T. Limitations of current definitions of miscarriage using mean gestational sac diameter and crown–rump length measurements: a multicenter observational study. Ultrasound Obstet Gynecol. 2011;38:497–502.
33. Society Obstetricians Gynecologists of Canada. Ultrasound evaluation of first trimester pregnancy complications. SOGC clinical practice guidelines. J Obstet Gynaecol Can. 2005;161:581–585.
34. Jauniaux E, Johns J, Burton J. The role of ultrasound imaging in diagnosing and investigating early pregnancy failure. Ultrasound Obstet Gynecol. 2005;25:613–24.
35. VanMello NM, Mol F, Ankum W, Mol BW, van der Veen F, Hajenius PJ. Ectopic pregnancy: how the diagnostic and therapeutic management has changed. Fertil Steril. 2012;98(5):1066–73.
36. Doubliet PM, Benson CB. First, do no harm…to early pregnancies. J Ultrasound Med. 2010;29:685–9.

37. Branch DW, Gibson M, Silber R. Clinical practice. Recurrent miscarriage. N Engl J Med. 2010;363(18): 1740–7.
38. Hatley W, Chase J, Campbell S. Establishing the death of an embryo by ultrasound: report of a public inquiry with recommendations. Ultrasound Obstet Gynecol. 1995;5:353–7.
39. Chang HJ, Chang SS. Ectopic pregnancy after assisted reproductive technology: what are the risk factors? Curr Opin Obstet Gynecol. 2010;22:202–7.
40. Banerjee S, Aslam N, Zosmer N, Woelfer B, Jrkovic D. The expectant management of early pregnancy of unknown location. Ultrasound Obstet Gynecol. 1999;14:231–6.
41. Barnhart K, van Mello NM, et al. Pregnancy of unknown location: a consensus statement of nomenclature, definitions and outcome. Fertil Steril. 2011; 95(3):857–66.
42. Condous G, Okaro E, Bourne T. The conservative management of early pregnancy complications: a review of the literature. Ultrasound Obstet Gynecol. 2003;22:420–30.
43. Rubal L, Chung K. Do you need to definitively diagnose the location of a pregnancy of unknown location? The case for "yes". Fertil Steril. 2012;98(5): 1078–84.
44. Barnhart K. Early pregnancy failure: beware of the pitfalls of modern management. Fertil Steril. 2012; 98(5):1061–5.
45. Jeve Y, Rana R, Bhide A, Thangaratinam S. Accuracy of first-trimester ultrasound in the diagnosis of early embryonic demise: a systematic review. Ultrasound Obstet Gynecol. 2011;38:489–96. doi:10.1002/uog.10108.
46. Royal College of Obstetricians and Gynaecologists. The management of early pregnancy loss. Guideline no. 21. London: RCOG; 2006.

Ultrasound Evaluation of Ectopic Pregnancy

25

Donald L. Fylstra

Ectopic pregnancy, the implantation of a fertilized ovum outside the uterine cavity, has been increasing in number at a staggering pace and now accounts for 2 % of all pregnancies in the United States [1]. Since many ectopic pregnancies are now treated in an outpatient setting, true current numbers are hard to obtain. Nearly all ectopic pregnancies (97 %) are implanted within the fallopian tube, and a common factor for the development of such ectopics is the presence of a pathological fallopian tube. Causes of such pathology include genital tract infection caused by gonorrhea and chlamydia, tubal surgery including tubal sterilization, previous ectopic pregnancy, and in utero exposure to diethylstilbestrol [2, 3]. Other risk factors for tubal ectopic pregnancy include conception with an intrauterine contraceptive device in place and conception while using a progesterone-only contraceptive method [4, 5].

Ectopic implantation can also occur outside of the fallopian tube, within the cervix, ovary, abdomen, uterine cornua, and cesarean scars. These extratubal implantations may not be associated with tubal pathology or the expected preexisting risk factors for tubal ectopic implantation.

D.L. Fylstra, MD
Department of OBGYN, Medical University of South Carolina, 96 Jonathan Lucas St., LSB 634 F, Charleston 29425, SC, USA
e-mail: fylstrad@musc.edu

The imaging modality of choice for the diagnosis of early pregnancy, regardless of implantation site, is transvaginal ultrasound.

The discriminatory zone of human chorionic gonadotropin (hCG) is that level of hCG, which, when reached, an intrauterine pregnancy should be identified within the endometrial cavity with transvaginal ultrasound, when the pregnancy is *normal and singleton*. The discriminatory zone of hCG is usually 1,500 mIU/ml. Normal and singleton is important because of the frequent misinterpretation of the hCG discriminatory zone. Waiting until the discriminatory zone of hCG is reached before performing a transvaginal ultrasound could miss early gestational pathology such as an extrauterine implantation (abnormal pregnancies may have hormone levels that are lower at any given gestation age). Likewise, failure to identify an intrauterine gestation with transvaginal ultrasound when the hCG level is greater than the discriminatory zone may miss an early multiple gestation, particularly those pregnancies that are the result of assisted reproductive technologies.

The confirmation of an intrauterine pregnancy with transvaginal ultrasound relies upon recognition, initially of a true gestational sac, followed soon thereafter, by recognition of structures within the sac consistent with a developing embryo. The term "gestational sac" is a sonographic term and not an anatomical structure. A true gestational sac has a thick echogenic rim, a trophoblastic decidual reaction, surrounding a sonolucent center, the chorionic sac. The intradecidual sign is the presence

L.A. Stadtmauer, I. Tur-Kaspa (eds.), *Ultrasound Imaging in Reproductive Medicine*,
DOI 10.1007/978-1-4614-9182-8_25,

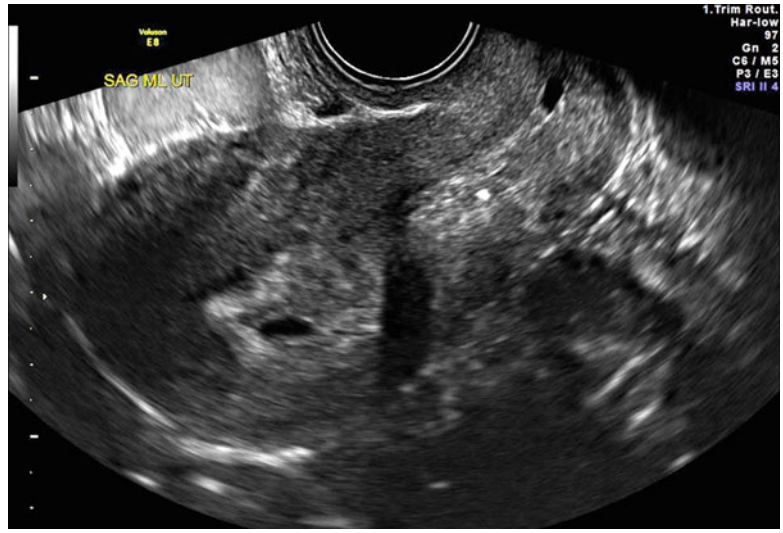

Fig. 25.1 Transvaginal ultrasound: early intrauterine gestational sac, "the intradecidual sign"

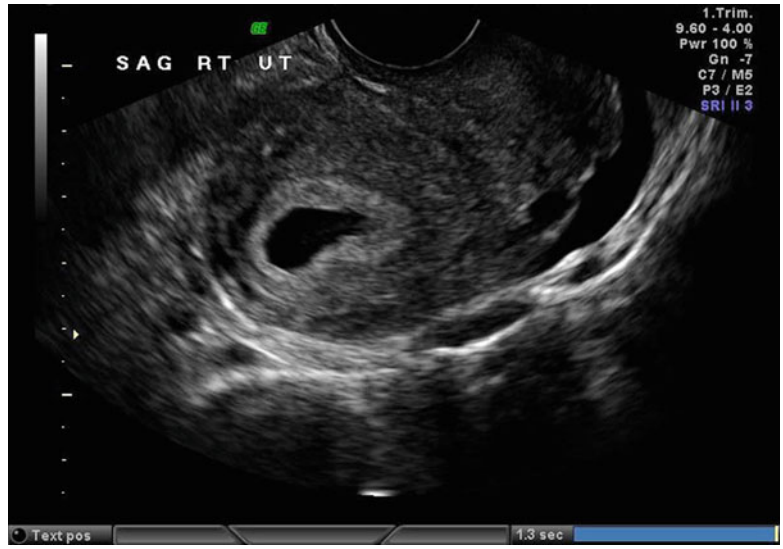

Fig. 25.2 Transvaginal ultrasound: intrauterine pseudosac associated with an ectopic pregnancy

of such a sac buried *beneath* the surface of the endometrium, appearing eccentrically positioned within the endometrium (Fig. 25.1). A "pseudosac" is a collection of fluid *within* the endometrial cavity itself, created by bleeding from the decidualized endometrium associated with an extrauterine pregnancy implantation (Fig. 25.2). The precise location of such an early sonolucent uterine fluid collection should distinguish between a true gestational sac and a pseudosac.

The yoke sac is the first visible structure within the gestational sac and is a distinct circular structure with a bright echogenic rim and sonolucent center (Fig. 25.3) and is recognized 3 weeks post-conception (5 weeks after the last menstrual period). The embryo is first recognized as a thickening along an edge of the yoke sac (Fig. 25.4), and embryonic cardiac motion can be first observed 3 1/2 to 4 weeks post-conception (5 1/2–6 weeks after last menstrual period). When exact pregnancy dating is available, an intrauterine pregnancy, regardless of embryonic number, should be identified within the endometrial cavity with transvaginal ultrasonography by 24 embryonic days or 38 menstrual days (exact 28 day menstrual cycle). This exact

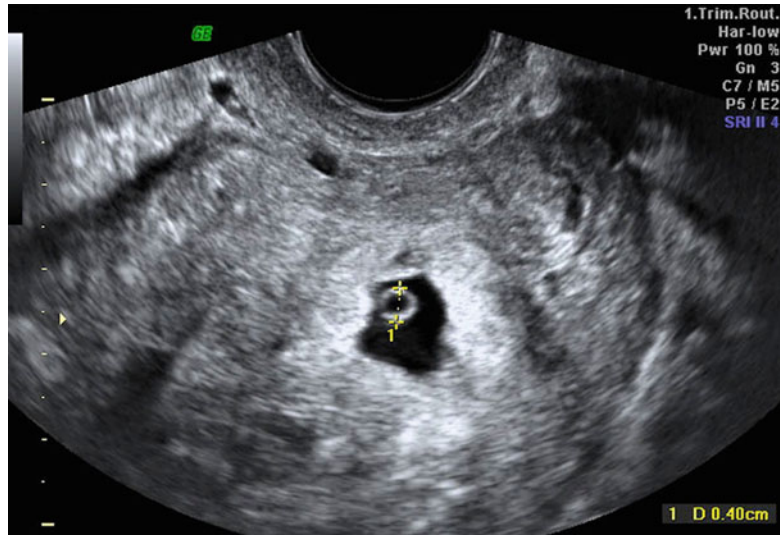

Fig. 25.3 Transvaginal ultrasound: intrauterine gestational sac containing a yolk sac

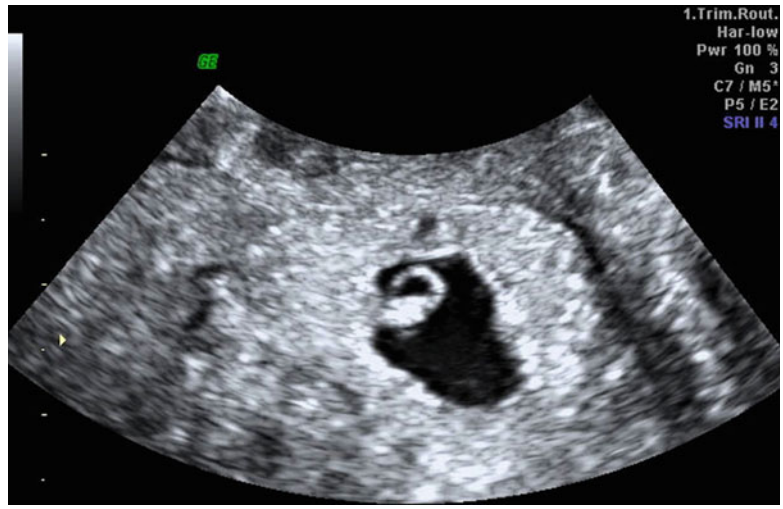

Fig. 25.4 Transvaginal ultrasound: thickened edge of a yolk sac representing an early developing embryo (embryonic cardiac activity may be present)

pregnancy dating does not rely on human chorionic gonadotropin, hCG, levels. Without such exact pregnancy dating and with no intrauterine pregnancy identified with transvaginal sonography, the "nondiagnostic ultrasound," a serum level of hCG is needed for ultrasound interpretation [6]. A word of caution, because of the variation in vaginal ultrasound technical and interpretive abilities and lab hCG levels, before embarking on treatment for a presumed ectopic pregnancy, especially with methotrexate, give every pregnancy the "benefit of the doubt." Be certain of the diagnosis or use diagnostic laparoscopy for confirmation.

Additional information can be gained from transvaginal ultrasound measurement of the endometrial echo in early gestation, before the recognition of a gestational sac. Spandorfer and Barnhart reported statistically different endometrial echo thicknesses between patients with normal intrauterine, failed intrauterine, and ectopic gestations [7]. Patients with normal pregnancies had endometrial echo thicknesses of 13.42 ± 0.68 mm. In contrast, those with failed intrauterine and ectopic gestations measured 9.28 ± 0.88 and 5.95 ± 0.35 mm, respectively ($P < .01$). In this report, 97 % of patients with an echo no greater than 8 mm

had abnormal pregnancies, and 71 % of these abnormal pregnancies were ectopic in location. Only 41 % of those patients with an echo thickness greater than 8 mm were abnormal, and only 14.7 % were ectopic in location. No patient with an endometrial echo thickness greater than 13 mm had an ectopic pregnancy, and no patients with an echo thickness less than 6 mm had a normal pregnancy. These are well-stratified differences, but other authors have seen much more overlap with endometrial echo measurements.

Usually, the transvaginal ultrasound identification of an intrauterine pregnancy reliably excludes an extrauterine implantation, except in the case of heterotopic pregnancy: the coexistence of an extrauterine implantation with an intrauterine pregnancy. The natural occurrence of heterotopic pregnancy is 1 in 4,000 pregnancies, but the frequency is much greater with pregnancies conceived with assisted reproductive technologies. Should a clinical presentation or abnormal pelvic ultrasound appearance suggest an ectopic pregnancy, despite visualization of an intrauterine gestation, the diagnosis of heterotopic pregnancy should be considered, with the probable need for diagnostic laparoscopy confirmation and treatment.

The possibility of ectopic pregnancy is frequently considered before hCG has reached the discriminatory zone and before ultrasound recognition [8]. Human chorionic gonadotropin rises exponentially in early normal pregnancy and should rise at least by 53 % in 48 h [9]. This exponential rise is less reliable after 10,000 mIU/ml, and at this level, pregnancy is better evaluated with ultrasound. Fifteen percent of normal intrauterine pregnancies can demonstrate an abnormal early rise of hCG, but for the majority of gestations, when the hCG rise is abnormal, at a plateau, or falling, an abnormal pregnancy is confirmed but not its location [10].

Cervical Pregnancy

Less than 1 %, and the rarest, of ectopics are implanted within the cervical canal below the level of the internal cervical os [11, 12]. The etiology of such implantations is unknown, but predisposing factors include prior uterine curettage, induced abortion, Asherman's syndrome, leiomyomata, presence of an intrauterine device, in vitro fertilization, and prior in utero exposure to diethylstilbestrol [13–16].

Before the now common use of early pregnancy transvaginal ultrasound, cervical pregnancies were frequently diagnosed at the time of spontaneous abortion or reached the second trimester, both associated with life-threatening hemorrhage frequently requiring hysterectomy as treatment. Usually, the first complaint is painless vaginal bleeding and speculum examination may reveal an open external cervical os with a fleshy-type endocervical mass presenting. With early transvaginal ultrasound, these implantations are easily identified (Fig. 25.5) and can, thus, be treated with conservative fertility-sparing options.

Rankin suggested that the diagnosis by ultrasound examination of cervical pregnancy required 4 criteria: enlargement of the cervix, uterine enlargement, diffuse amorphous intrauterine echoes, and absence of an intrauterine pregnancy [17]. Timor-Tritsch et al. refined the criteria to include the placenta and entire chorionic sac containing the pregnancy must be below the internal cervical os and the cervical canal must be dilated and barrel shape [18].

If necessary to exclude the diagnosis of a spontaneous abortion in progress, the presence of embryonic cardiac activity and/or Doppler ultrasound indicating vascular attachment confirms a living pregnancy.

Ovarian Pregnancy

One half of one percent to almost 3 % of ectopics are implanted within the ovary [11, 19]. Ovarian pregnancy like other non-tubal ectopic pregnancies may occur without the usual expected antecedent risk factors for ectopic pregnancy but does seem to have a strong association with conceptions with an intrauterine contraceptive device in place [20, 21]. The presenting signs and symptoms are similar to other ectopic pregnancies: positive pregnancy test, abdominal pain, and vaginal bleeding.

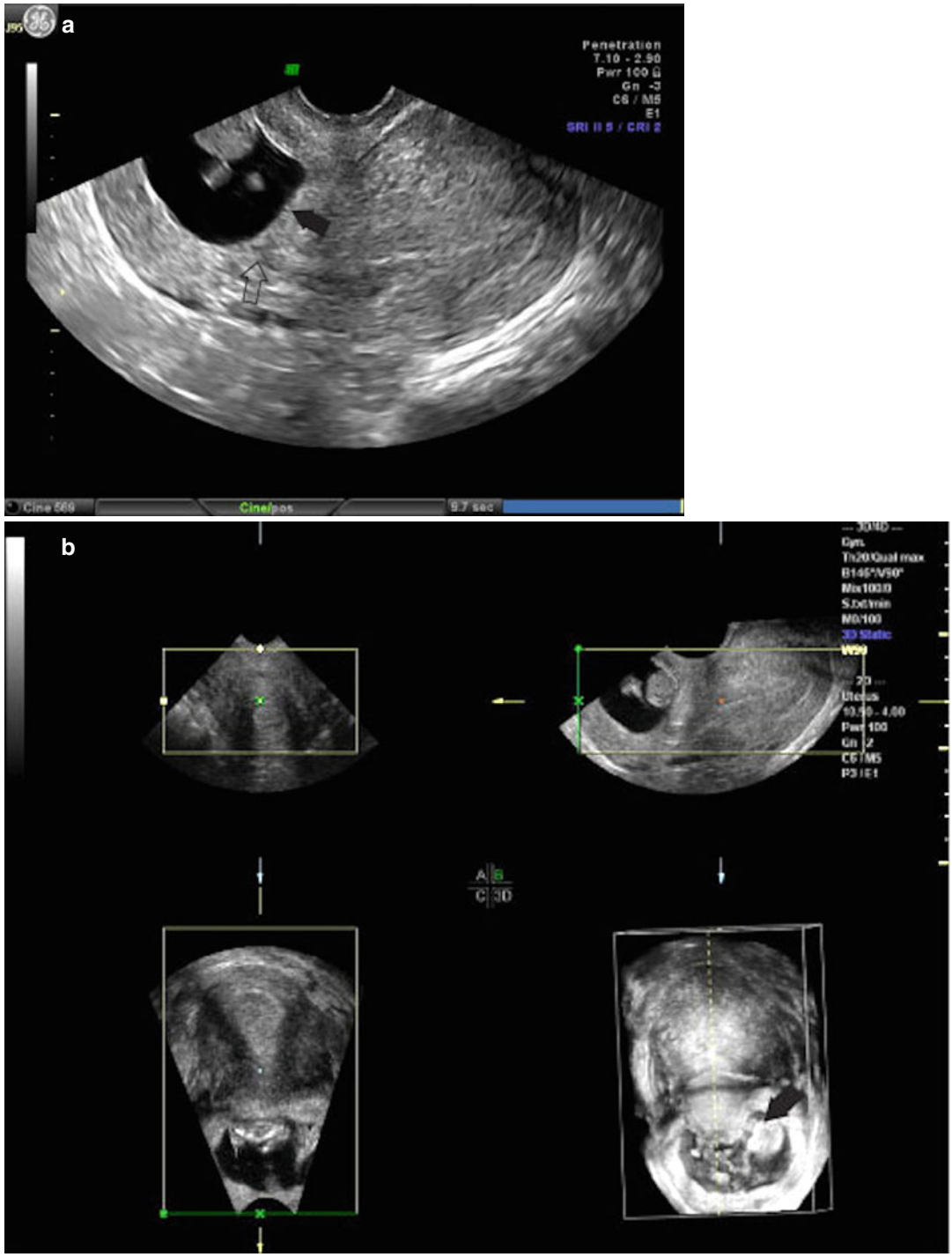

Fig. 25.5 (**a**) Transvaginal ultrasound, midline sagittal image: cervical pregnancy, (*closed arrow*) points to the cervical pregnancy within the (*open arrow*) points to cervical canal. (**b**) Transvaginal ultrasound: 3D rendering of a cervical pregnancy, (*closed arrow*) points to the internal cervical os

It is difficult to preoperatively make the diagnosis of ovarian pregnancy. An ultrasound finding suggesting ovarian implantation is a walled cystic mass within or adjacent to an ovary, but this does not exclude a corpus luteum and a tubal implantation. Doppler cannot

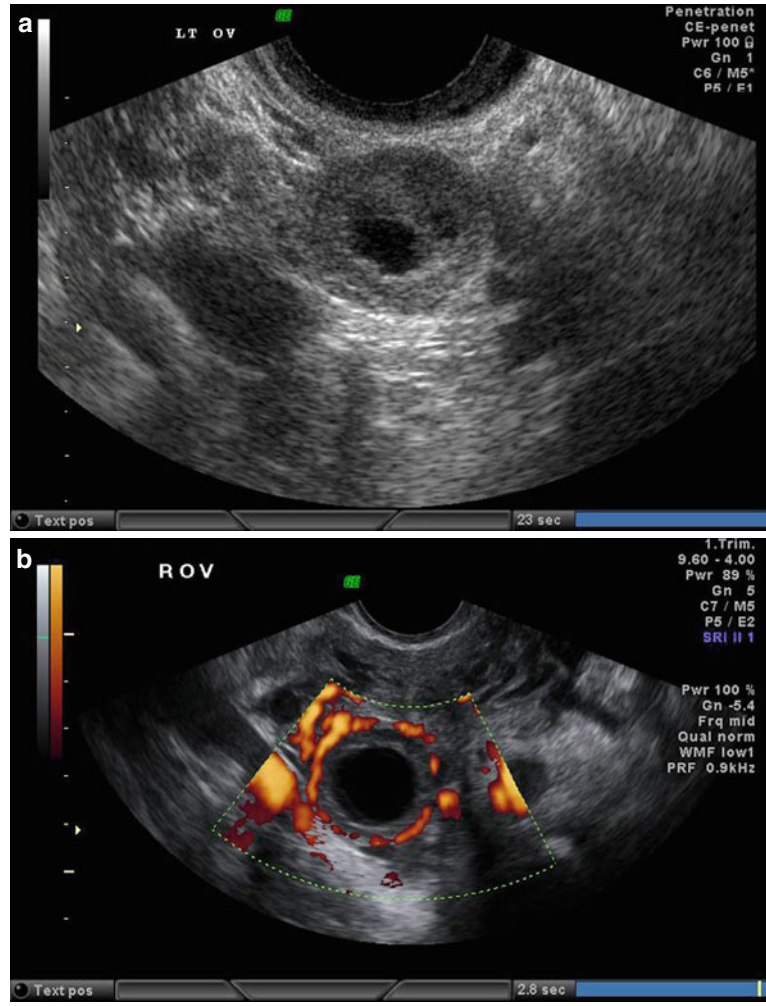

Fig. 25.6 (**a**) Transvaginal ultrasound of an ovarian corpus luteum cyst. (**b**) Transvaginal ultrasound: color Doppler imaging of an ovarian corpus luteum cyst

distinguish between a corpus luteum and an ovarian pregnancy implantation (Fig. 25.6). This diagnosis is usually a pathological diagnosis: made by microscopic examination of a surgically removed adnexal mass, via laparotomy or laparoscopy, based on Speigelberg's criteria: the tube must be intact and distinctly separate from the ovary, the gestational sac must occupy the normal anatomical location of the ovary, the gestational sac must be connected to the uterus by the utero-ovarian ligament, and unquestioned ovarian tissue must be demonstrated in the wall of the gestational sac [22].

It is important for the laparoscopic surgeon to understand that an ovarian pregnancy can look like a corpus luteum ovarian cyst upon direct inspection, and cystectomy and pathology only will reveal the true diagnosis. However, when an adnexal ectopic is diagnosed with a nonsurgical algorithm, conservative medical therapy can be successful without a true diagnosis of location.

Abdominal Pregnancy

Less than 1 % of ectopic pregnancies are implanted within the abdominal cavity [11, 23]. The pathogenesis of abdominal implantation is controversial. Many are the result of secondary nidation within the peritoneal cavity after tubal abortion, tubal rupture or uterine rupture [24]. True primary abdominal implantation must

satisfy the criteria of Studdiford. Studdiford, reporting a primary peritoneal implantation in 1942, established three criteria for such a primary abdominal pregnancy: normal fallopian tubes with no evidence of recent or remote trauma, the absence of any uteroperitoneal fistula, and the presence of a pregnancy related exclusively to the peritoneal surface and early enough to eliminate the possibility of secondary implantation following a primary nidation within the tube [25].

The most common abdominal implantation site is the posterior cul-de-sac, followed by the mesosalpinx, the omentum, the bowel and its mesentery, and the peritoneum of the pelvic and abdominal walls, including the anterior cul-de-sac [23]. Other reported locations include the retroperitoneal space, the appendix, the liver, and the spleen [26–31].

With the universal use of early pregnancy imaging, the diagnosis can be confirmed at an early gestational age, but this requires imaging demonstrating a continuity of the cervix and uterus without pregnancy contents, like other ectopic implantations. The presence of an adnexal mass suggestive of ectopic pregnancy, when no intrauterine gestation is identified, could be an ectopic pregnancy of any location, including an abdominal implantation. Failure to follow basic ultrasound principles can miss the diagnosis. Such early diagnosis can spare maternal mortality at the expense of fetal mortality, with a perinatal mortality rate of 40–95 % [32].

Cesarean Scar Ectopic Pregnancy

Although previously rare, the incidence of pregnancy implantation within the scar of a prior cesarean is increasing due to the increasing number of cesarean deliveries. The natural history of such a condition is unknown, but uterine scar rupture and hemorrhage, even in the first trimester, seems likely if the pregnancy is allowed to continue, with possible serious maternal morbidity and the possible need for hysterectomy and loss of subsequent fertility. Early diagnosis of such implantation is made only with a high level of suspicion: early ultrasound in a woman with a prior cesarean delivery (Fig. 25.7).

Endometrial and myometrial disruption or scarring can predispose to abnormal pregnancy implantation. Trophoblast adherence or invasion is enhanced when the scant decidualization of the lower uterine segment is impaired further by previous myometrial disruption. Implantation of a pregnancy within the uterine scar of a prior cesarean delivery is different from an intrauterine pregnancy with placenta accreta. Cesarean scar implantation is a gestation completely surrounded by myometrium and the fibrous tissue of the scar and separated from the endometrial cavity or fallopian tube (Fig. 25.7). The mechanism that most probably explains scar implantation, like intramural implantation, is invasion of the myometrium through a microscopic tract. Like intramural pregnancy, such a tract is believed to develop from the trauma of previous uterine surgery, such as curettage, cesarean delivery, myomectomy, metroplasty, hysteroscopy, and even manual removal of the placenta [33–35]. The time interval between such trauma and a subsequent pregnancy may impact upon implantation events. Some of the reported cases were diagnosed and treated within a few months of a prior cesarean delivery suggesting that incomplete healing of the uterine scar may contribute to scar implantation [36, 37].

Early diagnosis with ultrasound can offer treatment options capable of avoiding uterine rupture and hemorrhage and, thereby, preserve the uterus. The differential diagnosis between spontaneous abortion in progress, cervico-isthmic pregnancy, and implantation within a cesarean scar can be difficult. Strict ultrasound imaging criteria must be used to assess the diagnosis of cesarean scar pregnancy. Ultrasound should reveal an empty uterine cavity, an empty cervical canal, development of the gestational sac in the anterior part of the uterine isthmus, and an absence of healthy myometrium between the bladder and the gestational sac, this last criterion allowing differentiation from cervico-isthmic implantation [38].

Although cesarean scar pregnancy is an uncommon occurrence, only with a high index of suspicion and the use of early endovaginal sonography can the diagnosis be made early

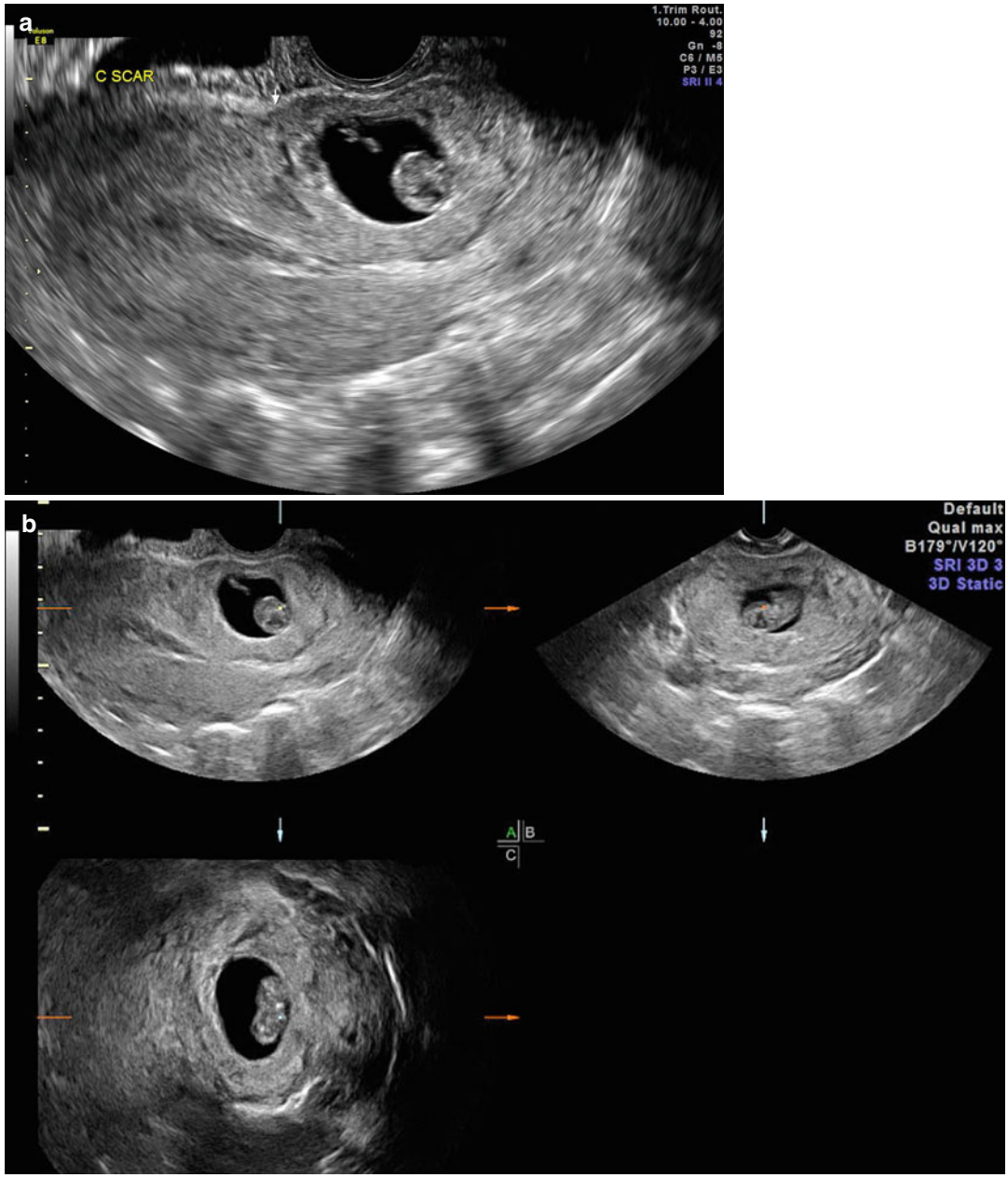

Fig. 25.7 (**a**) Transvaginal ultrasound: midline sagittal image with gestation in the anatomical location of a prior cesarean scar. (**b**) Transvaginal ultrasound: 3D rendering of cesarean scar ectopic

enough to prevent rupture leading to significant maternal morbidity and loss of future fertility. Clinical history and endovaginal ultrasound can aid in differentiating cesarean scar pregnancy from incomplete abortion and cervico-isthmic pregnancy. Precise localization of the early pregnancy by transvaginal ultrasound should be encouraged in all patients with threatening gestational pathology. A sagittal ultrasound view along the long axis of the uterus, through the gestational sac, can localize precisely a cesarean scar implantation (Fig. 25.7).

Interstitial Ectopic Pregnancy

Two to three percent of ectopics are implanted within the interstitial portion of the fallopian tube, that portion of the tube that transitions from the endometrial cavity to the tubal isthmus through a wall of myometrium [11]. The interstitial, or cornual, portion of the fallopian tube is tortuous, 0.7 mm in diameter, and 1–2 cm in length [39]. This is a relatively thick segment of fallopian tube with a greater capability to expand before rupture than more distal portions of the fallopian tube [40]. Since implantation within this portion of the fallopian is still "within the tube," it is associated with the same commonly recognized risk factors for tubal ectopic pregnancy. No single factor clearly differentiates women with an interstitial pregnancy from those with isthmic or ampullary ectopic pregnancies.

Transvaginal ultrasound is the primary method for diagnosing interstitial implantation (Fig. 25.8). However, many early ultrasounds

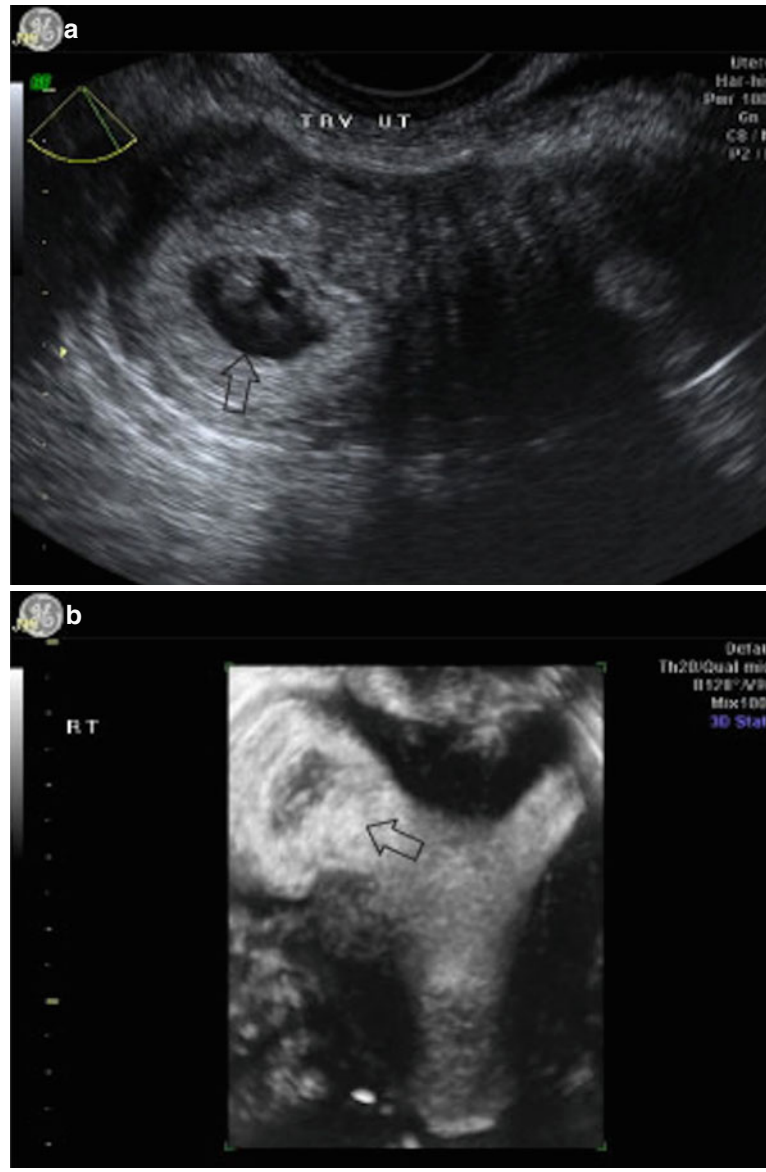

Fig. 25.8 (**a**) Transvaginal ultrasound: transverse view across uterine fundus demonstrating an asymmetrically implanted gestation, concern for interstitial ectopic. (**b**) Transvaginal ultrasound: 3D rendering confirming interstitial pregnancy implantation. (*open arrows*) Point to gestational sac

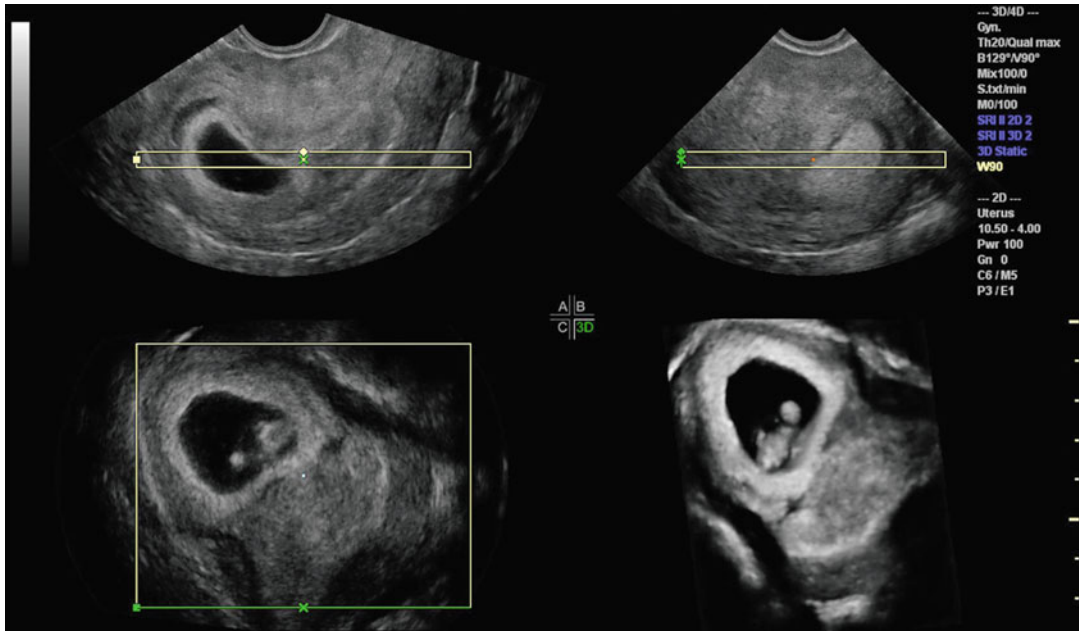

Fig. 25.9 Transvaginal ultrasound: angular pregnancy

show that these pregnancies are surrounded by myometrium and can be mistaken for normally implanted pregnancies. Ultrasound findings that are highly suggestive of interstitial implantation are the identification of an echogenic line between the gestational sac and the endometrial cavity, "the interstitial line sign," an empty uterine cavity with a gestational sac eccentrically located outside the endometrial cavity with a thin mantle of surrounding myometrium less than 5 mm in thickness [41]. Collectively, these ultrasound findings are 88–93 % specific but with a sensitivity of only 40 % [42, 43]. Coronal images generated by 3D sonography are helpful in identifying these features [44] (Fig. 25.8).

Interstitial ectopic pregnancies are frequently mislabeled as "cornual ectopics." Cornual pregnancy refers to a pregnancy within the horn of a bicornuate uterus, communicating or noncommunicating, and the clinical outcome of this implantation varies greatly and depends upon the size and expansile capacity of the affected horn [40].

Angular pregnancies are implanted in one of the lateral angles of the uterine cavity, medial to the uterotubal junction, and must be distinguished from interstitial implantations. Angular pregnancies lead to an asymmetric enlargement of the uterus (Fig. 25.9). What distinguishes an interstitial ectopic pregnancy from an angular pregnancy is that the laparoscopic appearance of the bulge of an interstitial pregnancy is lateral to the round ligament, whereas the bulge of an angular pregnancy is medial to the round ligament, displacing the round ligament laterally. Over one third of angular pregnancies end in early abortion, but for those that continue pelvic pain, persistent vaginal bleeding, placental retention during the third stage of labor, and rarely uterine rupture can be expected complications.

Ectopic After Hysterectomy

Only 56 cases of ectopic pregnancy after hysterectomy have been reported in the world's literature and are rarely suspected before surgical intervention [45]. Over half of such pregnancies have been "early presentations," this occurring because an unrecognized, preclinical pregnancy existed at the time of hysterectomy:

a preimplanted fertilized ovum was in transit and confined to the fallopian tube, or sperm was present within the fallopian when the hysterectomy was performed during a peri-ovulatory period, allowing postoperative fertilization and tubal implantation. An immediate pre-hysterectomy pregnancy test would not be expected to be positive under such circumstances. "Late presentation" ectopics have occurred after all types of hysterectomy and as remote as 12 years after the hysterectomy. These post-hysterectomy ectopic pregnancies occur with retention of one or both ovaries with the presence of a vaginal-tubal or vaginal-peritoneal fistula allowing vaginally implanted sperm access to ovulated ova.

Because the symptoms of ectopic pregnancy can be mimicked by common immediate complications after hysterectomy, such as protracted abdominal pain, pelvic hematoma formation, vaginal cuff infection, and vaginal bleeding, ectopic pregnancy is rarely expected in most post-hysterectomy cases until additional imaging or repeat operation confirms the diagnosis.

Summary

Ectopic pregnancy occurs in one out of every 50 pregnancies. Early transvaginal ultrasound can locate most, if not all early pregnancies, and should be performed on every early pregnancy with symptoms of gestational pathology or a high likelihood of ectopic pregnancy based on gynecologic history. With suspected gestational pathology, early vaginal sonography should be performed regardless of hCG level. The late diagnosis of an ectopic pregnancy increases the risk for loss of fertility and for maternal morbidity and mortality. Many non-tubal ectopic locations can be diagnosed with early transvaginal sonography, then with successful medical management. The pregnancy of unknown location, when diagnosed early and confirmed to be extrauterine, can, likewise, be managed conservatively and successfully. Medical management fails more commonly with more advanced, living ectopic pregnancies, which may occur with non-tubal ectopic pregnancies, requiring surgical intervention [46]. Therefore, it is extremely prudent to diagnose gestational pathology early with transvaginal sonography.

References

1. Centers for Disease Control and Prevention (CDC). MMWR. Ectopic pregnancy – United States, 1990–1992. MMWR Morb Mortal Wkly Rep. 1995;44:46–8.
2. Ankum WM, Mol BWJ, Van der Veen F, Bodduyt PM. Risk factors for ectopic pregnancy: a meta-analysis. Fertil Steril. 1996;65:1093–9.
3. Peterson HB, Xia Z, Hughes JM, Wilcox LS, Tylor LR, Trussell J. The risk of ectopic pregnancy after tubal sterilization: US Collaborative Review of Sterilization Working Group. N Engl J Med. 1997; 336:762–7.
4. Borgatta L, Murphy M, Chuangb C, Beardsley L, Burnhill MS. Pregnancies diagnosed during depo-provera use. Contraception. 2002;66:169–72.
5. Furlong LA. Ectopic pregnancy risk when conception fails: a review. J Reprod Med. 2002;47:881–5.
6. Kadar N, Bohrer M, Kemmann E, et al. The discriminatory human chorionic gonadotropin zone for endovaginal sonography: a prospective, randomized study. Fertil Steril. 1994;61:1016–20.
7. Spandorfer SD, Barnhart KT. Endometrial stripe thickness as a predictor of ectopic pregnancy. Fertil Steril. 1996;66:474–7.
8. Ankum WM, Van der Veen F, Hamerlynck JVTH, et al. What to do when human chorionic gonadotropin levels are below the discriminatory zone. J Reprod Med. 1995;40:525–8.
9. Barnhart KT, Sammel MD, Rinaudo PF, Zhou L, Hummel AC, Guo W. Symptomatic patients with an early viable intrauterine pregnancy: HCG curves redefined. Obstet Gynecol. 2004;104:50–5.
10. Kadar N, Caldwell BV, Romero R. A method of screening for ectopic pregnancy and its indications. Obstet Gynecol. 1981;52:162–6.
11. Bouyer J, Coste J, Fernandez H, Pouly JL, Job-Spira N. Site of ectopic pregnancy: a 10 year population-based study of 1800 cases. Hum Reprod. 2002;17:3224–30.
12. Ushakov FB, Elchalal U, Aceman PJ, Schenker JG. Cervical pregnancy: past and future. Obstet Gynecol Surv. 1997;52:45–59.
13. Dicker D, Feldberg D, Samuel N, Goldman JA. Etiology of cervical pregnancy: association with abortion, pelvic pathology, IUDs, and Asherman's syndrome. J Reprod Med. 1985;30:25–7.
14. Ginsburg ES, Frates MC, Rein MS, Fox JH, Hornstein MD, Friedman AJ. Early diagnosis and treatment of cervical pregnancy in an in vitro fertilization program. Fertil Steril. 1994;61:966–9.
15. Shinagawa S, Nagayama M. Cervical pregnancy as a possible sequela of induced abortion. Am J Obstet Gynecol. 1969;105:282–4.

16. Thomas RL, Gingold BR, Gallagher MW. Cervical pregnancy: a report of two cases. J Reprod Med. 1991;36:459–62.
17. Raskin MM. Diagnosis of cervical pregnancy by ultrasound: a case report. Am J Obstet Gynecol. 1978;130:234–5.
18. Timor-Tritsch IE, Monteagurdo A, Mandeville EO, Peisner DB, Anaya GP, Pirronw EC. Successful management of a viable cervical pregnancy by local injection of methotrexate guided by transvaginal ultrasonography. Am J Obstet Gynecol. 1994;170:737–9.
19. Grimes HG, Nosal RA, Gallagher JC. Ovarian pregnancy: a series of 24 cases. Obstet Gynecol. 1983;61:174–80.
20. Kraemer B, Kraemer E, Guengoer E, Juhasz-Boess I, Solomayer EF, Wallwiener D, Rajad TK. Ovarian ectopic pregnancy: diagnosis, treatment, correlation to Carnegie Stage 16 and review based on a clinical case. Fertil Steril. 2009;92:392. e13–5.
21. Sandvei R, Ulstein M. History and finding of ectopic pregnancies in women with and without an IUD. Contracept Deliv Syst. 1980;1:131–8.
22. Spiegelberg O. Zur Casuistik der Ovariaschwangerschaft. Arch Gynakol. 1873;13:73.
23. Shaw SW, Hsu JJ, Chueh HY, Han CM, Chen FC, Chang YL, Chao AS, Cheng PJ, Hsieh TT, Soong YK. Management of primary abdominal pregnancy: twelve years of experience in a medical centre. Acta Obstet Gynacol. 2007;86:1058–62.
24. Clark JFJ, Guy RS. Abdominal pregnancy. Am J Obstet Gynecol. 1996;96:511–20.
25. Studdiford WE. Primary peritoneal pregnancy. Am J Obstet Gynecol. 1942;44:487–91.
26. Anderson PM, Opfer EK, Busch JM, Megann EF. An early abdominal wall ectopic pregnancy successfully treated with ultrasound guided intralesional methotrexate: a care report. Obstet Gynecol Intern. 2009;2009:247252.
27. Chui AK, Lo KW, Choi PC, Sung MC, Lau JW. Primary hepatic pregnancy. Aust N Z J Surg. 2001;71:260–1.
28. Nama V, Gyampoh B, Karoski M, McRea R, Opemuyi I. Secondary abdominal appendicular ectopic pregnancy. J Minim Invasive Gynecol. 2007;14:516–7.
29. Shippey SH, Bhoola SM, Royek AB, Long ME. Diagnosis and management of hepatic ectopic pregnancy. Obstet Gynecol. 2007;109:544–6.
30. Thompson RJ, Hawe MJ. A rare pathological trinity: an appendiceal ectopic pregnancy, acute appendicitis, and a carcinoid tumor. Ir J Med Sci. 2011;180(2):579–80.
31. Yagil Y, Beck-Razi N, Amit A, Kerner H, Gaitini D. Splenic pregnancy: the role of abdominal imaging. J Ultrasound Med. 2007;26:1629–32.
32. Martin JN, Sessums JK, Martin RW, Proyer JA, Morrison JC. Abdominal pregnancy: current concepts of management. Obstet Gynecol. 1988;71:549–62.
33. Fait G, Goyert G, Sundareson A, Pickens Jr A. Intramural pregnancy with fetal survival: case history and discussion of etiologic factors. Obstet Gynecol. 1987;70:472–4.
34. McGowan L. Intramural pregnancy. JAMA. 1965;192:637–8.
35. Miller DA, Chollet JA, Goodwin TM. Clinical risk factors for placenta previa-placenta accreta. Am J Obstet Gynecol. 1997;177:210–4.
36. Huang KH, Lee CL, Wang CJ, Soong YK, Lee KF. Pregnancy in a previous cesarean section scar: case report. Changgeng Yi Xue Za Zhi. 1998;21:323–7.
37. Marcus S, Cheng E, Goff B. Extrauterine pregnancy resulting from early uterine rupture. Obstet Gynecol. 1999;94:804–5.
38. Godin PA, Bassil S, Donnez J. An ectopic pregnancy developing in a previous cesarean section scar. Fertil Steril. 1997;67:398–400.
39. Tulandi T, Al-Jaroudi D. Interstitial pregnancy: results generated from the 92. Society of Reproductive Surgeons Registry. Obstet Gynecol. 2004;103:47–50.
40. Lau S, Tulandi T. Conservative medical and surgical management of interstitial ectopic pregnancy. Fertil Steril. 1999;72:207–15.
41. Moawad NS, Mahajan ST, Moniz MH, Taylor SE, Hurd WW. Current diagnosis and treatment of interstitial pregnancy. Am J Obstet Gynecol. 2010;202:15–29.
42. Ackerman TE, Levi CS, Dashefsky SM, Holt SC, Lindsay DJ. Interstitial line: sonographic finding in interstitial (cornual) ectopic pregnancy. Radiology. 1993;189:83–7.
43. Timor-Tritsch IE, Monteagudo A, Matera C, Veit CR. Sonographic evolution of cornual pregnancy treated without surgery. Obstet Gynecol. 1992;79:1044–9.
44. Rastogi R, Meena GL, Rastogi N, Rastogi V. A rare and difficult clinicosonographic diagnosis. J Hum Reprod Sci. 2008;1:81–2.
45. Fylstra DL. Ectopic pregnancy after hysterectomy: a review and insight into etiology and prevention. Fertil Steril. 2010;94:431–5.
46. American College of Obstetricians and Gynecologists. ACOG Practice Bulletin No. 94. Medical management of ectopic pregnancy. Obstet Gynecol. 2009;111:1479–85.

Focused Ultrasound for Treatment of Fibroids

26

Gloria Richard-Davis and Elosha Eiland

Introduction

Uterine leiomyomas (fibroids) are the most common pelvic tumors in women. These benign smooth muscle tumors have a less than 0.5 % chance of undergoing malignant transformation. It is estimated that 20–25 % of women have uterine fibroids [1]. Fibroids are derived from smooth muscle cells of the uterus or the myometrium. Fibroids exist in a variety of sizes, ranging from millimeters in diameter to large tumors that can extend to reach the costal margin. Fibroids can occur singularly or in multiples. The exact etiology of fibroids continues to remain a mystery, although many studies suggest a genetic component. Studies have also shown that the growth of fibroids is related to the presence of estrogen in circulation. Many women with uterine fibroids are asymptomatic. Women that experience symptoms may have irregularities in their menstrual cycles, such as intermenstrual bleeding or menorrhagia. Other symptoms include pelvic pressure, dyspaurenia, urinary frequency, weight gain, bloating, or constipation complaints.

Several treatment options for uterine fibroids exist. Hysterectomy is the definitive treatment of symptomatic fibroids. Hysterectomy is a highly invasive surgical procedure to remove the uterus. Hysterectomy for uterine fibroids can be performed vaginally, abdominally, or laparoscopically. Hysterectomy is limited to women who have completed child bearing. Fertility-sparing treatment options for symptomatic uterine fibroids include the following: myomectomy, uterine artery embolization (UAE), cryoablation, and magnetic resonance-guided focused ultrasound (MRgFUS). Myomectomy, surgical excision of the fibroid tissue, has long been the ideal method for removing fibroids to preserve fertility. Myomectomy can be performed laparoscopically, hysteroscopically, or via laparotomy incision. UAE is a minimally invasive procedure performed by interventional radiology that decreases the blood supply to uterus and ultimately the fibroid, causing the fibroid to undergo necrosis. Cryoablation is also a minimally invasive treatment usually performed under magnetic resonance guidance, wherein fibroids are ablated by placing cryoablation probes percutaneously directly into the fibroid [2]. In 2003, MRgFUS was introduced as a noninvasive alternative procedure in the treatment of fibroids. With MRgFUS, fibroid tissue is heated and destroyed using targeted ultrasonic energy passing through the anterior abdominal wall.

A comparison of uterine-sparing surgeries such as myomectomy with the most common nonsurgical options (MRgFUS and UAE) is listed in the Table 26.1. There are multiple factors that affect the choice of procedures for treatment, such as the size of fibroids, location, and patient symptoms. All three procedures result in 70–80 %

G. Richard-Davis, MD, FACOG (✉)
E. Eiland, MD
Department of Obstetrics and Gynecology, Meharry Medical College, 1005 Dr. D.B. Todd Jr. Drive, Nashville 37208, TN, USA
e-mail: gdavis@mmc.edu; eeiland@mmc.edu

L.A. Stadtmauer, I. Tur-Kaspa (eds.), *Ultrasound Imaging in Reproductive Medicine*,
DOI 10.1007/978-1-4614-9182-8_26,

Table 26.1 MRgFUS in comparison to UAE and myomectomy

	Myomectomy	UAE	MRgFUS
Success rate	80 % with complete resolution or significant improvement of menorrhagia	80 % with improvement in menorrhagia, bulk-related symptoms, or both; reduced uterine volume >60 % by 9 months	70–80 % reduction in clinical symptoms
Recurrence rate (RR) of symptoms and repeat procedures (RP)	RR 7.5 % RP 6.8 % by 2 years	RR 10 % by 3 years RP 20 % by 5 years	Data unavailable
Complications	Febrile morbidity Intraperitoneal bleeding	Major complication rate of less than 1 %	Few FDA reportable adverse events Skin burns Nerve damage
Recovery period	2–3-day hospital stay Recovery period of 2–4 weeks	Outpatient procedure Recovery period of 13 days	Outpatient procedure Recovery period 1–4 days
Pregnancy outcomes	Overall conception rate of 57 %; spontaneous abortion rate 19 %	Future fertility not intended; limited long-term data. Pregnancies reported with increase preterm birth and spontaneous abortion	Clinical trials ongoing; 54 pregnancies in 51 women reported Spontaneous abortion rate –28 %

Based on data from Refs. [3–6]

improvement in symptoms. Retreatment rates are low with all options but lowest for myomectomy (7.4 %) versus UAE (10 %) followed by MRgFUS (14 %). Complication rates across the board are relatively low. The greatest differences are in the recovery time, where myomectomy is an inpatient procedure with 2–4 weeks of recovery time. UAE is an outpatient procedure but does require an average 13 days' recovery, while MRgFUS is also an outpatient procedure but has a 1–4 days' recovery time. This is the primary distinguishing factor. Pregnancy outcome data is more challenging to compare, as UAE and MRgFUS have been limited to women not planning future pregnancies. Therefore, data on pregnancies post procedure is limited. Recent clinical trials are focusing on MRgFUS and pregnancy outcomes. Therefore, data should be forthcoming in the near future.

Magnetic resonance-guided focused ultrasound—approved by the FDA in October 2004—has the potential to completely revolutionize the treatment of uterine fibroids [7]. MRgFUS provides a nonsurgical outpatient method of ablating fibroids that preserves the uterus and enables patients to return to normal activity within 1 or 2 days. Based on two groundbreaking core technologies, MRgFUS gives physicians the ability to destroy fibroid masses by producing precise amounts of heat and vibration within the body with pinpoint accuracy. It uses heat rather than radiation to destroy tissue and can be used again and again without harmful side effects. MRgFUS has only a few serious FDA reportable adverse events including skin burns, which result from poor coupling from hair and scars on the skin, and nerve damage, which resolved within a year [8]. There is also a slight risk of damage to adjacent organs, such as bowel perforation.

Currently, MRgFUS treatment for uterine fibroids is offered at medical centers in 15 states in the United States and in 14 countries around the world. Over 3,000 patients have been treated worldwide, including 370 who are being followed for the FDA post market. Four more companies are developing and testing similar technology for fibroid treatment [9]. The technology is evolving, as are guidelines for treatment. Several studies have shown that MRgFUS significantly improves clinical symptoms in 70–80 % of women with uterine fibroids [6–8, 10, 11]. Studies have demonstrated a correlation between the treated volume of the fibroids, improvement in symptoms, and lesion shrinkage [12].

How Does It Work?

In conventional diagnostic ultrasound, ultrasound waves pass through the anterior abdominal wall. Significant heating only occurs where the waves converge at the focus. However, because lower levels of energy proximal and distal to the focus have the potential to damage normal tissue, real-time monitoring of the entire beam is critical.

When transmitting the ultrasonic energy continuously, high-intensity focused ultrasound can raise tissue temperature at the focal point. We quantify the level and duration of this temperature elevation as the tissue's "thermal dose." Thermal effect can be used to create either a low-level thermal rise over several hours (local hyperthermia) or, conversely, a short, highly localized high temperature rise that cooks the tissue (thermal ablation).

Depositing a high level of ultrasonic energy causes an intense increase in temperature, thermal coagulation, and cell death. Exposing tissue, for even 1 s, to a temperature of 56 °C/130 °F is enough to induce irreversible thermal damage to cells. Thermal necrosis results from the denaturation of the cell proteins, just like cooking an egg. Researchers and physicians use focused ultrasound's thermal coagulation effect to noninvasively treat a variety of diseases, including symptomatic uterine fibroids; breast, liver, and prostate cancer; low back pain; and brain disorders (essential tremor and neuropathic pain) (see Fig. 26.1).

ExAblate uses a "sonication" process in which focused ultrasound (FUS) concentrates a high-energy beam on a specific point, raising its temperature to 60–85 °C resulting in destruction of fibroid tissues by coagulation necrosis [8]. High intensities of energy are accumulated in a relatively small tissue volume, which effectively results in tissue destruction through heat and cavitation effects [13].

Multiple sonications are required to ablate the fibroid tissue. The MRI system provides essential data including the location of the intended target (fibroid) and internal organs where non-target treatment could result in complications. Additionally, the MRI allows for real-time thermometry, so that the treating physician can adjust power to achieve intended necrosis of the fibroid while minimizing injury to normal tissue from too high a temperature. This magnetic resonance thermometry provides instant feedback as to the thermal dose delivered during each sonication (see Fig. 26.1).

Fig. 26.1 Doctors communicate with patient during procedure (Courtesy of Insightec, Inc)

In contrast to UAE where occlusion of vascular supply causes destruction of fibroid and normal myometrium, MRgFUS spares normal myometrium. Specific leiomyomata are targeted for treatment with MRgFUS, also sparing myometrium. However, some leiomyomata may go untreated due to time limitations or safety problems in targeting, potentially resulting in variable in treatment outcome (Fig. 26.2).

Patient Selection

In early clinical trials for MRgFUS technology, the inclusion and exclusion criteria were identical. All women in these studies were premenopausal and at least 18 years old, had significant leiomyoma symptoms (as defined by a transformed symptom severity score greater than 41 out of 100 points on a validated leiomyoma specific quality of life measure (Uterine Fibroid Symptoms Quality of Life Questionnaire)), and did not desire future childbearing. Exclusion criteria included women with uteri larger than 24 weeks gestational size, a hematocrit less than

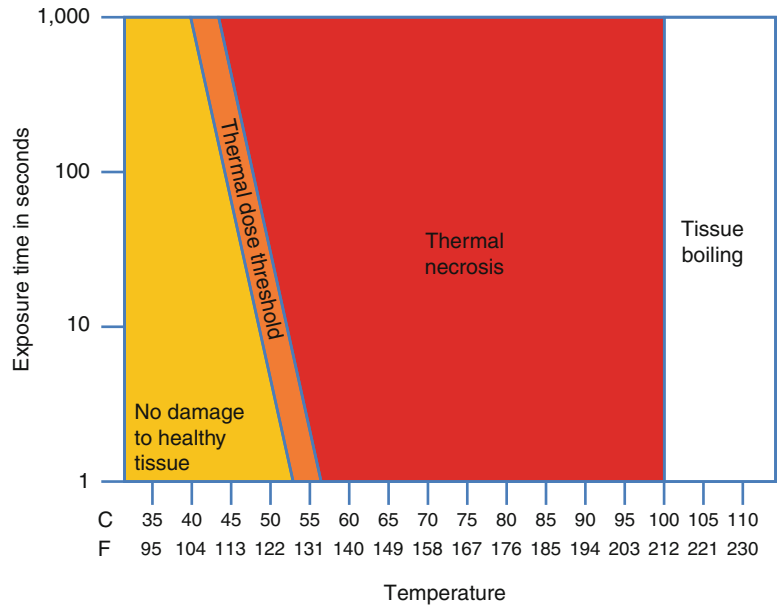

Fig. 26.2 Different levels of thermal dose applied versus their biological outcome (Courtesy of Focused Ultrasound Foundation)

25 %, a positive pregnancy test, major medical disease, or contraindication to magnetic resonance imaging such as a pacemaker or weight over 250 lb.

The FDA relaxed treatment protocols on April 30, 2004, so that patients treated after that date in phase 3 continued-access protocol and the post-market study, both in the United States and abroad ($n=64$ and 61, respectively, overall 34 %), were allowed to have more extensive treatment. Treatment volume allowances were increased from 33 to 50 % for all leiomyomata except submucosal ones, and maximal treatment volume was increased to 150 mL per leiomyoma. Extension of treatment time from 120 to 180 min and treatment border restrictions increased to 1.5 cm from the endometrium and 0.5 cm from the leiomyoma capsule to the serosal surface were eliminated. This allowed more patients to be treated with MRgFUS safely based on clinical trial data.

A post-marketing study of African-American women was mandated by the FDA and required treatment candidates to be "consistent with product labeling," thus making the same enrollment criteria as noted previously implicit rather than explicit.

A pretreatment magnetic resonance imaging scan was required for treatment planning to assess the accessibility of leiomyomata to treatment without injury to the bowel, bladder, or pelvic nerves; exclude adenomyosis or lesions suspicious for uterine sarcomas; and demonstrate pretreatment vascularization of the leiomyoma by using the intravenous contrast agent gadolinium. African-American women have an increased incidence of fibroids, earlier onset of disease, and more severe symptoms [14–16]. Despite their increased risk of disease, African-American women historically comprise only approximately 15 % of subjects in fibroid studies [17]. Recent ongoing Fibroid Interventions: Reducing Symptoms Today and Tomorrow (FIRSTT) trial is focused on recruitment of African-American women to analyze differences. This trial will provide for sub-analysis of the data specific to African-American women and explore further the genetic linkage [18].

Current inclusion criteria to receive MRgFUS as a viable treatment option include the following: (1) a patient must first have a uterine fibroid(s), (2) the fibroid(s) must be relevant to the patient's symptoms, and (3) the location and size of the fibroids must correlate with the patient's symptoms. For example, subserosal fibroids located just underneath the serosa of the uterus grow outward resulting in compression symptoms to adjacent organs, i.e., bladder (urinary frequency) and intestines (constipation) (see Table 26.2). Subserosal fibroids associated

Table 26.2 Patient inclusion criteria for MRgFUS

1. Patient should have a definitive diagnosis of a uterine fibroid(s) as the cause for her symptoms
2. Patient's uterus should be <24 cm without the cervix (alternatively, maximal fibroid volume should be <900 cc)
3. Patient may have up to six clinically significant fibroids less than 4 cm in size
4. Patient should be pre- or perimenopausal
5. Patient should be able to have a catheter during treatment

Table 26.3 Patient exclusion criteria for MRgFUS

1. Hemoglobin <10 mg/dL
2. Hemolytic anemia
3. Unstable cardiac status including:
(a) Unstable angina pectoris on medication
(b) Documented myocardial infarction within 6 months of protocol entry
(c) Congestive heart failure requiring medication (other than diuretic)
(d) Currently taking antiarrhythmic drugs
(e) Severe hypertension (diastolic BP >100 on medication)
(f) Presence of cardiac pacemaker
4. Severe cerebrovascular disease (multiple CVA or CVA with 6 months)
5. Currently on anticoagulation therapy
6. Presence of underlying bleeding disorder
7. Current pregnancy
8. Presence acute pelvic infection
9. Evidence of uterine pathology other than leiomyoma
10. Presence of undiagnosed pelvic mass outside of the uterus
11. Presence of symptomatic pedunculated submucosal or pedunculated subserosal myoma
12. Presence of severe adenomyosis (only for United States)
13. Evidence of high-grade SIL by pap smears or HPV testing
14. Weight >110 kg (250 lb)
15. Presence of extensive longitudinal abdominal scarring in an area of the abdomen directly anterior to the treatment area that may block the energy path (only for United States)
16. Presence of standard contraindications for MR imaging, such as non-MRI compatible implanted metallic devices, does not have severe claustrophobia. Size and weight should allow fitting in MRI device, etc.
17. Individuals who are not able or willing to tolerate the required prolonged stationary prone position during treatment (approximately 3 h)

with uterine bleeding instead of compression symptoms may not be a candidate for removal by MRgFUS [8]. Exclusion criteria are extensive and include pregnancy, other uterine pathology, severe anemia, and other medical conditions (see Table 26.3).

Patients with scars or moles in the mid-abdominal region could possibly be excluded from having this procedure performed because scars have high ultrasound absorption and may lead to pain or damage to the skin [7]. Individuals that have been diagnosed with other pelvic diseases should also be excluded from this procedure. Women who weigh more than 250 lb. are not candidates for MRgFUS [7]. Communication is important throughout the procedure and it is vital that the patient is able to do so. Pre- or perimenopausal women, pregnant women, or women with an active pelvic infection will not be able to undergo therapy. The MRgFUS treatment also requires a urinary catheterization. Patients should be aware that a catheter will be in place. Severe adenomyosis is also a contraindication to receiving treatment. However, recent studies have shown that MRgFUS can be used to ablate adenomyosis and improve symptoms during a period of 3–6 months. However, no long-term evidence exists that demonstrates that there is a clinical benefit in the treatment of adenomyosis [8].

The location of fibroids is one of the primary concerns with this MRgFUS technique. MRI is used to precisely measure fibroids and location to determine eligibility of treatment. Fibroids must be reachable by the MRgFUS device and not be too far away from the skin line but at least 4 cm from the sacrum. This distance decreases the amount of heating of the bone and reduces nerve damage which can occur as a result of nerves lying next to heated bone surfaces [8]. Bone absorbs ultrasound waves more readily than soft tissue. As a result, low energies can cause high temperatures in bone surfaces and result in nerve damage to adjacent nerves.

Patients should not have more than 6 fibroids that are more than 4 cm in size each, as this is usually associated with the fibroids being in close proximity to the sacrum or being inaccessible, i.e., hidden behind bowel [8]. Patients should not

Table 26.4 Technical suitability for MRgFUS

1. Fibroid(s) should be clearly visible on non-contrast MRI
2. Fibroid(s) should be device accessible (i.e., positioned in the uterus such that they can be accessed without being shielded by bowel or bone)
3. Fibroid(s) center should be at least 4 cm from the sacrum surface
4. Fibroid(s) should be hypo- or iso-intense on MR T2 images (relative to the uterus muscle)
5. Fibroid(s) should enhance on MR contrast imaging
6. Fibroid(s) envelope should not be significantly calcified
7. Patients should not have imaging suggestive of malignant disease of uterus, ovary, or cervix
8. Patients should not have severe adenomyosis (only for US patients)

have fibroids that have more than a significant proportion of the fibroid 12 cm in depth away from the skin line, as the maximum depth of penetration of the sound is 12 cm. Mitigation techniques can sometimes be used to decrease the depth. However, if the mitigation techniques are unsuccessful, the fibroid must be excluded. Examples of mitigation techniques include filling the rectum with ultrasound gel to elevate the uterus and fibroids anteriorly and using a thinner acoustic coupling gel pad, which reduces the distance between the patient and the transducer [8] (see Table 26.4).

Patients who have a calcified fibroid envelope (capsule) are excluded from this procedure due to the ultrasound's inability to penetrate the calcified capsule and enter the body of the fibroid mass [8]. Pedunculated fibroids attached to the uterus by a stalk are excluded because during the procedure, they may become detached and enter the abdominal cavity, requiring further surgical, perhaps invasive, interventions [8].

Impact on Future Fertility

Review of the literature on pregnancy outcome after MRgFUS revealed 88 women became pregnant. The mean time to conception was 8 months after treatment [4]. Of those 88 pregnancies, there were 45 (51 %) total deliveries, 67 % SVD (spontaneous vaginal deliveries), and 33 % C/S (cesarean section). However, 19 of those 88 (22 %) women experienced spontaneous abortions. Rabinovici noted that uterine rupture, preterm labor, placental abruption, and abnormal placentation leading to fetal growth restriction were not observed in any of the cases [11].

Several case reports of women conceiving after MRgFUS ablation have been published [19].The largest series was published by Rabinovici. In 2003, he reported on 54 pregnancies in 51 women who were treated with MRgFUS for symptomatic uterine fibroids and/or focal adenomyosis. Of the delivered pregnancies in which gestational age was reported, there was a 93 % (14 of 15) term delivery rate and one preterm birth which occurred at 36 weeks. The current series of pregnancies reassures that term (and ongoing) pregnancies can be achieved in a substantial percentage of women conceiving after MRgFUS treatment of uterine fibroids [4]. Clinical studies are ongoing to evaluate fertility outcomes after MRgFUS.

Other Conditions That Can Be Treated

Adenomyosis

The MRgFUS procedure can ablate adenomyosis tissue sufficiently and can improve symptoms significantly during a period of 3–6 months posttreatment especially those with low-signal intensity adenomyosis on T2-weighted MR images [8]. It is not yet an approved FDA indication. Additional clinical data is still needed. A case report submitted by Rabinovici et al. details a patient who underwent MRgFUS to ablate focal uterine adenomyosis [20]. The patient experienced significant reduction in menometrorrhagia in the weeks following therapy, and at her 6-week follow-up visit, her adenomyotic tumor was noted to decrease in size from 6.5×4.9×4.8 cm pretreatment to 3.5×4.3 cm posttreatment. The patient went on to conceive spontaneously three menstrual cycles after therapy. She had an uneventful pregnancy, labor, and vaginal delivery that resulted in the delivery of a full term, normal weight neonate.

Patient Preparation

Before the procedure can go forth, the patient is asked to fast overnight. The abdomen area is shaved to remove any hair and check for the presence of scars. The patient is positioned abdomen down over a water bath which contains a transducer. The patient's abdomen is fixed with the transducer via the water bath using a gel pad. Vital signs and comfort level are monitored throughout the 3 h treatment. It is vital the patient remains in a comfortable position for the procedure. Communication is maintained through an intercom system and emergency button given to the patient.

Generally, treating and ablating an 8 cm fibroid takes approximately 3 h of sonication (excluding patient preparation and planning), depending on energy absorption and location of the fibroid. However, two options are available: First, the fibroid is treated over two sessions, performed preferably with the fibroid volume being split into a superior and an inferior region for each of the treatment. This is to avoid the ultrasound beam in the second treatment from passing through already treated regions if anterior-posterior division was made. Second option is pretreatment with GnRH agonist prior to MRgFUS to shrink the fibroid and improve treatment outcomes [7].

Treatment

Patients remain awake during the 2–3-h procedure to provide feedback regarding any pain or discomfort experienced during therapy. Therapy can be stopped at any moment by the signal of the emergency button given to the patient prior to treatment. During this surgery, ultrasound energy is released in the form of heat through the body. The beam carries high levels of heat energy to cause cell death or apoptosis. The result of death is the decrease in size of the fibroid(s).

The region of treatment (ROT) is placed on the coronal images. The ROT is drawn with a margin of at least 1 cm to serosal surfaces to minimize the risk of ablating the serosa resulting in severe pain and possible bowel injury. There is no limit to the percentage of fibroid volume that can be treated though generally a 60–70 % of ablation is necessary for good outcomes [9]. The operator then chooses the treatment plan depending on the size and type of fibroid being treated. For "white fibroids," a nominal high-density plan should be selected; otherwise a medium-density plan would be suitable. The length of the sonications can then be selected and may vary from 10 to 45 mm. Based on the treatment plan chosen, the FUS system automatically displays a series of sonications to cover the region of treatment. Each spot is cylindrically shaped, 25–45 mm in length and 5 mm in diameter for a nominal fibroid (see Fig. 26.3).

The system will display the total number of sonication spots on the defined ROT. These spots are green, yellow, or red (just like traffic lights) to indicate the safety of each sonication spot. Each sonication treatment varies from 20 to 30 s. This is followed by cooling periods of 24–90 s. For the patient's safety, a cooling period between each sonication is programmed into the treatment plan, to allow cooling of tissue outside and anterior to the treatment zone. Immediately following treatment, the patient's skin is checked for the presence of any burns [8].

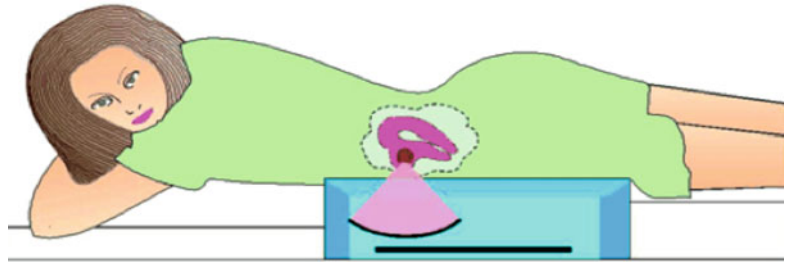

Fig. 26.3 MR-guided focused ultrasound surgery (Courtesy of Insightec, Inc.)

MRgFUS offers a safer treatment with a much faster recovery time than other surgeries. Patients are generally able to return to the normal activities the day after the procedure with little to no medication. Patients follow up 2 weeks after the procedure both with their gynecologist and at the interventional radiologist. Those patients with larger or multiple fibroids in which the treatment could not be completed can have a repeat treatment planned from 1 week onward [8]. After 6 months, a follow contrast-enhanced MRI is performed to assess fibroid size [8].

Outcomes

In 2004, early reports by Hindley demonstrated greater improvement in the Uterine Fibroid Symptoms and Quality of Life Questionnaire (UFS-QLQ) by patients who had a greater proportion of the fibroid treated [7]. The UFS-QLQ is a validated uterine fibroid-specific questionnaire developed to evaluate the symptoms of uterine fibroids and their impact on health-related quality of life [21]. It consists of an eight-item symptom scale and 29 health-related quality of life (HRQL) items comprising 6 domains: concern, activities, energy/mood, control, self-consciousness, and sexual functioning. All items are scored on a five-point Likert scale, summed and transformed into a 0–100 point scale. Patients had to have a minimum of 21 points, out of a total of 40 points, on the symptom severity scale to be included in the study. One hundred nine patients qualified and were treated at seven sites. Fifty-two patients were treated in the United States, and 57 patients were treated in Europe and Israel. The mean age was 44.8 ± 4.9 [SD] years (the range was 30–58). 11 % of patients were AA with mean body mass index of 25.8 ± 5.2. Of the fibroids treated, 22 % were submucosal, 57 % were intramural, and 21 % were subserosal. The mean fibroid volume in patients with only a single fibroid treated (n =60) was 346, ± 245 cm^3. In patients with multiple fibroids treated (n = 32), the mean fibroid volume was less at 294, ± 188 cm^3. The region of treatment was 39 cm^3 (± 27 cm^3) for single fibroids and 38 cm^3 (± 24 cm^3) for multiple fibroids. The actual volume that received a thermal dose as measured using MR thermometry was 36 cm^3 (± 18 cm^3), around 10 % of the fibroid volume for single fibroids, and 32 cm^3 (± 23 cm^3) about 11 % for multiple fibroids. At 6-month follow-up, the mean fibroid volume was reduced by 13.5 %, ± 32. Although the change in fibroid volume is modest, the average non-perfused volume at the end of the treatment was approximately 25 %. The expected impact was modest shrinkage of the fibroid. In addition, the mean non-perfused volume was 51.2 cm^3 (± 62.2 cm^3). Overall, 79.3 % of patients achieved a greater than 10-point reduction in the UFS-QLQ score (n = 82, p < 0.0001). The mean reduction in the symptom severity score on UFS-QLQ was 27.3 points (p < 0.0.0001; range, 18.75 to –81.25 points), and although most of this improvement occurs in the first 3 months after treatment (24.1 points), improvement continued up to 6 months.

Hindley reported that the greater percentage of the non-perfused volume (NPV) of fibroids posttreatment correlated to improvement in symptoms. The average improvement in the scores was 25.8 at 6 months in those patients with NPV after treatment of less than 30 %, compared to 31.7 in patients who had more than 30 % NPV. The volume of the fibroid treated in early studies was limited by safety margins imposed by the regulatory authorities.

Stewart et al. report longer follow-up confirmed a positive correlation in the volume reduction of the fibroid to symptom improvement after 2 years [15]. Stewart et al. in 2007 [12] reported women undergoing MRgFUS for symptomatic uterine leiomyomata had durable symptom relief, as measured by the symptom severity score at 24 months with significantly greater improvement with more complete ablation (p < .001). Patients also reported an "improved quality of life" months after the treatment had taken place [7]. Treated fibroid decreased by 12 % volume at 1 month and 15 % by 3 months. Higher mean NPV ration immediately posttreatment correlated with higher probability of intervention-free survival (Fig. 26.4).

As restrictions were lifted, an increase proportion of the fibroid could be treated [22].

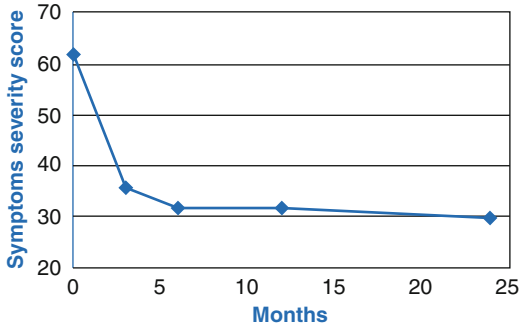

Fig. 26.4 Symptoms severity score (Courtesy of Insightec, Inc.)

Therefore, later investigators reported on safely treating larger percentage of fibroid. Recently, Zhang et al. treated 21 out of 23 patients with a mean fibroid volume of 97.0 ± 78.3 cm^3. An average of 75 ± 11.4 % of fibroid volume was treated. The average NPV was 83.3 ± 71.7. Zhang reported no statistical difference between the treatment volume and the NPV. An MRI at 3 months in 12 patients revealed a decrease in fibroid volume of 31.4 ± 29.3 %, which was statistically significant by paired t-test ($p = 0.002$). The average treatment time was 2.5 ± 1.4 h which was well tolerated by patients with few side effects [23].

Overall, MRgFUS treatment has had few side effects. Taran noted in a survey of 12 experts underreporting of adverse events. The author searched the FDA's Manufacturer and User Facility Device Experience Database (MAUDE) from January 1, 2004, to October 31, 2008, with the search terms "Product Class: Ablation System, High-Intensity Focused Ultrasound (Hifu), MR-Guided," "Manufacturer: InSightec," and "Brand Name: ExAblate and ExAblate 2000" and found 11 reported adverse events. Twelve participants reported 17 adverse events not previously reported and found in searching MAUDE. These included five neuropathies, four grade 1–2 skin burns, performance of two emergent hysterectomies, two abdominal wall edemas, one bowel injury, one bladder injury, one deep vein thrombosis (DVT), and one fat necrosis. There were no patient deaths. The authors concluded there is an underreporting of adverse events in MAUDE [9].

Cost

Other than the limitations listed previously, the cost of the therapy seems to remain the most challenging barrier to treatment with MRgFUS. The cost of the procedure ranges between $5,000 and $15,000 at 90 % of the treatment centers. Despite several studies that have shown that MRgFUS is cost-effective compared to other treatment modalities, such as UAE, myomectomy, and hysterectomy, reimbursement for the procedure by major insurance companies is not universal and patients are responsible for the entire cost of the procedure [24–26]. Many insurance companies still consider MRgFUS treatment of fibroids experimental and will not cover the cost. A physician survey conducted by Taran et al. during an international symposium in October 2008 reported that 81 % ± 19 of patients do not receive MRgFUS treatment secondary to declined reimbursement [9]. It was noted that reimbursement of services by insurance companies occurred more frequently when services were provided at academic institutions compared with private practices. A retrospective study conducted by Behera et al. of patients who were referred for minimally invasive treatment of fibroids during the time period of November 2007 and February 2009 showed that 12 % of patients declined MRgFUS for financial reasons but that another 48 % declined MRgFUS for unstated reasons, often after obtaining financial and insurance coverage information [26].

Conclusion

In October 2004, the FDA approved the ExAblate 2000 for treatment of uterine fibroids [7]. ExAblate is the only commercially approved noninvasive therapeutic system. Several studies have shown that MRgFUS significantly improves clinical symptoms in 70–80 % of women with uterine fibroids. MRgFUS is noninvasive and can be performed as an outpatient procedure and allows the majority of patient to return to work and their normal activities in 1–2 days. MRgFUS is a technique that has minimum complications, requires no general anesthesia, and has no overnight stay. Clinical trials are ongoing to

evaluate future fertility in patients that have undergone MRgFUS and look promising. Other uses for MRgFUS are also under investigation, such as treatment of adenomyosis. Several other companies are developing similar technology that may be launched soon, adding to nonsurgical therapeutic options, body of work, and standardization of insurance coverage.

References

1. Cramer SF, Patel A. The frequency of uterine leiomyomas. Am J Clin Pathol. 1990;94:435.
2. Sakuhara Y, Shimizu T, Kodama Y, Sawada A, Endo H, Abo D, Hasegawa T, Miyasaka K. Magnetic resonance-guided percutaneous cryoablation of uterine fibroids: early clinical experiences. Cardiovasc Intervent Radiol. 2006;29(4):552–8.
3. Breech LL, Rock JA. Leiomyomata uteri and myomectomy. In: Rock JA, Jones HW, editors. Telinde's operative gynecology. Tenthth ed. Philadelphia: Lippincott Williams & Wilkins; 2008. p. 719–21.
4. Rabinovici J, David M, Fukunishi M, Morita Y, Stewart EA, MRgFUS Study Group. MR guided focused ultrasound pregnancies: pregnancy outcome following magnetic resonance guided focused ultrasound surgery (MRgFUS) for conservative treatment of uterine fibroids. Fertil Steril. 2008;93(1): 199–209.
5. Stovall DW. Alternatives to hysterectomy: focus on global endometrial ablation, uterine fibroid embolization, and magnetic resonance-guided focused ultrasound. Menopause. 2011;18(4):443–50.
6. Fennessy FM, Tempany CM, McDannold NJ, et al. Uterine leiomyomas: MR imaging-guided focused ultrasound surgery-results of different treatment protocols. Radiology. 2007;243(3):885–93.
7. Hindley J, Gedroyc W, Regan L, Stewart E, Tempany C, et al. MRI guidance of focused ultrasound therapy of uterine fibroids: early results. AJR Am J Roentgenol. 2004;183(6):1713–9.
8. Abdullah B, Subramaniam R, Omar S, Wragg P, Ramli N, Wui A, Lee C, Yusof Y. Magnetic resonance-guided focused ultrasound surgery (MRgFUS) treatment for uterine fibroids. Biomed Imaging Interv J. 2010;6(2):e15. Epub 2010 Apr 1.
9. Taran FA, Hesley G, Gorny KR, Stewart E. What factors currently limit magnetic resonance – guided focused ultrasound of leiomyomas? A survey conducted at the first international symposium devoted to clinical magnetic resonance-guided focused ultrasound. Fertil Steril. 2010;94:331–4.
10. Stewart EA, Rabinovici J, Tempany CM, et al. Clinical outcomes of focused ultrasound surgery for the treatment of uterine fibroids. Fertil Steril. 2006;85(1):22–9.
11. Rabinovici J, David M, Fukunishi M, Morita Y, Gostout BS, Stewart EA, MRgFUS Study Group. Fertil Steril. 2010;93(1):199–209.
12. Stewart EA, Gostout B, Rabinovici J, et al. Sustained relief of leiomyoma symptoms by using focused ultrasound surgery. Obstet Gynecol. 2007;110(2 Pt 1):279–87.
13. Al Hilli MM, Stewart EA. Magnetic resonance-guided focused ultrasound surgery. Semin Reprod Med. 2010;28(3):242–9. Epub 2010 Apr 22.
14. Baird DD, Dunson DB, Hill MC, Cousins D, Schectman JM. High cumulative incidence of uterine leiomyoma in black and white women: ultrasound evidence. Am J Obstet Gynecol. 2003;188:100–7. PubMed: 12548202.
15. Stewart EA. Uterine fibroids. Lancet. 2001;357: 293–8. PubMed: 11214143.
16. Huyck KL, Panhuysen CI, Cuenco KT, Zhang J, Goldhammer H, Jones ES, et al. The impact of race as a risk factor for symptom severity and age at diagnosis of uterine leiomyomata among affected sisters. Am J Obstet Gynecol. 2008;198(168):e1–9. PubMed: 18226615.
17. Taran FA, Brown HL, Stewart EA. Racial diversity in uterine leiomyoma clinical studies. Fertil Steril. 2010;94(4):1500–3. Epub 2009 Dec 6. Review.
18. Bouwsma EV, Hesley GK, Woodrum DA, Weaver AL, Leppert PC, Peterson JG, Stewart EA. Comparing focused ultrasound and uterine artery embolization for uterine fibroids – rationale and design of the fibroid interventions: reducing symptoms today and tomorrow (FIRSTT) trial. Fertil Steril. 2011;96(3):704–10. Epub 2011 Jul 27.
19. Hanstede MM, Tempany CM, Stewart EA. Focused ultrasound surgery of intramural leiomyomas may facilitate fertility: a case report. Fertil Steril. 2007;88(2):497.e5–e7.
20. Rabinovici J, Inbar Y, Eylon SC, Schiff E, Hananel A, Freundlich D. Pregnancy and live birth after focused ultrasound surgery for symptomatic focal adenomyosis: a case report. Hum Reprod. 2006;21(5):1255–9.
21. Harding G, Coyne KS, Thompson CL, et al. The responsiveness of the uterine fibroid symptom and health-related quality of life questionnaire (UFS-QOL). Health Qual Life Outcomes. 2008;6:99.
22. Orsi F, Arnone P, Chen W, Zhang L. High intensity focused ultrasound: a new therapeutic option for solid tumors. J Cancer Res Ther. 2010;6(4):414–20.
23. Zhang L, Chen WZ, Liu YJ, Hu S, Zhou K, Chen L, et al. Feasibility of magnetic resonance imaging – guided high intensity focused ultrasound therapy for ablating uterine fibroids in patients with bowel lies anterior to uterus. Eur J Radiol. 2010;73:396–403.
24. Zowall H, Cairns JA, Brewers C, Lamping DL, Gedroyc WM, Regan L. Cost effectiveness of magnetic resonance-guided focused and ultrasound surgery for treatment of uterine fibroids. BJOG. 2008;115:653–62.
25. O'Sullivan AK, Thompson D, Chu P, Lee DW, Stewart EA, Weinstein MC. Cost-effectiveness of magnetic resonance guided focused ultrasound for the treatment of uterine fibroids. Int J Technol Assess Health Care. 2009;25(1):14–25.
26. Behera MA, Leong M, Johnson L, Brown H. Eligibility and accessibility of magnetic resonance-guided focused ultrasound (MRgFUS) for the treatment of uterine leiomyomas. Fertil Steril. 2010;94(5):1864–8.

Index

L.A. Stadtmauer, I. Tur-Kaspa (eds.), *Ultrasound Imaging in Reproductive Medicine*,
DOI 10.1007/978-1-4614-9182-8, © Springer Science+Business Media New York 2014